Fundamentals, Design & Control of

Air-conditioning Systems

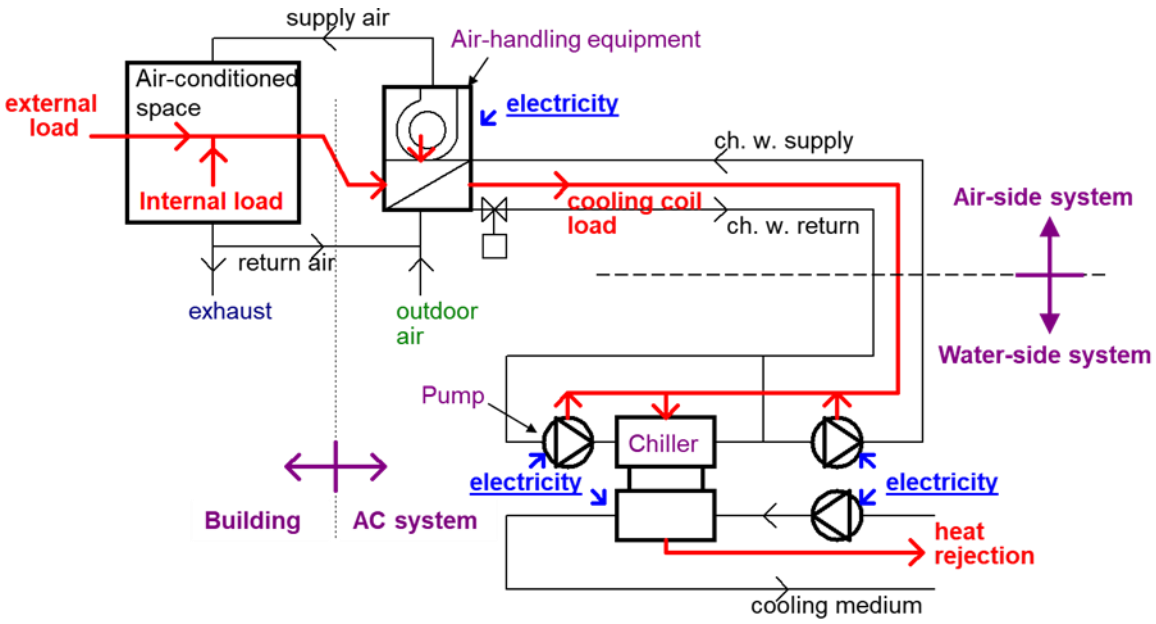

Francis W. H. Yik

Fundamentals, Design & Control of Air-conditioning Systems

By

Francis W. H. Yik, BSc, MSc, PhD, DEng, MHKIE, MIMechE, FCIBSE

This book is dedicated to students and practitioners in the field of building services engineering in Hong Kong and elsewhere.

About the author

Francis Yik graduated from the University of Hong Kong in 1980 with a bachelor's degree in mechanical engineering. He practiced as a building services consulting engineer and was awarded an MSc degree in mechanical engineering, also by the University of Hong Kong, before joining the Department of Building Services Engineering of the Hong Kong Polytechnic University (then called Hong Kong Polytechnic) in 1987 as a lecturer. Francis became a Professor in 1999 and was awarded a higher doctorate in engineering (DEng) in 2009 by his alma mater, the University of Northumbria at Newcastle, UK where he acquired his PhD degree in 1993. He re-joined the industry in 2013 and worked for ATAL Engineering Group. He retired from full time employment as Technical Director of the group in 2017, and part-time employment as a Technical Consultant in 2020.

The following was said about Francis during the ceremony in which he was awarded the higher doctorate in 2009:

> "*Professor Wai Hung Francis Yik is a professor in the Department of Building Services Engineering at the Hong Kong Polytechnic University and we are delighted to be awarding him the Higher Doctorate today in recognition of the significant contribution he has made to the field of Building Services Engineering.*
>
> *His extensive record of published academic research has made a real contribution to his profession and is likely to have a lasting impact on the lives of others.*
>
> *Professor Yik, 52, qualified with a PhD in Building Services Engineering at Northumbria in 1993. A recognised expert in this field, he has made a significant contribution to the science and engineering practice of air conditioning design and operation through his teaching, research and consultancy.*
>
> *A recipient of the Dufton Silver Medal from the Chartered Institution of Building Services Engineers, Professor Yik has acted as a visiting professor at Northumbria and collaborated with academics from the School of Built Environment in a number of published works, including a joint project to raise the professional profile of building services engineers in Hong Kong.*
>
> *Professor Yik's Higher Doctorate marks his vital contribution to our understanding of air conditioning design and operation in humid sub-tropical climates and complements his most recent work, which has focused on construction, economics and research in support of the various professions that contribute to the wider built environment.*"

Preface

This book on air-conditioning systems is dedicated to students and practising engineers in the field of building services engineering or, as is more widely known in North America, mechanical, electrical, and plumbing (MEP) in buildings. It focuses on the range of central air-conditioning systems that are common or emerging in modern buildings. Nevertheless, adequate coverage is given to the fundamentals underpinning air-conditioning engineering, especially on psychrometric principles, heat transfer in buildings related to cooling load calculation and thermal comfort of building occupants, and on air and water flows in air-conditioning systems and equipment.

Selection of topics to be covered in the book was based on the knowledge that one would need to carry out design and operation & maintenance of air-conditioning systems in modern buildings, especially on designs and measures for enhancing energy efficiency. The breadth and depth of coverage of the topics were tuned in the light of the author's experience in system design, teaching on under- and post-graduate courses, and delivering technical training for practising engineers. The objectives are to enable the targeted readers to understand the working principles and, on that basis, to carry out design for new systems as well as performance evaluation and analysis for existing systems.

Although the book may be used as a textbook for under- and post-graduate courses on air-conditioning engineering, its coverage on individual topics has not been adjusted to suit the limits on teaching hours of standard modules offered in universities. The instructor will need to be selective in using the materials in classes, but students are encouraged to read the complete chapters on the relevant topics. Practising building services engineers, especially air-conditioning system design engineers, will find the book a useful reference to their work, including for refreshment and supplement of their knowledge, and for new knowledge that had not been covered in the courses they attended previously.

In Chapter 1 of this book, a brief review is given of the impact of air-conditioning on the form and shape of buildings and the efficiency of land use, with Hong Kong taken as an example. A brief introduction is given on the types of air-conditioning systems that are employed in various types of buildings. An overview is then given of the dominance of air-conditioning in the energy consumption of buildings and, in turn, of buildings in the overall energy use of a modern city in a subtropical climate region, followed by a world energy scene and concerns about climate change.

Chapter 2 is dedicated to psychrometry, with emphasis on the definitions of psychrometric properties and their evaluation from two known properties, and on the heat and mass transfers in air-conditioning processes and cycles. These serve as the basis for measurement of moist air state, evaluation of human thermal comfort, and for air-conditioning system design. Appendix A covers the calculations involved in the development of a computing tool for plotting a digital psychrometric chart and for psychrometric properties evaluation.

Cooling load estimation, another topic on basics, is covered in Chapter 3, which includes techniques employed to model heat transfer in buildings and an outline of the current standard cooling load calculation method, the radiant time series (RTS) method, with the key steps illustrated by numerical examples. The methods for generating the required data for design cooling load calculation for buildings in a particular location are covered in this chapter. The design cooling load calculation data for Hong Kong are summarized in Appendix B.

Chapter 4 is on the functions, features, working principles, and performance of various air-side air-conditioning systems commonly used and emerging in modern buildings. Details of the steps and calculations involved in the design process will be explained and illustrated by numerical examples. Besides conventional systems, chilled ceiling/beam systems are covered in detail. Space air diffusion design, duct sizing, fan-duct systems, mechanical ventilation analyses and duct leakage test are covered in Chapter 5. Air balancing is deferred to Chapter 7 where air and water balancing are covered in one go. Likewise, estimation of variable speed fan power demand is deferred to Chapter 9 where the method for estimation of variable speed pump/fan power demand is discussed.

Water side air-conditioning systems are covered in Chapters 6 to 8. The major kinds of equipment in typical water-side air-conditioning systems are covered in Chapter 6, which includes chillers, pumps, cooling towers and heat exchangers. Substantial coverage is given on the theory and application of cooling towers for condenser heat rejection, which is widely used as a much more energy efficient alternative to air-cooled chillers. The cause and treatment of white plumes from cooling towers are also discussed in detail.

The configuration, operating principle and performance of various chilled water pumping systems, including the variable primary flow systems that are increasingly used nowadays, are discussed in Chapter 7. As mentioned above, air and water system balancing are covered in this chapter. Chapter 8 covers pipe sizing and selection of control valves, including in depth discussions on control characteristics of systems and various problems that may arise with improper selection of control valve.

Chapter 9 is dedicated to operational control and control optimization for minimizing the energy use of central chiller plants and air-side systems, and their integration into a method for whole system control optimization. Its coverage includes methods for modelling chillers and cooling towers that can cope with a much wider range of system parameters that may be varied in control optimization. For completeness, Chapter 10 is included to cover heating load estimation and heating system designs and equipment, including boilers, radiators, floor heating panels, hot water piping systems, heat recovery chillers and heat pumps, and absorption and adsorption chillers. Some materials in this chapter were adapted from teaching materials of Prof. Chris Underwood, my PhD supervisor and good friend, and ex-colleague, Dr. T. Y. Chen.

F W H Yik
Hong Kong, 2020

Table of Contents

Chapter/section Contents

Chapter 1 Introduction

1.1 Air-conditioning

In modern cities in tropical and subtropical regions, such as Singapore, Kuala Lumpur, Bangkok, Macau, Hong Kong, Shenzhen, Guangzhou, and Taipei, air-conditioning has become a common provision in buildings, to shelter people from the hot and humid outdoor weather. In those cities, air-conditioning is needed not just on scorching summer days but throughout the whole, or a large part, of the year, and this applies to nearly all kinds of buildings, including commercial, office, industrial, residential, and leisure and cultural buildings in which people work, shop, rest and recreate.

Consequent upon global warming, many cities in temperate climate zones are experiencing higher and higher summer peak temperatures and longer and more frequent periods of heat waves (see e.g. [1]). As a result, buildings in these climate zones may also need to be equipped with air-conditioning systems which, hitherto, was considered largely unnecessary. This, however, will boost energy use, and hence more greenhouse gas emissions, which would exacerbate the problem giving rise to a vicious circle.

In the above, the term 'air-conditioning' refers mainly to cooling and dehumidification of indoor air but, in fact, air-conditioning covers heating, cooling, humidifying, dehumidifying, and removal of contaminants in the air in an indoor space, as appropriate, for maintaining the state of the indoor air within desirable limits. Indoor air contaminant control is typically done through ventilation, i.e. by replacing the air inside the air-conditioned space by fresh outdoor air, and by filtration, i.e. through sieving out the particulates suspended in air. Nevertheless, it is a common perception that air-conditioning means cooling, dehumidification, and ventilation. For clarity, such a system may be described as a mechanical ventilation and air-conditioning (MVAC) system while a system that can perform all functions of air-conditioning is referred to as a heating, ventilating, and air-conditioning (HVAC) system.

Although providing occupants with a comfortable indoor environment is the major purpose that most air-conditioning systems are meant to serve, many industrial processes, such as electronic component manufacturing and drug production, rely on purposely designed HVAC systems to provide a stringently controlled indoor environment essential to the process. As would be expected, there will be a huge difference in the involved first and running costs between an air-conditioning system just for thermal comfort control and a sophisticated HVAC system for stringent indoor environmental and air quality control.

However, this book focuses only on air-conditioning systems for thermal comfort control in buildings. Whereas the basics covered in this book may apply, readers in desirous to know in-depth knowledge about specialized systems for various industrial or healthcare settings should consult specialized references on such topics.

1.2 Benefits of air-conditioning

Providing air-conditioning in buildings brings about huge economic benefits. In addition to the gain in productivity of people in a comfortable environment and making possible certain processes that can only be carried out under specific environmental conditions, a more fundamental effect is the impact it makes (in conjunction with other building services) on building design and urban development.

Before electricity supply became available to buildings, building services like air-conditioning systems, electric lights, and lifts were simply non-existent. Buildings in those days were mainly masonry buildings built from heavy materials with large thermal capacity, such as stones and bricks (Figure 1.1). The high thermal mass of the building fabric can help moderate conduction heat transfer into and out of the indoor space (see Chapter 3), resulting in smaller diurnal and seasonal variations in the indoor temperature. In other words, the indoor space would be cooler in daytime and warmer at night, and cooler in summer and warmer in winter compared to a lightweight building.

Availability of ventilation and lighting is prerequisite to indoor spaces meant for occupants to stay and work or live to serve their purposes. Ventilation and lighting are needed to keep the quality of indoor air within acceptable health limits and to enable the occupants to move about safely. Ventilation can also provide a certain amount of cooling whenever the outdoor temperature is significantly lower than the indoor temperature.

Before the emergence of air-conditioning equipment and electric lights, buildings relied mainly on windows to obtain and regulate light and ventilation. However, where strong solar radiation could enter an indoor space through a window, the indoor space could become too hot and the ventilation rate achievable by opening wide the window could hardly be sufficient to bring the indoor temperature down to comfortable levels. When it rained, the window had to be tightly shut notwithstanding that this would also diminish daylight and natural ventilation.

For ensuring occupants could enjoy an acceptable indoor environment as often as possible, verandahs were included in the designs of many old buildings, around their perimeter (Figure 1.1). With this design, all windows would be shaded by the roof or the floor plate above the verandah, which would also keep rain water from reaching the doors and windows, allowing windows to be kept open to admit daylight and outdoor air into indoor spaces even on rainy days (Figure 1.2). For more extensive buildings, the same approach is extended to include court yards and semi-open corridors (Figure 1.3).

Incorporating verandahs and court yards into building designs implies less usable floor area could be built on a given piece of land. With air-conditioning, which includes supply of fresh outdoor air into indoor spaces for ventilation, verandahs and court yards for facilitating natural air movement for cooling and ventilation can be eliminated.

a) Murray House was built in the present-day business district of Central, Hong Kong in 1844 as officers' quarters of the Murray Barracks

b) The Victorian era building was moved to Stanley in the southern part of Hong Kong Island during the 2000s

Figure 1.1 The Murray House, a classic historic building in Hong Kong

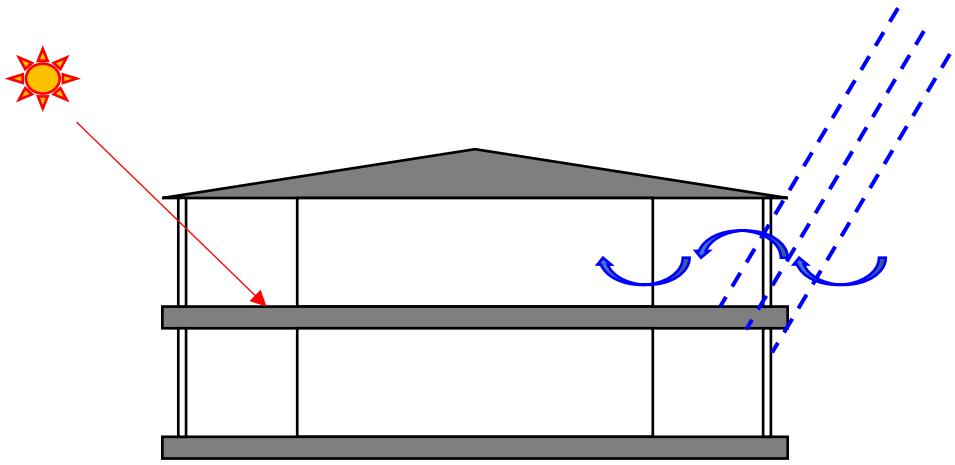

Figure 1.2 Cross-section of a building with verandah along the perimeter

a) The Main Building

b) The corridor beside a court yard

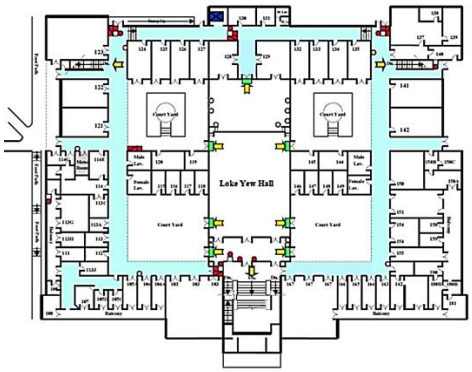

c) First floor plan of the Main Building

Figure 1.3 Main Building of The University of Hong Kong

When electric lights became available, the function of verandahs and court yards in maximizing daylight availability is no longer needed either. In conjunction with lifts and escalators for vertical transportation, and fire services for ensuring fire safety in buildings, much more floor area can now be built on a piece of land. Furthermore, with the building services systems, the quality of the indoor environment can be substantially raised, and the buildings may be utilized over a longer period every day, or even round the clock, throughout the year.

Economic development would be restrained without concurrent urban development, and the latter could only take place when it was possible to supply the needed number of dwellings for the people moving into a city to work and live, as well as the indoor spaces for accommodating all the associated industrial, commercial, and public services activities. It is, therefore, fair to say that the invention of air-conditioning system in 1902 by Willis Carrier [2], and the continued improvements in the design and performance of air-conditioning systems and equipment, have been a key supporting factor to mankind's economic, technical, and social developments.

1.3 Common air-conditioning systems in buildings

The most widely used air-conditioning equipment in residential buildings are window type air-conditioners and split-type air-conditioners (Figure 1.4), which may be referred to simply as window units and split units. These air-conditioning units serve relatively small areas, and each may be operated independently. These are characteristics that suit well residential buildings where the time of operation and the required indoor temperature set point may vary from room to room in a flat or house, and from one flat or house to another, and each household will pay for the energy cost for running their own air-conditioners. These small air-conditioners, however, would consume much more energy than the central air-conditioning systems employed in commercial buildings, if both are to cope with the same cooling demands for the same durations under the same environmental conditions.

As its name suggests, a window type air-conditioner is installed through a window in the building envelop and thus are visible from outside the building. Besides the impact on the outlook, it means that, only rooms at the perimeter of a building may be equipped with a window unit, unless ducts are installed for conveying the supply and return air between the air-conditioned room and the unit. Water seepage is possible when rain is driven by strong wind through the crevices between the unit and the opening through which the unit is installed, which may happen during a typhoon period. They may also be rather noisy, especially when their compressors start, are running, or stop, which will take place cyclically while they are operating. The units are typically equipped with just rough air filters due to the limited fan pressure available to overcome the pressure losses.

Just like a window type air-conditioner that is split into two parts, a split-type air-conditioner comprises an indoor unit and an outdoor unit. The outdoor unit houses the compressor and the condenser, and the indoor unit comprises a fan and a refrigerant coil for cooling the air drawn by the fan to flow through it. The outdoor and indoor units are connected by refrigerant pipes, and only a small hole through the building envelop would be needed for the refrigerant pipes and the cable for feeding electricity to the

outdoor unit to pass through. Where applicable, a condensate drain pipe may also pass through the same or another hole, and all such openings would be sealed before completion of the installation work.

Compared to window units, split units can provide greater flexibility to cope with room layout and, with the compressors installed outdoors, a much quieter indoor environment can be achieved. Nowadays, split units are increasingly equipped with variable speed drives for their compressors and supply air fans, which can reduce energy consumption as well as lowering their noise during operation. However, the appearance of outdoor units outside the building envelop, the lower energy efficiency compared to central air-conditioning systems, and the limitation on the type of air filter that may be used remain valid.

Figure 1.4 A residential development where a mix of split and window-type air-conditioners are in use

Split type air-conditioners, and their extended version, called variable refrigerant flow (VRF) systems, are also common in small commercial buildings or discrete premises in

larger commercial buildings. For larger buildings, central air-conditioning systems would be a natural choice for the lower running costs and better indoor environmental conditions that may be achieved. These central air-conditioning systems typically comprise a central chiller plant and air-side systems serving individual air-conditioned spaces connected to the chiller plant by a chilled water piping network. There will also be a fresh air supply system for ensuring adequate indoor air quality.

Discussions on air-conditioning systems is adjourned at this point because designs of central air-conditioning systems are a major topic of this book and elaborations on various types of central air-conditioning systems are covered from Chapter 4 onward. In the remaining part of this introductory chapter, attention will be turned to the energy consumption and the associated environmental burdens that air-conditioning would incur, and mitigation of the problems.

1.4 Energy consumption and environmental burdens and mitigation measures

While we continue to enjoy the benefits that air-conditioning brings forth, we have begun, since the oil crisis in the 1970s [3], to concern more and more about depletion of the earth's limited fossil fuel reserve, because running our air-conditioning systems requires substantial amounts of energy input. Furthermore, climate change due to anthropogenic greenhouse gas (GHG) emissions has emerged as an imminent threat to sustainable development of mankind while electricity generation from burning fossil fuels, including coal, petroleum, and natural gas, is one of the key sources of anthropogenic GHG.

In the discussion below, the energy use statistics of Hong Kong in recent years is used as an example to demonstrate the dominance of air-conditioning systems in the energy use of buildings, of buildings in the city-wide energy consumption, and of electricity generation in the GHG emission of a modern city [4-6]. This will be followed by a brief picture of the global energy scene [7] and the key messages from the Intergovernmental Panel on Climate Change (IPCC) [8], which stress that the same rates of energy use and GHG emission are simply unsustainable, while reducing energy use in buildings, especially that for space heating and air-conditioning, is a key measure to take.

1.4.1 Energy end-use statistics of Hong Kong

Reported energy statistics [4, 5] shows that more than 40% of the world's energy use is due to buildings. About 90% of the life cycle energy use of buildings is consumed over their occupied or in-use stage, which spans from completion of construction till demolition, and most of the rest is used for constructing the buildings, including for making the required building materials. In Hong Kong, buildings consume predominantly electricity and are collectively responsible for about 90% of the amount generated for the entire city (Figure 1.5) [6]. Although the share of electricity in the total energy use of Hong Kong is about 55% (Figure 1.6), about 70% of the total GHG emission of Hong Kong is incurred by electricity generation (Figure 1.5).

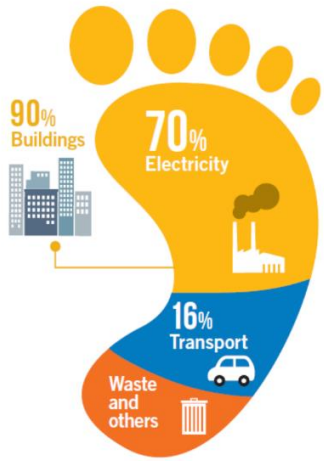

Figure 1.5 Shares of greenhouse emission by sectors in Hong Kong (Source: Hong Kong's Climate Action Plan 2030+, 2017 [5])

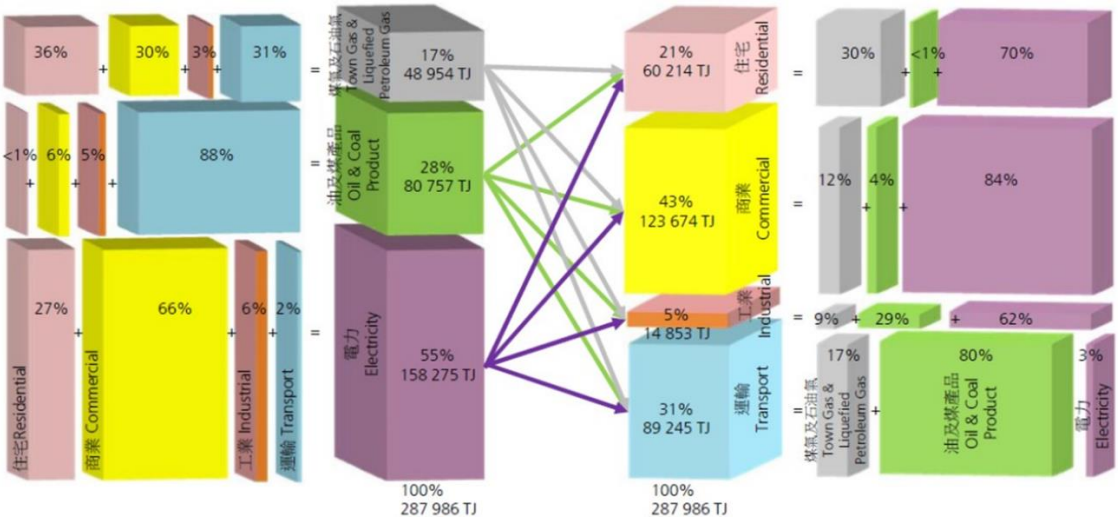

Figure 1.6 Shares of energy use by fuel types and sectors in Hong Kong (Source: Hong Kong Energy End-use Data 2017 [6])

According to the Energy End-use Data of Hong Kong in 2005 to 2015, published by the Electrical and Mechanical Services Department [6], the largest energy end-use in the commercial and the residential sectors are both air-conditioning, each accounted for about 25% of the total energy consumption of the respective sector (Figure 1.7). With respect to just the total amount of electricity consumed, air-conditioning had a share of 29% in the commercial sector (Figure 1.8) and 36% in the residential sector (Figure 1.9).

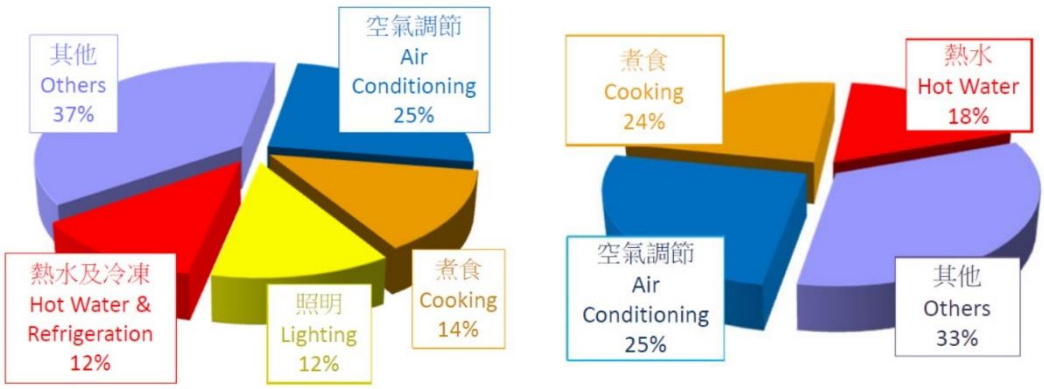

a) Energy end-uses in the commercial sector

b) Energy end-uses in the residential sector

Figure 1.7 Energy end-uses in the commercial and residential sectors of Hong Kong (Source: Hong Kong Energy End-use Data 2017 [6])

Compared to year 2005, the shares of the electricity consumed for air-conditioning and lighting in the commercial sector in 2015 had both dropped (Figure 1.8), which reflected the effects of energy efficiency enhancements in new and old buildings, including use of new air-conditioning equipment that are more efficient, retrofitting of existing systems and equipment, and use of more energy efficiency lighting equipment and appliances. Reductions in the energy use of lighting and appliances lead to double benefits, including saving in the electricity they consumed directly as well as in the electricity consumed by the air-conditioning system due to reduced heat gains from them.

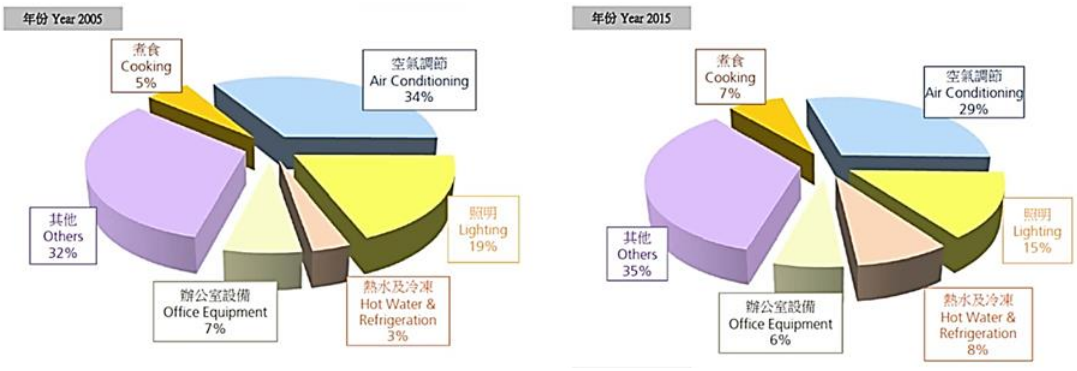

Figure 1.8 Electricity end-uses in the commercial sector of Hong Kong in 2005 and 2015 (Source: Hong Kong Energy End-use Data 2017 [6])

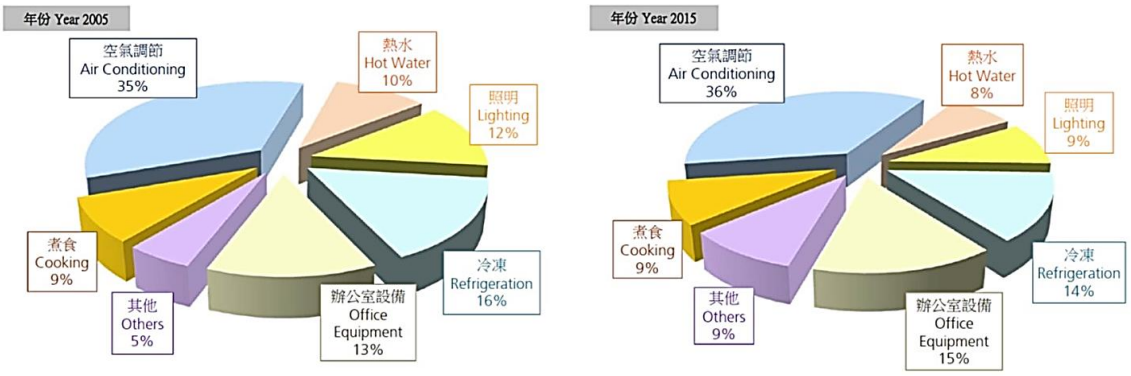

Figure 1.9 Electricity end-uses in the residential sector of Hong Kong in 2005 and 2015 (Source: Hong Kong Energy End-use Data 2017 [6])

For the residential sector (Figure 1.9), the share of the electricity consumed for lighting dropped significantly (from 12% to 9%) over the period from 2005 to 2015, which was due to the emergence and widening use of energy efficient lamps, including compact fluorescent lamps, T5 fluorescent tubes, LED lights, etc. The share of the electricity consumed for air-conditioning, however, rose slightly (from 35% to 36%) over the same period, despite that the energy efficiency of new window or split-type air-conditioners has improved over the years. This should have been due to the greater market penetration of air-conditioning equipment into the residential sector. Along with economic growth, more and more households in the low-income class can afford equipping their dwellings with air-conditioners.

1.4.2 The world energy scene

The world energy scene described in the following was based on information given in, and the related graphs were extracted from, *BP Statistical Review of World Energy 2017* [7]. However, the descriptions given below were the interpretations of the author who is solely responsible for any misinterpretations of information in the source.

As shown in Figure 1.10, the world primary energy consumption, generally, had been on an increasing trend, although it had occasionally dropped over a limited period when the world economy was hit by global recession, e.g. in 2009, consequent upon the subprime mortgage crisis that happened in the United States in 2008. In the past quarter of a century, oil, coal and natural gas remained the major forms of consumed primary energy; nuclear power stayed at a relatively steady level; there was a slight increase in the share of hydroelectricity; and a substantial growth in renewables could be seen, although still rather small in absolute term. The growth in world primary energy consumption in 2016 was about 1%, which was significantly smaller than the average of earlier years, with the reduction in growth of consumption in China being a key contributor (Figure 1.11).

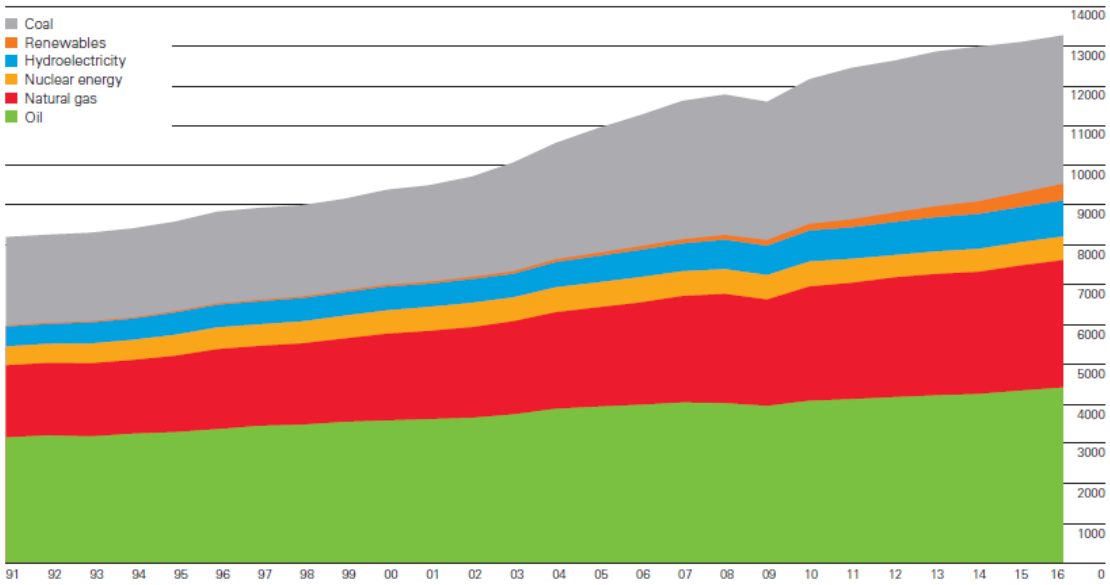

Figure 1.10 World primary energy consumption (Million tonnes oil equivalent) (Source: BP Statistical Review of World Energy 2017 [7])

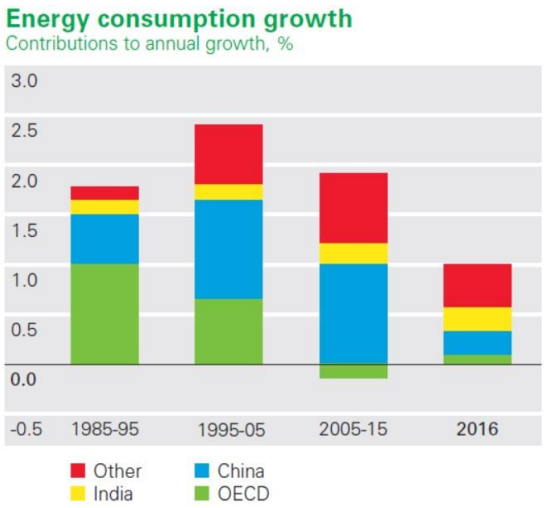

Figure 1.11 Energy consumption growth (Contributions to annual growth, %) (Source: BP Statistical Review of World Energy 2017 [7])

For oil (Figure 1.12), the world-wide reserves-to-production (R/P) ratio stood at about 50 years, which was substantially higher than the figures in the late 1980s, due mainly to new reserves being found at a rate surpassing growth in consumption over the years. This was most significant for the Central and South America region and, as a result, the share of Middle East in the global proved reserves dropped to less than a half (Figure 1.13). Notwithstanding this, the message that the total amount of oil reserves known to us today would be exhausted in 50 years, if we keep the current production rate, is an alarming signal urging for reduction in consumption as well as substitution of oil (and other fossil fuels as well) by renewables.

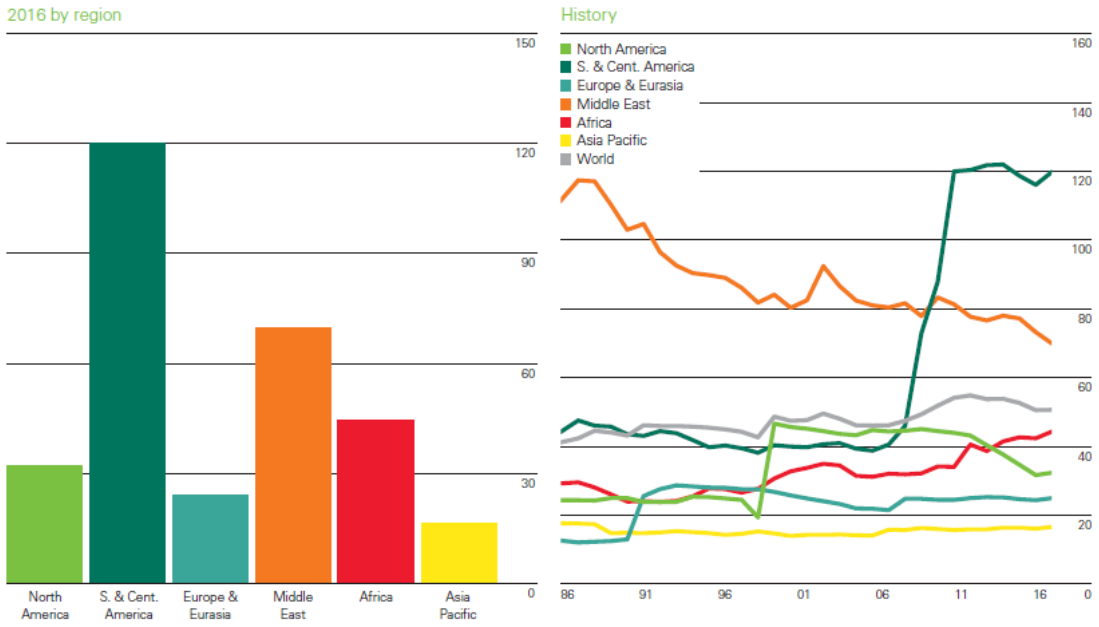

Figure 1.12 Reserves-to-production (R/P) ratios of oil (Years) (Source: BP Statistical Review of World Energy 2017 [7])

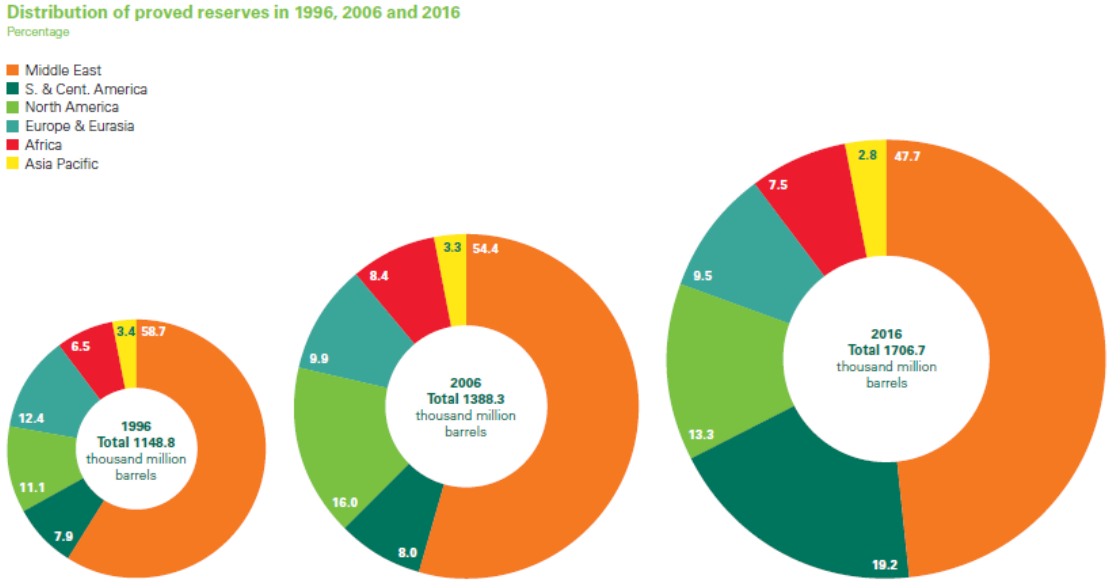

Figure 1.13 Distribution of proved reserves in 1996, 2006 & 2016 (Percentage) (Source: BP Statistical Review of World Energy 2017 [7])

1.4.3 Climate change and mitigation measures

As pointed out in the *Climate Change Synthesis Report 2014* [8] published by IPCC:

"*Human influence on the climate system is clear, and recent anthropogenic emissions of GHG are the highest in history. Recent climate changes have had widespread impacts on human and natural systems. Warming of the climate system is unequivocal, and since the 1950s, many of the observed changes are unprecedented over decades to millennia.*"

In the 21st Convention of Parties (COP21) held in Paris in 2015, after the delegates of the Parties had worked hard for two weeks plus one day, the President of COP21 declared in the morning of 12 December 2015 that the Paris Agreement had been reached. The salient points of the Agreement included:

- 187 countries had participated and declared to make Intended Nationally Determined Contributions (INDC) on carbon reduction, and many of them did.

- The estimated aggregate GHG emission levels in 2025 and 2030 resulting from the INDC would lead to a projected level of 55 gigatonnes in 2030, which well exceeds the levels required to hold the increase in global average temperature to below 2°C above the pre-industrial levels, not to mention the level required to limit the temperature increase to 1.5°C above pre-industrial levels (Figure 1.14). There is an urgent need to address the significant gap between the aggregated effect of the INDC and the target levels for realizing the 2°C and 1.5°C scenarios.

- The total global carbon should be capped as soon as possible and achieve balance of emission with the assimilative capacity of the sinks (forest, ocean, etc.) by 2050.

- Parties to communicate their first INDC no later than when the Party submits its respective instrument of ratification, accession, or approval of the Paris Agreement.

- Parties whose INDC pursuant to decision contains a time frame up to 2025 to communicate by 2020 a new INDC and to do so every five years thereafter.

As Figure 1.15 shows, buildings were responsible for 18.4% (12% indirect + 6.4% direct) of the 49 gigatonnes of GHG emitted by various economic sectors in 2010. The measures highlighted in the IPCC Report [8] for reducing GHG emissions due to buildings include:

1. Carbon and/or energy taxes (either sectoral or economy-wide)

2. Tradable certificates for energy efficiency improvements (white certificates)

3. Subsidies or tax exemptions for investment in efficient buildings, retrofits and products, and subsidized loans

4. Building codes and standards; equipment and appliance standards; and mandates for energy retailers to assist customers invest in energy efficiency

5. Energy audits; labelling programmes; and energy advice programmes

6. Public procurement of efficient buildings and appliances, and

7. Labelling programmes for efficient buildings; product eco-labelling.

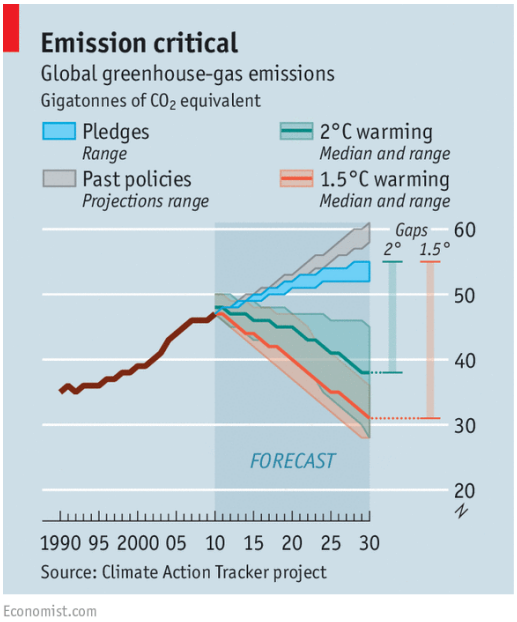

Figure 1.14 Emission reductions required for capping global warming by 2 °C and 1.5°C. (Source: The Economist)

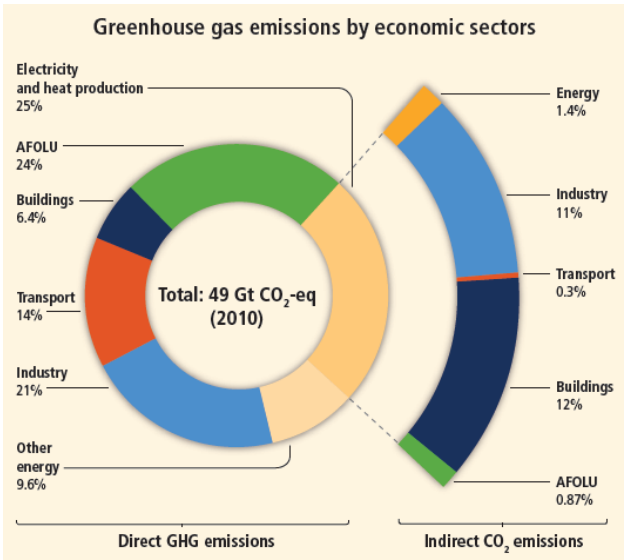

AFOLU = agriculture, forestry and other land use

Figure 1.15 Total anthropogenic greenhouse gas (GHG) emissions (gigatonne of CO2-equivalent per year, GtCO2-eq/yr) from economic sectors in 2010. (Source: Climate Change 2014 Synthesis Report, IPCC)

1.4.4 Steps being taken in Hong Kong

Hong Kong has been making efforts to reduce energy consumption and CO_2 emissions over the years but finds it necessary to step up her effort to meet the upcoming challenges. Except taxation and emission trading measures, which are yet to be considered, the measures listed above have been taken to various extents by the government and the private sector of Hong Kong to control and promote energy efficiency of buildings, which include both mandatory and voluntary measures. The Building Energy Efficiency Ordinance (Cap 610), which regulates the energy efficiency of building services installations in buildings, including air-conditioning installations, was enacted, and has come into full operation since 21 September 2012.

Consequent upon China's commitment to lower CO_2 emissions per unit of GDP (referred to as carbon intensity) by 60% to 65% from the 2005 level by 2030, the Hong Kong government has set the target of reducing carbon intensity by 65% - 75% from the 2005 level by 2030 [5]. This is an ambitious target that could only be achieved with concerted efforts from all stakeholders. The key strategies being taken to realize the goal include [5]:

- Phasing down coal for electricity generation and replacing it with natural gas by 2030.
- Optimize the introduction of renewable energy in a more systematic manner with the government taking the lead.
- While continuing to improve energy saving for new buildings, focus will be put on energy saving for existing buildings and public infrastructure; and
- Facilitate walking as well as continue to provide a safe, efficient, reliable, and environment-friendly transport system with multi-modal choices that meets the community's needs.

1.5 Concluding remarks

The price of electricity is expected to become higher and higher for various reasons, such as taxation and increase in cost due to scarcity of fossil fuels, the use of additional cleansing technologies (e.g. carbon capture and storage), switching to a less carbon intensive but more expensive fuel, use of more expensive plants for generation from renewable sources, etc. Therefore, energy conservation will become a key means for minimizing operating cost of buildings. Furthermore, the energy efficiency standard to be met will be raised from time to time due to tightening of regulatory requirements, which can be made possible by enhancement of relevant systems and equipment.

As pointed out in this chapter, air-conditioning is a technology that has made substantial contributions to the prosperity of modern cities and well being of the citizens, but air-conditioning systems are also energy intensive to run. Therefore, engineers responsible for their design, installation and operation and maintenance shoulder great responsibilities, including ensuring the systems will not only function well in indoor climate control, they will run reliability, and will consume the least possible energy while they serve their functions.

References

[1] Jenkins, G.J., Perry, M.C., and Prior, M.J. The climate of the United Kingdom and recent trends. Met Office Hadley Centre, Exeter, UK, 2008.

[2] Oremus, W., A history of air conditioning – From ancient mountains of snow to the window units of today, The Slate Group LLC, 2011. (Visited Oct. 2017: http://www.slate.com/articles/arts/culturebox/2011/07/a_history_of_air_conditioning.html)

[3] 1973 Oil Crisis, Wikipedia (https://en.wikipedia.org/wiki/1973_oil_crisis; visited in Oct 2017)

[4] Environment Bureau, Energy Saving Plan for Hong Kong's Built Environment 2015~2025+, Hong Kong SAR Government, 2015.

[5] Environment Bureau, Hong Kong's Climate Action Plan 2030+, Hong Kong SAR Government, 2017.

[6] Electrical and Mechanical Services Department, Hong Kong Energy End-use Data 2017, Hong Kong SAR Government, 2017.

[7] BP Statistical Review of World Energy, British Petroleum, June 2017.

[8] IPCC Climate Change 2014 Synthesis Report, Intergovernmental Panel on Climate Change, 2014.

Chapter 2 Psychrometry

2.1 Basic concepts

2.1.1 Dry air, water vapour and moist air

Since air-conditioning is about treating air, we need to know the composition of air that is assumed in the analyses and how we can quantify the effects of heating, cooling, humidifying, and dehumidifying air. In chemistry lessons, we learnt that atmospheric air is in fact a mixture of a variety of gases, including nitrogen, oxygen, carbon dioxide, argon, etc. Although water vapour is also present in air, the quantity is insignificant compared to the major constituent gases and thus, it is often ignored in analyses of most engineering fields.

However, air-conditioning leads not only to a change in the temperature of the air, changing the amount of water vapour in it is also a key objective. The importance of the latter function of air-conditioning can be seen from the assumption made in air-conditioning analyses that air is regarded as a binary mixture, i.e. a mixture of two "pure substances", with water vapour singled out as one of the two pure substances while all the other gases present in air are lumped and regarded as the second pure substance, referred to collectively as dry air. Air is also called moist air to signify that it is a mixture of dry air and water vapour.

Regarding dry air as a pure substance is a good approximation provided that when the mixture of gases undergo thermodynamic processes together, the composition of dry air remains unchanged and the properties defined for representing the state of the dry air remain a good representation of the aggregate properties of the individual constituent gases. Together with the assumption that water vapour is absent, these assumptions have been proven to be reliable simplifications and have been widely applied to analyses of many thermodynamic processes involving air, such as processes and cycles in air compressors, internal combustion engines and gas turbines. For air-conditioning, the assumption regarding dry air is equally valid but, as highlighted above, presence of water vapour cannot be neglected.

Psychrometry, also known as (aka) psychrometrics or hygrometry, is the field of engineering concerned with the physical and thermodynamic properties of gas-vapour mixtures. The mixture to which psychrometry is most frequently applied is moist air because of its key role in heating, ventilating, and air-conditioning (HVAC), and meteorology.

Psychrometry is a key foundation of air-conditioning engineering as it provides a basis for defining the properties of moist air and how such properties change when the moist air is heated or cooled and humidified or dehumidified. This allows us to estimate the heat and mass transfer rates that will take place in air-conditioning processes and, in turn, the capacities required of components and equipment in an air-conditioning system, which is a key task of system design.

2.1.2 Properties and states of a substance

The rates of heat and work transfers taking place in a thermodynamic process can be evaluated provided that we know the thermodynamic states of the working fluid when the process starts and ends. The thermodynamic state (hereinafter referred to simply as the state) of the working fluid under a given condition is defined by the properties of the working fluid under that condition, e.g. the temperature and pressure of steam entering or leaving a turbine. The major properties of a fluid include temperature, pressure, density, specific heat, enthalpy, entropy, etc.

If the working fluid is a pure substance, e.g. steam or dry air (when regarded as a pure substance), its state will be fully defined when two of its properties are fixed. Once the state of the working fluid is defined, all the other properties at the same state are also fixed and can be evaluated from the known properties. Other than equations, the relations among properties of a substance may be presented in the form of charts or tables, such as T-s (temperature – entropy) diagram, p-h (pressure – enthalpy) diagram, and transport properties tables.

Among the properties of a working fluid, only some can be measured. Those that are measurable, either directly or indirectly, are important, as their measured values can be used to define the state of the working fluid. Analyses of thermodynamic processes may then proceed from evaluation of the other required properties by using the relations among the various properties of the working fluid at a given state. Using again a steam turbine as an example, the enthalpies of steam entering and leaving a turbine, which are not measurable, can be determined from the measured temperatures and pressures of the steam flowing into and out of the turbine. The power output of the turbine can then be determined from the mass flow rate and the loss in enthalpy of the stream as it flows through the turbine.

For moist air, which is regarded as a mixture of two pure substances, namely dry air and water vapour, its state can only be defined when we know three of its properties. Nevertheless, for most air-conditioning processes, it may be assumed that the total pressure of the air, which equals the atmospheric pressure (p_{atm}), is held steadily at one standard atmospheric pressure (= 101.325kPa), unless the location concerned is subject to a significantly different atmospheric pressure, such as places at high altitudes. Once the total pressure is defined, we just need to find out two more properties of moist air to define its state and evaluate its other properties.

Like thermodynamic process analyses, measurable properties, and knowledge about the relations among the properties of moist air, are crucial to psychrometric analyses. Tables and charts are available in handbooks on heating and air-conditioning, including the ASHRAE Handbook [1] and CIBSE Guide [2], to facilitate psychrometric analyses.

2.1.3 Intensive, extensive and specific properties

The properties of a substance may be classified into intensive and extensive properties (aka intrinsic and extrinsic properties, respectively). Intensive properties, such as density and temperature, are independent of the amount of the substance but, extensive properties, such as volume, enthalpy and entropy are proportional to the amount of the

substance involved. The properties mentioned above for defining the state of a working fluid must be intensive or specific properties.

Specific properties of a substance, which are properties relative to a specific quantity, are derived from the intensive and extensive properties of that substance, or the same property of that substance and another substance. Using again density as an example, it is an intensive property as well as a specific property. As a specific property, it denotes the mass per unit volume of the substance. Note that a specific property is also an intensive property, but the reverse is not necessarily true. For example, temperature is an intensive property but not a specific property. The ratio of the densities of oil and water (two intensive properties) is called the specific gravity of oil, where water is taken as the reference liquid and its density is used as the base value for normalization of the oil density.

In a psychrometric process that causes a change in the humidity of (i.e. the amount of water vapour in) moist air, the mass of the moist air will rise or drop accordingly, but the dry air mass will remain unchanged. In psychrometry, therefore, instead of the total mass of dry air and water vapour, the dry air mass alone is used as the base value for normalization of extensive properties of moist air into specific properties. For example, dividing the volume of a moist air sample by the mass of dry air in it yields the specific volume of the moist air. Calculations of the heat and mass transfers taking place in a psychrometric process can be done far more conveniently by using specific properties defined based on the dry air mass.

2.2 Psychrometric properties

2.2.1 Dalton's laws and perfect gas law

Consider an amount of moist air that fills up a vessel with an internal volume V, as shown in Figure 2.1. Under steady state condition, the dry air and water vapour of the moist air will both attain the same steady temperature T. Let p_a be the pressure inside the vessel under this condition.

Now, if we take all water vapour molecules out of the vessel leaving only dry air inside, and keep the temperature of the dry air in the vessel steadily at T, by injecting an adequate amount of heat, when we then measure the pressure inside the vessel, we shall find that the pressure will become p_{da}, which will be slightly lower than p_a. If we take all dry air out instead and leave water vapour only inside the vessel, and keep the water vapour in the vessel steadily at T, the pressure that we shall find by measurement will become p_w, which will be much lower than p_a.

The Dalton's law in chemistry and physics states that the total pressure exerted by a mixture of non-reacting gases is equal to the sum of the partial pressures of the individual gases. Here, the partial pressure of each gas is the pressure exerted by the gas when it alone occupies the same volume and is kept at the same temperature as the mixture (Figure 2.1). Applying the Dalton's law to the case of the moist air in the vessel described above, we can write:

$$p_a = p_{da} + p_w \tag{2.1}$$

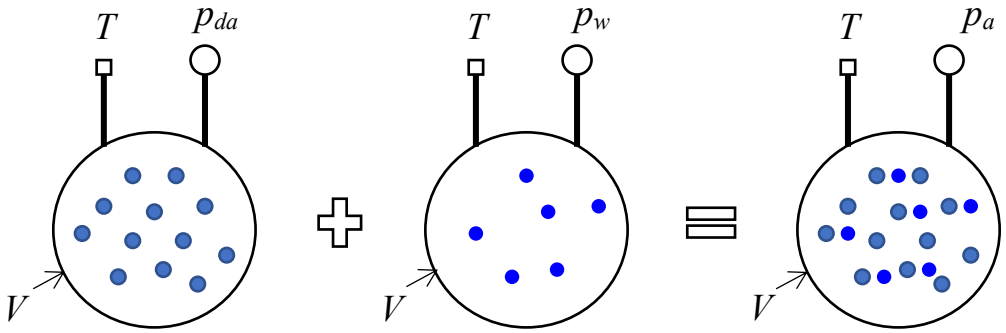

	Dry Air	Water Vapour	Moist Air
t (°C)	24	24	24
T (K)	297.15	297.15	297.15
m_{da} (kg)	1	0	1
m_w (kg)	0	0.006199	0.006199
p_{da} (Pa)	100325	0	100325
p_w (Pa)	0	1000	1000
p_a (Pa)	100325	1000	101325

Figure 2.1 Moist air in a vessel

By regarding both the dry air and the water vapour in moist air as perfect gases, the perfect gas law (Equation (2.2)) may be applied to each of them.

$$pV = mRT \tag{2.2}$$

Where

p = pressure of the gas, Pa
V = volume of the gas, m^3
m = mass of the gas, kg
R = gas constant of the gas, J/kg-K
T = absolute temperature of the gas, K

Because the dry air and the water vapour, when present alone in the vessel, occupied the same volume V and were at the same temperature T, we may write:

$$p_{da}V = m_{da}R_{da}T \tag{2.3}$$

$$p_wV = m_wR_wT \tag{2.4}$$

Where

p_{da} = partial pressure of the dry air, Pa
p_w = partial pressure of the water vapour, Pa
m_{da} = mass of the dry air, kg
m_w = mass of the water vapour, kg
R_{da} = gas constant of the dry air = 287 J/kg-K
R_w = gas constant of the water vapour = 461.5 J/kg-K

By conservation of mass, the mass of the moist air, m_a, is given by:

$$m_a = m_{da} + m_w$$

The moist air may also be regarded as a perfect gas and the perfect gas law that applies to it is:

$$p_a V = m_a R_a T \tag{2.5}$$

From the above equations, the following relation between the moist air gas constant, R_a, and the gas constants of dry air and water vapour can be derived:

$$m_a R_a = p_a \frac{V}{T} = (p_{da} + p_w)\frac{V}{T} = p_{da}\frac{V}{T} + p_w \frac{V}{T} = m_{da} R_{da} + m_w R_w$$

$$R_a = \frac{m_{da}}{m_a} R_{da} + \frac{m_w}{m_a} R_w \tag{2.6}$$

Equation (2.6) may be obtained directly by applying the Gibbs-Dalton law, as expressed below:

$$m\psi = m_1\psi_1 + m_2\psi_2 + \cdots + m_n\psi_n \tag{2.7}$$

Where

m = mass of a mixture of n non-reacting gases = $m_1 + m_2 + \ldots + m_n$.
m_i = mass of the i^{th} constituent gas in the mixture, for i = 1, 2, ..., n.
ψ = a specific property of the mixture of the n constituent gases.
ψ_i = the same specific property of the i^{th} constituent gas in the mixture, for i = 1, 2, ..., n.

The specific property, ψ, in Equation (2.7) may be any specific property of the gases, such as gas constant (as in Equation (2.6)), specific heat, specific enthalpy, etc. Note should be taken that in Equations (2.6) & (2.7), the total mass instead of the dry air mass was adopted as the base of normalization for specific properties but, in later discussions, the latter will be adopted.

As temperature and pressure are thermodynamic properties of gaseous substances, in the above discussions, temperature and partial vapour pressure of each constituent of moist air have already been used to define the state of water vapour and dry air in the moist air and they, indeed, are psychrometric properties of moist air. Besides

temperature and pressure, other psychrometric properties that are used in air-conditioning engineering are defined in the following sub-sections.

2.2.2 Moisture content

In psychrometry, how much water vapour is there in a moist air sample is a key moist air property that needs to be quantified to facilitate comparison and analysis. This is a measure of how humid the air is, and thus is generally called humidity. The proper specific property used in psychrometry for quantification of air humidity is called moisture content (aka humidity ratio), w, which is defined as the mass of water vapour per unit mass of dry air in the moist air sample, as shown in Equation (2.8).

$$w = \frac{m_w}{m_{da}} \tag{2.8}$$

Where

w = moisture content, kg/kg dry air
m_w = mass of water vapour in the moist air sample, kg
m_{da} = mass of dry air in the moist air sample, kg

Making use of Equations (2.3) and (2.4), Equation (2.8) may be re-written as:

$$w = \frac{p_w V}{R_w T}\frac{R_{da} T}{p_{da} V} = \frac{R_{da}}{R_w}\frac{p_w}{p_{da}} = \frac{287}{461.5}\frac{p_w}{p_{da}} = 0.622\frac{p_w}{p_{da}}$$

From the Dalton's law (Equation (2.1)),

$$w = 0.622\frac{p_w}{p_a - p_w} \tag{2.9}$$

As can been seen by inspecting Equation (2.9), it represents a relation between two psychrometric properties, namely moisture content, w, and partial pressure of water vapour, p_w, under a constant total pressure, p_a. Other relations among psychrometric properties will be derived later and, as mentioned above, they collectively are an important means for analyses of air-conditioning processes and cycles.

2.2.3 State of saturation

If we put liquid water and air into a concealed chamber situated inside a steady environment (Figure 2.2), the water and the air inside the chamber may initially exchange heat and moisture but after a long enough time, the two will attain thermodynamic equilibrium with each other and with the surrounding environment. In this equilibrium state, the water and the air will both be at the same temperature as the surrounding environment and, therefore, there will be no more heat exchange between them nor there is heat exchange between either the moist air or the liquid water with the environment.

For the water that is in thermodynamic equilibrium with the air in the chamber, a liquid water molecule at the air/water interface is at state 'f' in the T-s diagram shown in Figure 2.2. It may break away from the liquid and become vapour to join the air only if

heat is supplied to it such that its state becomes 'g' as shown in Figure 2.2. Without any supply of the required latent heat of vaporization, the only chance for a liquid water molecule at the water surface to leave and join the air is when a vapour molecule in the air condenses into liquid and join the water at the same time, giving up an amount of latent heat of condensation that equals the latent heat of vaporization of one liquid water molecule. The total number of water vapour molecules in the moist air, therefore, is conserved.

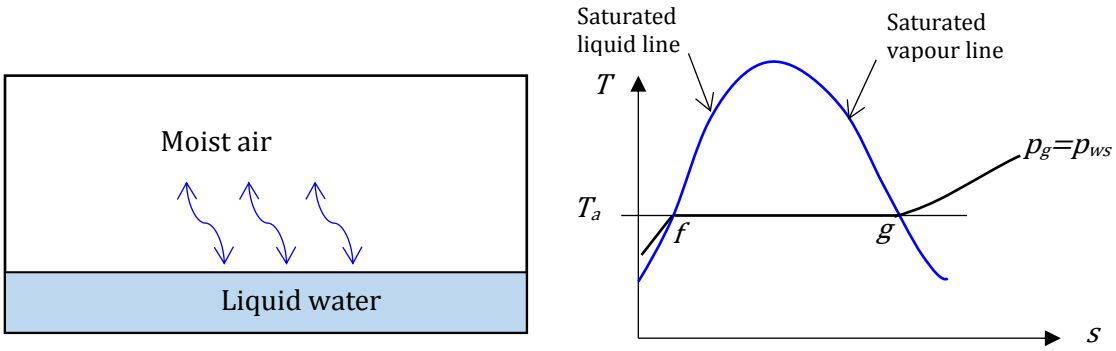

Figure 2.2 Moist air and liquid water in a concealed chamber and T-s diagram for the water

The above implies that there is a limit to the holding capacity of an amount of moist air for water vapour at a given temperature, and the moist air reaching this full-capacity state is in a saturated state. This equilibrium state of the moist air and the water would happen when the saturation vapour pressure of the moist air (p_{ws}) equals the saturation pressure of the water (p_g) at the water surface (at state 'g' in Figure 2.2). Equation (2.9) can also be applied to evaluate the moisture content of the saturated moist air with a vapour pressure of p_{ws}:

$$w_s = 0.622 \frac{p_{ws}}{p_a - p_{ws}} \tag{2.10}$$

Where

w_s = saturated moisture content, kg/kg dry air
p_{ws} = partial pressure of saturated water vapour, Pa

For moist air that is saturated under the pressure of one standard atmosphere, p_{atm}, and at temperature T, the partial pressure of water vapour in a moist air, p_{ws}, is fixed. In other words, saturation may be regarded as a property which, together with temperature (and total pressure = p_{atm}), would define the state of a moist air sample. Therefore, it is possible to express the partial pressure of water vapour of a saturated moist air, p_{ws}, and also its moisture content, w_s, as functions of temperature, T, given that it is saturated at the total pressure of p_{atm}, as depicted by the equations below.

$$w_s = w_s(T) \tag{2.11}$$

$$p_{ws} = p_{ws}(T) \tag{2.12}$$

The relationships depicted by Equations (2.11) and (2.12) are non-linear, and curve-fit models have been derived for prediction of saturated air moisture content or vapour pressure for use in psychrometric calculations. The following equation is given in the ASHRAE Handbook [1] for saturated water vapour pressure as a function of temperature within the range from 0 to 200°C:

$$\ln(p_{ws}) = \frac{C_8}{T} + C_9 + C_{10}T + C_{11}T^2 + C_{12}T^3 + C_{13}\ln(T) \tag{2.13}$$

$$T = t + 273.15$$

Where

T = absolute temperature of the saturated moist air, K;
t = temperature in degree Celsius, °C
C_8 to C_{13} are coefficients with values as shown in Table 2.1.

Table 2.1 Values of Coefficients in Equation (2.13)

Coefficient	Value	Coefficient	Value
C_8	$-5.8002206 \times 10^{+03}$	C_{11}	$4.1764768 \times 10^{-05}$
C_9	$1.3914993 \times 10^{+00}$	C_{12}	$-1.4452093 \times 10^{-08}$
C_{10}	$-4.8640239 \times 10^{-02}$	C_{13}	$6.5459673 \times 10^{+00}$

Once the saturated water vapour pressure for moist air at a given temperature can be evaluated, e.g. by using Equation (2.13), Equation (2.10) can be used to evaluate its moisture content.

Example 2.1

Determine the saturation moisture content of air at 15, 25 and 35°C, assuming the air is under one standard atmospheric pressure in all cases. Comment on the results.

Solution

The saturation vapour pressure of the air, p_{ws}, at each of the given temperatures can be determined using Equation 2.13 and values of the coefficients given in Table 2.1. Having evaluated p_{ws}, the corresponding saturation moisture content, w_s, can be determined using Equation 2.10. The calculation results are as summarized in Table 2.2.

It can be seen from the saturation moisture content values shown in Table 2.2 that over the range of temperature from 15 to 35°C, the saturation moisture content of air is in the range of about 1% to less than 4%; the higher the

temperature, the higher the saturation moisture content. Although this small percentage justifies the simplification assumption of neglecting the presence of water vapour in air in a wide range of thermodynamic analyses (e.g. on processes in air power cycles), a change of moisture content within this range would make large differences in thermal comfort sensation of human beings and substantial energy input is required to bring about such change in moisture content in air.

Table 2.2 Calculation results of Example 2.1

t	°C	15	25	35
T	K	288.15	298.15	308.15
C_8/T		-20.12917	-19.45404	-18.82272
C_9		1.39150	1.39150	1.39150
$C_{10}\ T$		-14.01568	-14.50209	-14.98849
$C_{11}\ T^2$		3.46775	3.71261	3.96583
$C_{12}\ T^3$		-0.34577	-0.38303	-0.42288
$C_{13}\ \ln(T)$		37.07296	37.29628	37.51223
$\ln(p_{ws})$		7.44158	8.06124	8.63548
p_{ws}	Pa	1705.45	3169.22	5627.82
p_a	Pa	101325	101325	101325
w_s	kg/kg	0.01065	0.02008	0.03658

2.2.4 Degree of saturation

The ratio of the moisture content of a moist air sample, w, to the moisture content of a saturated moisture air sample, w_s, at the same temperature and pressure (one standard atmospheric pressure), as shown in Equation (2.14), is the definition of the moist air property called degree of saturation, μ, or percentage saturation, if expressed in percent.

$$\mu = \frac{w}{w_s} \tag{2.14}$$

Degree of saturation, with a value in the range of 0 to 1, is a measure of how close a moist air sample is to saturation. The air is dry if its degree of saturation is low and air at such condition will be able to hold much more water vapour before reaching the saturation limit (unless there is, at the same time, a large drop in its temperature). Objects exposed to such air will be dried, i.e. they are ready to give up their moisture to the air. Degree of saturation, therefore, is a specific property of moist air for quantification of air humidity, which can provide a useful quantification of how readily the air is to gain moisture from objects exposed to it.

2.2.5 Dew point

Figure 2.3 shows a plot of the moisture content of saturated air against temperature, $w_s(t)$, where the moisture content values were determined by using the same method as in Example 2.1. The following observations can be made from this graph:

1. The temperature and moisture content of saturated air are one-one correspondent, i.e. to each temperature, there is one, and only one, value of moisture content of saturated air.

2. The moisture content of saturated air drops monotonically with temperature, and the rate of reduction in moisture content with temperature also drops, i.e. for the same temperature reduction, the corresponding drop in moisture content will be higher the higher the initial temperature.

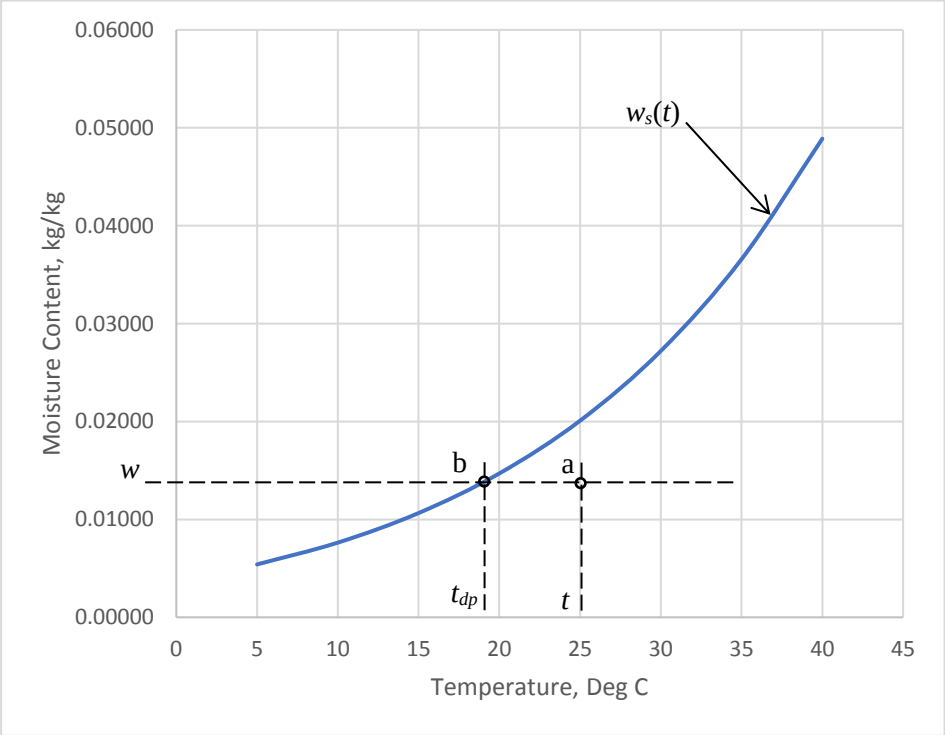

Figure 2.3 Moisture Content of Saturated Air as a Function of Temperature, $w_s(t)$

The relationship between moisture content and temperature of saturated air implies that corresponding to an unsaturated moist air sample at temperature t and moisture content w, which is represented by state point 'a' shown in Figure 2.3, there is a saturated moist air sample with moisture content w_s that equals w, as represented by state point 'b' in the same figure. The temperature of the saturated moist air sample, denoted as t_{dp}, will be lower than t, and t_{dp} can be regarded as a property of the state of the moist air sample at t and w, as it bears a definite relationship with t and w, and t_{dp} is given the name 'dew point' temperature.

This concept of dew point is expressed mathematically in Equation (2.15):

$$w_s(t) > w = w_s(t_{dp});\ t_{dp} < t \tag{2.15}$$

Instead of comparing two moist air samples side-by-side, if the moist air sample at state point 'a' shown in Figure 2.3 is cooled down from t to t_{dp} with its moisture content held constant, the moist air will become same as the saturated moist air at state point 'b' shown in Figure 2.3. Further cooling of the moist air sample will cause the original moisture content in the air to become higher than the saturation moisture content at the new temperature, and it will no longer be possible for the excessive moisture to stay in vapour state but to condense out as liquid.

This explains why condensate will appear on a cold surface when the surface is exposed to humid air. For example, it is a common experience that the outer surface of a can of cold soft drink will be covered by water droplets after it has been taken out of a fridge for a short while. The appearance of dew on leaf and grass surfaces in cold mornings is because of the same phenomenon, which justifies calling this temperature the dew point.

Since moisture content is a property of moist air and moisture content and dew point of air is one-one-correspondent, dew point is also a property of moist air. Besides a measure of moisture content in air, dew point is the lowest temperature to which the air may be cooled without giving rise to condensation. The absence or presence of condensation is highly sensitive to whether the temperature of the surface exposed to the air is above or below the dew point of the air, and this characteristic is utilized in a method for accurate measurement of moisture content in air (further elaboration on this issue will be given in Section 2.3.2).

2.2.6 Relative humidity

Relative humidity, ϕ, as defined in Equation 2.16, is a moist air property that serves a similar function as degree of saturation, μ, i.e. a measure of humidity of moist air or more precisely how close a moist air is to saturation.

$$\phi = \frac{p_w}{p_{ws}} \tag{2.16}$$

Where

p_w = partial pressure of water vapour in moist air at temperature t and pressure p_a, Pa
p_{ws} = partial pressure of water vapour in saturated moist air also at temperature t and total pressure p_a, Pa

Like degree of saturation, the value of relative humidity, ϕ, may vary between 0 and 1; $\phi = 0$ if the air is completely dry ($w = 0$ & $p_w = 0$) and $\phi = 1$ if the air is saturated ($p_w = p_{ws}$). Other than the cases where its value equals 0 or 1, the value of relative humidity is greater than the value of degree of saturation, μ, for unsaturated moist air at the same

state, but by just a rather small amount. In practice, relative humidity and degree of saturation are often used interchangeably.

Nevertheless, relative humidity is better known to the public than degree of saturation as a measure of humidity of air because it is widely used in weather reports, and nearly all hygrometers available in the market show readings in relative humidity but hardly any show degree of saturation. It is also more commonly used in defining the design conditions of indoor and outdoor air for air-conditioning system design.

Readers may find that in some handbooks and references [e.g. 1, 3], the definition of relative humidity is given as the ratio of mole factions of water vapour in the air and in saturated air at the same temperature and pressure. This definition will boil down to the definition introduced above in terms of ratio of partial pressures of water vapour in the air and in saturated air at the same temperature and pressure. In fact, after deriving the alternative definition in partial pressure ratio, the original definition will hardly be used again, and it tends to be forgotten. Therefore, for simplicity sake, relative humidity has been defined here based directly on partial pressure ratio.

2.2.7 Specific volume

Specific volume, v, is defined as the volume of moist air per kg of dry air in the moist air:

$$v = \frac{V}{m_{da}} \tag{2.17}$$

Where

$V =$ volume occupied by moist air, m^3
$m_{da} =$ mass of dry air in the moist air, kg

Being the reciprocal of density, specific volume, is needed in conversions between the mass and volume flow rates of moist air. Both ways of quantification of the moist air flow rate are needed in air-conditioning system design because mass flow rate is used in estimation of the heat and mass transfer rates, and hence the heating or cooling capacities required of equipment and system components, while volume flow rate is used in determining the physical sizes required of equipment and system components, especially fans, coils, ducts and grilles for handling the air flow.

How can specific volume of a moist air be determined from other properties of known values will be illustrated in Example 2.2, which will appear later.

2.2.8 Specific enthalpy

Equation (2.18) is the steady flow energy equation [1], which is applicable to a thermodynamic system under a steady state where there is one stream of working fluid entering and leaving the system while the rate of heat input to the system is Q and the rate of work done by the system is W (see Annex A in Chapter 5).

$$\dot{m}\left(h_1 + \frac{u_1^2}{2} + gz_1\right) - \dot{m}\left(h_2 + \frac{u_2^2}{2} + gz_2\right) + Q - W = 0 \tag{2.18}$$

Where

$\dot{m}$ = mass flow rate of working fluid flowing through the system, kg/s
h_1 & h_2 = specific enthalpy of working fluid entering and leaving the system, kJ/kg
u_1 & u_2 = velocity of working fluid flowing into and out of the system, m/s
g = gravitational acceleration = 9.81m/s^2
z_1 & z_2 = elevation of working fluid entering and leaving the system with reference to a datum, m
And, subscripts 1 & 2 denote the locations where the working fluid enters and leaves the system, respectively.

When applied to a psychrometric process, the steady flow energy equation may be simplified by assuming that compared to the enthalpy terms, the kinetic ($u^2/2$) and potential (gz) energy terms are insignificant and may be ignored. Furthermore, there will be no work done in a psychrometric process. With these assumptions, Equation (2.18) can be largely simplified to:

$$\dot{m}(h_2 - h_1) = Q \tag{2.19}$$

In psychrometry, the working fluid is moist air, which is a mixture of dry air and water vapour, and the mass base of specific properties of moist air is the mass of dry air in the moist air. Accordingly, the steady flow energy equation becomes:

$$\dot{m}_{da}(h_2 - h_1) = Q \tag{2.20}$$

Where h is the specific enthalpy of moist air defined, according to the Gibbs-Dalton law (Equation (2.7)), as the sum of the enthalpies of the dry air and water vapour components, per kg of dry air in the moist air:

$$m_{da}h = m_{da}h_{da} + m_w h_w$$

$$h = h_{da} + \frac{m_w}{m_{da}} h_w$$

$$h = h_{da} + wh_w \tag{2.21}$$

Where

h_{da} = specific enthalpy of dry air, kJ/kg dry air
h_w = specific enthalpy of water vapour, kJ/kg water vapour
w = moisture content of moist air, kg water vapour/kg dry air

Like temperature, a reference datum must be established for measurement of specific enthalpy. The reference datum for temperature measurement is the freezing point of water under one standard atmospheric pressure, which is defined as 0^{o}C. For the dry air, the following differential equation holds:

$$dh_{da} = Cp_{da}dt \tag{2.22}$$

Where Cp_{da} is the specific heat of dry air under constant pressure (≈ 1.005kJ/kg-K). Defining dry air at 0°C as the reference datum at which h_{da} is equal to zero, and assuming Cp_{da} is a constant, the specific enthalpy of dry air at temperature t (in °C) above zero can be evaluated using the following equation, obtained by integrating Equation (2.22), as a good approximation:

$$h_{da} = Cp_{da} \cdot t \tag{2.23}$$

For the water vapour, saturated liquid water at 0°C is taken as the reference datum and assigned a specific enthalpy value of zero. The specific enthalpy of saturated water vapour at 0°C will then be equal to the latent heat of vaporization of water at 0°C, denoted by the symbol h_{fg0} (= 2501kJ/kg). On this basis, the specific enthalpy of water vapour at a given temperature t (in °C) above zero is:

$$h_w = h_{fg0} + Cp_w \cdot t \tag{2.24}$$

Where Cp_w is the specific heat of water vapour under constant pressure (≈ 1.87kJ/kg-K), also assumed to be a constant.

Substituting Equations (2.23) and (2.24) into (2.21), we get:

$$h = Cp_{da} \cdot t + w\left(Cp_w \cdot t + h_{fg0}\right) \tag{2.25}$$

This may be rearranged into:

$$h = (Cp_{da} + wCp_w) \cdot t + wh_{fg0} \tag{2.26}$$

Let Cp_a be the specific heat of moist air as defined below,

$$Cp_a = Cp_{da} + wCp_w \tag{2.27}$$

Equation (2.26) may be re-written as:

$$h = Cp_a \cdot t + wh_{fg0} \tag{2.28}$$

Based on Equation (2.27), the value of Cp_a will vary from 1.024 to 1.061 kJ/kg-K over the range of w from 0.01 to 0.03. For applications where error by a few percent is acceptable, Cp_a may also be regarded as a constant, as we do for Cp_{da} and Cp_w.

At this juncture, readers' attention is drawn to the following points of clarification related to the materials covered in this subsection:

a) In thermodynamics, heat input to a system, Q, and work done by a system, W, are conventionally taken as positive. Accordingly, rates of heat leaving a system and work done on a system are negative quantities. In an air-conditioning process, rate of cooling of the air in the process is, according to the convention of thermodynamics, a negative quantity. Nevertheless, we may, for convenience, regard the rate of cooling of air by an air-conditioning system as a positive

quantity. Care, therefore, needs to be exercised in interpreting the definition and meaning of the stated values.

b) In the above, the specific enthalpy of saturated liquid water (h_f) at 0°C was taken as the datum for measuring specific enthalpy of water vapour in air, i.e. $h_f = 0$ at 0°C. This is different from the conventional datum adopted in thermodynamics, which is the triple point of water at which the solid, liquid and vapour phases co-exist. This happens at the temperature of 0.01°C and the pressure of 611.2Pa and, at this state, the specific internal energy of liquid water (u_f) is defined as zero. The specific enthalpy of liquid water at this state ($h_f = u_f + p \cdot v$) is slightly greater than zero (= 0.0006112 kJ/kg). However, the datum and method (Equation (2.24)) adopted here are justified as the difference is small while their use make the datums for both dry air and water vapour consistent.

c) The specific enthalpy of water vapour is measured from the datum of saturated liquid water at 0°C, and the liquid is assumed to have undergone vaporization into saturated vapour and has been superheated thereafter to the temperature of the vapour under concern. This method can be used to quantify specific enthalpy of water vapour because there are little differences among the specific enthalpy values of water vapour samples, if all of them are at the same temperature, be they saturated or superheated by different temperature rises from the respective saturated vapour states (see also Section 2.2.10, on explanations for Equations (2.46) & (2.47)).

Meanwhile, we shall digress for a while to discuss on the sensible, latent and total heat transfers in a psychrometric process and on an imaginary process called adiabatic saturation, as applications of specific enthalpy, but shall return to an important psychrometric property, the thermodynamic wet-bulb temperature at the end of this discussion.

2.2.9 Sensible, latent and total heat

Consider the process undergone by a stream of moist air flowing through a system during which heat and moisture are injected into the air stream at constant rates of Q kW and M kg/s, respectively, as shown in Figure 2.4. The mass flow rate of the air stream is $\dot{m}_a$ kg/s, which is the mass flow rate of dry air in the moist air, and it stays unchanged throughout the process. The moist air entering the system is at temperature t_{a1} °C with a moisture content of w_{a1} kg/kg. After the simultaneous heat and moisture transfer involving a total heat transfer of Q kW and moisture transfer of M kg/s, the moist air is leaving the system at temperature t_{a2} °C and moisture content w_{a2} kg/kg.

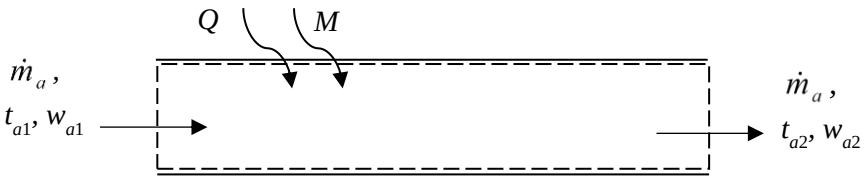

Figure 2.4 Process with heat and moisture inputs to a stream of moist air

The mass flow rate of water vapour being carried into the system by the moist air stream is given by $\dot{m}_a w_{a1}$, and the mass flow rate of water vapour leaving is $\dot{m}_a w_{a2}$. By mass balance, we get:

$$M = \dot{m}_a(w_{a2} - w_{a1}) \tag{2.29}$$

Referring to the steady flow energy equation shown as Equation (2.20):

$$Q = \dot{m}_a(h_{a2} - h_{a1}) \tag{2.30}$$

Where

h_{a1} & h_{a2} = the specific enthalpy of the moist air entering and leaving the system, kJ/kg dry air

Using Equation (2.25), Equation (2.30) can be expanded to:

$$Q = \dot{m}_a\left[Cp_{da}t_{a2} + w_{a2}\left(Cp_w t_{a2} + h_{fg0}\right) - Cp_{da}t_{a1} - w_{a1}\left(Cp_w t_{a1} + h_{fg0}\right)\right]$$

Which can be simplified, by collecting like terms, to:

$$Q = \dot{m}_a[Cp_{da}(t_{a2} - t_{a1}) + w_{a2}Cp_w t_{a2} - w_{a1}Cp_w t_{a1} + h_{fg0}(w_{a2} - w_{a1})] \tag{2.31}$$

Let:

$$w_m Cp_w(t_{a2} - t_{a1}) = w_{a2}Cp_w t_{a2} - w_{a1}Cp_w t_{a1} \tag{2.32}$$

It can be seen from the above equation that w_m is a temperature weighted mean of the moisture contents of the entering and leaving moist air.

Substituting Equation (2.32) into Equation (2.31), and after collecting like terms, we get:

$$Q = \dot{m}_a\left[(Cp_{da} + w_m Cp_w)(t_{a2} - t_{a1}) + h_{fg0}(w_{a2} - w_{a1})\right] \tag{2.33}$$

Let the specific heat of moist air be defined for this case as:

$$Cp_a = Cp_{da} + w_m Cp_w \tag{2.34}$$

Equation (2.33) may be rewritten as:

$$Q = Q_{Sen} + Q_{Lat} = \dot{m}_a\left[Cp_a(t_{a2} - t_{a1}) + h_{fg0}(w_{a2} - w_{a1})\right] \tag{2.35}$$

As shown in Equation (2.35), the total heat imparted to the moist air, Q, may be broken down into two components, a sensible heat component, Q_{Sen}, which is manifested by a rise in temperature of the air, and a latent heat component, Q_{Lat}, which is manifested by a rise in moisture content of the air, as shown below:

$$Q_{Sen} = \dot{m}_a Cp_a (t_{a2} - t_{a1}) \tag{2.36}$$

$$Q_{Lat} = \dot{m}_a h_{fg0} (w_{a2} - w_{a1}) \tag{2.37}$$

Recalling Equation (2.29), the result of mass balance on the system, Equation (2.37) may be written as:

$$Q_{Lat} = M \cdot h_{fg0} \tag{2.38}$$

From Equations (2.34), (2.36) to (2.38), we can see that the moisture input into the air stream will affect directly the latent heat gain of the air, as well as indirectly, but to a much lesser extent, the sensible heat gain of the air, through the change in moisture content of the air that will result.

2.2.10 Adiabatic saturation and thermodynamic wet-bulb temperature

Consider a horizontal, extremely long, and well-insulated chamber, with openings at its two ends and with its bottom surface covered by a layer of water over its entire length, as shown in Figure 2.5. A stream of moist air is flowing steadily, at a dry air mass flow rate of $\dot{m}_a$ kg/s, through the chamber from the opening at one end to that at the other end. The air enters the chamber at the temperature of t_a °C, and its moisture content is w_a kg/kg.

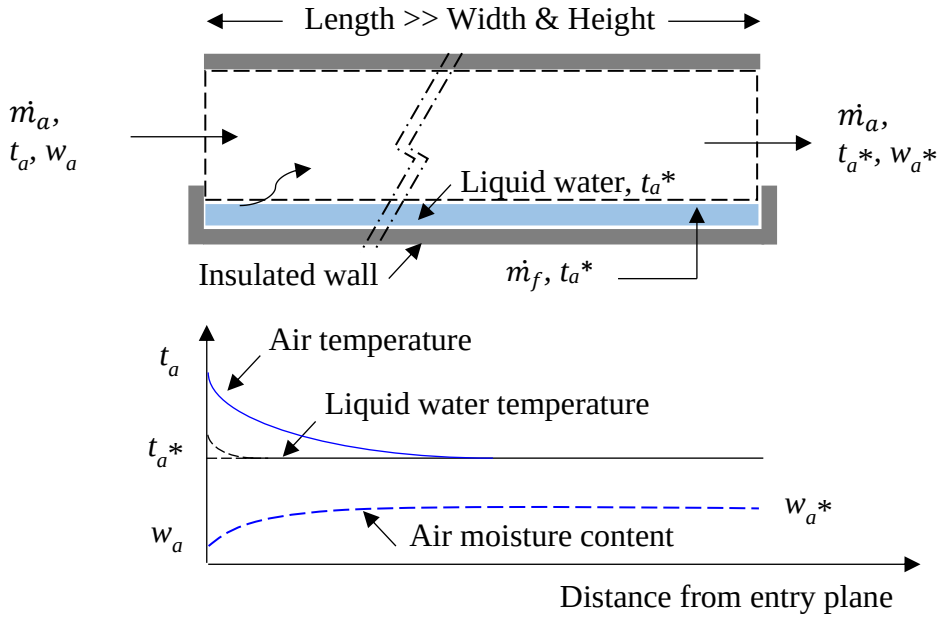

Figure 2.5 An imaginary adiabatic saturation process

The ensuing discussions on the adiabatic saturation process are based on the following assumptions:

1. The chamber is well-insulated such that no heat and moisture exchange with the surroundings of the chamber can take place when air flows along the length of the chamber.

2. Air at the same entry condition as defined above has been flowing steadily through the chamber for a long time such that the air and the water inside the chamber have reached their respective steady state conditions in all parts inside the chamber.

3. The air leaving the chamber is at a steady state denoted by the temperature t_a* ^oC, and moisture content w_a* kg/kg.

4. The make-up water supply is under control such that its flow rate would match with the rate of loss in liquid water due to evaporation, and its temperature is same as the equilibrium temperature between the air and water in the region that ends at the exit of the chamber, i.e. t_a* ^oC.

From heat and mass transfer studies, we learnt that heat transfer will take place by conduction, convection, or radiation whenever there is a temperature difference and a possible heat flow path. Whereas a temperature difference is the driving force for heat transfer, water vapour (mass) transfer is driven by a difference in partial vapour pressure (representing concentration of water vapour), which may take place by diffusion or convection. Therefore, the air in the chamber discussed above will exchange sensible heat with the liquid water layer wherever there is a temperature difference between them. Furthermore, water molecules in the liquid water will evaporate into water vapour and join the air stream if the saturation water vapour pressure at the temperature of the water surface is higher than the water vapour pressure in the air.

Evaporation of liquid water into water vapour must be sustained by a supply of heat to compensate for the latent heat of evaporation (denoted as h_{fg}*). In the case of the well-insulated chamber in question, the only possible source of this heat supply is from either the air flowing above the water, or the water in the chamber, driven by a temperature difference between the air and the water, i.e. through sensible heat exchange between them, or by heat transfer between different parts of the water, which will lead to a drop in the air or the water temperature depending on from which source heat is supplied to sustain the evaporation process.

It is possible that evaporation is sustained partly by the heat supplied by the water, leading to a drop in water temperature, but this will only happen in the transition region nearby the entrance of the chamber. Further down the chamber, the water temperature will approach and reach the temperature t_a* which will be lower than t_a if the air entering the chamber is not saturated. The heat transfer between the air and the water will diminish and stop as the air and water temperatures converge. The equilibrium state is reached when the saturation water vapour pressure at the surface of the liquid water equals the saturation water vapour pressure in the air above the water, which will happen when the air temperature and the water surface temperature are equalized.

As explained above, if the air entering the chamber is unsaturated, it will be able to hold more water vapour as it is exposed to liquid water, which will cause the air to drop in temperature. This simultaneous heat and moisture exchange will continue within a region downstream of the air entry plane and will diminish and stop as the air and water attain thermodynamic equilibrium after the air has flown along the chamber over a sufficiently long distance. The equilibrium state will continue up to the exit plane (Figure 2.5). To the steady state condition of the chamber, we may apply the principles of energy and mass conservation to relate the conditions at the entry and exit planes.

Consider overall water mass balance:

$$\dot{m}_a w_a^* = \dot{m}_a w_a + \dot{m}_f \tag{2.39}$$

Where

$\dot{m}_f =$ liquid make-up water supply flow rate, kg/s

By overall energy balance, with the specific enthalpy of the liquid water approximated by the product of its specific heat and temperature:

$$\dot{m}_a h_a^* = \dot{m}_a h_a + \dot{m}_f C_f t_a^* \tag{2.40}$$

Where

$h_a =$ specific enthalpy of air entering the chamber, kJ/kg
$h_a^* =$ specific enthalpy of (saturated) air leaving the chamber, kJ/kg
$C_f =$ specific heat capacity of liquid water, kJ/kg-K

From Equation (2.39),

$$\dot{m}_f = \dot{m}_a (w_a^* - w_a) \tag{2.41}$$

Substituting Equation (2.41) into Equation (2.40) and cancelling the dry air mass flow rate ($\dot{m}_a$) that appears at every term at both sides of the equation, we get:

$$h_a^* = h_a + (w_a^* - w_a) C_f t_a^* \tag{2.42}$$

Expanding the specific enthalpy h_a in the above equation into an expression in terms of the temperature and moisture content of the air at the entry plane, the above equation becomes:

$$h_a^* = Cp_{da} t_a + w_a (Cp_w t_a + h_{fg0}) + (w_a^* - w_a) C_f t_a^* \tag{2.43}$$

Solving for w_a from the above equation, we get:

$$w_a = \frac{h_a^* - Cp_{da} t_a - w_a^* C_f t_a^*}{Cp_w t_a + h_{fg0} - C_f t_a^*} \tag{2.44}$$

Inspection of Equation (2.44) unveils that the right-hand side of the equation comprises:

- Thermodynamic properties of air, water vapour and liquid water (Cp_{da}, Cp_w, C_f & h_{fg0}), which may be taken as constants with known values.
- Variables that can be measured conveniently by using thermometers (t_a & t_a^*).
- Variables that can be ascertained once the value of t_a^* is known (w_a^* & h_a^*) because the state of the air leaving the chamber is saturated.

The important implication of this observation is that if we can measure the entering and leaving air temperatures (t_a & t_a^*) of an adiabatic saturation process, the moisture content in the entering air, w_a, can be evaluated (Equation (2.44)). In other words, the adiabatic saturation process can serve, in theory, as a means for measurement of the moisture content of air, which otherwise cannot be directly measured. Furthermore, t_a^*, called the 'thermodynamic wet bulb temperature', can be taken as a psychrometric property because the state of moist air is fully defined when t_a & t_a^* are fixed, which has the same effect as fixing t_a & w_a.

To get a more detailed insight into the adiabatic saturation process, let us continue with also expanding the h_a^* term in Equation (2.43), which yields:

$$Cp_{da}t_a^* + w_a^*\left(Cp_w t_a^* + h_{fg0}\right) = Cp_{da}t_a + w_a\left(Cp_w t_a + h_{fg0}\right) + (w_a^* - w_a)C_f t_a^*$$

The above may be further manipulated into:

$$(Cp_{da} + w_a Cp_w)t_a - (Cp_{da} + w_a^* Cp_w)t_a^* = (w_a^* - w_a)h_{fg0} - (w_a^* - w_a)C_f t_a^*$$

Adding and subtracting $w_a Cp_w$ inside the brackets in the second term at the left-hand side of this equation, we get:

$$(Cp_{da} + w_a Cp_w)t_a - (Cp_{da} + w_a Cp_w - w_a Cp_w + w_a^* Cp_w)t_a^* = (w_a^* - w_a)h_{fg0} - (w_a^* - w_a)C_f t_a^*$$

Collecting terms with ($t_a - t_a^*$) as a factor, and likewise terms with ($w_a^* - w_a$),

$$(Cp_{da} + w_a Cp_w)(t_a - t_a^*) - (w_a^* - w_a)Cp_w t_a^* = (w_a^* - w_a)h_{fg0} - (w_a^* - w_a)C_f t_a^*$$

And finally,

$$(Cp_{da} + w_a Cp_w)(t_a - t_a^*) = (w_a^* - w_a)(h_{fg0} + Cp_w t_a^* - C_f t_a^*) \qquad (2.45)$$

Note that the specific enthalpy of water vapour, h_w, at a given temperature, t_w, may be evaluated from:

$$h_w = h_{fg0} + Cp_w t_w \tag{2.46}$$

The above expression assumes that the water vapour was brought to a state with specific enthalpy equals the given value of h_w, first by evaporating saturated liquid water at 0°C (with zero enthalpy) to saturated vapour at 0°C, and then super-heating the saturated vapour to t_w.

Alternatively, we may first heat up the saturated liquid from 0 to t_w, and then evaporate the saturated liquid to saturated vapour at t_w°C, which will lead to the same specific enthalpy value h_w, as expressed below:

$$h_w = C_f t_w + h_{fgw} \tag{2.47}$$

Where h_{fgw} is the latent heat of evaporation of water at temperature t_w.

Equating the right-hand sides of Equations (2.46) & (2.47), replacing t_w by t_a^* and h_{fgw} by h_{fg}^*, and solving for h_{fg}^*, we get:

$$h_{fg}^* = h_{fg0} + Cp_w t_a^* - C_f t_a^* \tag{2.48}$$

The right-hand side of the above equation is identical to the terms within the second bracket at the right-hand side of Equation (2.45). Therefore, Equation (2.45) can be simplified to:

$$(Cp_{da} + w_a Cp_w)(t_a - t_a^*) = (w_a^* - w_a)h_{fg}^* \tag{2.49}$$

Where h_{fg}^* is the latent heat of evaporation of water at temperature t_a^*.

Now, Equation (2.49) makes it apparent that the heat input rate for sustaining vaporization of the liquid water at the rate needed to raise the moisture content of the air from w_a to w_a^*, which is given by the right-hand side of the equation, is at the expense of a sensible heat loss of the air at the rate as given by the left-hand side of the equation, resulting in the drop in its temperature from t_a to t_a^*. There is no need for any external supply of heat, which is the essence of the adiabatic saturation process.

At this juncture, let us turn our attention to methods and instruments for measurement of humidity. We shall return to the adiabatic saturation process when we discuss psychrometric processes.

2.3 Humidity measurement

2.3.1 Wet-bulb temperature

In the preceding section, the following psychrometric properties have been defined:

1) Total pressure, p_a (usually taken as equal to $p_{atm} = 101{,}325$Pa)
2) Temperature (more precisely, dry-bulb temperature), t (°C)
3) Vapour pressure, p_w (Pa)
4) Moisture content, w (kg/kg)

5) Specific volume, v (m^3/kg)
6) Specific enthalpy, h (kJ/kg)
7) Degree of saturation, μ
8) Relative humidity, ϕ
9) Dew point, t_{dp} (°C)
10) Thermodynamic web-bulb temperature, t^* (°C)

The total pressure and temperature of air can be measured by using unsophisticated instruments, such as barometers and thermometers, which were already available since the advent of air-conditioning technology. We, however, need to be able to measure at least one more property to enable us to define the state of moist air. Before sufficiently accurate instruments for measuring relative humidity or dew point became available, humidity measurement was a problem that needed to be resolved. Although the use of a long, well-insulated chamber for measurement of the thermodynamic wet bulb temperature is simply not practicable, the concept of the adiabatic saturation process provided a direction for development of humidity measurement.

Simple, low cost hygrometers comprising two thermometers, with the sensing bulb of one covered by a wetted wick, had been successfully developed for humidity measurement (Figure 2.6). The temperature measured by the thermometer with a dry bulb, and is thus called the dry bulb temperature, t, is simply the temperature of the air surrounding its sensing bulb. The temperature measured by the thermometer with a wetted sensing bulb (when a steady state is attained) is called the wet bulb temperature, t', which will be the temperature at which the sensible heat transfer from the surrounding air to the wet wick surface is just sufficient to sustain liquid water to evaporate into vapour and be carried away from the wick by the air. The difference between the dry and wet bulb temperatures, $t - t'$, is called wet bulb depression, which will be a finite positive value unless the air being measured is already saturated in which case the wet bulb depression will be zero.

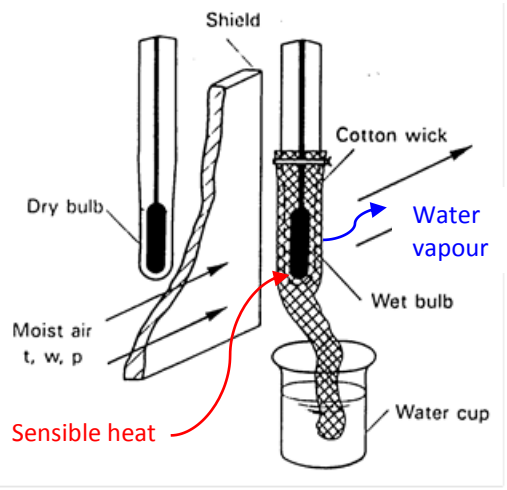

Invention of hygrometer with dry and wet bulb thermometers:

1799: French Leslie first measured the humidity using a differential thermometer with a dry-bulb and a wet-bulb.

1815: French Joseph Louis Gay-Lussac derived the formula for calculating humidity from readings of the dry- and wet-bulb thermometers.

(Source: http://www.cwb.gov.tw/V7e/knowledge/encyclopedia/in008.htm)

Figure 2.6 Dry and wet bulb thermometers

The heat and moisture transfer at the wetted surface of the wet bulb thermometer can be described by the following equation:

$$(h_c + h_r)A(t - t') = h_m A(p'_{ws} - p_w)h_{fg,t'} \quad (2.50)$$

Where

h_c, h_r & h_m = the convective heat transfer coefficient, radiant heat transfer coefficient and convective mass (moisture) transfer coefficient, respectively.
A = the heat and mass transfer area on the wetted wick.
p'_{ws} & p_w = the saturation water vapour pressure at the wet bulb temperature and the water vapour pressure of the air, respectively.
$h_{fg,t'}$ = the latent heat of vaporization at t'.

From Equation (2.50), it can be seen that:

1. When t & t' have been measured, the water vapour pressure in the air, p_w, can be evaluated and, therefore, the state of the air can be defined once the two properties t and p_w are fixed (together with $p_a = p_{atm}$), and so will be all the other psychrometric properties of the air, which can then be evaluated; and

2. The value of p_w that will be calculated, however, is dependent on the values of the transport coefficients h_c, h_r & h_m, which can be affected by a range of factors, including the speed and direction of movement of the air over the wetted wick, and the temperatures of surfaces that are surrounding and can exchange radiant heat with the wetted wick.

For the reasons given above, using hygrometers that differ in design to measure the same air condition may lead to different wet bulb temperature readings, and the readings may also be affected by the conditions of the air and the surrounding environment. Hygrometers of improved designs are available (Figure 2.7), such as sling hygrometers, which include a swivel handle for rotating the thermometers during a measurement ensuring there will be a sufficiently high and relatively steady speed of air movement round the sensing bulbs. Aspiration hydrometers, which include radiation shield and a fan to draw air to flow steadily over the sensing bulbs are another type of improved hydrometers.

Given that wet bulb temperature measurement is dependent on a variety of extrinsic factors, wet bulb temperature should not be regarded as a property of moist air. Nevertheless, measurement of wet bulb temperature has become a key means for air humidity measurement, which has been extensively used, even the air temperature leaving an idealistic adiabatic saturation process, which is indeed a psychrometric property, is given the name thermodynamic “wet bulb” temperature.

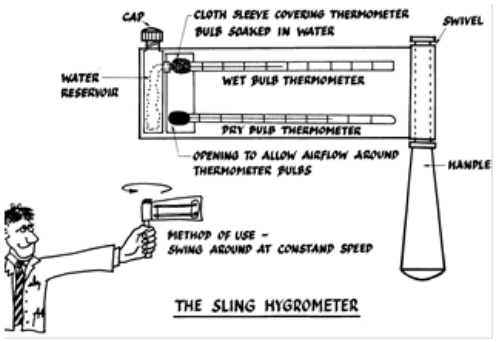

Aspiration Hygrometer

Figure 2.7 Sling and aspiration hygrometers

2.3.2 Other types of instruments for humidity measurement

Besides measuring wet bulb temperature, air humidity may also be determined by measuring the mechanical or electrical characteristics of materials that may vary with the ambient air humidity, such as elongation of the sensing element under a constant tension, the conductivity or capacitance of the sensing element, etc. In addition to accuracy, the time it would take for the sensing element to respond to a change in humidity is an important consideration in sensor selection. For automatic control or monitoring and logging of performance of air-conditioning systems, sensors that can output an electrical signal are essential.

Among various types of hygrometers available, the dew point hygrometer with cyclic chilled mirror sensor is, so far, the most accurate type for air humidity measurement. In the sensor of this type of hygrometer (Figure 2.8), there is a small mirror that will reflect an incident light beam, and the reflected light will be picked up by a light sensor. When the mirror surface is at a temperature below the dew point of the air to which the mirror is exposed, condensate will appear on the mirror surface which will diminish the intensity of the reflected light.

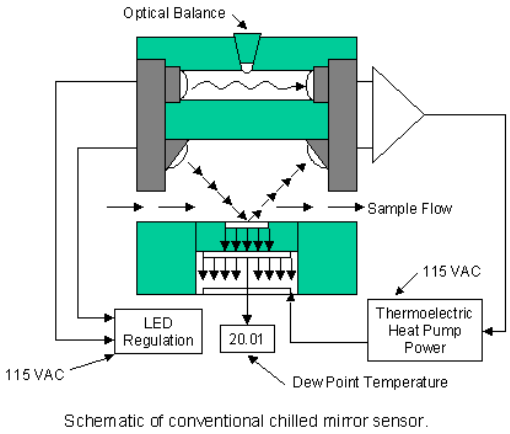

Schematic of conventional chilled mirror sensor.

Figure 2.8 Cyclic chilled mirror dew point sensor

Therefore, by chilling and heating cyclically the mirror in the sensor, and measuring its surface temperature by an accurate temperature sensor, the temperature at which there is a sudden change in intensity of the reflected light beam due to formation and clearance of condensate upon the mirror surface can be determined, which is the dew point of the air being measured.

Details about the designs and operating principles of various types of hygrometers can be found in handbooks and references on air-conditioning systems, e.g. ASHRAE Handbook [1], and references on measurement, e.g. [4].

2.4 Psychrometric chart

Before introducing the psychrometric chart, its key features, and how to use it to find values of properties of moist air at a given state, an example is given on calculation of psychrometric properties based on data available from psychrometric tables in relevant handbooks. This example is intended to serve two purposes: as a worked example for the calculation methods, and for illustrating the burden it could become if such calculations are to be repeated time after time in practical applications.

For interested readers, details about how a psychrometric chart can be plotted with the use of a computer, and methods for calculating psychrometric properties for various states of moist air, are given in Appendix A.

2.4.1 Psychrometric property evaluation using tabulated data

Psychrometric property tables for moist air typically provide values of key properties, including moisture content, specific volume, and specific enthalpy, of saturated moist air under one standard atmospheric pressure. Properties of unsaturated moist air will need to be calculated based on the known saturated property values.

Example 2.2

> We can find from Table 2 in Chapter 1 of the *ASHRAE Handbook – Fundamentals* [1] the following for saturated moist air at 24°C:
>
> Moisture content, $w_s = 0.018965$kg/kg
> Specific volume, $v_s = 0.8671$m^3/kg
> Specific enthalpy, $h_s = 72.388$kJ/kg
>
> If we want to know the moisture content, specific volume, and specific enthalpy of moist air at 24°C and 50% relative humidity, we should carry out the following calculations.
>
> Saturation water vapour pressure, p_{ws}, at 24°C is related to moisture content, w_s, by:
>
> $$w_s = 0.622 \frac{p_{ws}}{p_a - p_{ws}}$$

Solving for p_{ws},

$$p_{ws} = \frac{p_a}{1+(0.622/w_s)} = \frac{101325}{1+(\frac{0.622}{0.018965})} = 2998\text{Pa}$$

The water vapour pressure, p_w, at 24°C and 50% relative humidity is:

$$p_w = \phi \cdot p_{ws} = 0.5 \times 2998 = 1499\text{Pa}$$

The moisture content of air, w, at 24°C and 50% relative humidity can now be evaluated, as follows:

$$w = 0.622\frac{p_w}{p_a - p_w} = 0.622\frac{1499}{101325-1499} = 0.00934 \text{ kg/kg}$$

The specific volume of moist air, v, at 24°C and 50% relative humidity can be determined using the perfect gas law for the dry air part, as follows:

$$p_{da}V = m_{da}R_{da}T$$

$$v = \frac{V}{m_{da}} = \frac{R_{da}T}{p_{da}} = \frac{R_{da}T}{p_a - p_w} = \frac{287.1\times(24+273.15)}{101325-1499} = 0.855\text{m}^3/\text{kg}$$

The specific enthalpy of air, h, at 24°C and 50% relative humidity can also be determined, as follows:

$$h = Cp_{da}t + w(Cp_w t + h_{fg0})$$
$$= 1.005 \times 24 + 0.00934 \times (1.87 \times 24 + 2501) = 47.9\text{kJ/kg}$$

The above example demonstrates the steps of calculation required to evaluate the moisture content, w, specific volume, v, and specific enthalpy, h, of unsaturated moist air from values of saturated properties available from a psychrometric table, which are relatively straightforward. Some combinations of unknown property and known properties, e.g. to calculate dew point, t_{dp}, from a known value of saturated moisture content, w_s, will involve solving for the solution from non-linear equations and, therefore, an iterative procedure will be needed.

In air-conditioning system design or when tackling a problem involving moist air, properties of moist air at many different states may need to be evaluated, which could become rather tedious. Such calculations can be largely cut down by referring to a psychrometric chart, which is an indispensable tool to air-conditioning engineers. However, the paper chart will be, and to a certain extent may have already been, replaced by electronic chart.

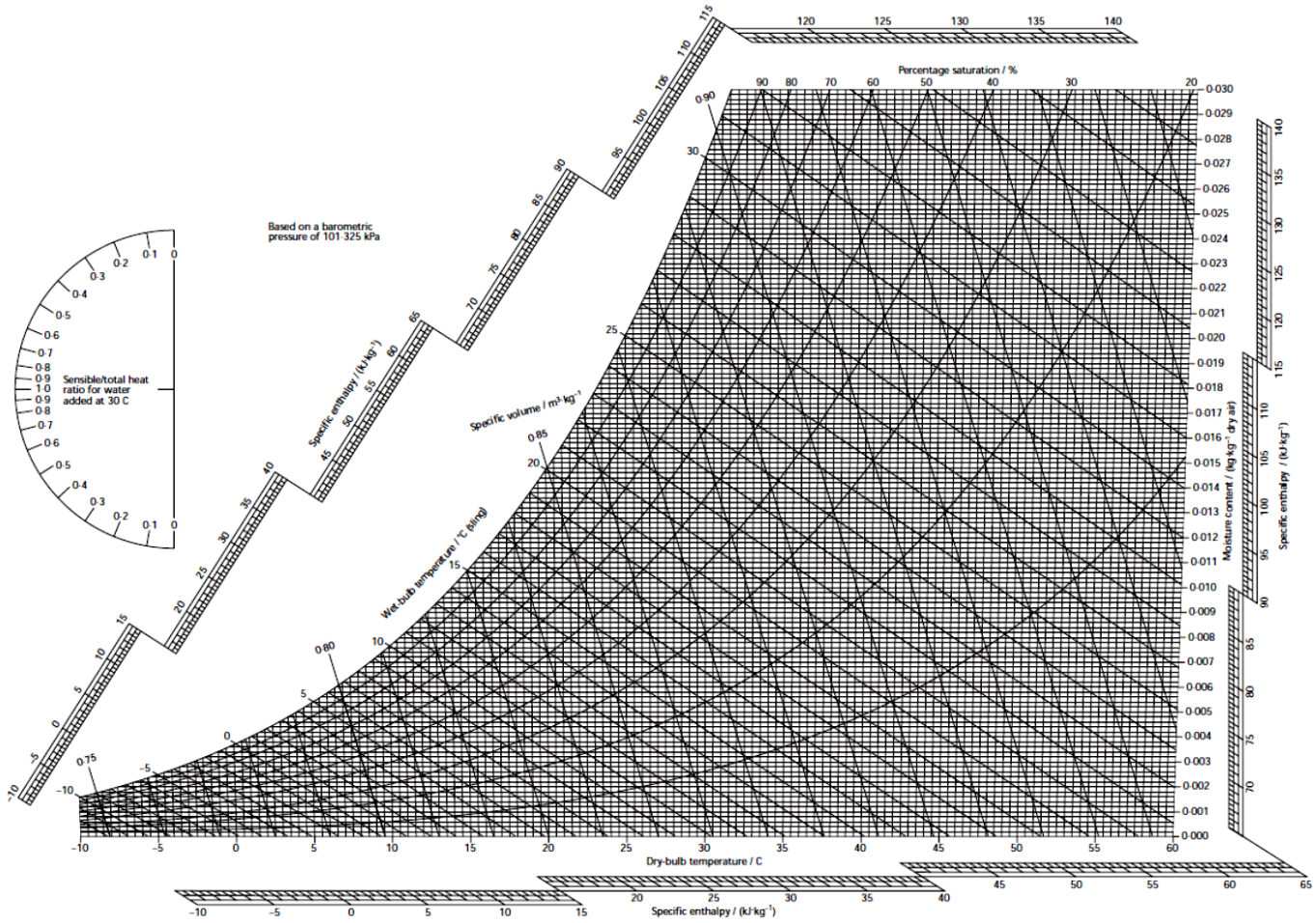

Figure 2.9 Psychrometric chart (CIBSE)

2.4.2 Key features of a psychrometric chart

2.4.2.1 Properties shown on the chart

Figure 2.9 shows the psychrometric chart available from the CIBSE Guide [2]. In this chart, dry bulb temperature (t) values are aligned horizontally along the bottom side, with the corresponding constant temperature lines extending upward (which are straight lines but not vertical lines except one; see Section A.2.1 in Appendix A). The axis for moisture content (w) is vertical and, therefore, constant moisture content lines are horizontal lines on the chart.

Two families of inclined lines, at different inclination angles, are shown on the chart, which are constant specific volume (v) and constant wet bulb temperature (t') lines. The wet bulb temperature lines shown are based on wet bulb temperatures measured by using sling hygrometers. This allows measured wet bulb temperature to be used directly to define the state of moist air in conjunction with the known value of another property, e.g. dry bulb temperature, although, strictly speaking, only thermodynamic wet bulb temperature is a property and could be shown on the chart.

The chart is surrounded by scales of specific enthalpy (h) but there are no constant specific enthalpy lines on the chart. Constant specific enthalpy (h) lines are omitted because they nearly overlap with the constant wet bulb (t') lines (Figure 2.10), and it would be confusing if both sets of lines are shown on the same chart (but the psychrometric chart developed by ASHRAE [1] indeed shows both sets of lines).

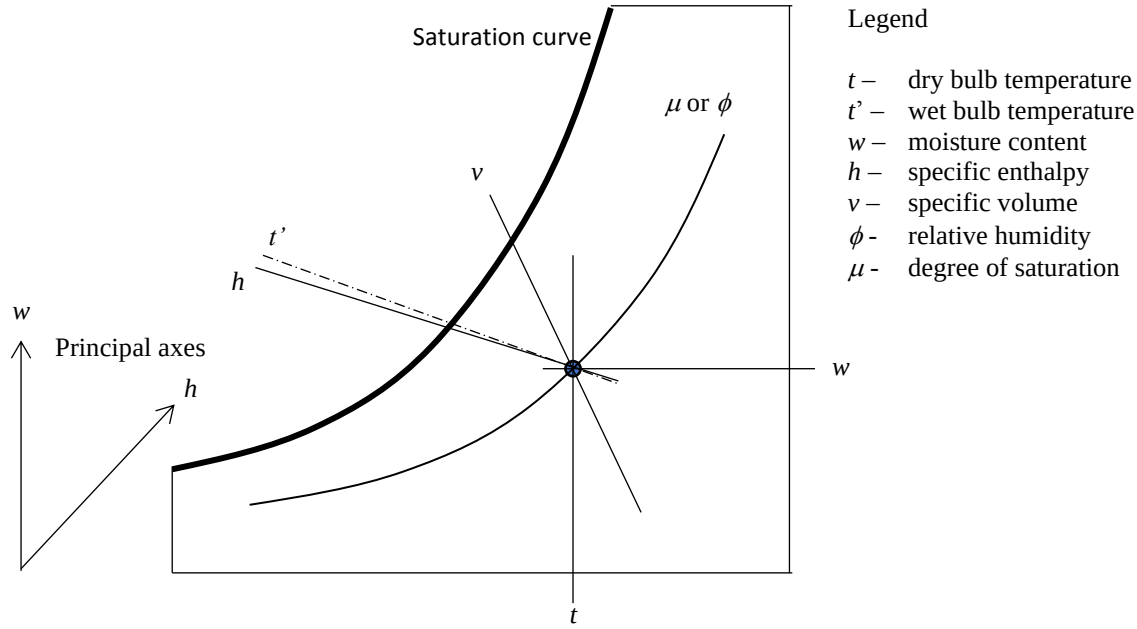

Figure 2.10 Principal axes of a psychrometric chart and constant property lines passing through a state point on the chart

The leftmost curve on the chart is the saturation curve, representing saturated states of moist air over a wide range of temperature, from -10°C to over 30°C. The other curves below the saturation curve are constant degree of saturation (μ) lines (constant relative humidity (ϕ) lines are shown instead on the psychrometric chart developed by ASHRAE [1]).

2.4.2.2 The principal variables of the chart

When we plot a graph to show the relation between two variables, say x and y, we would typically choose to plot the dependent variable, y, along the vertical axis and the independent variable, x, along the horizontal axis. The two axes, therefore, are orthogonal. If there are more than two variables to be plotted, we may choose two variables, referred to here as the principal variables, to be represented by the horizontal and vertical axes, and plot a graph that shows how they are related when the other independent variables are held constant. For example, if there are three variables x, y & z that bear a specific mathematical relationship among them, we could plot curves corresponding to a range of constant z values on a graph with y along the vertical axis and x along the horizontal axis (Figure 2.11).

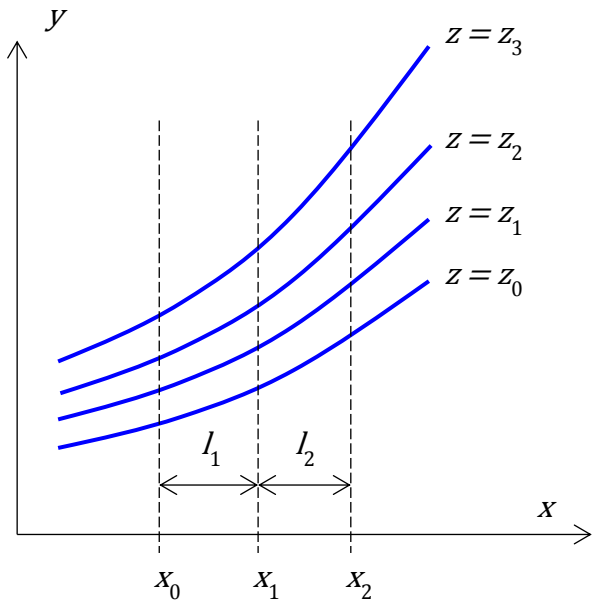

$$\frac{x_2 - x_1}{x_1 - x_0} = \frac{l_2}{l_1}$$

Figure 2.11 Curves showing relations between y and x at constant values of z and relation between lengths on a graph and a linear scale

Furthermore, we would use linear scales in both axes unless there is an obvious reason for not doing so. With linear scales, we can use linear distances on the graph to represent changes in the values of the variables represented by the axes, as they are proportional to each other (Figure 2.11).

In the case of a psychrometric chart, the properties plotted along the linear axes of the chart are specific enthalpy (h) and moisture content (w) (Figure 2.10). They are

selected as the principal variables because changes in their values are proportional to the total heat and moisture transfers taking place in a process that causes the changes in these properties. If we fix the value of only one psychrometric property, for example, the dry bulb temperature, which is not any one of the two principal variables, a curve can be plotted on the chart to show how specific enthalpy and moisture content are related when the dry bulb temperature of the moist air is held constantly at the stated value, which will result in a constant temperature curve.

Whereas most graphs employ orthogonal axes, in the psychrometric chart, the axis representing specific enthalpy and the axis representing moisture content are not perpendicular to each other (Figure 2.10). The angle between the two principal axes may be varied and the angle chosen is typically for making the constant temperature lines appear to be vertical (but they are actually not vertical and are diverging from each other with increase in moisture content).

2.4.3 Reading moist air properties from a psychrometric chart

Each point on the psychrometric chart represents a specific state of moist air (Figure 2.10). The state point defined by the fixed values of two properties is located at the intersecting point of the two lines that represent the respective values of the two properties on the chart. Once the location of a state point is identified, the values of all the other properties may be read directly from the chart. This will be a straightforward task if constant value lines of the property to be evaluated are available.

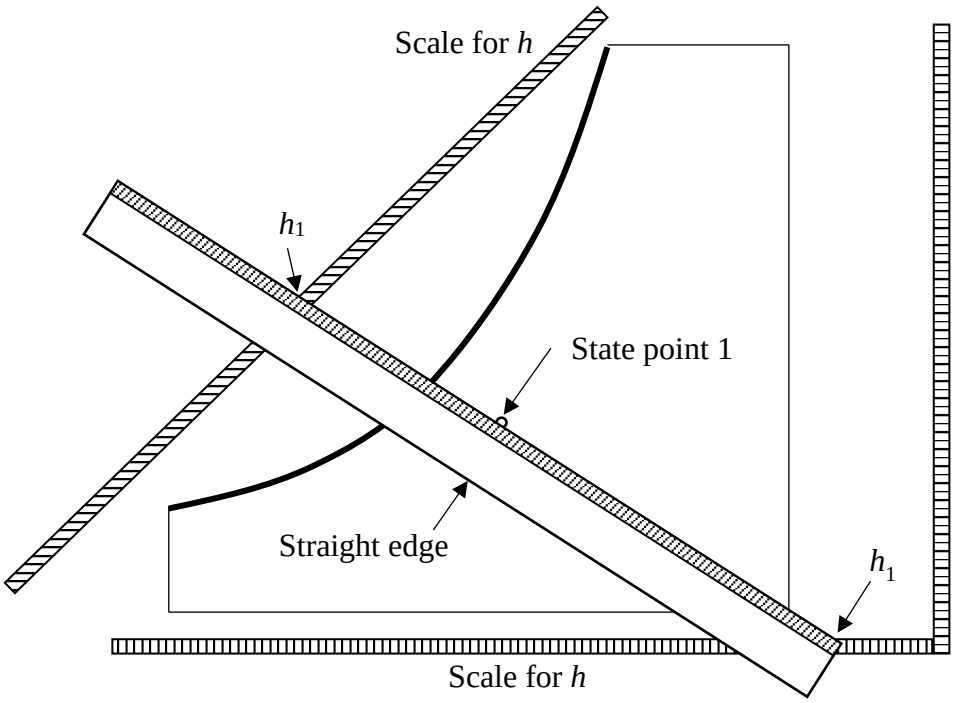

Figure 2.12 Reading specific enthalpy from a psychrometric chart

As mentioned above, constant specific enthalpy lines are absent, but the chart is surrounded by scales of specific enthalpy (Figure 2.9). One way to read specific enthalpy from a psychrometric chart is to use a straight edge. With the side of the straight edge touching the state point in question and rotating the straight edge about the state point until the straight edge cuts the specific enthalpy scales at two sides of the chart at the same value on the scales, that value is the specific enthalpy value for the state point (Figure 2.12).

2.5 Psychrometric processes

2.5.1 The general process

Section 2.2.9 described a process that will cause heat and moisture to be injected into a stream of moist air flowing steadily through a system in which this process takes place. By using Equations (2.29), (2.30) and (2.36), we can evaluate the state of the moist air at the end of this process, as follows:

$$w_{a2} = w_{a1} + \frac{M}{\dot{m}_a} \tag{2.51}$$

$$h_{a2} = h_{a1} + \frac{Q}{\dot{m}_a} \tag{2.52}$$

$$t_{a2} = t_{a1} + \frac{Q_{Sen}}{\dot{m}_a Cp_a} \tag{2.53}$$

Where

$\dot{m}_a =$	the dry air mass flow rate, kg/s
$M =$	the rate of moisture input into the air stream, kg/s
$Q =$	the rate of total heat input into the air stream, kW
$Q_{Sen} =$	the rate of sensible heat input into the air stream, kW
w_{a1} & $w_{a2} =$	the moisture content of the moist air entering and leaving the system, kg/kg
h_{a1} & $h_{a2} =$	the specific enthalpy of the moist air entering and leaving the system, kJ/kg
t_{a1} & $t_{a2} =$	the temperature of the moist air entering and leaving the system, ^{o}C
$Cp_a =$	the specific heat capacity of moist air, kJ/kg-K

The sensible heat input rate can also be evaluated from:

$$Q_{Sen} = Q - Q_{Lat} \tag{2.54}$$

Where Q_{Lat} is the latent load, given by:

$$Q_{Lat} = \dot{m}_a(w_{a2} - w_{a1})h_{fg0} \tag{2.55}$$

As Equations (2.51) to (2.53) show, there will be increases in the values of the respective properties of the moist air when heat and moisture are injected into the

moist air. With reference to the initial state point of the moist air on a psychrometric chart, the state point of the moist air will be shifted to a new position, because of the gains in heat and moisture in the process. Figure 2.13 shows the direction along which the state point of the air will move as the air undergoes a process that involve adding or removing heat and/or moisture from the moist air.

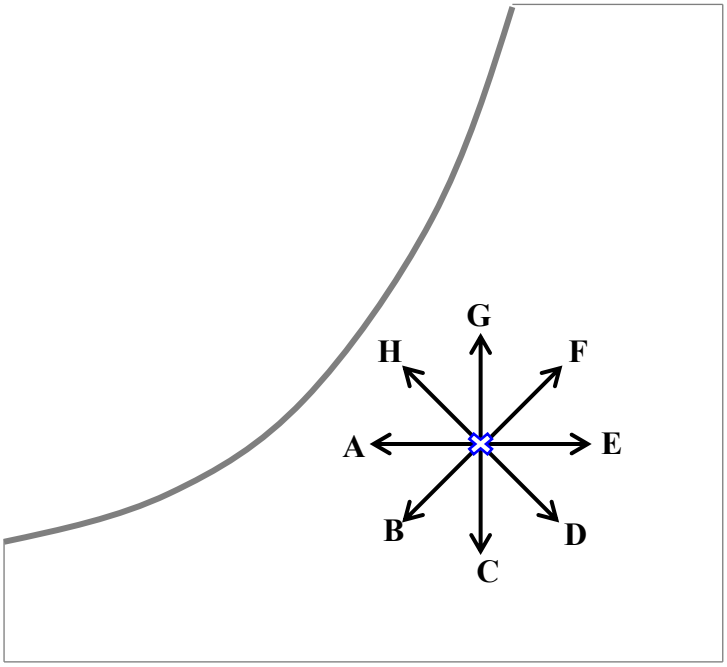

Psychrometric Processes:

A – Sensible cooling

B – Cooling and dehumidification

C – Isothermal dehumidification

D – Heating and dehumidification

E – Sensible heating

F – Heating and humidification

G – Isothermal humidification

H – Cooling and humidification

Figure 2.13 Movement direction of state point of moist air when undergoing a psychrometric process

Air-conditioning typically involves treating air through a series of processes that make up a cycle. These processes, and the conventional all air cycle, which is the starting point of air-conditioning system design, are discussed in the ensuing sub-sections.

2.5.2 Sensible heating or cooling process

When an air-conditioning equipment is adding or removing sensible heat to or from a stream of moist air flowing through it, without adding or removing any moisture to or from the air at the same time, the process is called a sensible heating process if heat is added to the air, or a sensible cooling process if heat is removed from the air. The equipment may be an electric heater, which converts electrical energy into heat and imparts the heat to the air, or a heating coil or a cooling coil, which is a heat exchanger that facilitates heat transfer between a medium and the air stream. The heat transfer medium may be chilled or hot water, steam, or condensing or evaporating refrigerant.

In a sensible heating or cooling process, the temperature of the air will be raised or lowered (see Equation (2.53), with $Q_{Sen} > 0$ or $Q_{Sen} < 0$) but its moisture content will remain unchanged (see Equation (2.51) with $M = 0$). Therefore, the state points of the moist air at the beginning and the end of the process will both lie on the same constant moisture content line on a psychrometric chart, which is a horizontal line (Figure 2.14a).

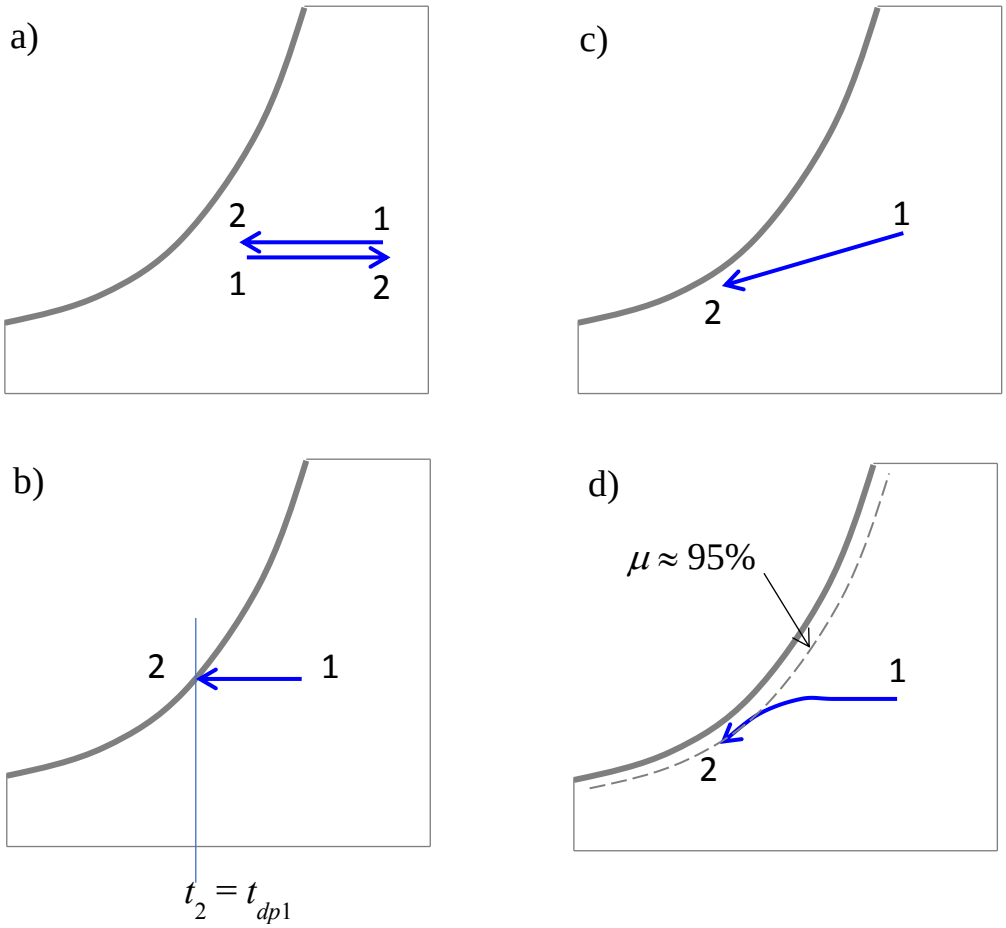

Figure 2.14 Sensible Heating and Cooling, and Cooling and Dehumidification Processes

For a sensible cooling process, there is a limit to the temperature of the air to which the air can be cooled, which is the dew point of the air (Figure 2.14b). Cooling air beyond its dew point will incur water vapour in the air to condense out as liquid, which will lead to a drop in the moisture content of the air, and hence the process is no longer just a sensible cooling process.

2.5.3 Cooling and dehumidification process

If moist air is cooled to below its dew point, its moisture content will drop together with its temperature (Figure 2.14c). This requires cooling of the heat transfer surface in a cooling coil, which is in contact with the air stream, to a temperature below the dew

point of the entering air. It, in turn, will cause some water vapour in the air stream to condense out and become liquid droplets deposited upon the heat transfer surface. The liquid water arising from condensation of water vapour is called condensate, which will leave the coil as the water droplets drip onto the pan beneath the coil and be drained away.

If we regard the cooling coil as a counter flow heat exchanger, which is a model widely used to simulate the performance of a cooling coil [5], the coil surface temperature will be the highest at the side the air enters the coil, and will be the lowest at the side the air leaves the coil (Figure 2.15). If the coil surface temperature at the side air enters the coil stays above the dew point of the air, the air will only be cooled sensibly until the air has moved deeper into the coil to the position where the coil surface temperature starts to fall below the dew point of the air. From that point onward, condensation of water vapour in the air will take place till the air leaves the coil. The process undergone by the air, therefore, will initially be a sensible cooling process followed by a cooling and dehumidifying process, as shown in Figure 2.14d.

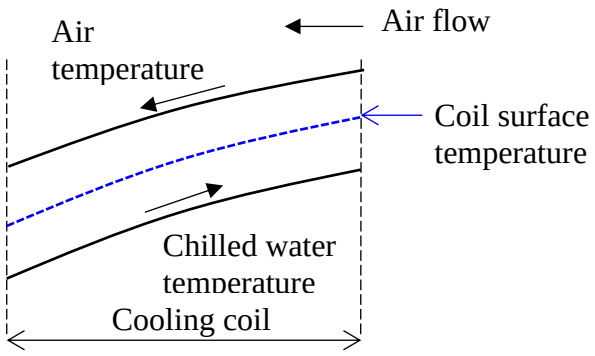

Figure 2.15 Temperature distributions inside a cooling and dehumidifying coil

The air that is in contact with the cold coil surface at a temperature below its dew point and is having its water vapour condensing out as liquid must be saturated air, and its temperature is close to the temperature of the coil surface. However, not all the air in the air stream flowing through the coil will have close contact with the coil surface. The air that is not in contact with the coil surface will stay at a slightly higher temperature and will be unsaturated. Nevertheless, air at various positions within the coil will mix and, by the time the air leaves the cooling and dehumidifying coil, its state will be close to but still not saturated.

In air-conditioning system design, the concepts of apparatus dew point and contact factor have been used for prediction of the leaving coil air state. We shall examine this method when the adiabatic mixing process is covered below. However, a simpler approach is to assume that the leaving coil air state is approximately 95% saturated (Figure 2.14d), which is the method we shall adopt in construction of the conventional all air cycle, as will be explained in detail later.

With the condensate leaving a cooling and dehumidifying coil (Figure 2.16) accounted for, the following moisture and heat balance equations can be derived:

$$M_{CC} = \dot{m}_{da}(w_{a1} - w_{a2}) \quad (2.56)$$

$$Q_{CC,Tot} = \dot{m}_{da}(h_{a1} - h_{a2}) - M_{CC}C_f t_{CC} \quad (2.57)$$

$$Q_{CC,Sen} = \dot{m}_{da}Cp_a(t_{a1} - t_{a2}) \quad (2.58)$$

Where

M_{CC} =	rate of condensation from the air, kg/s
$Q_{CC,Tot}$ =	rate of total heat removal from the air through the cooling coil, kW
$Q_{CC,Sen}$ =	rate of sensible heat removal from the air through the cooling coil, kW
$\dot{m}_{da}$ =	the dry air mass flow rate, kg/s
w_{a1} & w_{a2} =	moisture content of the moist air entering and leaving the coil, kg/kg
h_{a1} & h_{a2} =	specific enthalpy of the moist air entering and leaving the coil, kJ/kg
t_{a1} & t_{a2} =	temperature of the moist air entering and leaving the coil, ^{o}C
Cp_a =	specific heat capacity of moist air, kJ/kg-K
C_f =	specific heat capacity of liquid water, kJ/kg-K
t_{CC} =	temperature of the condensate leaving the coil, ^{o}C

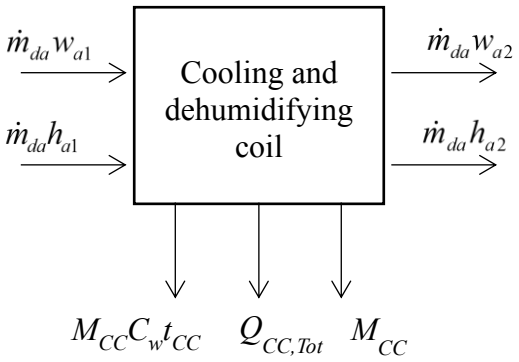

Figure 2.16 Heat and moisture transfers at a cooling and dehumidifying coil

Example 2.3

A fresh air (FA) handling unit is treating outdoor air from 33.3^{o}C, 66% relative humidity (RH) to 16^{o}C and 95% RH. The dry air mass flow rate of the FA being treated is 1 kg/s. The temperature of condensate leaving the coil may be taken as 10^{o}C. Determine:

i) The condensate flow rate

ii) The rate of heat carried away by the condensate
iii) The total cooling coil output required.

Solution

Table 2.3 summarizes the given and calculated values of properties of the fresh air entering and leaving the cooling coil in the fresh air-handling unit.

The condensate flow rate
$= M_{CC} = \dot{m}_{da}(w_{a1} - w_{a2}) = 0.01067$ kg/s

The rate of heat carried away by the condensate
$= Q_{Cds} = M_{CC}\, C_f\, t_{CC} = 0.448$ kW

The total cooling coil output required
$= Q_{CC,Tot} = \dot{m}_{da}(h_{a1} - h_{a2}) - M_{CC} C_f t_{CC} = 44.64$kW

Table 2.3 Calculation results of Example 2.3

On coil condition			Leaving coil condition		
$\dot{m}_{da}$	1	kg/s			
t_{a1}	33.3	°C	t_{a2}	16	°C
ϕ_{a1}	0.66		ϕ_{a2}	0.95	
p_{ws1}	5119.74	Pa	p_{ws2}	1818.44	Pa
p_{w1}	3379.03	Pa	p_{w2}	1727.52	Pa
w_{a1}	0.021458	kg/kg	w_{a2}	0.010789	kg/kg
h_{a1}	88.47	kJ/kg	h_{a2}	43.39	kJ/kg

As the above example shows, the rate that heat will be carried away by the condensate will account for just about 1% of the required cooling coil output. The last term at the right-hand side of Equation (2.57), therefore, may be omitted in practical calculations.

2.5.4 Room air diffusion process

The room air diffusion process, shown as process 1-2 in Figure 2.17, is the process undergone by the air supplied into an air-conditioned space for providing the space with air-conditioning, which, to the air under concern, is a heating and humidifying process. When the cooled and dehumidified air at state 1 (Figure 2.17) is supplied into the air-conditioned space, both the temperature and the moisture content of the air will rise as it picks up the heat and moisture from external and internal sources of the space (we shall deal with cooling loads in the next chapter). Equations (2.51) to (2.53) can be used to evaluate the temperature, moisture content and specific enthalpy of the air at the end of the process, i.e. at state 2 in Figure 2.17.

If state 2 represents the design state of the air in the air-conditioned space, Q, Q_{Sen} and M in Equations (2.51) to (2.53) will be the total cooling load, sensible cooling load and

moisture load of the space, respectively. With the room air maintained at the design state steadily, Q, Q_{Sen} and M are equal to the total cooling, sensible cooling, and dehumidification rates that are output by the air-conditioning system for the space.

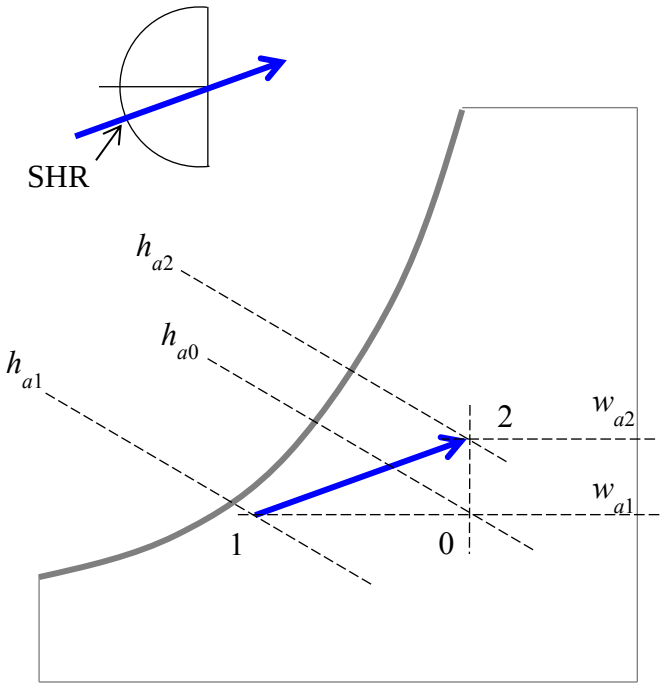

Figure 2.17 The room air diffusion process

The sensible cooling load, Q_{Sen}, may also be expressed, with reference to the state points shown in Figure 2.17, as:

$$Q_{Sen} = \dot{m}_{da}(h_{a0} - h_{a1}) \tag{2.59}$$

Where, at the state point 0, $t_{a0} = t_{a2}$ and $w_{a0} = w_{a1}$. It follows that process 1-0 is a sensible heating process and thus:

$$h_{a0} = h_{a1} + Cp_a(t_{a2} - t_{a1}) \tag{2.60}$$

The ratio of the sensible load to the total load, referred to as the sensible heat ratio, or *SHR*, can be written as:

$$\frac{Q_{Sen}}{Q} = SHR = \frac{h_{a0} - h_{a1}}{h_{a2} - h_{a1}} \tag{2.61}$$

As can be seen by referring to Figure 2.17, the *SHR* is related to the slope of the process line 1-2 on the psychrometric chart. The value of *SHR* may vary between 0 and 1, corresponding to a process that involves solely latent heat transfer ($h_{a0} = h_{a1}$; $SHR = 0$) to a process that involves solely sensible heat transfer ($h_{a0} = h_{a2}$; $SHR = 1$). In other words, if we know the *SHR* of a process, we can determine the slope of the process line

on a psychrometric chart even if we do not know yet the starting or ending state points of the process.

On a psychrometric chart (Figure 2.9), there is a protractor with graduations for different *SHR* values at its circumference. A line joining the centre of the protractor and a graduation mark (Figure 2.18) will have a slope corresponding to the *SHR* value as represented by the mark. As shown in Figure 2.18, the upper half of the protractor is for processes involving cooling & humidification or heating & dehumidification whereas the lower half is for processes involving cooling & dehumidification or heating and humidification.

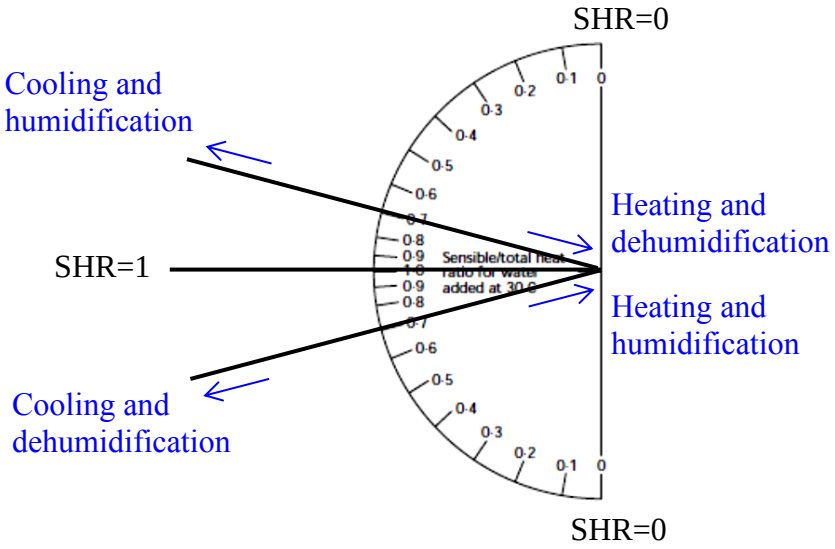

Figure 2.18 The sensible heat ratio (SHR) protractor on a psychrometric chart

Although *SHR* is introduced above with reference to the room air diffusion process, the concept in fact is applicable to various other processes that involve sensible and latent heat transfers, such as the cooling and dehumidification process of a cooling coil.

2.5.5 Adiabatic mixing process

Merging of two air streams into one, with the air in the two streams thoroughly mixed, is common in air-conditioning. Since the mixing process will complete, with the mixture achieving a uniform state, within a short period of time, the assumption is usually made that no loss or gain of heat and moisture to or from the surrounding will take place. For this reason, the process is called an adiabatic mixing process.

Let $\dot{m}_{da}$, h_a and w_a be the dry air mass flow rate, specific enthalpy and moisture content of air in the air streams, and subscripts 1, 2 & 3 of these variables denote the three air streams where stream 3 is the mixture of streams 1 & 2 (Figure 2.19). From conservation of mass, we have:

$$\dot{m}_{da1} + \dot{m}_{da2} = \dot{m}_{da3} \tag{2.62}$$

Balancing the water vapour in the air streams, we get:

$$\dot{m}_{da1} w_{a1} + \dot{m}_{da2} w_{a2} = \dot{m}_{da3} w_{a3} \tag{2.63}$$

Based on conservation of energy, we can write:

$$\dot{m}_{da1} h_{a1} + \dot{m}_{da2} h_{a2} = \dot{m}_{da3} h_{a3} \tag{2.64}$$

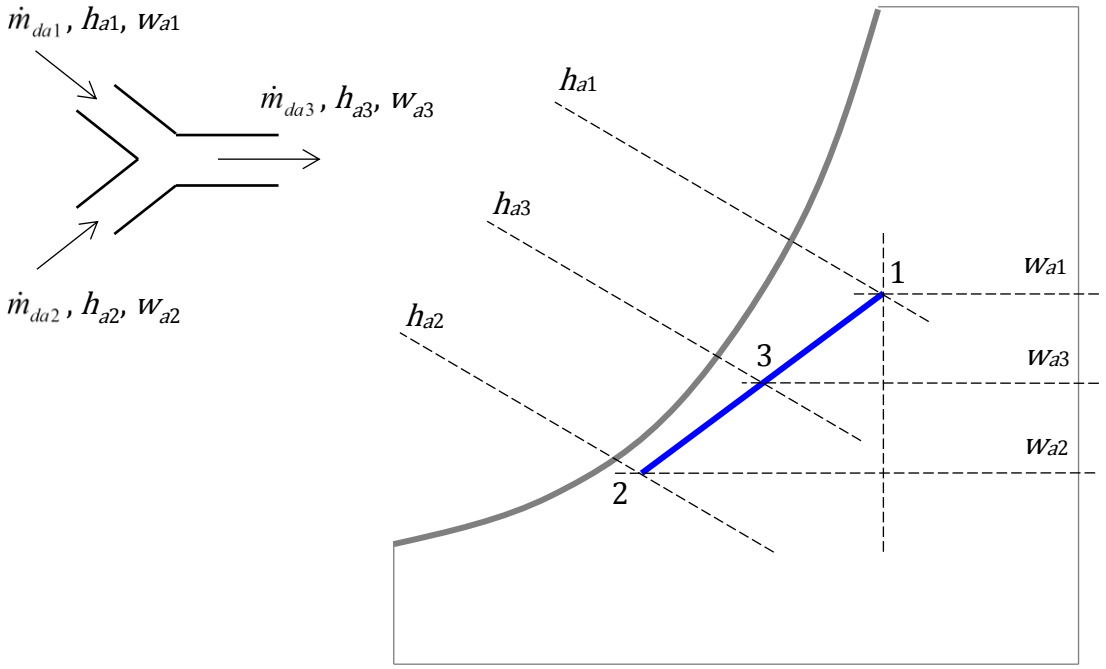

Figure 2.19 An adiabatic mixing process

From Equations (2.63) & (2.64), the mixture state can be evaluated as follows:

$$w_{a3} = \frac{\dot{m}_{da1}}{\dot{m}_{da3}} w_{a1} + \frac{\dot{m}_{da2}}{\dot{m}_{da3}} w_{a2} \tag{2.65}$$

$$h_{a3} = \frac{\dot{m}_{da1}}{\dot{m}_{da3}} h_{a1} + \frac{\dot{m}_{da2}}{\dot{m}_{da3}} h_{a2} \tag{2.66}$$

Using Equations (2.62) and (2.63):

$$\dot{m}_{da1} w_{a1} + \dot{m}_{da2} w_{a2} = (\dot{m}_{da1} + \dot{m}_{da2}) w_{a3}$$

$$\dot{m}_{da1} (w_{a1} - w_{a3}) = \dot{m}_{da2} (w_{a3} - w_{a2})$$

$$\frac{\dot{m}_{da1}}{\dot{m}_{da2}} = \frac{w_{a3} - w_{a2}}{w_{a1} - w_{a3}} \tag{2.67}$$

Similarly, using Equations (2.62) and (2.64):

$$\frac{\dot{m}_{da1}}{\dot{m}_{da2}} = \frac{h_{a3}-h_{a2}}{h_{a1}-h_{a3}} \tag{2.68}$$

Since the left-hand sides of Equations (2.67) & (2.68) are identical, we can write:

$$\frac{h_{a3}-h_{a2}}{h_{a1}-h_{a3}} = \frac{w_{a3}-w_{a2}}{w_{a1}-w_{a3}}$$

$$\frac{h_{a3}-h_{a2}}{w_{a3}-w_{a2}} = \frac{h_{a1}-h_{a3}}{w_{a1}-w_{a3}} \tag{2.69}$$

Referring to Figure 2.19, it becomes apparent that both the left- and the right-hand sides of the above equation are a ratio of the specific enthalpy difference and the moisture content difference between two state points. Given that specific enthalpy and moisture content are the two principal variables plotted in linear scales on a psychrometric chart, this ratio represents the slope of the straight line joining up the two state points.

Therefore, Equation (2.69) implies that the straight-line between states 1 &3 and that between states 2 & 3 are having the same slope. As the two straight lines are connected at point 3, they are co-linear, and they make up one continuous straight-line right from state 1 to state 2, with state 3 lying on this straight line between states 1 & 2.

Equation (2.68) may be further manipulated to:

$$\frac{\dot{m}_{da1}}{\dot{m}_{da2}} = \frac{\dot{m}_{da3}-\dot{m}_{da2}}{\dot{m}_{da2}} = \frac{h_{a3}-h_{a2}}{h_{a1}-h_{a3}}$$

$$\frac{\dot{m}_{da3}}{\dot{m}_{da2}} = \frac{h_{a3}-h_{a2}}{h_{a1}-h_{a3}} + 1 = \frac{h_{a1}-h_{a2}}{h_{a1}-h_{a3}}$$

Inverting both sides, we get:

$$\frac{\dot{m}_{da2}}{\dot{m}_{da3}} = \frac{h_{a1}-h_{a3}}{h_{a1}-h_{a2}}$$

Let l_{12} be the linear distance between state points 1 and 2, and l_{13} the distance between state points 1 and 3, on the psychrometric chart (Figure 2.19). Since h_a and w_a are in linear scales on the chart,

$$\frac{\dot{m}_{da2}}{\dot{m}_{da3}} = \frac{h_{a1}-h_{a3}}{h_{a1}-h_{a2}} = \frac{l_{13}}{l_{12}} \tag{2.70}$$

The implication of this result is that we can determine the state point of the mixture of two air streams, i.e. state 3, by a graphical method. The first step is to measure the linear distance between the two state points representing the states of the two air streams to be mixed, i.e. between states 1 & 2, on the psychrometric chart. This distance, denoted by l_{12}, when scaled down by the mass flow rate ratio, as shown in Equation (2.70), will yield:

$$l_{13} = \frac{\dot{m}_{da2}}{\dot{m}_{da3}} l_{12}$$

By measuring, along the straight-line joining up states 1 and 2, a distance that equals l_{13} from state point 1 will allow us to locate state point 3.

Example 2.4

Explain how the state of the air leaving a cooling and dehumidifying coil can be determined when the on-coil air condition and the sensible heat ratio (SHR) of the process are known.

Solution

In this example, the concepts of "apparatus dew point" and "contact factor", which may be employed to find the condition of the air leaving a cooling and dehumidifying coil, are explained. Furthermore, the concept of the adiabatic mixing process is also employed in this method.

The "apparatus dew point" of a cooling and dehumidifying coil refers to the intersecting point (point *c* shown in Figure 2.20) of the saturation curve and the straight-line obtained by extending the cooling and dehumidifying process line from state point 1, which represents the known on-coil air condition, along a slope determined by the sensible heat ratio (SHR) of the process (see Section 2.5.4).

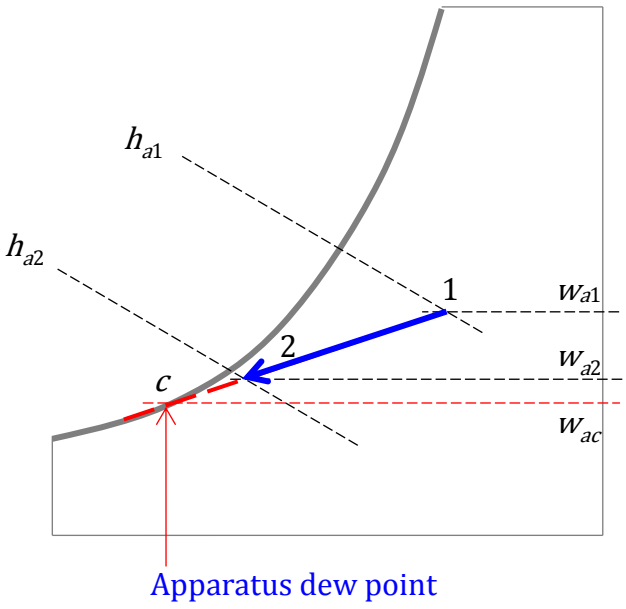

Figure 2.20 Apparatus dew point of a cooling and dehumidifying coil

The apparatus dew point may be interpreted as the temperature of air leaving an idealistic cooling and dehumidifying coil where the air flowing through the coil could all be brought to saturation when the air leaves the coil (Figure 2.20). The

real process may then be modelled by regarding a portion of the air flow is treated by such an idealistic coil and the rest not treated at all. The actual leaving coil air state would then be the mixture of the air leaving the idealistic coil and the air that bypassed it (and untreated).

The following ratio (β) of the moisture content and specific enthalpy differences of air at the on- and off-coil air states (1 & 2) and the apparatus dew point state (c) may be regarded as a measure of the effectiveness of a cooling and dehumidifying coil:

$$\beta = \frac{w_{a1} - w_{a2}}{w_{a1} - w_{ac}} = \frac{h_{a1} - h_{a2}}{h_{a1} - h_{ac}} \tag{2.71}$$

Where β is called the "contact factor" and $(1 - \beta)$ the "bypass factor".

Therefore, if the contact or bypass factor of a coil is known, the leaving coil air state can be evaluated using Equation (2.71), or graphically by measuring the linear distances between state points 1 & c and 1 & 2 on a psychrometric chart.

2.5.6 Adiabatic saturation process

In Section 2.2.10, the idealistic adiabatic saturation process has been discussed with reference to a long, well-insulated chamber with water on the bottom surface, through which air may flow. Based on this process, the property thermodynamic wet bulb temperature, t_a^*, was derived and defined.

By using Equation (2.42), which is shown again as the first equation below, we can derive equations (Equations (2.72) to (2.74)) to describe the adiabatic saturation process and understand how the process line will appear on a psychrometric chart:

$$h_a^* = h_a + (w_a^* - w_a) C_f t_a^*$$

$$h_a = (C_f t_a^*) \cdot w_a + (h_a^* - w_a^* C_f t_a^*) \tag{2.72}$$

$$h_a = f(w_a)|_{t_a^* = Const} = a \cdot w_a + b \tag{2.73}$$

$$\frac{\Delta h_a}{\Delta w_a} = C_f t_a^* \tag{2.74}$$

For a given air state, say state 1 as shown in Figure 2.21, if air at this state flows through the long, well-insulated chamber, it will leave saturated at t_a^*, meaning that the thermodynamic wet bulb temperature of state 1 is t_a^*. As the air flows through the chamber, its state will change gradually from state 1 to a series of intermediate states until the air reaches the equilibrium state that is saturated at t_a^*. If, instead of state 1, air starts to flow into the chamber at any one of such intermediate states, it will still end up leaving the chamber at the state that is saturated at t_a^*. Therefore, if we plot state 1 and all these intermediate states on the psychrometric chart, we will get a constant thermodynamic wet bulb temperature line, as depicted by Equation (2.73).

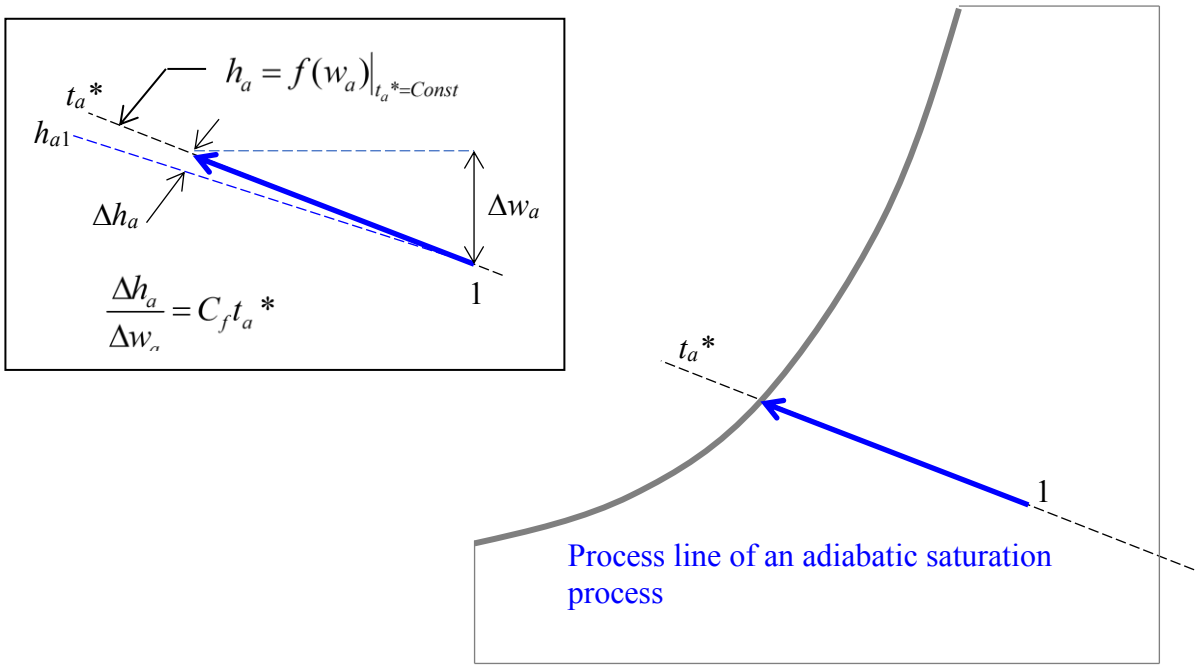

Figure 2.21 Adiabatic saturation process on a psychrometric chart

It can also be seen from Equation (2.72) that when the value of t_a* is fixed, which accordingly will fix the values of h_a* and w_a*, the terms in the two brackets at the right-hand side of this equation becomes constants, and therefore the equation can be re-written as shown in Equation (2.73) where a & b are two constants. It, therefore, becomes apparent from Equation (2.73) that the constant thermodynamic wet bulb temperature lines are straight lines on a psychrometric chart with h and w being the principal variables.

Furthermore, as Equation (2.74) shows, in an adiabatic saturation process, while the moisture content in the air increases, there will be a corresponding rise in the specific enthalpy of the air (see the figure in the box in Figure 2.21). Therefore, the constant thermodynamic wet bulb temperature line will rise above the constant specific enthalpy line when both lines extend from the initial state of the air at the beginning of the process (Figure 2.21).

In realistic adiabatic saturation processes, such as those that take place inside spray humidifiers and air washers (Figure 2.22), the state of the air cannot reach the saturation state but will stop at a high degree of saturation, albeit unsaturated. In such equipment, water is sprayed inside a chamber and the water droplets will be in direct contact with the air stream being induced to flow through the chamber by a fan. The water droplets will fall onto a basin at the bottom and the water will be pumped to the nozzles and sprayed inside the chamber again.

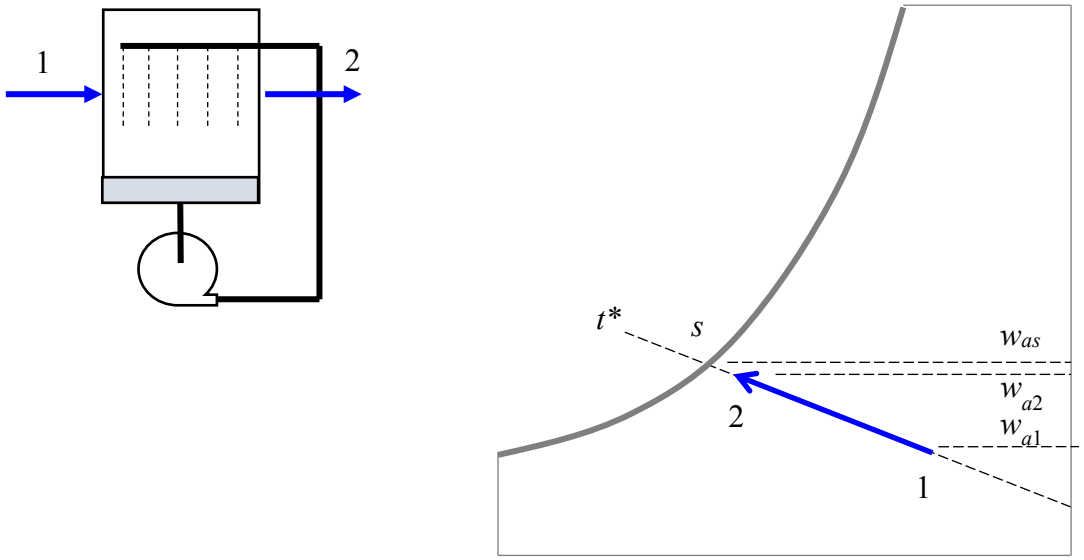

Figure 2.22 Realistic adiabatic saturation process in a spray humidifier

In the process, some liquid water from the water droplets will vaporize and join the air, thus adding moisture to the air. Water losses will be made up by an external water supply. In the absence of an external heat source, and, therefore, the process is an adiabatic saturation process, the heat required to sustain the heat of vaporization comes from the air, resulting in a drop in the air temperature. The process line coincides with the constant thermodynamic wet bulb temperature line passing the state point of the initial state of the air.

A parameter called effectiveness, η, is defined to gauge how close to saturation the air can be made by a spray humidifier (Figure 2.22), as follows:

$$\eta = \frac{w_{a2} - w_{a1}}{w_{as} - w_{a1}} \tag{2.75}$$

Knowing the value of η for a spray humidifier and the entering state of air, the leaving air state point can be found using the above equation in conjunction with a psychrometric chart.

2.6 The conventional all air cycle

2.6.1 Processes in an air-conditioning cycle

In an air-conditioning system, treated air is supplied into the air-conditioned space and the air will be induced to flow back to the system and be treated again, ready for another round of circulation between the air-conditioned space and the system. The air, therefore, is undergoing cyclic changes in its thermodynamic state as it is being recirculated. In each cycle, the air will undergo several psychrometric processes in turn. The end state of a process will become the starting state of the next process and hence two consecutive processes will be connected when shown on a psychrometric chart. All

the processes, with each connected to the preceding and the following processes, form an air-conditioning cycle.

With reference to the air-conditioning system schematic diagram shown in Figure 2.23, the air-conditioning cycle comprises the following processes:

1. The room air diffusion process, involving V_s m³/s of supply air (SA) from the air-handling unit entering the air-conditioned space at state *s*, which will gain heat and moisture from the internal and external sources, ending up at state *r*.

2. The adiabatic mixing process, taking place after V_{fa} m³/s of the air returning from the air-conditioning space at state *r* has been disposed of as exhaust air (EA), leaving (V_s – V_{fa}) m³/s of return air (RA) at state *r* to mix with V_{fa} m³/s of outdoor fresh air (FA) at state *o*, leading to V_s m³/s of air at state *m* at the end of the adiabatic mixing process.

3. The cooling and dehumidifying process that follows the adiabatic mixing process where V_s m³/s of air at state *m* is cooled and dehumidified by the cooling coil inside the air-handling unit to state *l*.

4. The sensible heating process, which is due to heat dissipation of the fan causing the air downstream of the cooling and dehumidifying coil to rise in temperature, and change from state *l* to *s*, before the air is supplied into the air-conditioned space again.

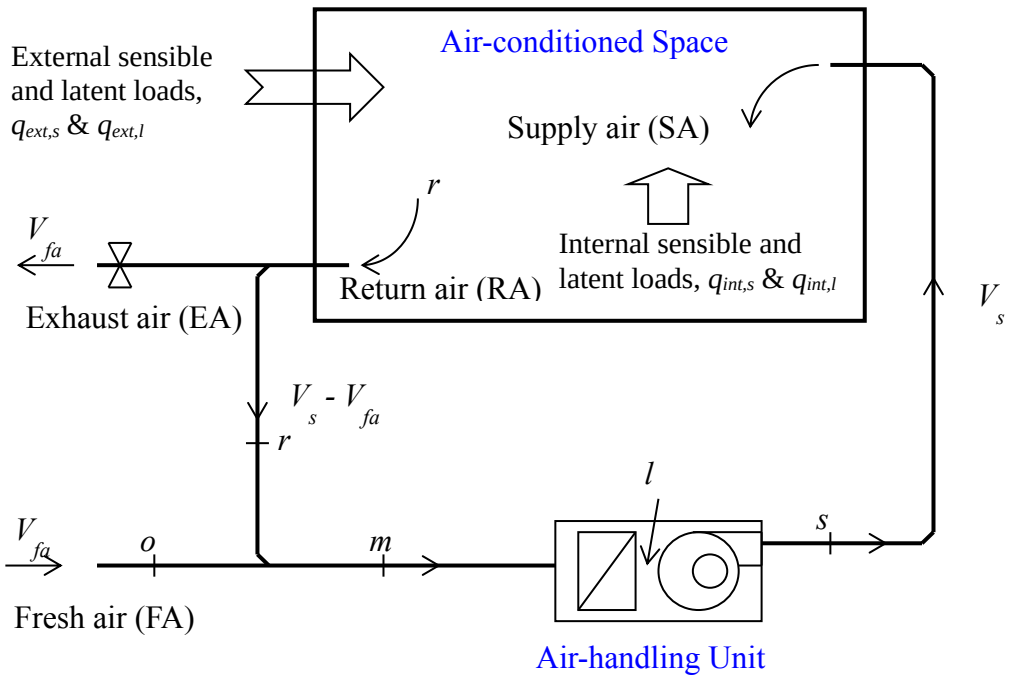

Figure 2.23 Air-conditioning system schematic diagram

Adhering to the set of symbols (*r*, *o*, *m*, *l* & *s*) used to denote the states of the air at various locations in the air-conditioning cycle as shown in Figure 2.23, the psychrometric processes that cause the state of the air to change from one to another, when shown on the psychrometric chart, will be as shown in Figure 2.24. The cycle formed by the psychrometric processes under the design condition for an all air system is called the conventional all air cycle, which is the starting point of system design for all kinds of air-side air-conditioning systems.

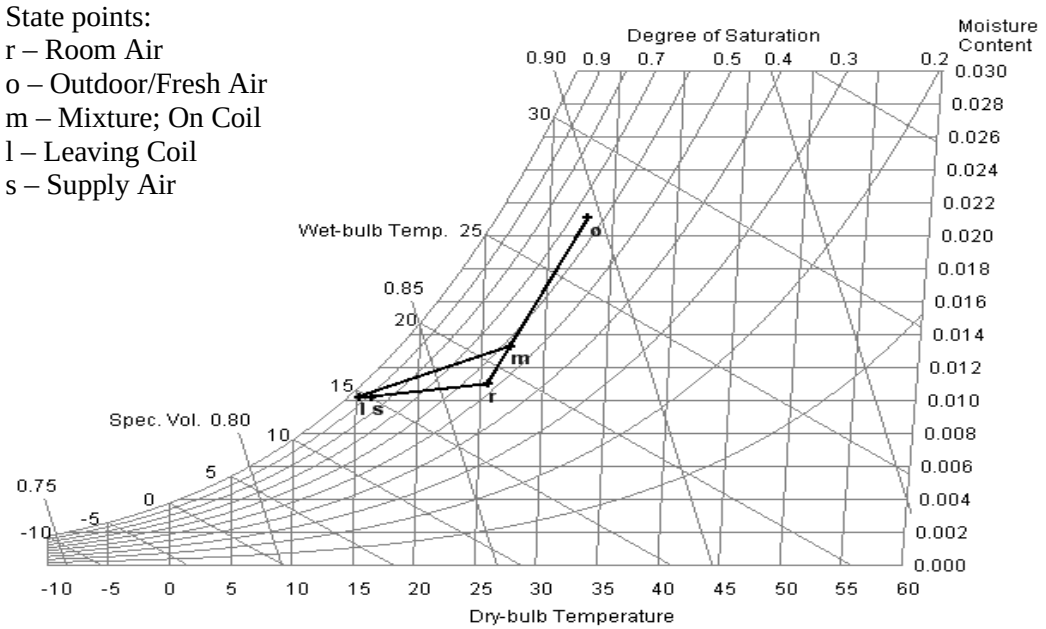

Figure 2.24 Air-conditioning processes and cycle on a psychrometric chart

2.6.2 Construction of the conventional all air cycle

Construction of the conventional all air cycle will involve the following steps:

1. Based on the design indoor air condition, e.g. t_r and ϕ_r, locate the state point representing the room air state, *r*, on the psychrometric chart (Figure 2.25a).

2. Let q_{rs} and q_{rl} be the design room sensible and latent loads, and based on their values as determined in design cooling load estimation, calculate the room sensible heat ratio (*RSHR*), as follows:

$$RSHR = \frac{q_{rs}}{q_{rs}+q_{rl}} \tag{2.76}$$

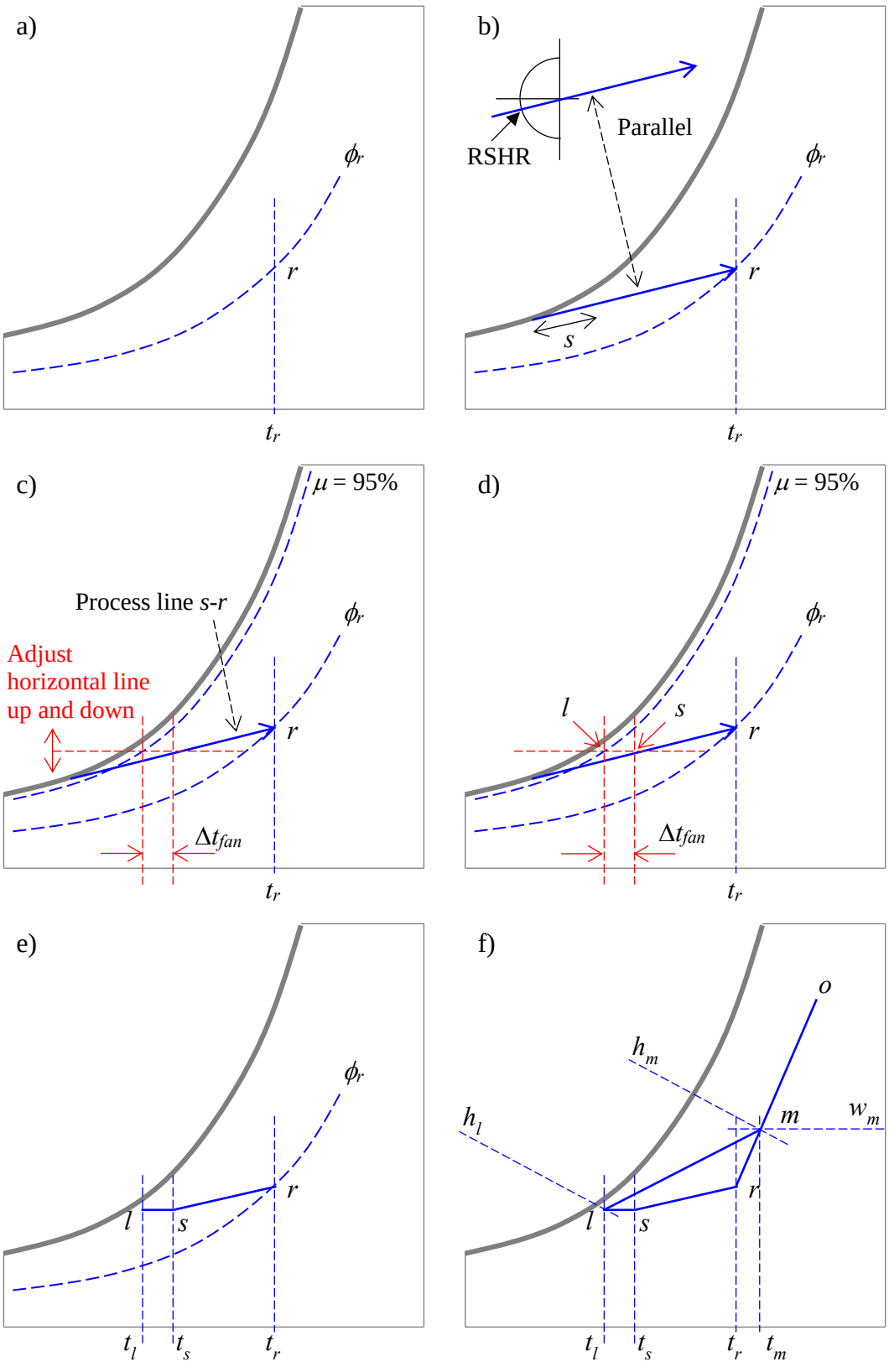

Figure 2.25 Steps of constructing the conventional all air cycle

3. Determine the slope of the process line *s-r* based on the *RSHR* using the protractor provided in the chart (Figure 2.25b) and draw a line at the protractor at the slope corresponding to the *RSHR*. Draw a line passing through the room air state *r* that is parallel to the line drawn at the protractor according to the *RSHR*. The supply air state point, *s*, will line on this process line but, at this juncture, the exact location of state point *s* remains unknown.

4. Assume that the state of air leaving a cooling and dehumidifying coil, *l*, will have a degree of saturation of 95%, and the temperature rise due to fan heat gain, ΔT_{fan}, is known (typically in the range of 0.5-1.5°C). The state points *l* and *s* can then be determined simultaneously by adjusting the location of a horizontal line until it crosses the 95% saturation line and the process line *s-r*, with the intersecting points separated from each other by ΔT_{fan} in the temperature scale (Figure 2.25c). The state point *l* lies at the intersecting point of the horizontal line with the 95% saturation line, and the state point *s* lies at the intersecting point of the horizontal line with the process line *s-r* (Figure 2.25d). Having determined the state points *l* and *s*, their psychrometric properties can be read from the psychrometric chart (Figure 2.25e).

5. The required supply air flow rate, V_s, can now be determined as follows:

$$V_s = \frac{q_{rs}}{\rho_a Cp_a (t_r - t_s)} \tag{2.77}$$

Where ρ_a = density of moist air = $1/v_a$, ≈1.2 kg/m^3.

6. Based on the design outdoor / fresh air state, locate its state point, *o*, on the psychrometric chart (Figure 2.25f). The mixture air state, *m*, can be determined with reference to the supply air flow rate (V_s) and the known fresh air flow rate (V_{fa}). Assuming the mixing of the outdoor air and the return air from the room is an adiabatic mixing process:

$$w_m = \frac{V_s - V_{fa}}{V_s} w_r + \frac{V_{fa}}{V_s} w_o \tag{2.78}$$

The state point *m* lies on the straight line joining up state points *o* and *r*, and having evaluated w_m, it can be located on the psychrometric chart (Figure 2.25f).

All state points of the conventional all air cycle have now been determined. The sensible ($q_{cc,s}$) and total ($q_{cc,t}$) cooling output required of the cooling and dehumidifying coil can also be determined as follows:

$$q_{cc,s} = \rho_a V_s Cp_a (t_m - t_l) \tag{2.79}$$

$$q_{cc,t} = \rho_a V_s (h_m - h_l) \tag{2.80}$$

If the fresh air is already pre-treated centrally when it is supplied to the air-handling unit (see Section 4.4.2), the supply air state of the fresh air should replace state point o in the above equations.

2.7 Thermal comfort

Since most air-conditioning systems are for providing occupants in buildings with a comfortable indoor environment, an understanding of the conditions in an indoor environment that would be perceived by the occupants as comfortable is essential to air-conditioning system design. However, a detailed treatment of the topic involves a considerable amount of deliberations, but this is considered not crucial to the purpose of this book. Therefore, only the essential concepts and the key parameters used to define environmental conditions for thermal comfort for adoption as the design indoor condition will be covered here. Interested readers may consult the ASHRAE Handbook [1] and references on this specific topic [6] for more detailed coverage.

In this section, an overview of heat balance on a human body and the factors that affect the heat exchanges between a human body and the surrounding indoor environment will be given, followed by an introduction to the thermal comfort envelop of indoor conditions defined by ASHRAE which provides guidance on selection of design indoor environment for air-conditioned spaces.

2.7.1 Heat exchanges between the human body and the environment

A human body will continue to output energy, which is derived from the food consumed, to sustain various activities of the body, including basic activities like heart beats, breathing, digestion, thinking, etc., and doing mechanical work. The rate of energy output of a human body is called metabolic rate, M, which will vary with the level of activity carried out by the person. The metabolic rate of a seated, quiet person is about 58.1W per m^2 skin surface area, which is taken as the reference value for one unit of metabolic energy output rate, called one met. When a man is doing physical exercises, his metabolic rate may rise to 4 met or even higher.

The rate of metabolic energy output, M, deducted by the rate of work done, W, is the net rate of heat to be dissipated to keep balance of energy in the body, as depicted by the following equation:

$$M - W = q_{sk} + q_{res} + S$$

$$M - W = C + R + E_{sk} + q_{res} + S \tag{2.81}$$

Where

M = Metabolic rate, W/m^2
W = Rate of mechanical work done, W/m^2
q_{sk} = Total rate of heat loss through skin, W/m^2 ($= C + R + E_{sk}$)
q_{res} = Total rate of heat loss through respiration, W/m^2
C = Rate of sensible heat loss from skin by convection, W/m^2
R = Rate of sensible heat loss from skin by radiation, W/m^2
E_{sk} = Rate of evaporative heat loss from skin, W/m^2
S = Rate of heat storage, W/m^2

As shown in Equation (2.81), heat dissipation from a human body is through the skin, q_{sk}, and respiration, q_{res}. Heat may be loss to the surrounding environment from the skin by convection, C, radiation, R, and by evaporation of moisture over the skin, E_{sk}. The convective and radiant heat losses are sensible heat losses, which will take place under all conditions (Figure 2.26).

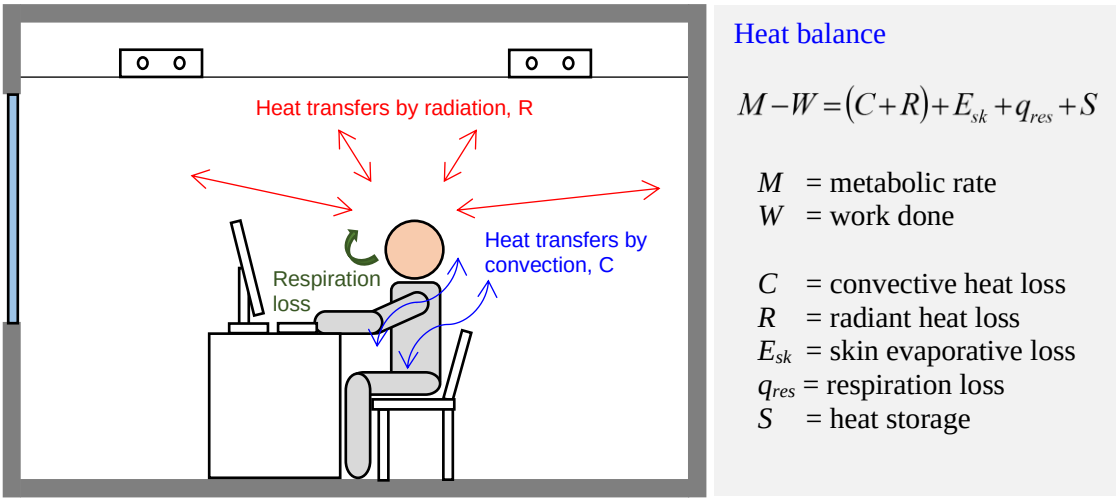

Figure 2.26 Heat exchanges between the human body and the environment

When metabolic rate is high, which requires the heat loss rate to be elevated at the same time, sweating followed by evaporation of the sweat is a physiological regulation for stepping up heat loss rate. Respiration loss, which includes both sensible and latent heat losses, will increase with breathing rate which, in turn, is regulated to match with the intensity of the metabolic rate.

If there is imbalance between the required net heat dissipation rate and the rate actually achieved, there will be heat storage in the body leading to a rise in body temperature or, in the case of a net loss, regulatory actions like quivers will happen to quickly raise heat to compensate. Neither would be regarded as a comfortable state.

A person will feel comfortable provided that his/her:

- Body temperature is held relatively stable ($S = 0$).
- Skin moisture is low, i.e. no sweating (E_{sk} is limited to diffusion of water vapour from skin to air without evaporation of sweat).
- Physiological effort of regulation is minimized, i.e. no sweating or panting for boosting heat dissipation rate (q_{res} is normal and stable).

2.7.2 Factors affecting thermal comfort sensation

The convective (C) and the radiant (R) heat losses from the skin can be expressed as:

$$C = f_{cl} h_c (t_{cl} - t_a) \qquad (2.82)$$

$$R = f_{cl} h_r (t_{cl} - \bar{t}_r) \tag{2.83}$$

Where

f_{cl} = Clothing area factor
h_c = Convective heat transfer coefficient, W/m^2-K
h_r = Linear radiant heat transfer coefficient, W/m^2-K
t_{cl} = Mean temperature of clothing surface, ^{o}C
t_a = Air temperature, ^{o}C
$\bar{t}_r$ = Mean radiant temperature of enclosing surfaces, ^{o}C

In Equation (2.83), the radiant heat loss is expressed as proportional to the difference between the cloth surface temperature and the mean radiant temperature of the surfaces enclosing the space. However, in theory, this rate of radiation heat loss is proportion to the fourth power of these temperatures in degree Kelvin (i.e. in absolute temperature). How a difference in the fourth power of two variables can be approximated by the difference of the two variables is explained in deriving Equation (3.45) in Chapter 3.

Adding Equations (2.82) & (2.83),

$$C + R = f_{cl}[(h_c + h_r)t_{cl} - (h_c t_a + h_r \bar{t}_r)] \tag{2.84}$$

Let

$$h = h_c + h_r \tag{2.85}$$

Equation (2.84) may be reorganized into:

$$C + R = f_{cl} h \cdot \left(t_{cl} - \frac{h_c t_a + h_r \bar{t}_r}{h}\right)$$

$$C + R = f_{cl} h \cdot (t_{cl} - t_o) \tag{2.86}$$

Where t_o, as defined below, is called operative temperature, which represents the combined effect of the air temperature, t_a, and the mean radiant temperature, $\bar{t}_r$.

$$t_o = \frac{h_c t_a + h_r \bar{t}_r}{h} \tag{2.87}$$

Note that the heat loss from the clothing surface (C+R), as given by Equation (2.86), must be sustained by the same rate of heat transmission from the skin surface through the thickness of the clothing to its surface, which can be described by:

$$C + R = \frac{t_{sk} - t_{cl}}{R_{cl}} \tag{2.88}$$

Where R_{cl} is the thermal resistance of clothing, (m^{2}K)/W.

Similar to defining met as the unit for metabolic rate at different activity levels, clo is defined as the unit for clothing insulation, and 1 clo is equivalent to 0.155 (m^2K)/W, the total clothing insulation of the business suit worn by men in winter. To facilitate calculation of the total clothing insulation of an ensemble of garments worn by a person, the clo values for various types of garment are given in the ASHRAE Handbook [1], which may be summed to yield the total clothing insulation value.

Regarding the evaporative loss from the skin, E_{sk}, the involved moisture transfer is driven by a vapour pressure differential across the skin surface and the ambient air, which implies that the ambient air humidity and clothing resistance to vapour transfer are factors that affect heat loss through this mechanism. Similarly, the temperature and humidity of the ambient air are factors that affect the rate of heat loss through respiration.

In summary, the factors that affect thermal comfort sensation of building occupants include:

- The activity level of occupants in the space.
- The thermal resistance of clothing worn by the occupants.
- The temperature and humidity of the air in the space.
- The temperature of surfaces enclosing the space.
- Other factors, such as air movement, which affect the heat and moisture transfer coefficients.

2.7.3 ASHRAE comfort envelops

The factors that can affect the heat and moisture exchanges between the human body and the environment and, in turn, the comfort sensation of occupants of buildings have been identified in the preceding sub-section. It is important to also note that the effect of varying one factor may be compensated by varying, at the same time, another factor. In other words, trade-offs can be made, within limits, among the factors without affecting the thermal comfort sensation of people.

For example, as shown in Equation (2.86), so long as the operative temperature, t_o, is kept at the same value, the sum of the convective and radiant ($C+R$) heat losses from the human body will remain unchanged. According to Equation (2.87), the same t_o value can be achieved if the indoor temperature, t_a, is raised and, at the same time, the mean radiant temperature, $\bar{t}_r$, is lowered by a commensurate amount. Furthermore, a dryer indoor environment will promote a higher rate of latent heat loss through skin moisture diffusion and respiration, which will allow a slightly higher indoor temperature to be kept without affecting the thermal comfort sensation of the occupants.

Figure 2.27 shows the ASHRAE Comfort Zone Chart, which provides information about the range of indoor thermal environment, defined by the combination of the operative temperature and relative humidity of the indoor air, that would be found acceptable to 80% of building occupants who are doing sedentary activity. There are two overlapping regions of the indoor thermal environment in this chart, pertaining to two clothing insulation values that apply to ensembles of garments typically worn by occupants in winter (clo = 1) and summer (clo = 0.5).

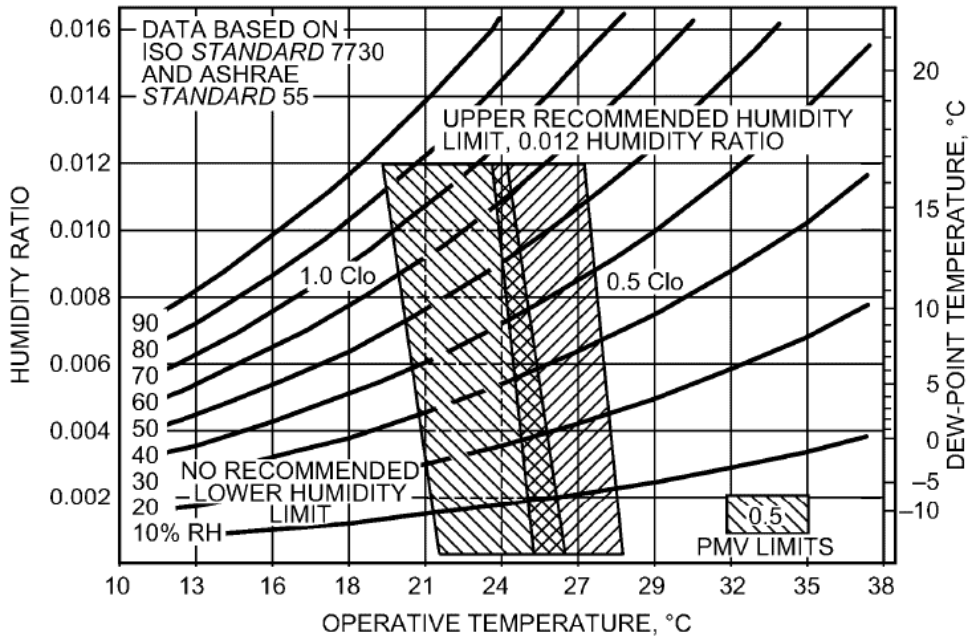

Note: Acceptable ranges of operative temperature and humidity with air speed ≤ 0.2 m/s for people wearing 1.0 and 0.5 clo clothing during primarily sedentary activity (≤ 1.1 met).

Figure 2.27 ASHRAE summer and winter comfort zones

Rather than the thermal comfort zone as shown in Figure 2.27, air-conditioning system designers may refer to air-conditioning design handbooks, such as the ASHRAE Handbook – Applications [7] or the CIBSE Guide A [8], for recommendations on design indoor thermal environments for air-conditioned spaces for difference occupation conditions.

References

[1] ASHRAE Handbook, Fundamentals, American Society of Heating, Refrigerating and Air-Conditioning Engineers, Inc., Atlanta, 2017.

[2] CIBSE Guide C – Reference Data, The Chartered Institution of Building Services Engineers, London, 2007.

[3] McQuiston FC, Parker JD & Spitler JD, Heating, Ventilating and Air Conditioning: Analysis and Design, 6th Ed., John Wiley & Sons, New York, 2005.

[4] Doebelin E, Measurement Systems: Application and Design, 5th Ed., McGraw-Hill Series in Mechanical and Industrial Engineering, 2004.

[5] Underwood CP, Yik FWH, Modelling Methods for Energy in Buildings, Blackwell Publishing Ltd., Oxford, 2004.

[6] ASHRAE Standard 55 -- Thermal Environmental Conditions for Human Occupancy, American Society of Heating, Refrigerating and Air-Conditioning Engineers, Inc., Atlanta, 2017.

[7] ASHRAE Handbook, Applications, American Society of Heating, Refrigerating and Air-Conditioning Engineers, Inc., Atlanta, 2015.

[8] CIBSE Guide A – Environmental Design, The Chartered Institution of Building Services Engineers, London, 2015.

Chapter 3 Building Heat Transfer and Cooling Load Calculation

3.1 Heat transfer fundamentals

3.1.1 Cooling load and heat transfers in buildings

As mentioned in Chapter 1, buildings provide occupants with shelter from adverse outdoor environments. With heating, ventilation, and air-conditioning (HVAC), the indoor thermal environment can be maintained steadily at a desirable condition, which may differ drastically from the outdoor condition. To ensure this can be achieved throughout the year, the HVAC system must have sufficient heating and cooling capacity to cope with the likely peak demands, and be able to regulate, from time to time, its output to match closely with any changes in the rate of heating or cooling required to allow a steady indoor condition to be maintained.

Estimation of the design heating load of a building is much simpler than estimation of the design cooling load. For design heating load estimation, heat gains from solar radiation and various internal sources may be ignored and, generally, steady-state heat transfer calculation would suffice. Design cooling load estimation, however, has to account for influences of the outdoor conditions and the use conditions within the air-conditioned spaces, and a dynamic analysis is needed for accurate results. Here, we would first deal with design cooling load estimation for determining the cooling capacity required of an air-conditioning system. The method for estimating heating load will be covered in Chapter 10.

The cooling load of an indoor space is the required rate of cooling for the air in the space for keeping the air steadily at its design state, which is typically expressed in terms of the desired values of the air temperature and relative humidity. For a building comprising multiple air-conditioned spaces, the design cooling load of the building, often referred to as the 'block cooling load', equals the cooling output required of the air-conditioning system serving the building to keep all the air-conditioned spaces at their respective design indoor conditions simultaneously, when the spaces are subject to the design outdoor conditions and their respective design usage conditions.

The cooling load of a space arises from heat gains of the space, which may be convective heat gains that will become cooling load instantaneously, or radiant heat gains that have occurred, from over ten hours before until the present moment, all contributing to the present cooling load. The heat gains of a space include the heat emitted by sources inside the space and the heat transported from the outdoors into the indoor spaces, through direct air transport or any one or combination of the possible modes of heat transfer, namely conduction, convection and radiation.

The distinction between heat gain, cooling load and heat extraction rate will be discussed in greater detail when we formally introduce the methods for cooling load calculation later in this chapter. Before that, methods for calculation of heat transfer rates under different modes of heat transfer are discussed, focusing on heat transfers that may take place in buildings, to provide a foundation for cooling and heating load calculation. An introduction to how the design outdoor and indoor conditions are defined is given together with the values of the design data applicable to Hong Kong,

which will appear within this chapter, and more comprehensively in Appendix B. Besides explaining how to carry out design cooling load estimation manually, the contents of this chapter are intended to enable readers to better understand the methods used in computer programs for cooling load estimation or detailed building energy simulation.

3.1.2 Dynamic conduction heat transfer in a wall or slab

Predicting the conduction heat transfers through the walls, roofs, partitions, and floor slabs of a building requires solution of the governing equation for conduction heat transfer, which will be derived below from first principle, based on some simplifying assumptions. As will also be discussed below, different solution schemes may be used to solve the governing equation. The algorithm for implementing the adopted solution scheme typically occupies the core of a building cooling load calculation program.

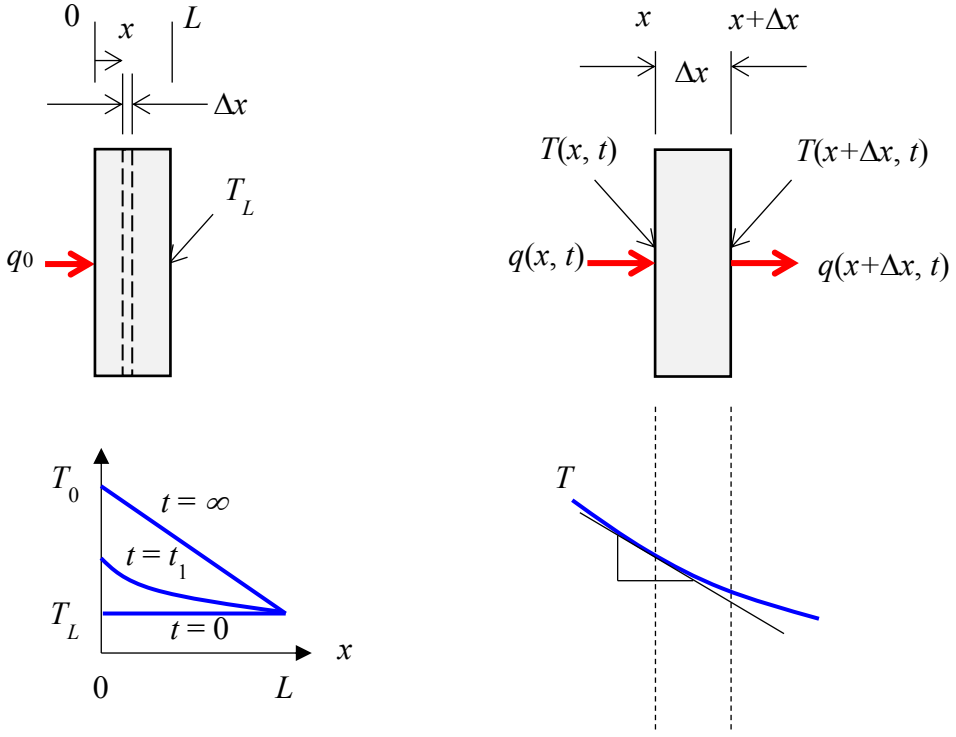

a) Wall of homogeneous material b) An elemental section in the wall

Figure 3.1 Heat conduction through a wall

Consider an opaque wall, as shown in Figure 3.1a. The wall is made of a slab of homogeneous material of constant heat transport properties, and has a uniform thickness, L, in the x-direction, which is much smaller than the width and height of the wall in the y and z-directions. Furthermore, the condition of the slab is uniform on every cross-sectional plane in the y-z directions throughout its thickness. These assumptions justify the use of a one-dimensional model. Furthermore, it has, initially, i.e. at time $t = 0$, a uniform temperature T_L across its thickness:

$$T(x, t) = T_L \quad \text{for } x = 0 \text{ to } L \text{ at time } t = 0 \tag{3.1}$$

Where $T(x, t)$ denotes temperature of the slab at position x and time t.

Assume that, starting from $t = 0$, heat flows into the surface of the wall at the side $x = 0$ at a steady rate of q_0, while the temperature of the surface at the side $x = L$, is maintained steadily at T_L,

$$\begin{cases} q(0,t) = q_0 \\ T(L,t) = T_L \end{cases} \quad \text{for } t = 0 \text{ to } t \tag{3.2}$$

Where $q(x, t)$ denotes the conduction heat flux through the cross-sectional plane in the slab at position x and at time t.

As a result of the steady rate of heat injection at the side $x = 0$, the temperature at this side of the wall, $T(0, t)$, will start to rise and become higher than the temperature of the adjacent layer of material (Figure 3.1a). This temperature difference will cause heat to flow by conduction to the adjacent layer thus bringing up its temperature. In this way, heat will flow, by conduction from one layer of material to the next, and reach the other side at $x = L$. When a steady state is reached, with $T(0, \infty)$ assuming a steady value of T_0, the temperature distribution across the thickness of the wall, $T(x, \infty)$, will become a straight line while the heat transfer rate, $q(x, \infty)$, will be the same at both surfaces as well as at all intermediate planes inside the wall (see further elaborations in the following section on steady-state conduction and convection).

A rise in temperature of the material means that the material has gained energy and the energy is stored inside the material. The amount of heat that a material can store per unit volume for each degree rise in temperature is dependent on its density, ρ, and specific heat, C. For an intermediate layer of material in the wall, the rise in its temperature, in turn, is dependent on how much heat can flow from and to the adjacent layers per unit time, which is proportional to the conductivity, k, of the material.

Given that major building materials, e.g. brick and concrete, have a substantial thermal mass (product of mass and specific heat, mC) and relatively low thermal conductivity (k), conduction heat transfer in a building takes time, and thus needs to be treated as a dynamic process. A dynamic conduction heat transfer model can be established, from first principle, to allow us to determine the conduction heat transfer rates from outside into a building through its external walls and roof.

Consider an elemental layer of material within the wall at position x, with a thickness Δx (Figure 3.1b). According to the Fourier's law of conduction, as shown in the following equation, the rate of conduction heat transfer through a cross-sectional plane in a material is proportional to the temperature gradient across the plane:

$$q(x,t) = -k\frac{\partial T(x,t)}{\partial x} \tag{3.3}$$

Where

k is the thermal conductivity of the material, W/m-K

$\partial T(x, t)/\partial x$ is the temperature gradient at position x and time t, K/m

The negative sign in Equation (3.3) results from the thermodynamic principle that heat flows only from a high to a low temperature region, in conjunction with the convention adopted in our analysis, which regards the rate of change of temperature w.r.t. x ($\partial T/\partial x$) as positive if T is increasing in the x direction, and heat flow (q) as positive if it is in the x direction.

We can relate the conduction heat flow rate at $x + \Delta x$, denoted by $q(x + \Delta x, t)$, to the conduction heat flow rate $q(x, t)$ at x as follows:

$$q(x + \Delta x, t) = q(x, t) + \frac{\partial q(x,t)}{\partial x}\Delta x \tag{3.4}$$

If the rate of heat flowing into, $q(x, t)$, and out of, $q(x+\Delta x, t)$, the elemental wall layer are not equal, the difference between them will lead to heat storage in, or loss form, the elemental wall layer, resulting in a rise or drop in its temperature at a rate given by:

$$q(x, t) - q(x + \Delta x, t) = \rho C \frac{\partial T(x,t)}{\partial t}\Delta x \tag{3.5}$$

Where

ρ = density of the material, kg/m^3
C = specific heat of the material, J/kg-K

From Equations (3.4) & (3.5), we can write:

$$\rho C \frac{\partial T(x,t)}{\partial t} = -\frac{\partial q(x,t)}{\partial x} \tag{3.6}$$

Substituting $q(x, t)$ given in Equation (3.3) into the above,

$$\rho C \frac{\partial T(x,t)}{\partial t} = -\frac{\partial}{\partial x}\left(-k \frac{\partial T(x,t)}{\partial x}\right)$$

$$\rho C \frac{\partial T(x,t)}{\partial t} = k \frac{\partial^2 T(x,t)}{\partial x^2}$$

$$\frac{\partial T(x,t)}{\partial t} = \alpha \frac{\partial^2 T(x,t)}{\partial x^2} \tag{3.7}$$

Where $\alpha = k/\rho C$ is the thermal diffusivity of the material, m^2/s.

Equation (3.7) is the governing partial differential equation for one-dimensional transient conduction heat transfer through a slab of homogeneous material. It can be solved when the initial condition ($T(x, 0)$) and the boundary conditions (e.g. $q(0, t)$, $q(L, t)$, $T(0, t)$ and $T(L, t)$, etc.) are defined. The solution can allow us to predict the temperature in the material at any position x and time t ($T(x, t)$), and from this the heat transfer rate ($q(x, t)$), using Equation (3.3).

For a composite wall comprising several layers of different materials, each layer may be modelled by the governing equation and the models are coupled by the boundary conditions that apply to the interface of each pair of adjoining materials, including the same temperature and conduction heat transfer rate that apply to each of the two surfaces that are in contact. For the two exposed surfaces of a wall, the boundary conditions are governed by the radiant and convective heat transfers from or to the environment to which the surfaces are exposed. Further elaboration on this issue will be given in the following sub-section, after a brief discussion on the methods for solving the governing equation.

Different methods may be used to solve the governing partial differential equation. Laplace transformation can be used to first reduce the partial differential equation into an ordination differential equation, which can be solved more easily. The type of solution that represents the impulse response of the wall or slab is particularly useful as it may be used to obtain the solution to any kinds of inputs, such as surface temperatures at different time steps of an arbitrary pattern.

The solution for boundary conditions that are triangular pulse functions provides the basis for the response factor method [1]. The response factor model (RFM) for a wall [2] is:

$$\begin{Bmatrix} q_0(n) \\ q_1(n) \end{Bmatrix} = \sum_{j=0}^{\infty} \begin{bmatrix} X(j) & -Y(j) \\ Y(j) & -Z(j) \end{bmatrix} \begin{Bmatrix} T_0(n-j) \\ T_1(n-j) \end{Bmatrix} \tag{3.8}$$

Where

$q_0(n)$ & $q_1(n)$ = the heat fluxes at the two surfaces of the wall at the current time step, n.

$X(j)$, $Y(j)$ & $Z(j)$ = the response factors of the wall to surface temperatures occurring at j time steps before the current time step, n.

$T_0(n-j)$ & $T_1(n-j)$ = the temperatures at the two surfaces of the wall at j time steps before the current time step, n.

The transfer function method, which can yield models that are more computationally efficient than the RFMs, is based on z-transformation in lieu of Laplace transformation. The transfer function model (TFM) for the response of a system due to inputs at the current and past time steps is given by:

$$\begin{aligned} g(n) &= a_0 f(n) + a_1 f(n-1) + a_2 f(n-2) + a_3 f(n-3) + \cdots \\ &-[b_1 g(n-1) + b_2 g(n-2) + b_3 g(n-3) + \cdots] \end{aligned} \tag{3.9}$$

Where

$g(n)$ is the response of the system at the current time step, n.

$f(n)$ is the input to the system at the current time step, n.

a_0, a_1, a_2, … and b_1, b_2, … are the weighting factors for the inputs and system responses at j time steps before the current time step, n, where $j = 0, 1, 2, \ldots$.

Both the RFM and TFM are suitable for implementation by using a computer but would be rather burdensome if it needs to be handled manually. These methods, in conjunction with the heat balance method [1], is the foundation underpinning the several generations of standard, simplified manual cooling load calculation methods developed by ASHRAE over the years. These include the cooling load temperature difference / solar cooling load / cooling load factor (CLTD/SCL/CLF) method, the total equivalent temperature difference / time averaging (TETD/TA) method, and the latest radiant time series (RTS) method.

The admittance method that CIBSE adopts [3, 4] is based directly on the Laplace transform of the governing equation and continues to deal with the problem in the frequency domain, including representing the boundary conditions by sinusoidal functions, and the solution is finally obtained based on the transfer function in the frequency domain. Of course, numerical methods, such as finite difference method (FDM), can be used to solve the differential equation for a given set of initial and boundary conditions.

The RTS method will be discussed in detail in Section 3.4. For more detailed descriptions on the other methods, interested readers may refer to [1-5].

3.1.3 Steady state conduction and convection

Whereas the solution for dynamic conduction heat transfer through a wall is complicated, the steady state solution is much simpler. The steady state solution is useful as it may be used to model members of the building fabric that have small thermal mass, such as glass panes of windows and skylights. In fact, the steady state solution, which represents the asymptotic condition, is also useful to the dynamic solutions for massive walls and slabs (see [5] and Section 3.4).

Continuing with the wall described above and, under the steady state ($t \to \infty$; see Figure 3.1a), there will be no more change in the temperature in the wall with time and thus the RHS of Equation (3.5) equals zero.

$$q(x,t) - q(x+\Delta x,t) = \rho C \frac{\partial T(x,t)}{\partial t} \Delta x = 0$$

In which case,

$$q(x,t) = q(x+\Delta x,t)$$

Referring to the Fourier's law of conduction (Equation (3.3)), the above result implies that the temperature gradient is the same at all intermediate sections in the wall, which is made of a homogeneous material (k is a constant throughout the wall) and thus the temperature profile is a straight line. Hence, Equation (3.3) may be re-written as:

$$q = -k \frac{dT}{dx} \tag{3.10}$$

Or, with reference to the wall shown in Figure 3.1,

$$q = k\frac{T_0 - T_L}{L} \tag{3.11}$$

In addition to a known surface temperature or heat flux, a common type of boundary condition of a wall or slab is defined through specifying the condition of the air to which the wall or slab surface is exposed. Assume that the wall shown in Figure 3.2 is exposed to air at both sides, and the air temperature at the side where $x = 0$ is T_{a0}, and that at the side where $x = L$ is T_{aL}.

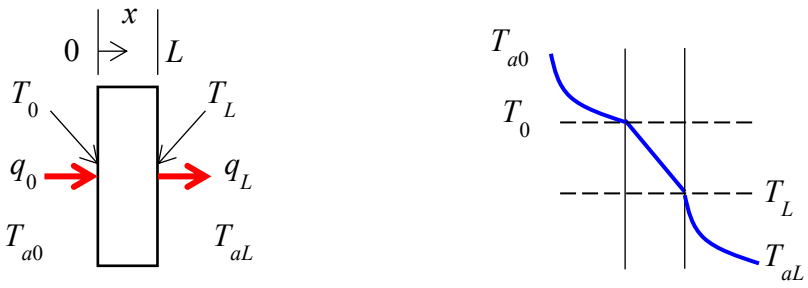

Figure 3.2 Steady-state conduction and convection heat transfers at a wall

If the air temperature T_{a0} is higher than T_0, the surface temperature of the wall at the side where $x = 0$, there will be convective heat transfer from the air to the surface, given by Equation (3.12), which is called the Newton's law of cooling:

$$q_0 = h_{c0}(T_{a0} - T_0) \tag{3.12}$$

Where h_{c0} is the convective heat transfer coefficient for the surface at $x = 0$, W/m^2-K.

In order to get heat flow in the same direction at the other surface, the surface temperature of the wall at the side where $x = L$, T_L, is assumed to be higher than T_{aL}, such that there will be convective heat transfer from the surface to the air, given by:

$$q_L = h_{cL}(T_L - T_{aL}) \tag{3.13}$$

Where h_{cL} is the convective heat transfer coefficient for the surface at $x = L$, W/m^{2}K.

In the steady state,

$$q_0 = q = q_L \tag{3.14}$$

Where q is the conduction heat transfer rate through the wall, W/m^2.

Equations (3.11), (3.12) & (3.13) may be re-arranged to as follows:

$$q_0 = \frac{T_{a0} - T_0}{1/h_{c0}} \tag{3.15}$$

$$q = \frac{T_0 - T_L}{L/k} \tag{3.16}$$

$$q_L = \frac{T_L - T_{aL}}{1/h_{cL}} \tag{3.17}$$

The equations above resemble the Ohm's law in electrical engineering ($I = V/R$) in that the temperature difference term at the RHS may be regarded as the potential difference that drives heat flow, and the denominator term as the resistance to heat flow, or simply thermal resistance. Under steady state condition, the above three heat transfer rates are equal (Equation (3.14)).

Reorganizing Equations (3.15) to (3.17) to as follows:

$$q\frac{1}{h_{c0}} = T_{a0} - T_0$$

$$q\frac{L}{k} = T_0 - T_L$$

$$q\frac{1}{h_{cL}} = T_L - T_{aL}$$

Adding the above three equations yields:

$$q\left(\frac{1}{h_{c0}} + \frac{L}{k} + \frac{1}{h_{cL}}\right) = T_{a0} - T_0 + T_0 - T_L + T_L - T_{aL} = T_{a0} - T_{aL}$$

$$q = \frac{T_{a0} - T_{aL}}{\frac{1}{h_{c0}} + \frac{L}{k} + \frac{1}{h_{cL}}} \tag{3.18}$$

Equation (3.18) can be re-written as:

$$q = U(T_{a0} - T_{al}) \tag{3.19}$$

Where U is called the overall heat transfer coefficient, or simply U-value, W/m^2-K, given by:

$$U = \frac{1}{\frac{1}{h_{c0}} + \frac{L}{k} + \frac{1}{h_{cL}}} \tag{3.20}$$

As can be seen from Equation (3.20), U can be calculated from the reciprocal of the sum of the thermal resistances of the surfaces and the wall material, which are in series.

For a composite wall comprising N layers of different materials of thermal conductivities k_1, k_2, …, k_N and thicknesses l_1, l_2, …, l_N, it can be shown that the U-value of this wall can be determined using:

$$U = \frac{1}{\frac{1}{h_{c0}} + \sum_{i=1}^{N}\left(\frac{L_i}{k_i}\right) + \frac{1}{h_{cL}}} \tag{3.21}$$

The term at the denominator at the RHS denotes the sum of thermal resistances of the surfaces and the material layers that appear in series. When the U-value is determined, the steady state rate of heat transfer through the wall when subjected to different ambient air temperatures at the two sides can be determined using Equation (3.19).

3.1.4 Radiant heat transfer

For refreshing readers on the subject, a very brief account of the key concepts of radiation heat transfer is given here. Detailed treatment on the subject can be found in various heat transfer textbooks (e.g. [6]).

Thermal radiation is a kind of electromagnetic wave: it can travel through vacuum; it travels along a straight line at the speed of light (c); and it may appear in different frequencies (f), and hence different wavelengths (λ), governed by the relation $c = f\lambda$. Any substance at a temperature above absolute zero emits thermal radiation, at a rate proportional to the fourth power of its absolute temperature.

When thermal radiation strikes a surface, it may be absorbed, reflected, or transmitted (Figure 3.3). The fractions that will be absorbed, reflected, and transmitted are called, respectively, absorptivity (α), reflectivity (ρ) and transmissivity (τ), which are properties of the surface. Consequent upon their definitions given above,

$$\alpha + \rho + \tau = 1 \tag{3.22}$$

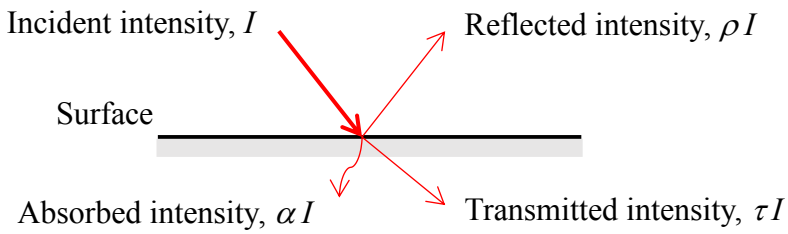

Figure 3.3 Interaction between a surface and the radiation incident upon the surface

A black body, by definition, absorbs all radiation, including light, incident upon it without any reflection or transmission, which explains for the name given to it. On the other hand, a black body emits radiation evenly in all directions, with intensity at different wavelengths varying according to a well-defined pattern, which, in turn, depends on the absolute temperature of the black body (Figure 3.4).

The rate of radiation emission of a black body at temperature T (in absolute temperature, K) is denoted by E_b (W/m^2), called the emissive power of the black body, and

$$E_b = \sigma T^4 \tag{3.23}$$

Where σ is the Stefan-Boltzmann constant (= 5.67x10^{-8} W/(m^2 K^4)).

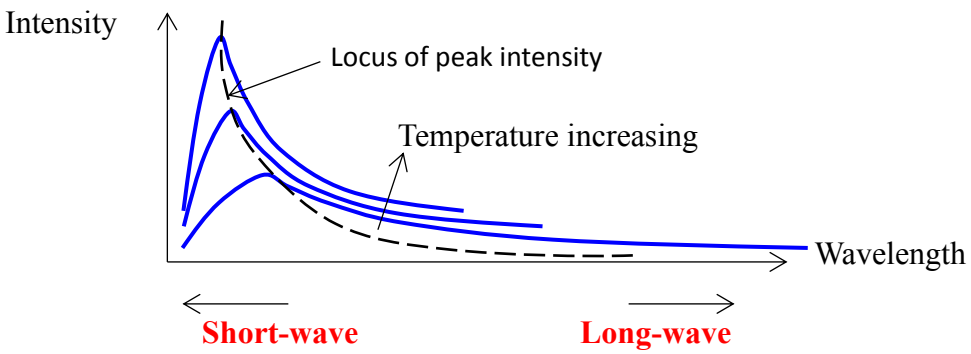

Figure 3.4 Distributions of intensity of radiation emitted by a black body

A gray body also emits radiation evenly in all directions but the intensity of radiation it emits is just a fraction of the intensity that a black body at the same temperature can emit. This fraction, ε, is called the emissivity of the gray body. Its emissive power (E, W/m^2), therefore, is:

$$E = \varepsilon\sigma T^4 \tag{3.24}$$

In radiation heat transfer calculations, wall and slab surfaces are often assumed to be gray opaque surfaces ($\tau = 0$). For this type of surfaces:

$$\alpha = \varepsilon \tag{3.25}$$

$$\rho = 1 - \varepsilon \tag{3.26}$$

The equality of the absorptivity and emissivity of a gray body is known as the Kirchhoff's Law. For two black surfaces (S_1 & S_2) that can "see" each other (Figure 3.5), they will exchange thermal radiation, resulting in a net radiant heat transfer from the surface at a higher temperature to that at a lower temperature at the rate of:

$$Q_{r1-2} = A_1 F_{12} \sigma T_1^4 - A_2 F_{21} \sigma T_2^4 \tag{3.27}$$

Where

$Q_{r1\text{-}2}$ is the net rate of radiant heat transfer from S_1 to S_2 (W)
A_1 & A_2 and T_1 & T_2 are the areas and absolute temperatures of S_1 & S_2
F_{12} is the fraction of radiation emitted by S_1 that can reach S_2
F_{21} is the fraction of radiation emitted by S_2 that can reach S_1

The factors F_{12} & F_{21} may be called shape factors, view factors, configuration factors or angle factors, and they are dependent solely on the geometric relationship of the pair of surfaces under concern. The value of shape factor may range from 0 (where a surface is hidden from the other) to 1 (where one surface cannot see itself and is completely enclosed by the other surface).

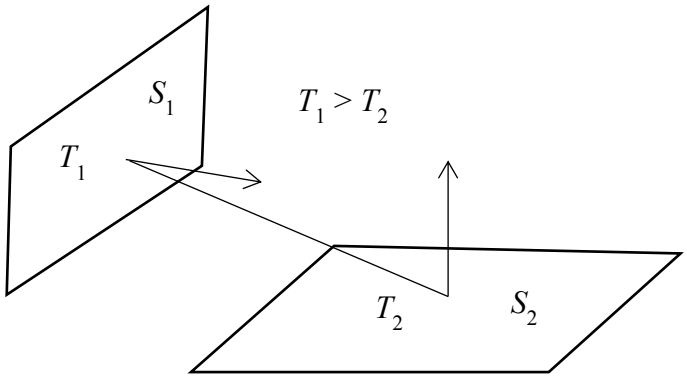

Figure 3.5 Two Surfaces Exchanging Thermal Radiation

Consider the special case where the temperatures of the two surfaces S_1 & S_2 are equal, i.e. $T_1 = T_2$. In this case, $Q_{r1\text{-}2}$ must be equal to zero. It follows from Equation (3.27) that the following reciprocity relation holds between a pair of surfaces:

$$A_1 F_{12} = A_2 F_{21} \tag{3.28}$$

Equation (3.27), therefore, becomes:

$$Q_{r1-2} = A_1 F_{12} \sigma (T_1^4 - T_2^4) \tag{3.29}$$

For a gray surface with emissivity ε, it will reflect radiation incident upon it as well as emit radiation at a rate dependent on its temperature (Figure 3.6). Let G be the intensity of radiant energy incident upon the gray surface (W/m^2), the total intensity of radiant energy leaving the surface, denoted by J, will be:

$$J = (1 - \varepsilon)G + \varepsilon E_b \tag{3.30}$$

Where G is called the irradiance on, and J the radiosity of, the surface (W/m^2).

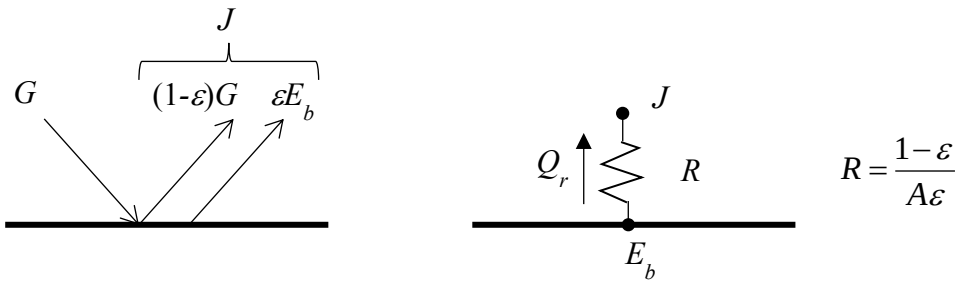

Figure 3.6 Radiation heat transfer upon a Gray Surface

From Equation (3.30), G may be expressed in terms of J as follows:

$$G = \frac{J - \varepsilon E_b}{1 - \varepsilon} \tag{3.31}$$

The net rate of radiant heat leaving a gray surface of area A, Q_r, is given by:

$$Q_r = A(J - G) \tag{3.32}$$

Substituting Equation (3.31) into the above, we get:

$$Q_r = A(J - \frac{J-\varepsilon E_b}{1-\varepsilon}) = A(\frac{J-\varepsilon J-J+\varepsilon E_b}{1-\varepsilon}) = A(\frac{\varepsilon(E_b-J)}{1-\varepsilon})$$

$$Q_r = \frac{E_b-J}{\frac{1-\varepsilon}{\varepsilon A}} \tag{3.33}$$

Equation (3.33) is in the form of the Ohm's law, and the denominator at the RHS may be regarded as the resistance to radiant heat leaving the surface.

For two gray surfaces (S_1 & S_2) that can see each other (Figure 3.5), the net rate of radiant heat transfer from S_1 to S_2 is given by:

$$Q_{r1-2} = A_1 J_1 F_{12} - A_2 J_2 F_{21} \tag{3.34}$$

Using the reciprocity relation (Equation (3.28)), Equation (3.34) becomes:

$$Q_{r1-2} = A_1 F_{12}(J_1 - J_2)$$

$$Q_{r1-2} = \frac{J_1-J_2}{\frac{1}{A_1 F_{12}}} \tag{3.35}$$

The net rate of radiant heat transfer between two gray surfaces S_1 & S_2, $Q_{r1\text{-}2}$, can be represented by a network model as shown in Figure 3.7. The two surfaces, however, can also exchange radiant heat with other surfaces. Therefore, the radiant heat transfer rates at the two surfaces (Q_{r1} & Q_{r2}) cannot be solved yet. The model will remain incomplete unless all surfaces that form an enclosed space are represented in the model. A complete model will then allow all the J's, and thus the Q_r's, to be solved.

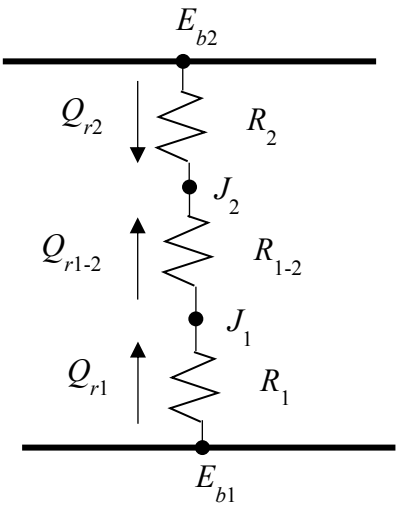

$$R_{1-2} = \frac{1}{A_1 F_{12}}$$

Figure 3.7 Equivalent circuit for radiation heat exchange between two gray surfaces

However, for the simplest case of two gray surfaces that form an enclosure, the radiant heat transfer rate between them can be solved. In this case (Figure 3.7),

$$Q_{r1} = Q_{r1-2} = -Q_{r2} \tag{3.36}$$

From Equation (3.33),

$$E_{b1} - J_1 = Q_{r1}\frac{1-\varepsilon_1}{\varepsilon_1 A_1}$$

$$J_1 = E_{b1} - Q_{r1}\frac{1-\varepsilon_1}{\varepsilon_1 A_1} \tag{3.37}$$

Similarly,

$$J_2 = E_{b2} - Q_{r2}\frac{1-\varepsilon_2}{\varepsilon_2 A_2} \tag{3.38}$$

From Equation (3.35),

$$J_1 - J_2 = Q_{r1-2}\frac{1}{A_1 F_{12}} \tag{3.39}$$

Substituting Equations (3.37) & (3.38) into (3.39), and taking note of Equation (3.36), we get:

$$E_{b1} - E_{b2} = Q_{r1-2}\left(\frac{1-\varepsilon_1}{\varepsilon_1 A_1} + \frac{1}{A_1 F_{12}} + \frac{1-\varepsilon_2}{\varepsilon_2 A_2}\right)$$

$$Q_{r1-2} = \frac{E_{b1}-E_{b2}}{\frac{1-\varepsilon_1}{\varepsilon_1 A_1}+\frac{1}{A_1 F_{12}}+\frac{1-\varepsilon_2}{\varepsilon_2 A_2}}$$

Using Equation (3.23),

$$Q_{r1-2} = \frac{\sigma(T_1^4-T_2^4)}{\frac{1-\varepsilon_1}{\varepsilon_1 A_1}+\frac{1}{A_1 F_{12}}+\frac{1-\varepsilon_2}{\varepsilon_2 A_2}} \tag{3.40}$$

For the special case where a flat surface (S_1) is exposed to an extremely large surface (S_2), we may assume F_{12} equals one, and the last term in the denominator equals zero due to the extremely large value of A_2. Equation (3.40) can then be simplified to:

$$Q_{r1-2} = A_1 \varepsilon_1 \sigma (T_1^4 - T_2^4) \tag{3.41}$$

Equation (3.41) is applicable to the (long wave) radiation heat transfer between a horizontal surface with the sky (Figure 3.8).

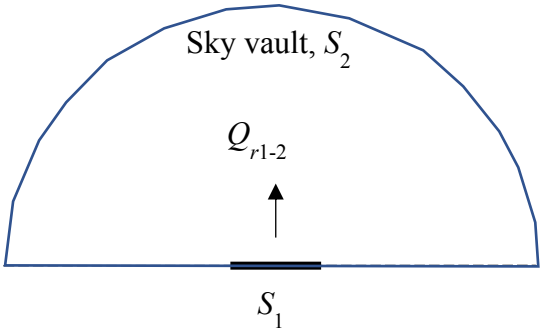

Figure 3.8 Radiation heat exchange between a horizontal surface and the sky vault

3.1.5 Short wave and long wave radiation

In calculating radiant heat transfer in buildings, distinction needs to be made between short-wave and long-wave radiation. As shown in Figure 3.4, the amount of energy emitted at short wavelength will increase with the temperature of the radiation source. Therefore, solar radiation and radiation emitted by some types of electric light would be mainly short-wave radiation.

For simplicity, however, the radiation emission from electric lights would simply be apportioned to indoor fabric surfaces. Hence, solar radiation will be the only short-wave radiation handled explicitly in cooling load calculations. Long-wave radiation to be accounted for includes, at the outdoor side, radiant heat exchanges of the external surfaces of the envelope with the sky and the ground, and, at the indoor side, among surfaces of building fabrics enclosing a space as well as between the surfaces and the internal sources.

3.2 Heat transfers into and out of an air-conditioned space

Any heat transported into an air-conditioned space is a heat gain of the space (Figure 3.9). The heat gains of a space include heat flows into the space from external sources and those from internal sources, and each source may incur radiant (R) or convective (C) heat gains, or both.

1. Heat gains from external sources:

    - Solar heat gains through fenestrations (transmitted: R; Absorbed: R+C)
    - Conduction heat gains through fenestrations (R+C)
    - Conduction heat gains through external and internal walls and slabs (R+C)
    - Infiltration (C)

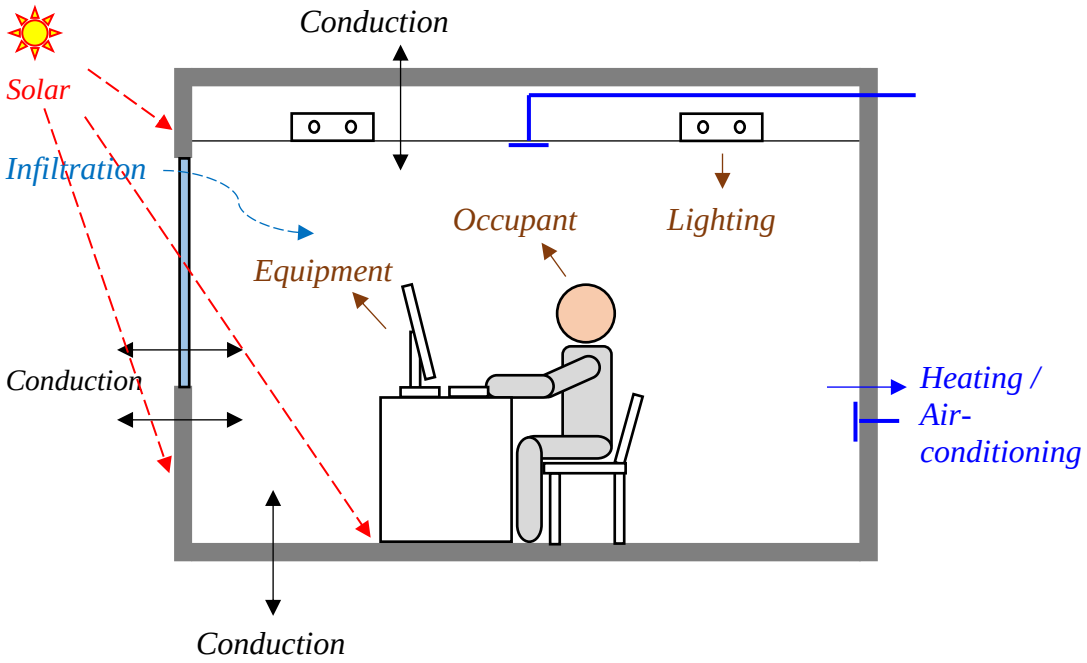

Figure 3.9 Heat gains of an air-conditioned space

2. Heat gains from internal sources:

- Lighting and appliances (R+C)
- Occupants (R+C)
- Materials at elevated temperatures brought into the space (R+C)

As will be discussed below, more elaborated methods are needed for determining heat gains through external walls and slabs, and fenestrations. Much simpler methods may be employed for determining the heat gains from internal sources.

3.2.1 Opaque wall or slab

3.2.1.1 Outer surface heat transfers

Figure 3.10 shows the heat transfers that may take place at the outer surface of an external wall, which include:

- Solar (short-wave) radiation incident upon and absorbed by the surface, q_{Sol}.
- Convection due to difference in temperature between the outdoor air and the wall surface, q_{co}.
- Net (long-wave) radiation gain, q_{ro}, from the surrounding surfaces (sky and ground).
- Conduction heat transfer into the wall, q_{wo}.

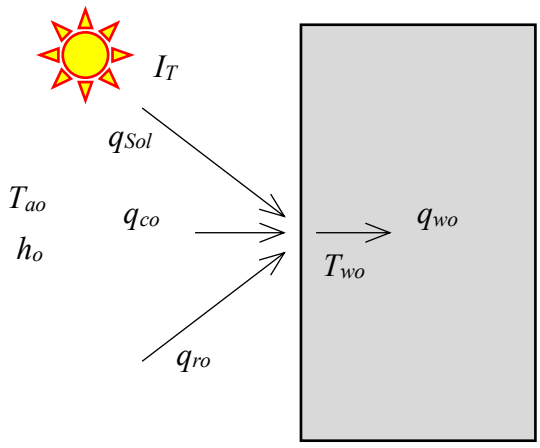

Figure 3.10 Heat transfers at the outer surface of an external wall

The solar (short-wave) radiation incident upon and absorbed by each unit area of the surface, q_{Sol}, is given by:

$$q_{Sol} = \alpha_o I_t \tag{3.42}$$

Where

α_o is the solar absorption coefficient; and
I_t is the total (beam and diffuse) intensity of solar radiation upon (normal to) the surface.

Convection due to difference in temperature between the outdoor air and the wall surface, q_{co}, is given by:

$$q_{co} = h_{co}(T_{ao} - T_{wo}) \tag{3.43}$$

Where

h_{co} is the external surface convection heat transfer coefficient; and
T_{ao} and T_{wo} are the outdoor air and wall external surface temperatures.

Applying Equation (3.41), the net gain in (long-wave) radiation (q_{ro}) from the surrounding surfaces may be expressed as:

$$q_{ro} = \varepsilon_o \sigma(T_{ao}^4 - T_{wo}^4) \tag{3.44}$$

Where ε_o is the emissivity of the external wall surface. Note that, for simplicity, all the surrounding surfaces (ground and sky included) are represented by a single fictitious black surface with extensive area, and the surface is assumed to be at the outdoor air temperature (T_{ao}).

The difference in the fourth power of the temperatures in Equation (3.44) is somewhat cumbersome to handle. It may be simplified by considering:

$$
\begin{aligned}
&a^4 - b^4 = (a^2 - b^2)(a^2 + b^2) \\
&= (a - b)(a + b)(a^2 + b^2) \\
&= (a - b)(a + b)(a^2 + 2ab + b^2 - 2ab) \\
&= (a - b)(a + b)[(a + b)^2 - 2ab] \\
&= (a - b)[(a + b)^3 - 2ab(a + b)] \\
&\approx (a - b)(8m^3 - 2m^2 \cdot 2m) \\
&\approx 4m^3(a - b)
\end{aligned}
$$

Where $a \approx b \approx m = (a + b) / 2$.

By denoting $h_{ro} = 4T_{avg}^3 \varepsilon_o \sigma$ where $T_{avg} = (T_{ao} + T_{wo})/2$, Equation (3.44) may be simplified to:

$$q_{ro} = h_{ro}(T_{ao} - T_{wo}) \tag{3.45}$$

And combined with Equation (3.43) to:

$$q_{cro} = h_o(T_{ao} - T_{wo}) \tag{3.46}$$

Where

h_{ro} is the radiant heat transfer coefficient;
q_{cro} is the total convection and long wave radiation heat transfer rate; and
h_o $(= h_{co} + h_{ro})$ is the combined convection and radiation heat transfer coefficient.

For vertical walls, the simplification above can give reasonably accurate estimation of the convection and long-wave radiation heat transfer at the external surface [1]. However, for a horizontal surface facing the sky, e.g. a roof, Equation (3.46) needs to be corrected for the radiant heat loss to the sky vault as follows:

$$q_{cro} = h_o(T_{ao} - T_{wo}) - \varepsilon_o \Delta R \tag{3.47}$$

Hence, Equation (3.47) can replace (3.46) by setting:

$\Delta R = 63 \text{W/m}^2$ for horizontal surface [1]
$\Delta R = 0$ for vertical surface

The heat transfers taking place at the external surface of a wall or slab can now be combined as:

$$q_o = q_{Sol} + q_{cro} \tag{3.48}$$

$$q_o = \alpha I_t + h_o(T_{ao} - T_{wo}) - \varepsilon_o \Delta R \tag{3.49}$$

Which can be re-arranged to:

$$q_o = h_o\left(\frac{\alpha I_t}{h_o} + T_{ao} - T_{wo} - \frac{\varepsilon_o \Delta R}{h_o}\right) \tag{3.50}$$

By defining sol-air temperature (T_{eo}) as:

$$T_{eo} = T_{ao} + \frac{\alpha I_t}{h_o} - \frac{\varepsilon_o \Delta R}{h_o} \tag{3.51}$$

Equation (3.50) can now be simplified to:

$$q_o = h_o(T_{eo} - T_{wo}) \tag{3.52}$$

Conduction heat transfer into the wall from the outer surface, q_{wo}, is given by:

$$q_{wo} = -k\frac{\partial T_w}{\partial x}\Big|_{x=0} \tag{3.53}$$

Where k is the thermal conductivity of the wall material.

From heat balance on the external surface:

$$q_o = q_{wo}$$

$$h_o(T_{eo} - T_{wo}) = -k\frac{\partial T_w}{\partial x}\Big|_{x=0} \tag{3.54}$$

Equation (3.54) is one of the needed boundary conditions for solving (the governing equation), Equation (3.7), for an external wall or roof.

3.2.1.2 Inner surface heat transfers

Heat transfers at the inner surface of an external wall include (Figure 3.11):

- Radiation from various sources, including transmitted solar radiation and radiation from other indoor sources, that is absorbed by the surface, q_{TS}.
- Convection from the surface to the indoor air due to the temperature difference between the wall surface and the indoor air, q_{ci}.
- Net (long wave) radiation loss from the surface to other surfaces enclosing the indoor space, q_{ri}.
- Conduction from within the wall toward the wall surface, q_{wi}.

The radiation that is absorbed by the surface, q_{TS}, includes solar radiation transmitted through windows and skylights, which falls onto the surfaces of building fabric elements enclosing an indoor space, such as walls, partitions, floor and ceiling; and radiation from various indoor sources, such as lighting, equipment, occupants, etc., which will also incident upon and absorbed by the surfaces. Assuming that the radiant energy from the sources is distributed evenly upon the building fabric element surfaces,

$$q_{TS} = \frac{Q_{TS,Tot}}{\sum_{k=1}^{N} A_k} \tag{3.55}$$

Where

$Q_{TS,\,Tot}$ is the total amount of transmitted solar radiation into the space and radiation from other sources.

A_k is the area at the indoor side of the k^{th} wall / slab enclosing the room.

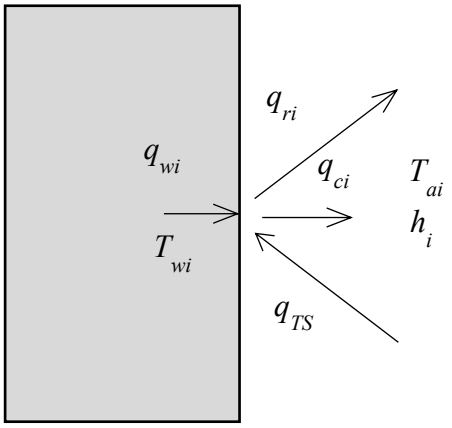

Figure 3.11 Heat transfers at the inner surface of an external wall

In practice, however, the transmitted solar radiation will be distributed to the floor surface only while other radiant heat gains, including the absorbed solar radiation that is transmitted into the space together with radiation from all other sources will be evenly distributed to the surfaces of the building fabric elements (usually with the window/skylight surfaces excluded) according to their surface areas. Furthermore, the energy apportioned to the surfaces is assumed to be absorbed completely by the surfaces without reflection and hence there would be no further stages of absorption and reflection.

Convection from the surface to the indoor air due to the temperature difference between the wall surface and the indoor air, q_{ci}, is given by:

$$q_{ci} = h_{ci}(T_{wi} - T_{ai}) \tag{3.56}$$

Where

h_{ci} = convection heat transfer coefficient
T_{wi} = internal surface temperature of wall
T_{ai} = indoor air temperature

Similar to the external surface, in determining the net (long wave) radiation loss from the surface to other surfaces enclosing the indoor space, q_{ri}, a fictitious surface at the room air temperature is used to represent all the surfaces enclosing the space, except the one under concern, and the net radiant heat transfer rate from the surface to the other surfaces is estimated using a linearized model as follows:

$$q_{ri} = h_{ri}(T_{wi} - T_{ai}) \tag{3.57}$$

Where

h_{ri} is the radiant heat transfer coefficient.

The combined convection and radiation heat transfer can be estimated by:

$$q_{cri} = h_i(T_{wi} - T_{ai}) \tag{3.58}$$

Where h_i $(= h_{ci} + h_{ri})$ is the combined convection and radiation heat transfer coefficient.

The net rate of heat transfer from the surface into the space, q_i, is given by:

$$q_i = h_i(T_{wi} - T_{ai}) - q_{TS} \tag{3.59}$$

By defining an environmental temperature, T_{ei}, as:

$$T_{ei} = T_{ai} + \frac{q_{TS}}{h_i} \tag{3.60}$$

Equation (3.59) can be re-written as:

$$q_i = h_i(T_{wi} - T_{ei}) \tag{3.61}$$

Conduction from within the wall toward the wall surface, q_{wi}, is given by:

$$q_{wi} = -k \frac{\partial T_w}{\partial x}\Big|_{x=L} = q_i \tag{3.62}$$

The equality of q_{wi} and q_i, as depicted by Equation (3.62), holds at all times because the surface of the wall has no thermal capacity and thus the rate of heat flowing towards it must be equal to the rate of heat flowing away from it. Equations (3.61) & (3.62) provide the next needed boundary condition for solving the governing equation for heat transfer through a wall or slab.

3.2.2 Fenestration

As for an external wall or slab discussed above, the same range of heat transfers will take place through a window or skylight. Additionally, a window or skylight will transmit a portion of the incident solar radiation and will absorb part of the solar energy as the radiation is penetrating the glass. The solar radiation transmitted into an air-conditioned space is often the dominant heat gain of the space. It, however, will not become cooling load until it is absorbed by the fabric or furniture surfaces inside the space, leading to a rise in the temperature of the surfaces, which, in turn, will cause heat to flow by convection to the indoor air.

Because the glass pane in a window or skylight is relatively thin, in the order of several mm and seldom exceeds 10 mm, its thermal mass is low and its resistance to conduction

heat transfer is small. These characteristics of glass pane allow the following simplifications to be made:

- Using a steady-state model will suffice for describing the state of, and the heat transfer through, a glass pane.
- The entire glass pane can be represented by a single temperature, T_G.

Note also that although a glass pane can transmit solar (short-wave) radiation, it can be regarded as opaque to long-wave radiation, which is the reason behind the greenhouse effect.

For simplicity, the heat transfer through a glass pane into an air-conditioned space due to incident solar radiation (called solar heat gain), and that due to indoor/ outdoor temperature difference (called conduction heat gain), are dealt with separately. However, similar to external walls and roofs, the long-wave radiation heat transfers at the external and internal surfaces of a glass pane are combined with the convection heat transfers at the respective surfaces.

Let the reflectivity, absorptivity and transmissivity of a glass pane be, respectively, ρ_G, α_G, and τ_G. When the glass pane is subject to an incident solar radiation of intensity I_T:

- The reflected portion ($\rho_G I_T$) does not enter the building and thus has no effect on the cooling load of the indoor space.
- The transmitted portion ($\tau_G I_T$) becomes part of the space heat gain but has no effect on the state of the glass pane.
- The absorbed portion ($\alpha_G I_T$) will affect the glazing temperature and thus the conduction, convection, and radiation heat transfer rates.

With reference to Figure 3.12, the heat transfer rate due to indoor/outdoor temperature difference, i.e. the conduction heat gain, q_{GT}, can be determined by using:

$$q_{GT} = U(T_{ao} - T_{ai}) \tag{3.63}$$

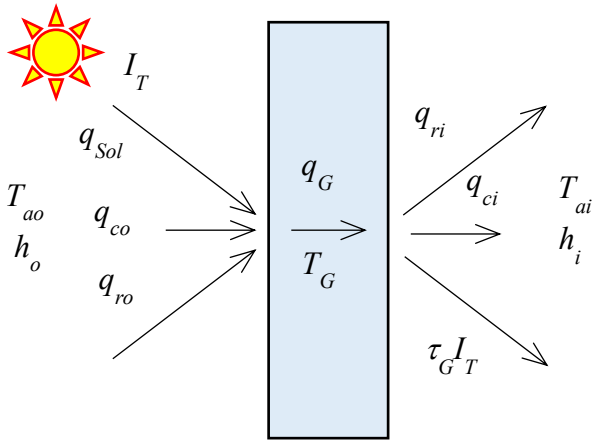

Figure 3.12 Heat transfers at a fenestration

Where, with thermal resistance of the glass pane ignored, U can be evaluated from:

$$U = \frac{1}{1/h_o + 1/h_i} = \frac{h_i h_o}{h_i + h_o} \tag{3.64}$$

With the use of combined convection and radiation heat transfer coefficients h_i and h_o, the long-wave radiation heat exchanges with the surrounding surfaces are accounted for.

As the conduction heat gain due to indoor/outdoor temperature difference has been dealt with separately, as shown above, the effect of the absorbed solar radiation can also be treated on its own right by assuming that both sides of the glass pane are exposed to the same ambient air temperature, T_a, and thus there will be no heat transfer due to an in/out temperature difference.

The absorbed solar radiation will raise the glass pane temperature, from T_a to T_G, and this temperature difference (value of T_a is arbitrary) will cause the absorbed heat to flow toward both the indoor and the outdoor sides.

The rate of heat flow toward the outdoor side, which will not affect the space, is:

$$q_{out} = h_o(T_G - T_a) \tag{3.65}$$

The rate of heat flow toward the indoor space is:

$$q_{in} = h_i(T_G - T_a) \tag{3.66}$$

Heat balance on the glass pane allows us to write:

$$\alpha_G I_t = h_i(T_G - T_a) + h_o(T_G - T_a)$$

$$\alpha_G I_t = (h_i + h_o)(T_G - T_a) \tag{3.67}$$

From Equations (3.66) & (3.67), q_{in}, the heat transfer rate that will contribute to the cooling load of the space can be expressed as:

$$q_{in} = \frac{h_i}{h_i + h_o} \alpha_G I_t \tag{3.68}$$

Using Equation (3.64),

$$q_{in} = \frac{U\alpha_G}{h_o} I_t \tag{3.69}$$

Therefore, the total rate of heat transfer through the fenestration into the indoor space is:

$$q_G = \left(\tau_G + \frac{U\alpha_G}{h_o}\right) I_t + U(T_{ao} - T_{ai}) \tag{3.70}$$

The term within the bracket in the first term at the RHS of the above equation is called the solar heat gain coefficient (*SHGC*). The *SHGC* of a double strength, heat absorbing (DSA) glass, $SHGC_{DSA}$, equals 0.87.

The Shading Coefficient (*SC*) of a fenestration is defined as:

$$SC = \frac{SHGC}{SHGC_{DSA}} = \frac{SHGC}{0.87} \tag{3.71}$$

With reference to the standard DSA glass, solar heat gain factor (*SHGF*), is defined as:

$$SHGF = SHGC_{DSA} \times I_t \tag{3.72}$$

To facilitate cooling load calculation, a series of *SHGFs* may be pre-evaluated for:

- A specific location on earth
- A range of standard exposure directions
- Different hours in a day

The solar heat gain from a particular glazing at a particular time can then be determined from the *SHGF* for the hour and the *SC* of the glazing:

$$q_{GSol} = SC \times SHGF \tag{3.73}$$

The method discussed above ignored the variation in the reflectance, transmittance, and absorptance of glazing with the incident angle (θ) of direct solar radiation (Figure 3.13). For more accurate calculation of solar heat gain through fenestration, solar heat gain coefficient that varies with the solar incident angle, $SHGC(\theta)$, would need to be used to calculate heat gain from direct radiation at a given incident angle. The heat gain due to diffuse radiation would need to be evaluated using a solar heat gain coefficient for all angles, $<SHGC>_d$.

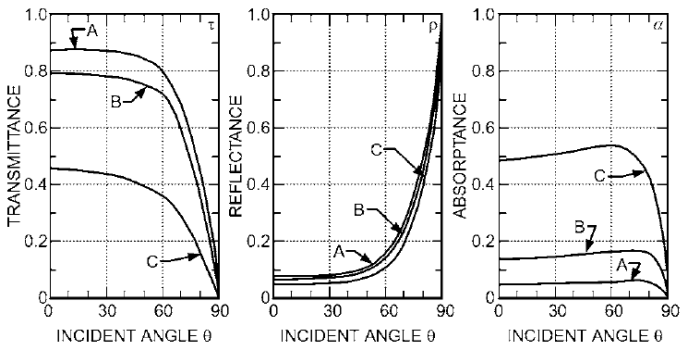

Figure 3.13 Variation of transmittance, reflectance, and absorptance with incident angle of solar radiation; A: double strength sheet glass; B: Clear plate glass; and C: heat absorbing plate glass (Source: ASHRAE Handbook, Fundamentals)

When the effects of external shading devices, such as overhang, side-fin, awning, etc., need to be accounted for, the areas of the parts of the glazing surface that are shaded and not shaded would need to be determined separately based on the incident angle of direct radiation and the geometry of the shading device. For internal shading devices, such as venetian blinds, drapers, etc., appropriate indoor solar attenuation coefficient (IAC) for direct and diffuse radiation for the specific device would need to be used to account for their effects. These more complicated methods, however, are not covered in this book. Interested readers should consult the ASHRAE Handbook [1] for details of the methods. To play safe, design cooling load calculation should ignore any shading device that is not a permanent provision.

Discussions on direct and diffuse radiation upon a surface and methods for their evaluation will be given in the following section. Further discussions on methods for handling transmitted and absorbed solar radiation and other radiant heat transfers in cooling load calculation are given in Section 3.4.

3.3 Outdoor and indoor design conditions

3.3.1 Intensity of solar radiation

As discussed above, solar radiation is a key source of heat gains of indoor spaces, through walls, roofs, windows, and skylights. Therefore, cooling load calculation requires evaluation of the intensity of solar irradiance upon building envelope components. The intensity under a clear sky is normally used in design cooling load calculations.

Although the sun emits radiation in all directions, due to the extremely long distance between the sun and the earth (Figure 3.14), it can be assumed that the sun's rays reaching the earth are along parallel straight lines. Before solar radiation can reach the surface of the earth, it must pass through the atmosphere (Figure 3.15). The air, water vapour and particulates in the atmosphere will scatter solar radiation while it passes through the atmosphere. Unlike the sun's ray which travels along a straight line, and hence called beam or direct radiation, the scattered radiation goes in all directions and is called diffuse radiation.

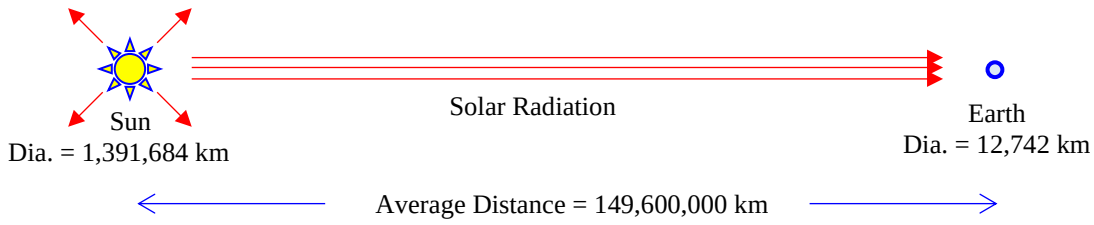

Figure 3.14 Distance between the sun and the earth

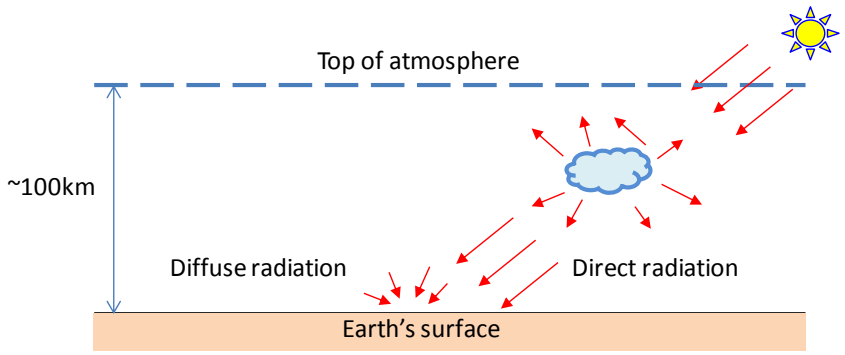

Figure 3.15 Scattering of solar radiation in the atmosphere

The intensity of direct solar radiation upon a surface is dependent on the incident angle of the sun's ray on the surface (θ), which is defined as the angle between the outward normal vector of the surface and the direction from which the sun's ray approaches the surface (Figure 3.16). Direct normal intensity of solar radiation, I_{DN}, is the intensity of direct solar radiation incident upon a surface (S_N) that is perpendicular to the direction of the direct solar radiation ($\theta = 0$).

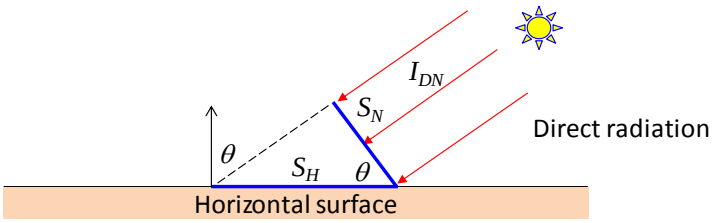

Figure 3.16 Incident angel of direct solar radiation upon a horizontal surface

If S_H is the horizontal surface covered by the shadow of S_N, S_H will receive the same amount of direct solar radiation as S_N, when S_N is removed. Therefore, the direct horizontal intensity of solar radiation, I_{DH}, can be related to the direct normal intensity, I_{DN}, with reference to the intensities of direct solar radiation upon S_N and S_H, as follows:

$$I_{DH} = \frac{I_{DN} A_{SN}}{A_{SH}}$$

Where A_{SN} and A_{SH} are respectively the area of the surfaces S_N and S_H (Figure 3.16).

Since

$$\frac{A_{SN}}{A_{SH}} = \cos\theta$$

$$I_{DH} = I_{DN} \cos\theta \qquad (3.74)$$

Likewise, for a surface S facing an arbitrary direction, if the solar incident angle is θ (Figure 3.17), the intensity of direct solar radiation on the surface, I_{DS}, will be given by:

$$I_{DS} = I_{DN} \cos\theta \tag{3.75}$$

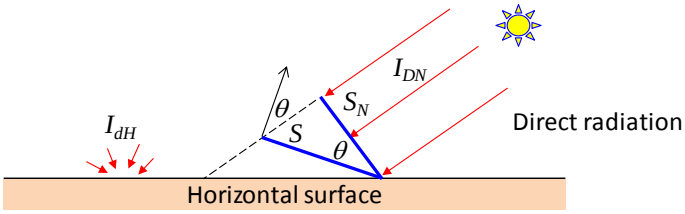

Figure 3.17 Direct solar radiation upon a titled surface

The amount of diffuse radiation that will reach a surface is proportional to the portion of the sky that the surface is exposed to, and hence a horizontal surface will receive the most diffuse radiation compared to any tilted surfaces. The intensity of diffuse solar radiation, therefore, is quantified by its intensity upon a horizontal surface, referred to as diffuse horizontal intensity, I_{dH}. The total of the direct horizontal (I_{DH}) and diffuse horizontal (I_{dH}) solar intensities is called the total horizontal intensity or global solar radiation (I_{TH}).

$$I_{TH} = I_{DH} + I_{dH} \tag{3.76}$$

The intensity of solar radiation a surface receives is affected mainly by the geometric relationship between the surface and the sun, which determine the incident angle θ of solar radiation, the attenuation and scattering effects, and the portion of the sky that the surface can "see". The sol-surface relationship, in turn, is dependent on:

- The location on earth under concern, measured by its longitude and latitude,
- The time of day and day of year, and
- The orientation and titling angle of the surface.

The earth orbits around the sun, at the rate of one cycle per a period of approximately 365.25 days. Because the earth's orbit is slightly elliptical, the intensity of solar radiation on a surface normal to the sun's ray outside the atmosphere, called extraterrestrial radiation (I_O), is variable. The extraterrestrial radiation intensity at the average sun-earth distance is called solar constant (I_{SC}), which equals 1367W/m^2.

I_O can be determined using [1]:

$$I_o = I_{SC}\left[1 + 0.033\cos\left(360^\circ \frac{n-3}{365}\right)\right] \tag{3.77}$$

Where n is the day of year ($n = 1$ for 1st Jan., 32 for 1st Feb., etc.)

Besides orbiting around the sun, the earth is also spinning about an axis through its north and south poles, referred to as self-rotation, at the rate of one cycle per day (24 hours). The axis of self-rotation of the earth is not perpendicular to its orbit plane but titled by an angle of 23.45°. The orbiting of the earth around the sun and self-rotation of the earth about an axis that is titled give rise to seasonal and diurnal variations in the weather condition on earth (Figure 3.18).

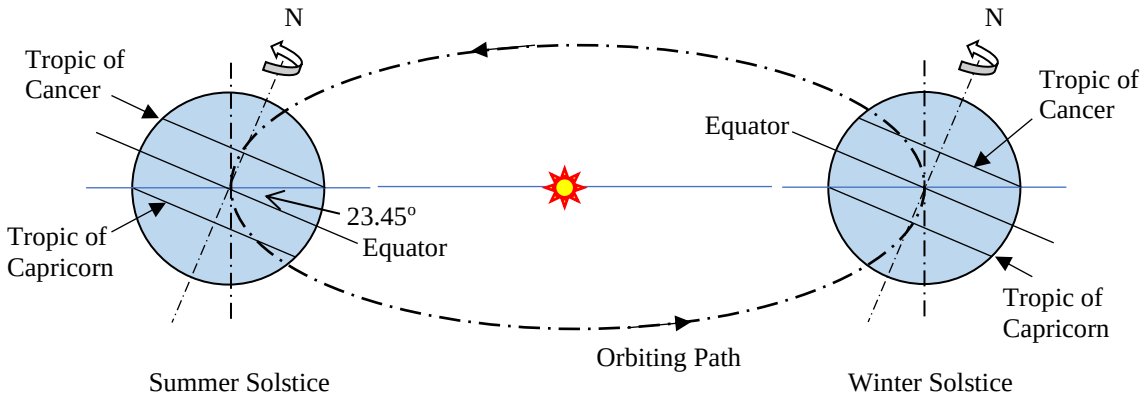

Figure 3.18 Orbiting and self-rotation of the Earth

The angle between the sun's ray and the equatorial plane of the earth is called declination angle, δ, which varies between -23.45° to +23.45° throughout a year (Figure 3.19), as given by the equation below, with n as defined for Equation (3.77):

$$\delta = 23.45^{\circ} \sin\left(360^{\circ} \frac{n+284}{365}\right) \tag{3.78}$$

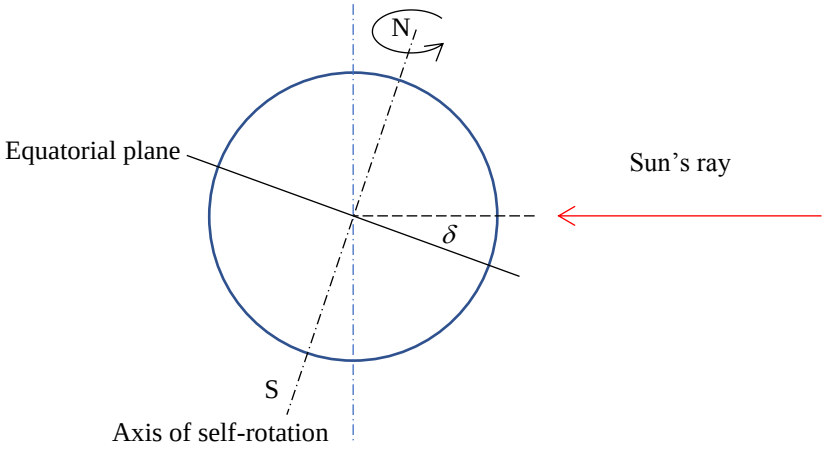

Figure 3.19 The declination angle

Since the earth will rotate by 360° a day, it will rotate by 15° in an hour. When the apparent solar time (*AST*) of a location on earth is at noon (12:00), the sun's rays will

be parallel to the meridian plane passing through the location, and the sun is at its highest position above the location on the same day. Note should be taken that apparent solar time (AST) may differ from the local time when an extensive region (e.g. a country) adopts a single standard time (all places in the region are then in the same time zone).

The AST can be determined from the longitude of the location under concern (LON), the local standard time (LST) and the longitude of the LST meridian (LSM), as follows:

$$AST = LST + (LON - LSM)/15 + ET/60 \tag{3.79}$$

Where ET in the above equation (in minutes) is called the equation of time, which is a correction required to account for the variation in the earth's orbiting velocity around the sun throughout the year. The monthly values of ET (on the 21st day of each month), in minutes, are as shown in Table 3.1. Refer to ASHRAE Handbook, Fundamentals [1] or other references for the formula for evaluating ET for other days in the year.

Table 3.1 Equation of time (minutes)

Month	Jan	Feb	Mar	Apr	May	Jun
ET	-10.6	-14	-7.9	1.2	3.7	-1.3
Month	Jul	Aug	Sep	Oct	Nov	Dec
ET	-6.4	-3.6	6.9	15.5	13.8	2.2

The hour angle, H, which is a measure of the direction from which the sun's ray approaches, is defined as (Figure 3.20):

$$H = 15 \cdot (AST - 12) \tag{3.80}$$

H is positive in the afternoon, negative in the morning.

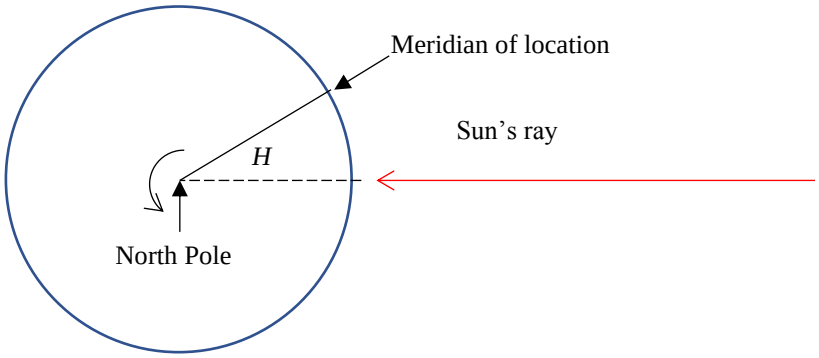

Figure 3.20 The hour angle

Solar position relative to a surface on earth is quantified by the solar altitude angle (β) and solar azimuth angle (ϕ) (Figrue 3.21), which can be determined by using the equations below.

$$\sin\beta = \cos L \cos\delta \cos H + \sin L \sin\delta \tag{3.81}$$

$$\sin\phi = \sin H \cos\delta / \cos\beta \tag{3.82}$$

$$\cos\phi = (\cos H \cos\delta \sin L - \sin\delta \cos L)/\cos\beta \tag{3.83}$$

Where L is the latitude angle of the location under concern.

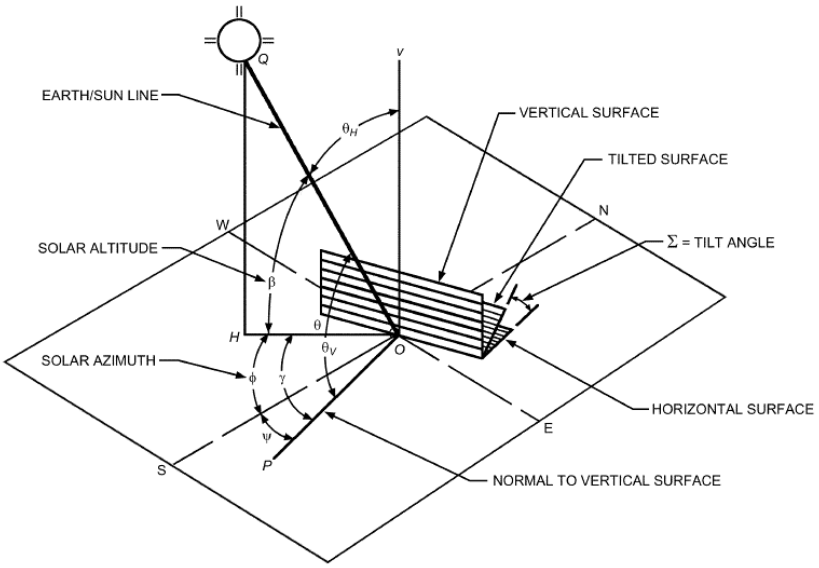

Figure 3.21 Various angles relating the sun and a surface on earth

Note that:

- Solar altitude angle, β, is measured from horizontal, upward positive.
- Solar azimuth angle, ϕ, is measured from South, clockwise positive.
- Both Equations (3.82) & (3.83) are needed to determine the correct solar azimuth angle, as the angle may be positive or negative, and its absolute value less or greater than 90°.

At solar noon, $H = 0$ and β reaches its maximum value, given by:

$$\beta_{max} = 90^{\circ} - |L - \delta| \tag{3.84}$$

Tables 3.2 and 3.3 provide values of solar altitude angles and solar azimuth angles at various local standard time and months in the year for Hong Kong ($LON = 114.17^{o}$E; $LAT = 22.30^{o}$N), which were evaluated using the method discussed above.

Table 3.2 Solar altitude angles in Hong Kong throughout the year (LON = 114.17°E; LAT = 22.30°N)

Month LST	**Jan**	**Feb**	**Mar**	**Apr**	**May**	**Jun**	**Jul**	**Aug**	**Sep**	**Oct**	**Nov**	**Dec**
5	-28.23	-26.03	-20.34	-13.14	-8.98	-9.00	-12.15	-16.13	-18.90	-20.85	-23.45	-26.36
6	-14.70	-12.17	-6.59	0.09	3.66	3.39	0.59	-2.67	-5.03	-7.19	-10.20	-13.15
7	-1.47	1.56	7.28	13.67	16.78	16.31	13.81	11.06	8.80	6.18	2.64	-0.32
8	11.28	15.02	21.11	27.45	30.22	29.58	27.33	24.92	22.45	19.07	14.86	11.92
9	23.27	27.98	34.74	41.32	43.86	43.09	41.06	38.77	35.67	31.13	26.09	23.22
10	33.99	40.01	47.86	55.14	57.64	56.74	54.90	52.42	48.01	41.73	35.70	33.04
11	42.57	50.22	59.70	68.58	71.50	70.49	68.77	65.36	58.35	49.68	42.67	40.44
12	47.67	56.87	67.99	79.71	85.33	84.24	82.29	75.36	64.12	53.21	45.75	44.25
13	48.00	57.68	68.18	77.38	80.57	81.78	82.17	74.65	62.31	51.10	44.13	43.57
14	43.47	52.26	60.13	65.13	66.70	68.02	68.64	64.10	54.03	44.12	38.26	38.57
15	35.26	42.72	48.38	51.53	52.86	54.29	54.77	51.04	42.58	34.07	29.36	30.33
16	24.76	31.02	35.29	37.67	39.12	40.65	40.93	37.35	29.76	22.31	18.56	20.00
17	12.90	18.24	21.67	23.82	25.54	27.18	27.21	23.49	16.30	9.60	6.60	8.37
18	0.23	4.88	7.84	10.08	12.20	13.96	13.68	9.64	2.55	-3.67	-6.08	-4.07
19	-12.95	-8.80	-6.03	-3.43	-0.78	1.12	0.46	-4.07	-11.31	-17.27	-19.21	-17.03

Note: a negative value means the hour is either before sun rise or after sun set.

Table 3.3 Solar azimuth angles in Hong Kong throughout the year (LON = 114.17°E; LAT = 22.30°N)

Month LST	Jan	Feb	Mar	Apr	May	Jun	Jul	Aug	Sep	Oct	Nov	Dec
5	-79.43	-90.06	-100.66	-110.73	-117.48	-119.88	-116.60	-107.32	-94.32	-82.41	-74.85	-74.26
6	-74.93	-84.56	-94.50	-104.52	-111.49	-113.85	-110.32	-101.04	-88.53	-77.30	-70.39	-70.08
7	-69.81	-79.03	-88.78	-99.15	-106.59	-109.02	-105.13	-95.46	-82.78	-71.61	-65.02	-64.99
8	-63.61	-72.81	-82.80	-94.03	-102.39	-105.02	-100.58	-89.96	-76.35	-64.73	-58.28	-58.60
9	-55.70	-65.12	-75.71	-88.52	-98.58	-101.67	-96.24	-83.76	-68.28	-55.77	-49.49	-50.31
10	-45.13	-54.69	-65.96	-81.43	-94.86	-98.91	-91.58	-75.48	-56.80	-43.38	-37.73	-39.30
11	-30.72	-39.42	-50.16	-69.08	-90.52	-97.11	-85.10	-61.23	-38.51	-25.88	-22.15	-24.75
12	-11.93	-17.01	-21.23	-31.64	-77.97	-101.39	-65.77	-27.24	-9.42	-3.16	-3.17	-6.78
13	9.22	10.50	19.69	47.08	85.52	98.84	66.20	32.44	23.96	20.37	16.41	12.37
14	28.51	34.66	49.30	73.32	92.19	97.30	85.18	63.22	47.94	39.37	33.22	29.46
15	43.49	51.51	65.47	83.57	96.17	99.36	91.63	76.50	62.58	52.94	46.13	42.90
16	54.50	62.89	75.37	90.05	99.87	102.23	96.28	84.46	72.22	62.64	55.75	53.01
17	62.69	71.11	82.54	95.38	103.78	105.69	100.62	90.54	79.39	69.96	63.05	60.66
18	69.07	77.60	88.55	100.51	108.19	109.81	105.18	96.02	85.42	75.89	68.80	66.61
19	74.30	83.24	94.26	106.05	113.42	114.83	110.37	101.64	91.11	81.10	73.51	71.40

Note: Solar azimuth angle is measured from South, clockwise positive.

The following angles are also defined for relating the sun's position to a surface (Figure 3.21):

ψ = surface azimuth angle, degree from South clockwise positive
γ = sol-surface azimuth angle
Σ = tilting angle of surface, from horizontal, positive upward

On the basis of the angles defined above,

$$\gamma = \phi - \psi \tag{3.85}$$

$\gamma > 90^o$ or $\gamma < -90^o$ means the surface is in shade.

The incident angle, θ, of direct solar radiation upon a surface can be determined from:

$$\cos\theta = \cos\beta \cos\gamma \sin\Sigma + \sin\beta \cos\Sigma \tag{3.86}$$

For a vertical surface, $\Sigma = 90^o$, hence:

$$\cos\theta = \cos\beta \cos\gamma \tag{3.87}$$

For a horizontal surface, $\Sigma = 0^o$, the incident angle is given simply by:

$$\theta = 90^\circ - \beta \tag{3.88}$$

The intensity of direct solar radiation upon a surface can be determined when θ and I_{DN} are known (Equation (3.75)). The intensities of direct and diffuse horizontal solar radiation under a clear sky (I_{DN} & I_{dH}) can be determined when the solar altitude angle (β) is known. The extent of scattering of solar radiation is proportional to the path length in the atmosphere that it travels through to reach the earth's surface (Figure 3.22), which is described by the relative air mass, m:

$$m = 1/[\sin\beta + 0.50572(6.07995 + \beta)^{-1.6364}] \tag{3.89}$$

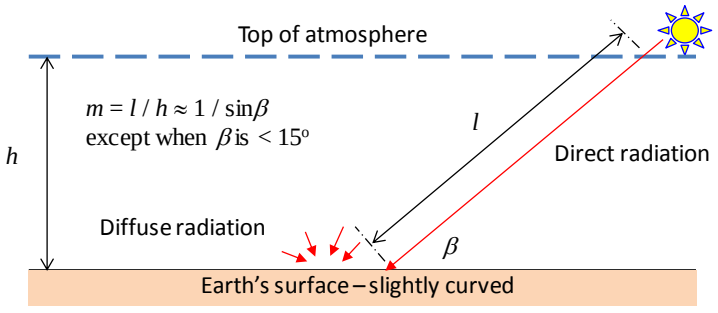

Figure 3.22 Path of direct radiation through the atmosphere

Under a clear sky,

$$I_{DN} = I_o exp(-\tau_b m^{ab}) \tag{3.90}$$

$$I_{dH} = I_o exp(-\tau_d m^{ad}) \tag{3.91}$$

Where

τ_b & τ_d = direct and diffuse radiation (pseudo) optical depths
ab & ad = direct and diffuse radiation air mass exponents, where

$$ab = 1.219 - 0.043\tau_b - 0.151\tau_d - 0.204\tau_b\tau_d \tag{3.92}$$

$$ad = 0.202 + 0.852\tau_b - 0.007\tau_d - 0.357\tau_b\tau_d \tag{3.93}$$

Values of τ_b & τ_d and ab & ad for various places can be found from the ASHRAE Handbook [1]. Those applicable to Hong Kong are given in Tables 3.4. Tables 3.5 & 3.6 summarize the clear sky direct normal and diffuse horizontal solar radiation intensities in Hong Kong, obtained by applying Equations (3.90) to (3.93) (see also Section B1 in Appendix B).

The total solar irradiance upon a receiving surface, I_t, comprises the following components (Figure 3.23):

$$I_t = I_D + I_d + I_G \tag{3.94}$$

Where

I_D is the direct intensity
I_d the diffuse intensity and
I_G the ground-reflected intensity

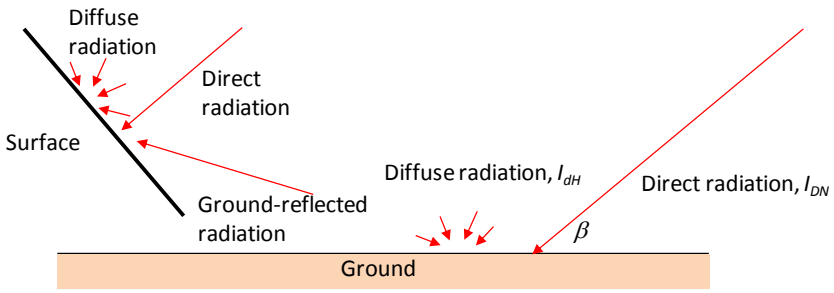

Figure 3.23 Components of solar radiation upon a surface

Table 3.4 The average values of τ_b & τ_d and ab & ad of each month for Hong Kong

Mth.	Jan	Feb	Mar	Apr	May	Jun	Jul	Aug	Sep	Oct	Nov	Dec
τ_b	0.631	0.658	0.766	0.775	0.701	0.659	0.617	0.682	0.741	0.725	0.621	0.604
τ_d	1.519	1.499	1.395	1.41	1.53	1.612	1.693	1.568	1.467	1.469	1.591	1.581
ab	0.76697	0.76314	0.75743	0.74984	0.73903	0.73054	0.72373	0.73475	0.74386	0.74874	0.75050	0.75949
ad	0.38680	0.40000	0.46339	0.46232	0.40565	0.37294	0.34292	0.39032	0.43499	0.42920	0.36724	0.36463

Table 3.5 Clear sky direct normal solar Intensity in Hong Kong

Month LST	Jun	Jul	Aug	Sep	Oct	Nov	Dec
6	14.56	0.89	0.01	0.00	0.00	0.00	0.00
7	253.27	236.99	140.61	74.18	36.40	8.67	0.04
8	439.74	449.31	370.88	300.30	261.50	254.51	196.99
9	554.29	574.31	511.87	450.34	422.55	445.47	416.85
10	624.43	649.11	596.05	540.16	517.91	553.91	542.77
11	664.86	692.07	643.96	590.09	569.35	611.17	610.55
12	682.77	711.77	665.40	610.29	587.86	632.05	638.68
13	681.04	711.68	664.27	604.47	577.09	621.35	633.92
14	659.41	691.79	640.37	571.60	534.94	576.66	595.17
15	614.34	648.58	589.31	505.37	452.64	486.92	512.82
16	537.62	573.41	500.50	391.57	311.39	326.63	363.45
17	412.61	447.81	351.86	205.29	92.48	70.15	112.89
18	209.87	234.45	112.62	3.19	2.60	0.00	33.20
19	1.24	0.70	24.70	0.00	0.00	0.00	0.00

Table 3.6 Clear sky diffuse horizontal solar intensity in Hong Kong

Month LST	Jun	Jul	Aug	Sep	Oct	Nov	Dec
6	17.90	5.64	1.18	0.00	0.00	0.00	0.00
7	100.45	84.47	69.45	52.01	34.10	16.35	2.76
8	162.77	145.54	149.21	147.00	129.75	103.21	86.84
9	206.47	187.57	203.92	213.12	197.25	163.69	154.00
10	236.20	216.05	240.44	256.42	240.74	202.03	196.71
11	254.62	233.84	262.88	282.07	265.71	224.01	221.90
12	263.11	242.40	273.38	292.82	275.00	232.37	232.91
13	262.29	242.36	272.81	289.70	269.58	228.06	231.02
14	252.08	233.72	261.15	272.42	248.88	210.60	216.02
15	231.76	215.84	237.39	239.24	210.62	177.90	186.12
16	199.76	187.24	199.24	186.44	150.08	125.33	137.10
17	153.14	145.07	142.31	107.57	60.78	45.15	60.95
18	86.83	83.78	59.70	9.07	8.76	0.00	31.62
19	6.12	5.19	24.29	0.00	0.00	0.00	0.00

The direct intensity, I_D, is given by:

$$I_D = I_{DN} \cos\theta \tag{3.95}$$

The diffuse intensity upon a vertical surface, I_{dV}, is given by:

$$I_{dV} = I_{dH} Y \tag{3.96}$$

Where Y is as evaluated by the following equation, or equal to 0.45, whichever is the greater.

$$Y = 0.55 + 0.437 \cos\theta + 0.313 \cos^2\theta \tag{3.97}$$

For a non-vertical surface, diffuse intensity, I_d, can be estimated from the following equation, with Y evaluated based on a vertical surface with the same azimuth:

$$I_d = \begin{cases} I_{dH}(Y \sin\Sigma + \cos\Sigma) & \Sigma \le 90^\circ \\ I_{dH} Y \sin\Sigma & \Sigma > 90^\circ \end{cases} \tag{3.98}$$

The ground-reflected intensity, I_G, is given by:

$$I_G = (I_{DN} \sin\beta + I_{dH}) \rho_G \frac{1-\cos\Sigma}{2} \tag{3.99}$$

Where ρ_G is ground reflectance, often taken to be 0.2 (see Table 5 in Chapter 14 of ASHRAE Handbook, Fundamentals (2017) [1] for values of specific kind of ground surfaces, e.g. surfaces covered by snow).

The clear sky total solar intensity upon surfaces facing various standard directions, and incident angle data, for Jun. to Dec. (W/m^2) in Hong Kong, which were calculated using the methods summarized above, are given in Sections B.2 & B.3 in Appendix B.

3.3.2 Outdoor air temperature and humidity

The preceding section has addressed the intensities of clear sky solar radiation incident upon the surfaces of the envelop of a building, which are to be used for calculation of the design cooling load for the building. Besides solar radiation, the outdoor air temperature and moisture content are key influential factors to the rate of heat transfer through the building envelop into indoor spaces, and the rate that heat is being carried by air flowing into a building. The latter includes infiltration, which is unintended but inevitable, and fresh air drawn in deliberately for ventilation.

For providing a reference for design cooling load calculation, a suitable design outdoor air state must be defined, typically by specifying the values of the dry- and wet-bulb temperatures. A simplistic approach is to select an extreme outdoor weather condition that has never been surpassed. This, however, will lead to oversized plants and thus energy inefficient operation. Because outdoor air dry-bulb and wet-bulb temperatures both vary from time to time, and even their annual general pattern may vary slightly from year to year, selection of the design outdoor weather condition needs to be based on statistical analysis of weather records of a specific region over a long enough period of time (typically 25 years).

From the statistical analysis, outdoor air dry-bulb temperatures that could be exceeded by different percentages of time in the cooling period, such as 0.4, 1.0, 2.0 and 5.0%, can be identified. The expected value of wet-bulb temperature given each of these outdoor air temperatures with known probability of exceedance can also be determined. This expected value is called 'mean coincident wet bulb (MCWB) temperature'. Alternatively, design outdoor wet bulb temperatures at known probabilities of exceedance and mean coincident dry bulb (MCDB) temperatures may be compiled for use in designs with specific concern on dehumidification capacity. With the statistical results, selection of the dry and wet bulb temperatures as the reference for design cooling load calculation can be made based on the acceptable risk level related to the probability that a plant sized based on the design weather condition may not have sufficient capacity to cope with the load.

A commonly used design weather condition for Hong Kong is 33.3°C dry bulb, 28°C wet bulb. A comparison can be made of this design condition with statistical figures shown in Tables 3.7 and 3.8. The data given in these tables are the design dry bulb (*DB*) and mean coincident wet bulb (*MCWB*) temperatures and design wet bulb (*WB*) and mean coincident dry bulb (*MCDB*) temperatures, at 0.4% exceedance level, obtained from ASHRAE Handbook [1].

The hourly design outdoor dry and wet bulb temperatures (t_{ao} & t'_{ao}), which are needed for design cooling load calculations, are to be evaluated based on the design dry bulb (*DB*) and wet bulb (*MCWB*) temperatures for individual months, adjusted to hourly values by using the daily range (*DR*) of the design temperatures for the month and the percentage of the daily range (*X*) for individual hours.

$$t_{ao} = DB - DR \cdot X \tag{3.100}$$

$$t'_{ao} = MCWB - DR \cdot X \tag{3.101}$$

Table 3.7 Outdoor design dry bulb temperature and mean coincident wet bulb temperature of Hong Kong at 0.4% risk level

Month	Jan	Feb	Mar	Apr	May	Jun
DB	22.1	23.1	26.0	28.6	31.2	32.2
MCWB	18.5	19.8	22.7	24.3	26.2	26.5
Month	Jul	Aug	Sep	Oct	Nov	Dec
DB	**33.0**	32.9	32.5	30.6	26.9	24.0
MCWB	**26.8**	26.6	25.6	25.2	21.9	19.3

Table 3.8 Outdoor design wet bulb temperature and mean coincident dry bulb temperature of Hong Kong at 0.4% risk level

Month	Jan	Feb	Mar	Apr	May	Jun
WB	19.5	21.1	23.6	25.3	26.9	27.7
MCDB	21.0	22.4	25.2	27.1	29.8	30.6
Month	Jul	Aug	Sep	Oct	Nov	Dec
WB	**27.7**	27.7	27.3	26.2	23.9	20.1
MCDB	**30.9**	31.1	30.3	28.9	25.6	22.6

Tables 3.9 and 3.10 summarize the values of *DR* and *X* to be used for evaluating the hourly design outdoor dry and wet bulb temperatures for Hong Kong. Note that the same *DR* and *X* values are applicable to both the design dry bulb and wet bulb temperatures, and there is only one daily profile of outdoor weather condition for each month. Table 3.11 shows the design hourly dry bulb temperatures and mean coincident wet bulb temperatures for Hong Kong at 0.4% risk level, compiled using the methods introduced above.

Table 3.9 Daily range (*DR*) for different months in Hong Kong

Month	Jan	Feb	Mar	Apr	May	Jun
DR for *DB/WB*	3.5	3.1	3.4	3.3	3.3	3
Month	Jul	Aug	Sep	Oct	Nov	Dec
DR for *DB/WB*	3.5	3.5	3.4	3.2	3.5	3.8

Table 3.10 Percentage daily range (X) for individual hours in Hong Kong

Time, hr	X	Time, hr	X	Time, hr	X	Time, hr	X
1	0.88	7	0.91	13	0.05	19	0.39
2	0.92	8	0.74	14	0	20	0.5
3	0.95	9	0.55	15	0	21	0.59
4	0.98	10	0.38	16	0.06	22	0.68
5	1	11	0.23	17	0.14	23	0.75
6	0.98	12	0.13	18	0.24	24	0.82

3.3.3 Indoor design conditions

The following indoor design conditions are influential to the cooling load of air-conditioned spaces and thus need to be defined before design cooling load calculations can proceed:

- Indoor air state, including dry bulb temperature and relative humidity that are comfortable to the occupants or suitable for the activity or process to be carried out in individual spaces.
- Occupancy rate, in terms of number of occupants per unit floor area (p/m^2) or square meters of floor area occupied by each person (m^2/p).
- Activity level of the occupants, in terms of the sensible and latent heat emitted by each person.
- Ventilation rate, in *l*/s per person, m^3/s or air-change per hour.
- Casual heat gains, including heat gains from all indoor heat sources, such as lighting and appliances, and any specific equipment that is present in the space.

Selection of indoor design conditions is largely determined by the choices of end-users and situations that would arise from use of the spaces, but building and air-conditioning system designers may also make appropriate recommendations. Some associated data, e.g. sensible and latent heat gains from occupants, may be obtained from standard references, such as ASHRAE Handbook [1], but some others would need to be ascertained from knowledge about the operating conditions, such as electricity consumption of equipment / machines for specific processes. Table 3.12 shows a set of typical indoor design conditions for office buildings in Hong Kong.

Table 3.11 Design dry and wet bulb temperatures for Hong Kong

	Jun		Jul		Aug		Sep		Oct		Nov		Dec	
Time	DB	WB	DB	WB	DB	WB	DB	WB	DB	WB	DB	WB	DB	WB
1	29.6	23.9	29.9	23.7	29.8	23.5	29.5	22.6	27.8	22.4	23.8	18.8	20.7	16.0
2	29.4	23.7	29.8	23.6	29.7	23.4	29.4	22.5	27.7	22.3	23.7	18.7	20.5	15.8
3	29.4	23.7	29.7	23.5	29.6	23.3	29.3	22.4	27.6	22.2	23.6	18.6	20.4	15.7
4	29.3	23.6	29.6	23.4	29.5	23.2	29.2	22.3	27.5	22.1	23.5	18.5	20.3	15.6
5	29.2	23.5	29.5	23.3	29.4	23.1	29.1	22.2	27.4	22.0	23.4	18.4	20.2	15.5
6	29.3	23.6	29.6	23.4	29.5	23.2	29.2	22.3	27.5	22.1	23.5	18.5	20.3	15.6
7	29.5	23.8	29.8	23.6	29.7	23.4	29.4	22.5	27.7	22.3	23.7	18.7	20.5	15.8
8	30.0	24.3	30.4	24.2	30.3	24.0	30.0	23.1	28.2	22.8	24.3	19.3	21.2	16.5
9	30.6	24.9	31.1	24.9	31.0	24.7	30.6	23.7	28.8	23.4	25.0	20.0	21.9	17.2
10	31.1	25.4	31.7	25.5	31.6	25.3	31.2	24.3	29.4	24.0	25.6	20.6	22.6	17.9
11	31.5	25.8	32.2	26.0	32.1	25.8	31.7	24.8	29.9	24.5	26.1	21.1	23.1	18.4
12	31.8	26.1	32.5	26.3	32.4	26.1	32.1	25.2	30.2	24.8	26.4	21.4	23.5	18.8
13	32.1	26.4	32.8	26.6	32.7	26.4	32.3	25.4	30.4	25.0	26.7	21.7	23.8	19.1
14	32.2	26.5	33.0	26.8	32.9	26.6	32.5	25.6	30.6	25.2	26.9	21.9	24.0	19.3
15	32.2	26.5	33.0	26.8	32.9	26.6	32.5	25.6	30.6	25.2	26.9	21.9	24.0	19.3
16	32.0	26.3	32.8	26.6	32.7	26.4	32.3	25.4	30.4	25.0	26.7	21.7	23.8	19.1
17	31.8	26.1	32.5	26.3	32.4	26.1	32.0	25.1	30.2	24.8	26.4	21.4	23.5	18.8
18	31.5	25.8	32.2	26.0	32.1	25.8	31.7	24.8	29.8	24.4	26.1	21.1	23.1	18.4
19	31.0	25.3	31.6	25.4	31.5	25.2	31.2	24.3	29.4	24.0	25.5	20.5	22.5	17.8
20	30.7	25.0	31.3	25.1	31.2	24.9	30.8	23.9	29.0	23.6	25.2	20.2	22.1	17.4
21	30.4	24.7	30.9	24.7	30.8	24.5	30.5	23.6	28.7	23.3	24.8	19.8	21.8	17.1
22	30.2	24.5	30.6	24.4	30.5	24.2	30.2	23.3	28.4	23.0	24.5	19.5	21.4	16.7
23	30.0	24.3	30.4	24.2	30.3	24.0	30.0	23.1	28.2	22.8	24.3	19.3	21.2	16.5
24	29.7	24.0	30.1	23.9	30.0	23.7	29.7	22.8	28.0	22.6	24.0	19.0	20.9	16.2

Table 3.12 Typical indoor design conditions for office buildings in Hong Kong

Parameter	Value
Indoor design temperature	24 – 25.5°C
Indoor design relative humidity	50 – 60%
Occupancy density	7 – 10m²/p
Sensible heat gain from occupant	65 – 75 W/p
Latent heat gain from occupant	45 – 55 W/p
Ventilation rate	7 – 10 l/s-p
Lighting heat gain	10 – 15 W/m²
Appliances heat gain	10 – 30 W/m²

Though it may sometimes be inevitable, use of conservative data for design cooling load calculations can lead to oversized plants and equipment and degraded energy efficiency. There may also be regulatory requirements that govern certain indoor design conditions, such as lighting power density and ventilation rate. Table 3.13 shows the requirements on indoor/outdoor design temperature and relative humidity given in the Building Energy Code of Hong Kong [7]. The requirement on lighting power density is shown in Table 3.14.

Table 3.13 Building Energy Code requirements on indoor/outdoor design temperature and relative humidity in Hong Kong [7]

Table 6.4 : Air-conditioning System Load Design Conditions				
Condition	Season	Applications	Temperature / Relative Humidity	
Indoor, for human comfort applications	Summer	Office and Classroom	Minimum dry bulb temperature	23°C
			Minimum relative humidity	50%
		Other applications	Minimum dry bulb temperature	22°C
			Minimum relative humidity	50%
	Winter	Hotel	Maximum dry bulb temperature	24°C
			Maximum relative humidity	50%
		Other applications	Maximum dry bulb temperature	22°C
			Maximum relative humidity	50%
Outdoor	Summer	All applications	Maximum dry bulb temperature of 35°C with wet bulb temperature lower than 29°C, or Maximum wet bulb temperature of 29°C with dry bulb temperature lower than 35°C	
	Winter	All applications	Minimum dry bulb temperature	7°C

Table 3.14 Building energy code requirements on lighting power density [7]

Table 5.4 : Lighting Power Density and Automatic Lighting Control for Various Types of Space

Type of Space	Maximum Allowable LPD (W/m^2)	Automatic Lighting Control Required (Yes / No)
Atrium / Foyer with headroom over 5m	17	Yes
Bar / Lounge	13	No
Banquet Room / Function Room / Ball Room	17	No
Canteen	11	No
Car Park	5	Yes, at parking spaces only
Changing Room/ Locker Room	10	Yes
Classroom / Training Room	12	Yes
Clinic	15	No
Common Room/ Break Room	8	Yes
Computer Room / Data Centre	15	Yes
Conference / Seminar Room	14	Yes
Confinement Cell	12	No
Copy/ Printing Room, Photocopy Machine Room	10	Yes
Corridor	8	Yes
Court Room	15	Yes
Covered Playground (underneath building)/ Sky Garden	12	Yes
Dormitory	8	Yes
Entrance Lobby	13	Yes
Exhibition Hall / Gallery	15	No
Fast Food / Food Court	14	No
Guest room in Hotel or Guesthouse	13	No
Gymnasium / Exercise Room	11	Yes
Indoor Swimming Pool, for recreational or leisure purposes	15	No
Kitchen	13	No
Laboratory	15	No
Lecture Theatre	13	Yes
Library – Reading Area or Audio Visual Centre	12	No
Library – Stack Area	15	No
Lift Car	11	Yes
Lift Lobby	10	Yes
Loading & Unloading Area	8	Yes
Long Stay Ward for elderly	15	No
Nurse Station	13	No
Office, enclosed (Internal floor area at or below $15m^2$)	12	Yes
Office, Internal floor area above $15m^2$ and of or below $200m^2$	10	Yes
Office, Internal floor area above $200m^2$	9	Yes
Pantry	12	Yes

Table 5.4 : Lighting Power Density and Automatic Lighting Control for Various Types of Space

Type of Space	Maximum Allowable LPD (W/m^2)	Automatic Lighting Control Required (Yes / No)
Passenger Terminal Building • Arrival Hall / Departure Hall, with headroom not exceeding 5m • Arrival Hall / Departure Hall, with headroom over 5m • Passenger circulation area	14 18 13	No No No
Patient Ward / Day Care	13	No
Plant Room / Machine Room / Switch Room	10	No
Porte Cochere	13	No
Porte Cochere with headroom over 5m	15	No
Public Circulation Area	13	Yes
Railway Station • Concourse / Platform / Entrance / Adit / Staircase, with headroom not exceeding 5 m • Concourse / Platform / Entrance / Adit / Staircase, with headroom over 5 m	14 18	No No
Refuge Floor	11	Yes
Restaurant	17	No
Retail	16	No
School hall	14	Yes
Seating Area inside Theatre / Cinema / Auditorium / Concert Hall / Arena	10	No
Server Room / Hub Room	10	No
Sports Arena, Indoor, for recreational purpose	17	No
Staircase	7	No
Storeroom / Cleaner	9	Yes
Toilet / Washroom / Shower Room	11	Yes
Workshop	13	No
Multi-functional Space	See below	

LPD of each combination of function-specific luminaires should not exceed the maximum allowable value corresponding to the type of space illuminated by that combination of luminaires, detailed as follows:

LPD_{F1} not to exceed LPD_{S1} ,

LPD_{F2} not to exceed LPD_{S2} ,…….,

LPD_{Fn} not to exceed LPD_{Sn}

where LPD_{F1} , LPD_{F2} .,...., LPD_{Fn} respectively refers to the lighting power density corresponding to function F1, F2, ..., Fn, and

LPD_{S1} , LPD_{S2} .,...., LPD_{Sn} respectively refers to the maximum allowable value of lighting power density corresponding to the classified Space S1, S2,....., Sn based on the respective function F1, F2, ..., Fn.

3.4 Design cooling load calculation

3.4.1 Heat gain, cooling load and heat extraction rate

The cooling load of a space is the rate that (sensible and latent) heat must be taken out of the space in order to maintain the indoor air state of the space at the design condition. Since air-conditioning is provided primarily through treating the air inside the space, the cooling load comprises only the (sensible and latent) heat that is imparted to the room air, which must be through convection.

Accordingly, all convective heat gains will instantaneously become parts of the cooling load of a space. Radiant heat gains will not become cooling load until their energy is absorbed by objects inside the space, thus raising up the temperatures of the objects, which will then lead to convective heat transfer to the indoor air. Note that sensible heat gains may be radiant or convective, but latent heat gains are all convective.

Heat extraction rate is the rate that heat is removed from the space by the air-conditioning system. Room air temperature can be kept at set-point value only if the sensible heat extraction rate equals the room sensible cooling load – any imbalance between the two will lead to drifting of the room air temperature from its set-point. Figure 3.24 shows the relation among heat gains, cooling load and heat extraction rate of a space with respect to their contributions to the design cooling load of a space.

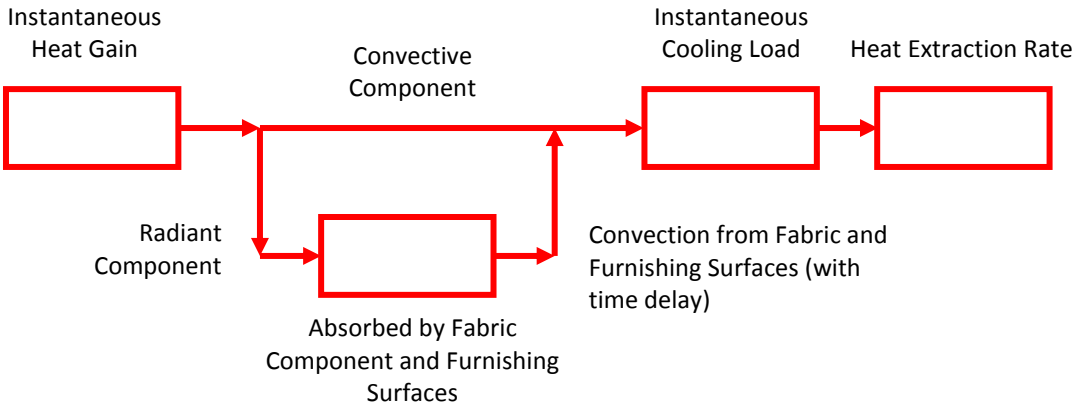

Figure 3.24 Heat gains, cooling load and heat extraction rate

Conduction heat gains from walls and roofs/ceilings are subject to the influence of the thermal storage effect of the fabric components and exhibits a time lag. They are to be evaluated from the solution of the governing equation (Equation 3.7) and appropriate boundary conditions. In the ASHRAE Method, the solution is called the conduction transfer function (CTF), which was obtained by using the transfer function method.

The other heat gains, as listed below, may all be regarded as instantaneous heat gains:

- Transmitted direct and diffuse solar heat gain through fenestrations
- Conductive heat gain from fenestrations
- Occupant heat gains

- Lighting & appliances heat gains
- Heat gains due to infiltration

The heat balance method is a rigorous method for determining the rate of heat flow to the air zone and thus the cooling load. Based on a detailed heat balance model, a transfer function model can be developed to allow the cooling load of a space due to heat gains of the space to be calculated. All simplified cooling load calculation methods introduced by ASHRAE were developed based on the transfer function method (TFM).

Among the simplified manual cooling load calculation methods, the Cooling Load Temperature Difference / Solar Cooling Load / Cooling Load Factor (CLTD/SCL/CLF) method was most widely used. In this method:

- Cooling load due to conduction through walls and roofs = A×U×CLTD
- Cooling load due to solar heat gain through fenestrations = A×SC×SCL
- Other cooling load = Heat Gain × CLF for the type of load concerned

3.4.2 The radiant time series method

A new manual cooling load calculation method, called the Radiant Time Series (RTS) method, was published in the 2001 edition of the ASHRAE Handbook – Fundamentals. This was meant to be the standard hand calculation method, replacing all previous methods for the same purpose. The RTS method is based on the assumptions that the 24-hourly design outdoor weather conditions for a given month would repeat day after day, and the indoor air state is kept steadily at the design value. It adheres much more closely to the RFM and TFM and should be able to yield more accurate results than other simplified methods, such as the CLTD/SCL/CLF method.

The Conduction Time Series (CTS), as shown below, is used in the RTS method to estimate conduction heat gain, q_n, from an external wall or roof at a particular time step (n).

$$q_n = c_0 q_{i,n} + c_1 q_{i,n-1} + c_2 q_{i,n-2} + \cdots + c_{23} q_{i,n-23} \tag{3.102}$$

Where

q_n is the conduction heat gain for the surface at the current time (n).

$q_{i,n-j}$, for $j = 0, 1, \ldots 23$, are respectively the input conduction heat gains j hours ago if the outdoor state were to stay at the same level steadily as at that hour, which is given by:

$$q_{i,n-j} = AU(T_{eo,n-j} - T_{ai}) \tag{3.103}$$

c_j is the conduction time factor (CTF) for j hours ago, and:

$$\sum_{j=0}^{23} c_j = 1 \tag{3.104}$$

Values of CTFs for representative walls and roofs can be found in the ASHRAE Handbook, Fundamentals [1].

When the conduction heat gains and other heat gains (except 'convective-only' heat gains) have been calculated, each would need to be split into its radiant and convective components. Typical splits between radiant and convective components of major types of heat gains of a space are given in Table 3.15. The convective components will immediately become parts of the total cooling load of the space at the time under concern (Figure 3.24). The radiant components, however, would need to be converted into cooling load by using the appropriate radiant time series (RTS), as depicted by the following equation:

$$Q_{r,n} = r_0 q_{r,n} + r_1 q_{r,n-1} + r_2 q_{r,n-2} + \cdots + r_{23} q_{r,n-23} \tag{3.105}$$

Where

$Q_{r,n}$ is the radiant cooling load for the current hour;
$q_{r,n-j}$ is the radiant heat gain at j hours ago, for $j = 0, 1, 2, \ldots, 23$; and
r_j is the radiant time factor (RTF) for heat gain at j hour ago, for $j = 0, 1, 2, \ldots, 23$.

Interested readers may refer to [2] on how the RTS model, Equation (3.105), can be derived from the TFM (Equation (3.9)).

Table 3.15 Recommended split between radiant and convective components of major types of heat gains

Heat Gain	Radiant portion	Convective portion
Wall, window conduction	0.63	0.37
Roof conduction	0.84	0.16
People	0.70	0.30
Lighting	0.67	0.33
Equipment	0.20	0.80
Transmitted solar	1.00	0.00
Absorbed solar	0.63	0.37
Infiltration	0.00	1.00

Two types of radiant time factors (RTFs) are used in design cooling load calculations, for solar heat gains and for non-solar radiant heat gains in an air-conditioned space. RTFs for solar heat gains are applied to transmitted solar heat gains through fenestrations. RTFs for non-solar radiant heat gains are applied to every other type of heat gain. The difference was due to the practice that transmitted solar heat gains were assumed to be distributed to the floor only whilst the non-solar radiant heat gains were assumed to be distributed to all surfaces (see Section 3.2.1.2) when the heat balance model was used to predict cooling loads from the heat gains for determination of the RTFs.

Representative RTFs for spaces with different thermal mass, denoted by light, medium and heavy weight constructions are provided in ASHRAE Handbook, Fundamentals [1] (*see Tables 19 & 20 of Chapter 18 in ASHRAE Handbook, Fundamentals, 2017*).

A simplified method for calculating solar heat gain through windows and skylights, which employs solar heat gain factors (SHGFs) based on the standard DSA glass and a shading coefficient (SC) for the glass concerned, has been introduced earlier. However, as mentioned above, in using the RTS method for design cooling load calculation, the transmitted solar heat gain and absorbed solar heat gain need to be dealt with separately, as different sets of radiant time factors (RTFs) are to be used for converting the heat gains into cooling loads.

Therefore, the method for calculating solar heat gains through fenestrations needs to be modified. The modified method utilizes separate transmitted and absorbed solar heat gain factors, also derived from the DSA glass.

$$\text{Transmitted solar heat gain } (TSHG) = A \cdot SC \cdot TSHGF \tag{3.106}$$

$$\text{Absorbed solar heat gain } (ASHG) = A \cdot SC \cdot ASHGF \cdot N_i \tag{3.107}$$

Where

A & SC are respectively the area and shading coefficient of the window glazing under concerned.

TSHGF & *ASHGF* are, respectively, the transmitted solar heat gain factor and absorbed solar heat gain factor, both based on the standard DSA glass.

N_i is the fraction of absorbed solar heat that flows toward the indoor space, given by:

$$N_i = \frac{h_i}{h_i + h_o} \tag{3.108}$$

Where h_o and h_i are the combined convection and radiant heat transfer coefficients for the external and internal surfaces of the glass, respectively.

The transmitted and absorbed solar heat gain factors are given by:

$$TSHGF = \tau_D I_D + \tau_d I_d \tag{3.109}$$

$$ASHGF = \alpha_D I_D + \alpha_d I_d \tag{3.110}$$

Where I_D and I_d are respectively the direct and diffuse solar intensities incident upon the glass (diffuse intensity includes diffuse radiation from the sky as well as ground reflectance).

Transmittance and absorptance of DSA glass are given by:

$$\tau_D = \sum_{j=0}^{5} t_j (\cos\theta)^j \quad (3.111)$$

$$\tau_d = 2 \cdot \sum_{j=0}^{5} \frac{t_j}{j+2} \quad (3.112)$$

$$\alpha_D = \sum_{j=0}^{5} a_j (\cos\theta)^j \quad (3.113)$$

$$\alpha_d = 2 \cdot \sum_{j=0}^{5} \frac{a_j}{j+2} \quad (3.114)$$

Where

τ_D = Transmittance for direct radiation
τ_d = Transmittance for diffuse radiation
α_D = Absorptance for direct radiation
α_d = Absorptance for diffuse radiation
θ = incident angle of direct radiation

Values of a_j and t_j are as given in Table 3.16.

Table 3.16 Values of a_j and t_j for calculation of ASHGF & TSHGF

j	a_j	t_j
0	0.01154	-0.00885
1	0.77674	2.71235
2	-3.94657	-0.62062
3	8.57811	-7.07329
4	-8.38135	9.75995
5	3.01188	-3.89922

Calculated values of *TSHGF* and *ASHGF* N_i for fenestrations of buildings in Hong Kong for 9 principal directions are given in Sections B.4.1 & B.4.2 in Appendix B. The *TSHGF* and *ASHGF* N_i values were determined based on h_o = 22.7 W/m²-K, h_i = 8.29 W/m²-K for vertical glasses, and h_i = 6.13 W/m²-K for horizontal glasses.

At this juncture, several numerical examples are given to illustrate the steps involved in design cooling load calculations.

Example 3.1 Cooling load due to solar and conduction heat gains through a window

Calculate the cooling load due to heat gains from the following window in a building in Hong Kong on a design day in August:

Area, A = 5 m²
Shading coefficient, SC = 0.45
Orientation = Southwest
Indoor design temperature = 24°C

It may be assumed that the window belongs to an air-conditioned room with heavy construction, with carpet on the floor, and the window area accounts for 50% of the external wall area.

Solution:

The heat gains through the window include:

Transmitted solar heat gain, $TSHG = A \cdot SC \cdot TSHGF$
Absorbed solar heat gain, $ASHG = A \cdot SC \cdot ASHGF \cdot N_i$
Conduction heat gain, $CHG = AU(T_{ao} - T_{ai})$

The *TSHG* is purely radiant but *ASHG* & *CHG* comprise a radiant and a convective component. The split between radiant and convective components of the *ASHG* and *CHG* is assumed to be 63% radiant; 37% convective (Table 3.15).

The other data required for the cooling load calculation can be collected from Table 19 & 20 in Chapter 18 of the *ASHARE Handbook, Fundamentals* [1], Table 3.11 and Section B.4 in Appendix B, which are summarized in Table 3.17.

For illustration purpose, the heat gain components are calculated step-by-step for 15:00 on the design day, with reference to the data shown in Table 3.17:

$TSHG = A\ SC\ TSHGF = 5 \times 0.45 \times 477.53 = 1074.4$ W
$ASHG = A\ SC\ ASHGF\ N_i = 5 \times 0.45 \times 8.78 = 19.76$ W

$ASHG(R) = 0.63 \times 19.76 = 12.45$ W
$ASHG(C) = 0.37 \times 19.76 = 7.31$ W

$U = h_i h_o / (h_i + h_o) = 6.072$ W/m^{2}K
$CHG = A\ U\ (T_{ao} - T_{ai}) = 5 \times 6.072 \times (32.9 - 24) = 270.2$ W

$CHG(R) = 0.63 \times 270.2 = 170.2$ W
$CHG(C) = 0.37 \times 270.2 = 99.98$ W

$NSHG(R) = ASHG(R) + CHG(R) = 12.45 + 170.2 = 182.65$ W
$NSHG(C) = ASHG(C) + CHG(C) = 7.31 + 99.98 = 107.29$ W

The same results for the other hours are summarized in Table 3.18.

Table 3.17 Data required for Example 3.1

Hour	RTF(TS) [a]	RTF(NS) [b]	LST	*TSHGF* [c]	*ASHGF* N_i* [d]	T_{ao} [e]	T_{ai}
0	0.49	0.38	1	0	0	29.82	24
1	0.12	0.09	2	0	0	29.68	24
2	0.06	0.06	3	0	0	29.575	24
3	0.04	0.04	4	0	0	29.47	24
4	0.03	0.04	5	0	0	29.4	24
5	0.02	0.03	6	0.424560409	0.007686915	29.47	24
6	0.02	0.03	7	32.67692801	0.591634943	29.715	24
7	0.02	0.03	8	78.0568297	1.413264673	30.31	24
8	0.02	0.03	9	115.2241169	2.086200202	30.975	24
9	0.02	0.03	10	143.4050955	2.596433344	31.57	24
10	0.02	0.02	11	173.4912323	3.141160494	32.095	24
11	0.02	0.02	12	211.114938	4.350582768	32.445	24
12	0.01	0.02	13	319.4409225	6.905321454	32.725	24
13	0.01	0.02	14	428.919906	8.141874269	32.9	24
14	0.01	0.02	**15**	**477.5264002**	**8.780180711**	**32.9**	**24**
15	0.01	0.02	16	444.7918261	8.180069102	32.69	24
16	0.01	0.02	17	321.0957847	5.897064503	32.41	24
17	0.01	0.02	18	109.3854519	2.008959019	32.06	24
18	0.01	0.02	19	28.19469403	0.51611458	31.535	24
19	0.01	0.02	20	0	0	31.15	24
20	0.01	0.01	21	0	0	30.835	24
21	0.01	0.01	22	0	0	30.52	24
22	0.01	0.01	23	0	0	30.275	24
23	0.01	0.01	24	0	0	30.03	24

[a] From Table 20 and [b] From Table 19 of ASHRAE Handbook, Fundamentals [1]; [c] & [d] From Appendix B.4; [e] From Table 3.11.

Table 3.18 Heat gains in Example 3.1

LST	TSHG	ASHG	CHG	ASHG(R)	ASHG(C)	CHG(R)	CHG(C)	NSHG(R)	NSHG(C)
1	0	0	176.7062	0	0	111.3249	65.3813	111.3249	65.3813
2	0	0	172.4555	0	0	108.647	63.80855	108.647	63.80855
3	0	0	169.2675	0	0	106.6386	62.62899	106.6386	62.62899
4	0	0	166.0795	0	0	104.6301	61.44943	104.6301	61.44943
5	0	0	163.9542	0	0	103.2912	60.66306	103.2912	60.66306
6	0.955261	0.017296	166.0795	0.010896	0.006399	104.6301	61.44943	104.641	61.45583
7	73.52309	1.331179	173.5182	0.838643	0.492536	109.3165	64.20174	110.1551	64.69427
8	175.6279	3.179846	191.5835	2.003303	1.176543	120.6976	70.88591	122.7009	72.06245
9	259.2543	4.69395	211.7742	2.957189	1.736762	133.4177	78.35645	136.3749	80.09321
10	322.6615	5.841975	229.8395	3.680444	2.161531	144.7989	85.04062	148.4793	87.20215
11	390.3553	7.067611	245.7795	4.452595	2.615016	154.8411	90.93842	159.2937	93.55343
12	475.0086	9.788811	256.4062	6.166951	3.62186	161.5359	94.87028	167.7028	98.49214
13	718.7421	15.53697	264.9075	9.788293	5.74868	166.8917	98.01577	176.68	103.7645
14	965.0698	18.31922	270.2208	11.54111	6.77811	170.2391	99.98171	181.7802	106.7598
15	**1074.434**	**19.75541**	**270.2208**	**12.44591**	**7.3095**	**170.2391**	**99.98171**	**182.685**	**107.2912**
16	1000.782	18.40516	263.8448	11.59525	6.809908	166.2222	97.62259	177.8175	104.4325
17	722.4655	13.2684	255.3435	8.359089	4.909306	160.8664	94.4771	169.2255	99.3864
18	246.1173	4.520158	244.7168	2.847699	1.672458	154.1716	90.54523	157.0193	92.21769
19	63.43806	1.161258	228.7768	0.731592	0.429665	144.1294	84.64743	144.861	85.0771
20	0	0	217.0875	0	0	136.7651	80.32238	136.7651	80.32238
21	0	0	207.5235	0	0	130.7398	76.7837	130.7398	76.7837
22	0	0	197.9595	0	0	124.7145	73.24503	124.7145	73.24503
23	0	0	190.5209	0	0	120.0281	70.49272	120.0281	70.49272
24	0	0	183.0822	0	0	115.3418	67.74041	115.3418	67.74041

Table 3.19 Cooling load calculation results for Example 3.1

LST	CL(RTS)	CL(RNS)	CL(C)	CL(Total)
1	105.61	127.72	65.38	298.71
2	95.96	125.64	63.81	285.40
3	85.21	123.90	62.63	271.74
4	75.20	122.20	61.45	258.86
5	67.98	120.74	60.66	249.38
6	65.98	120.27	61.46	247.70
7	100.28	121.50	64.69	286.48
8	157.32	125.76	72.06	355.14
9	212.35	131.22	80.09	423.67
10	259.29	136.72	87.20	483.21
11	307.46	142.07	93.55	543.08
12	364.00	146.78	98.49	609.27
13	499.02	151.78	103.76	754.56
14	654.19	155.61	106.76	916.55
15	753.09	157.86	107.29	1018.24
16	754.99	157.68	104.43	1017.10
17	635.78	155.53	99.39	890.69
18	388.22	151.32	92.22	631.75
19	243.11	146.37	85.08	474.56
20	167.91	142.40	80.32	390.64
21	139.36	139.14	76.78	355.29
22	125.18	135.92	73.25	334.34
23	118.18	133.10	70.49	321.77
24	112.79	130.30	67.74	310.83

The cooling load due to transmitted solar heat gain for hour n is given by:

$$Q_{r,n} = r_0 q_{r,n} + r_1 q_{r,n-1} + r_2 q_{r,n-2} + \cdots + r_{23} q_{r,n-23} \qquad \text{(a)}$$

Values of r_j for $j = 0$ to 23 are available from Table 3.17, under column RTF(TS). Values of $q_{r,k}$, for $k = n$ to n-23, have already been calculated and summarized under column TSHG in Table 3.18. The cooling loads due to this heat gain at various hours in the day can now be determined by using Equation (a). For example, for $n = 15$,

$$\begin{aligned} Q_{r,n} = {} & 0.49 \times 1074.43 + 0.12 \times 965.07 + 0.06 \times 718.74 + \\ & 0.04 \times 475.01 + 0.03 \times 390.36 + 0.02 \times 322.66 + \\ & 0.02 \times 259.25 + 0.02 \times 175.63 + 0.02 \times 73.52 + \\ & 0.02 \times 0.96 + 0.02 \times 0 + \ldots + 0.01 \times 63.44 + \\ & 0.01 \times 246.12 + 0.01 \times 722.47 + 0.01 \times 1000.78 \\ = {} & 753.08 \end{aligned}$$

Note that for $n = 15$, $q_{r,\,n-13} = q_{r,2}$; $q_{r,\,n-14} = q_{r,1}$; $q_{r,\,n-15} = q_{r,24}$; $q_{r,\,n-16} = q_{r,23}$; and so on.

Equation (a) can also be used to calculate the radiant portions of absorbed solar and conduction heat gains. Here, values of r_j for $j = 0$ to 23 are available from Table 3.17, under column RTF(NS). Values of $q_{r,k}$, for $k = n$ to n-23, are given under column NSHG(R) in Table 3.18. For example, again with $n = 15$,

$$\begin{aligned} Q_{r,n} = {} & 0.38 \times 182.69 + 0.09 \times 181.78 + 0.06 \times 176.68 + \\ & 0.04 \times 167.70 + 0.04 \times 159.29 + 0.03 \times 148.48 + \\ & 0.03 \times 136.37 + 0.03 \times 122.70 + 0.03 \times 110.15 + \\ & 0.03 \times 104.64 + 0.02 \times 103.29 + 0.02 \times 104.63 + \\ & 0.02 \times 106.64 + 0.02 \times 108.65 + 0.02 \times 111.32 + \\ & 0.02 \times 115.34 + 0.02 \times 120.03 + 0.02 \times 124.71 + \\ & 0.02 \times 130.74 + 0.02 \times 136.77 + 0.01 \times 144.86 + \\ & 0.01 \times 157.02 + 0.01 \times 169.23 + 0.01 \times 177.82 \\ = {} & 157.86 \end{aligned}$$

The overall results of the above calculations are summarized in Table 3.19. Figure 3.25 shows the thermal storage effect of the room fabric in redistributing the heat energy into the room over time: the heat gain is attenuated when transformed into cooling load; the cooling load exits throughout the day even when heat gain has already dropped to zero; and there is a time lag between the peak time of heat gain and that of cooling load.

As shown in Figure 3.26, the cooling load due to transmitted solar radiation dominates the overall cooling load due to heat gains through a window, and the other cooling load components are relatively stable compared to that due to transmitted solar radiation.

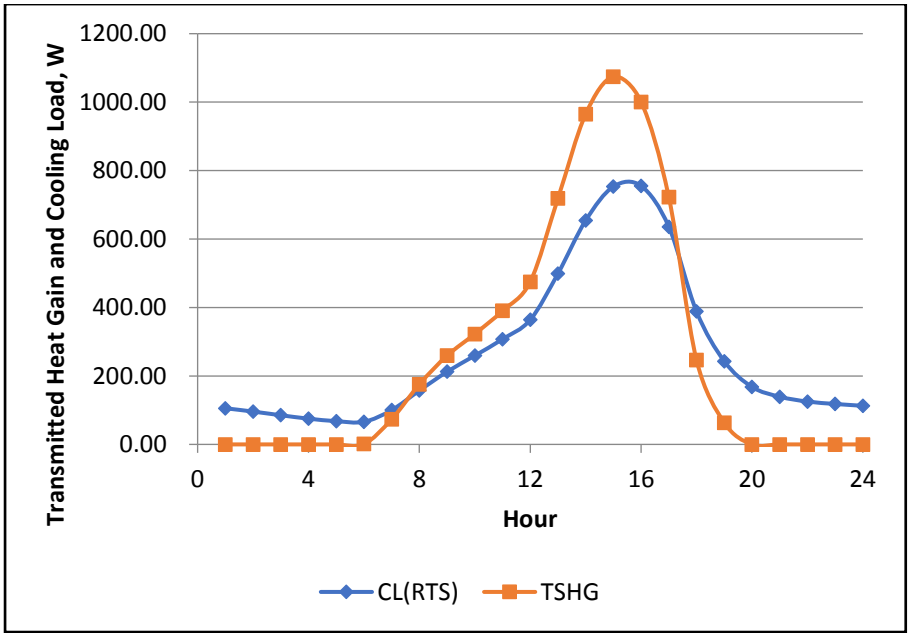

Figure 3.25 Transmitted solar heat gain and resultant cooling load

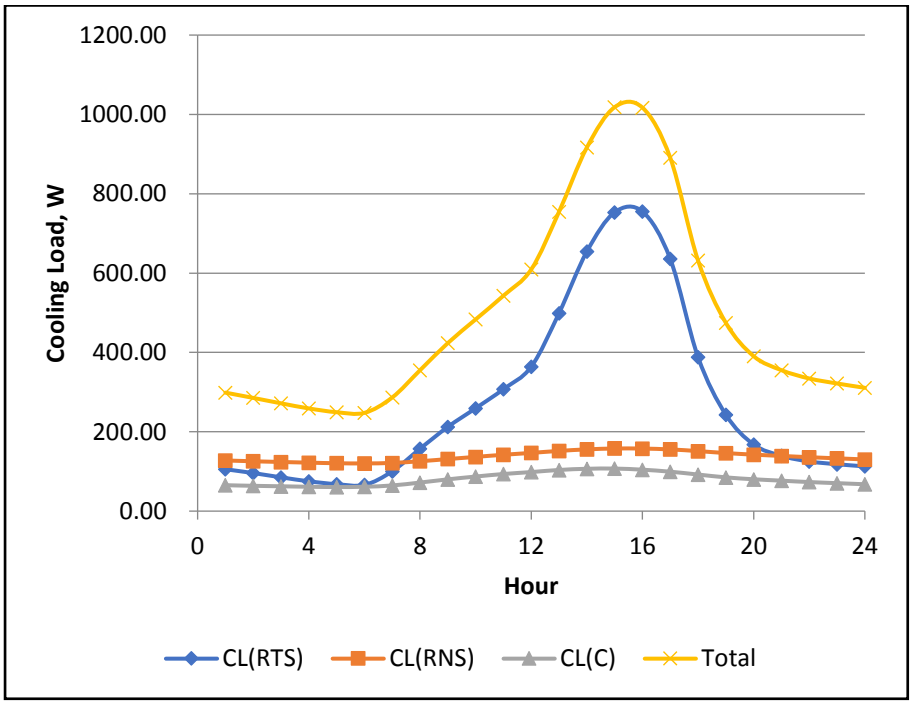

Figure 3.26 Cooling load components due to transmitted solar heat gain, radiant portion of absorbed and conducted heat gains and convective heat gains

Example 3.2 Calculation of sol-air temperature for a surface

Calculate the sol-air temperature for a wall with the following characteristics at 15:00 on a design day in August. The wall belongs to a building in Hong Kong.

Surface characteristics:

Orientation: Vertical facing Southwest
Solar absorption coefficient, $\alpha = 0.9$
Outdoor combined convective and radiant heat transfer coefficient, $h_o =$ 22.7 W/m^{2}K

Outdoor temperature, $T_{ao} = 32.9^oC$

Intensity of solar radiation upon the surface, $I_T = 593.1$ W/m^2

Solution:

The sol-air temperature is given by:

$$T_{eo} = T_{ao} + \frac{\alpha I_t}{h_o} - \frac{\varepsilon_o \Delta R}{h_o}$$

Substituting the given values of the parameters in the equation, we get:

$$T_{eo} = 32.9 + \frac{0.9 \times 593.1}{22.7} - 0 = 56.4^oC$$

Example 3.3 Calculation of conduction heat gain through a wall

Calculate the conduction heat gain through a wall of the following characteristics, by using the conduction time series. The wall belongs to a building in Hong Kong.

Surface area, $A = 11.5$m^2

$h_o = 22.7$ W/m^2-K and U-value $= 0.45$ W/m^2-K

Orientation: Vertical facing South-west

Solar absorption coefficient, $\alpha = 0.9$

Indoor temperature, $T_{ai} = 24^oC$

Design month: August

The wall is a cast concrete wall, with Conduction Time Factors (CTFs) as follows:

Hour	0	1	2	3	4	5
CTF	0.01	0.1	0.2	0.18	0.14	0.1
Hour	6	7	8	9	10	11
CTF	0.07	0.05	0.04	0.03	0.02	0.02
Hour	12	13	14	15	16	17
CTF	0.01	0.01	0.01	0.01	0	0
Hour	18	19	20	21	22	23
CTF	0	0	0	0	0	0

Solution

The first step is to calculate the sol-air temperatures (T_{eo}) throughout the day based on design outdoor air temperatures and total solar intensities incident upon the external surface of the wall at various hours in the day, and the characteristics of the wall. Data for clear sky total solar irradiance upon vertical and horizontal surfaces are available from Section B.2 in Appendix B, and design outdoor air temperatures are available from Table 3.11.

For example, at 15:00 in an August design day, the outdoor air temperature (Table 3.11) is 32.9°C. The total solar irradiance upon a SW facing vertical surface (Section B.2 in Appendix B) is 593.1 W/m^2. These are actually the conditions based upon which sol-air temperature was determined in the preceding example. The sol-air temperature, therefore, is 56.4 °C.

The same calculation is to be repeated for h=1 to 24. Note that, for a vertical surface, the sol-air temperature before sun rise and after sun set equals the outdoor air design temperature of the corresponding hour.

Having determined the sol-air temperatures, the input conduction heat gain at each hour in the day ($q_{i,h}$) can be determined as follows:

$$q_{i,h} = AU(T_{eo,h} - T_{ai})$$

For example, at 15:00,

$$q_{i,h} = 11.5 \times 0.45 \times (56.4 - 24) = 167.7$$

The calculation is to be repeated for $h = 1$ to 24.

The conduction heat gains at different hours in the day can now be determined using the input conduction heat gains at various hours and the CTFs given in the question part above:

$$q_n = c_0 q_{i,n} + c_1 q_{i,n-1} + c_2 q_{i,n-2} + \cdots + c_{23} q_{i,n-23}$$

For example, for $h = 15$, q_h is given by:

0.01 x 167.74 + 0.1 x 159.83 + 0.2 x 137.38 +
0.18 x 105.89 + 0.14 x 86.44 + 0.1 x 76.00 +
0.07 x 65.68 + 0.05 x 52.70 + 0.04 x 37.97 +
0.03 x 28.42 + 0.02 x 27.95 + 0.02 x 28.31 +
0.01 x 28.85 + 0.01 x 29.39 + 0.01 x 30.12 +
0.01 x 31.21 + 0
= 95.82

Table 3.20 summarizes the results obtained.

Table 3.20 Heat gain calculation results for Example 3.3

h	T_{ao}	T_{eo}	$q_{i,h}$	q_h
1	29.82	29.82	30.12	51.59
2	29.68	29.68	29.39	46.41
3	29.575	29.575	28.85	42.35
4	29.47	29.47	28.31	39.15
5	29.4	29.4	27.95	36.38
6	29.47	29.49107	28.42	34.11
7	29.715	31.33646	37.97	32.27
8	30.31	34.18324	52.70	31.81
9	30.975	36.69251	65.68	34.21
10	31.57	38.68588	76.00	39.77
11	32.095	40.70377	86.44	47.26
12	32.445	44.46143	105.89	55.80
13	32.725	50.54738	137.38	65.88
14	32.9	54.88496	159.83	79.22
15	32.9	**56.41393**	**167.74**	**95.82**
16	32.69	54.25682	156.58	112.65
17	32.41	47.90747	123.72	125.57
18	32.06	37.36845	69.18	130.38
19	31.535	32.92345	46.18	124.02
20	31.15	31.15	37.00	108.98
21	30.835	30.835	35.37	92.22
22	30.52	30.52	33.74	77.68
23	30.275	30.275	32.47	66.48
24	30.03	30.03	31.21	58.08
		Sum	1628.116	1628.116

Example 3.4 Calculation of cooling load due to conduction heat gain through a wall

Calculate the cooling load due to conduction heat gain through the wall discussed in Example 3.3, assuming that the radiant time factors (RTFs) used in Example 3.1 are applicable to this example.

Solution:

The same method as used in Example 3.1 for converting radiant heat gains due to conduction and absorbed solar radiation heat gains to cooling load applies. In fact, it can also be used to convert radiant heat gains from occupants, lighting, and appliances. The method involves the following processes:

- Each heat gain is split into its convective and radiant components.
- The convective components are summed to become part of the cooling load at the hour of occurrence of the heat gain.
- Radiant components summed to become part of the total non-solar heat gain for the corresponding hour.
- Radiant time series for non-solar heat gain are used to convert heat gain into cooling load.

Detail steps of the calculations are omitted here. Table 3.21 summarizes the overall results of the calculations. Figures 3.27 & 3.28 shows the results plotted in graphs.

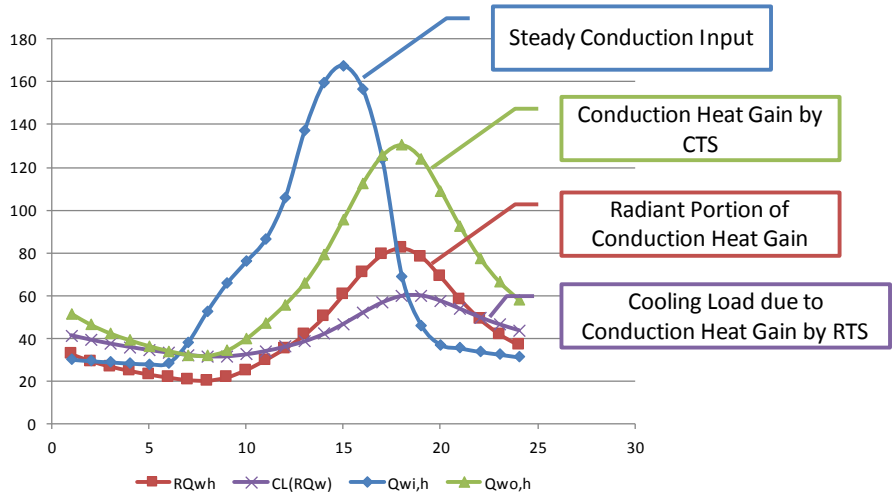

Figure 3.27 Input conduction heat gain, conduction heat gain, radiant portion of the conduction heat gain and cooling load due to the conduction heat gain

Table 3.21 Cooling load calculation results for Example 3.4

Hour	RTF(NS)	LST	RQwh	CQw	CL(RQw)	CL(Wall)
0	0.38	1	32.50055	19.08762	41.34694	60.43456
1	0.09	2	29.23996	17.17267	39.29952	56.47219
2	0.06	3	26.68174	15.67023	37.50161	53.17184
3	0.04	4	24.66673	14.48681	35.92271	50.40952
4	0.04	5	22.91897	13.46035	34.50138	47.96173
5	0.03	6	21.49237	12.6225	33.27127	45.89377
6	0.03	7	20.32874	11.9391	32.20805	44.14715
7	0.03	8	20.04283	11.77118	31.51767	43.28885
8	0.03	9	21.55205	12.65755	31.55922	44.21677
9	0.03	10	25.05797	14.71659	32.47853	47.19512
10	0.02	11	29.77594	17.48745	34.03779	51.52524
11	0.02	12	35.15574	20.64702	36.02224	56.66926
12	0.02	13	41.50579	24.37642	38.53146	62.90787
13	0.02	14	49.90813	29.31113	42.02701	71.33814
14	0.02	15	60.36862	35.45459	46.68067	82.13526
15	0.02	16	70.96844	41.67988	51.90548	93.58536
16	0.02	17	79.10725	46.45981	56.64924	103.1091
17	0.02	18	82.14	48.24095	59.65867	107.8996
18	0.02	19	78.13141	45.8867	59.82065	105.7073
19	0.02	20	68.65691	40.32231	57.29908	97.62139
20	0.01	21	58.10051	34.12252	53.56657	87.68909
21	0.01	22	48.93645	28.74045	49.76654	78.50699
22	0.01	23	41.88501	24.59913	46.453	71.05213
23	0.01	24	36.59103	21.48997	43.68786	65.17783
Sum			1025.713		1025.713	

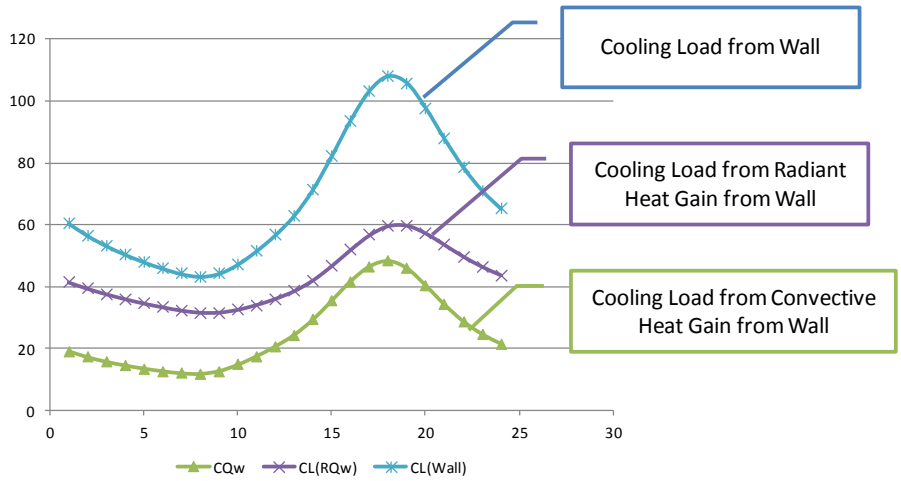

Figure 3.28 Radiant and convective components of cooling load from a wall

3.4.3 Internal and other heat gains and cooling load

Sensible and latent heat gains from occupants, $Q_{occ,s}$ & $Q_{occ,l}$ are to be determined based on the heat gain per person and the total number of occupants in the space, as follows:

$$Q_{occ,s} = q_{occ,s} N_{occ} \tag{3.115}$$

$$Q_{occ,l} = q_{occ,l} N_{occ} \tag{3.116}$$

Where

$q_{occ,s}$ & $q_{occ,l}$ are, respectively, the sensible and latent heat gains per occupant (dependent on activity level of the occupant); and

N_{occ} is the number of occupants in the space (often determined from an occupancy density and floor area of space).

The sensible part of the heat gain comprises a radiant and a convective portion, and the radiant portion needs to be converted into cooling load using the non-solar RTFs.

Heat gains from lighting and appliances, Q_{lgt} & Q_{app}, are often estimated from a load density figure and the floor area of the space involved:

$$Q_{lgt} = A \cdot q_{lgt} \tag{3.117}$$

$$Q_{app} = A \cdot q_{app} \tag{3.118}$$

Where

q_{lgt} & q_{app} are, respectively, the lighting and appliances heat gains per unit floor area (both are sensible heat gains); and

A is the floor area of the space

Each of the above heat gains comprises a radiant and a convective portion, and the radiant portion needs to be converted into cooling load using the non-solar RTFs.

Calculation of the sensible and latent cooling load due to fresh air supply, $Q_{fa,s}$ & $Q_{fa,l}$, is based on the flow rate and the indoor and outdoor air states:

$$Q_{fa,s} = \rho V_{fa} Cp_a (T_{ao} - T_{ai}) \quad (3.119)$$

$$Q_{fa,l} = \rho V_{fa} (w_{ao} - w_{ai}) h_{fg0} \quad (3.120)$$

Where

V_{fa} is the fresh air supply rate for the space(s), often determined from the occupancy density, floor area and ventilation rate per person to be allowed.

T_{ao} and w_{ao} are the dry bulb temperature and moisture content of outdoor air at the design condition for the month and hour under concern.

T_{ai} and w_{ai} are the dry bulb temperature and moisture content of indoor air at the design condition.

Note that the above equations can be applied directly for the purposes of determining the block cooling load on the central chiller plant. In determining the capacity required of a fresh air-handling equipment, however, the leaving coil condition should be used in lieu of the indoor air condition (see later discussions on air-side air-conditioning systems).

The sensible and latent cooling load due to infiltration, $Q_{inf,s}$ & $Q_{inf,l}$ are to be evaluated by:

$$Q_{inf,s} = \rho V_{inf} Cp_a (T_{ao} - T_{ai}) \quad (3.121)$$

$$Q_{inf,l} = \rho V_{inf} (w_{ao} - w_{ai}) h_{fg0} \quad (3.122)$$

Where

V_{inf} is the infiltration rate for the space, often determined from the air change rate of infiltration (e.g. 0.5 air change per hour) and the internal volume of the space.

T_{ao} and w_{ao} are the dry bulb temperature and moisture content of outdoor air at the design condition for the month and hour under concern.

T_{ai} and w_{ai} are the dry bulb temperature and moisture content of indoor air at the design condition.

3.4.4 Remarks

Hourly design cooling load calculation for each air-conditioned space needs to be carried out for one design day per month from June to Dec. This is needed to allow the peak cooling load of individual spaces, which may arise at different times among different spaces, to be identified from the results.

The peak value of the total cooling load of a group of spaces, such as rooms on the same floor served by a common air-handling system, may differ from the sum of peak cooling loads of the spaces. The air-handling system serving a group of spaces should be sized with reference to the simultaneous peak cooling load of the spaces while terminal devices serving individual spaces should be sized according to the peak cooling load of the space concerned.

In sizing the cooling capacity of the central chilled water plant, the following allowances should be made to cater for the fan and pump heat gains:

- An allowance of about 5% of the block total sensible cooling load, to cater for the fan heat gain.

- An allowance of about 3% of the block total cooling load (including the above allowance for fan heat gain) to cater for the heat gains from the chilled water pumps.

References

[1] ASHRAE Handbook, Fundamentals, American Society of Heating, Refrigerating and Air-Conditioning Engineers, Inc., Atlanta, 2017.

[2] Underwood CP, Yik FWH, Modelling Methods for Energy in Buildings, Blackwell Publishing Ltd., Oxford, 2004.

[3] Jones WP, Air-conditioning Engineering, 3rd ed., Edward Arnold, 1992.

[4] CIBSE Guide A – Environmental Design, The Chartered Institution of Building Services Engineers, London, 2015.

[5] McQuiston FC, Parker JD & Spitler JD, Heating, Ventilating and Air Conditioning: Analysis and Design, 6th Ed., John Wiley & Sons, New York, 2005.

[6] Bergman TL, Lavine AS, Incropera FP, DeWitt DP, Fundamentals of Heat and Mass Transfer, 8th Edition, John Wiley & Sons, Inc., 2017.

[7] Code of Practice for Energy Efficiency of Building Services Installation, Electrical and Mechanical Services Department, Government of the Hong Kong SAR, 2018.

Chapter 4 Air Side Air-conditioning Systems

4.1 Introduction

A central air-conditioning system typically comprises a central water-side system and multiple air-side systems. The air-side systems are responsible for treating the air in the air-conditioned spaces, or the air drawn-in from outdoors for ventilation, while the water-side system supplies chilled and/or hot water to the air-side systems to enable them to perform their functions (Figure 4.1). There may be several to hundreds of air-side systems in an air-conditioned building, depending on the size of the building, the kind of air-side system design adopted, and the zoning of spaces served by the systems.

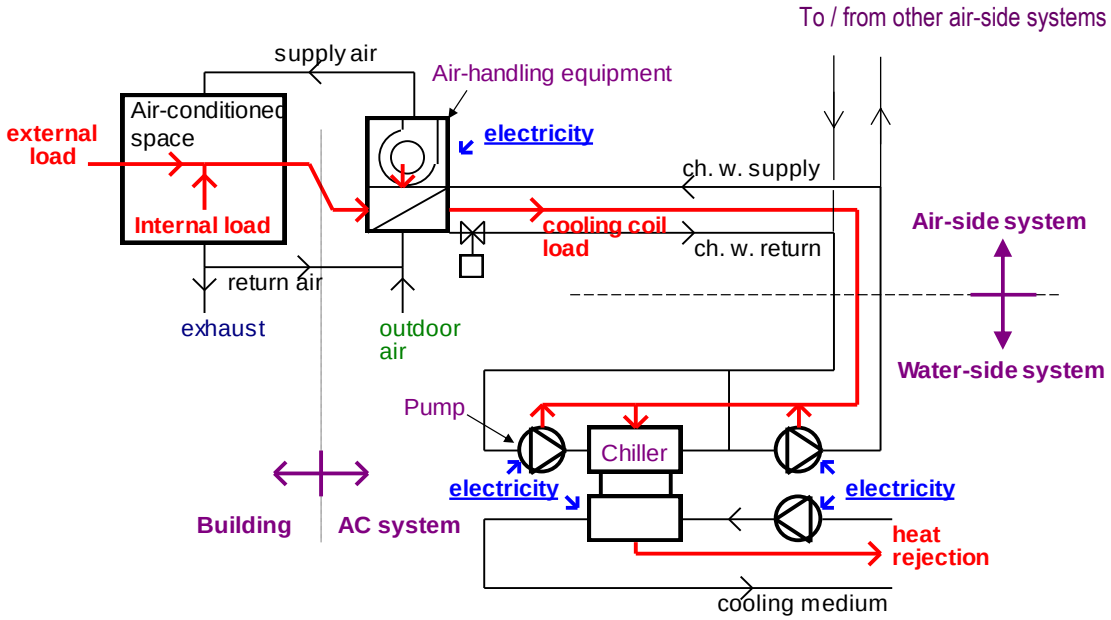

Figure 4.1 Relation between air-side and water-side systems in a central air-conditioning system

An air-side system is composed of one or more air-handling equipment, a ducting system, automatic control supply and power systems, and associated accessories. For an air-side system that serves one or a few air-conditioned spaces in a building, the air in the space(s) is drawn by a fan in the air-handling equipment to flow toward and through the filter(s) and coil(s) in the equipment that treat the air. The treated air is then supplied by the fan through a ducting network back to the space(s), thus completing a cycle. Within this cycle, some air may be disposed of and replenished by fresh outdoor air, which may or may not have been pre-treated. The kind of air-side system dedicated for treating outdoor fresh air is called a fresh air handling system, which will also distribute the treated fresh air to the air-conditioned spaces directly or through the air-side systems serving the spaces.

A piece of air-handling equipment typically comprises an insulated metal casing, a fan, a coil, air-filters, control devices and other accessories, and may be called, depending on its capacity, an air-handling unit (AHU) or a fan-coil unit (FCU). Large AHUs are normally housed inside dedicated plant rooms, often called AHU rooms, and may have

separate supply and return fans, cooling and heating coils, and rough and high efficiency air-filters, as well as other components, e.g. humidifier, total heat recovery wheel, heat pipes, etc. Small AHUs and FCUs may be installed inside the air-conditioned spaces, e.g. inside the false ceiling void above an occupied space.

The air-handling equipment of the air-side systems rely on the water-side system to feed them with chilled water and, where applicable, also hot water, for performing the cooling, dehumidifying, and heating functions. After exchanging heat with the air inside the coil in the air-handling equipment, the chilled or hot water will return to the main plant of the water-side system for treatment, after which it will be distributed again to the air-side systems.

The focus of this and the next chapter is on the design and operating principles of the types of air-side air-conditioning system most commonly adopted in commercial buildings. Water-side systems, each comprising a central chiller plant, a chilled water circulation system and, where applicable, heating equipment and a hot water circulation system, will be discussed in Chapters 6 to 8 & Chapter 10. Air-side systems discussed in this and the next chapter may also serve as heating equipment and will not be repeated in Chapter 10, but brief coverage will be given there on those types of space heating systems and equipment that have not yet been mentioned.

4.1.1 Characteristics of space cooling load

An understanding of the cooling load characteristics of the spaces to be served by an air-side system is essential to proper system selection and sizing of the associated air-handling equipment, air ducts and water pipes. The key characteristics to be examined include:

1. The peak cooling loads of individual air-conditioned spaces, and by how much the cooling loads may vary, i.e. the range between the peak and minimum cooling loads of the spaces within a day and throughout the year.

2. Whether heating will be required by the spaces in winter and, if so, the peak heating loads of the spaces and the range of variation of the heating loads.

3. When heating is needed in some spaces, whether cooling will still be called for in the other spaces at the same time.

4. The simultaneous peak cooling loads and, where applicable, the simultaneous peak heating loads, of collections of spaces served by the air-side system and its equipment and components (e.g. main duct section), and the possible range of variation of the loads.

5. Any specific requirements with respect to the temperature, humidity, pressure relative to adjoining spaces, and cleanliness of the air in the air-conditioned spaces, and whether or not re-circulation of the air is allowed.

Some or all requirements stated in item 5 in the above list are relevant to systems serving healthcare buildings, laboratories, archives, datacentres, premises for

manufacturing hi-tech products, etc. Air-conditioning systems that can meet such requirements are specialized systems and each would require a thorough treatment to enable readers to adequately carry out design work for such systems. However, to avoid making this book too voluminous, no coverage on these systems is given here. Our focus remains buildings and premises where only comfort air-conditioning is needed.

Many factors can affect the cooling load of an air-conditioned space, such as thermal characteristics of the building fabric elements, location of the space relative to the building envelop and non-air-conditioned spaces, changes in solar position, cloud cover, outdoor air temperature and humidity, the occupation schedule, characteristics of the internal loads, etc. As shown in Figure 4.2, for a floor with substantial area, the space would typically be partitioned, and there will be rooms around the perimeter, referred to here as the perimeter zone, and spaces in the central part, the interior zone.

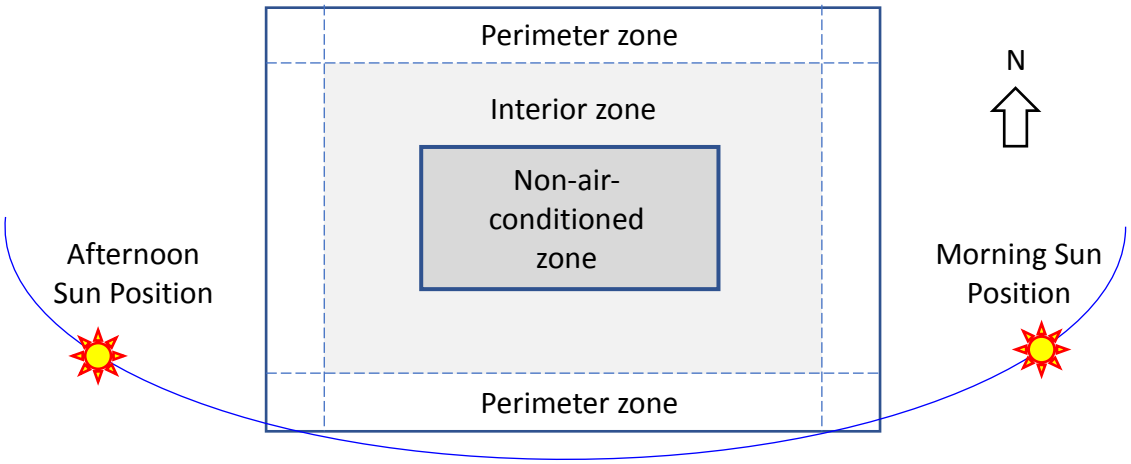

	Perimeter Zone	Interior Zone
Cooling load due to solar heat gains and conduction heat gains	Dominant	Absent or small*
Cooling load due to internal heat gains	Present	Dominant
Cooling load pattern	Variable	Relatively steady*
Summer operation	Cooling	Cooling
Winter operation	Cooling &/or Heating	Cooling*

* Spaces on a floor immediately below the roof level may be exceptions.

Figure 4.2 Characteristics of perimeter and interior zones in a building

On a sunny day, the direct and diffuse solar radiation transmitted through windows into a room in the perimeter zone will be intercepted by the partition walls and the ceiling and floor slabs enclosing the room. Therefore, having entered a room, solar radiation cannot reach any other rooms in the building. Similarly, heat gains of a room due to conduction through the external wall and window, and the roof and skylight, if applicable, will affect primarily that room, with little effect on adjacent rooms. With temperatures of the rooms in both the perimeter and the interior zones controlled at

the same level, those spaces in the interior zone are subject primarily to internal heat gains, including heat gains from lighting and equipment, the occupants, and any processes in the space that generate sensible and/or latent heat.

In general, the cooling loads of perimeter zones of a building may vary by much greater extents compared to those of interior zones. In winter when the outdoor temperature is low and solar heat gain is absent or small, the cooling load of the perimeter zone may drop below zero, in which case heating is required. The internal heat gains tend to be more stable and may vary according mainly to the occupancy schedule of the space. As the interior zone is isolated from the outdoors, there is no path through which the heat gains from the internal sources may be taken away except through the air-conditioning system, and this remains applicable irrespective of the outdoor weather. Therefore, cooling would be required throughout the year for the interior zones of an extensive building, even when heating is called for in some spaces in the perimeter zone.

4.1.2 Air-side system equipment and components

The air-handling equipment of an air-side air-conditioning system plays a crucial role in the function served by the system; it is at the front-line, responsible for treating (including heating, cooling, humidifying, dehumidifying, and filtering) the air and driving the air to re-circulate between the equipment and the air-conditioned space. The major components of an air-handling equipment include (Figure 4.3):

- Coil(s) for facilitating heat exchange between the air and the medium of cooling/heating, chilled or hot water.

- Fan(s) for delivering the treated air to the air-conditioned space, i.e. the supply air (SA), and extracting air from the air-conditioned space back to the equipment, i.e. the return air (RA) (a single fan can serve both purposes).

- Filters for removal of particulates suspended in the air, which may involve rough filters and high efficiency filters.

- An insulated casing made up of a steel structural frame and sheet metal panels with insulation, for housing the above components.

As mentioned above, air-handling equipment that is large in size is called an air-handling unit (AHU) and a small one a fan coil unit (FCU) (Figure 4.3a & 4.3b). In a variable air volume (VAV) system (see later descriptions), there are also VAV terminals (Figure 4.3c) that regulate the amount of air to be supplied into the air-conditioned spaces for controlling the temperature in the spaces. Some equipment, such as chilled ceilings and chilled beams, do not have a fan. The systems mentioned here, including CAV and VAV systems, primary air fan coil systems, and chilled ceiling and beam systems, and the equipment in such systems, will be discussed in detail in later sections.

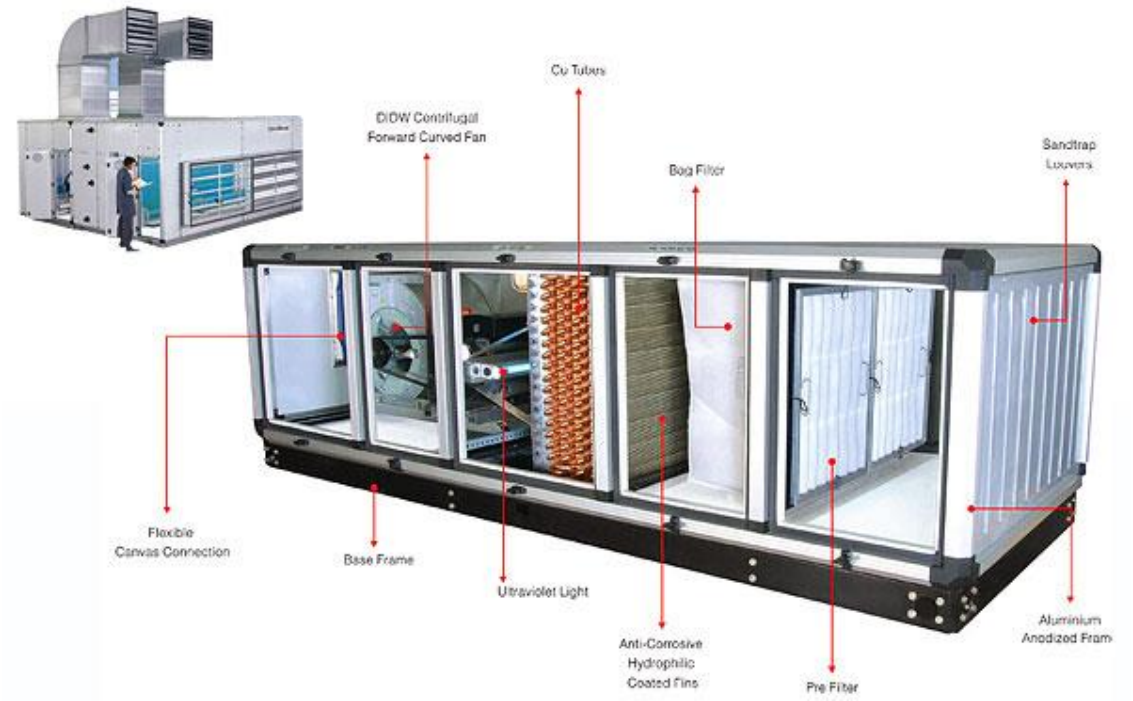

a) An air-handling unit (AHU)

b) A fan coil unit (FCU)

c) A VAV terminal

Figure 4.3 Air-handling equipment in a central air-conditioning system

The component in an air-handling equipment that outputs cooling or heating is the cooling or heating coil, which is typically made of copper tubes that pass through and are bonded to a stack of aluminium (or sometimes copper) plate fins at regular spacing (often quantified in terms of number of fins per inch) (Figure 4.4). The copper tubes are arranged into several rows, and the chilled or hot water may be distributed to tubes in half, one or two rows, and will make a few passes before returning to the central chilled and hot water plant.

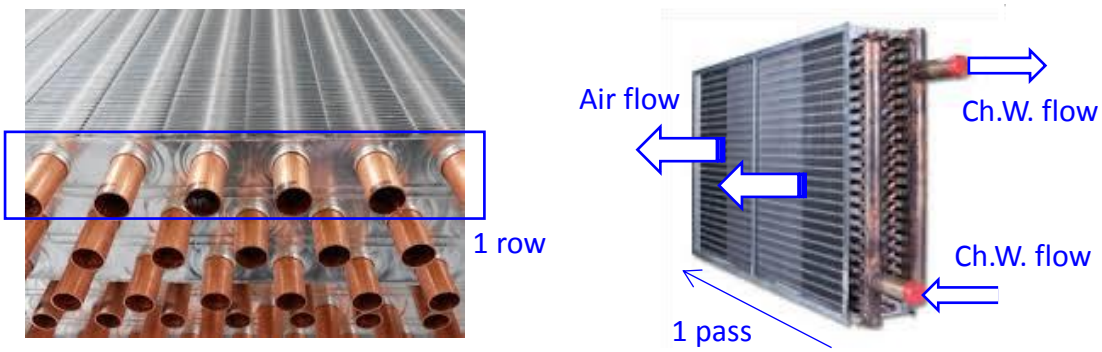

Figure 4.4 Fins and tubes inside a cooling or heating coil

The air is cooled and dehumidified, or heated, when it is induced by the fan to flow through the gaps between the fins. Dehumidification will take place only when the air is in contact with fin surfaces that are maintained at a temperature below the dew point of the air, resulting in condensation of water vapour in the air into liquid water droplets, which will eventually fall from the fin surfaces onto a drain pan below the coil.

4.1.3 Basic automatic control for HVAC systems

Note that for comfort air-conditioning, most air-conditioning systems would have active control over only the dry bulb temperature of the indoor air. Nevertheless, while providing cooling for indoor temperature control, the system will output a certain amount of dehumidification, but the amount of latent cooling that can be provided is not subject to active control. Consequently, the indoor air moisture content or relative humidity may vary (float) dependent on the balance between the rate that moisture is added to the indoor air by external and internal sources and the rate that moisture is removed by the air-conditioning system. This is referred to as 'passive humidity control'. Of course, systems that can provide active control over both indoor temperature and humidity are available, but they involve extra equipment and consume more energy.

As will be highlighted in the next section, the way in which an air-side air-conditioning system is controlled defines the type of air-side system it belongs. In fact, the operating performance of an air-side system, and its suitability for the cooling load characteristics of a particular type of premises, are largely influenced by the control strategy applied. Therefore, a good understanding of the control system associated with an air-side system is essential to system designers and operation and maintenance (O&M) personnel.

A brief summary of the basic features of automatic control systems employed in air-conditioning systems is given in Annex A of this chapter, to facilitate readers who need to refresh their knowledge in automatic control. The functions of the control system for each type of air-side air-conditioning system covered in the following sections will be discussed in detail.

4.2 Operating and control principles of CAV and VAV systems

Figure 2.23 in Chapter 2 shows the schematic diagram applicable to a large family of air-side systems called 'all air' systems. The reason for this name is that only air will be supplied into, and return from, the air-conditioned space for providing it with air-conditioning. There is another family of air-side systems, called 'air-water' systems, which will have both air and water flowing into and out of the air-conditioned space via the associated air ducts and water pipes when the air-conditioning systems are running. The primary air fan coil system and chilled ceiling/beam system, which will be discussed later, belong to the air-water systems.

Except the chilled ceiling/beam system, the conventional all air cycle discussed in Section 2.6 in Chapter 2 is the starting point of system design for all kinds of air-side air-conditioning systems. The design cooling coil capacity, the design supply air flow rate and the design chilled water flow rate are to be determined in an analysis of the conventional all air cycle. The distinction between different types of air-side system are often based on the way in which indoor temperature control is performed.

4.2.1 Room air temperature control for an air-conditioned space

Consider an air-conditioned space with internal volume V_r, as shown in Figure 4.5. The temperature of the air inside the space is denoted by T_r. The sensible cooling load of the room due to heat gains from external sources is $q_{ext,s}$ and that from the internal sources $q_{int,s}$. At the same time, the air-conditioning system is extracting sensible heat from the space at the rate of q_s.

The deviation between the sensible cooling load of the air-conditioned space and the sensible cooling output of the system, δq_s, is given by:

$$\delta q_s = q_{ext,s} + q_{int,s} - q_s \tag{4.1}$$

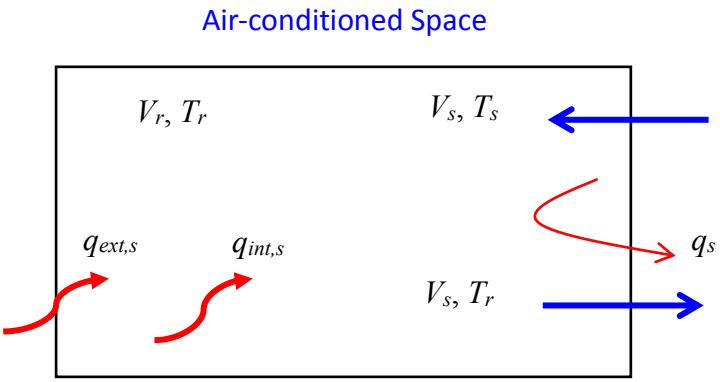

Figure 4.5 Sensible Heat Balance in an Air-conditioned Space

Whenever the deviation differs from zero, the space air temperature, T_r, will rise or drop at a rate as depicted by the following equation:

$$\rho_a V_r Cp_a \frac{dT_r}{dt} = q_{ext,s} + q_{int,s} - q_s \quad (4.2)$$

Where

ρ_a = density of air
Cp_a = specific heat of air
t = time

However, the major objective of designing and operating an air-conditioning system is to achieve a stable indoor temperature ($T_r \cong$ Const.) that equals the design indoor temperature for the premises concerned. If T_r is kept at a constant level, the dT_r/dt term, and the left-hand side of Equation (4.2), will be equal to zero, which can be satisfied only if the sensible cooling output of the air-conditioning system matches exactly with the sensible cooling load of the space, even though the latter may vary from time to time:

$$q_s = q_{ext,s} + q_{int,s} \quad (4.3)$$

The rate of sensible cooling provided by the air-conditioning system, q_s, is given by the following equation:

$$q_s = \rho_a V_s Cp_a (T_r - T_s) \quad (4.4)$$

Where V_s is the supply air flow rate and T_s the supply air temperature.

The crux of room temperature control, therefore, is to regulate from time to time the sensible cooling output of the air-side system such that it will match closely with the dynamic room sensible cooling load. Inspection of Equation (4.4) unveils that the air density, ρ_a, and specific heat, Cp_a, cannot be varied while keeping the room air temperature, T_r, at a stable level is a major objective to be achieved (Figure 4.6a). The remaining variables that can be varied to regulate the sensible cooling output of the system for controlling T_r include V_s and T_s (Figure 4.6b).

Given that varying any one of the two variables can already change the sensible cooling output to match with the total external and internal sensible cooling loads, for simplicity sake, we should avoid varying both of them at the same time, as this may lead to system reactions that counter each other. Therefore, between the two variables V_s and T_s, we have to choose one to regulate for indoor air temperature control. If we choose to fix V_s and vary T_s, the system will be a constant air volume (CAV) air conditioning system. If we choose to fix T_s and vary V_s instead, the system will become a variable air volume (VAV) air conditioning system.

4.2.2 Constant air volume (CAV) system

As shown in Figure 4.7, a CAV system comprises a fan driven by a constant speed motor, which will deliver a constant supply air volume flow rate; a cooling and dehumidifying coil fed with chilled water from a water-side system; and a control system that includes a room temperature sensor, a controller, and a control valve that regulates the flow rate

of chilled water flowing through the cooling and dehumidifying coil. Variation of the supply air temperature, T_s, to cope with variation in the room sensible cooling load is done by regulating the flow rate of chilled water flowing through the cooling and dehumidifying coil.

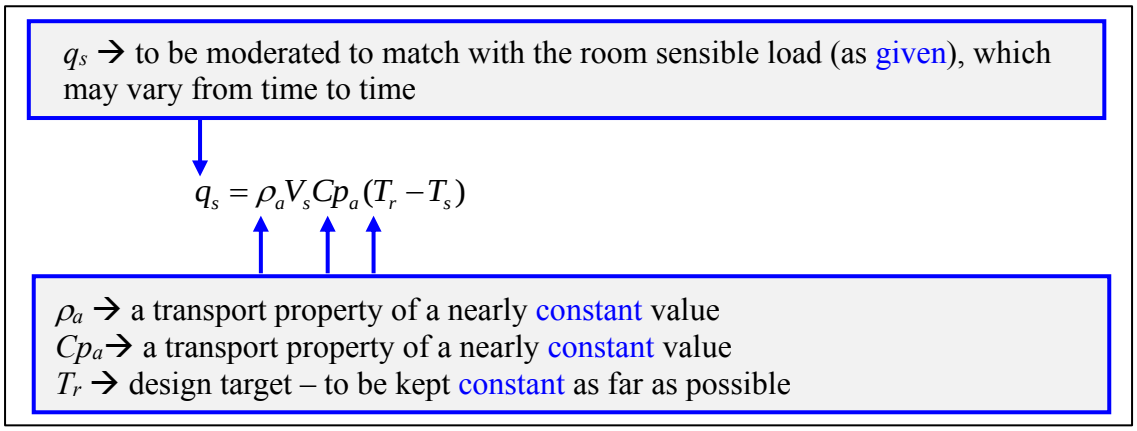

a) Terms that cannot be varied for control purpose

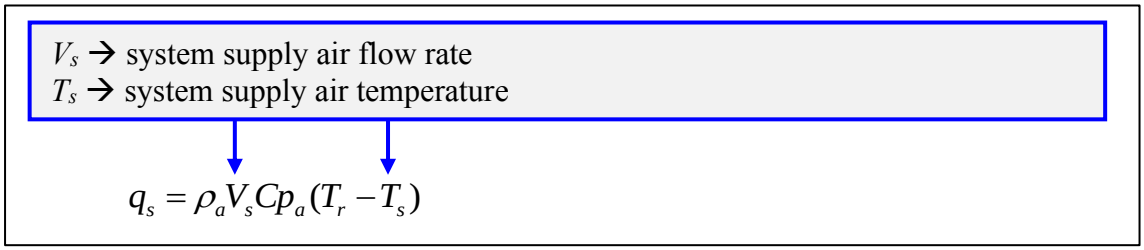

b) Terms that can be varied for control purpose

Figure 4.6 Terms that can and cannot be varied to regulate the sensible cooling output of an air-side air-conditioning system

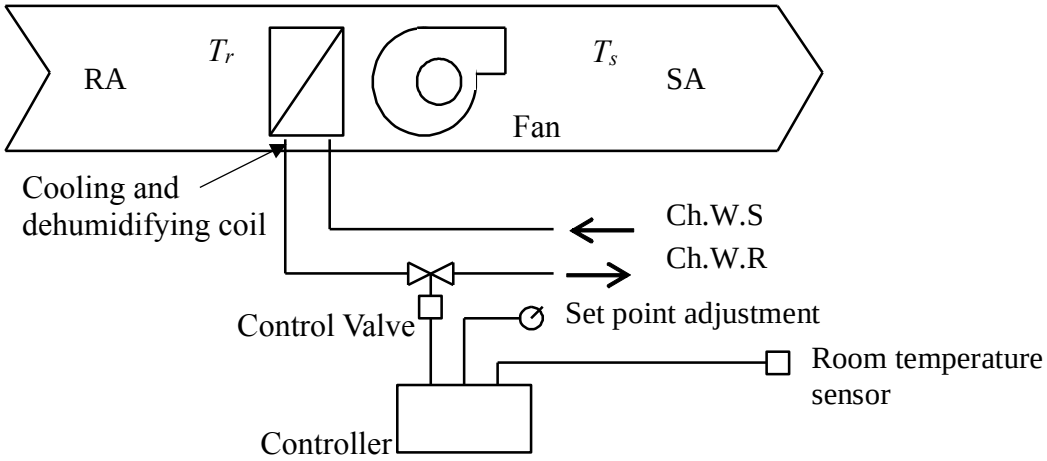

Figure 4.7 A constant air volume (CAV) system

Assume that the CAV system (Figure 4.7) is initially operating steadily under a specific operating condition, with the room air temperature T_r and supply air temperature T_s achieving steady values but, since then, the sensible cooling load of the room has risen by a finite amount. Before the system can respond to this change, the return air temperature T_r will rise and, consequently, the supply air temperature T_s will rise too.

When the room temperature error, e ($e = T_r - T_{r,sp}$; $T_{r,sp}$ = set point value of T_r), increases, the controller will step up its output signal to the control valve, which will then open wider to allow more chilled water to flow through the cooling and dehumidifying coil (this definition of e for a cooling system will be used consistently in this book; see also 4A.2.3 in Annex A). With increased chilled water flow rate, the coil will provide a greater cooling output, which will cause T_s to drop. As a result, the sensible cooling effect to the room will increase which will cause T_r to drop. This corrective action will stop when T_r settles on a steady value within the throttling range, if proportional (P) control is used, or on the set-point, if proportional plus integral (PI) or proportional plus integral plus derivative (PID) control is used.

If the sensible cooling load of the room is now reduced, the room / return air temperature T_r and the supply air temperature T_s will both drop. Therefore, the deviation between T_r and the set-point value (e) will decrease, and, in response, the controller will step down its output signal to the control valve, which will then close by a commensurate amount to reduce the rate of chilled water flowing through the cooling and dehumidifying coil. With a smaller chilled water flow rate, the coil will provide less cooling output, which will cause T_s to rise. As a result, the sensible cooling effect to the room will drop which will cause T_r to rise. This corrective action will stop when T_r settles again on a steady value within the throttling range, or on the set-point, depending on whether P or PI or PID control is used.

It follows from the above analysis of the response of the CAV system to changes in room sensible load that the supply air temperature T_s would be the lowest, and the value of ($T_r - T_s$) the highest, when the system is operating steadily under the design load. After adjustment of the chilled water flow rate in response to a load reduction and steady operation attained once again, T_s will assume a higher value under the part-load condition, and it will approach the room air temperature T_r if the room sensible load drops to a very low value. Figure 4.8 shows the psychrometric cycles for a CAV system when the system is operating steadily under the design condition and a part-load condition with the sensible load approximately halved, as unveiled by the proportion of the width of ($T_r - T_s'$) to that of ($T_r - T_s$).

The supply air temperature under part-load condition, T_s', can be evaluated from the room sensible cooling load under the part-load condition, q_s', as follows:

$$T_s' = T_r - \frac{q_s'}{\rho_a V_s C p_a} \tag{4.5}$$

Recall our discussions in Chapter 2, Section 2.5.3, as long as the air is being dehumidified, the leaving coil condition of the air at the end of the cooling and dehumidification process in the coil may be taken as at 95% degree of saturation, which applies to both the design and the part-load conditions, i.e.:

$$\mu_l = \mu_l' = 0.95$$

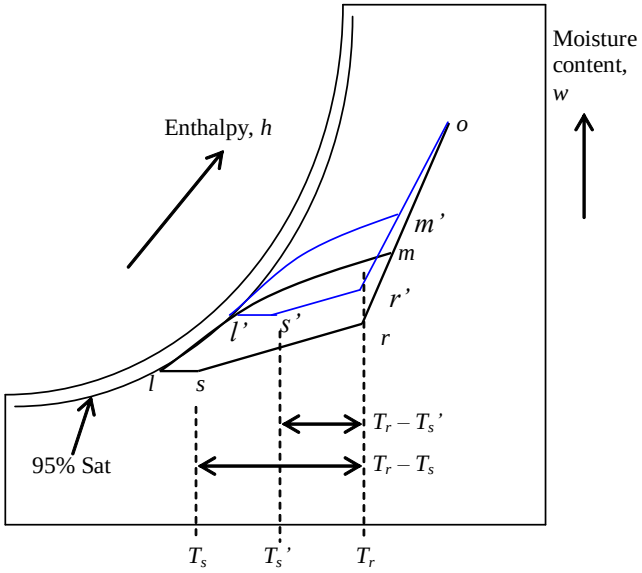

Note: In this figure, the design cycle is shown with state points denoted by *l*, *s*, *r*, *m* and *o*, and process lines in black. The part-load cycle is shown with state points denoted by the same range of alphabets with an apostrophe, and process lines in blue.

Figure 4.8 Design and part-load cycle of a CAV system

Given the following conditions:

- The control system is keeping the indoor air temperature T_r at or within a small margin about the set point temperature.

- The supply air temperature T_s will rise in part-load operation to T_s' and, therefore, the horizontal distance between the supply air and room air state points *s'* and *r'* on a psychrometric chart will be shortened in part-load operation, with the state point *s'* moved toward the room air state point *r'*.

- The temperature difference between the supply air and the air leaving the cooling coil, which represents the fan heat gain, should remain unchanged, i.e.:

  $$(T_s - T_l) = (T_s' - T_l)$$

The only way that all the above conditions on the leaving coil air state (*l'*), supply air state (*s'*) and the room air state (*r'*) can be fulfilled under a part-load condition is to have the three state-points *l'*, *s'* & *r'* all moved upward on the psychrometric chart (Figure 4.8). This implies that when a CAV system is running under part-load condition:

- The supply air flow rate and thus the fan power demand will remain unchanged.

- The supply air temperature and moisture content will both become higher than those corresponding to the design supply air state.

- The indoor air moisture content (and relative humidity) will rise, which is an inherent characteristic of a CAV system.

As stated above, when a CAV system is running under part-load condition, inevitably, the relative humidity of the indoor air state, *r*, will rise and it may rise beyond an acceptable limit. For preventing indoor air humidity from rising above a high limit, the air may be cooled down to well below the required leaving coil temperature such that the supply air moisture content is low enough to prevent a high indoor relative humidity. However, this will require reheating the air so as to keep the indoor temperature under control (Figure 4.9).

Figure 4.9a shows the space air diffusion process with (*s*"-*r*') and without (*s*-*r*) a preceding reheat process. In this example, *r* is the indoor air state that will result from reduced room sensible load, which is regarded as too humid. By further cooling the air from state *l* to *l'*, the moisture content of the new supply air state, *s'*, will be much lower than that at the original supply air state, *s*, which will ensure the moisture content of the new indoor air state will be lower than state *r*. The reheat process *s'* to *s*" brings the air temperature up from $T_{s'}$ to T_{s}", which equals T_s, such that the indoor temperature T_r can be kept.

Figure 4.9b shows the schematic diagram for a CAV system with a high-limit room air humidity control function included in the control system. As shown in this figure, the chilled water flow rate through the cooling coil is controlled according to either the return air temperature or humidity, depending on which represents a stronger demand. This means that if the humidity is low, chilled water flow rate control will be performed to keep the return air temperature under control. However, when the room air humidity is high, the signal from the humidity sensor will rise above the temperature signal and the higher-of-two selector switch (Module C) will then pass the humidity signal to the chilled water controller.

In this mode of operation, the leaving coil air temperature will be lowered for preventing the room air humidity from rising above a high limit (the set point) but the air will be too cold for the air-conditioned space. As a result, the room air temperature will drop, and this will be picked up by the return air temperature sensor which feeds the signal not only to Module C but also to Module B, which is the hot water flow controller, for reheating the air to a suitable temperature for maintaining the indoor air temperature at or nearby the set point value. The control schematic diagram shown in Figure 4.9b is based on the use of discrete control modules. With direct digital control (DDC), nowadays, the functions of these control modules will be replaced by a control algorithm embedded in a building management system (BMS).

Note should be taken that reheat is wasting energy as the air is first cooled and then heated up, which will involve cancellation of the cooling and heating efforts both of which require use of energy. Therefore, the reheat process should be avoided if at all possible, and it, if used solely for comfort air-conditioning, may be prohibited by regulatory controls over building energy performance.

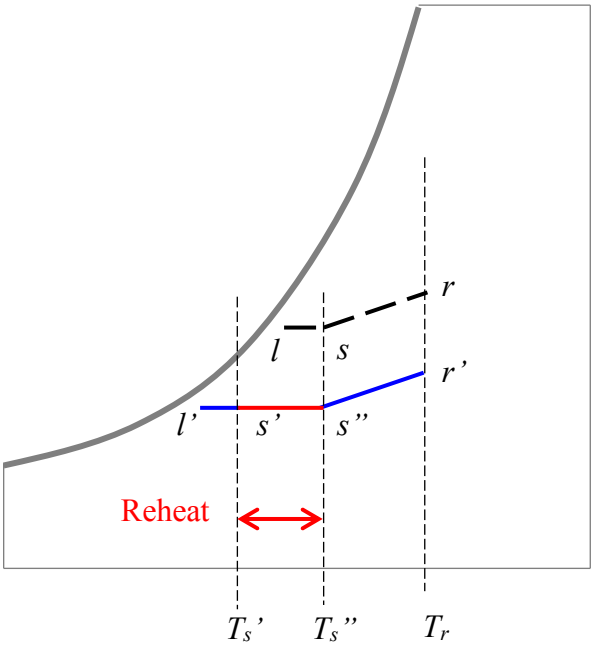

a) Space air diffusion process with and without preceded by a reheat process

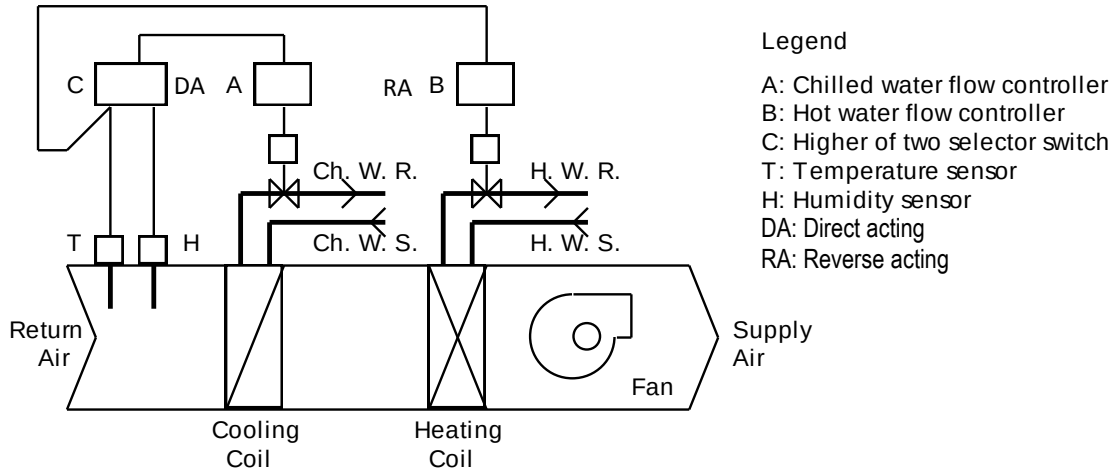

b) Control system schematic for a high-limit humidity control by reheat

Figure 4.9 CAV System with high-limit room air humidity control by reheat

Another limitation of a CAV system is that it can only respond to one room temperature feedback signal. If a CAV system is used to serve multiple rooms, only the temperature of the room where the temperature sensor is located can be put under control while all the other rooms may be over- or under-cooled. For example, if two rooms share the use of a CAV system and the temperature sensor is installed in room 1, the psychrometric cycle of the system may be as shown in Figure 4.10. Under the condition shown in the figure, room 2 will be over-cooled while room 1 has its temperature kept at the set-point value. An average of the temperatures of all the rooms, as reflected by the temperature of the mixed return air, can be used as the feedback signal but the rooms may still be over- or under-cooled from time to time.

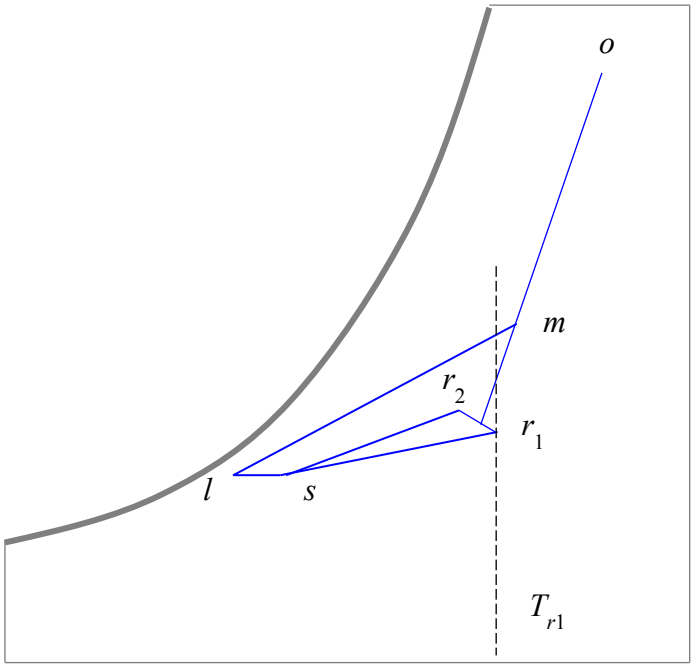

Figure 4.10 CAV system serving two rooms, with temperature sensor installed in room 1

4.2.3 Variable air volume (VAV) system

As mentioned above, in a VAV system, the supply air temperature T_s is fixed and the sensible cooling output of the air-side system, q_s, is moderated to match with the room sensible cooling load, $q_{r,s}$, by varying the supply air volume flow rate V_s. The matching of q_s with $q_{r,s}$ is manifested by the indoor air temperature T_r being kept at the set point value. Therefore, implementation of the VAV control scheme requires keeping T_s under the control of a dedicated control loop while another control loop is needed for controlling T_r by regulating V_s.

Figure 4.11 shows these control loops in a VAV system that serves just a single zone, i.e. there is only one room temperature sensor in the system for controlling the temperature inside one air-conditioned space. The control over T_s is through regulating the mass flow rate of chilled water flowing through the cooling and dehumidifying coil whereas V_s is regulated by either varying the fan speed or the angular position of an inlet guide vane (see discussions below) through which to control T_r.

To provide a convenient starting point for explanation of the actions that will be taken by the control loops in response to a load disturbance, we assume that the system shown in Figure 4.11 employs PI controllers for both T_s and T_r control. Furthermore, the system is assumed to be running steadily, with T_s and T_r equal to their respective set point values, and the water flow rate and the supply air flow rate, V_s, are each at a value between its maximum and minimum limits.

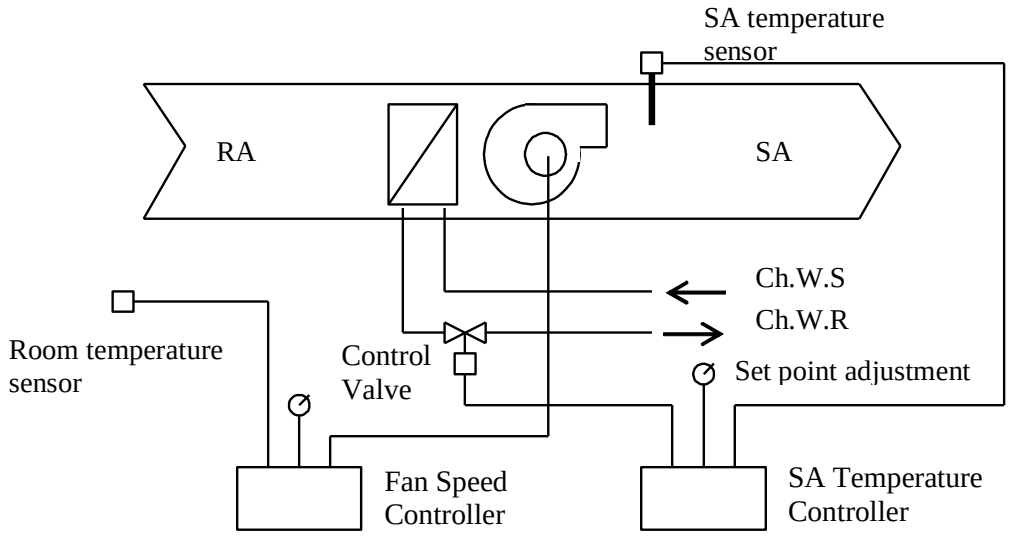

Figure 4.11 Schematic diagram for a single-zone VAV system

Assume that now the room sensible load is increased, there will be an increase in the room air temperature T_r before the system can respond to the load change and, as a result, a positive error, e ($e = T_r - T_{r,sp}$; $T_{r,sp}$ = set point value of T_r), will arise. The output of the fan speed controller will then increase which will cause V_s to be increased. As a corrective action that will increase the sensible cooling capacity of the system is yet to be taken, the cooling and dehumidifying coil will no longer be able to cool the air to the supply air temperature set point when the supply air flow rate is increased. As a result, the supply air temperature T_s will rise above its set point and, in response, the supply air temperature controller will command the control valve to open wider to allow more chilled water to flow through the coil. This will increase the sensible cooling capacity and pull down T_s, and T_r will then drop accordingly.

The corrective actions described above will continue until the indoor air temperature T_r returns to the set point value. The reader is encouraged to figure out the sequence of corrective actions when the disturbance is a reduction in room sensible load instead. Note, however, should be taken that the sequence of actions described above is just for a clear explanation of the way in which the control system copes with a load change. Actually, those control actions will take place simultaneously rather than one after another, as described in the discussion.

Regarding the means for regulation of the air flow rate in the system, a widely adopted method nowadays is to equip the fan of the air-handling unit with a variable speed drive (Figure 4.12). Inlet guide vanes had been extensively used before for their lower costs, but their use is becoming obsolete, although fans with inlet guide vanes may still be found in some existing buildings. The key drivers behind this substitution of technology include the superior part-load energy efficiency of the fan when put under variable speed control, as compared to the use of inlet guide vane (Figure 4.12), and the drop in price of variable speed drives, as the technology matures and the market widens.

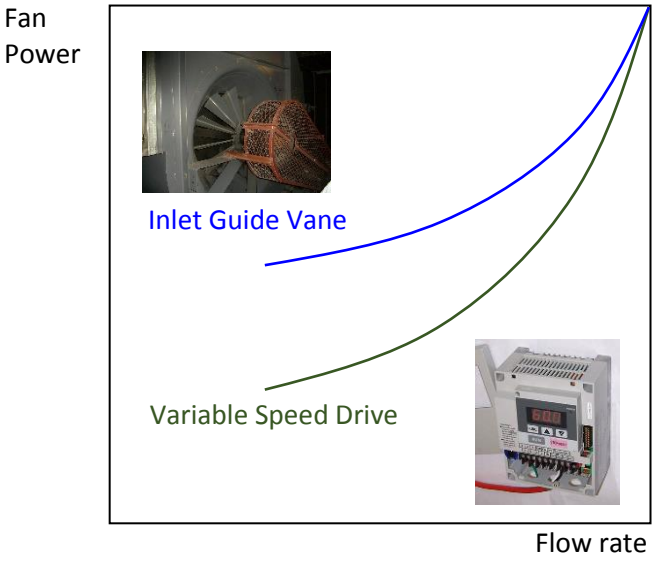

Figure 4.12 Power demand of a fan with inlet guide vane and variable speed drive

Since both the supply air temperature T_s and the room air temperature T_r are put under control in a VAV system, the difference between these temperatures and thus the supply air state, *s*, will vary only slightly no matter whether the system is operating under design or part-load conditions (Figure 4.13), unless the system runs into an uncontrollable operating condition which may indeed arise as will be explained below. The supply flow rate in part-load condition, V_s', which will vary with the room sensible cooling load, can be evaluated from:

$$V_s' = \frac{q_s'}{\rho_a Cp_a (T_r - T_s)} \tag{4.6}$$

Where q_s' is the room sensible cooling load in a part-load condition.

Figure 4.13 shows the design and part-load psychrometric cycles for a VAV system. By regarding the supply air state as fixed, the location of the room air state under part-load condition, *r'*, is dependent on the room sensible heat ratio and may deviate from the design room air state *r*. The deviation, however, will usually be small, which means that, compared to CAV systems, VAV systems will perform much better in passive humidity control under part-load conditions.

The major incentive of adopting VAV system is the reduction in fan energy use that is achievable when the required supply air flow rate drops in part-load conditions. Since the required supply air flow rate is linearly proportional to the room sensible cooling load (see Equation 4.6) but the latter may drop to very low or even negative levels (see Section 4.1.1), problems will arise if the supply air flow rate is allowed to drop with the room sensible load with zero flow rate as the limit, which will occur (in theory) when the inlet guide vane is fully closed or fan speed drops to zero.

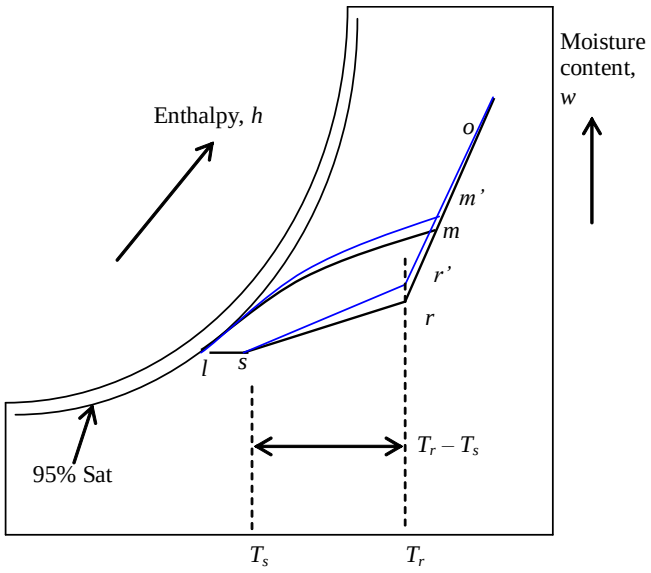

Figure 4.13 Design (black) and part load (blue) psychrometric cycles for a VAV system

However, substantial reduction in the supply air flow rate is undesirable for at least two reasons. First, because fresh air is typically mixed with the return air before the mixed air is treated in the cooling and dehumidifying coil to become the supply air (Figure 4.1), the fresh air supply to the air-conditioned space will also be reduced in proportion to the reduction in the supply air flow rate. The fresh air supply, therefore, may become insufficient to ensure adequate indoor air quality and/or oxygen supply for the occupants.[1] Second, when the flow rate through individual diffusers reduces, an adequate air flow pattern from outlets of supply diffusers may no longer be maintained. Under a rather low supply air flow rate, the cold supply air will dump onto occupants directly below them, but air movement will become stagnant at other locations, resulting in highly uneven temperature and indoor contaminant concentration distributions within the air-conditioned space.

Since both inadequate fresh air supply and inadequate space air diffusion are undesirable, a minimum flow rate needs to be set to avoid the supply air flow rate from falling below a minimum acceptable level, $V_{s,min}$. The ratio of the minimum supply flow rate to the design flow rate, $V_{s,design}$, is called the minimum turn down ratio (*MTDR*):

$$MTDR = \frac{V_{s,min}}{V_{s,design}} \tag{4.7}$$

MTDR is typically set at 30%. Once the *MTDR* is reached, no further reduction in the supply air flow rate will happen even if the room sensible cooling load is smaller than that which the minimum supply flow rate can cater for. This means the system will be out of control and the room will be over-cooled. As will be discussed later, this problem can be overcome by terminal reheat.

[1] The only exception to this drawback is a single-zone VAV system with constant supply of fresh air from a fresh air fan or fresh air handling unit as long as the supply air flow rate is higher than the fresh air flow rate.

A VAV system will seldom operate at or near to the design condition but is operating under part-load conditions for most of the time. However, once the flow rate is reduced, the air flow pattern will deviate from the pattern under the design condition. Supply air diffusers that can avoid dumping until the flow rate is reduced to the minimum level are preferred, and slot diffusers that can take advantage of the 'Coanda effect' (Figure 4.14) are widely used.

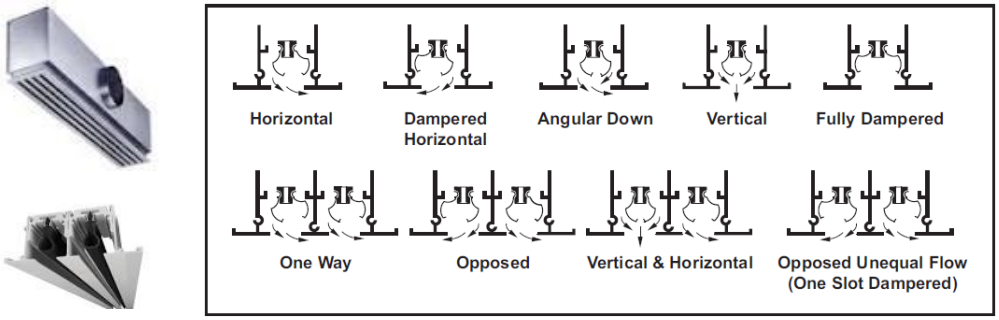

a) Slot diffusers commonly used for VAV systems

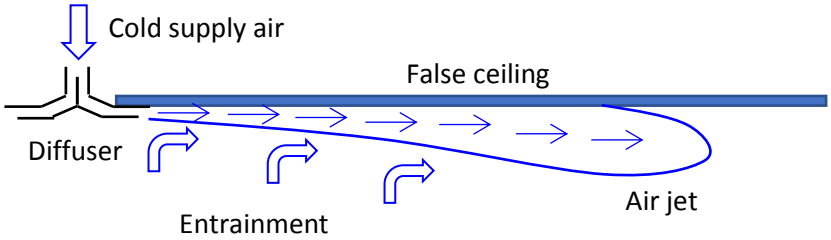

b) Coanda effect that keeps air jet attached to ceiling until entrainment becomes negligible

Figure 4.14 Diffusers of VAV systems and Coanda effect

The Coanda effect refers to the adherence of an air jet to a solid surface above it due to asymmetric entrainment of air from the surrounding, which occurs when an air jet is discharged into an air-conditioned space at the ceiling level, and the ceiling surface blocks entrainment of air into the jet from the top side. The vertical momentum of the air entrained to flow upward to join the jet will help sustain the jet from dropping until the entrainment diminished with the air velocity in the jet. By that time, the air temperature in the jet will become close to the room air temperature and hence will not cause any discomfort when it enters the occupied zone and impinges on occupants.

4.2.4 Variants of VAV system

The single-zone VAV system introduced above is not suitable for premises that comprise multiple rooms, which require independent temperature control for each room and may also require simultaneous heating and cooling among the rooms. However, as discussed above, this is a common situation among commercial buildings

with extensive floor areas. Several variants of the basic (single-zone) VAV system that can cope with these requirements are discussed below.

To enable a VAV system to serve multiple zones, the temperature control function needs to be delegated to a number of VAV terminals, also called VAV boxes, with each room requiring independent zone temperature control provided with at least one VAV terminal (Figure 4.15). A VAV terminal is basically a motorized air damper for regulation of the flow rate of supply air it will let pass into the room.

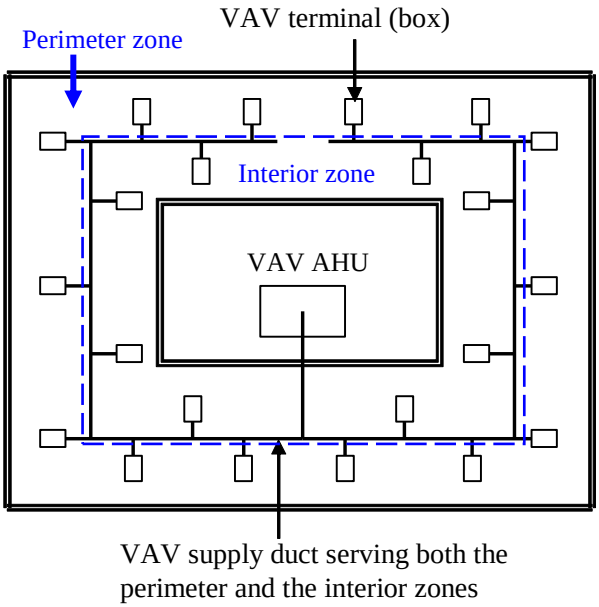

Figure 4.15 Layout of a VAV system serving multiple zones

As shown in Figure 4.16, each VAV terminal is equipped with a temperature control system that comprises a controller, a damper actuator, and a room temperature sensor. The position, or degree of opening, of the damper is dictated by the output of a controller which operates according to the feedback signal from the room temperature sensor and the pre-set temperature set point. In response to an increase in the room temperature, the controller will command the damper to open wider such that more supply air will be fed into the air-conditioned space which will bring the indoor temperature back to the set-point level.

Figure 4.17 shows the control arrangement for a VAV system with VAV terminals for serving multiple zones. The control loop for the supply air temperature is same as that for the single-zone VAV system (Figure 4.11). In lieu of a room temperature sensor, the static pressure in the main supply ductwork is used as the feedback signal for the fan speed control for regulation of the supply air flow rate that the VAV AHU will deliver. This is based on the premise that when the VAV terminals close their dampers for reducing supply air flow rate, the static pressure in the supply duct will rise. It will drop instead if the VAV terminals open wider their dampers for increasing supply air flow rate into the spaces they serve. This duct static pressure signal, therefore, can be utilized for fan speed (or inlet guide vane) control for flow rate regulation.

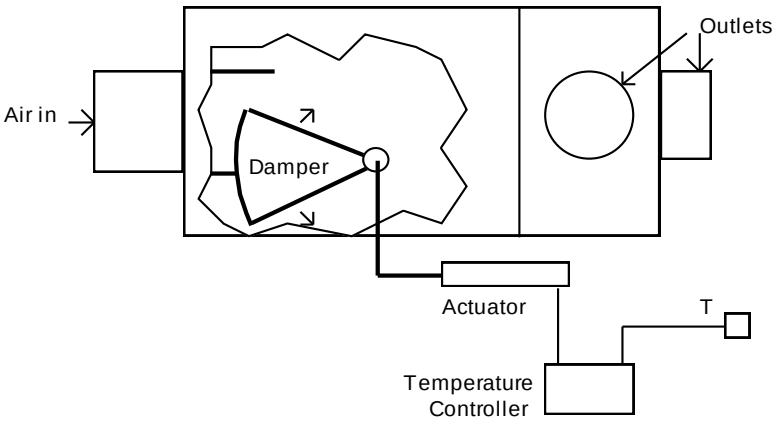

Figure 4.16 A simple VAV terminal

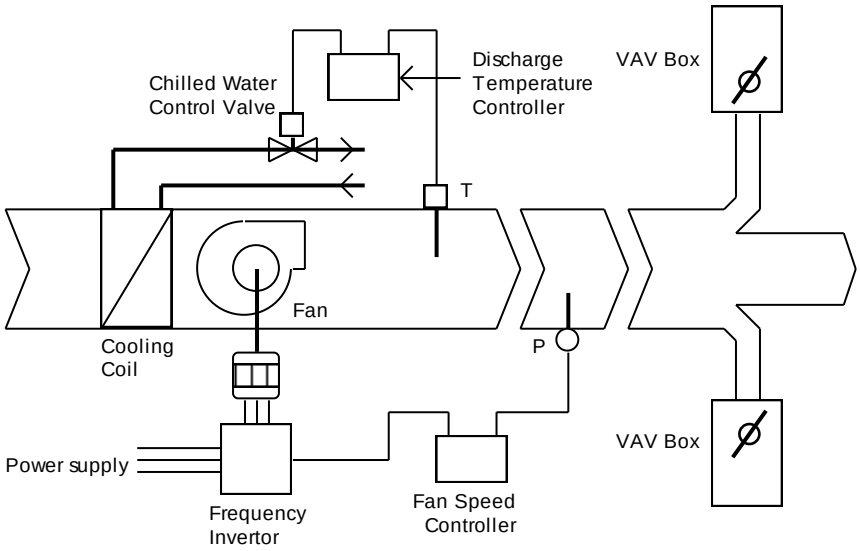

Figure 4.17 Control diagram for a VAV system with VAV terminals for serving multiple zones

However, the supply air flow rate through a VAV terminal, and thus the room temperature control performance, can be affected by pressure fluctuations upstream of the VAV terminal inlet, due to opening and closing of other VAV terminals connected to the same supply air ductwork. With an increase or a reduction in the upstream pressure, the air flow rate through a VAV terminal will increase or drop even though there is no change in the room air temperature. When this happens, the room air temperature will drift, which will call for a corrective action to be taken by the VAV terminal. Although the room air temperature may be under control once again later, there will be unnecessary fluctuation of the indoor temperature which is undesirable.

The pressure independent VAV terminal (Figure 4.18) is an enhanced version of the basic VAV terminal which can cope with the problem of upstream pressure fluctuations in a VAV system. An air flow sensor is installed at the inlet of a pressure independent

VAV terminal to measure the actual flow rate being let through into the air-conditioned space served by the terminal and the flow controller will moderate the damper according to the deviation of the flow rate from its set point.

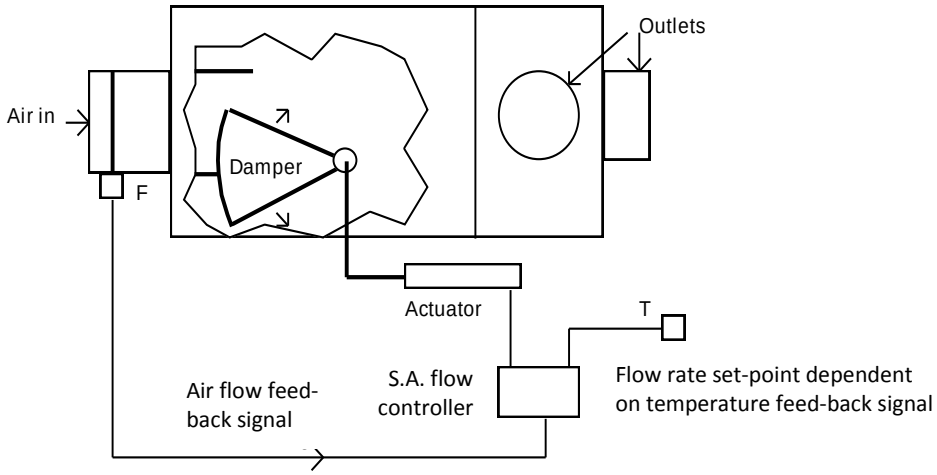

a) Control schematic

b) Physical outlook

Figure 4.18 Pressure independent VAV terminal (with velocity reset)

The supply air flow rate set point, however, is set according to the temperature sensor signal, and thus may vary from time to time. In other words, the flow rate set point is reset consistently according to the room air temperature, which will cause the damper control loop to vary the supply flow rate to counter act with the drift in room air temperature from its set point value.

If the room air temperature is being kept steadily within limits but the flow rate is changed due to a rise or drop in the upstream pressure, this change in flow rate will lead to a change in the flow rate error and the damper control loop will react immediately to correct the flow rate. Since this is a direct response of the damper control loop without the need to wait for a room air temperature change before action is taken, the room air temperature can be more stably controlled than when a simple VAV terminal is used.

Heating is required in a perimeter room if the cooling load of the room due to internal heat gains is insufficient to compensate for the heating load due to heat losses to the outdoors through the building envelop and infiltration of cold outdoor air, which may happen on a cold winter day. If just some rooms in a building are calling for heating and the others are still calling for cooling, both heating and cooling need to be provided at the same time.

For perimeter rooms that may require heating, the heating demand may be satisfied by installing a heater, which may be an electric heating coil or a hot water coil (Figure 4.19a), in the VAV terminals serving those rooms. The heater will be inactive when the temperature of the room it serves stays above a pre-set threshold, in which case the terminal will simply moderate the flow rate of supply air from the air-handling unit to the room, or keep the supply air at the minimum level. The heater will become active only when the room temperature falls below the threshold, and will heat up the supply air that has been cooled in the air-handling unit beforehand.

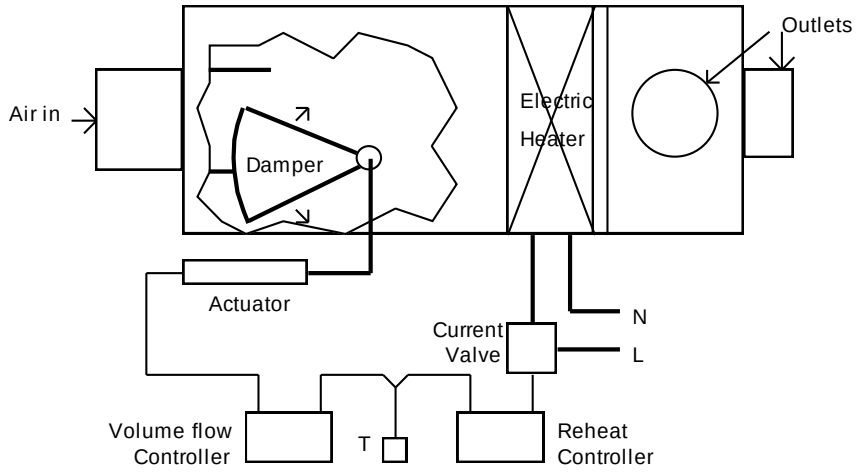

a) Control system of a VAV terminal with reheat

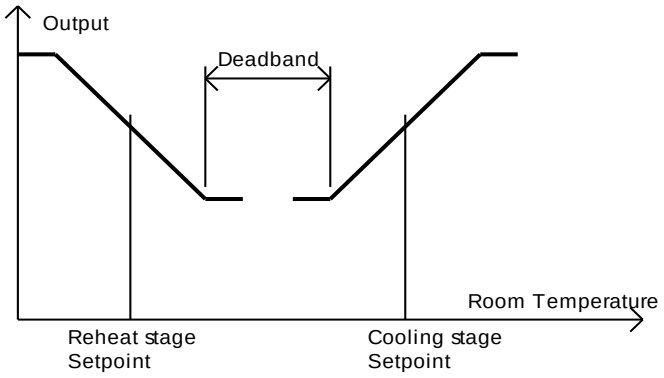

b) Control scheme for the cooling and heating stages of a VAV terminal with reheat

Figure 4.19 Controls for a VAV terminal with reheat

For those terminals with heaters, the cooling and heating set points must be set such that there is a dead band between the operating temperature ranges of the two stages (Figure 4.19b), to ensure heating is called for only when the supply flow rate has reached the minimum setting and the indoor temperature continues to drop due to excessive heat loss from the room. The heating coil should be sized according to the winter heating load of the room estimated based on the design temperature in the heating mode, plus the capacity for reheating up the supply air, at the minimum flow rate, from the supply air temperature from the air-handling unit to the design room temperature.

The dual conduit VAV system, which is a VAV system coupled with a skin CAV system, and the dual duct VAV system, which comprises both a hot and a cold air supply ducting circuit, had been used in luxurious office buildings. In a dual conduit system, the skin CAV system will cater for any heat loss through the building envelop due to indoor/outdoor temperature difference, leaving the VAV system to deal solely with cooling. In a dual duct system, both the cold and the hot air supply flow rates are regulated according to the room air temperature, and mixing of cold and hot air supplies will occur when the cooling load drops to below half of the design value until solely hot air is called for to keep control of the indoor temperature.

Both the dual conduit and dual duct systems can provide a higher degree of comfort for the occupants by maintaining at least a minimum air circulation rate inside the air-conditioned space. However, cancellation of cooling effort by heating will arise in cool months for both systems and, therefore, their use may be prohibited by building energy regulatory controls (which is the case in Hong Kong), and they are becoming obsolete. For this reason, no further discussion is given here on the design processes and control methods for these systems.

4.3 Economizer cycle

Modern buildings with extensive floor areas and good thermal insulation require air conditioning all year round, even in winter when the outdoor weather is cold. In the cool months, the outdoor air specific enthalpy may fall below that of the indoor air. On cold winter days, the outdoor temperature may even be lower than the design supply air temperature (Figure 4.20). When such conditions arise, the outdoor air may be utilized to meet the demand for cooling, which will require minimal energy input. Use of cool outdoor air to provide space cooling without turning on chillers is commonly referred to as “free cooling”.

An air-conditioning system can be purposely designed to take advantage of the free cooling effect of outdoor air for providing air-conditioning whenever the outdoor weather conditions permit, and the psychrometric cycles implemented are called the ‘economizer cycle’. Figure 4.21 is a schematic diagram showing the configuration of the air-conditioning system and the associated control systems and devices for an economizer cycle system.

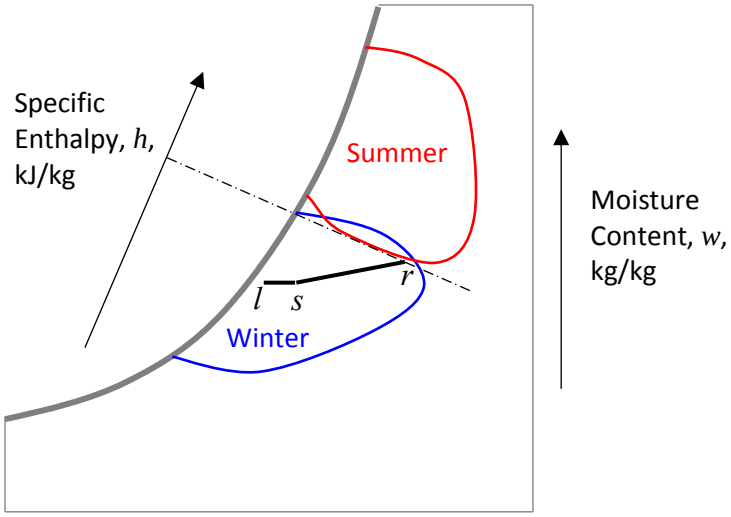

Figure 4.20 Range of outdoor air state in summer and winter in Hong Kong on a psychrometric chart in contrast against the leaving coil, supply, and room air states

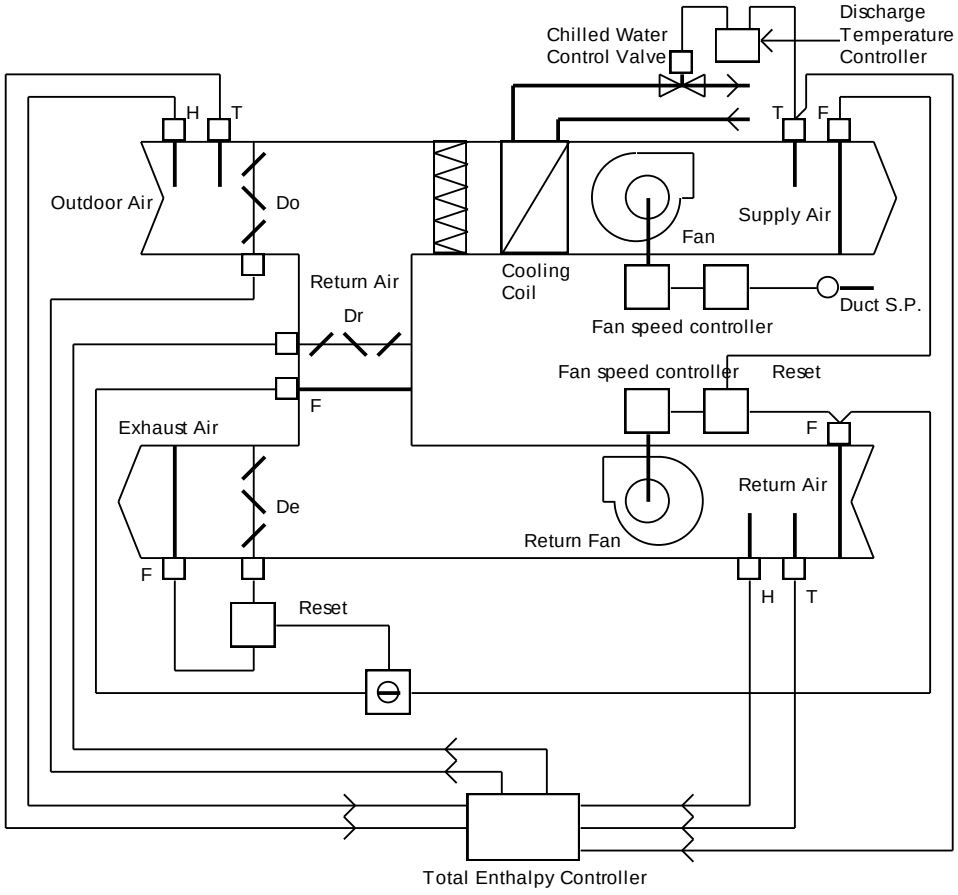

Figure 4.21 System and control schematic for economizer cycle system

In a system with economizer cycle control, the temperature and relative humidity of the indoor and outdoor air are consistently measured to enable the respective enthalpies to be computed and compared. When the outdoor air enthalpy is higher than that of the indoor air, the system will operate in just the same way as a conventional air-conditioning system (Figure 4.22a). The amount of fresh air drawn into the system will be the minimum flow rate that is required for providing ventilation for the occupants, or for other purposes as are required for the activities in the air-conditioned space.

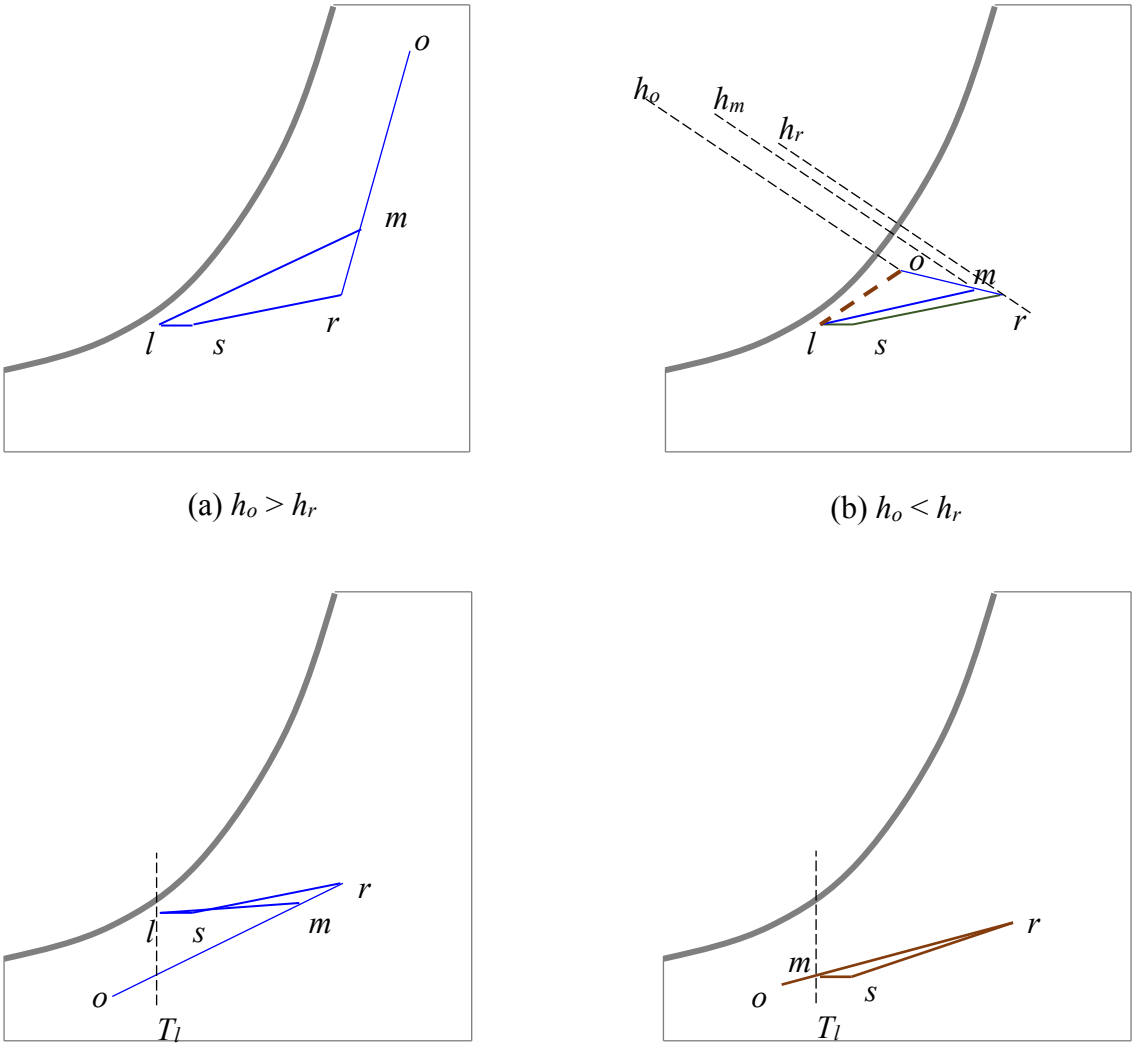

(a) $h_o > h_r$

(b) $h_o < h_r$

(c) $T_o < T_l$; Small V_{fa}

(d) $T_o < T_l$; Large V_{fa}

Figure 4.22 Psychrometric cycles of air-conditioning system operating under different outdoor air conditions

Whenever the outdoor air is found to have an enthalpy level lower than that of the indoor air (Figure 4.22b), the system will be switched to the mode of operation where all return air will be disposed of. The system will admit 100% of the system air flow

from the outdoor and let all the outdoor air be treated by the cooling coil for provision of air-conditioning.

Since cooling coil load is proportional to the difference in enthalpy of the air across the coil, the total amount of cooling load imposed upon the coil (for process *o* – *l* in Figure 4.22b) is less than if return air is allowed to flow through the air-handling unit (AHU) and cooled and dehumidified by the coil (for process *m* – *l* in Figure 4.22b). Hence, the amount of refrigeration load is reduced, and this will bring about a significant saving in energy consumption at the central chiller plant.

When the outdoor air temperature drops below the normal off-coil air temperature at the AHU, the air-conditioned space would be over-cooled if 100% outdoor air were still used for cooling. However, if we switch back to the mode of operation with minimum outdoor air, with a large amount of return air re-circulated through the system and mix with the outdoor air to make up the total supply volume flow rate required (Figure 4.22c), it would still require cooling from the central chiller plant for providing air-conditioning.

By increasing the amount of outdoor air and reducing the amount of return air at the same time, we can have the mixture temperature of the two air streams adjusted to the design leaving coil air temperature (Figure 4.22d). Under this mode of operation, there would in fact be no cooling load on the cooling coil as the amount of fresh air admitted into the system would be sufficiently cold for providing the required amount of cooling.

From the above description, it can be seen that there are three modes of operation in an economizer cycle system. The corresponding outdoor conditions will fall in three different regions, denoted as Zone I, II and III, on a psychrometric chart as shown in Figure 4.23. The operation of the outdoor air damper Do, the return air damper Dr, and the exhaust air damper De, as shown in Figure 4.21, corresponding to the three zones of operations are summarized in Table 4.1.

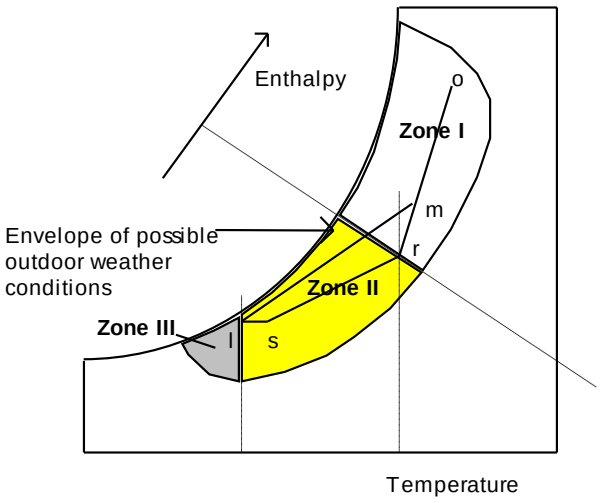

Figure 4.23 Outdoor weather condition for the three modes of operation

Table 4.1 Modes of operation of an economizer cycle system

Weather Zone	In/Out Condition	Damper position		
		Do	Dr	De
I	$h_o > h_r$	min.	open	min.
II	$h_o < h_r$ and $t_o > t_l$	open	closed	open
III	$t_o < t_l$	Under modulating control		

Besides the year-round weather conditions, if the economizer cycle may be adopted hinges on whether there are sufficient outdoor air intake and exhaust louvres at the building perimeter and spaces to accommodate the large air-ducts involved. It is ideal for large spaces, such as exhibition halls, but could be difficult to apply to typical commercial/ office buildings.

4.4 Central fresh air/primary air system

4.4.1 Local and centralized supply

Providing fresh air (FA) from outdoors to air-conditioned spaces for ventilation, and disposing off an equal amount of indoor air, are needed for supply of oxygen to meet the respiration needs of the occupants and for dilution and disposal of the carbon dioxide exhaled by the occupants as well as any odours and other emissions from indoor sources. FA supply may be provided by:

- Local intake: using the AHU serving a group of spaces or a dedicated fan to draw in the required FA (as assumed in construction of the conventional all air cycle discussed above), or

- Central supply: providing a central FA supply system, which may include pre-treatment (including cooling / heating, dehumidifying / humidifying, and filtering) of the outdoor air before delivering the FA to individual AHUs (Figure 4.24).

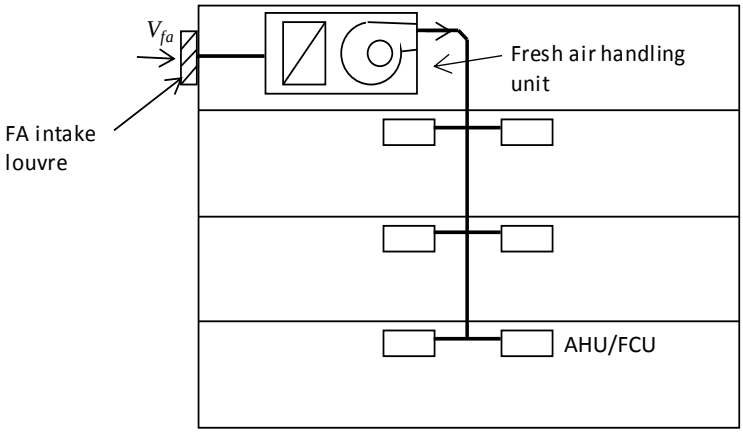

Figure 4.24 A central fresh air supply system

The benefits of using a central FA supply system include:

- Supply flow rate is less susceptible to influence of wind and thus is more stable.
- Prevention of ingress of rain.
- The dehumidification load for treating the fresh air supply is already taken care of by the fresh air-handling unit. Therefore, latent load on the AHU, and rate of condensate production at the coil, will be much reduced (Figure 4.25).

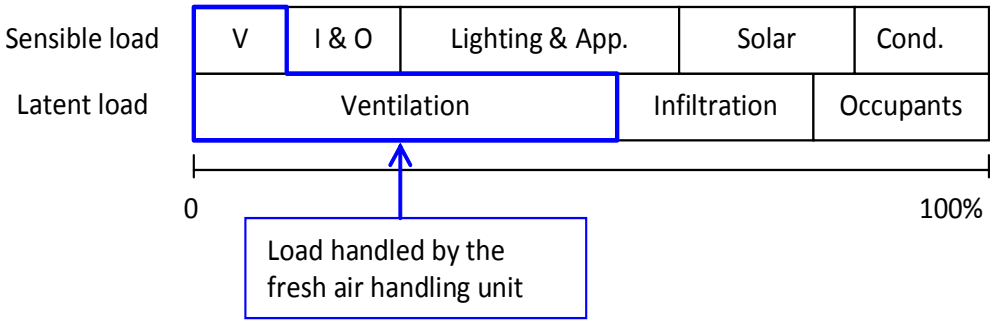

Abbreviations: V: Ventilation I & O: Infiltration and Occupants
App.: Appliances Cond.: Conduction

Figure 4.25 Sensible and latent portions of cooling load components

4.4.2 Choices of FA supply state

There is no hard and fast rule in respect of where to stop the treatment of outdoor air in a FA handling unit. Figure 4.26 shows the cooling and dehumidification process involved and the common choices of FA supply state:

- At the state where the specific enthalpy of the treated FA is same as that of the room air. There will be no increase in total cooling load on the AHU; the FA supply will provide an amount of sensible cooling but will impose an equal amount of latent load on the cooling coil.

- At the state where the moisture content of the treated FA is same as that of the room air. There will be no increase in latent load on the AHU for FA treatment and the FA will share a portion of the sensible cooling duty of the cooling and dehumidifying coil.

- At the same state as the leaving coil air of the AHU. The FA can offset a portion of the sensible and latent cooling loads of the AHU.

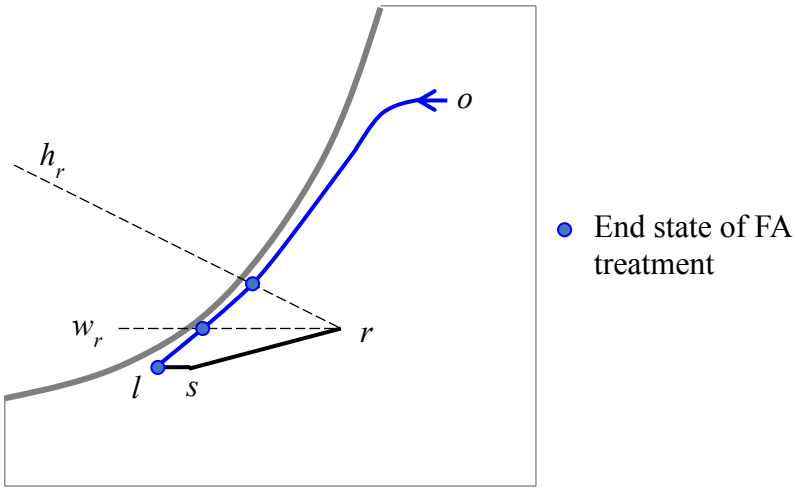

Figure 4.26 Choices of end state of central FA treatment

4.4.3 Air-to-air heat recovery wheel

On hot summer days, pre-treating outdoor air for providing air-conditioned spaces with ventilation accounts for a substantial portion of the total cooling load on the central chiller plant, and its energy consumption. At the same time, exhaust air will be extracted out of air-conditioned spaces, which is at the indoor temperature and moisture content, significantly lower than the temperature and moisture content of the outdoor air.

Therefore, considerable energy saving can be achieved by using the exhaust air to cool and dehumidify the outdoor air before the outdoor air is treated to the required state by the fresh air handling units. This can be achieved by using an 'air-to-air heat recovery wheel' (Figure 4.27) to facilitate total heat exchange between the outdoor air and the exhaust air. For air-conditioning systems in a place with hot and humid weather, such as Hong Kong, devices that can recover total heat will be much more beneficial than those that can only recover sensible heat from the exhaust air.

Rotary type air-to-air heat recovery wheels are commonly used for recovery of the cooling and dehumidifying potentials of exhaust air from air-conditioned spaces for pre-treatment of outdoor air. The wheel is typically made of thin sheets of light weight material (e.g. aluminium) that is coated on the surface with a layer of hygroscopic material (desiccant), such as silica gel or aluminium oxide, and rolled to form multiple passages through which air can flow (Figure 4.27).

The outdoor and exhaust air streams are channelled to flow through two different portions of the wheel, typically in opposite directions, and the wheel is driven by a motor to rotate at a steady speed such that each sector of the wheel will pass through the outdoor air steam and the exhaust air stream in turn. While a sector is in the outdoor air stream, it will absorb both sensible heat and moisture from the outdoor air. When the sector rotates to the exhaust air stream, the exhaust air will cool and dry the desiccant layer in that sector of the wheel by absorbing heat and moisture from it, making the sector of the wheel ready for the next cycle of operation.

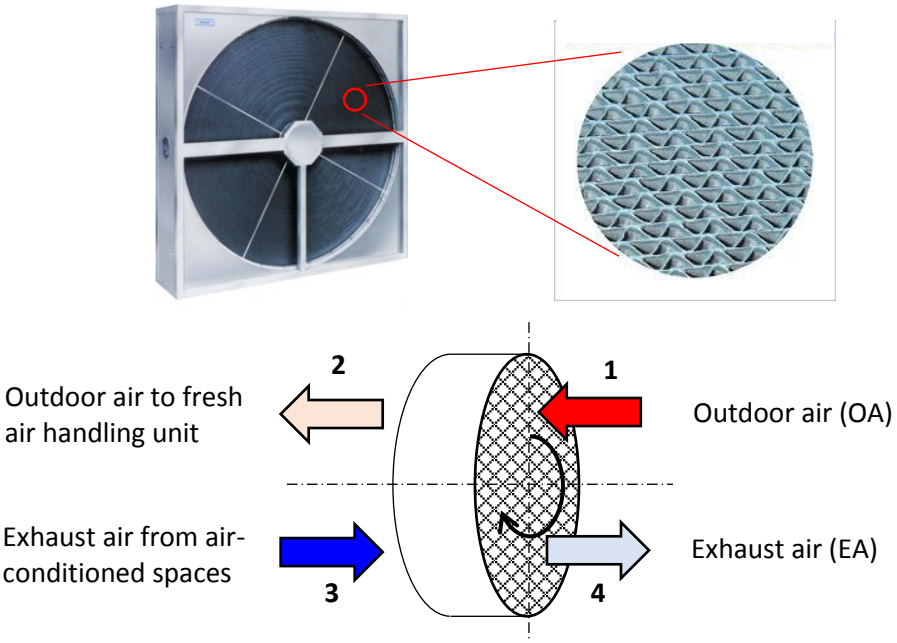

Figure 4.27 Rotary total heat recovery wheel

As a sector of the wheel leaves the exhaust air stream and enters the outdoor air stream, there will still be exhaust air trapped inside the air passages in the wheel. For ensuring no exhaust air will be carried back to the fresh air stream, a purge section is included to allow a small amount of outdoor air to flow through the wheel to purge the remaining exhaust air, which will be disposed of into the exhaust air stream (Figure 4.28). Furthermore, the fans that drive the exhaust air and outdoor air to flow through the total heat recovery wheel should be located at positions that will not cause cross-leakage of exhaust air (Figure 4.29).

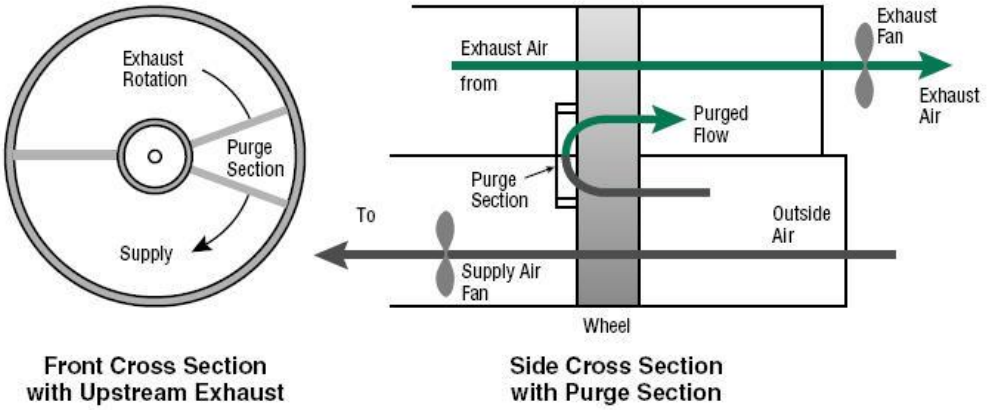

Figure 4.28 Purge section in a rotary total heat recovery wheel

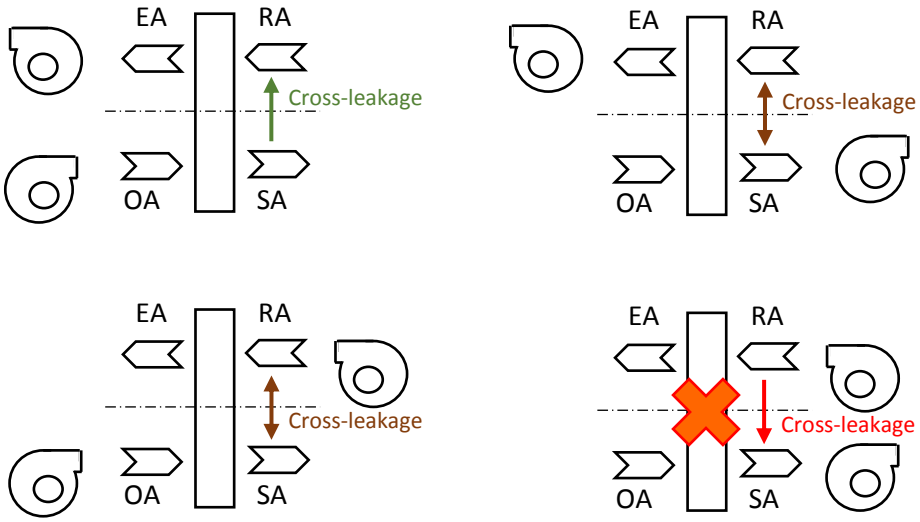

Note: Cross-leakage from RA stream to SA stream undesirable and should be avoided by installing fans at appropriate positions

Figure 4.29 Possible cross-leakage in a rotary total heat recovery wheel

By denoting the states of the outdoor and exhaust air entering and leaving a total heat recovery wheel as states 1 to 4 as shown in Figure 4.27, the total heat loss of the outdoor air, q_{OA}, can be determined by:

$$q_{OA} = \rho_a V_{OA}(h_1 - h_2) \tag{4.8}$$

And the total heat gain of the exhaust air, q_{EA}, is given by:

$$q_{EA} = \rho_a V_{EA}(h_4 - h_3) \tag{4.9}$$

Where

ρ_a = air density
V_{OA} and V_{EA} = volume flow rates of outdoor and exhaust air
h = air specific enthalpy
Subscripts 1 to 4 are as shown in Figure 4.27.

The maximum possible total heat transfer rate, q_{Max}, that could be achieved with the given entering outdoor and exhaust air states is:

$$q_{Max} = \rho_a V_{Min}(h_1 - h_3) \tag{4.10}$$

Where $V_{Min} = V_{OA}$ or V_{EA}, whichever is the smaller. Normally, $V_{Min} = V_{EA}$.

Therefore, the effectiveness of a rotary heat recovery wheel, η, is defined as:

$$\eta = \frac{q_{OA}}{q_{Max}} = \frac{V_{OA}}{V_{Min}} \frac{h_1 - h_2}{h_1 - h_3} \tag{4.11}$$

Knowing the value of the effectiveness of the rotary heat recovery wheel, the leaving outdoor air enthalpy, h_2, can be determined as follows:

$$h_2 = h_1 - \eta \frac{V_{Min}}{V_{OA}} (h_1 - h_3) \tag{4.12}$$

The leaving exhaust air enthalpy, h_4, can also be determined, as follows:

$$h_4 = h_3 + \eta \frac{V_{Min}}{V_{OA}} (h_1 - h_3) \tag{4.13}$$

Performance curves of rotary total heat recovery wheels are typically given by manufacturers in terms of the total effectiveness of the wheel as a function of the face velocity of air flow through the wheel and the ratio of the minimum to the maximum of the outdoor and exhaust air flow rates (see for example, Figure 4.30).

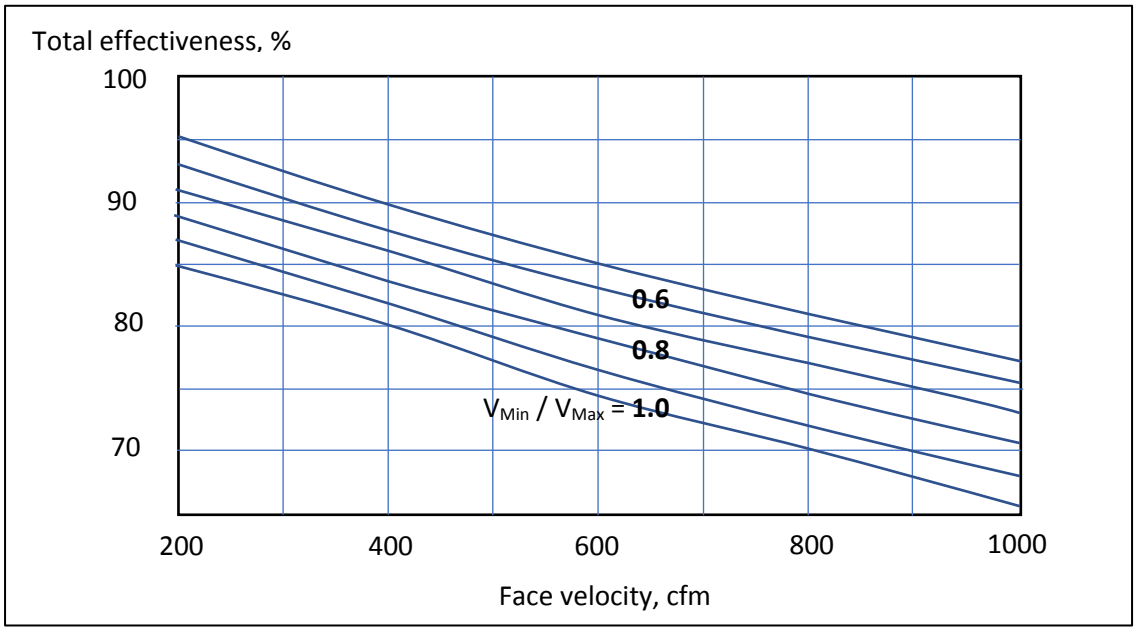

Figure 4.30 Typical performance curves of rotary total heat recovery wheel

The annual energy saving achievable by adopting total energy recovery wheels in a building can be estimated by using the method described below. The estimation requires data about:

- The year-round hourly weather data of the location under concern.
- The total fresh air supply flow rate determined from the total number of occupants in the building and the fresh air supply rate per person.

- The total flow rate of available exhaust air from the air-conditioned spaces for heat and moisture exchange with the outdoor air at the total energy recovery wheel.

The assumption could be made that the exhaust air would be at the same temperature and relative humidity as the indoor air, or suitable adjustment has to be made for any significant duct heat gain. The reduction in cooling load for cooling and dehumidifying the fresh air supply at each hour of operation can be estimated as shown below.

The original total cooling load for fresh air treatment, $Q_{FA,O}$, is:

$$Q_{FA,O} = \rho_a V_{FA}(h_o - h_s) \tag{4.14}$$

Where

ρ_a = air density, kg/m^3
V_{FA} = fresh air supply flow rate, m^3/s
h_o = outdoor air enthalpy, kJ/kg
h_s = fresh air supply enthalpy, kJ/kg

With the total energy recovery wheel, the outdoor air enthalpy entering the cooling and dehumidifying coil in the fresh air handling unit can be lowered to the air enthalpy leaving the wheel, h_w, which can be determined from:

$$h_w = h_o + \eta \frac{V_{EA}}{V_{FA}}(h_o - h_e) \tag{4.15}$$

Where

V_{EA} = exhaust air flow rate through the wheel (assumed $V_{EA} < V_{FA}$), m^3/s
η = effectiveness of the wheel
h_e = exhaust air enthalpy, kJ/kg

Hence, with the total energy recovery wheel, the total cooling load for fresh air treatment, $Q_{FA,W}$, becomes:

$$Q_{FA,W} = \rho_a V_{FA}(h_w - h_s) \tag{4.16}$$

Therefore, the reduction in fresh air cooling load, ΔQ_{FA}, is:

$$\Delta Q_{FA} = Q_{FA,O} - Q_{FA,W} = \rho_a V_{FA}(h_o - h_w) \tag{4.17}$$

The above hourly calculation would need to be repeated to cover all operating hours in a year to yield the annual total saving in cooling load. The cooling load saving would also need to be converted into electricity consumption saving taking due account of the energy performance of the chiller plant under different weather conditions throughout the year. Note should be taken that there may not be energy saving in some months in the year; there are times that the outdoor air enthalpy is low enough that no advantage

can be gained by using the total energy recovery wheel. Under Hong Kong weather conditions, saving is possible typically from April to October in a year.

Care should also be taken in system design to strike a good balance between using the general exhaust air from air-conditioned spaces for providing 'second-hand' air-conditioning to areas like toilets, which is a common practice in Hong Kong, and reserving sufficient flow rate of the general exhaust air for total heat exchange with the outdoor air at the total energy recovery wheel. In any case, only about 80%, at maximum, of the fresh air supply flow rate should be channeled to the total heat recovery wheels to ensure the air-conditioned spaces are positively pressurized to deter infiltration of hot and humid outdoor air.

4.5 Primary air fan coil system

4.5.1 Individual zone temperature control

When a VAV system with VAV terminals is used to serve multiple rooms, individual zone temperature control is "delegated" to the VAV terminals serving individual rooms. For a CAV system, however, it can only respond to one room temperature feedback signal. As mentioned in Section 4.2.2, when a CAV system is applied to serve multiple rooms, only the temperature of one of the rooms can be put under control while the other rooms may be over- or under-cooled. An average of the temperatures of all the rooms, as reflected by the mixed return air, can be used as the feedback signal but the rooms may still be over- or under-cooled.

Instead of using an all air system, the need for individual zone temperature control for multiple rooms can be met by replacing the central CAV air-handling equipment with a number of smaller units, such that each room is served by at least one small CAV unit. Such small air-handling equipment will comprise a fan and a cooling and/or a heating coil, and therefore is call a fan-coil unit (FCU).

Irrespective of the kind of air-side system being used, air-conditioned spaces have to be supplied with fresh air (FA) for ventilation, typically through a central FA supply system. The centrally supplied FA is also called primary air (PA) while the air re-circulated through the air-handling equipment is called secondary air. When FCUs are used, both air, which is the PA supply, and water, which is the chilled / hot water supply, will be circulated through the air-conditioned spaces, and thus such systems are often called primary air fan-coil systems and are in the category of 'air-water' systems.

4.5.2 Fan coil units and selection

To ease dismantling of the fan and the motor for maintenance, the vast majority of fan coil units (FCUs) used in buildings adopt the 'blow-through' arrangement, i.e. with the fan blowing air to flow through the cooling and dehumidifying coil (Figure 4.31), whereas most larger air-handling equipment adopt the 'draw-through' arrangement. A rough filter is typically installed for removing large suspended particulates in the air, which needs to be cleansed from time to time. The use of a small fan in FCUs, which would be able to provide just a low fan total pressure, precludes the use of air-filters with higher filtration efficiency.

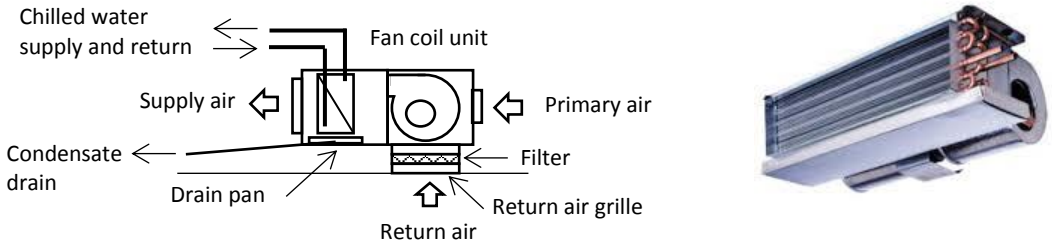

Figure 4.31 Typical ceiling mount fan coil unit

Since condensate will be generated when air is dehumidified as it flows through a cooling coil, there is, therefore, a condensate drain pan beneath the cooling coil in a FCU onto which the condensate droplets formed over the coil surface will fall. The condensate drain pan needs to be connected to a condensate drain pipe, which should be insulated and installed with a fall of at least 1:100, to facilitate drainage of the condensate by gravitational force. For air-conditioned spaces with extensive areas, design and installation of the condensate drain pipes can be a challenge if there is limited clearance within the ceiling void for accommodating the slopping condensate drain pipes. Small tanks and pumps for drainage of condensate may need to be installed if drainage by gravity is not possible in certain parts of a building.

Given that there can be hundreds or more of FCUs in a single building, and each has to be equipped with an independent control system, the cost of providing air-conditioning will become a concern. The cost of the FCUs can be largely cut down by mass production, with FCUs produced at standard modular sizes that can handle supply air flow rates that increase in steps, such as 200, 400, 600, 800 & 1200 cfm (cubic feet per minute; 1 cfm = 0.472 l/s).

In most cases, only the simplest, and cheapest, type of control system would be employed, such as on/off control provided by a thermostat installed inside the occupied area. A motorized on/off control (solenoid) valve is installed at the chilled water pipe (Figure 4.32a), which will be fully opened or closed under the command of the thermostat. Nevertheless, on top of the thermostat, there will be a selector switch for manual adjustment of fan speed, conventionally in 3 steps: High/Medium/Low, but variable speed FCUs have become available more recently (see below).

As a result of the use of on/off control, the indoor temperature will fluctuate from time to time between the on- and off-settings, with some degree of overshoot (Figure 4.32b). The difference between the on- and off-settings is called control differential, which may be adjusted. A smaller control differential will reduce the range of variation in the indoor temperature but will lead to more frequent cycling between open and close status of the control valve.

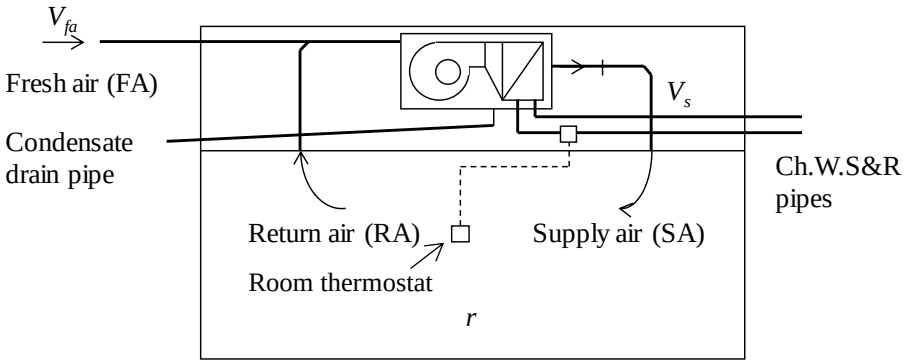

a) Thermostatic control over chilled water supply

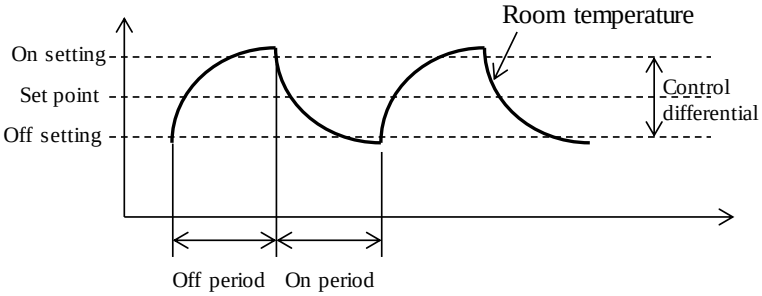

b) Cyclical room temperature fluctuations

Figure 4.32 On/off control for fan coil unit

Since FCUs are mass produced in modular sizes, the sensible and total cooling capacities, and the air flow rate, of a FCU cannot be adjusted to match closely with the design sensible and total cooling loads and the design supply air flow rate for the air-conditioned space it serves. FCU manufacturers will provide rated sensible and total cooling capacities of each modular size of their FCUs, but such ratings are based on a specific set of on-coil air dry and wet bulb temperatures and air flow rate.

Manufacturer's technical data manuals should also be consulted for information about the external static pressure available from a FCU and the noise data. The external static pressure is the net fan pressure available for overcoming the losses due to the supply and return ducts, diffusers and grilles and the filter, with pressure for overcoming losses through the coil and other components in the FCU already allowed for.

Because the fan in a FCU (typically forward curved centrifugal fan) is small in size, the fan pressure available is limited. Hence, the air ducts connected to a FCU have to be short in distance and large in cross sectional area; and, as mentioned above, only rough filter with low pressure drop can be used with FCUs (their ability to control air cleanliness is much lower compared to systems with central AHUs).

Whenever any operating conditions for a particular application deviate from the rated conditions, the performance of the FCU will be affected. FCU manufacturers used to provide correction factors for performance adjustments for each parameter that deviates from the rated condition. A FCU can be selected if both its sensible and total

capacities, and its external static pressure, exceed the respective requirements. The supply flow rate, and noise level, will be determined once a unit is selected, and must also be checked.

4.5.3 Variable speed fan coil units

For a FCU, the supply and return ducts and grilles, and the coil inside the FCU, are all flow elements with constant resistances. Therefore, if a variable speed fan is used, the fan motor power will be proportional to the cube of the flow rate, which means a substantial amount of fan energy may be saved in part-load operation. FCUs with variable speed drives and associated controls have become available in the last decade and have been adopted as a means to enhance the energy performance of new and existing buildings, including in Taiwan, Hong Kong and elsewhere.

Since the supply air flow rate and the chilled water flow rate may both be varied for indoor temperature control, a control strategy that can sequence the use of the two control methods is needed. One of the possible control strategies is shown in Figure 4.33.

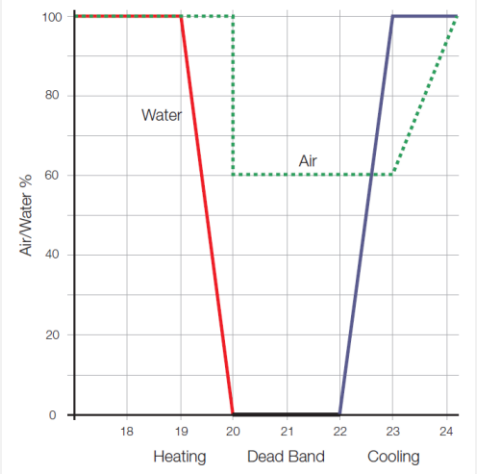

- Under this control strategy, the supply fan speed will be regulated from the minimum to the full speed within the range of indoor temperature from 23 to 24°C, while the chilled water flow rate will be kept at the full flow rate.
- When the indoor temperature falls below 23°C, indoor temperature control will be handled over to the control-loop for regulation of the chilled water flow rate while the supply fan speed will be fixed at the low limit (at 60% design flow in this example).

Figure 4.33 A control strategy for variable speed fan coil unit

4.6 Chilled ceiling and beam system

Chilled ceilings and chilled beams are unconventional air-conditioning systems originated in Europe in the 1980's and are penetrating the markets in other regions, including the United States and Asian countries. This is different from most other air-conditioning technologies, which were originated in North America and then spread to other continents. The success of chilled ceiling and chilled beam is mainly because they are regarded as energy efficient air-conditioning systems and, therefore, are adopted in various buildings that aim to be "low carbon / low energy" buildings.

Nevertheless, their suitability for application is conditional – they are only suitable for providing comfort air-conditioning for premises with moderate to low cooling load

intensity, especially low latent load intensity, such as offices. With the use of chilled ceilings and chilled breams, there will be lots of exposed cool surfaces in the air-conditioned space. Surely, condensation upon the exposed cool surfaces, should it happen, will be disastrous, and this has been a key concern of building developers and designers in places with hot and humid weather like Hong Kong, notwithstanding that there are already successful cases of their application in places with such weather, including Hong Kong, Guangzhou, Singapore, etc.

The potential condensation problem is still a key hindrance to wide adoption of chilled ceiling / beam systems but, as will be discussed below, the condensation problem can be avoided by limiting the moisture sources in the air-conditioned space, deterrence of infiltration of humid outdoor air into the air-conditioned space, and proper design of the associated primary air (PA) system.

4.6.1 Construction and characteristics of chilled ceiling and chilled beam

Chilled ceiling / beam systems are air-water systems, as they require delivery of both chilled water and primary air into the air-conditioned space. As shown in Figure 4.34a, a chilled ceiling panel comprises a coil made of copper tube that is bonded to a panel typically made of sheet metal, but other ceiling panel materials may also be used. The bonding between the tube and the panel ensures good heat conduction, and the tube is normally covered by a layer of thermal insulation at the top to minimize heat gain from other sources. The tube is connected to the chilled water supply and return pipes, typically by using flexible hoses to ease inspection and maintenance – this allows the penal to be hinged and swung opened for inspection and maintenance.

Chilled water is circulated through the tube to cool down the panel surface, such that both convective and radiant heat transfers will take place on the exposed surface of the panel (Figure 4.35), while radiant heat transfer would account for the dominant portion (up to 70% possible). The maximum total cooling capacity of chilled ceiling is only around 80W per square meter of the chilled ceiling surface area (see example calculation results in Table 4.2). Assuming equal areas between the floor and the false ceiling and taking into account the ceiling surfaces that are occupied by lighting fixtures and other building services components, the cooling capacity of a chilled ceiling system will be less than 60W per square meter of floor area. This relatively small cooling capacity is a limitation to application of chilled ceilings to premises with high sensible load intensities.

Passive chilled beam (Figure 4.34b) is basically a cooling coil through which air can flow into and out of it by natural convection. Air cooled by the chilled beam will drop into the air-conditioned space, which will induce air from the space to flow into it from the top, thereby creating a re-circulating flow. The convective portion of the total heat transfer is much greater compared to a chilled ceiling. A chilled beam may also be integrated with other services, such as lighting units to become a multi-service chilled beam (see, for example the photo in Figure 4.34b).

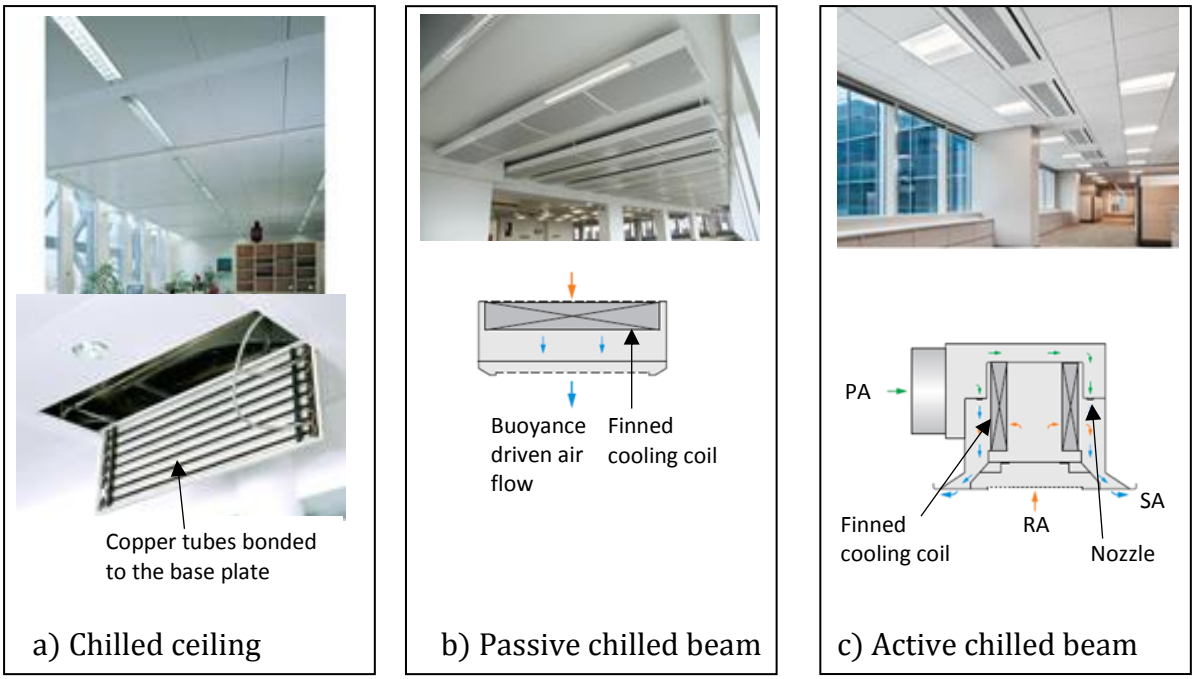

Figure 4.34 Chilled Ceiling and Passive and Active Chilled Beams

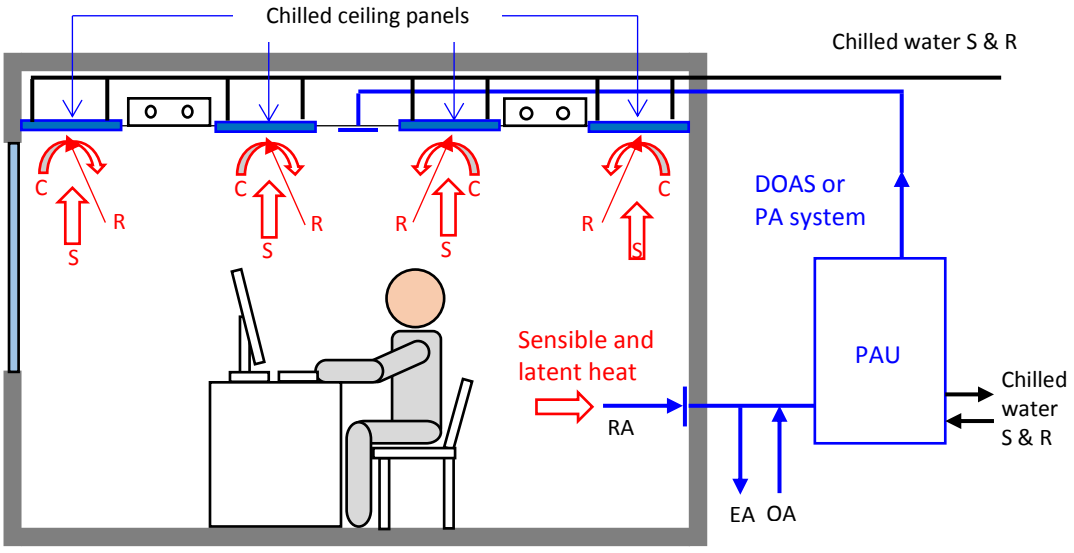

Figure 4.35 Heat transfers in a chilled beam system

Table 4.2 Example calculation of convective and radiant heat transfer on a horizontal surface (with heat transfer in upward direction)

a) Total convective and radiant heat transfer

Case		A	B
Surface temperature, T_s	°C	16	16
Room air temperature, T_a	°C	25	24
Rad.+conv. heat transfer coeff.[1]	W/m²K	9.26	9.26
Total heat transfer rate, Q_{tot}	W/m²	83.34	74.08

[1] Table 1, Ch. 26, ASHRAE Handbook – Fundamentals, 2009.

b) Radiant portion of total heat transfer

Case		A	B
Surface emissivity, ε_s	-	1	0.9
Radiant heat transfer rate, Q_{rad} [2]	W/m²	51.70	41.15

[2] The heat transfer rate is given by (Equation 3.41):

$Q_{r1-2} = A_1 \varepsilon_1 \sigma (T_1^4 - T_2^4)$

Hence, for our case,

$\frac{Q_{rad}}{A} = \varepsilon_s \sigma (T_a^4 - T_s^4)$

Where σ is the Stefan-Boltzmann constant (= 5.67x10^{-8} W/(m² K⁴)).

Compared to chilled ceilings, passive chilled beams may be used to provide a greater cooling capacity, up to 350 - 475W per square meter of the exposed face area of the chilled beam. However, clearances are needed between chilled beams to facilitate circulation of air from the room up to the top side of the chilled beam and back down through the chilled beam to the occupied space. The cooling capacity should be above 100W/m² floor area when passive chilled beams are used.

By using active chilled beams (Figure 4.34c), the cooling capacity may be further increased, up to 700 - 1250W per square meter of the exposed face area of the chilled beam. However, even greater distances need to be kept between active chilled beams to ensure proper space air diffusion.

When in operation, primary air (PA) will be fed into an active chilled beam and ejected inside the casing through jet nozzles at a high velocity (Figure 4.34c). Partial vacuum will arise in the region with high air flow velocity, which will cause air in the air-conditioned space to be drawn to flow into the chilled beam through the coil and mix with the PA. The mixture of PA and indoor air, after being cooled by the coil, will then be distributed into the air-conditioned space through the diffusers at the outlet. Dumping of cold air onto occupants can be avoided with proper layout design.

4.6.2 Configuration and characteristics of chilled ceiling / beam systems

Both chilled ceilings and chilled beams may be used in the same system for serving different areas with different cooling load intensities. However, a chilled ceiling/beam system can function properly provided only that there is a primary air (PA) system, or

dedicated outdoor air system (DOAS), operating in parallel at the same time (Figure 4.35).

Because chilled ceilings and chilled beams can only handle sensible cooling loads from the space, a PA system is needed to supply fresh air for ventilation as well as to remove all latent cooling loads, i.e. moisture loads, of the space. The PA system, therefore, is a key companion of chilled ceiling / beam system and its performance is crucial to avoidance of occurrence of condensation. Being supplied at a temperature well below the indoor air temperature, the PA will, at the same time, offset a fraction of the sensible cooling load of the space.

For avoiding condensation, the surface temperature of a chilled ceiling or beam must be kept above the dew point temperature of the indoor air. A surface temperature in the range of 16 to 18°C is often used as a design criterion for a chilled ceiling / beam system. For maintaining such surface temperature at the chilled ceiling / beam, a supply chilled water temperature between 14 and 16°C will suffice. However, given that the PA supply is responsible for removal of moisture gains in the air-conditioned space, the PA handling unit must supply air at a low enough moisture content and, therefore, the unit would require chilled water supply at a temperature of around 7°C, as in a conventional air-conditioning system.

According to the ASHRAE Handbook [1], the principal advantages of using chilled ceiling systems include:

- Total human thermal comfort may be better satisfied because not only indoor air temperature but also mean radiant temperature can be controlled.

- Comfort levels can be better than those of other space-conditioning systems because thermal loads are satisfied directly and air motion in the space corresponds to required ventilation only.

Readers may refer to Section 2.7.3 for a discussion on the thermal comfort issue. Besides thermal comfort, using chilled ceiling and chilled beam systems can lead to energy saving, due to:

- The possible use of a higher indoor temperature.

- The elevated chilled water supply temperature required by the chilled ceilings and beams.

- The much-reduced volume flow rate of air to be transported into the air-conditioned space as primary air.

Additionally, the height of the ceiling void required for installation of chilled ceilings / beams is less than that for a conventional all air system, permitting the use of a lower floor-to-floor height. Furthermore, the maintenance cost should be lower as well due to the simple maintenance work required, which is limited to vacuuming of the dry coils, with the possible bacterial and mould growth due to presence of condensate and cleansing of drain pans, fans and filters all absent.

The benefit due to the possible use of a higher chilled water supply temperature can be realized only if the building is large enough to justify the use of separate chiller plants or more complicated plant designs, such as chillers in series, such that chillers that deliver the higher supply temperature will run at a much higher coefficient of performance (COP) compared to those that will need to deliver chilled water at a lower temperature (see Chapter 6 for more detailed elaboration on chiller COP).

For smaller buildings, it may be more economical to install just one chiller plant, with the higher chilled water supply temperature achieved by directly mixing return chilled water with supply chilled water from the plant or through the use of a small heat exchanger between two chilled water circuits operating at different temperature ranges.

4.6.3 Design of chilled ceiling / beam system in conjunction with the PA system

As remarked above, in the design of chilled ceiling / beam systems, it is crucial to ensure the primary air (PA) supply flow rate, V_{PA}, and the difference in moisture content between the indoor air and the PA supply ($w_r - w_s$), are large enough for the PA to offset the total moisture gain (M_r, in kg of moisture per second) of the room (Figure 4.36), i.e.:

$$M_r \leq \rho_a V_{PA}(w_r - w_s) \tag{4.18}$$

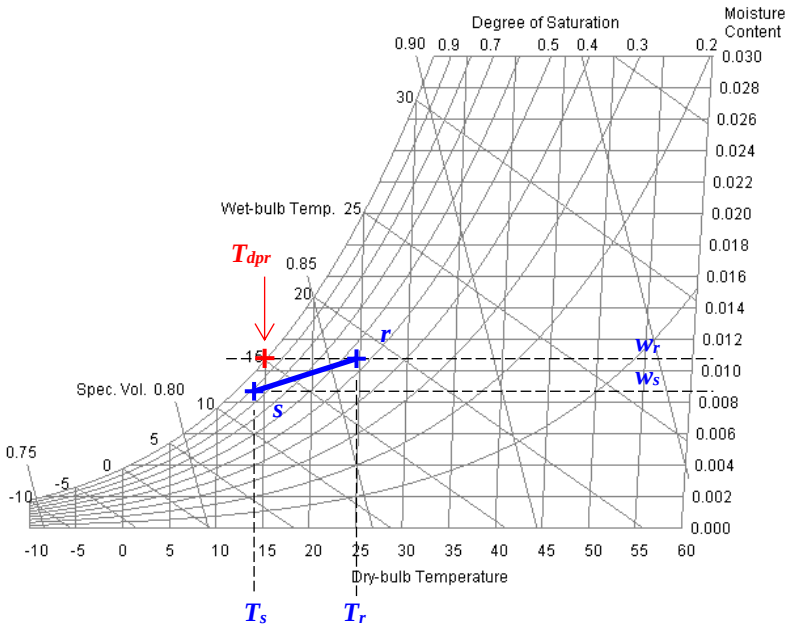

Remark:
For avoiding condensation, the surface temperatures of the chilled ceilings / beams must all be above the dew point temperature of the indoor air (T_{dpr}).

Figure 4.36 The primary air supply process

Therefore, the minimum supply flow rate of PA is:

$$V_{PA} \geq \frac{M_r}{\rho_a(w_r - w_s)} \tag{4.19}$$

Since the PA is supplied into the air-conditioned space at temperature T_s, which is below the room air temperature T_r, the PA will also provide an amount of sensible cooling, Q_{SPA}, given by:

$$Q_{SPA} \leq \rho_a V_{PA} Cp_a (T_r - T_s) \tag{4.20}$$

Therefore, the total sensible cooling capacity of the chilled ceilings / beams ($Q_{SCC/B}$) must be sufficient to offset the remainder of the room sensible load, with the sensible cooling effect of the PA discounted:

$$Q_{SCC/B} \geq Q_{SR} - Q_{SPA} \tag{4.21}$$

Where

Q_{SR} = Design room sensible cooling load, kW

The steps of design may be summarized as follows:

1. Careful selection of design conditions, including indoor air state, PA supply air state and chilled water supply temperatures for the PA handling unit and the chilled ceilings / beams. The supply PA state should have as low a moisture content as possible, subject to the available chilled water temperature, and the indoor air state should have as high a moisture content as possible, subject to the condition that its dew point should be well below the surface temperature of the chilled ceiling / beam. The indoor air temperature should also be as high as possible, subject to thermal comfort limit.

2. Design cooling load calculation for air-conditioned spaces, with breakdowns of the design load into sensible and latent design cooling loads for each space.

3. Determination of PA supply flow rate required to offset all latent load of the space.

4. Checking if the PA flow rate is acceptable; otherwise, adjust design conditions. If room air condition changed, start again from Step 1.

5. After determination of a suitable PA flow rate, calculation of its sensible cooling capacity and offsetting this from the room sensible cooling load (Equation 4.21).

6. Selection of chilled ceiling / beam that can meet the remainder of the design room sensible cooling load calculated in Step 5. For active chilled beams, their cooling output is dependent on the PA supply flow rate.

A typical floor in an office building model was used as a reference to demonstrate the design steps mentioned above. Table 4.3 summarizes the design conditions adopted for air-conditioning system design.

Table 4.3 Design conditions for an office floor

Design conditions	Unit	Value
Design OA temperature, T_o	°C	33.3
Design OA RH, RH_o	%	66
Design OA moisture content, w_o	kg/kg	0.02146
Design OA enthalpy, h_o	kJ/kg	88.47
Design RA temperature, T_r	°C	25
Design RA RH, RH_r	%	55
Design RA dew point, T_{dpr}	°C	15.4
Design RA moisture content, w_r	kg/kg	0.01093
Design RA enthalpy, h_r	kJ/kg	52.982
Room floor area (Interior Zone)	m^2	493.24
Room height	m	3.2
Room volume	m^3	1578.368
Lighting and app. power density	W/m^2	35
Lighting and appliances heat gain, Q_{si}	kW	17.2634
Occupancy rate	m^2/p	9
No. of Occupants	No.	54.8
Sensible heat gain per person	W/p	75
Rad. Sen. heat gain from occupant	%	60
Latent heat gain per person	W/p	55
Moisture gain per person	g/s-p	0.0219912
Sensible load from occupants, Q_{sp}	kW	4.1103333
Latent heat gain from occupants, Q_{lp}	kW	3.0142444
Moisture gain from occupants, M_p	kg/s	0.0012052
FA requirement	l/s-p	10
FA flow rate, V_{fa}	m^3/s	0.5480444
Infiltration ACH	ACH	0.1
Infiltration flow rate, V_{inf}	m^3/s	0.0438436
Sensible load from infiltration, Q_{sinf}	kW	0.4439598
Latent load from infiltration, Q_{linf}	kW	1.3855719
Moisture gain from infiltration, M_{inf}	kg/s	0.000554

The design cooling loads of the perimeter zones facing different directions and of the interior zone were calculated based on design weather conditions of Hong Kong, using a computer program and the results were as summarized in Table 4.4. Note should be taken that the room sensible cooling loads are to be shared between the PA system and the chilled ceilings / beams. Therefore, the room sensible cooling load that the PA system can offset should be determined before selection of chilled ceiling or beam can be carried out.

Table 4.4 Design cooling load predictions for an office Floor

Floor	Space	DSL	DLL	DTL	Area	DSL	DLL	DTL
		kW	kW	kW	m^2	W/m^2	W/m^2	W/m^2
Typical	North	11.33	1.46	12.79	144.44	78.42	10.13	88.54
Typical	West	14.39	1.20	15.58	144.44	99.59	8.30	107.90
Typical	East	13.07	1.86	14.94	144.44	90.51	12.91	103.42
Typical	South	12.33	1.12	13.45	144.44	85.34	7.77	93.11
Typical	Interior	25.75	6.04	31.79	493.24	52.20	12.25	64.45
Typical	Total	73.67	11.05	84.73	1071.00	68.79	10.32	79.11

Legend: DSL = Design sensible load or load intensity
DLL = Design latent load or load intensity
DTL = Design total load or load intensity

Note: The DSL is shared between the PA system and the chilled ceilings / beams;
The DLL is undertaken solely by the PA system.

A parametric study had been done to examine the impacts of different combinations of indoor air temperature and relative humidity, and PA supply condition, on the required flow rate of PA. As shown in Figure 4.37, the required PA supply flow rate is indeed highly sensitive to these parameters; each rise or drop in the temperature of the room air or PA supply by one-degree Celsius, or in the relative humidity of the room air by 5%, may lead to a dramatic increase or drop in the required PA supply air flow rate.

For the case being studied, the condition of 12°C for the PA supply dew point temperature and 25°C, 55% RH for the indoor air state are an optimal combination to be selected, as the PA supply flow rate required is just slightly higher than the minimum fresh air flow rate that should be supplied for the occupants. At this condition, the PA can offset room sensible load at the rate of 18.1 W/m^2 (Figure 4.37). Table 4.5 summarizes the cooling capacities required of the chilled ceilings / beams for different zones on the floor, found after deducting the cooling capacity of the PA from the design room sensible loads of the respective zones.

As Table 4.5 shows, chilled ceiling panels may be adopted for the interior zone but either passive or active chilled beams are needed for the perimeter zones. With this result, one may proceed to the next step of selection of the models of chilled ceiling and chilled beams, and the layout design, for the office floor.

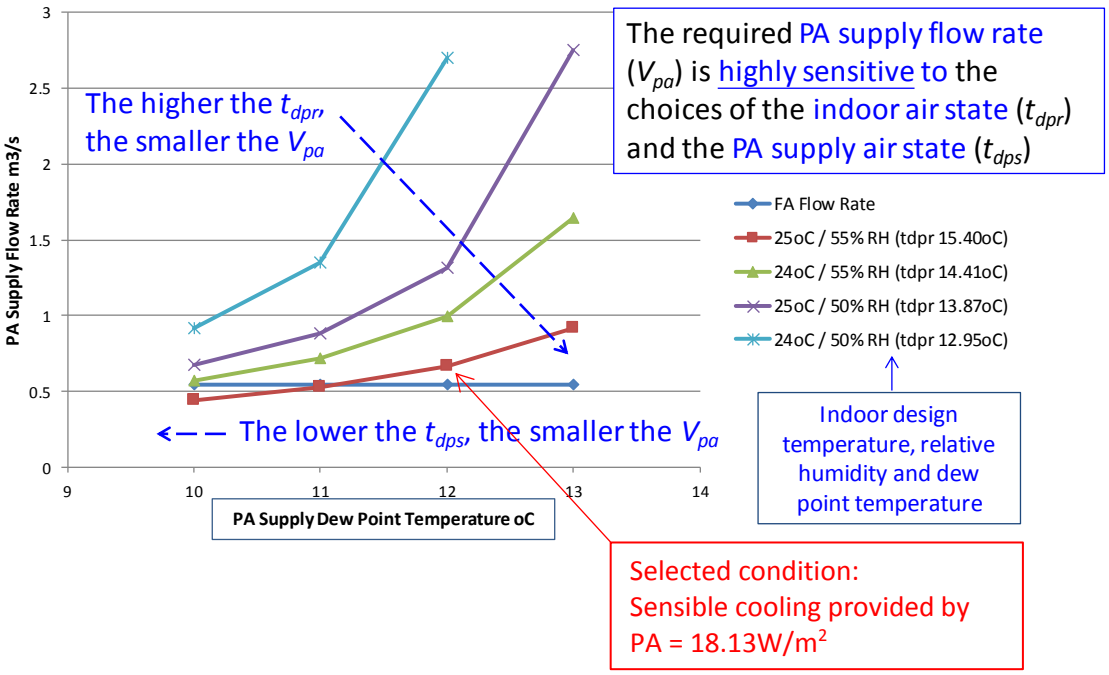

Figure 4.37 Impacts of the indoor air state and primary air supply state on the required PA flow rate

Table 4.5 Required chilled ceiling / beam capacity

Floor	Space	DSL	PA S Cap	CC/B Cap
		W/m²	W/m²	W/m²
Typical	North	78.42	18.13	60.29
Typical	West	99.59	18.13	81.46
Typical	East	90.51	18.13	72.38
Typical	South	85.34	18.13	67.21
Typical	Interior	52.20	18.13	34.07

Legend: DSL = Design sensible load intensity
PA S Cap = Primary Air Sensible Cooling Capacity
CC/B Cap = Chilled Ceiling / Beam Sensible Cooling Capacity

4.6.4 Control of chilled ceiling / beam system

Like fan-coil systems, chilled ceiling / beam systems are normally provided with simplistic automatic control systems for controlling the indoor temperatures of the zones they serve. For a zone served by multiple chilled ceiling panels or beams, the ceiling panels or beams may be grouped into one circuit and controlled by a single 2-way valve for on/off control of chilled water flow through the panels / beams (Figure 4.38).

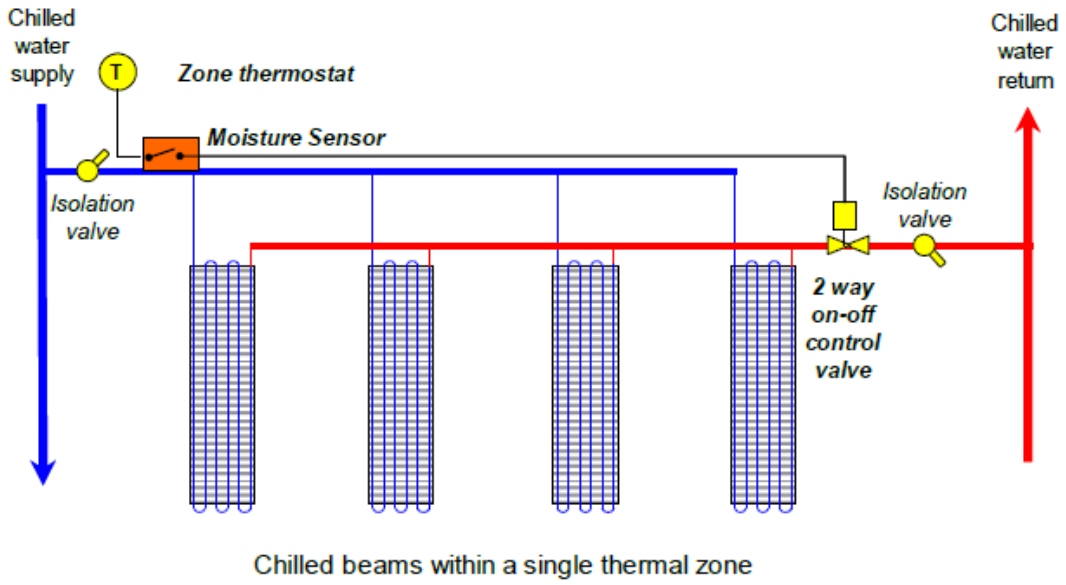

Figure 4.38 Automatic control for chilled ceiling / beam

As a measure to avoid damages that condensation could incur, a moisture sensor may be installed at an exposed section of the supply water pipe, with thermal insulation removed (Figure 4.38). Once moisture is detected, the sensor will cause the chilled water flow to be shut-off, thereby eliminating the occurrence of condensation upon the chilled ceiling / beam surfaces. However, once chilled water supply needs to be stopped to avoid occurrence of condensation, the system can only be restored to normal working order again when the accompanying PA system is able to pull down the humidity level in the space.

Annex 4A Essence of automatic control for air-conditioning systems

4A.1 Automatic control system and components

Automatic control is crucial to air-conditioning systems and equipment; so crucial that the different types of air-side system, e.g. the constant air volume (CAV) and variable air volume (VAV) systems, are distinguished by the control methods they adopt. With automatic control, an air-conditioning system or equipment will react automatically to disturbances, such as an increase in cooling load or duct static pressure, while keeping the "controlled variable", such as air or water temperature or flow rate, at or near to the desired value, referred to as the "set-point".

In order to keep the controlled variable within accepted limits, its value must be measured and compared to the set-point value from time to time. Deviation of the measured value from the set-point value is called "error". The error signal is amplified and converted by a "controller" into an output to an "actuator", which will drive a "controlled device" such that the operating condition of the system (e.g. its heating or cooling output) will be changed in a manner that will cause the error to be minimized or eliminated. This kind of control is called "closed-loop control" as the output is fed back and used in the control process (Figure 4A.1).

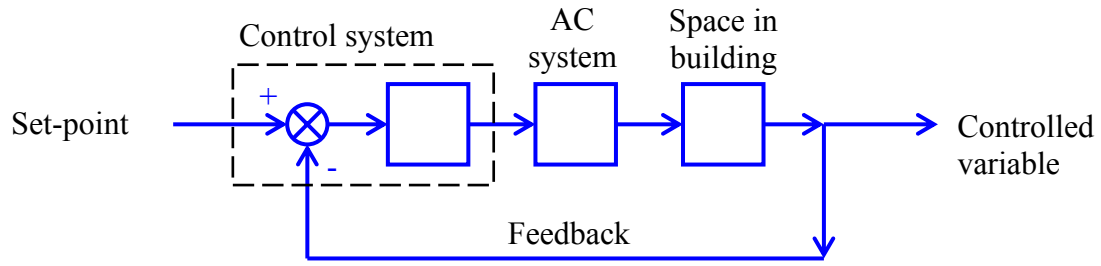

Figure 4A.1 Block diagram for a closed-loop control system

The "sensor" for measuring the controlled variable together with the controller and actuator are "control devices" of an automatic control system. Figure 4A.2 shows the relation between the control devices and the system under its control which, in our case, includes the air-conditioning system and the space in the building served by the system, as the response of both would affect the controlled variable.

Figure 4A.3 shows the relations among control devices and the air-conditioning system in a control schematic diagram for a fresh air handling unit. The function of the control system for the fresh air handling unit is to maintain the temperature of the fresh air leaving the unit at or near to the set-point value.

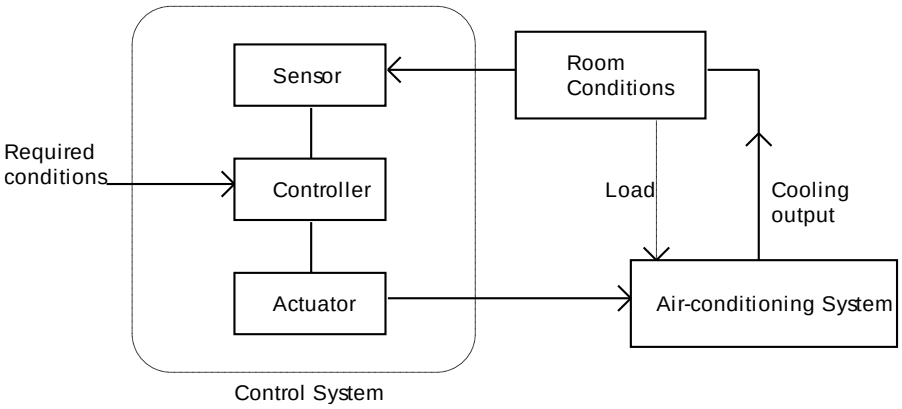

Figure 4A.2 Relations among control system, air-conditioning system, and building

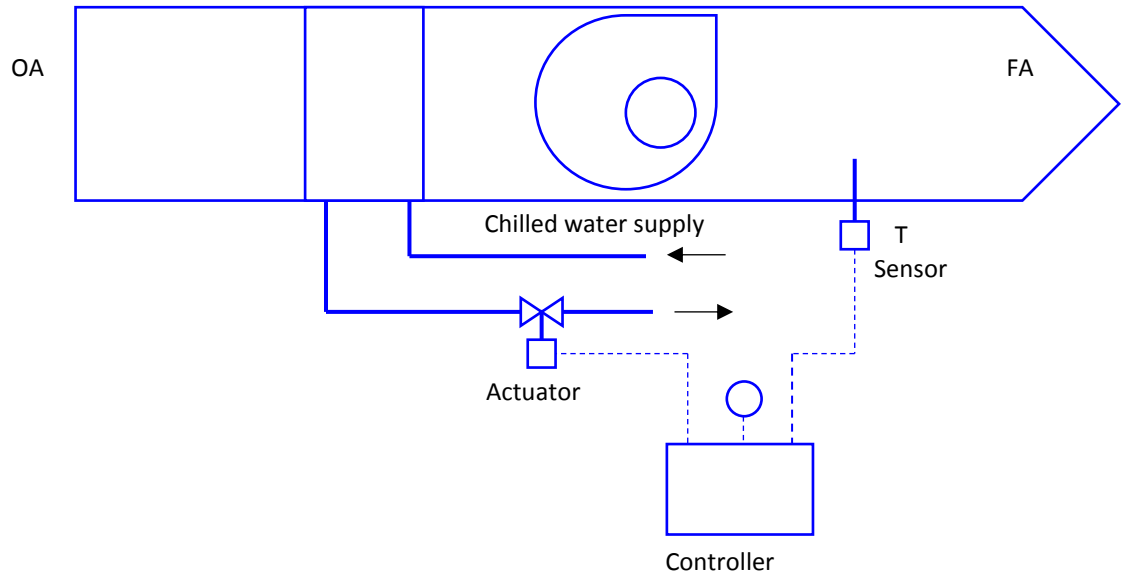

Figure 4A.3 Control schematic for a fresh air handling unit showing relations among control devices and the air-conditioning system

4A.2 Control actions

There are 5 types of control action that are commonly used in air-conditioning systems, which include:

- On/off control
- Floating point control
- Proportional (P) control
- Proportional plus Integral (PI) control
- Proportional plus Integral plus Derivative (PID) control

4A.2.1 On/off control

On/off control, also called two-position control, is the type of control action that may be implemented with the use of the simplest, and hence the least expensive, control devices, such as thermostats with a bi-metallic strip coupled to an on/off switch (Figure 4A.4a) or a solenoid valve. For on/off control, there are two control settings, namely the on-setting and off-setting (Figure 4A.4b). When the controlled variable goes beyond the on-setting, the controlled device will be set to the maximum output, or simply turned on. When the controlled variable passes the off-setting, the controlled device will be set to zero output, or simply turned off.

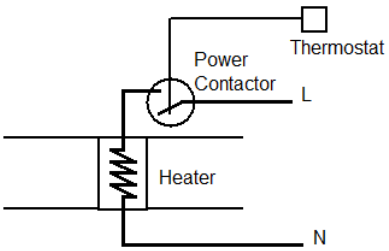

a) Thermostatic control of an electric heater

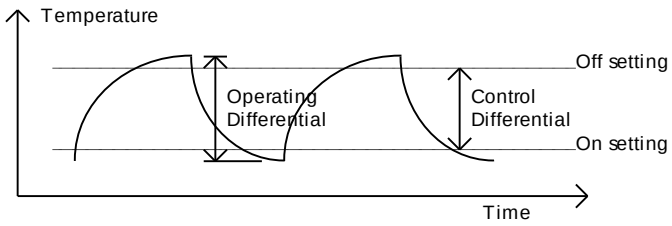

b) Variation of the controlled variable

Figure 4A.4 On/off control system and response

The difference between the on- and off-settings is called “control differential” (Figure 4A.4b) and their mid-value is the set-point. In lieu of the on- and off-settings, the more common settings for an on/off controller are the set-point and control differential based upon which the on- and off-settings used in the control action are defined.

Using winter indoor air temperature control by switching an electric heater on and off as an example, which is the function served by the system shown in Figure 4A.4, electricity supply to the heater will be cut when the indoor temperature overshoots the off-setting. Without power supply to the heater, no heating is supplied to the room and therefore the room temperature will start to fall, but no action will be taken until the room temperature falls below the on-setting, at which point electricity supply to the heater will be resumed and the heater will output its full capacity. This will bring up the room air temperature and, once the temperature overshoots the off-setting again, the power supply to the heater will be cut. Such cycles of on and off operation of the heater will continue until the heating system is put out of operation. Within an on and off cycle,

the ratio of the on time to the period of the cycle is proportional to the sensible load on the system.

With on/off control, the frequency of the on/off cycle is dependent on the width of the control differential; the narrower the differential, the more frequent the controlled device will be turned on and off. Although a smaller control differential will result in more accurate control over the controlled variable, it will lead to increased wear and tear of the control devices and the system under control due to the more frequent on/off switching actions.

4A.2.2 Floating point control

Floating point control is an enhancement of the basic on/off control. Instead of turning a system to either full or no output, the output of the system will be gradually increased or reduced, by an incremental step per unit time step, as long as the controlled variable stays outside the control differential; the output will be increased if the on-setting is overshoot and reduced if the off-setting is passed. When the controlled variable stays inside the control differential, no action will be taken, and the controlled device will stay at its last position.

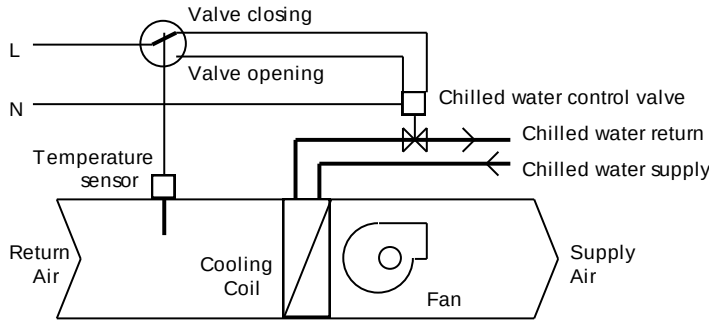

a) System schematic

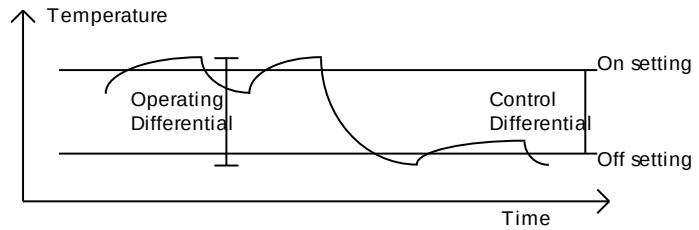

b) Room temperature response

Figure 4A.5 Floating point control system and response

As shown in Figure 4A.5b, the controlled variable, indoor temperature in this example of a space cooling system, may wander within the control differential with no definite path, but will be brought back when it goes outside the control differential. The controlled variable, therefore, may still vary within a margin called “operating differential”, but the response of the system is gradual instead of cycling between fully on or off.

Floating point control can be easily implemented with digital control devices. However, with micro-processor-based control, implementation of more sophisticated control actions, such as P, PI or even PID control, will not incur significant increase in cost.

4A.2.3 Proportional (P) control

In proportional (P) control, the controller output is linearly proportional to the error, and the correlation between the two may be positive (direct acting) or negative (reverse acting). The following are the definitions of some terms used in P control (apply also to PI & PID controls) (Figure 4A.6):

- Set point ($V_{o,sp}$): this is the desired level of the controlled variable at which the controller is set to maintain as a target.
- Error or offset (e): this is the difference between the set point and the actual level of controlled variable as fed-back by the sensor.
- Throttling range (TR): this is the range between the levels of the controlled variable over which the controlled device would be commanded by the controller to move from the maximum to minimum position or vice versa.

The P control action may be expressed mathematically as:

$$V_o = K_P e + M \tag{4A.1}$$

Where:

$$K_P = \frac{V_{o,max} - V_{o,min}}{TR} \tag{4A.2}$$

V_o = output from the controller
K_P = proportional gain
e = error
M = manually offset (output level when $e = 0$)
$V_{o,max}$ = maximum controller output
$V_{o,min}$ = minimum controller output
TR = throttling range

The error, e, is often defined in control textbooks as:

$$e = V_{o,sp} - V_o \tag{4A.3a}$$

The above definition is suitable for application to heating systems with a reverse acting controller the output of which is inversely proportional to the controlled variable (see Figure 4A.6.c as opposed to Figure 4A.6.a), i.e. the lower the value of the controlled variable (the indoor temperature), the higher its output which will lead to a higher heating output.

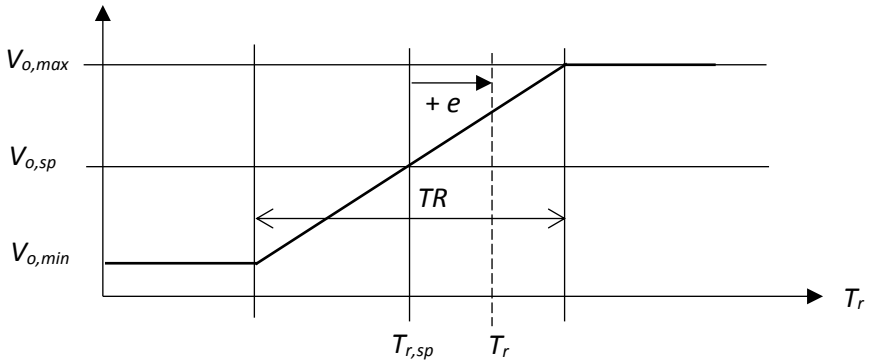

a) Error or offset, *e*, and throttling range, *TR*, of a direct acting P

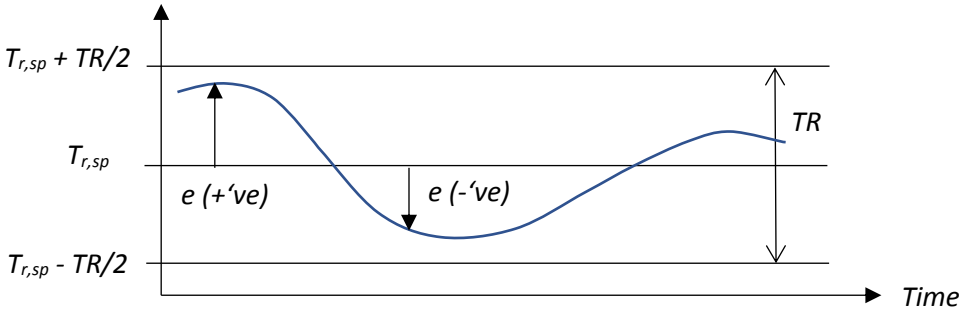

b) Variation in error, *e*, of a direct acting P controller

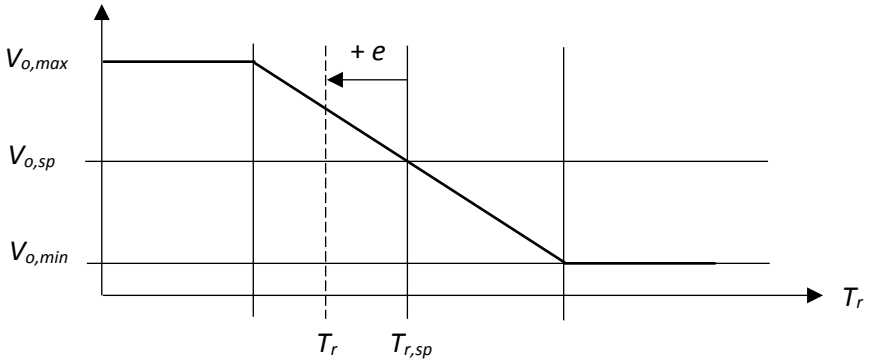

c) Error or offset, *e*, of a reverse acting P controller

Figure 4A.6 Error of offset and throttling range in control

For cooling systems, however, we need a controller that will output a higher value that will lead to a higher cooling output the higher the value of the controlled variable (the indoor temperature). Therefore, for cooling systems with direct acting controllers the output of which will be higher the higher the value of the controlled variable (Figure 4A.6.a), the definition of the error, *e*, term is as shown below.

$$e = V_o - V_{o,sp} \qquad (4A.3b)$$

The error term in both Equations (4A.3a) & 4A.3b) are compatible with Equation (4A.1) as well as other equations for describing P, PI & PID control actions. Throughout the book, the definition as given in Equation (4A.3b) is used for error.

The set point is mid-way between the upper and lower limits of the throttling range (*TR*). With P control, a larger error means a greater control action to be taken by the controlled device. However, there are limits to the movement of a controlled device and, hence, if the error (in absolute value) is greater than half the *TR*, the controlled device will just stay at its maximum or minimum position. The system will be out of control when such a condition arises.

With P control, the controller output is proportional to the error. At zero error, the output will be at the pre-set value *M*, also called the manual off-set. However, it is far more often to have a positive or negative error, i.e. the controlled variable deviates from the target set point value for most of the time.

The spread of the error range, i.e. the throttling range, can be adjusted at the controller. Note, however, should be taken that the values of the proportional gain K_P and the throttling range are interrelated. Spread of the throttling range should neither be too wide (i.e. K_P too small) nor too narrow (i.e. K_P too large). If K_P is too small, system response will be slow, and accuracy of control will be poor. If K_P is too large, however, control action becomes virtually on/off and it may even cause hunting (rapid cycling) of the system, which is highly undesirable and should be avoided.

4A.2.4 Proportional plus integral (PI) control

To minimize the error that will inevitably occur in simple P control, an additional term is added which is called integral action as shown mathematically below:

$$V_o = K_P e + K_I \int e \cdot dt + M \qquad \text{(4A.4a)}$$

Alternatively, the equation may be modified to:

$$V_o = K_P \left(e + \frac{1}{T_I} \int e \cdot dt \right) + M \qquad \text{(4A.4b)}$$

Where

K_I = integral gain;
T_I = the integral (reset) action time ($= K_P / K_I$)

As can be seen from the above expressions, with PI control, control action will continue to increase (or drop) as long as error exists; it will stabilize only when the error is brought to zero eventually. Figure 4A.7 compares how the controlled variable will become when there is a step change in disturbance to the system, e.g. a step reduction in the cooling load on an air-side system.

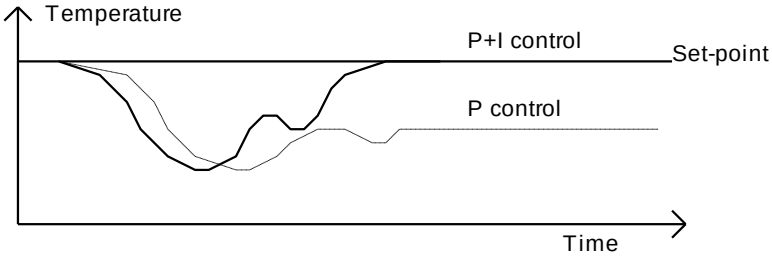

Figure 4A.7 Indoor temperature response to a step reduction in sensible load with P and PI control

During the start-up period of an air-side system, there would inevitably be a large deviation between the set point and the actual value of the controlled variable. With PI control, large action would be incurred within a short time due to the integral action. This phenomenon is called "integral windup", which can be prevented by limiting the 'I' action to take effect until the controlled variable stays within the proportional band.

4A.2.5 Proportional plus integral plus derivative (PID) control

As discussed in the preceding sections, P control suffers from a steady state error. Whereas PI control can eliminate the steady state error, the integral action needs a finite time to become effective, i.e. it takes time for the integral signal to become significant. If prompt action is desired to cope with sudden change in load whilst steady state error is to be removed as well, an additional control action, the derivative action, may be included and the resultant control action can be expressed as:

$$V_o = K_P e + K_I \int e \cdot dt + K_D \frac{de}{dt} + M \qquad (4A.5)$$

Where K_D = derivative gain

With PID control, the overall control action includes a part which is proportional to the rate of change of the error signal, de/dt. Use of PID control has the advantage that it can respond quickly to a sudden load change. Since thermal response of buildings, and hence the required rate of response on the air-conditioning systems, are normally slow, PID control was seldom used in conventional HVACR systems.

However, with the advent of direct digital control (DDC) and building management system (BMS), implementation of PID control will not entail significant increase in cost and hence this type of control is becoming increasingly widely used. The control parameters, however, have to be finely tuned to get desired results [2, 3].

4A.2.6 Digital implementation

With digital controllers or direct digital control (DDC) systems, the integral and derivative actions are implemented with reference to a constant sampling interval, Δt. Here, the sampled value of the error at time step t is denoted by e_t, and the error at one time step later, i.e. $t+\Delta t$, by e_{t+1}.

By replacing the integral of error over time by summation, and the differentiation by finite difference, Equation (4A.5) may be re-written, for time = t, as:

$$V_{o,t} = K_P e_t + K_I \sum_{j=0}^{t} e_j \cdot \Delta t + K_D \frac{e_t - e_{t-1}}{\Delta t} + M \tag{4A.6}$$

For time step $t + \Delta t$,

$$V_{o,t+1} = K_P e_{t+1} + K_I \sum_{j=0}^{t+1} e_j \cdot \Delta t + K_D \frac{e_{t+1} - e_t}{\Delta t} + M \tag{4A.7}$$

From the above equations, we can define an incremental controller output, $\Delta V_{o,t+1}$ as:

$$\Delta V_{o,t+1} = V_{o,t+1} - V_{o,t} \tag{4A.8}$$

Substituting Equations (4A.6) & (4A.7) into (4A.8), we get,

$$\Delta V_{o,t+1} = K_P(e_{t+1} - e_t) + K_I e_{t+1} \cdot \Delta t + K_D \frac{e_{t+1} - 2e_t + e_{t-1}}{\Delta t} \tag{4A.9}$$

Note that the manual offset term, M, has been eliminated in the subtraction process, and hence becomes immaterial in the digital control process.

Having calculated $\Delta V_{o,t+1}$, the required output $V_{o,t+1}$ can be determined from:

$$V_{o,t+1} = V_{o,t} + \Delta V_{o,t+1} \tag{4A.10}$$

References

[1] ASHRAE Handbook, HVAC Systems and Equipment, Chapter 6 Panel Heating and Cooling, American Society of Heating, Refrigerating and Air-conditioning engineers, Inc., 2008.

[2] Underwood, C.P., HVAC Control Systems Modelling, Analysis and Design, E & FN Spon, 1999.

[3] Haines, R.W., Hittle, D.C., Control Systems for Heating, Ventilating, and Air Conditioning, 5th Ed., Chapman & Hall, 1993.

Chapter 5 Space Air Diffusion, Fan Duct System, and Mechanical Ventilation

5.1 Introduction

Chapter 4 has elaborated on the major air-side air-conditioning systems that may be selected for comfort air-conditioning in buildings, including constant air volume (CAV) and variable air volume (VAV) systems, primary air fan coil systems, and chilled ceiling / beam systems. The operating principles and characteristics of these air-side systems and the associated primary air system and the optional heat recovery wheels, as well as the considerations to be given to their design, have been discussed in detail. System design calculations may be carried out according to the principles and methods discussed in that chapter, in conjunction with the methods for psychrometric analyses and cooling load calculation covered in Chapters 2 & 3.

Subsequent to system selection and determination of the capacities of the air-handling equipment and the design flow rates of supply air, fresh air, and chilled water, there are further design work to be done before the air-side system design is complete. These include selection and layout of supply air diffusers and return air grilles, and layout and sizing of air ductworks connecting the air-handling equipment and the supply diffusers and return grilles. The first part of this chapter is dedicated to these design steps for the air-side air-conditioning systems. To complement the discussions on air-side systems, analysis of fan duct systems, guidance on fan selection, and design of mechanical ventilation systems for temperature and airborne contaminant control are included in the second part of this chapter.

Furthermore, an annex is appended to this chapter to provide readers with a concise review of basic fluid mechanics that supports the section on duct sizing (and as well the section on pipe sizing in Chapter 8).

5.2 Space air diffusion design

In the last chapter, the discussions on design of air-side air-conditioning systems assumed implicitly that the air inside an air-conditioned space could be represented by a single air state. In other words, the assumption was made that the states of air at various locations in an air-conditioned space were uniform throughout the space. How close is this idealistic condition to the real situation hinges on the performance of the supply air diffusers, which is dependent on the layout and the air flow characteristics of the air diffusers.

As a part of the air-conditioning system design process, space air diffusion design deals with selection and layout design of supply air diffusers for an air-conditioned space. Proper space air diffusion design is vital to ensuring the temperature and movement of air inside an air-conditioned space would be found acceptable by most of the occupants. Unfortunately, it is often not given adequate attention or compromised on aesthetic consideration for the false ceiling.

Compared to other aspects of air-conditioning system design, space air diffusion design is not as well supported by clear principles and rigorous methods. The method covered in the ASHRAE Handbook [1, 2] is based on the air diffusion performance index (ADPI)

but the prediction of ADPI achievable in a space due to a specific diffuser type and layout is based largely on limited empirical findings and may be considered somewhat vague. A more rigorous method, i.e. computation fluid dynamics (CFD) simulation, is available. However, whilst its application to some complex situations are justified, applying it to every project may be considered too costly. In this section, the basic concepts of space air diffusion design that is based on the ADPI method are introduced and discussed.

5.2.1 Effective draft temperature

The heat transfer between the surface of a human body and the ambient air, and hence the thermal comfort sensation of an occupant, is dependent not only on the temperature but also the moving speed of the surrounding air (see Section 2.7). The effects of the two can be combined and quantified by a single parameter, called the effective draft temperature (θ_{ed}) [2], as defined below:

$$\theta_{ed} = (T_x - T_c) - 8(V_x - 0.15) \tag{5.1}$$

Where

T_x = local air temperature, °C
T_c = average (set point) air temperature, °C
V_x = local air speed, m/s

Equation (5.1) implies that the effect of an increase in the temperature of the air surrounding an occupant by 1°C can be compensated by also increasing the air speed by 0.125 m/s, leaving the value of the effective draft temperature unaffected. A high percentage of people in sedentary condition would find it comfortable when exposed to an effective draft temperature between −1.5 and +1°C, provided that the air speed is less than 0.35m/s [3].

Closer examination of Equation (5.1) unveils that irrespective of the actual value of T_c, as long as T_x equals T_c and V_x equals 0.15, the effective draft temperature (θ_{ed}), will be equal to zero. Obviously, fulfilling such condition does not necessarily mean that the indoor thermal environment will be regarded as acceptable to most occupants. A prerequisite to applying Equation (5.1) is that the average (set point) temperature T_c must be within the range considered to be comfortable by the occupants (see discussions on thermal comfort in Chapter 2).

If measurements of air temperature and speed are made at a number of different locations within an air-conditioned space, the effective draft temperature can be evaluated for each location. The percentage of the locations that have their effective draft temperature and air speed meeting the abovementioned comfort criteria (i.e. $-1.5 < \theta_{ed} < +1$°C and $V_x < 0.35$m/s) is called the air diffusion performance index (ADPI).

A common design objective is to achieve an ADPI value above 80%. However, ADPI is applicable only to space cooling and the air temperature and speed measurements should be conducted according to ASHRAE Standard 113 [4], which defines the number of measurement points, their locations, the method of measurement, etc.

5.2.2 Diffuser selection

Many types of air diffusers are available in the market, such as ceiling diffusers, high sidewall grilles, slot diffusers, jet nozzles, etc. (Figure 5.1). Figure 5 in Chapter 20 of the ASHRAE Handbook, Fundamentals, 2009 [5] is included here as Figure 5.2, which shows the air movement and vertical temperature distributions in a space with a high sidewall supply grille and a ceiling diffuser. As illustrated in this figure, the air flow and temperature patterns in a space will vary with the type of diffuser adopted. For the same diffuser, its performance can be largely different when used for heating and cooling.

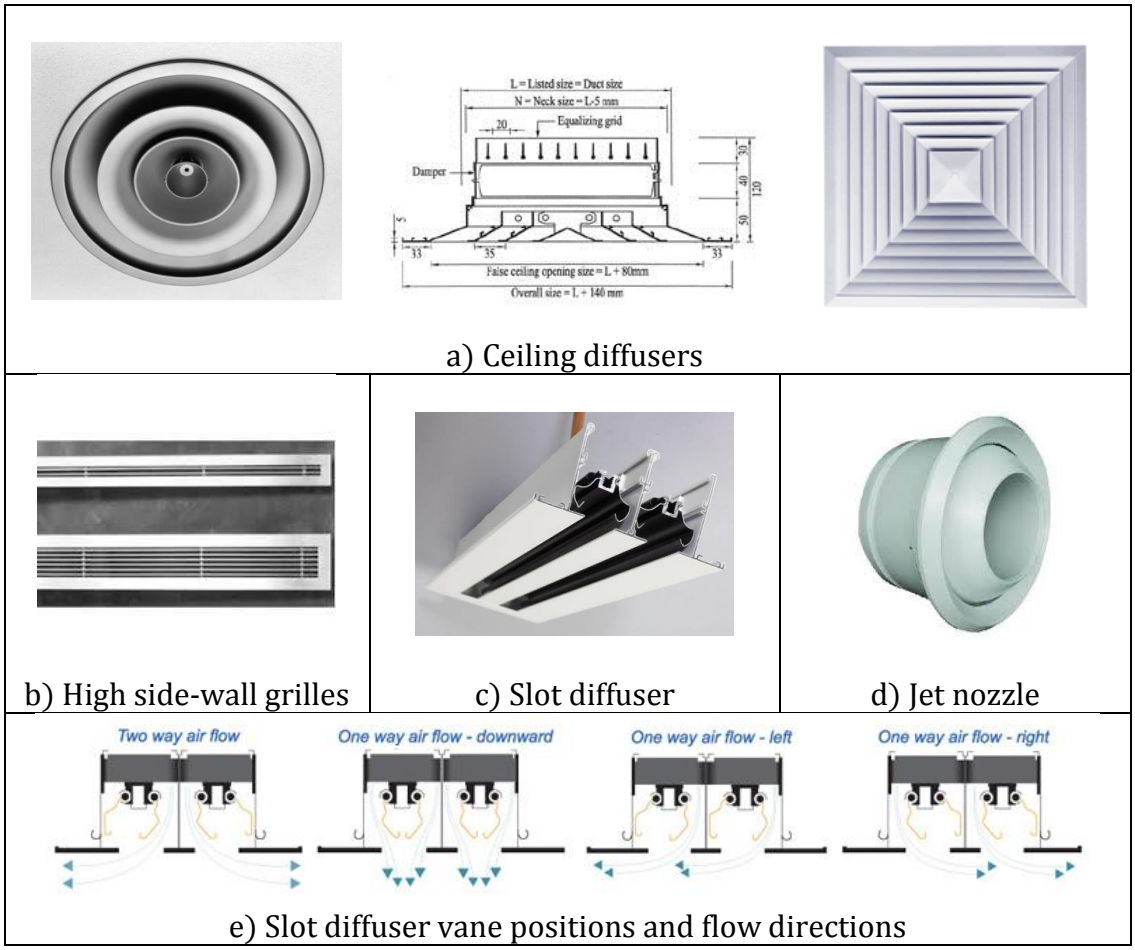

a) Ceiling diffusers

b) High side-wall grilles

c) Slot diffuser

d) Jet nozzle

e) Slot diffuser vane positions and flow directions

Figure 5.1 Common air diffusers types

Given the variations in performance characteristics among different types of diffusers, each type of diffuser may be suitable for application to a limited number of system types and to indoor spaces with geometric configuration and cooling load intensity falling within given ranges. For example, ceiling diffusers are suitable for a CAV system but could result in highly uneven air temperature and speed distributions when used in a VAV system. Furthermore, a diffuser that can perform well when the air-conditioning

system is providing cooling may perform badly when the mode of operation is switched to heating (Figure 5.2).

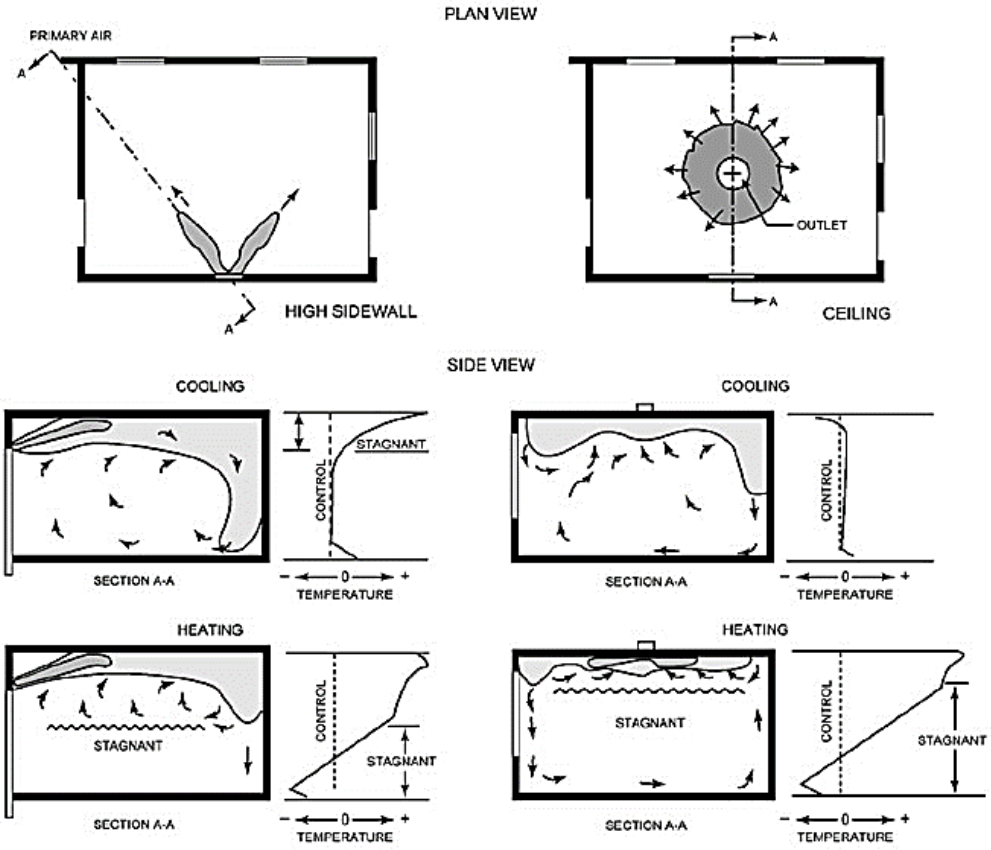

Figure 5.2 Air movement and temperature characteristics of high sidewall grilles and ceiling diffusers (Source: Figure 5 in Chapter 20 of ASHRAE Handbook, Fundamentals, 2009 [5])

The characteristics of the air stream discharged by various types of diffuser used in air-conditioning systems can be described by referring to the characteristic parameters of an air jet. As shown in Figure 5.3, a non-isothermal air jet is formed inside a large space when cool air at a temperature below the temperature of the air in the space is discharged horizontally into the space through an opening in one of the walls enclosing the space.

When the air enters the room through the wall opening, the air in the jet is moving at a speed, v_0, which is higher than the speed of the air surrounding the jet. As air is a viscous fluid, the surrounding air will be 'entrained' into the air jet as long as the speed of the air in the jet is higher than that of the surrounding air, resulting in an expansion in size of the jet as well as a reduction in the speed and an increase in temperature of the air in the jet. The lost in momentum will be greater for air at the circumference of the jet than that in the core. Being cooler than the air inside the space, the air jet will also fall in height as the air in it flows further away from the wall opening.

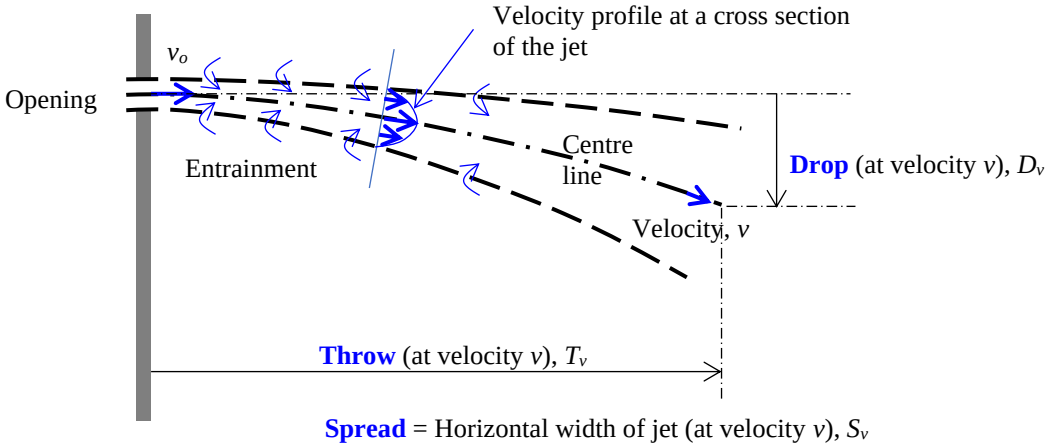

Figure 5.3 Throw, drop and spread of a cool air jet

As shown in Figure 5.3, the horizontal distance between the wall and a point along the centreline of the jet, where the air velocity has slowed down from v_o to v, is called the throw, T_v. The horizontal width of the jet at the same point is called the spread, S_v. The vertical distance between this point and the centre-line level of the wall opening through which the air enters the space is called the drop, D_v. Since T_v, S_v and D_v are all dependent on v, a reference velocity, called terminal velocity, is defined for their quantification. Unless otherwise specified, the value of $v = 0.25$m/s is adopted as the terminal velocity for diffuser selection. Throw and drop data for diffusers may be obtained from the diffuser manufacturers for use in space air diffusion design.

The geometric configuration of the room for which diffusers are to be selected is quantified by a parameter called the characteristic length, L, defined according to Table 3 in Chapter 57 of ASHRAE Handbook, HVAC Applications [2], which is shown here as Table 5.1. Figure 5.4 is a graphical illustration of the definition of characteristic length for different types of diffuser.

Table 5.1 Characteristic room length for several diffusers (measured from center of air outlet) (Source: Table 3 in Ch. 57 of ASHRAE Handbook, HVAC Applications [2])

Diffuser Type	Characteristic Length L
High sidewall grille	Distance to wall perpendicular to jet
Circular ceiling diffuser	Distance to closest wall or intersecting air jet
Sill grille	Length of room in direction of jet flow
Ceiling slot diffuser	Distance to wall or midplane between outlets
Light troffer diffusers	Distance to midplane between outlets plus distance from ceiling to top of occupied zone
Perforated, louvered ceiling diffusers	Distance to wall or midplane between outlets

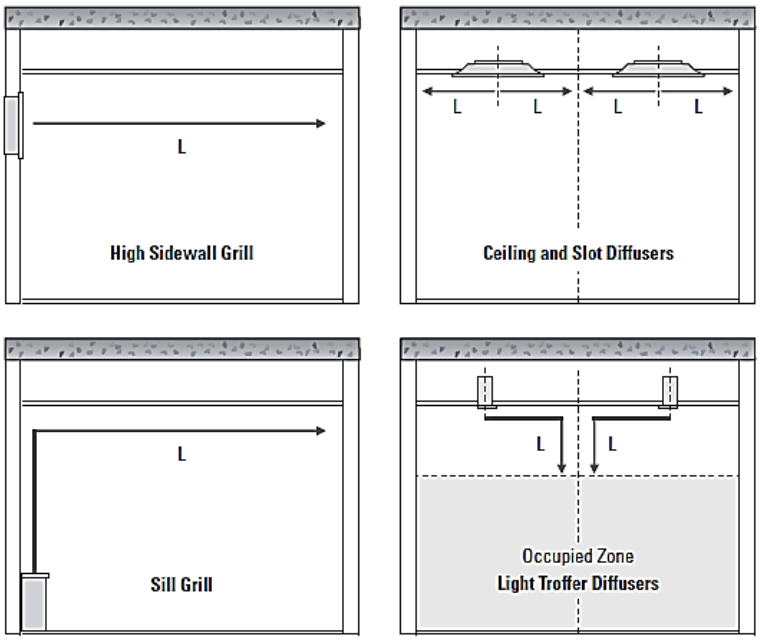

Figure 5.4 Characteristic room length for several diffusers

Recommended throw to characteristic length ratio ($T_{0.25}/L$) for the target ADPI value can be found from Table 4 in Chapter 57 of the ASHRAE handbook, HVAC Applications, 2015 [2], which is shown here as Table 5.2. As the data in this table show, ADPI is affected by room load intensity (W/m^2); the larger the load (or the higher the $T_{0.25}/L$ value), the smaller the ADPI value. Though not explicitly stated, the load should be the design room sensible load.

The procedures involved in space air diffusion design are as summarized below:

1. Ascertain load intensity from design cooling load calculation results.

2. Select a type of grille, find out the supply flow rate each unit can handle within pressure drop and noise limits, the corresponding throw value, and determine the number of units of such grille required for the room.

3. Work out a layout design of the grilles and evaluate the characteristic length for each.

4. Evaluate the throw to characteristic length ratio ($T_{0.25}/L$) for each grille and check if the target ADPI value can be achieved.

5. If ADPI is lower than target value, modify the grille selection and/or layout design and evaluate the performance again.

6. The above design steps should be repeated until the required spare air diffusion performance is achieved.

Table 5.2 Air Diffusion Performance Index (ADPI) Selection Guide (Source: Table 4 in Ch. 57 of ASHRAE Handbook, HVAC Applications [2])

Terminal Device	Room Load, W/m²	$T_{0.25}/L$ for Maximum ADPI	Maximum ADPI	For ADPI Greater Than	Range of $T_{0.25}/L$
High sidewall grilles	250	1.8	68	—	—
	190	1.8	72	70	1.5 to 2.2
	125	1.6	78	70	1.2 to 2.3
	60	1.5	85	80	1.0 to 1.9
Circular ceiling diffusers	250	0.8	76	70	0.7 to 1.3
	190	0.8	83	80	0.7 to 1.2
	125	0.8	88	80	0.5 to 1.5
	60	0.8	93	90	0.7 to 1.3
Sill grille, straight vanes	250	1.7	61	60	1.5 to 1.7
	190	1.7	72	70	1.4 to 1.7
	125	1.3	86	80	1.2 to 1.8
	60	0.9	95	90	0.8 to 1.3
Sill grille, spread vanes	250	0.7	94	90	0.6 to 1.5
	190	0.7	94	80	0.6 to 1.7
	125	0.7	94	—	—
	60	0.7	94	—	—
Ceiling slot diffusers (for $T_{0.50}/L$)	250	0.3	85	80	0.3 to 0.7
	190	0.3	88	80	0.3 to 0.8
	125	0.3	91	80	0.3 to 1.1
	60	0.3	92	80	0.3 to 1.5
Light troffer diffusers	190	2.5	86	80	<3.8
	125	1.0	92	90	<3.0
	60	1.0	95	90	<4.5
Perforated, louvered ceiling diffusers	35 to 160	2.0	96	90	1.4 to 2.7
				80	1.0 to 3.4

5.2.3 Return grilles

Because the locations and characteristics of return air grilles have much less influence on the air temperature and speed distributions in an air-conditioned space, there is much freedom in locating return air grilles in space air diffusion design, provided the face velocity and the noise emitted from the grilles stay within acceptable limits. Consult the ASHRAE Handbook [2] for recommendations on high limits of face velocity upon return grilles. A simple criterion is to limit the face velocity at or below 2.5m/s.

5.3 Air duct system design

In a central air-conditioning system, the supply air diffusers, and the return air grilles, are connected to the air-handling unit by air ducts to facilitate circulation of air between the air-conditioned space and the air-handling unit. The air ducts are typically made of galvanized mild steel sheets and clad with thermal insulation. There are well established standards on ductwork construction [6, 7], which are widely adopted in supply and installation contracts for air-conditioning systems to govern the quality of ductwork in the systems.

5.3.1 Energy and pressure lost due to air flow through a duct

In determining the required size of a piece of air duct, attention must be paid to its dynamic performance, in respect of the air flow velocity in the duct and the pressure drop that will be incurred across the duct, which are dependent on the flow rate of air to

be conveyed and the cross-sectional area and length of the duct, including any duct fittings (e.g. bends, Tee-offs, etc.) involved. Duct sizing must strike a proper balance between initial cost of the ductwork and the long-term operating cost of fans for overcoming the pressure losses. There could also be other constraints, such as ceiling void spaces and structural opening sizes, that limit sizes of ducts that could be installed, and flow induced noise and vibration must not be overlooked.

For readers' quick reference, a concise summary of the basic fluid mechanics principles that underpin duct sizing methods (and pipe sizing and fan/pump selection methods) is given in Annex 5.A. The steady flow energy equation (Equation 5A.22) given in the Annex may be applied to the case of a fan-duct system (same applies to a pump-pipe system). In a fan-duct system, there will not be heat input and the heat gain or loss from or to the surrounding may be neglected (i.e. $Q = 0$). However, account must be taken of the increase in internal energy (e) of the air, which is due to the flow incurred energy loss and will eventually be dissipated as heat to the surrounding.

Ignoring any heat transport, Q, dividing all terms by the mass flow rate, m, replacing specific volume by the reciprocal of density ($v = 1/\rho$), and after re-arrangement, the steady flow energy equation becomes:

$$\frac{p_1}{\rho_1} + \frac{u_1^2}{2} + gz_1 + \frac{W_{in}}{m} = \frac{p_2}{\rho_2} + \frac{u_2^2}{2} + gz_2 + l \tag{5.2}$$

Where the last term in the equation, l, stands for the energy loss per unit mass flow rate of the fluid ($= e_2 - e_1$). Note also that in Equation 5.2, W_{in}, which denotes the work input to a fan or pump, replaced the work output of the system, W, which will be negative when work is input to the system as in the case of a fan or pump, where $W_{in} = -W$.

By assuming that the density of the fluid will remain unchanged when the fluid is subject to a pressure change (i.e. the fluid is essentially incompressible), Equation (5.2) may be expressed with reference to a mean air density (ρ), and with each term converted to a pressure term, as follows:

$$p_1 + \rho\frac{u_1^2}{2} + \rho g z_1 + \rho\frac{W_{in}}{m} = p_2 + \rho\frac{u_2^2}{2} + \rho g z_2 + \rho l \tag{5.3}$$

The $\rho u^2/2$ terms in the above equation are called velocity pressures, which may be combined with the respective static pressure (p) to become the total pressure (p_t):

$$p_{t1} + \rho g z_1 + \rho\frac{W_{in}}{m} = p_{t2} + \rho g z_2 + \rho l \tag{5.4}$$

For a fan (or a pump), Equation (5.4) may be further simplified by ignoring the height difference between the inlet and exit:

$$p_{t1} + \rho\frac{W_{in}}{m} = p_{t2} + \rho l$$

Solving for W_{in}, we get:

$$W_{in} = \frac{m}{\rho}(p_{t2} - p_{t1}) + ml = V(p_{t2} - p_{t1}) + ml \quad (5.5)$$

Where V is the volume flow rate ($= m/\rho$).

Defining fan (pump) efficiency, η, as shown in Equation (5.6), the fan power can be evaluated by using Equation (5.7):

$$\eta = \frac{V(p_{t2} - p_{t1})}{W_{in}} \quad (5.6)$$

$$W_{in} = \frac{V(p_{t2} - p_{t1})}{\eta} \quad (5.7)$$

When analysing just the ducting (or piping) system, the work term in Equation (5.3) can be ignored ($W_{in} = 0$), and the energy loss may be replaced by a total pressure loss term (Δp_l):

$$p_1 + \rho\frac{u_1^2}{2} + \rho g z_1 = p_2 + \rho\frac{u_2^2}{2} + \rho g z_2 + \Delta p_l \quad (5.8)$$

Equation (5.8) is actually the Bernoulli's equation, which is the basic analytical tool for many fluid flow problems, including air flow through ducting systems (and water flow through piping systems). For air-conditioning system design, the Bernoulli's equation provides the means for determining the sizes of ducts for conveying a given air flow rate and the associated pressure losses that would need to be overcome, and the duties required of the fan for driving the air flow.

5.3.2 The Darcy-Weisbach equation and friction factor

The pressure loss (Δp_l) incurred by air flow in ducts, as shown in Equation (5.8), can be determined by using the Darcy-Weisbach equation, as shown below:

$$\Delta p_l = f\frac{L}{D_h}\rho\frac{u^2}{2} \quad (5.9)$$

Where:

$$D_h = 4\frac{A}{P} \quad (5.10)$$

In Equation (5.9), f is the Darcy-Weisbach friction factor, L the duct length, D_h the duct hydraulic diameter, u the air flow velocity and ρ the air density. In Equation (5.10), A and P are the cross-sectional area and perimeter length of the duct.

Note that the Darcy–Weisbach friction factor is 4 times the Fanning friction factor. Attention must be paid to distinguish which one of these is meant by the "friction factor" shown in a chart or an equation to be used for finding appropriate values of the friction factor for duct loss calculations.

The Moody diagram is a chart that can be used to evaluate the friction factor applicable to a pipe of a given relative roughness when the pipe is conveying fluid flow corresponding to a certain Reynolds number. Figure 5.5 is a diagrammatic illustration of a Moody diagram. A proper diagram is available in the ASHRAE Handbook [1] and various references on fluid mechanics.

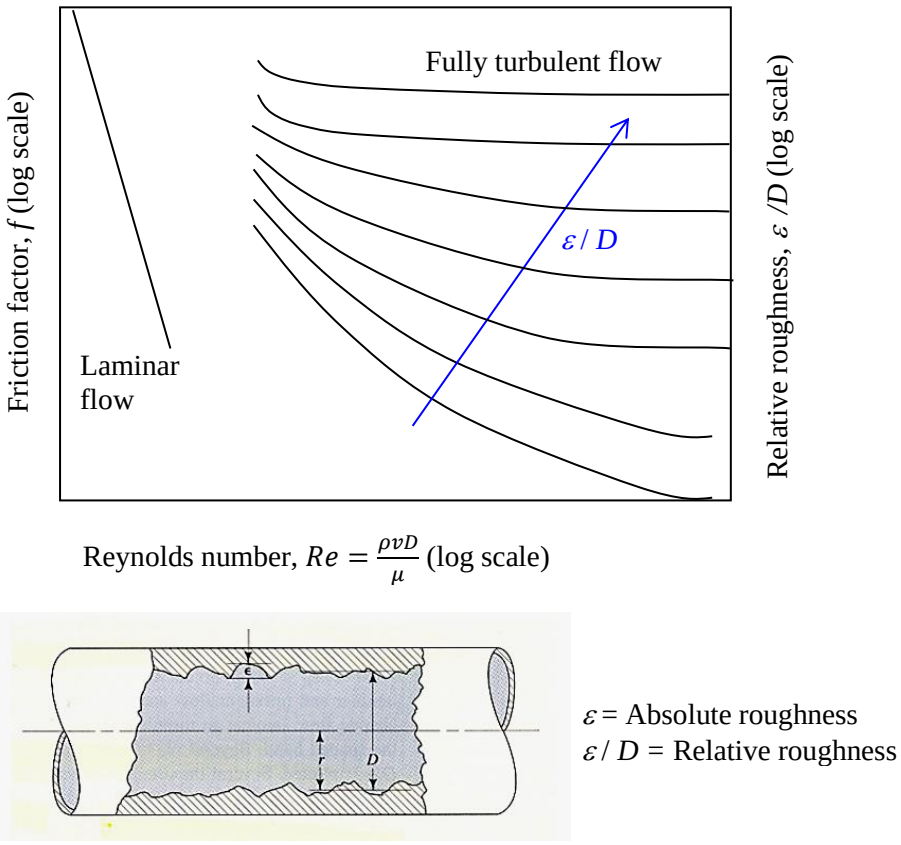

Figure 5.5 Moody diagram for Darcy-Weisbach friction factor

It can be observed from the Moody diagram (Figure 5.5) that when the flow is fully turbulent, the friction factor will be dependent mainly on the relative roughness and is nearly independent of the flow velocity (and hence the Reynolds number). In other words, for a given pipe with fixed roughness, the friction factor tends to be a constant rather than a function of the flow rate through the pipe, provided the flow is fully turbulent, which is an assumption very often made in analyses of fluid flow through pipes, ducts, and pipe/duct system components. According to the Darcy–Weisbach equation (Equation 5.9), with a constant friction factor, the pressure drop per unit length of the pipe will be proportional to the square of the flow velocity or flow rate through the pipe, which is the case when the flow is fully turbulent.

Instead of using the Moody diagram, the friction factor may be evaluated by using the Colebrook's equation (Equation 5.11)) [1]:

$$\frac{1}{\sqrt{f}} = -2\log\left(\frac{\varepsilon}{3.7D_h} + \frac{2.51}{Re\sqrt{f}}\right) \tag{5.11}$$

Where

$$Re = \frac{\rho u D_h}{\mu} \tag{5.12}$$

And ε is the absolute roughness factor, D_h the hydraulic diameter, and Re the Reynolds number to be evaluated from Equation (5.12), and in it, μ is the fluid's viscosity.

As shown in Equation (5.11), the friction factor term appears at both sides of the Colebrook's equation. This means that the equation is implicit and solution for the friction factor needs to be solved by an iterative procedure.

Data on the roughness of typical types of air duct material can be found from the ASHRAE Handbook [1], CIBSE Guide [8], and other relevant references.

5.3.3 Equivalent duct diameter

Note that unlike the hydraulic diameter (Equation 5.10) of a round duct, which is equal to its diameter, the hydraulic diameter of a rectangular or flat oval duct is different from the diameter of an equivalent circular duct, D_e, of the same length that will incur the same pressure drop when conveying the same flow rate. The equivalent circular duct diameter (D_e) of a rectangular duct and a flat oval duct can be evaluated respectively from Equations (5.13) and (5.14) [1]:

$$D_e = \frac{1.3(a \cdot b)^{5/8}}{(a+b)^{1/4}} \tag{5.13}$$

$$D_e = \frac{1.55(AR)^{5/8}}{P^{1/4}} \tag{5.14}$$

Where:

a & b are the lengths of the sides of the cross-section of a rectangular duct ($a > b$).

AR & P are the cross-sectional area and perimeter length of a flat oval duct, as shown in Figure 5.6 and the equations below:

For a flat oval duct,

$$AR = \frac{\pi b^2}{4} + b(a-b) \tag{5.15}$$

$$P = \pi b + 2(a-b) \tag{5.16}$$

Since equivalent diameters can be determined for rectangular and flat oval ducts, duct loss data, in tables or charts, can be developed just for round ducts to facilitate duct sizing.

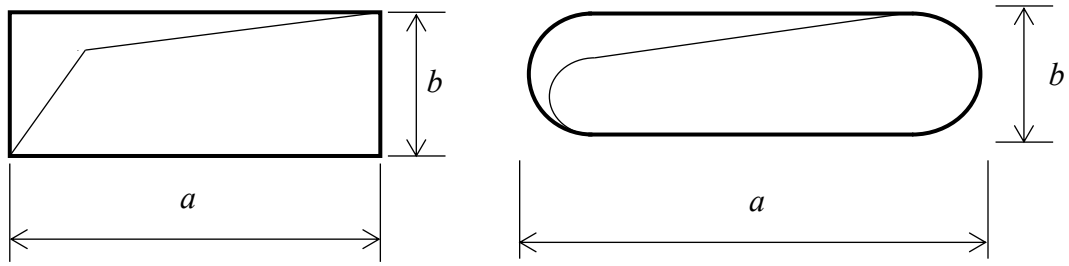

Figure 5.6 Width and height of a rectangular and a flat oval duct

It is interesting to note that Equations (5.13) and (5.14) differ from what can be derived directly from the definition of equivalent diameter, i.e. the diameter of an equivalent circular duct, D_e, of the same length that will incur the same pressure drop when conveying the same flow rate. For a non-circular duct with cross-sectional area AR, and perimeter P,

$$\Delta p = \frac{\rho f L}{2}\frac{u^2}{D_h} = \frac{\rho f L}{2}\frac{1}{D_h}\left(\frac{Q}{AR}\right)^2 \tag{5.17}$$

For a circular duct with diameter that equals the equivalent diameter of the rectangular duct (D_e) and is conveying the same flow rate (Q),

$$\Delta p = \frac{\rho f L}{2}\frac{1}{D_e}\left(\frac{Q}{A_e}\right)^2 \tag{5.18}$$

Where A_e is the cross-sectional area of the circular duct with diameter D_e.

Equating Equations (5.17) & (5.18) and after cancellation of identical terms,

$$D_e\left(\frac{\pi D_e^2}{4}\right)^2 = D_h AR^2 \tag{5.19}$$

It follows from the above equation that:

$$D_e^5 = \left(\frac{4}{\pi}\right)^2 D_h AR^2 \tag{5.20}$$

For a rectangular duct,

$$D_e^5 = \left(\frac{4}{\pi}\right)^2 \frac{4(ab)}{2(a+b)}(ab)^2$$

$$D_e = 1.265\frac{(ab)^{3/5}}{(a+b)^{1/5}} \tag{5.21}$$

For a flat oval duct,

$$D_e^5 = \left(\frac{4}{\pi}\right)^2 \frac{4AR}{P} AR^2$$

$$D_e = 1.453 \frac{AR^{3/5}}{P^{1/5}} \quad (5.22)$$

CIBSE adopted the above equations in developing their duct sizing tables in lieu of those given in the ASHRAE Handbook which were based on Huebscher [9] whose approach was criticized to be invalid [10]. Between the ASHRAE and CIBSE methods, there are just minor differences, as shown by the equivalent diameters calculated using the two methods, as summarized in Table 5.3.

Table 5.3 Equivalent diameters (D_e) calculated using the ASHRAE and CIBSE methods

Rectangular				ASHRAE	CIBSE
a	*b*	*ab*	(*a*+*b*)	D_e	D_e
300	100	30000	400	182.7	185.3
300	125	37500	425	206.8	209.3
300	150	45000	450	228.5	230.9
300	175	52500	475	248.2	250.5
300	200	60000	500	266.4	268.7
300	225	67500	525	283.3	285.5
300	250	75000	550	299.1	301.3
300	300	90000	600	327.9	330.4

Flat oval				ASHRAE	CIBSE
a	*b*	*AR*	*P*	D_e	D_e
300	100	27854.0	714.2	179.9	181.3
300	125	34146.8	742.7	202.3	203.3
300	150	40171.5	771.2	221.8	222.4
300	175	45927.8	799.8	239.0	239.3
300	200	51415.9	828.3	254.2	254.3
300	225	56635.8	856.9	267.8	267.6
300	250	61587.4	885.4	279.9	279.6
300	300	70685.8	942.5	300.3	299.9

5.3.4 Data and tool for duct sizing

As mentioned above, equivalent diameters can be determined for rectangular and flat oval ducts and, hence, duct loss data tables or charts can be developed just for round ducts to facilitate duct sizing.

Typical duct sizing charts show the pressure loss per unit duct length due to friction, and the corresponding flow velocities, for galvanized steel ducts of given sizes when conveying different air flow rates, as exemplified in Figure 5.7. The duct sizes shown are for circular ducts, but the chart can be used to size rectangular or flat oval ducts with

reference to their equivalent diameters. In sizing air ducts, the air pressure drop should be in the range of 0.65 to 1.23 Pa/m for low-velocity ducts and 3.3 to 5.7 Pa/m for high velocity ducts, and flow velocity should stay within the range of 9 to 20m/s.

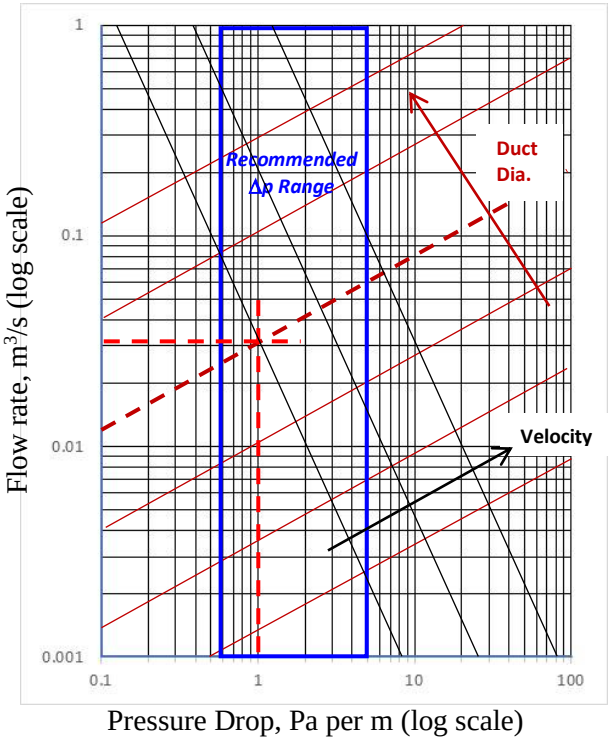

Figure 5.7 Duct sizing chart (Not to scale)

The Ductulator (Figure 5.8) is a convenient tool widely used by air-conditioning practitioners for manual duct sizing. For a given air flow rate, the pressure drop per unit length, flow velocity and equivalent diameter, and the different combinations of the cross-sectional width and height of a rectangular duct corresponding to the equivalent diameter, can be seen at a glance on a Ductulator. It is a good companion of air-conditioning system designers and is preferred by most of them to duct sizing charts and tables.

The friction chart and Ductulator were typically developed based on the surface roughness of galvanized sheet steel, which is the most common material used for duct fabrication. If the surface roughness of the material of the duct under concern differs from that assumed in the duct friction chart or Ductulator, duct pressure loss will need to be estimated based on the known roughness (see for example data in Table 1 of Chapter 21 in ASHRAE Handbook, Fundamentals [1]) and the equations given above.

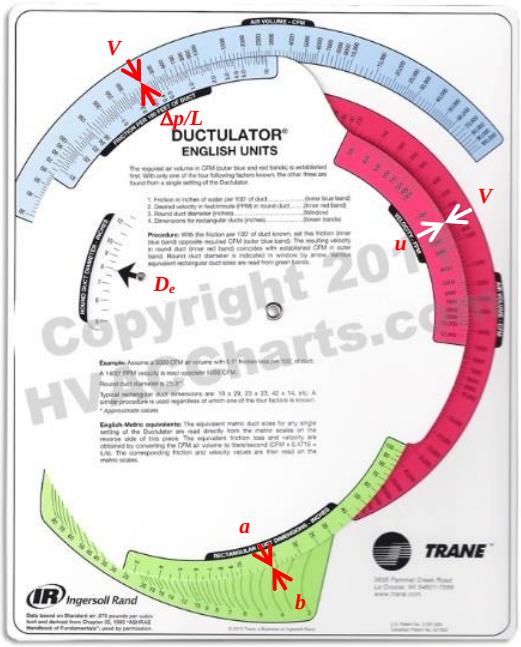

Figure 5.8 A Ductulator

5.3.5 Local loss coefficients and equivalent length for duct fittings

The following is a general description of the relation between the pressure loss (Δp) that a ducting system component will incur when air is flowing through it at the velocity (u):

$$\Delta p = C \cdot \rho \frac{u^2}{2} \tag{5.23}$$

When applied to duct fittings, the dimensionless coefficient C in the above is called the local loss coefficient, and the pressure losses dynamic losses.

Comparing Equation (5.23) against Equation (5.9), it can be seen that for a piece of duct with a uniform cross section and a length L, C is given by:

$$C = f \frac{L}{D_h} \tag{5.24}$$

Local loss coefficients for various types of duct fitting can be found from handbooks on air-conditioning system design (e.g. ASHRAE Handbook, Fundamentals [1] or CIBSE Guide C [8]), or databases that contain the relevant data (ASHRAE have developed one such database).

Note that dynamic loss calculation is based on the actual velocity in the duct rather than the velocity in an equivalent circular duct (equivalence is in flow rate, not velocity). For a duct section or elbow, there will be a single value of the velocity (u) to be used for determining the velocity pressure ($\rho\, u^2/2$) but u may have different values for a converging or diverging section or a Tee or Wye section (Figure 5.9). Attention must be

paid to which inlet / outlet is referred to in using a loss coefficient to determine duct fitting pressure loss.

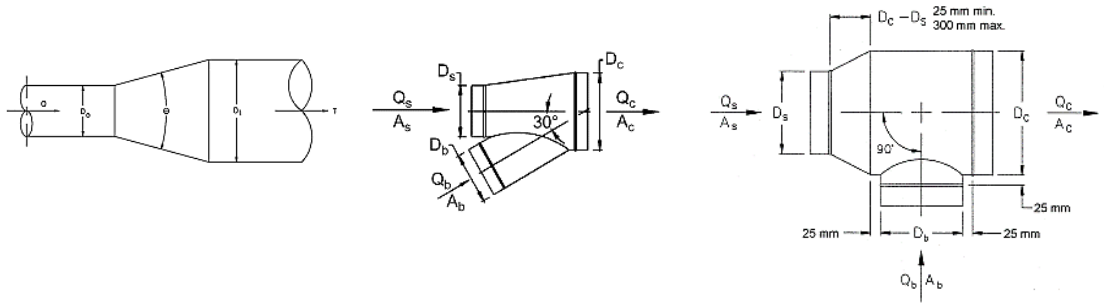

Figure 5.9 Duct fittings – diverging, wye and tee sections

For example, if we know the flow rate Q and the diameters D_0 and D_1 at the entry section (0) and exit section (1) of an expansion fitting, as well as the local loss coefficient based on section 0 (C_0), the pressure drop across the fitting is given by:

$$u_0 = \frac{Q}{\pi D_0^2/4} \tag{5.25}$$

$$\Delta p = C_0 \frac{1}{2}\rho u_0^2 \tag{5.26}$$

If the loss coefficient (C_1) is based on section 1 instead, its relationship with C_0 is as follows:

$$\Delta p = C_0 \frac{1}{2}\rho u_0^2 = C_1 \frac{1}{2}\rho u_1^2$$

$$C_1 = C_0 \left(\frac{u_0}{u_1}\right)^2 \tag{5.27}$$

For a Wye or Tee, the coefficient of pressure loss from the common section to the straight through section (C_s) or the branch (C_b), or vice versa, are dependent on:

A_s/A_c, A_b/A_c, Q_s/Q_c, and Q_b/Q_c

Where

A = cross sectional area
Q = volume flow rate
Subscripts c, s & b denote the common section, straight through section and branch section, respectively.

Readers may find from relevant references negative values of loss coefficients for converging Wye or Tee sections, which means that, in those cases, an increase rather than a drop in pressure will result after mixing.

The concept of equivalent length (L_e) is sometimes used for quantification of the pressure losses of duct fittings. It is the length of a straight duct of the same size as the fitting which will incur the same pressure loss when passing the same air flow rate.

Given that for a fitting:

$$\Delta p = C \cdot \rho \frac{u^2}{2}$$

From Equation (5.24), for a straight duct section with length L_e:

$$\Delta p = f \frac{L_e}{D_h} \cdot \rho \frac{u^2}{2}$$

Equating the two yields:

$$L_e = C \frac{D_h}{f} \tag{5.28}$$

When expressed in equivalent lengths, the effects of the fittings may then be accounted for as if the total duct run were extended by a length that equals the total equivalent lengths of the fittings.

5.3.6 Duct size calculation methods

Although the T-method had been developed by Tsal et al in 1988 [11] and has been introduced in the ASHRAE Handbook, Fundamentals since 1997, this method, which includes optimization of the life cycle cost of the ducting system, has seldom been used in practice by air-conditioning engineers. The most widely used duct sizing methods include (and remain):

- The equal friction method
- The static regain method

In the equal friction method, ducts are sized for a constant pressure loss per unit length ($\Delta p/L$). The value of the $\Delta p/L$ criterion to be used is a choice of the designer. Use of a higher $\Delta p/L$ value will reduce the initial cost of a ducting system but will incur a higher fan pressure requirement and thus a higher operating cost, and vice versa.

Equivalent lengths are particularly suitable for application in conjunction with the equal friction method, as the total system pressure loss can be estimated from the $\Delta p/L$ value and the total equivalent length of the critical circuit in the system. Air flow velocity in the ducting system will drop as flow rate is reduced along the duct run, which is a desirable feature for noise control.

The static regain method takes advantage of the rise (regain) in static pressure that will result from a reduction in the velocity pressure in the main duct after a portion of the air flow is diverted to flow into a branch. The objective is to make use of the static pressure regain to compensate for the pressure loss of the duct section immediately downstream.

Taking the section of a ducting system as shown in Figure 5.10 as an example, the static pressure and flow velocity at planes 1 & 2 are related by the Bernoulli's equation, as shown below:

$$p_1 + \rho\frac{u_1^2}{2} = p_2 + \rho\frac{u_2^2}{2} + \Delta p_{t,1-2} \tag{5.29}$$

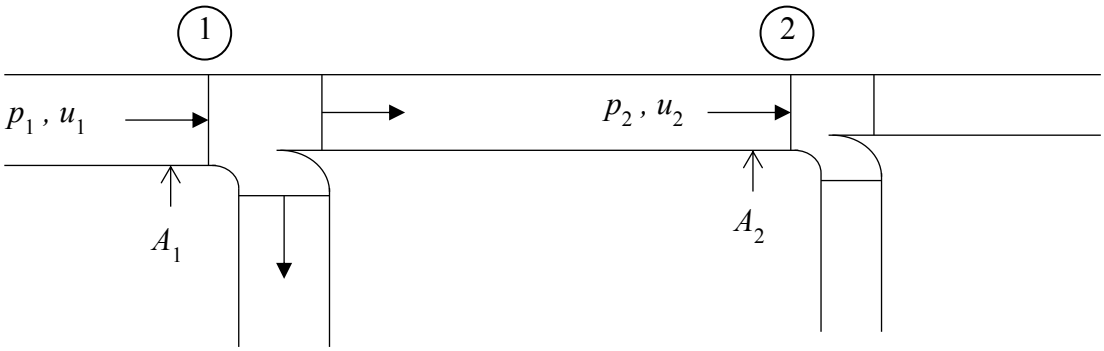

Figure 5.10 A section of a supply air duct system with branches

Achieving the abovementioned objective will lead to equalization of the static pressures at cross sectional planes 1 and 2 in the ducting system. With $p_1 = p_2$, Equation (5.29) can be simplified to:

$$\Delta p_{t,1-2} = \rho\frac{u_1^2}{2} - \rho\frac{u_2^2}{2} \tag{5.30}$$

The above equation will allow the air flow velocity u_2 to be solved, which will in turn allow the size of the duct section between planes 1 & 2 to be determined. However, because the pressure loss between planes 1 and 2 ($\Delta p_{t,1\text{-}2}$) is also dependent on u_2, solution for u_2 requires the use of an iterative procedure.

Note also that $\Delta p_{t,1\text{-}2}$ will include pressure losses across the straight-through branch of the diverting Wye fitting, the duct section(s) that follow(s), as well as any elbow(s) in between if the duct run needs to turn in direction, up to plane 2.

Ducting system design using the static regain method will start from a maximum velocity selected for the root section (immediately downstream of the supply fan), and each downstream section can then be sized using Equation (5.30). A ducting system sized according to this method will have approximately the same static pressure at the entrance to each branch, which will simplify terminal unit selection and system balancing.

Nevertheless, this method has the following disadvantages:

- Unreasonably low velocities and large duct sizes may result at the end of a long duct run.

- The trial and error procedures are tedious.
- The total pressure requirements of each part of the system are not apparent.
- The method does not yield a balanced system.

5.4 Operating characteristics of a fan-duct system

5.4.1 Fan duty

Once the layout of a ducting system has been worked out and individual duct sections in the system have been sized, the total pressure loss of the system, and hence, the duty required of the fan unit for delivering the required air flow rate through the system, can be determined. For a fan-duct system with multiple branches (Figure 5.11), the air delivered by the fan will be split and diverted at the branches to flow along different circuits, and the required total pressure for delivering air through a branch circuit at its design flow rate can differ from branch to branch. The critical branch is the one belonging to the circuit that has the greatest pressure drop round the circuit (the critical circuit), and the critical branch is typically the furthest branch from the fan, but this may not always be the case.

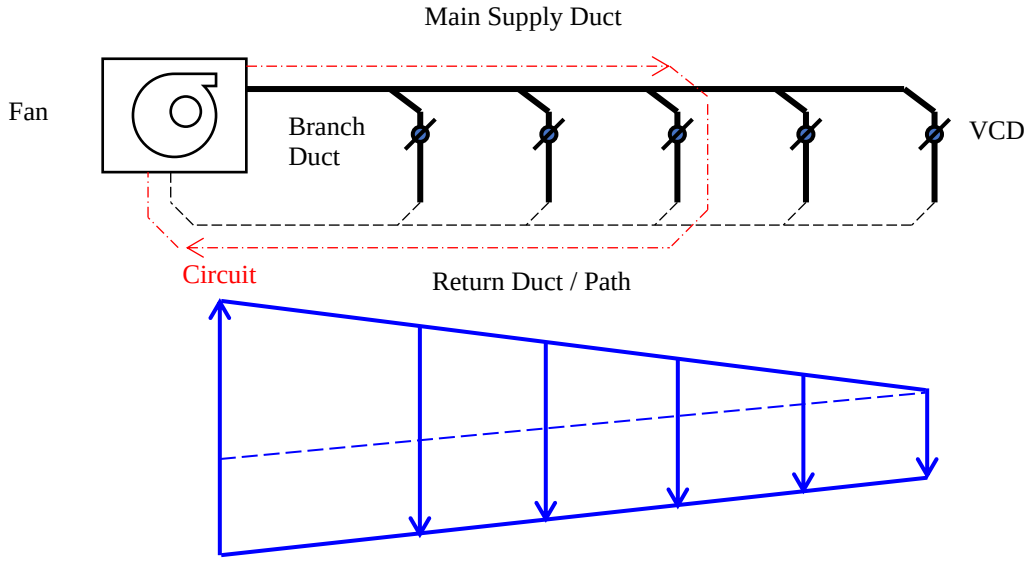

Figure 5.11 Pressure distribution in an air duct system with branches

Before the duty required of the fan can be determined, the critical circuit needs to be identified and the total pressure drop round the critical circuit should be taken as the required fan total pressure. Consequently, except the critical branch, all other branches in the system will be subject to excessive pressure. Before the required adjustment is made, the actual air flow rates through the branches may exceed or fall below their respective design values. Volume control dampers (VCDs) are installed at the branches to throttle off any excessive pressure, such that the branch air flow rates can be adjusted to their respective design values. The process of adjusting the VCDs in the

system such that each branch will receive its design flow rate is called air flow balancing, which is an important part of the commissioning work for air-side systems.

Discussions on air flow balancing, however, will be omitted here because discussions on water flow balancing, which involves the same basic principles and the approach to be used are equally applicable to air ducting systems, will be covered in Chapter 7. Nevertheless, the procedures for air flow balancing for a VAV system will involve more complex procedures not implemented in simply air flow and water flow balancing [2].

The fan in a fan-duct system must be able to overcome the total pressure loss incurred by air flow in the ducting system while it delivers the required total air flow rate through the system. Hence, reference needs to be made to both the air flow rate and the fan total pressure in defining the duty of a fan. The fan total, static and velocity pressures that are used to quantify the characteristics of a fan are as defined in Figure 5.12. Additionally, the performance of a fan includes its power demand (or its efficiency) while it performs the duty. The performance of a fan is typically presented graphically as a curve showing the variation in the fan total (or static) pressure with flow rate. Additional curves may be included to show the corresponding power demand and/or efficiency.

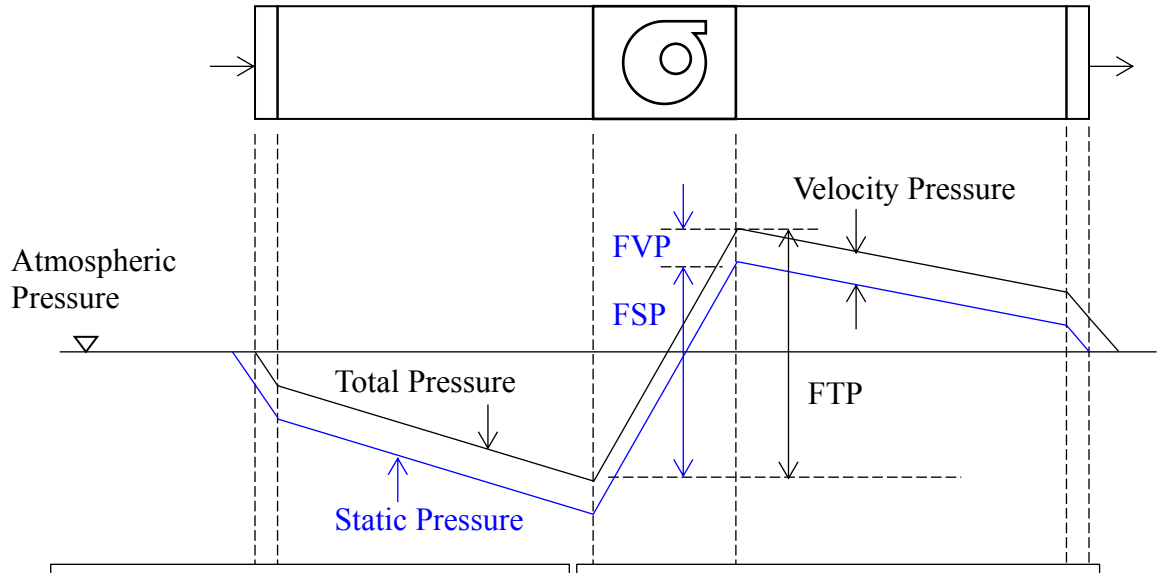

FTP = FSP + FVP

FTP = Fan Total Pressure = $p_{T,1} - p_{T,e}$
FSP = Fan Static Pressure = $p_{S,1} - p_{T,e}$
FVP = Fan Velocity Pressure= $\rho V_1^2/2$

Legend:

$p_{T,1}$ = Total pressure leaving fan
$p_{T,e}$ = Total pressure entering fan
$p_{S,1}$ = Static pressure leaving fan
V_1 = Velocity leaving fan

Figure 5.12 Fan total, static and velocity pressures in a fan-duct system

Note that:

- Fan power (W) and efficiency (η) are alternative variables; either one of them together with the fan total pressure ($\Delta p_{T,f}$) and flow rate (V) are sufficient to define the state of operation of a fan while running at a given speed (see Equations (5.6) & (5.7)).

- The performance of a fan, including the $\Delta p_{T,f}$-V and the W-V relations, is further dependent on the running speed of the fan (N), as shown in Figure 5.13 (see also earlier discussions on VAV system).

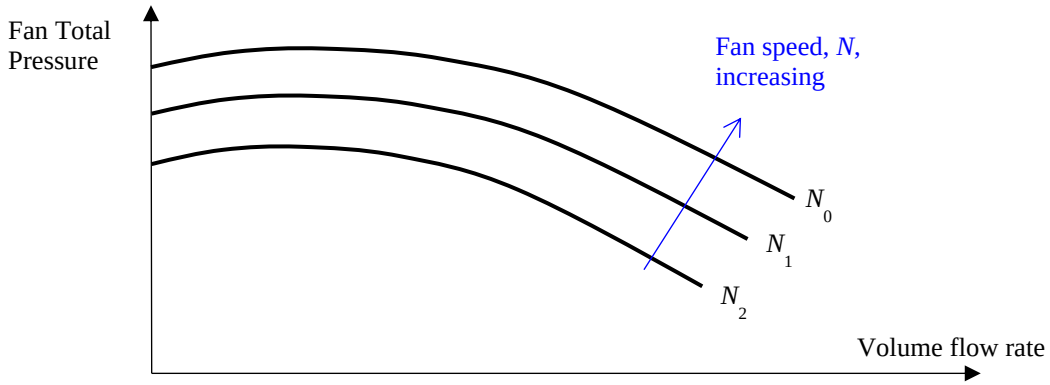

Figure 5.13 Fan total pressure curves at different speeds

Fans of different types (e.g. centrifugal, axial and propeller) and component designs (e.g. impeller with forward or backward curved blades) may be used for mechanical ventilation and air-conditioning (Figure 5.14). Figure 5.15 shows the general performance characteristics of centrifugal and axial fans to which attention should be paid in fan selection.

Centrifugal Fan

Forward Curved Impellor

Backward Curved Impellor

Axial Fan

Propeller Fan

Figure 5.14 Types of fans in air-conditioning and ventilation systems

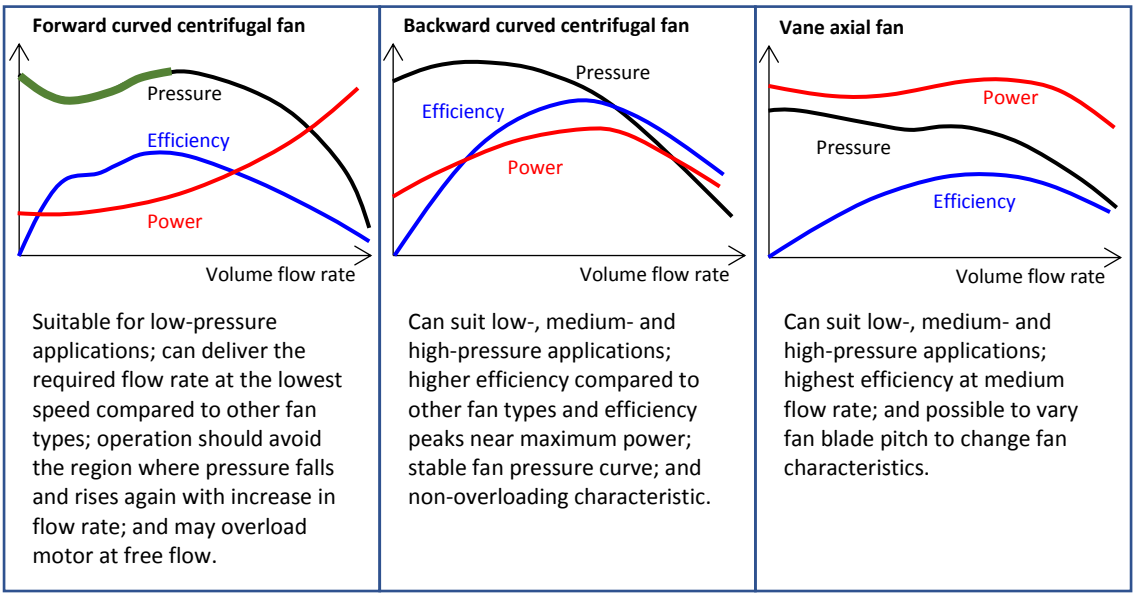

Figure 5.15 Performance characteristics of centrifugal and axial fans

5.4.2 System component characteristics and operating point

Similar to a fan, the hydraulic characteristics of a ducting system may be represented by the relationship between the total pressure loss through the system ($\Delta p_{T,s}$) and the system total air flow rate (V). For a ducting system comprising only components of fixed (i.e. not variable) characteristics, and the air flow in the system may be regarded as fully turbulent, the total pressure-flow rate relationship may be expressed as:

$$\Delta p_{T,s} = K_s V^2 \qquad (5.31)$$

Where K_s is the flow resistance of the entire ducting system.

The components of a ducting system are typically a collection of duct sections and fittings, and each of them may be represented by a flow resistance model of a form similar to Equation (5.31) above (with its flow resistance denoted here by K_i – see Equations (5.23) & (5.24)). The flow resistance of the entire system (K_s) can be evaluated from the flow resistances of the components of the system (K_i for $i = 1, 2, \ldots$), through condensing the flow resistance models of the duct sections and fittings, taking into account the ways in which the components are interconnected.

For example, consider two components in series (Figure 5.16a)) where the pressure drop-flow rate relation of each of the components can be described by:

$$\Delta p_1 = K_1 V^2$$

$$\Delta p_2 = K_2 V^2$$

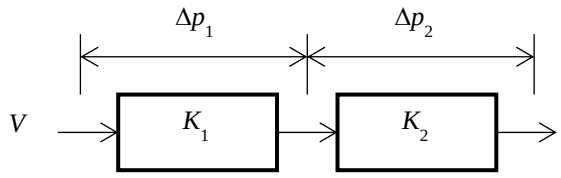

a) Two components in series

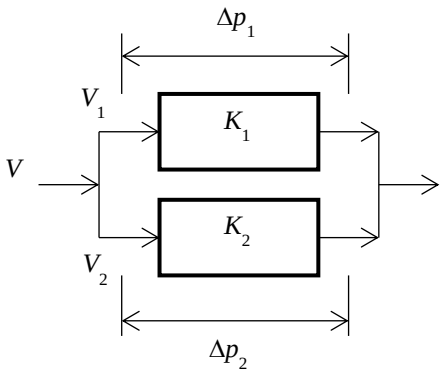

b) Two components in parallel

Figure 5.16 Basic ducting system configurations

An equivalent component that will incur the same total pressure drop while passing the same flow rate can be expressed as:

$$\Delta p_s = \Delta p_1 + \Delta p_2 = (K_1 + K_2)V^2$$

Or

$$\Delta p_s = K_s V^2 \tag{5.32}$$

Where

$$K_s = K_1 + K_2 \tag{5.33}$$

For the same two components but arranged in parallel (Figure 5.16b)):

$$V_1 = \sqrt{\frac{\Delta p_1}{K_1}}$$

$$V_2 = \sqrt{\frac{\Delta p_2}{K_2}}$$

Since, in this case of two components in parallel,

$$\Delta p_s = \Delta p_1 = \Delta p_2$$

$$V = V_1 + V_2$$

It follows that

$$V = \sqrt{\Delta p_s} \cdot \left(\frac{1}{\sqrt{K_1}} + \frac{1}{\sqrt{K_2}}\right)$$

Or

$$\Delta p_s = K_s V^2 \tag{5.34}$$

Where

$$K_s = \left[1/\left(\frac{1}{\sqrt{K_1}} + \frac{1}{\sqrt{K_2}}\right)\right]^2 \tag{5.35}$$

Knowing how the fan total pressure of a fan, and the total pressure drop of a ducting system, would vary with the air flow rate through them, the pressure-flow rate characteristic curves for both the system and the fan can be constructed. The operating condition of the fan and the ducting system, when the two are coupled together, is defined by the intersecting point of the system and fan characteristic curves, as shown in Figure 5.17. The operating point of the fan in a fan-duct system will shift as the system resistance or running speed of the fan, or both, is/are changed (Figure 5.18), which will happen from time to time in systems that handle variable air flow rate (e.g. a variable air volume system).

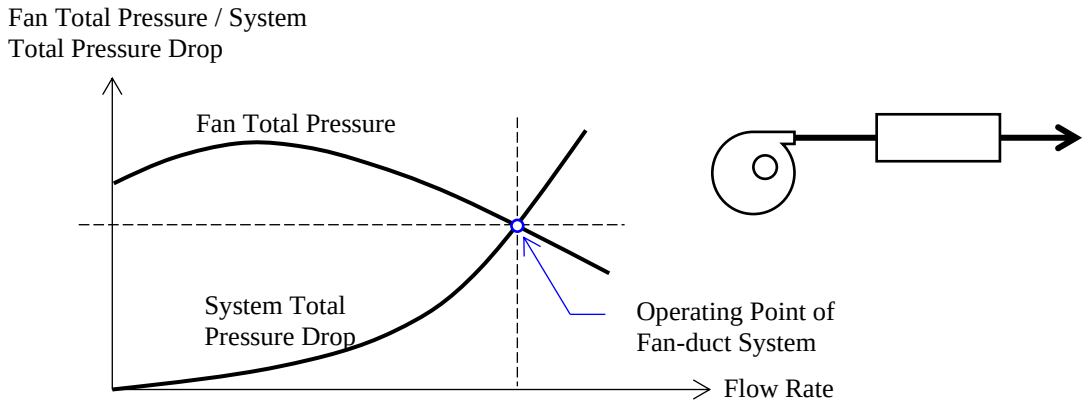

Figure 5.17 Operating point of a fan-duct system

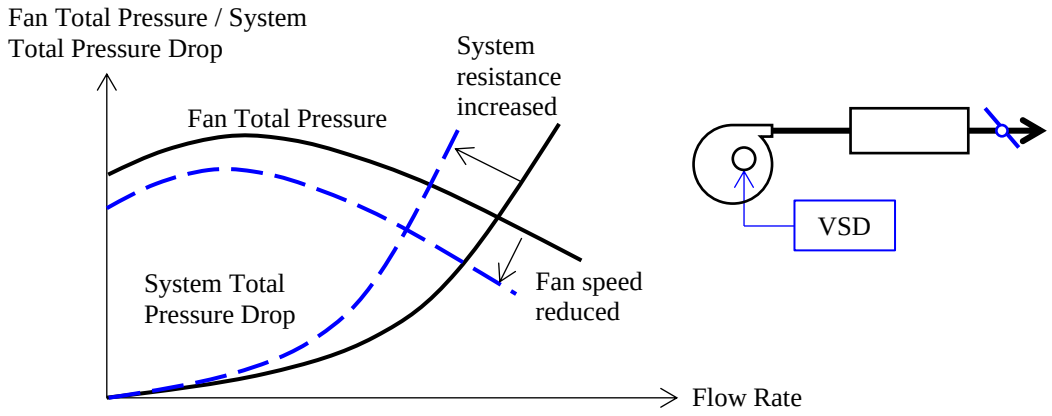

Figure 5.18 Shift of the operating point of a fan-duct system

5.4.3 Fans in series and parallel

For two fans connected in series, the air flow rate through the two fans (V) will be the same but the total pressure that the two fans collectively deliver (Δp_f) will be equal to the sum of the fan total pressures of the two fans (Figure 5.19a)).

$$\Delta p_f = \Delta p_1 + \Delta p_2 \tag{5.36}$$

Two fans in series may need to be used when a single fan is unable to deliver the required air flow rate at the required fan total pressure. Having two fans operating in series but with the ventilated space situated in between (Figure 5.19b)) provides a means for adjustment and control of the static pressure inside the space, which in turn enables containment of the air inside the space or prevention of ingress of air from the surrounding into the space.

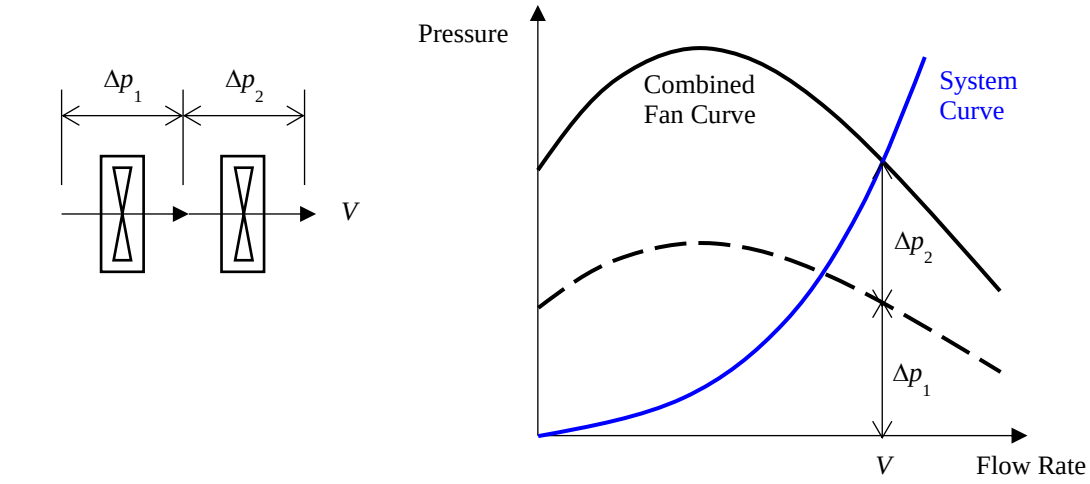

a) Combined Characteristics

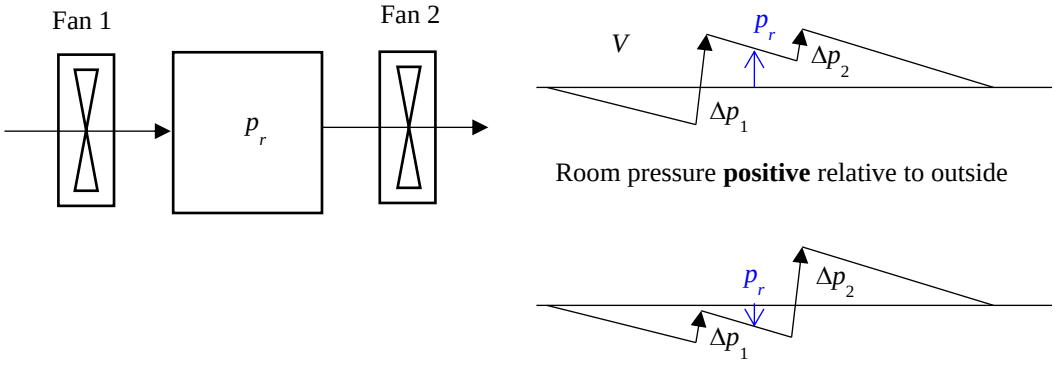

b) Example Application

Figure 5.19 Two fans in series

For two fans connected in parallel, the total air flow rate (V) equals the sum of the air flow rate through the two fans (V_1 & V_2) while the two fans will run at the same total pressure (Δp_s) (Figure 5.20a)).

$$V = V_1 + V_2 \tag{5.37}$$

$$\Delta p_s = \Delta p_1 = \Delta p_2 \tag{5.38}$$

Fans in parallel is a commonly adopted system configuration where the total system flow rate is shared by several fans, allowing some of the fans to be shut down when the total flow rate demand is reduced. Note should be taken that when putting fans in parallel, their sizes (total pressure-flow rate capacities) should not differ significantly. Otherwise, the fan that can only provide a smaller fan total pressure may be stalled by the total pressure output by the larger fan (Figure 5.20b)).

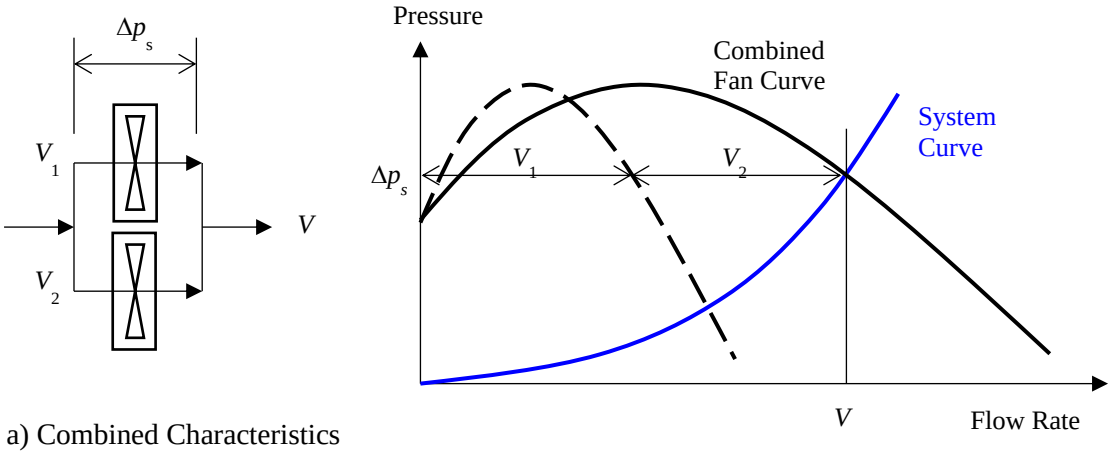

a) Combined Characteristics

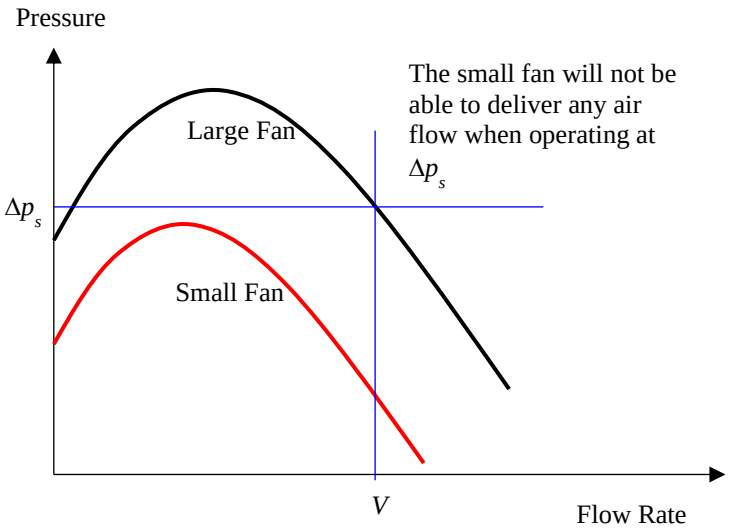

b) Small fan stalled when pressure is too high

Figure 5.20 Two Fans in Parallel

5.4.4 Fan surge

There is a limit to the reduction in flow rate that a fan can handle without giving rise to unstable operation. When operating under the unstable condition, which is referred to as fan surge, severe vibration and noise will arise. Fan surge must be avoided as it may lead to damage to the system and undesirable disturbances. The region that fan surge will occur is wider the higher the fan total pressure to be delivered, and the fan surge zone is typically shown in the fan characteristic curves available from the fan manufacturers (see for example Figure 5.21).

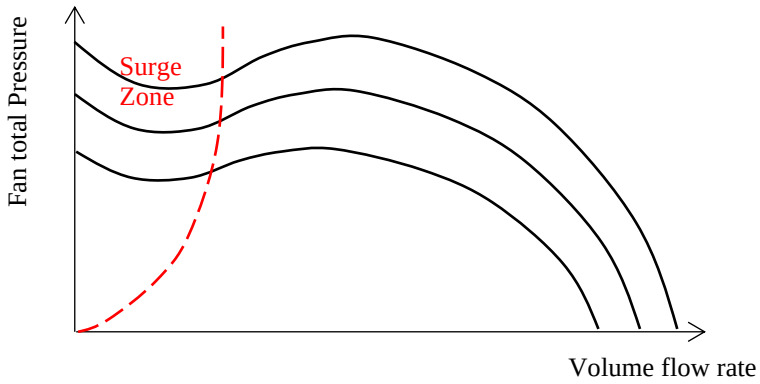

Figure 5.21 Typical fan characteristic curve of a forward-curved fan

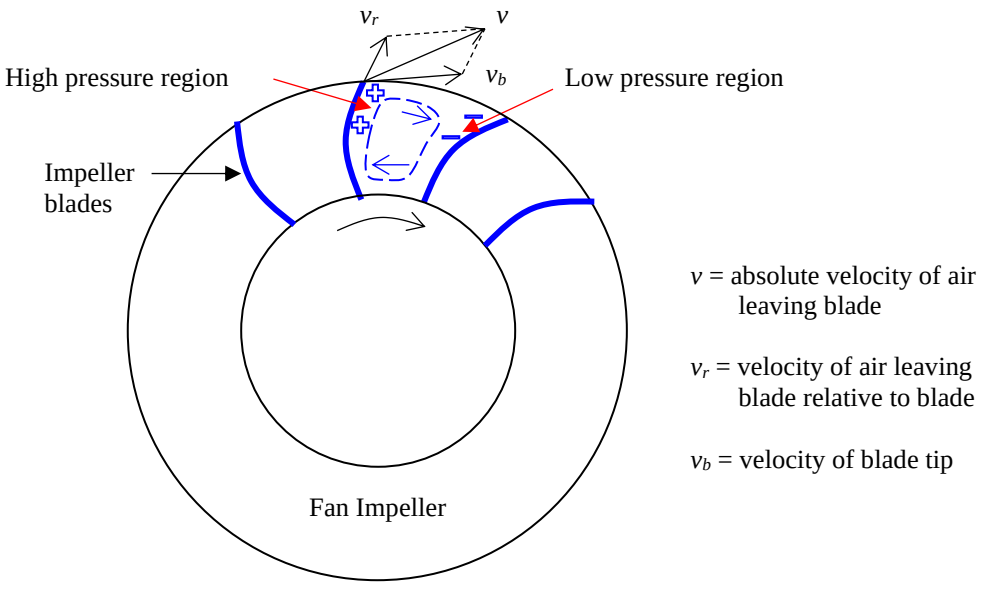

Figure 5.22 Air Flow Through a Fan Impeller

The following is a simplified explanation for why fan surge arises (with reference to Figure 5.22):

- Air is discharged in the direction of v which is dependent on v_r and v_b.

- When the flow rate through the fan drops, v_r will reduce in magnitude and v will turn toward the circumference of the impeller.

- When close enough, the discharged air can be induced to flow back into the impeller by the negative pressure in the low-pressure region, giving rise to re-circulating flow between the impeller blades.

- The re-circulated flow will increase the flow rate and v will then turn away stopping the re-circulating flow. This cycle will repeat, giving rise to strong vibration and noise.

5.4.5 Fan selection

As a matter of course, the key considerations to be taken in selecting a fan for a particular application include:

- The function to be served by the fan (e.g. for supply, return or exhaust) and characteristics of the system (e.g. variable air volume or constant volume).

- Whether or not the fan under consideration is capable of performing the required duty, which includes the fan total pressure and air flow rate to be delivered.

Additionally, consideration must be given to a number of other factors, including:

- The rated and part-load performance of the fan, including its pressure-flow rate characteristics, potential of fan surge, and energy efficiency.

- The need for and the method of regulation of the fan operation (e.g. flow rate adjustment through fan speed or blade pitch control).

- Air flow direction and the space available for installation (e.g. a straight-through vane axial fan is needed if there is not enough space for installing the connecting ducts for a centrifugal fan).

- The noise of the fan in operation (generally, the higher the efficiency the quieter the fan) vis-à-vis the required noise level in the spaces served.

- The initial cost.

For special applications, further consideration should also be given to certain issues, such as the temperature of and contaminants in the air to be handled (e.g. substances that make the air erosive or corrosive, or inflammable), etc.

5.5 Mechanical ventilation for temperature and contaminant control

5.5.1 Functions of mechanical ventilation systems

Instead of air-conditioning, mechanical ventilation (MV) is required in a variety of premises in buildings, such as underground carparks, various plant rooms, storerooms, changing rooms, toilets, etc. The MV systems may range from just a simple propellor fan in conjunction with a pair of intake and exhaust louvres, to an elaborated fan-duct system with automatic operational and safety control devices.

The major purpose of some MV systems is to remove the heat transported into and generated within a ventilated space, to ensure the temperature inside the space would stay below a high limit. At the same time, odours and/or air borne contaminants generated within the space would also be removed by the MV system. Conversely, some other MV systems are meant to remove contaminants from the indoor air while cooling is a by-product. Some MV systems would be run according to pre-set time schedules or round the clock but some others would normally be in standby mode and would be started only when certain event arises, such as outbreak of a fire, leading to a need for ventilation, in this case for smoke extraction.

HVAC system designers have to ensure the ventilation rate provided by an MV system is sufficient to serve its purpose, such as keeping the temperature or contaminant concentration in the ventilated space from exceeding a high limit, or lowering the temperature or contaminant concentration from an initially high level to a low level within an allowable maximum period of time. Once the design air flow rate is determined, sizing of the required ductwork and selection of fan for the application can be done following the methods for air-side air-conditioning systems discussed in preceding sections. The fan-duct system analysis discussed above is also appliable to MV systems.

5.5.2 Applications that require a constant rate of ventilation

In determining the required ventilation rate for an application, the assumption is very often made that the air in the ventilated space is 'perfectly mixed'. This means that the properties of the indoor air, such as temperature and humidity, and the concentrations of any airborne contaminants, are assumed to be uniformly distributed inside the space. As a result, a single value of the air temperature or contaminant concentration may be used to represent the air in the entire indoor space, which can greatly simplify the problem.

If the heat or contaminant source is a steady source, the ventilation rate that should be provided consistently can simply be determined as follows:

$$V_s = \frac{S}{C(\theta_i - \theta_s)} \tag{5.39}$$

Where

$V_s =$ the required ventilation rate.

$S =$ the rate of heat or contaminant generated within and transported into the ventilated space.

$\theta_i =$ the maximum allowable indoor temperature or contaminant concentration (assumed to be uniformly distributed in the ventilated space).

$\theta_s =$ the temperature or contaminant concentration of the air that will be drawn in for ventilation (assumed to stay at a constant value).

$C =$ a constant coefficient depending on the problem at hand, e.g. $C =$ the product of density and specific heat of air (ρCp) for a temperature control problem; and C simply equals 1 (or may be ignored) for a contaminant concentration control problem.

This design approach is applicable to MV systems serving a plant room, e.g. a transformer room or lift machine room, where the maximum rate of heat dissipation of the equipment inside the room, the tolerable high limit of temperature in the room, and the likely peak ambient air temperature, are all known. The required ventilation rate for dilution of steady emissions of particulates or gases from indoor sources may be determined in the same way.

On the other hand, the required ventilation rate for many MV systems may simply be determined with reference to a given design criterion, e.g. a flow rate per square meter of floor area or a number of air-changes per hour (ACH), as in the case of ventilation for a toilet, workshop or general storeroom, or a ventilation rate per person present, as in the case of fresh air provision for air-conditioned spaces.

5.5.3 Dynamic analysis

Consider a room as shown in Figure 5.23, which has a fixed internal volume, V, and air inside it is perfectly mixed. There is an internal source that releases steadily a contaminant into the room at the rate of S mg/s. The initial concentration of the contaminant in the room (at time $t = 0$) is $C(0)$, and concentration is quantified here in mass of the contaminant per unit volume, e.g. mg/m^3. Ventilation at a constant volume flow rate of V_s m^3/s is used to purge the contaminant in the room, starting from $t = 0$, and the concentration of the contaminant in the outdoor air drawn in for ventilation is C_s mg/m^3, which may be taken as a constant.

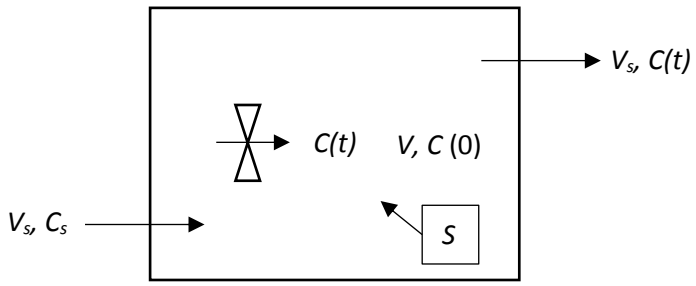

Figure 5.23 Ventilation for a room in which air is perfectly mixed

For this room, the following equation may be derived from conservation of the mass of the contaminant in the room at time t.

$$V\frac{dC(t)}{dt} = V_s\big(C_s - C(t)\big) + S \tag{5.40}$$

After ventilation has been provided for a long enough time, the indoor air will reach a steady-state contaminant concentration, $C(\infty)$. At this state, there will be no more changes in the contaminant concentration and hence, Equation (5.40) will become:

$$0 = V_s\big(C_s - C(\infty)\big) + S \tag{5.41}$$

$$C(\infty) = C_s + S/V_s \tag{5.42}$$

Note that the steady-state concentration, $C(\infty)$, evaluated by the above equation is the lowest concentration that can be achieved by the ventilation arrangement for purging from an initially high concentration $C(0)$. If the source is absent ($S = 0$), the steady state concentration will simply be equal to the outdoor air concentration.

Rearranging Equation (5.41) into the following and substituting it into Equation (5.40), we get Equation (5.43) below.

$$S = V_s(C(\infty) - C_s)$$

$$V\frac{dC(t)}{dt} = -V_s\big(C(t) - C(\infty)\big) \tag{5.43}$$

Further re-arrangement of the above yields:

$$\frac{dC(t)}{C(t)-C(\infty)} = -\frac{V_s}{V}dt$$

Which may be integrated into:

$$\ln\big(C(t) - C(\infty)\big) = -\frac{V_s}{V}t + K$$

$$C(t) - C(\infty) = A\exp\left(-\frac{V_s}{V}\cdot t\right) \tag{5.44}$$

Where K is an integration constant, and $A = e^K$ which may be evaluated by using the initial condition that at $t = 0$, $C(t) = C(0)$. Therefore,

$$A = C(0) - C(\infty)$$

Substituting this result back into Equation (5.44),

$$C(t) - C(\infty) = [C(0) - C(\infty)]\exp\left(-\frac{V_s}{V}\cdot t\right)$$

$$C(t) = C(\infty) + [C(0) - C(\infty)]\exp\left(-\frac{V_s}{V}\cdot t\right) \tag{5.45}$$

Which may be re-written as:

$$C(t) = C(0)\exp\left(-\frac{V_s}{V}\cdot t\right) + C(\infty)\left[1-\exp\left(-\frac{V_s}{V}\cdot t\right)\right] \tag{5.46}$$

Replacing $C(\infty)$ by Equation (5.42),

$$C(t) = C(0)\exp\left(-\frac{V_s}{V}\cdot t\right) + (C_s + S/V_s)\left[1-\exp\left(-\frac{V_s}{V}\cdot t\right)\right] \tag{5.47}$$

As shown in Equation (5.47), the evolution of $C(t)$ may be regarded as the combined effect of two processes, namely the decay in concentration from $C(0)$ that would result if C_s & S are both equal to zero (as given in Equation (5.48)); and the growth in concentration due to C_s & S if the initial concentration in the room $C(0)$ equals zero (as given in Equation (5.49)) (Figure 5.24).

$$C(t) = C(0)\exp\left(-\frac{V_s}{V}\cdot t\right) \tag{5.48}$$

$$C(t) = (C_s + S/V_s)\left[1-\exp\left(-\frac{V_s}{V}\cdot t\right)\right] \tag{5.49}$$

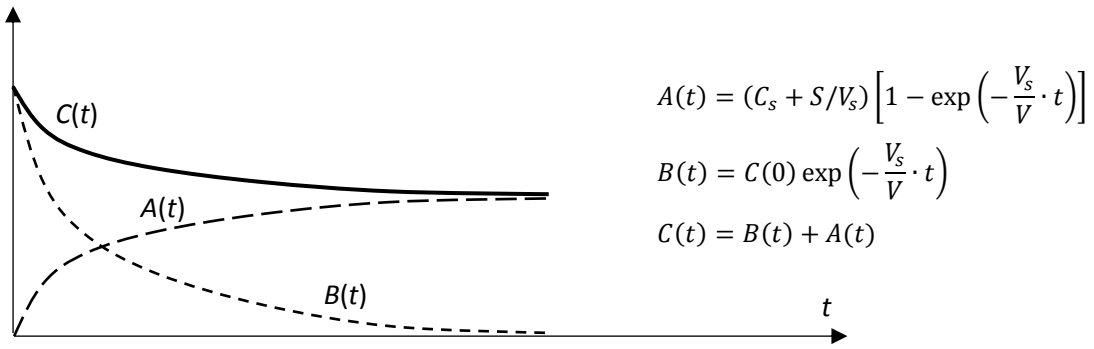

Figure 5.24 Evolution of $C(t)$ (Equation (5.47))

Again, for the room shown in Figure 5.23, which has a fixed internal volume, V, and air inside it is perfectly mixed, we assume now that there is, instead of the contaminant source, an internal heat source that releases a steady rate of S kW of heat into the room. The initial temperature of the room air (at time $t = 0$) is $T(0)$ °C and ventilation at a constant volume flow rate of V_s m³/s is used to cool down the room, starting from $t = 0$, and the temperature of the outdoor air drawn in for ventilation is T_s °C, which may be taken as a constant. The heat conservation equation for the room air is:

$$\rho V Cp\frac{dT(t)}{dt} = \rho V_s Cp\big(T_s - T(t)\big) + S \tag{5.50}$$

Following similar steps for solving Equation (5.40) above, the solution for Equation (5.50) can be derived, as shown below:

$$T(t) = T(0)\exp\left(-\frac{V_s}{V}\cdot t\right) + \left(T_s + \frac{S}{\rho V_s Cp}\right)\left[1 - \exp\left(-\frac{V_s}{V}\cdot t\right)\right] \quad (5.51)$$

An example is given below to illustrate application of the above theory.

Example 5.1

A fire occurred in a motel room ($V = 85\text{m}^3$) in which a sofa containing polyurethane foam was burned and filled the room with smoke containing HCN (hydrogen cyanide). Immediately after the fire was extinguished, the smoke concentration was 100g/m^3, of which 10% by mass was HCN.

The firemen evacuated the smoke with an extract fan and blew outside air into the room at the same rate of V_s, which equals 28.33m^3/ min. Because of the fire, the outside air contained HCN at a concentration C_s of 1mg/m^3.

On the basis of the well-mixed model, estimate the length of time that must elapse, t_1, before individuals could enter the room after the fire had been extinguished, given that the Short Time Exposure Limit (STEL) of HCN concentration to be achieved before individuals can enter the room, $C(t_1)$, is 5mg/m^3.

Solution

Equation (5.47) can be applied to this problem, by setting $S = 0$.

$$C(t) = C(0)\exp\left(-\frac{V_s}{V}\cdot t\right) + C_s\left[1 - \exp\left(-\frac{V_s}{V}\cdot t\right)\right]$$

Which can be re-written as:

$$C(t) - C_s = C(0)\exp\left(-\frac{V_s}{V}\cdot t\right) - C_s\exp\left(-\frac{V_s}{V}\cdot t\right)$$

$$C(t) - C_s = (C(0) - C_s)\exp\left(-\frac{V_s}{V}\cdot t\right)$$

$$\frac{C(t)-C_s}{C(0)-C_s} = \exp\left(-\frac{V_s}{V}\cdot t\right)$$

$$\ln\left(\frac{C(t)-C_s}{C(0)-C_s}\right) = -\frac{V_s}{V}\cdot t$$

$$t = -\frac{V}{V_s}\ln\left(\frac{C(t)-C_s}{C(0)-C_s}\right) \quad (5.52)$$

At $t = t_1$,

$$C(t) = C(t_1) = 5\text{mg/m}^3$$

Given that

$C(0) = 100\ \text{g/m}^3 \times 1000\ \text{mg/g} \times 10\% = 10{,}000\ \text{mg/m}^3$

$C_s = 1\ \text{mg/m}^3$

$V = 85\text{m}^3$ and

$V_s = 28.33\text{m}^3/\ \text{min}$

Substituting the above into Equation (5.52),

$$t_1 = -\frac{85}{28.33}\ln\left(\frac{5-1}{10000-1}\right) = 23.47\text{min}$$

5.5.4 Ventilation rate measurement

The dynamic analysis method outlined above, in conjunction with the use of a tracer gas and measurement of the dynamic variation in the concentration of the tracer gas in a room, may be applied to determine the ventilation rate in the room, which otherwise is difficult to ascertain. Examples include determination of ventilation rate due to natural ventilation or infiltration, which are difficult to find except by experimental measurement.

The following three methods are the most widely adopted for ventilation rate measurement:

1. Constant injection method
2. Constant concentration method
3. Decay method

All the above three methods rely on the assumption that the air in the room being measured is perfectly mixed.

A gas is preferred for use as a tracer gas if it is benign and stable, is not normally present in the ambient air, is readily mixed with air, and its concentration can be measured to high degree of accuracy. A common choice of tracer gas used in indoor air quality (IAQ) studies is sulphur hexafluoride, SF_6, which does not normally exist in air. Carbon dioxide, CO_2, is sometimes used instead for its lower cost but the concentration of CO_2 in the ambient air must also be measured. Portable propeller fans are often used to ensure the air and the tracer gas are thoroughly mixed.

a) *Constant injection method*

Constant injection method may be used to measure ventilation rate which may vary from time to time ($V_s(t)$). For a room with internal volume V, which is ventilated at an unknown air flow rate $V_s(t)$, the ventilation rate can be determined by injecting a tracer gas at a fixed rate S, and by measuring continuously the concentration of the tracer gas in the room or in the exhaust air path, $C(t)$.

Assuming that the air entering the space does not contain any tracer gas, i.e., $C_s = 0$,

$$V\frac{dC(t)}{dt} = S - V_s \cdot C(t) \tag{5.53}$$

Therefore,

$$V_s = \frac{S}{C(t)} - \frac{V}{C(t)}\frac{dC(t)}{dt}$$

Within a period from $t = 0$ to $t = T$, the time averaged flow rate, $\overline{V_s}$, is:

$$\overline{V_s} = \frac{1}{T}\int_0^T V_s dt \tag{5.54}$$

It follows that

$$\overline{V_s} = \frac{1}{T}\int_0^T \frac{S}{C(t)}dt - \frac{1}{T}\int_{C(0)}^{C(T)} V\frac{dC(t)}{C(t)}$$

$$\overline{V_s} = S\overline{\left(\frac{1}{C(t)}\right)} - \frac{V}{T}[\ln C(T) - \ln C(0)]$$

$$\overline{V_s} = S\overline{\left(\frac{1}{C(t)}\right)} - \frac{V}{T}\ln\left(\frac{C(T)}{C(0)}\right) \tag{5.55}$$

Note should be taken that

$$\overline{\left(\frac{1}{C(t)}\right)} \neq \frac{1}{\overline{C(t)}} \tag{5.56}$$

It can be seen from the above that by continuing with the tracer gas injection at a constant rate (S) and measuring the concentration in the room ($C(t)$) over a range of consecutive periods, the time averaged ventilation rate for each period can be determined from the measured data.

b) *Constant concentration method*

There is a problem with the constant injection method introduced above that what the appropriate injection rate, S, should be is not known beforehand. If it is too low, it would be difficult to accurately measure the tracer gas concentration in the room or in the exhaust air stream. It may also be too high, which will make the measurement too costly or may even lead to measurement problems, e.g. upper concentration measurement limit of sensors exceeded. Such problems can be avoided by using the constant concentration method.

As its name suggests, the injection rate is under control in the constant concentration method such that the concentration of the tracer gas in the room or the exhaust stream will stay at a steady level. The mass balance equation for the tracer gas, as shown below, can be equated to zero given that the concentration ($C(t)$) is now controlled at a steady value whereas the source term, $S(t)$, may now vary from time to time.

$$V\frac{dC(t)}{dt} = S(t) - V_s \cdot C(t) = 0 \tag{5.57}$$

It follows that:

$$V_s(t) = \frac{S(t)}{C(t)}$$

Over a period of measurement,

$$\overline{V_s(t)} = \frac{\overline{S(t)}}{C(t)} \tag{5.58}$$

c) *Decay method*

In this method, after dosing a room with a tracer gas that is absent in the ambient air ($C_s = 0$) to a high enough initial concentration $C(0)$, injection of tracer gas will be stopped (thus $S = 0$). At this juncture (taken as $t = 0$), measurement of the concentration of the tracer gas in the room or the exhaust air stream will start. The ventilation rate in the room, V_s, can then be determined from the concentration records as follows.

For the case where $S = 0$ and $C_s = 0$, Equation (5.48) can be applied to find the ventilation rate:

$$C(t) = C(0) \exp\left(-\frac{V_s}{V} \cdot t\right) \tag{5.59}$$

From the above equation, it can be seen that if the measured concentrations at various time intervals ($C(t)$) are normalized by the initial concentration ($C(0)$) and the logarithmic values of the concentration ratio are plotted against time (Figure 5.25), a linear, downward sloping straight line can be fitted to the data. The slope of the line, G, when determined, can be used to evaluate the ventilation rate, V_s.

$$\ln \frac{C(t)}{C(0)} = -\frac{V_s}{V} \cdot t$$

$$G = -\frac{V_s}{V} \tag{5.60}$$

$$V_s = |G| \cdot V \tag{5.61}$$

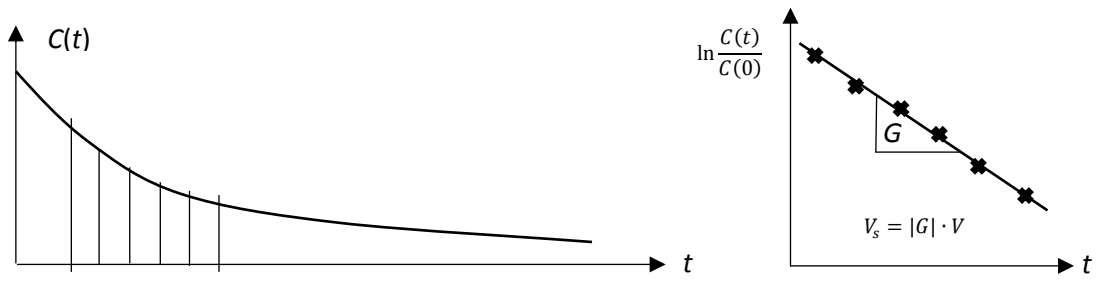

Figure 5.25 Decay method for determination of ventilation rate

There are alternative approaches in using the decay method for measuring ventilation rate in a room, as shown Figure 5.26, and briefly discussed below.

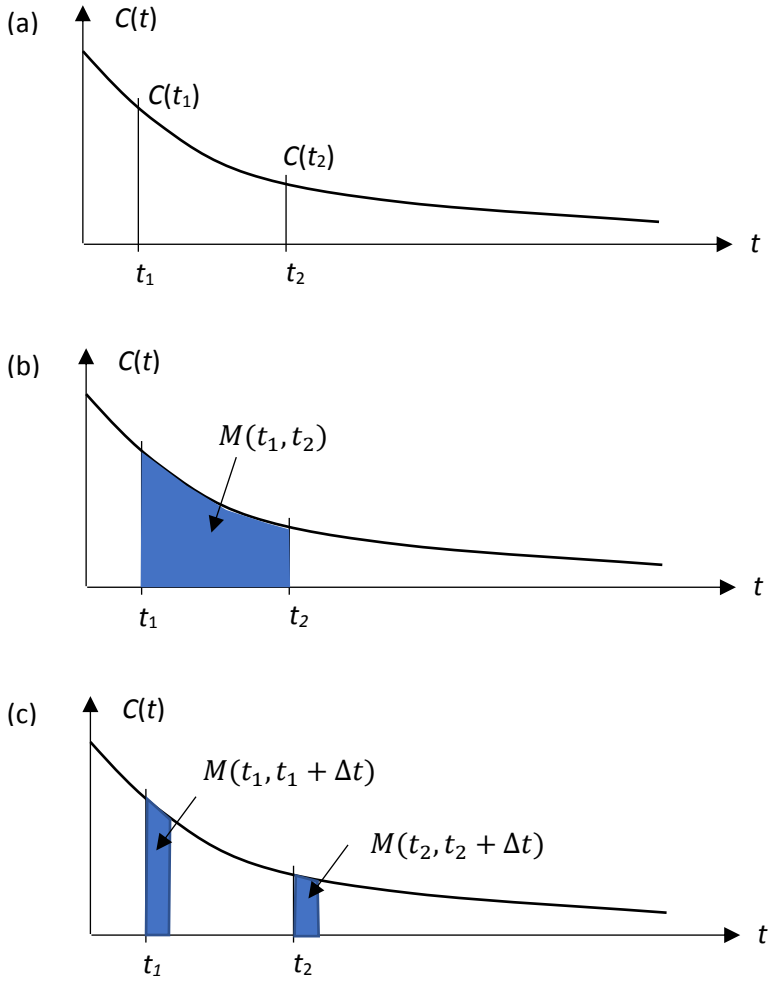

Figure 5.26 Three alternative ways of measuring ventilation rate using the decay method

i) By sampling concentrations at two time instants, t_1 and t_2 (Figure 5.25 (a)).

Using Equation (5.59),

$$C(t) = C(0)\exp\left(-\frac{V_s}{V}\cdot t\right)$$

$$C(t_1) = C(0)\exp\left(-\frac{V_s}{V}\cdot t_1\right)$$

$$C(t_2) = C(0)\exp\left(-\frac{V_s}{V}\cdot t_2\right)$$

Therefore,

$$\frac{C(t_1)}{C(t_2)} = \frac{\exp\left(-\frac{V_s}{V}\cdot t_1\right)}{\exp\left(-\frac{V_s}{V}\cdot t_2\right)} = \exp\left(-\frac{V_s}{V}\cdot(t_1 - t_2)\right)$$

$$\ln\left(\frac{C(t_1)}{C(t_2)}\right) = -\frac{V_s}{V}\cdot(t_1 - t_2)$$

$$V_s = -\frac{V}{(t_1 - t_2)}\ln\left(\frac{C(t_1)}{C(t_2)}\right) \tag{5.62}$$

ii) By integrating the concentration measurement between two time instants, t_1 and t_2 (Figure 5.25 (b)).

Let

$$M(t_1, t_2) = \int_{t_1}^{t_2} C(t)dt \tag{5.63}$$

Using Equation (5.59),

$$M(t_1, t_2) = \int_{t_1}^{t_2} C(0)\exp\left(-\frac{V_s}{V}\cdot t\right)dt$$

$$M(t_1, t_2) = -C(0)\frac{V}{V_s}\left[\exp\left(-\frac{V_s}{V}\cdot t\right)\right]_{t_1}^{t_2}$$

$$M(t_1, t_2) = -\frac{V}{V_s}\left[C(0)\exp\left(-\frac{V_s}{V}\cdot t_2\right) - C(0)\exp\left(-\frac{V_s}{V}\cdot t_1\right)\right]$$

$$M(t_1, t_2) = -\frac{V}{V_s}[\mathrm{C}(t_2) - \mathrm{C}(t_1)] \tag{5.64}$$

$$V_s = -\frac{V}{M(t_1, t_2)}[\mathrm{C}(t_2) - \mathrm{C}(t_1)] \tag{5.65}$$

iii) By integrating the concentration measurement at two time instants, t_1 and t_2, each for a time duration Δt (Figure 5.25 (c)).

Using Equation (5.64),

$$M(t_1, t_1 + \Delta t) = -\frac{V}{V_s}[\mathrm{C}(t_1 + \Delta t) - \mathrm{C}(t_1)]$$

$$M(t_1, t_1 + \Delta t) = -\frac{V}{V_s}\left\{C(0)\exp\left[-\frac{V_s}{V}\cdot(t_1 + \Delta t)\right] - \mathrm{C}(t_1)\right\}$$

$$M(t_1, t_1 + \Delta t) = -\frac{V}{V_s}\left\{C(0)\exp\left[-\frac{V_s}{V}\cdot t_1\right]\exp\left[-\frac{V_s}{V}\cdot \Delta t\right] - \mathrm{C}(t_1)\right\}$$

$$M(t_1, t_1 + \Delta t) = -\frac{V}{V_s}\left\{C(t_1)\exp\left[-\frac{V_s}{V}\cdot \Delta t\right] - \mathrm{C}(t_1)\right\}$$

$$M(t_1, t_1 + \Delta t) = \frac{V}{V_s}C(t_1)\left\{1 - \exp\left[-\frac{V_s}{V}\cdot \Delta t\right]\right\}$$

Similarly,

$$M(t_2, t_2 + \Delta t) = \frac{V}{V_s} C(t_2) \left\{1 - \exp\left[-\frac{V_s}{V} \cdot (\Delta t)\right]\right\}$$

Therefore,

$$\frac{M(t_1, t_1+\Delta t)}{M(t_2, t_2+\Delta t)} = \frac{C(t_1)}{C(t_2)} = \exp\left[-\frac{V_s}{V} \cdot (t_1 - t_2)\right]$$

$$\ln\left\{\frac{M(t_1, t_1+\Delta t)}{M(t_2, t_2+\Delta t)}\right\} = -\frac{V_s}{V} \cdot (t_1 - t_2)$$

$$V_s = \frac{V}{(t_2 - t_1)} \ln\left\{\frac{M(t_1, t_1+\Delta t)}{M(t_2, t_2+\Delta t)}\right\} \qquad (5.66)$$

5.6 Duct leakage test

A ductwork in an air-side air-conditioning or mechanical ventilation system is assembled from straight duct sections, bends, tees and wyes, reducers and expanders, and other fittings with a joint between each pair of such components. Although ductwork components are primarily manufactured in duct factories nowadays, rather than fabricated on site as in the older days, they are assembled together manually on site, through the use of rivets, screws, or flanges together with clamps or bolt and nuts. Therefore, air leakage is expected from any ductwork. Reference [6] & [7] provide details of ductwork constructions widely adopted in the HVAC industry and reference [13] is a common reference for pressure tests on ducting systems.

As noted above, discussion on air flow balancing is deferred until water flow balancing is covered in Chapter 7. However, the same approach is not applicable to air leakage test, notwithstanding that pipe leakage test is also covered in Chapter 7. The key difference is that leakage is inevitable in air ducts and is considered acceptable if the leakage rate is below a threshold whereas no water leakage would be tolerable in water piping systems.

Although air leakage through the seams and joints of ductwork is inevitable, serious leakage will lead to insufficient cooling or ventilation, waste of energy, and possibly noise and condensation problems. Therefore, the leakage rate must be kept to the least possible and tests have to be conducted after ductworks are assembled to verify if the leakage rate is within acceptable limits. The air leakage rate of a metal duct (Q_L), in l/s per m^2 of duct surface, is quantified by:

$$Q_L = C \cdot \Delta p_s^N \qquad (5.67)$$

Where

$\Delta p_s =$ the difference in static pressure between the interior of the duct and outside (in Pa)
$N =$ an exponent which is typically taken as 0.65
$C =$ a constant reflecting the area characteristics of the leakage path

The Code of Practice for Energy Efficiency of Building Services Installations [12] specified the leakage thresholds as given in Table 5.4. The Code specified also that at least 25% in area of ductwork which is designed to operate at operating static pressure in excess of 750 Pa should be leakage tested. Notwithstanding this, DW143 [13] provides that designers may waive tests for low pressure ductworks and require for a maximum of 10% of medium pressure ductworks and all high pressure ductworks to be leakage tested. The pressure ranges and the corresponding leakage limits specified in DW143 are as shown in Table 5.5.

Table 5.4 Duct leakage thresholds in The Code of Practice for Energy Efficiency of Building Services Installations [12]

Leakage Class	Operating Static Pressure (Pa)	Air Leakage Limit (L/s per m^2 of duct surface)
I	above 750 to 1000	$0.009 \times p^{0.65}$
II	above 1000 to 2000	$0.003 \times p^{0.65}$
III	above 2000	$0.001 \times p^{0.65}$

Note: p is the operating static pressure in Pascal

Table 5.5 Duct leakage thresholds in DW143 [13]

System classification	Design static pressure (Pa)		Max. air vel. (m/s)	Max. leakage (liter per m^2)
	Max. +'ve	Max. –'ve		
Low pressure (Class A)	500	500	10	$0.027 \times p^{0.65}$
Medium pressure (Class B)	1000	750	20	$0.009 \times p^{0.65}$
High pressure (Class C)	2000	750	40	$0.003 \times p^{0.65}$

p = static gauge pressure in duct (Pa)

Figure 5.27 shows the typical set up for a duct leakage test. The section of the ductwork to be tested must be sealed off at connections to other parts of the ductwork and at all openings. A blower with volume control and instruments for air pressure and flow rate measurements (Figure 5.28) are required for the test. For the piece of ductwork to be tested, besides identifying its working pressure, its dimensions are to be measured to enable its total surface area to be calculated. The maximum tolerable leakage flow rate for the ductwork can then be calculated from this surface area and the relevant formula given in Table 5.4 or Table 5.5 for the pressure class of the ductwork.

After blanking off all openings, connecting the blower to the ductwork, and connecting the pressure and flow meter to the relevant tapings at the ductwork and across the orifice plate for pressure and flow measurements, the blower would be turned on and regulated to achieve the working pressure in the ductwork. With the ductwork kept pressurized at the working pressure steadily, the reading of the flow rate discharged by the blower into the ductwork is to be read and compared against the leakage flow rate threshold allowed for the ductwork as determined earlier. Should the ductwork fail to

meet the requirement, smoke tubes may be used to detect the leakage sites and remedial work could then be done to improve the air-tightness of the ductwork. After that, the ductwork should be tested again.

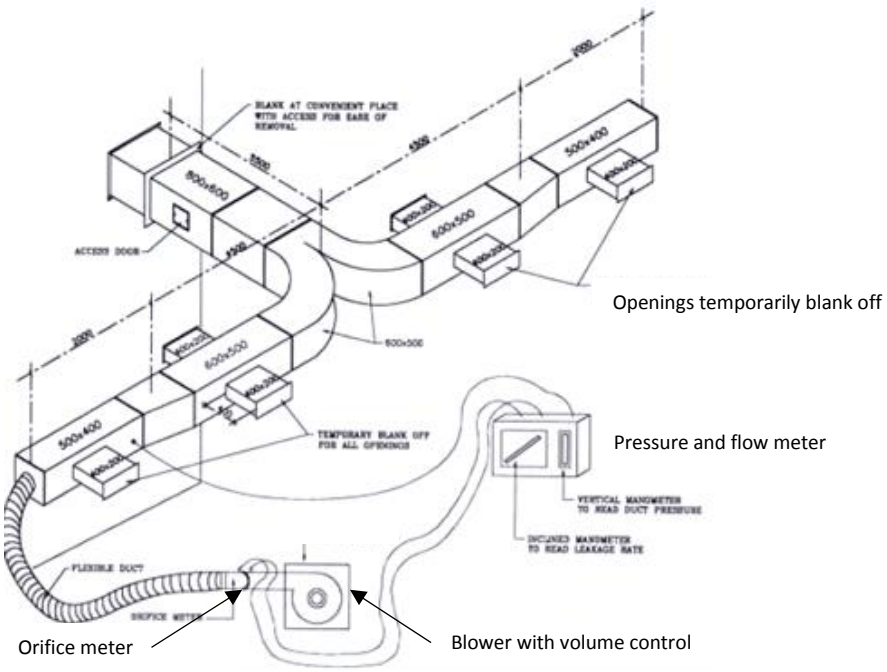

Figure 5.27 Typical duct leakage test set-up

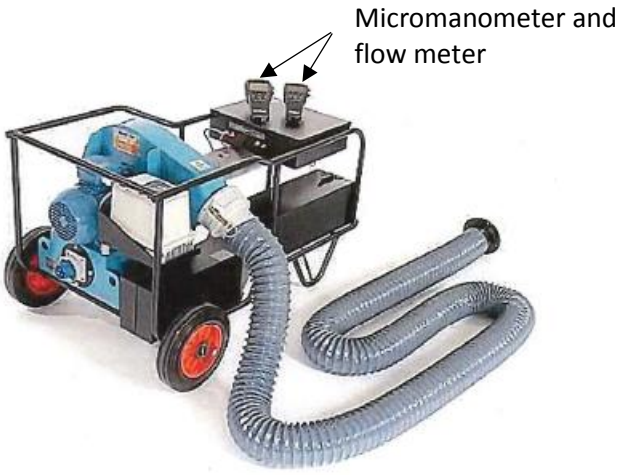

Figure 5.28 Duct leakage test kit complete with blower and measuring devices

Annex 5A Basic fluid mechanics

5A.1 Displacement, velocity, and acceleration

The following terms are used for description of the dynamics of an object:

- Displacement, *s*, the length of the path of movement of an object from one position to another, measured in m.
- Speed, the displacement of an object per unit time, in m/s.
- Velocity, *v*, speed in a given direction, in m/s.
- Acceleration, *a*, the rate of change of velocity per unit time, in m/s^2.

For an object that is stationary and will move along a straight line at a constant acceleration *a* starting from time = 0, at time = *t*,

$$v = a \cdot t \tag{5A.1}$$

$$s = \left(\frac{0+v}{2}\right) t = \frac{1}{2} a \cdot t^2 \tag{5A.2}$$

5A.2 Gravitational force, potential energy, and kinetic energy

Gravitational acceleration (*g*) is the acceleration of an object when it falls freely toward the ground from a high level above under the influence of gravity only (Figure 5A.1(a)).

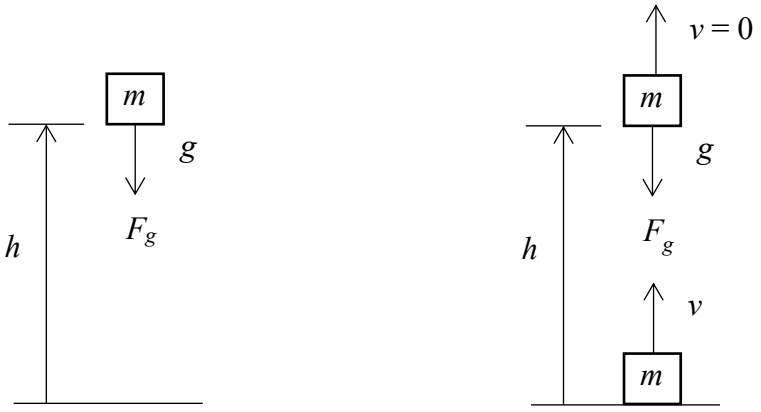

Figure 5A.1 (a) An object falling from a height *h* toward the ground; (b) An object moving upward from ground level at a velocity *v*.

If the object is initially stationary ($v = 0$ at $t = 0$) at a height of *h* above ground level and it starts to fall freely, at time *t* when it hits the ground, its downward velocity (v) will be:

$$v = g \cdot t$$

And hence,

$$t = v/g \tag{5A.3}$$

$$h = \frac{1}{2}g \cdot t^2 = \frac{1}{2}g \cdot \left(\frac{v}{g}\right)^2 = \frac{v^2}{2g} \tag{5A.4}$$

If the mass of the object is m, the gravitational force acting on the object (F_g), which is the weight of the object, is given by:

$$F_g = mg \tag{5A.5}$$

The amount of work (J) that will be done by the force F_g by pulling the object with mass m to move over a distance h is given by:

$$J = F_g h = mgh \tag{5A.6}$$

It follows that when an object of mass m is at a height h above a datum level, it has the potential to do an amount of work that equals mgh. Hence, mgh is the 'potential energy' of the object.

At the time the object falls to the datum level, its height, and hence its potential energy, will drop to zero but its velocity will increase to v. From Equation (5A.4), the following relation between h and v can be seen:

$$mgh = mg\left(\frac{v^2}{2g}\right) = \frac{1}{2}mv^2 \tag{5A.7}$$

Conversely, if an object is moving upward at an initial velocity of v (Figure 5A.1(b)), it will decelerate to zero velocity when it reaches a height of h above the initial level.

It can be seen that:

- The quantity $\frac{1}{2}mv^2$, which can be acquired by the object at the expense of its potential energy mgh, is energy associated with the motion of the object, called 'kinetic energy'.

- The loss in potential energy of the object will lead to an increase in its kinetic energy, and vice versa, which means that potential energy and kinetic energy may be converted from one to the other, while the total energy is conserved (implicit assumption: no loss of energy in the processes).

5A.3 Potential and kinetic energy of fluid

Consider a fluid particle originally at rest at the free surface of the fluid inside a vessel and it starts to flow downward toward the outlet at the low level of the vessel, as shown in Figure 5A.2.

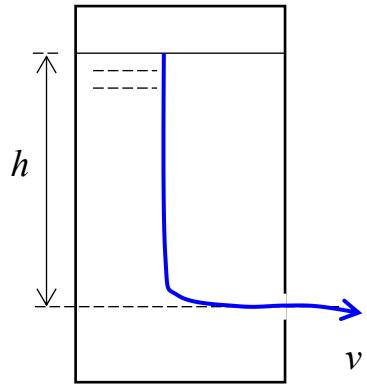

Figure 5A.2 Fluid flowing out of a vessel

By the time the fluid particle reaches the outlet, it will have dropped in level by h, i.e. it has lost potential energy by an amount of gh per unit mass. If the fluid particle is flowing at a velocity v at the exit, its kinetic energy per unit mass is $v^2/2$. Assuming there is no loss of energy,

$$gh = \frac{v^2}{2} \quad \text{or} \quad h = \frac{v^2}{2g} \quad \text{and hence} \quad v = \sqrt{2gh} \tag{5A.8}$$

The above result, which is same as Equation (5A.7) above, provides a relation between the height of the free surface in the vessel above the opening and the velocity of the fluid flowing out of the opening.

Will the outflow velocity of the fluid change if we consider another fluid particle in the vessel which is initially stationary but at a level below the free surface? The answer is no but to explain this, we need a relation between the static pressure and the potential and kinetic energy of fluid.

5A.4 Pressure and energy of fluid

When in contact with a surface, a fluid will exert a force on and normal to the surface, and the magnitude of the force per unit area of the surface is pressure (in N/m^2) in the fluid. The static pressure of a fluid is the pressure in a stationary fluid, or the pressure in a moving fluid with the pressure component due to motion discounted. Fluid static pressure is given rise by an externally applied force on the fluid within a system, e.g. the force exerted by a piston on the fluid within a cylinder, or gravitational force on the fluid. There can only be one static pressure value at a single point within a fluid, and the pressure is isotropic, i.e. the same in all directions.

The static pressure of a fluid given rise by gravity is called hydrostatic pressure. The hydrostatic pressure at a point in a fluid is proportional to the depth of the point from the free surface of the fluid.

Consider a vertical vessel with uniform cross-sectional area (A), which is open at the top, as shown in Figure 5A.3. The vessel is filled with a liquid with density ρ up to a height of h from the horizontal bottom surface.

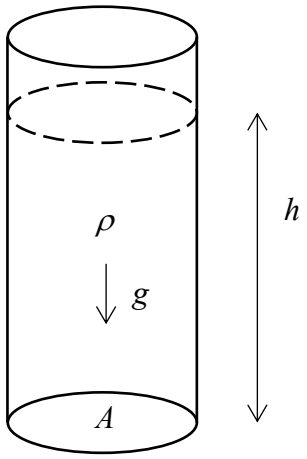

Figure 5A.3 A Fluid Column

The total volume (V), mass (m) and weight (w) of the fluid in the vessel are:

$$V = hA$$
$$m = \rho V$$
$$w = mg = \rho gV = \rho ghA$$

Since w is the downward force acting on the bottom horizontal surface of the vessel by the liquid due to its weight, the hydrostatic pressure at the bottom of this fluid column (p) is:

$$p = \frac{w}{A} = \rho gh \qquad (5A.9)$$

The above equation shows that the hydrostatic pressure in a liquid is proportional to the depth from the free surface of the liquid.

Figure 5A.4 shows a horizontal pipe with an internal cross-sectional area A that is connected to a reservoir through a vertical pipe. The water surface in the reservoir is at a vertical distance h above the horizontal pipe. The horizontal area of the reservoir is many times greater than the cross-sectional area of the pipe such that water leaving the reservoir through the pipe will cause a negligible rate of loss in height of the free surface in the reservoir.

As shown in the enlarged diagram in Figure 5A.4, there is a frictionless piston inside the horizontal pipe that seals up the pipe. Let F be the force acting on the piston resulting from the water pressure, and the piston is moved by this force over a distance s over a short time period, the work done by the force (J) is given by:

$$J = F \cdot s \tag{5A.10}$$

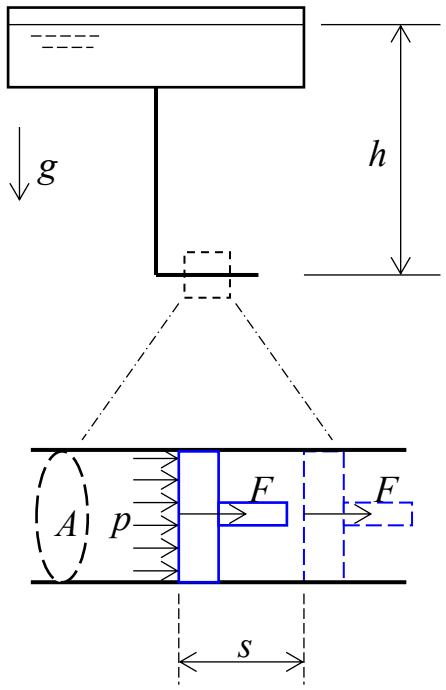

Figure 5A.4 A Horizontal Pipe Connected to a Reservoir

Since the water pressure acting on the piston, p, equals ρgh,

$$F = pA = \rho gh \cdot A$$

$$J = F \cdot s = pA \cdot s = \rho gh \cdot A \cdot s$$

Note that A·s equals the volume (V) swept through by the piston, which equals the volume of water that has flown through the pipe over the period. Therefore, each volume of water V at pressure p flowing through the pipe over the same period has the capacity to produce an amount of work that equals J.

From the above discussion, and considering that energy is capacity to perform work, it can be deduced that:

$$J = pV = \rho gh \cdot V$$

$$p = \rho gh = \frac{J}{V} = \text{Energy per unit volume}$$

$$\frac{p}{\rho} = gh = \frac{J}{\rho V} = \text{Energy per unit mass}$$

$$\frac{p}{\rho g} = h = \frac{J}{\rho V g} = \text{Energy per unit weight} = \text{head}$$

Recall the earlier example on fluid flowing out of a vessel (Figure 5A.2), and regard the process of a fluid particle flowing out of the vessel as two processes in series: first, the fluid particle dropped in height very slowly (v can be regarded as nearly zero) from the free surface to the level of the exit, thus losing potential energy by an amount of gh per unit mass but, in return, gaining pressure by p (where $p/\rho = gh$ = energy per unit mass). When the fluid particle flows out through the opening, its pressure will drop to zero, but its kinetic energy will increase to $v^2/2$ per unit mass.

Having established the relationship between pressure and potential energy, it can be seen that it does not matter whether a fluid particle that flows out of the vessel was initially from the free surface or any other intermediate point in the fluid within the vessel (e.g. point 1 or 2 in Figure 5A.5). This is because the velocity of a fluid particle was zero at any point before it moves toward the exit, and at that static state:

$$p_0 + \rho g z_0 = p_1 + \rho g z_1 = p_2 + \rho g z_2 = \rho g h$$

Where z_0, z_1 and z_2 are the heights of the respective points, all measured from the datum level, which is the level of the exit as shown in the figure, positive upward. Once the fluid particular starts to flow, a part of the energy (total potential and pressure energy) will be converted into kinetic energy.

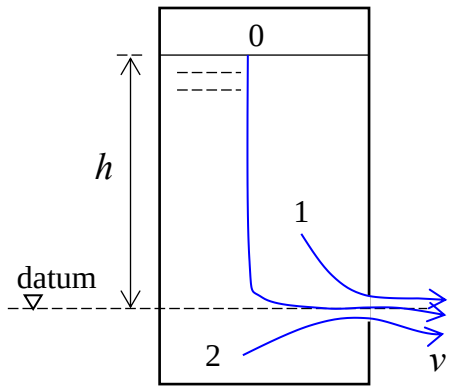

Figure 5A.5 Fluid flowing out of a vessel from different locations in the vessel

Assuming no loss in energy in the entire process, at any point along the flow path of the fluid particle (called a streamline), the total energy will be conserved, i.e.:

$$p + \frac{1}{2}\rho v^2 + \rho g z = const \qquad (5A.11)$$

Where z is the vertical distance above a datum level.

The above equation is called the Bernoulli's equation, which applies to any point along a streamline if frictional loss due to fluid flow can be ignored.

The Bernoulli's equation has numerous applications in fluid mechanics and one of which is for measurement of fluid flow velocity using a device called the Pitot tube, as

shown in Figure 5A.6. Assuming no loss of energy and according to the Bernoulli's equation (Equation (5A.11)), at any point along a streamline, the sum of the pressure energy, kinetic energy and potential energy of the fluid particle at the point is same as that at any other point on the same streamline. If all streamlines of the fluid flowing in the undisturbed region as shown in Figure 5A.6 are horizontal, along the particular streamline that impinges onto the nose of the tube (denoted as Point 0), the velocity of the fluid will be brought to zero at that point (call the stagnation point as shown in the figure).

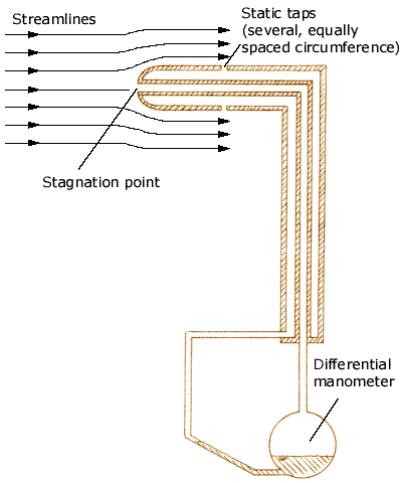

Figure 5A.6 Fluid flow velocity measurement using a Pitot tube

Hence, the fluid pressure at the stagnation point is given by:

$$p_0 = p + \frac{1}{2}\rho v^2 \qquad (5A.12)$$

It can be seen from the above that the flow velocity of a fluid may also be expressed as a pressure, called velocity pressure (p_v), which is given by:

$$p_v = \frac{1}{2}\rho v^2 \qquad (5A.13)$$

Furthermore, by measuring the stagnation pressure (p_0) and the static pressure (p), or the difference between the two, the velocity pressure and hence the flow velocity (v) in the undisturbed region can be measured. An important condition in the measurement as implied by the above discussion is that the openings in the Pitot tube for measurement of static pressure in a stream of fluid must be tangential to the streamline. Otherwise, the opening will obstruct fluid flow, leading to conversion of a part of the velocity pressure into static pressure, and thus the measurement could be erroneous.

5A.5 Pressure drop and energy loss due to fluid flow

Now, consider a horizontal pipe of uniform cross-sectional area, A, and a fluid is flowing through it, as shown in Figure 5A.7.

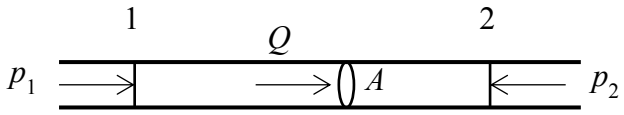

Figure 5A.7 Fluid flow through a pipe

If the volume flow rate of the fluid is Q (m^3/s), over a time lapse of t, a total volume of the fluid, V, will have flown through any intermediate cross-sectional plane in the pipe, and

$$Q = V/t \tag{5A.14}$$

Let J be the energy loss incurred by the fluid flow between planes 1 & 2 over the time period t. Given that the kinetic energy and potential energy of the fluid at planes 1 & 2 remain the same (as velocity and level are the same), this rate of energy loss (J/t) will lead to a drop in the pressure energy of the fluid as it flows from plane 1 to plane 2.

If the pressure drops from p_1 at plane 1 to p_2 at plane 2, the energy loss (J) is given by:

$$J = (p_1 - p_2)As$$

Where s is the distance between plane 1 and plane 2.

It follows that:

$$J = (p_1 - p_2)A(Q/A)t$$

$$J = (p_1 - p_2)Qt$$

$$J/t = (p_1 - p_2)Q \tag{5A.15}$$

Conversely, if water is driven to flow from a lower to a higher pressure, e.g. from p_1 to p_2, by a pump, as shown in Figure 5A.8, the pump has to impart to the water an amount of energy per unit time that equals J/t, which is the pumping power for raising the pressure of the water from p_1 to p_2 at the flow rate Q.

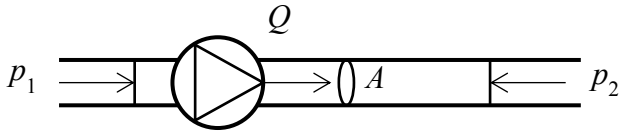

Figure 5A.8 Pump driven fluid flow

Applying the result for flow induced pressure loss in a reversed manner, we get:

$$J/t = (p_2 - p_1)Q \tag{5A.16}$$

If the efficiency of the pump is η, the power input required by the pump, W, is:

$$W = \frac{(p_2 - p_1)Q}{\eta} \tag{5A.17}$$

Note that because the pressure difference in this equation is a static pressure difference, the pumping power determined by the equation is correct only if the inlet and exit velocities across the pump are equal. As discussed in the main text, the pressure difference should be the total pressure difference, where total pressure (p_t) at a point in a flow field (same as stagnation pressure discussed above) is the sum of the static pressure and the velocity pressure at the same point, as depicted by the following equation:

$$p_t = p + \frac{1}{2}\rho v^2 \tag{5A.18}$$

Dropping in the pressure of a fluid along the direction that the fluid is flowing inside a pipe or pipe fitting is a natural phenomenon given rise by the viscosity of the fluid, which is commonly referred to as the effect of friction between the moving fluid and the internal surface of the pipe. Applying Bernoulli's equation between two cross-sectional planes at different positions along a streamline,

$$\left(\frac{p_1}{\rho g} + \frac{v_1^2}{2g} + z_1\right) - \left(\frac{p_2}{\rho g} + \frac{v_2^2}{2g} + z_2\right) = h_f \tag{5A.19}$$

Where h_f is the head loss due to friction.

For a horizontal pipe with uniform cross-sectional area along its entire length, the above equation can be simplified to:

$$p_1 - p_2 = \rho g h_f \tag{5A.20}$$

The head loss due to friction in fluid flow through a circular pipe, h_f, can be evaluated from the Darcy-Weisbach equation below:

$$h_f = \frac{fL}{d}\frac{v^2}{2g} \tag{5A.21}$$

Where f is the friction factor; L the pipe run length between the two cross-sectional planes, v the velocity of fluid flow and d the internal diameter of the pipe (assumed to be circular).

5A.6 The steady flow energy equation

The above theory can be extended by considering the steady flow energy equation shown below (typically covered in a thermodynamics course), which applies to a system with a fluid flowing steadily into and out of the system, as shown in Figure 5A.9.

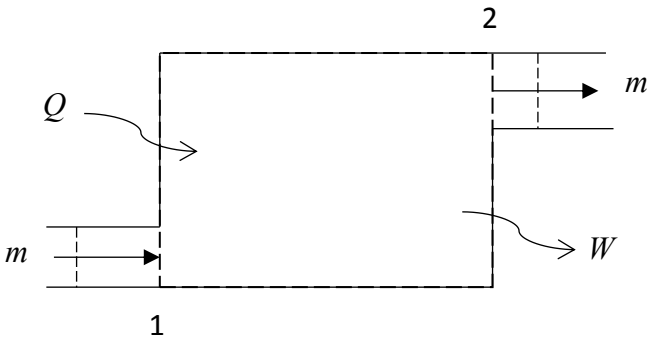

Figure 5A.9 Fluid flowing steadily through a system

$$Q - W = m(e_2 - e_1) + mg(z_2 - z_1) + \frac{1}{2}m(u_2^2 - u_1^2) + m(p_2v_2 - p_1v_1) \quad (5A.22)$$

Here, Q is the heat input into the system, W the work done by the system, m the mass flow rate of the fluid flowing through the system, and g the gravitational acceleration. For the fluid at the inlet (plane 1) and at the exit (plane 2), distinguished by the subscripts 1 & 2 respectively, e is specific internal energy, z height from a common datum, u flow velocity, p pressure and v specific volume.

Noting that specific enthalpy, h, is defined in thermodynamics as:

$$h = e + pv \quad (5A.23)$$

Equation (5.A.22) may be re-written as:

$$Q - W = m(h_2 - h_1) + mg(z_2 - z_1) + \frac{1}{2}m(u_2^2 - u_1^2) \quad (5A.24)$$

Compared to the Bernoulli's equation, the steady-flow energy equation (SFEE) accounts for heat and work exchanges with the surrounding as well as change in the internal energy of the fluid in the energy balance consideration. The energy balance analyses on air-conditioning processes discussed in this book may be regarded as an application of the SFEE, with work exchange and changes in energy due to motion and height of air in the process ignored.

References

[1] ASHRAE Handbook, Fundamentals, American Society of Heating, Refrigerating and Air-Conditioning Engineers, Inc., Atlanta, 2017.

[2] ASHRAE Handbook, Applications, American Society of Heating, Refrigerating and Air-Conditioning Engineers, Inc., Atlanta, 2015.

[3] McQuiston FC, Parker JD & Spitler JD, Heating, Ventilating and Air Conditioning: Analysis and Design, 6th Ed., John Wiley & Sons, New York, 2005.

[4] ASHRAE Standard 113, Method of Testing For Room Air Diffusion, American Society of Heating, Refrigerating and Air-Conditioning Engineers, Inc., Atlanta, 2013.

[5] ASHRAE Handbook, Fundamentals, American Society of Heating, Refrigerating and Air-Conditioning Engineers, Inc., Atlanta, 2009

[6] SMACNA HVAC Duct Construction Standards - Metal and Flexible (ANSI/SMACNA 006-2006), Sheet Metal and Air Conditioning Contractors' National Association, 2006.

[7] DW 144: Specification for Sheet Metal Ductwork, Building Engineering Services Association, 2016.

[8] CIBSE Guide C – Reference Data, The Chartered Institution of Building Services Engineers, London, 2007.

[9] Huebscher, R.G., Friction equivalents for round, square and rectangular ducts, ASHVE Transactions 1948, 54:101-118.

[10] Koch, P., Equivalent diameters of rectangular and oval ducts, Building Services Engineering Research and Technology, 2008, 29(4): 341–347.

[11] Tsal, R.J., Behls, H.F., and Mangel, R, T-method duct design, Part I: Optimization theory, Part II: Calculation procedure and economic analysis. ASHRAE Transactions 1988, 94(2): 90-111, 112-151.

[12] Code of Practice for Energy Efficiency of Building Services Installation, Electrical and Mechanical Services Department, Government of the Hong Kong SAR, 2018.

[13] DW143: Guide to Good Practice – Ductwork Air Leakage Testing, Building Engineering Services Association, 2013.

Chapter 6 Water-side Systems and Equipment

6.1 Introduction

Depending on the climatic conditions of its location, a building may be equipped with, for HVAC purposes, a major chilled water plant with or without an ancillary hot water plant, or a major hot water plant with or without an ancillary chilled water plant. As there are fundamental differences between a hot water system and a chilled water system, they are covered separately in this book, with chilled water systems discussed first and in greater detail. A concise account of hot water systems for space heating will be given in Chapter 10, together with brief discussions on heat recovery chillers, heat pumps, and absorption / adsorption chillers.

Figure 6.1 shows a schematic diagram of a central air-conditioning system with the demarcation between the air-side and the water-side systems highlighted. The air-handling equipment rely on the chilled water supply from the central chiller plant to provide cooling to air-conditioned spaces. The chilled water is driven by the chilled water pumps in the central chiller plant to circulate between the plant and the air-handling equipment via a chilled water piping network, transporting the heat extracted from the air-conditioned spaces by the air-handling equipment to the central chiller plant. The chilled water, having been warmed up while it picks up the heat, will return to the central chiller plant and be fed through the chillers there, which will cool it back down to the supply temperature such that the chilled water is ready to be delivered to the air-handling equipment once again.

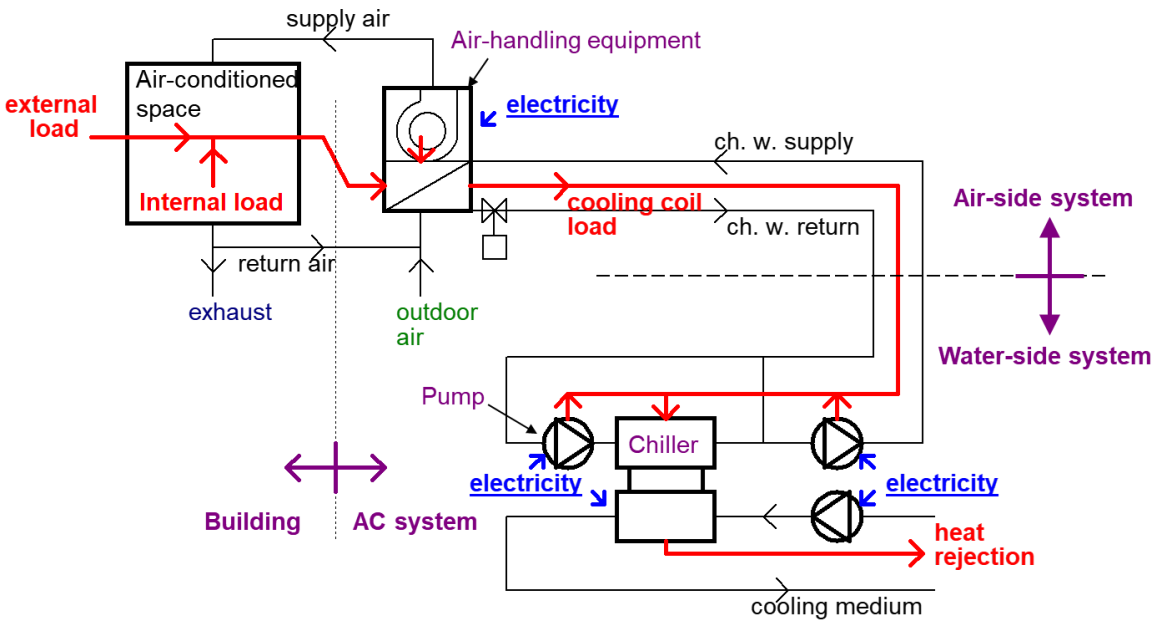

Figure 6.1 Schematic diagram showing the air-side and water-side systems in a central air-conditioning system

While the chillers cool the chilled water, the heat extracted from the chilled water, together with the energy consumed by the chillers for outputting cooling, must be

carried away by a cooling medium and rejected to a heat sink (this point will be re-visited when the refrigeration cycle is discussed). Depending on the type of heat rejection method employed, the central chiller plant may include other equipment, such as condenser water pumps and heat exchangers, and there may also be other equipment which may be installed outside the plant, such as cooling towers or seawater pumps. Associated with the system and equipment include automatic control systems and plant performance monitoring devices.

The above description highlights the functions of a central chilled water system and its major equipment and sub-systems, including a chilled water distribution network, which are collectively referred to as the water-side air-conditioning system. The designs, operating principles and controls of water-side air-conditioning systems and equipment will be discussed in this and the following two chapters, including:

- Operating principles of chillers, with focus on vapour compression type refrigeration equipment.
- Heat rejection methods, including the system configurations and equipment involved.
- Operating principles of water pumps, cooling towers and heat exchangers, and methods for evaluation of their performance.
- Chilled water pumping system designs, including the configurations and operating principles and controls of the range of commonly used systems, such as single-loop, two-loop, and variable primary flow (VPF) systems.
- Water pressure losses through pipes and fittings, pipe sizing and pump selection and control valve selection.
- Variable speed (VS) pump energy use estimation.

Chiller plant equipment sequencing control and control optimization are covered in Chapter 9.

6.2 Water chillers

6.2.1 The medium of heat transport

As the introduction above depicts, the function of the central air-conditioning system in a building is, in essence, to move heat from the air-conditioned spaces to the central chiller plant and finally to a heat sink for disposal, which may be the atmosphere or a river, a lake or the sea. Unless for a special reason, either air or water is used as the medium for heat transport as both are abundantly available, either freely or at a small cost. However, water is preferred to air, unless air has a crucial role to play in the process, e.g. it is the substance that fills up the air-conditioned space and, therefore, is the only choice of medium for picking up the heat from the air-conditioned space and carrying it to the air-handling equipment.

The specific advantage of using water over air as a heat transport medium is due to the preferable properties of water: it has a higher specific heat capacity (4.2 kJ/kg-K vs 1.02 kJ/kg-K) and a much higher density (1000 kg/m^3 vs 1.2 kg/m^3) compared to air. This implies that for the same amount of heat to be transported, the volume of air required is about 3,400 times that of water, if both are subject to the same rise in temperature. Therefore, not only the required sizes of pipes for conveying water are much smaller than the air ducts for the same heat transport duty, the energy required to drive the cooling medium to recirculate between the heat source and the heat sink can be drastically reduced by using water. This is the major reason why water is so widely used for transport of heat, especially over long distances.

For air-conditioning provision in buildings, using chilled water as the heat transport medium allows the use of a central chiller plant to serve a large number of spaces in a single or a cluster of building(s), which is a much better solution than discrete air-conditioning units (see Section 1.3) in respect of the quality of indoor environmental control and energy efficiency that can be achieved. In modern cities with hot weather, nearly all medium- to large-size buildings are equipped with air-conditioning systems that comprise a central chiller plant. In the case of a district cooling system, buildings served by the central plant may even be at a distance of over a kilometre away. The key equipment in a chiller plant responsible for cooling the chilled water are the chillers, which are a kind of refrigeration equipment.

6.2.2 Refrigeration processes and cycle

Most water chillers used in buildings for provision of air-conditioning are vapour compression refrigeration equipment that function as a reversed heat engine – a machine that transports heat from a heat source at a low temperature (T_E) to a heat sink at a higher temperature (T_C, $T_C > T_E$) with input of work (Figure 6.2).[2]

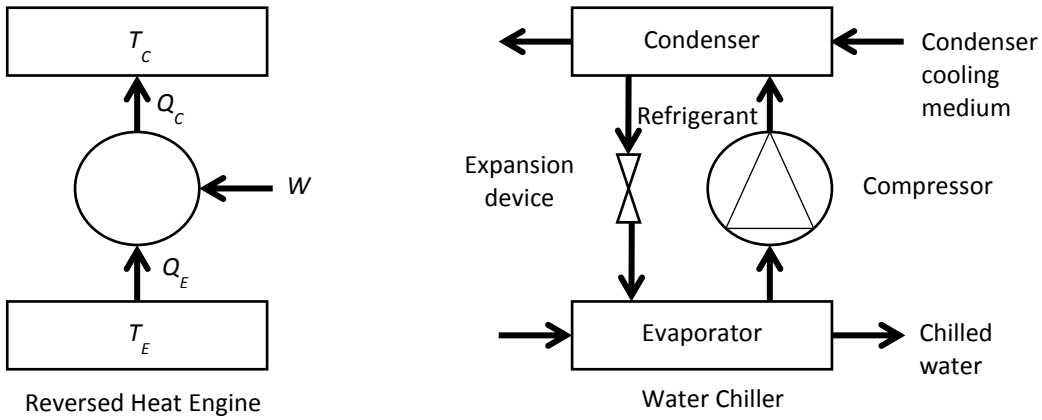

Figure 6.2 Water chiller as a reversed heat engine

[2] Vapour compression chillers are not the only type of machine that may be used; absorption / adsorption chillers are another kind of chiller that can provide refrigeration effect, which require input of heat, instead of work. Obviously, their applicability is constrained by the availability of a low-cost heat source and thus they are seldom used in commercial buildings. Discussions on this type of chillers are given in Chapter 10.

The working fluid being circulated through the components inside a vapour compression chiller is a refrigerant. The refrigerants currently in common use include R22, R32, R134a, R410a, and R744 (CO_2), and more recently the HFO refrigerants, e.g. HFO-1234yf (see Chapter 30 in the ASHRAE Handbook Fundamentals 2017 [1] for thermo-physical properties of these refrigerants). Like air and water, the refrigerant is also a heat transport medium but, unlike air and water, it will undergo phase changes in the processes, from liquid to vapour and back to liquid as it absorbs and rejects heat.

The processes undergone by the refrigerant inside a chiller form a cycle, called the Reversed Rankine cycle (Figure 6.3). The processes include:

- Compression (1-2), assumed to be isentropic
- Condensation (preceded by de-superheating and followed by sub-cooling) (2-3), assumed to be isobaric
- Expansion (3-4), assumed to be adiabatic
- Evaporation (followed by super-heating) (4-1), assumed to be isobaric

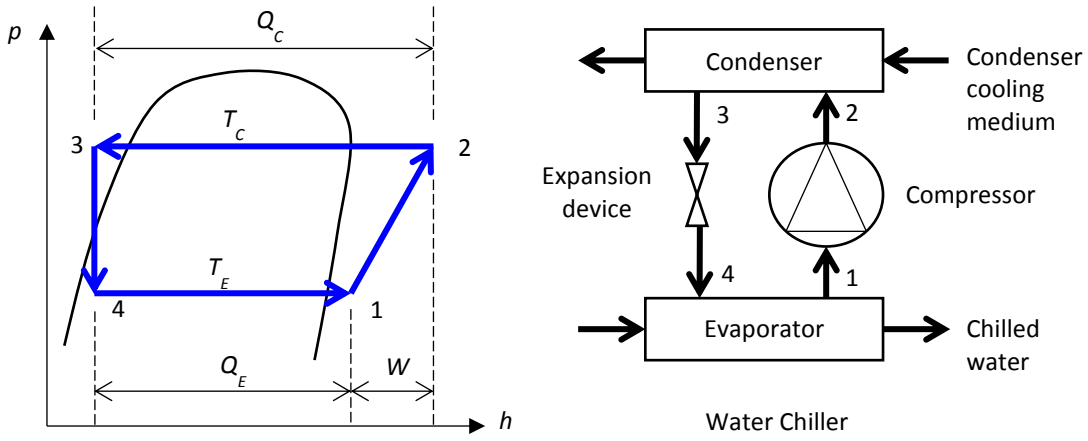

Figure 6.3 Water chiller and the refrigerant cycle

Note that the de-superheating, sub-cooling, and superheating processes are processes upstream or downstream of the isothermal condensation or evaporation processes, which are taking place outside the phase-changing zone under the dome-shaped saturation liquid and vapour curves in the p-h diagram (i.e. the refrigerant stays in the same phase and its temperature will change in each of these processes) (Figure 6.3).

By applying the steady-flow energy equation (see Annex 5A.1.6), the rate of heat or work transfer taking place in the processes can be evaluated from the change in the enthalpy of the refrigerant in each process. Accordingly, the rate of work input in the compression process (W) is:

$$W = h_2 - h_1 \qquad (6.1)$$

The rate of heat output in the condensation process (Q_C) is:

$$Q_C = h_2 - h_3 \tag{6.2}$$

Assuming there is no heat gain or loss (i.e. adiabatic) and since no work is done in the throttling process:

$$h_4 = h_3 \tag{6.3}$$

The refrigeration effect of the evaporation process (Q_E) is:

$$Q_E = h_1 - h_4 \tag{6.4}$$

It follows that (Figure 6.3):

$$Q_C = Q_E + W \tag{6.5}$$

The coefficient of performance of a chiller (COP) is defined as:

$$COP = Q_E/W \tag{6.6}$$

If, instead of refrigerating effect (Q_E), the heat output of the reversed heat engine (Q_C) is the desired output, the machine is called a heat pump and its coefficient of performance (COP_{HP}) is then:

$$COP_{HP} = Q_C/W = 1 + COP \tag{6.7}$$

The above coefficients of performance are widely used as a metric for gauging and comparing the energy performance of chillers and heat pumps.

6.2.3 Components of a vapour compression chiller

The major components of a vapour compression chiller in which the four processes of the refrigeration cycle take place include: the compressor, the condenser, the expansion device, and the evaporator (Figure 6.3). To suit different capacity ranges, physical sizes and operational requirements and constraints, each of these chiller components may be selected from devices of different designs. Only an outline is given here for each of these components. Interested readers may refer to relevant books and handbooks [2 - 5], as well as technical information provided by chiller manufacturers, for more in-depth treatments on these components.

i) Compressors

Common types of chiller compressors fall into two categories, viz. centrifugal or positive displacement, that differ in the way in which the compression process is carried out. In a centrifugal compressor (Figure 6.4), there is an impeller which will be driven to rotate at high speed such that the vapour refrigerant inside it will be pushed by the impeller blades to move along with the rotating impeller and, consequently, compelled by centrifugal force to leave at high speed through the openings at the outer perimeter of the impeller. As the refrigerant vapour gushes out of the impeller and slows down in the

volute casing, its pressure will be boosted before being discharged into the condenser. The refrigerant leaving the impeller will be replenished by vapour refrigerant from the evaporator that is induced to flow into the impeller through its eye.

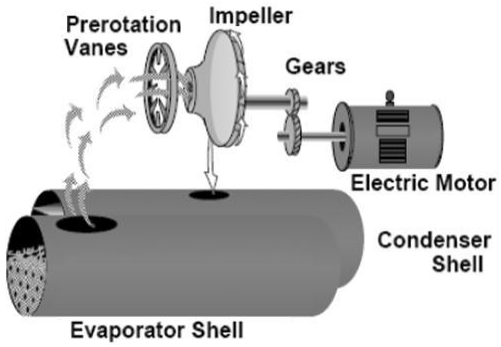

Figure 6.4 Operation of a centrifugal compressor in a chiller

Capacity control of a centrifugal chiller is performed mainly through regulation of the flow rate of refrigerant through the compressor. This is typically done by varying the blade angle of inlet guide vanes (also called pre-rotation vanes) just outside the eye of the impeller. Although modern centrifugal chillers may be equipped with variable speed drives for their compressors for capacity control, which can significantly improve the energy performance of the chillers when operating under part-load, they are still equipped with inlet guide vanes for ensuring stable capacity control in the low speed / low output range, e.g. $< 50\%$ of their rated capacity.

Conventional centrifugal chillers have their impellers supported by bearings, and the high rotational speed of the impeller is achieved by using a gear train to step the speed up from the motor speed. These devices, however, incur considerable energy losses. Recently, centrifugal chillers with gearless, high speed direct drive and magnetic bearings for their impellers are available, which can offer superior part-load performance over the conventional chillers and yield energy cost savings that can well payback the increase in chiller cost. As the impeller shaft is suspended in air by the magnetic bearings, lubricant for the compressor is no longer needed. Therefore, such chillers are often nicknamed as 'oil-free' chillers. Oil-free chillers are, at time of this writing, available only within the maximum unit cooling capacity of about 1,400kW (dual compressors) (bigger units may have become available by now).

In the category of positive displacement compressors, refrigerant compressors of a variety of designs are available. These include the traditional reciprocating compressors, and screw and scroll compressors that emerged later. They share a common feature that the compression process is carried out by a moving physical boundary such that the volume occupied by the refrigerant vapour is reduced (hence the name positive displacement) thereby raising the pressure and temperature of the refrigerant vapour, before the refrigerant is discharged toward the condenser.

For a reciprocating compressor (Figure 6.5), the back and forth motions of the piston inside a cylinder cause the volume inside the cylinder to vary, which, together with the

coordinated opening and closing of the intake and discharge valves, will induce refrigerant to flow into the cylinder when the piston is drawn to move backward, and will compress the refrigerant when the piston is pushed to move forward. This reciprocating action of the piston is driven by the connecting rod linked to a rotating crank shaft which, in turn, is driven to rotate by a motor drive. Capacity output of a reciprocating compressor may be controlled by turning on and off the compressor (like most window type air-conditioners). For a compressor comprising multiple cylinders, however, capacity control in steps can be done by unloading some cylinders as the load drops (by controlling the valve openings such that no compression work is done).

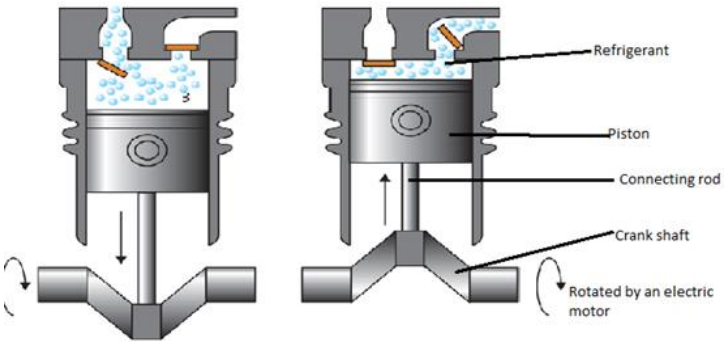

Figure 6.5 A reciprocating compressor

Figure 6.6 shows a pair of helical screws inside a screw compressor together with diagrams that show how the compressor works. The clearance between the casing and the screws is the space into which the refrigerant would be induced to enter and be compressed. This volume is expanded at the side where the lobes of the screws disengage and is reduced at the other side where the lobes of the screws mesh. Capacity control is performed through a slide valve that regulates the amount of refrigerant that will go through the compression process. Capacity control may also be done by varying the rotational speed of the compressor.

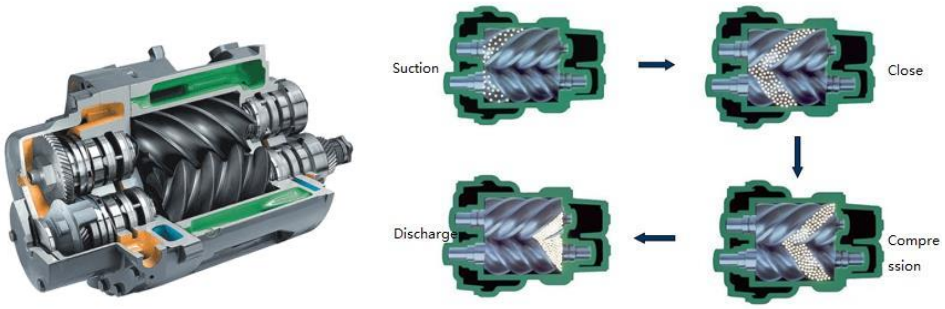

Figure 6.6 A typical screw compressor

Scroll compressors are used in smaller chiller units. A scroll compressor comprises two scrolls (Figure 6.7), with one fixed in position and the other driven to rotate in an

orbiting manner, giving rise to expansion and contraction of the space between the two scrolls, which are utilized to compress refrigerant. Compared to reciprocating chillers of the same capacity, scroll chillers are more energy efficient and will incur less noise and vibration in operation. A chiller may comprise multiple scroll compressors and by unloading some compressors, the output can be reduced in steps.

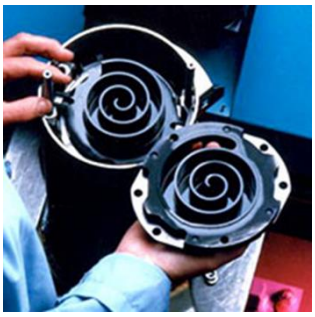

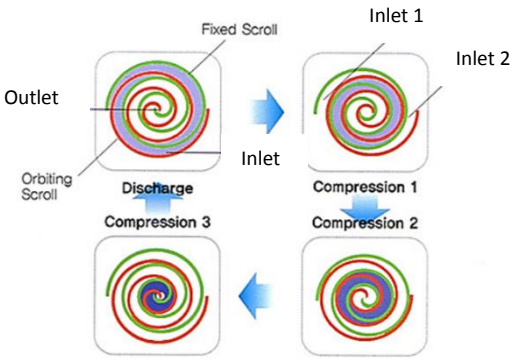

Figure 6.7 A scroll compressor

ii) Condenser and evaporator

Both the condenser and the evaporator of a chiller are basically heat exchangers. In a condenser, heat is disposed from the refrigerant vapour to the cooling medium such that the vapour may condense into liquid. In an evaporator, the liquid refrigerant will vaporise at a low temperature commensurate with the evaporator pressure such that heat will flow from the chilled water to the refrigerant, thereby cooling the chilled water down to the desired temperature. Shell-and-tube type heat exchangers are most commonly used for evaporators and condensers of water-cooled chillers. Air-cooled chillers are typically equipped with finned coil type condensers (Figure 6.8).

iii) Expansion device

As shown in Figure 6.3, in order that the refrigerant vapour may condense into liquid by disposing heat to the cooling medium, the pressure in the condenser must be high enough to allow the condensation process to take place at a sufficiently high temperature. On the other hand, the evaporator pressure must be low enough such that the liquid refrigerant may vaporise at a sufficiently low temperature to cool the chilled water. The pressure difference between the condenser and the evaporator is the outcome of the compression process. Between the condenser outlet and the inlet of the evaporator, the pressure difference is maintained by an expansion device the major duty of which is to throttle the refrigerant so as to lower its pressure.

Expansion devices of different designs are available, including capillary tube, thermostatic expansion valve, electronic expansion valve, orifice plate, float ball expansion valve, etc. to meet the need of various refrigeration machines (Figure 6.9). In addition to their major duty, expansion devices do serve other important functions, such as ensuring refrigerant entering a compressor is fully vaporized and regulating mass flow rate of refrigerant in a chiller. In-line with the objectives of this book, the

design and working principles of each kind of expansion device are not elaborated here but interested readers may refer to relevant books and handbooks for details [2 – 5].

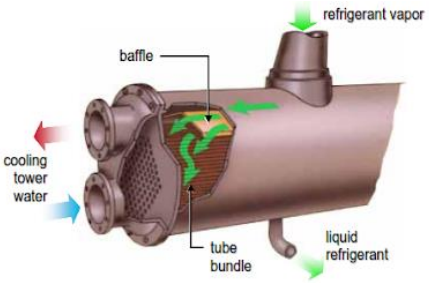

a) Shell-and-tube condenser

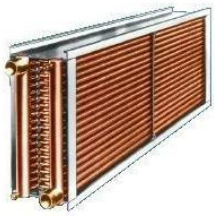

b) finned-tube condenser

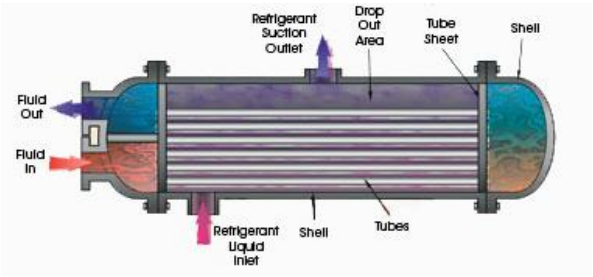

c) Shell-and-tube evaporator

Figure 6.8 Chiller condenser and evaporator

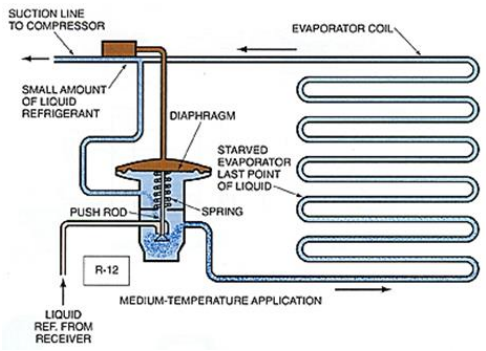

a) Thermostatic expansion valve

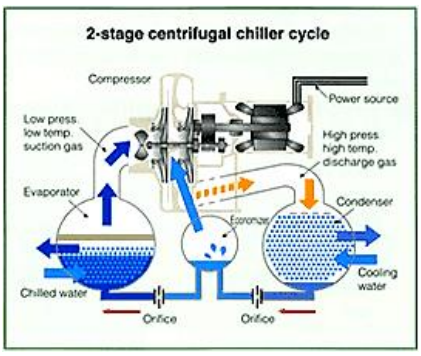

b) Orifice plate

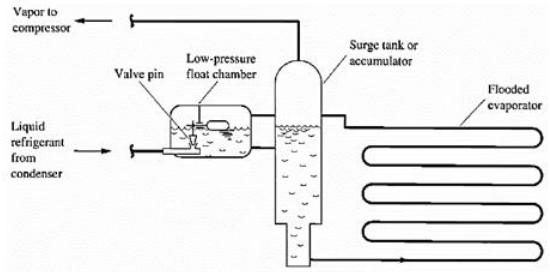

c) Float ball

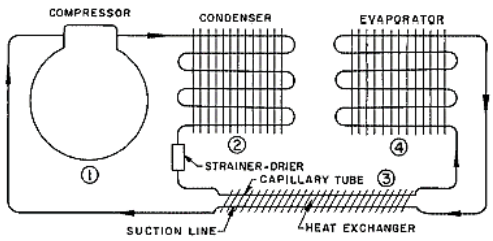

d) capillary tube

Figure 6.9 Expansion devices

6.3 Chiller heat rejection method

The heat of condensation of the refrigerant inside a chiller is transferred to the condenser cooling medium and transported through it to a sink for disposal, which would either be the outdoor air or, if available, a river, a lake, or the sea. As already remarked above, a chiller is called an air-cooled chiller if air is used, and a water-cooled chiller if water is used, as the condenser cooling medium (Figure 6.10).

a) An air-cooled packaged chiller

b) A water-cooled packaged chiller

c) Cross-flow cooling towers

d) Plate-type heat exchangers

Figure 6.10 Major equipment of a central chilled water plant

If atmospheric air is the final heat sink but air is not utilized directly as the condenser cooling medium, a heat transfer equipment, such as a cooling tower or radiator (like that used in cars for engine cooling), is needed for disposal of the heat to the outdoor air. Similarly, if water from a water source is not fed directly through the chiller condensers (e.g. when seawater is used), a heat exchanger would need to be used for transferring the heat to the water.

6.3.1 Heat rejection system configurations

i) Direct air-cooled system

The simplest way of rejecting the condenser heat is to use air to cool the condenser, which is the case when air-cooled chillers are used. An air-cooled chiller (Figure 6.10a) is equipped with finned-tube coils as its condenser and fans for drawing outdoor air to flow through the gaps between the fins of the condenser coils to cool the refrigerant

being fed through the tubes. The condenser and the fans, as well as the compressor, evaporator, expansion device, a control panel and other accessories are typically assembled into a package unit, which can be used once fixed on site and with chilled water pipes and electricity supply connected. Air-cooled chillers are normally installed outdoors but, if needed, may be installed indoors with ducted exhaust.

ii) Direct water-cooled system with cooling tower

Cooling towers are heat transfer equipment that allow the condenser heat of water-cooled chillers to be disposed of to the atmosphere. Detailed analysis on the operating principle and process of cooling towers will be given later in this chapter. In using this heat rejection method, water pumps are installed to circulate the condenser water between the chillers and the cooling towers (Figure 6.11a). Water supply is required to replenish water losses in the process, and water treatment is needed to control water quality and prevent outbreak of legionnaire's disease. A low limit temperature control system is typically installed to prevent condenser water temperature entering chiller from falling below a low limit (~16^{o}C), which may happen in winter and cause unstable operation of the chiller.

iii) Indirect water-cooled system with cooling tower

The condenser water circuit in the abovementioned heat rejection system may be split into two that are thermally connected by a heat exchanger in between (Figure 6.11b). This design may be used when seawater is used in the circuit through the cooling tower and fresh water is used in the circuit through the chiller, to protect the chiller condenser from the corrosion and erosion effects of seawater. Pumps are needed in each water circuit for heat transport.

iv) Direct seawater-cooled system

For a building nearby a harbour, a pump station may be built to draw seawater for condenser cooling. The seawater drawn-in by the seawater pumps may be fed directly through chiller condensers, and the used seawater will be pumped back to the harbour for disposal (Figure 6.11c). Filtration equipment and chemical / biocide dosing are needed to control water quality and prevent growth of micro-organisms.

v) Indirect seawater-cooled system with heat exchanger

For protection of the chiller condensers, the condenser water circuit in the abovementioned system may be split into two that are thermally connected by heat exchangers between them (Figure 6.11d). This allows fresh water to be used in the circuit through the chiller, although one more group of pumps is needed.

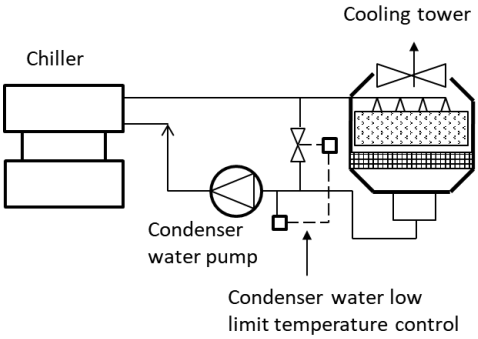

a) Water-cooled system with cooling towers

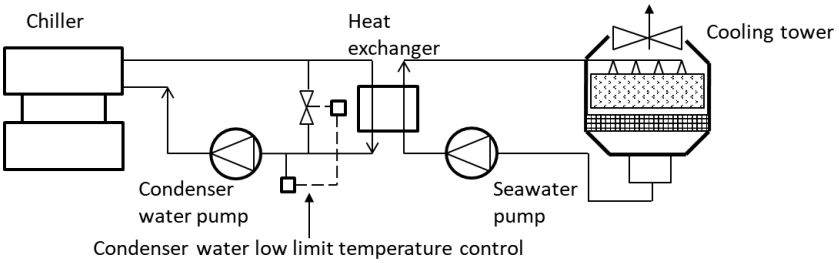

b) Indirect water-cooled system with cooling towers

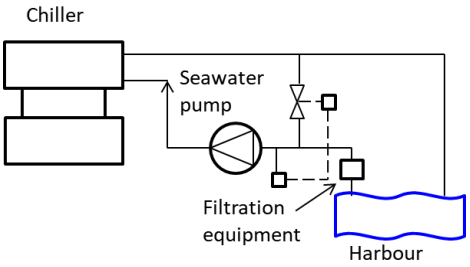

c) Direct seawater-cooled system

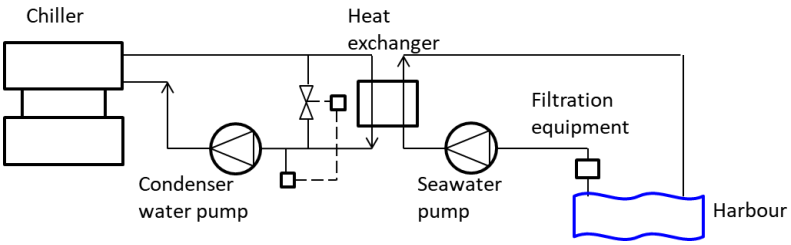

d) Indirect seawater-cooled system

Figure 6.11 Configurations of central chiller plants using different heat rejection methods

6.3.2 Impact on energy performance and equipment

In designing a chiller plant, a selection can be made from the range of heat rejection methods introduced above such that the plant may be run at the highest possible energy efficiency. This choice is highly significant to the running cost of the plant because the temperature of the available condenser cooling medium ($T_{CM,e}$) has a profound impact on the work input required for producing the cooling output (Figure 6.12): the condensing temperature of the refrigerant inside the condenser (T_C) has to be sufficiently higher than the cooling medium temperature whereas the higher the condensing temperature, the higher the work input required (W) and, at the same time, the smaller the refrigeration effect (Q_E).

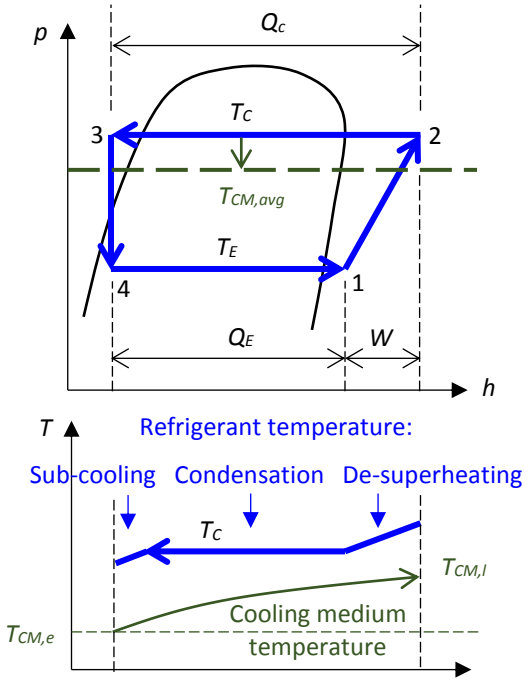

Figure 6.12 Relation between condensing temperature and temperature of cooling medium

Table 6.1 shows the typical design cooling medium entering temperatures adopted in Hong Kong for chillers with different heat rejection methods. Cooling medium of the lowest temperature that could be made available is seawater from the harbour which is used directly for condenser cooling. Protecting the condenser with a freshwater circuit would raise the entering condenser water temperature by at least 1 ~ 2°C compared to using seawater direct. Without seawater supply, the next best option is to use water-cooled chillers together with cooling towers. Using air-cooled chillers would be the only option if no water source is available, at the price of the highest condenser cooling medium temperature.

Table 6.1 Typical design cooling medium entering temperatures adopted in Hong Kong

Heat Rejection Method	Design Cooling Medium Entering Temp.
Direct air-cooled	35°C
Direct water-cooled with cooling tower (CT)	31 – 32°C (air wet-bulb temp. entering CT 28°C)
Indirect water-cooled with cooling tower (CT) and heat exchanger (HX)	32°C (air wet-bulb temp. entering CT 28°C)
Direct seawater-cooled	27 – 28°C
Indirect seawater-cooled with heat exchanger (HX)	29 – 30°C (seawater temperature entering HX 27°C)

Since the choice of cooling medium to be used for a central chilled water plant may be restricted by the availability of alternatives, rather than restricting the use of certain chiller type or heat rejection method, regulatory control on energy performance of air-conditioning systems and equipment is typically through setting minimum acceptable limits on COP of various types of chillers (see for example the building energy code in force in Hong Kong [6]).

To cope with the characteristics of the cooling medium adopted, the design or choice of material for certain components of the major equipment may need to be adjusted to ensure the system and equipment are adequately protected from any adverse effects, e.g. the corrosion and erosion effects that seawater may cause. Table 6.2 lists the requirements on the design and materials of major chiller plant equipment to be used for various heat rejection methods.

Table 6.2 Equipment selection considerations for different heat rejection methods

Heat Rejection Method	Chiller Condenser Tube and Related Equipment
Direct air-cooled	Finned coil condenser with copper tubes and aluminium/copper plate fins
Direct water-cooled with cooling tower (CT)	Shell-and-tube condenser with copper tubes. Fibre glass, metal, or wood cooling tower
Indirect water-cooled with cooling tower (CT) and heat exchanger (HX)	Shell-and-tube condenser with copper tubes (for fresh water); titanium plate HX for fresh water /seawater
Direct seawater-cooled	Shell-and-tube condenser with 70/30 cupro-nickel or titanium tubes
Indirect seawater-cooled with heat exchanger (HX)	Shell-and-tube condenser with copper tubes (for fresh water); titanium plate HX for fresh water / seawater

6.4 Water pumps

6.4.1 Key features of pumps in air-conditioning systems

The function of water pumps in the water-side system of a central air-conditioning system has already been highlighted in the preceding sections. Nearly all water pumps used in central air-conditioning systems are centrifugal pumps. Centrifugal pumps of the horizontal split case design are the dominant type used but end suction pumps are used for supplying smaller flow rates of water at moderate pressures (Figure 6.13).

Double inlet double width horizontal split case centrifugal pump

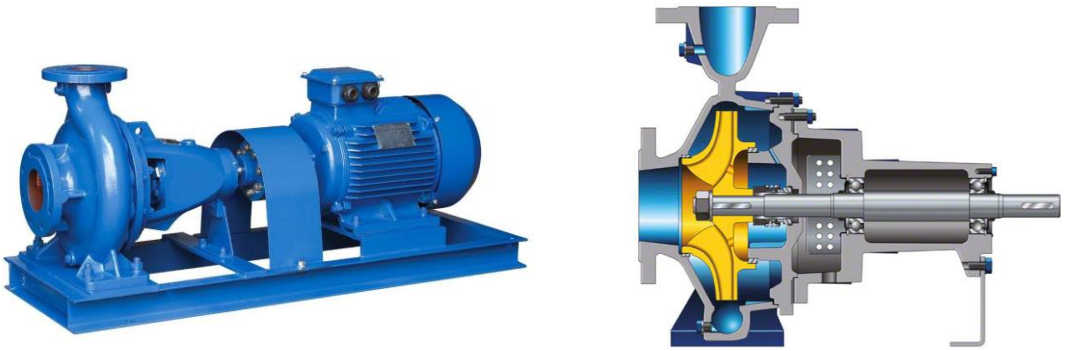

Single inlet single width end suction centrifugal pump

Figure 6.13 Centrifugal pumps commonly used in central air-conditioning systems

The horizontal split case design allows adoption of the double inlet double width (DIDW) arrangement where water may enter the impeller from both sides thus increasing the flow capacity of the pump without much increase in physical size. Direction of water flow entering the pump is same as the direction of water flow leaving. Another major advantage of the horizontal split case design is that, for repair and maintenance, there is no need to disconnect the suction and discharge pipes connected to the pump, or to remove the pump motor, even if the impeller needs to be taken out.

The end suction pump draws in water from the end connection in the axial direction and discharges water in the transverse direction perpendicular to the pump axis. Since the impeller has inlet at one side only, end suction pumps are single inlet single width (SISW) pumps. This kind of pump can discharge water at similar pressure as a DIDW pump with the same impeller diameter but at nearly half the flow rate. The back-pull-out design is widely used to provide similar convenience for repair and maintenance as a horizontal split case pump. This requires the use of a spacer between the motor and pump shafts such that the spacer can be dismantled giving space for pulling out the impeller from the back side without disturbing connections to the pipes of the air-conditioning system or the pump motor mounting.

6.4.2 Pump performance

Both centrifugal pumps and fans are rotodynamic machines and are governed by the same fluid mechanics principles. The methods for evaluation and analysis of fan performance introduced in Chapter 5 are equally applicable to pumps, such as:

Pump efficiency, $$\eta = \frac{V \cdot \Delta P}{W} \tag{6.8}$$

Pump power, $$W = \frac{V \cdot \Delta P}{\eta} \tag{6.9}$$

Where

ΔP = pumping pressure (difference between discharge and suction pressures)
V = water volume flow rate

The required performance of pumps for a chilled, condenser, or sea water distribution system is primarily to deliver the flow rate of water as required to meet the heat transport duty at the pumping pressure sufficient to overcome the losses through the piping system. Other important performance include the power or efficiency of the pump corresponding to the required duty, and the net positive suction pressure (NPSP) for systems involving drawing water from a tank with free surface below the pump (as could occur in a seawater pumping system). The noise and vibration that would arise during operation may also be performance of concern.

The key performance of a centrifugal pump is often presented as a curve that shows the pumping pressure, P, that the pump can discharge over a range of flow rate (V) at a given rotational speed (N) of the impeller of a given diameter (D). Since the same pump casing may house any impeller of the same design as long as its outer diameter is within a limited range, which is a measure for fine tuning pump performance by trimming the impeller, pump manufactures typically provide a family of P-V curves that correspond to a series of diameters (Figure 6.14). In the same graph, other curves may be included, such as constant pump power and/or efficiency contours, and a NPSP curve. Such performance charts are the key references for selection of pumps for a system, considering not only the design operating condition but also the possible operating conditions in the year round.

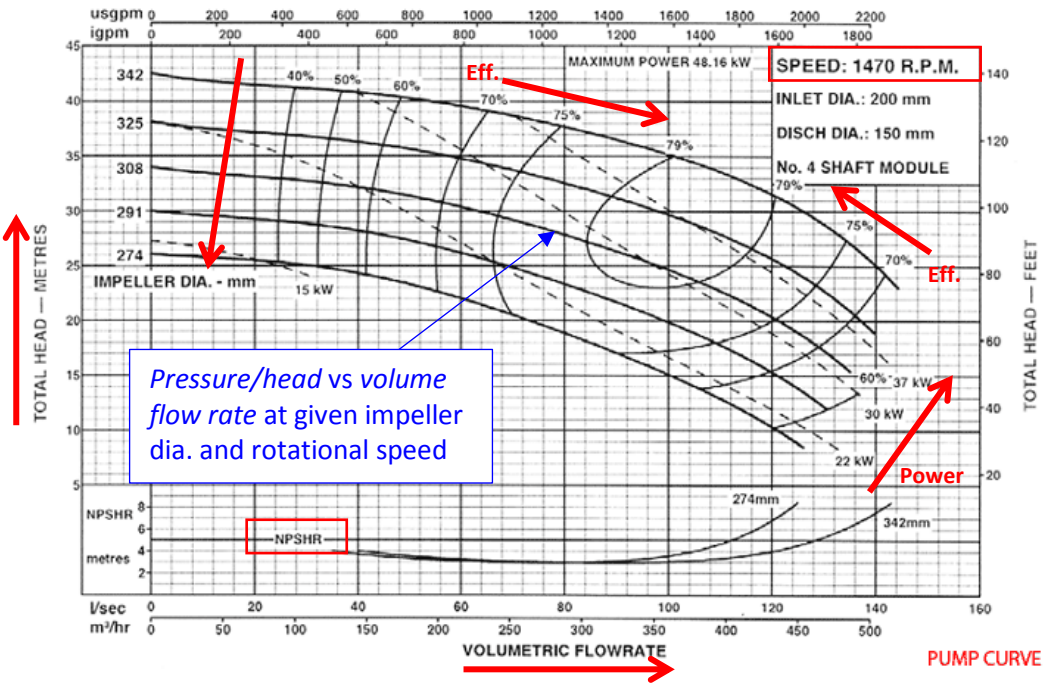

Figure 6.14 Performance curves of a centrifugal pump

6.4.3 Materials of key components

Other than the pump performance, selection of pumps needs to look into the suitability of the component materials for the expected service conditions, especially the medium it would handle. Table 6.3 provides some advice on the materials to be used for various components when the pump is for handling fresh water and seawater.

Table 6.3 Materials of pump components for handling fresh water and seawater

Pump component	For fresh water	For seawater
Casing	Cast Iron	Cast Iron
Impeller	Gunmetal*, Zinc-free Bronze, Stainless Steel	Zinc-free Bronze, Stainless Steel
Shaft	Carbon Steel, Stainless Steel	Stainless Steel
Bearing	Bronze	Bronze, Stainless Steel

* Gunmetal, also known as red brass in the United States, is a type of bronze – an alloy of copper (88%), tin (10%), and zinc (2%).

6.5 Cooling towers

Cooling towers are widely used in buildings for rejection of the chiller condenser heat to the atmosphere. With cooling towers, the more energy efficient water-cooled chillers can be used even if an abundant source of water supply is lacking. Figure 6.15 shows various types of cooling towers available in the market.

Blow through type cooling tower with centrifugal fans, counter-flow

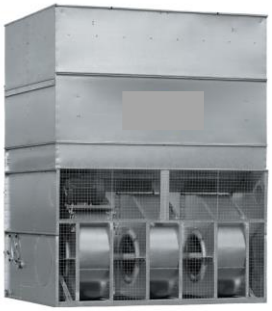

Draw through type cooling towers with propeller fans

Wooden cooling tower, crossflow

Natural draft cooling tower

Fibre glass cooling tower, counter-flow

Figure 6.15 Types of cooling towers

The condenser water leaving a chiller is fed into a cooling tower and, for maximising the heat and mass transfer area available, the water is broken into fine water droplets by forcing it through the spray nozzles in the cooling tower (Figure 6.16). Air from the surrounding is drawn or blown into the cooling tower such that the air will have direct contact, and thus heat and mass exchanges, with the water droplets inside the cooling tower. As a minute part of the condenser water evaporates from liquid state to vapour state and joins the air stream, the latent heat of evaporation is sustained primarily by sensible heat loss of the water itself, which is the reason why the condenser water temperature will drop in the cooling tower. The air, after picking up heat and vapour from the water, is disposed of into the atmosphere.

An analysis on the heat and mass transfer processes taking place in a cooling tower, based on the counter-flow arrangement (Figure 6.16), is given in the following sub-section. This analysis, however, is a simplified treatment based on the assumption that

the mass flow rate of the water is regarded as unchanged in accounting for the effect of heat loss on the water temperature (as will be pointed out below). More rigorous treatments can be found from [3, 7, 8].

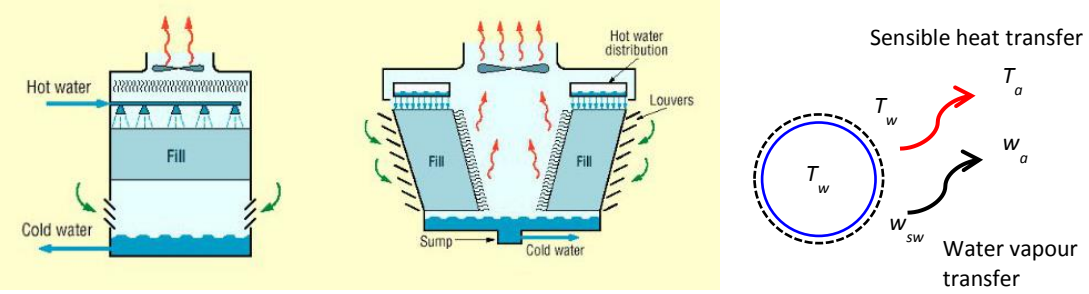

Figure 6.16 Air and water flows in counter-flow and crossflow cooling towers and heat and moisture transfer between water droplet and air

6.5.1 Heat and moisture transfer in a cooling tower

Migration of water vapour (i.e., mass transfer) from the droplet surface to the air is driven by the difference in moisture content between the saturated air on the surface of the water droplet and the air ($w_{sw} - w_a$) (Figure 6.16). Since any vapour leaving the water droplet comes from vaporization of the liquid water in the droplet, the required latent heat of vaporization needs to be sustained by supply of heat at the same rate. Given that the droplet is isolated from any external source of heat except the air surrounding it, the latent heat of vaporization has to be sustained either by sensible heat transfer from the air to the water droplet and/or by a drop in temperature of the water droplet itself.

Concurrent with the vapour transfer, sensible heat transfer between the air and the water droplet will take place as long as there is a temperature difference between the surface of the water droplet and the air ($T_w - T_a$), regarded as positive if the sensible heat transfer is from the droplet to the air as for the vapour transfer. Within a cooling tower, sensible heat transfer from the air to the water is possible but, if it does happen, it will happen within a small portion of the cooling tower, at the air inlet side, and is much smaller than the heat loss of the water as it drops in temperature for sustaining vaporization, and thus the condenser water may be cooled down in the cooling tower.

The total heat transfer between the water droplet and the air surrounding it is the sum of the sensible heat transfer and the latent heat transfer associated with the water vapour transfer. It can be shown that specific enthalpy (h) may be regarded as the driving potential for total heat transfer [3, 7, 8], which allows the rate of total heat exchange between the water droplet and the air per unit area of the droplet surface (q_{tot}) to be described by:

$$q_{tot} = h_d(h_{sw} - h_a) \tag{6.10}$$

In the equation above:

h_d = total heat or mass transfer coefficient (in m^{-2} s^{-1})
h_{sw} = specific enthalpy of air saturated at T_w
h_a = specific enthalpy of surrounding air

Since there are many droplets of different sizes inside a cooling tower, an average value (a), which denotes the total surface area of all the droplets per unit volume in the cooling tower, is used in the analysis. The analysis is based on the assumptions that the cooling tower has the counter-flow arrangement, the cross-sectional area for air and water flows is uniform throughout the tower, and the conditions of the air and the water across any intermediate plane perpendicular to the air/water flow directions are uniform. These assumptions jointly justify the use of a one-dimensional treatment for the analysis. Figure 6.17 shows the idealized cooling tower model used in the analysis.

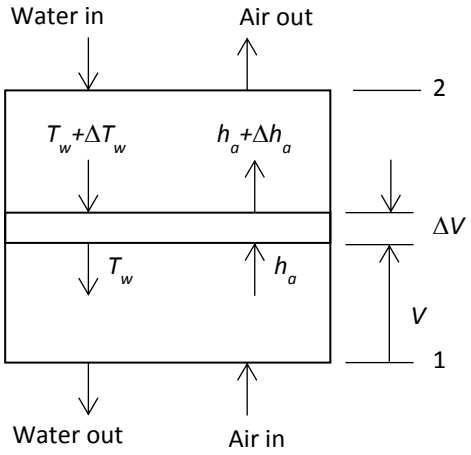

Figure 6.17 An idealized counter-flow cooling tower model

As shown in Figure 6.17, the air enters the cooling tower from the bottom, through plane 1, and leaves the cooling tower from the top, through plane 2. The water flow is in the reversed direction, from plane 2 down to plane 1. As the air and the water flow through the cooling tower, both will change in properties as a result of the heat and mass exchanges between them.

The reference dimension adopted for the analysis is V, the internal volume of the cooling tower, measured from plane 1 until plane 2, positive upward. Accordingly, as shown in Figure 6.17, the change in the specific enthalpy of air is regarded as positive upward, i.e. if at the plane denoted by V, the specific enthalpy of air is h_a, its specific enthalpy is regard as $h_a + \Delta h_a$ as the air flows by an incremental distance to the plane denoted by $V + \Delta V$. As to the water, its temperature would be regarded as changing from $T_w + \Delta T_w$ at the plane $V + \Delta V$ to T_w at the plane V.

Across the elemental section (ΔV), the rate of total heat gain of the air (ΔQ_a) can be related to the change in state of the air, as follows:

$$\Delta Q_a = m_a(h_a + \Delta h_a) - m_a h_a = m_a \Delta h_a \tag{6.11}$$

Where m_a is the mass flow rate of dry air through the cooling tower and Δh_a is the change in specific enthalpy of air as it flows through the elemental section.

Across the elemental section (ΔV), the corresponding heat loss of the water (ΔQ_w) is given by (it is a heat loss as it is evaluated by subtracting the heat carried by the leaving water from that of the water entering the elemental section):

$$\Delta Q_w = m_w C_w(T_w + \Delta T_w) - m_w C_w T_w = m_w C_w \Delta T_w \tag{6.12}$$

Where m_w is the mass flow rate of water through the cooling tower and C_w is specific heat of water.

The changes in the states of the air and the water are made possible by the total heat transfer from the water to the air (as water is assumed to be having a heat loss and air is having a heat gain) taking place within the elemental section (ΔV) in the cooling tower (Figure 6.17). Using Equation (6.10), this total heat transfer rate (ΔQ_{tot}) is given by:

$$\Delta Q_{tot} = h_d a(h_{sw} - h_a)\Delta V \tag{6.13}$$

From heat balance consideration on the elemental section, we can see that:

$$\Delta Q_a = \Delta Q_w = \Delta Q_{tot} \tag{6.14}$$

Equating the right-hand sides of Equations (6.12) and (6.13), and re-arranging, we get:

$$\frac{h_d a}{m_w}\Delta V = \frac{C_w}{h_{sw} - h_a}\Delta T_w \tag{6.15}$$

Integrating both sides of the above equation,

$$\frac{h_d a}{m_w} V_T = C_w \int \frac{1}{h_{sw} - h_a}\Delta T_w \tag{6.16}$$

Where V_T is the total internal volume of the cooling tower from plane 1 to plane 2.

Note that:

- As shown in Equation (6.12), the mass flow rate of water (m_w) was assumed to be a constant, which is a simplifying assumption made in this analysis, but in reality, it will drop across the elemental section as there will be evaporation loss within the elemental section.

- Once again, m_w was assumed to be a constant in the integration process to arrive at Equation (6.16). As will be shown below, the water loss is so small compared to the water flow rate that the impact of this assumption is negligible.

- The LHS of Equation (6.16), called the Number of Transfer Units (NTU) of a cooling tower, is dimensionless and hence the RHS is also dimensionless.

Equating Equations (6.11) and (6.12),

$$m_w C_w \Delta T_w = m_a \Delta h_a \tag{6.17}$$

Rearranging and taking limit,

$$\frac{dh_a}{dT_w} = \frac{m_w C_w}{m_a} \tag{6.18}$$

The RHS of the above equation will be a constant if m_w and m_a are held constant (the assumption that m_w = const. is made once again here). In this condition, the enthalpy of the air (h_a), when plotted against the water temperature (T_w) at the corresponding plane along the direction of air flow, will be a straight line, as its slope (dh_a/dT_w) equals a constant (Figure 6.18). Hence, when h_{a1}, T_{w1} & T_{w2}, and m_w & m_a are known, and these are typically design parameters of a heat rejection system for which a cooling tower is to be selected, h_a corresponding to any intermediate water temperature T_w within the range of T_{w1} to T_{w2} can be evaluated:

$$h_a = h_{a1} + \left(\frac{m_w C_w}{m_a}\right)(T_w - T_{w1}) \tag{6.19}$$

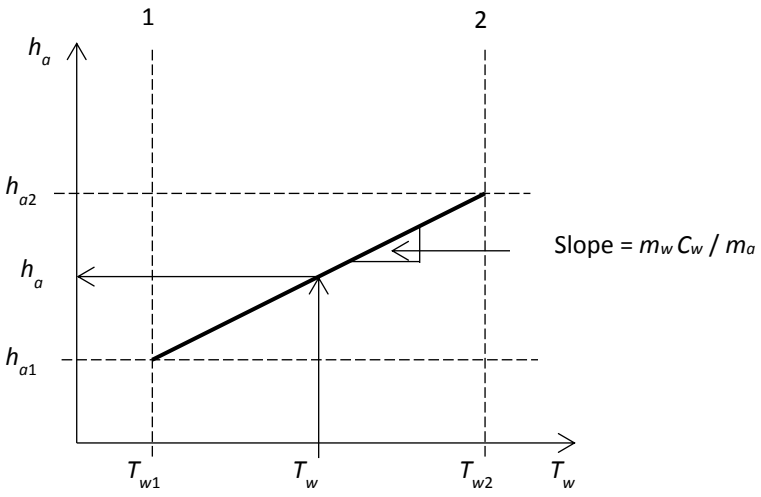

Figure 6.18 Air specific enthalpy vs water temperature in a cooling tower

Since saturation air enthalpy is dependent only on the air temperature, the enthalpy of the saturated air film above the water droplets, with same temperature as the water, can also be plotted in the same graph. This graph (Figure 6.19) enables the parameters required for numerical integration of Equation (6.16) to be obtained conveniently:

$$NTU = \frac{h_d a}{m_w} V_T = C_w \sum_{T_{w1}}^{T_{w2}} \frac{\Delta T_w}{h_{sw} - h_a} \tag{6.20}$$

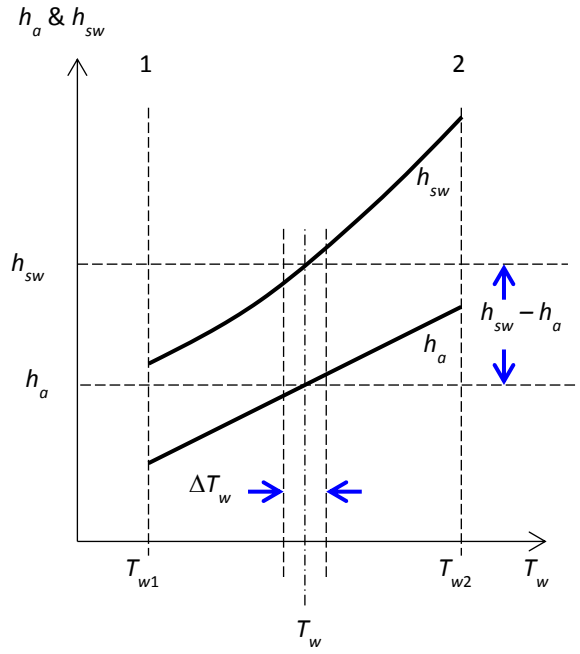

Figure 6.19 Graphical illustration of the numerical integration process for evaluation of the NTU of a cooling tower

The value of NTU evaluated from the required water entering and leaving temperatures, design outdoor (entering) air state and the air and water mass flow rates is the required NTU value (NTU_R). The NTU value that a cooling tower is able to provide, referred to as the available NTU (NTU_A) can then be compared with the required NTU. The cooling tower is suitable for the application if $NTU_A \geq NTU_R$.

The numerical calculation steps may also be carried out systematically through the use of a table, as shown in Example 6.1.

In practice, cooling tower selection is seldom based on NTU value. Evaluation of NTU, however, is still useful because, for a given cooling tower, as long as the air and water mass flow rates are held constant, its NTU value will not vary significantly over not too wide ranges of the water and air temperatures. Therefore, the NTU value of a cooling tower may be used for analysis of its part-load performance (see further elaborations in Section 9.3.2).

For cooling tower selection, manufacturers would typically provide performance curves based on the following two parameters (Figure 6.20):

Range = Difference between the entering and leaving water temperatures

Approach = Difference between the leaving water temperature and the entering air wet bulb temperature

Example 6.1

Given the following design parameters, evaluate the NTU_R of the cooling tower.

m_w	m_a	T_{wb1}	T_{w1}	T_{w2}
64kg/s	51.2kg/s	28°C	32°C	37°C

The table with which the calculations are carried out is as follows:

[a]	[b]	[c]	[d]	[e]	[f]	[c]/[f]
T_w	h_{sw}	ΔT_w	h_a	h_{sw}-h_a	Avg[e]	
32	110.7		89.7	20.9		
33	116.5	1	95.0	21.5	21.24	0.0471
34	122.6	1	100.2	22.4	21.98	0.0455
35	129.1	1	105.5	23.6	23.01	0.0435
36	135.8	1	110.7	25.1	24.34	0.0411
37	142.8	1	116.0	26.9	25.98	0.0385
					Sum	0.2156
					NTU_R	0.9056

Remarks:

The temperature range of water (32 to 37°C) is subdivided into intermediate values at 1°C interval (ΔT_w), as shown in columns [a] & [c] above.

Values in column [b] are specific enthalpies of saturation vapour at temperatures shown in the corresponding rows in column [a].

The h_a value of the air entering the cooling tower, which corresponds to $T_w = 32$°C and shown in the first row of column [d], was found from the given air entering condition. The other h_a values were determined based on Equation (6.19) and corresponding values of T_w shown in column [a].

Column [e] shows the difference in value between columns [b] & [d]. Since these values correspond to the water and air states at the boundaries of the elemental sections represented by the temperature values in column [a], the means of the values at a row and the row immediately above in column [e] were evaluated and shown in column [f], to represent the mid-plane values within each subdivision.

The last column shows the values in column [c] divided by values in column [f]. When summed and then multiplied by C_w, the result is the NTU required of the cooling tower,

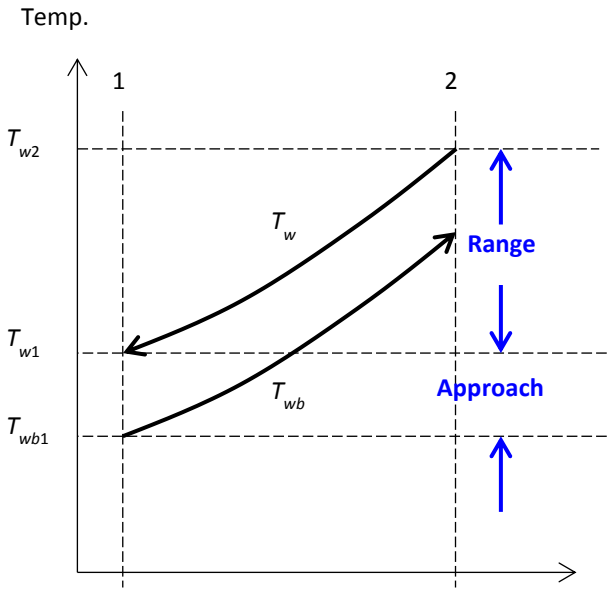

Figure 6.20 The range and approach of a cooling tower

Obviously, range is proportional to the heat rejection rate to be handled by the cooling tower per unit mass flow rate of water. The approach defined above is a measure of the driving force for total heat transfer, i.e. the difference in enthalpy between the saturated air above the water droplet and the air, and it is evaluated at the air entering plane. This is because the saturation air enthalpy is fully defined by its temperature, and wet bulb temperature may be taken as a proxy of specific enthalpy as constant wet bulb temperature lines are nearly parallel with constant specific enthalpy lines on a psychrometric chart. The approach therefore may be interpreted as a measure of how easy or difficult the total heat transfer duty can be accomplished, the smaller the value of the approach, the smaller the driving force for the total heat transfer and thus the larger the required cooling tower.

6.5.2 Water losses in cooling tower

Given that water can be cooled inside a cooling tower through evaporating a small amount of the water, the amount of water in the condenser water system will drop with time of operation. This water loss is called evaporation loss (E). Besides this loss, some fine water droplets will be carried away by the air stream, which is called drift loss (D). Therefore, eliminators are installed in cooling towers to minimize drift loss (Figure 6.21).

Since only pure water will be evaporated, when there is evaporation loss, the concentrations of dissolved solids (minerals and other impurities) in the water will increase, which can exacerbate condenser tube fouling as well as scale formation on pipe internal surfaces and corrosion. In order to control the concentration of total dissolved solids in the water, some water in the system will be bled-off from time to time. Bleeding off water from the condenser water system gives rise to the water loss that is called blowdown loss (B). The total water loss, therefore, equals $E + D + B$.

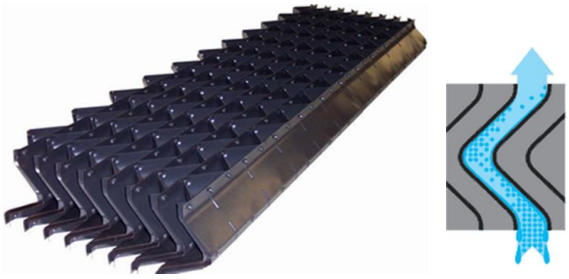

Air can turn in flow direction far more readily than water droplets. The water droplets, therefore, will impinge onto the curved flow channel surfaces and drop down back into the cooling tower.

Figure 6.21 Eliminators in a cooling tower for reducing drift loss

To make-up this loss, a supply system that can feed the cooling tower system with make-up water at the same flow rate is needed. The cycle of concentration (C_{cyc}), as defined below, is a reference parameter for determining the blowdown rate required:

$$C_{cyc} = C_s/C_m \tag{6.21}$$

Where C_s and C_m are the concentrations of dissolved solids in the cooling tower water and in the make-up water, respectively.

The amount of dissolved solids leaving the system is given by (Figure 6.22):

$$C_s(D + B)$$

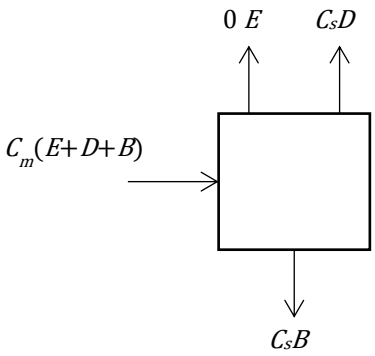

Figure 6.22 Mass balance on impurities in a cooling tower

The amount of dissolved solids entering the system with the make-up water is:

$$C_m(E + D + B)$$

As the incoming and outgoing amounts are equal under steady state, we can express C_{cyc} as follows:

$$C_{cyc} = \frac{C_s}{C_m} = \frac{E+D+B}{D+B} \tag{6.22}$$

Solving for B from the above,

$$B = \frac{E}{C_{cyc}-1} - D \tag{6.23}$$

The evaporation loss, E, can be estimated from the heat rejection rate (HR) to be handled by the cooling tower:

$$HR = m_w C_w (T_{w2} - T_{w1})$$

$$E = \frac{HR}{h_{fg,w}}$$

Where $h_{fg,w}$ is the latent heat of evaporation at the water temperature, T_w. Hence,

$$\frac{E}{m_w} = \frac{C_w(T_{w2}-T_{w1})}{h_{fg,w}} \tag{6.24}$$

The designs of many condenser water systems adopt a temperature difference of 5.5°C across the chiller condenser ($T_{w2} - T_{w1}$). Since the specific heat of water (C_w) is about 4.2 kJ/kgK and the latent heat of evaporation ($h_{fg,w}$) is about 2,400 kJ/kg, the evaporation loss is about 1% of the condenser water flow rate:

$$\frac{E}{m_w} = \frac{4.2\times5.5}{2400} \approx 0.01$$

The drift loss can be kept to a negligibly small level (< 0.005%; see below). Assuming a cycle of concentration of 2 and using Equation (6.23):

$$B = \frac{0.01}{2-1} - 0 = 0.01$$

The make-up rate required (= E+B+D) is, therefore, about 2% of the condenser water flow rate.

Prevention of spread of legionnaire's disease (LD) is a key issue to design, operation, and maintenance of cooling towers because the water temperature in cooling towers is suitable for the bacteria (legionella) to proliferate. In many places, implementing proper measures for LD prevention is a regulatory requirement. Additionally, since the make-up water is usually obtained from fresh water supplies, conservation of water is also a key concern. In Hong Kong, the Code of Practice for Water-cooled Air Conditioning Systems [9] requires:

- Drift emission of the drift eliminator installed in cooling tower shall not exceed 0.005% of the maximum design water circulation rate through the cooling tower.

- In order to prevent water wastage, the minimum cycle of concentration in designing water treatment program and bleed off requirement shall not be less than 6 and 2 for fresh water and seawater cooling tower system, respectively.

- The bleed-off water from cooling tower shall be reused for flushing purpose by discharging it to a retention tank before transferring it to the flushing water tank or discharging it directly to the flushing water tank by gravity.

6.5.3 Levelling and flow balancing of cooling towers

For reliability and maintenance considerations, multiple cooling tower units are often installed for parallel operation in central air-conditioning systems (Figure 6.22a). However, imbalance in the flow resistances of the supply and/or return pipe branches connecting the cooling towers to the condenser water circuit will cause mismatches in the flow rates of water entering and leaving individual cooling towers. If provisions are made to stop feeding water into a cooling tower when the cooling tower is taken out of operation, which is a common arrangement, but there is no isolation valve at the outlet of the cooling tower, water in the basin of the cooling tower would continue to be drawn out by the condenser water pumps.

The abovementioned situations would give rise to drying out of some cooling tower units and, in turn, air being sucked into the condenser water circuit while, at the same time, water overflow would happen at some other cooling tower units (Figure 6.22b). The condenser water circuit connected to the cooling towers, therefore, has to be well balanced to ensure water will be fed into and drawn out of each cooling tower at the correct flow rate, and the water flow rate will not be affected when individual cooling tower units are put into and out of operation.

A widely used method for mitigating the problems is to install a common equalizer pipe which is connected to all the cooling tower units such that the water levels inside different cooling tower basins will be close to each other at all times (Figure 6.22c). To achieve this, the equalizer pipe must be generously sized, typically with the same diameter as the main return header pipe, such that a small difference in the water level in the cooling tower basins (25mm) will be sufficient to drive water flow through the equalizer pipe to even out the water levels.

Cooling tower manufacturers typically recommend:

- All towers are installed so that their overflow levels are at the same elevation.
- All supply and return piping between towers are symmetrical, which helps ensure balanced flows through each tower.
- Installing valves at the inlet and outlet of each tower for final adjustment of water flow. These valves can also be used as shut-off valves to isolate each tower during maintenance.
- Make certain that the outlet valve is closed when the inlet valve is closed, and have both valves operate simultaneously if they are automatically controlled.
- Installing equalizing pipes with shut-off valves between tower basins in order to ensure the same water levels.

- As differences in water levels may arise due to dirty strainers, changes in valve position, and clogged nozzles, regular maintenance of cooling towers is essential.

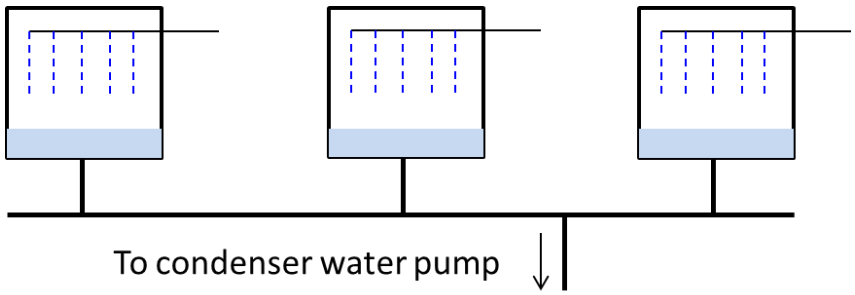

a) Cooling towers installed without measures to ensure balanced flow

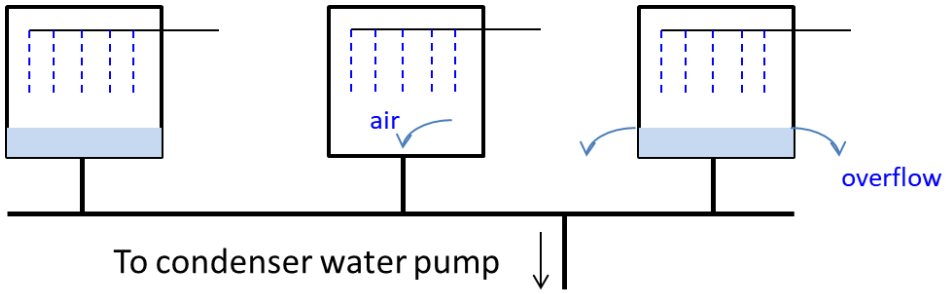

b) Ingress of air and overflow due to unbalanced flow among cooling

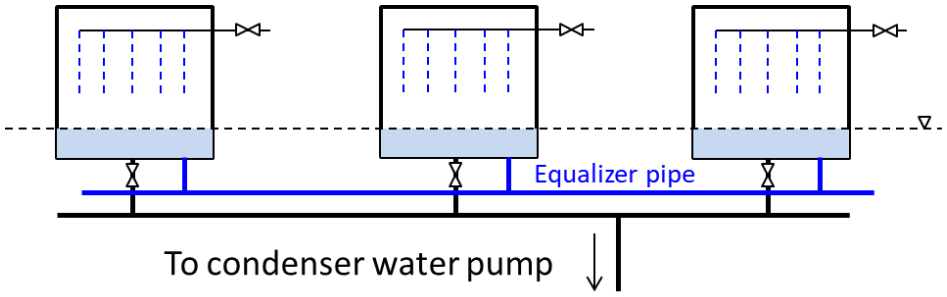

c) Leveling and equalizer pipe for balancing cooling towers and solenoid valves for isolation

Figure 6.23 Flow balance problems and mitigation measures for multiply cooling towers

6.5.4 Cooling tower plume abatement

Under certain operating conditions, instead of an invisible stream of warm moist air, cooling towers may emit visible white plumes (Figure 6.24). Appearance of white plume is undesirable because:

- It can be mistaken as smoke arising from outbreak of fire.

- In case the cooling tower is located on an intermediate floor, it may block the view of upper floors.
- It may increase the risk of spread of legionnaires' disease, or at least perceived to be so.
- It could be taken as substandard performance of the cooling towers.
- If severe enough, it could cause problems to aviation.

Figure 6.24 White plume emitted by cooling towers

White plume emission from a cooling tower is due to the presence of fine water droplets in the discharge air stream, which scatter light and thus making the discharge air steam look like white smoke. The reason behind the appearance of white plume from a cooling tower, and methods for mitigation, are analysed and discussed below.

i) Conditions under which white plume will appear

It has been shown above that the air enthalpy (h_a) inside a cooling tower is a linear function of the water temperature (T_w) (Equation 6.19 and Figure 6.18). It follows that, at the exit plane:

$$h_{a2} = h_{a1} + \frac{m_w C_w}{m_a}(T_{w2} - T_{w1}) \qquad (6.25)$$

Note that the heat rejection rate, Q, is given by:

$$Q = m_w C_w (T_{w2} - T_{w1})$$

$$h_{a2} = h_{a1} + \frac{Q}{m_a} \tag{6.26}$$

This clearly shows that the higher the value of Q and the smaller the value of m_a, the higher the value of h_{a2}.

Given that the air in a cooling tower is in direct contact with the water droplets while heat and moisture exchanges between them take place, the leaving air state can be taken as saturated. For the same heat rejection rate (Q) but with two different entering air states with the same enthalpy value (points 1 & 1' in Figure 6.25), the leaving air state will be the same, as stated in Equation (6.26), but the sensible heat and moisture exchanges between the air and the water will be different.

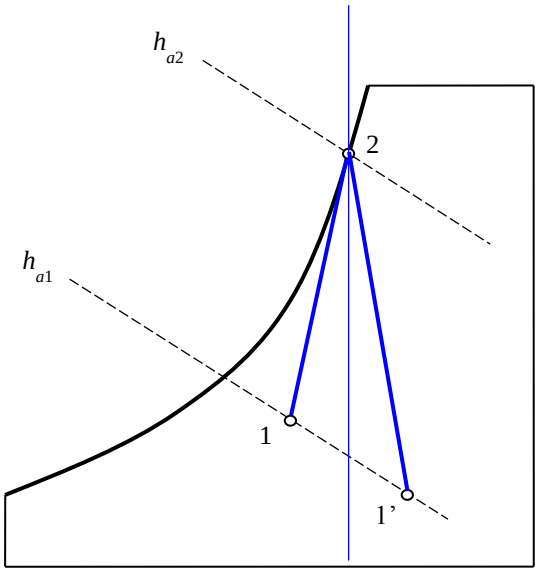

Figure 6.25 Inlet and outlet air states of a cooling tower

The air leaving a cooling tower (at state point 2) will mix with the ambient outdoor air (typically same as that of the air entering the cooling tower, at state point 1 or 1'). On a psychrometric chart, the state point of the mixture of two air streams will lie on a straight-line joining up the states of air in the two air streams, in this case state points 1 & 2 (Figure 6.26a). If the line joining up state points 1 & 2 has a portion of it lying above the saturation curve, the mixture of the air will have a moisture content greater than the maximum amount that the air can hold (Figure 6.26b). The air is said to be supersaturated and the excessive moisture will precipitate out as fine water droplets. If points 1 & 2 in this case are the states of ambient air and the air discharged by a cooling tower, the cooling tower will appear to be emitting a white plume.

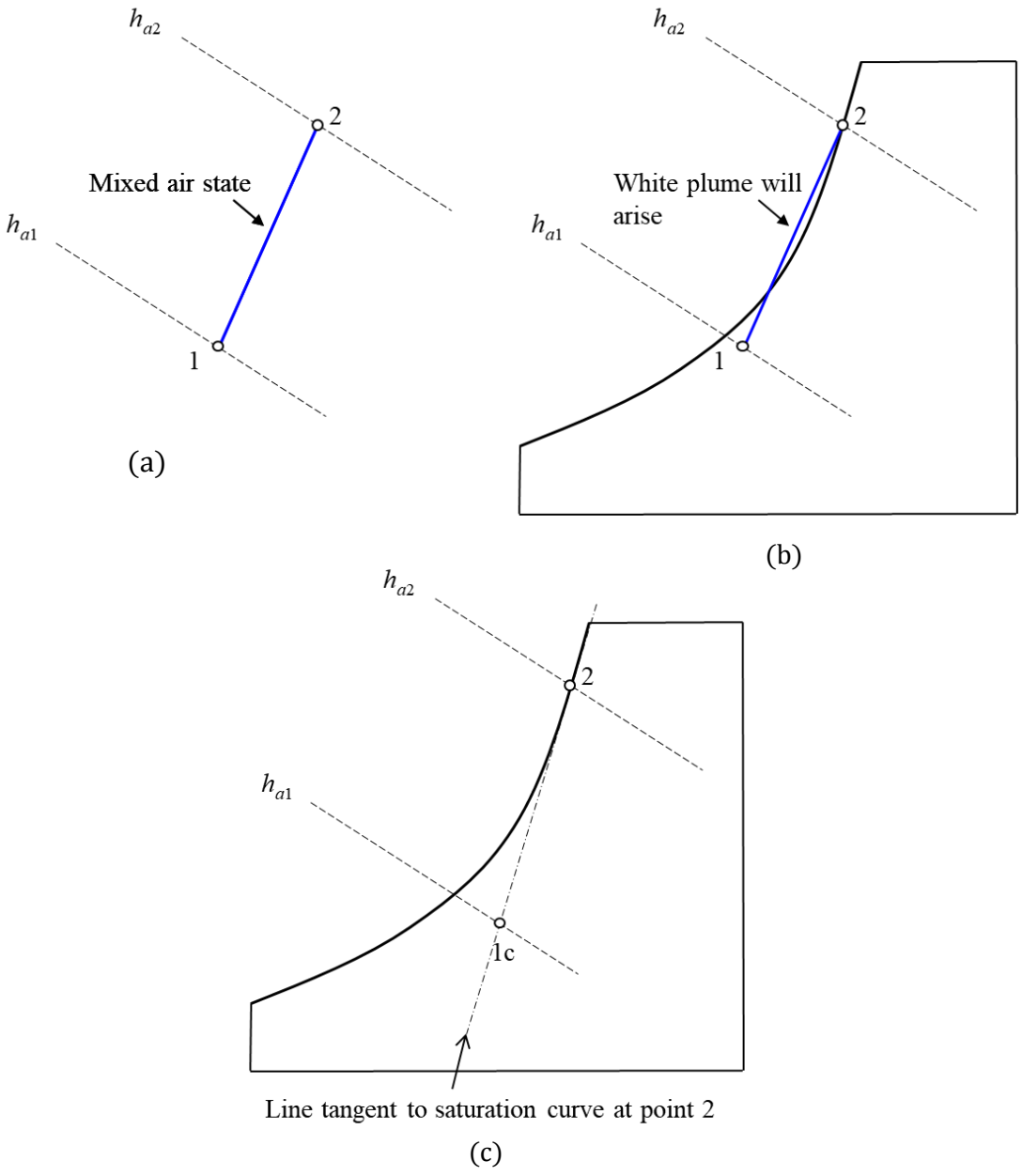

Figure 6.26 (a) State of mixture of air leaving a cooling tower and surrounding outdoor air; (b) mixture state being at a supersaturated state leading to emission of white plume; and (c) marginal case where white plume will not exist

However, as long as the straight line joining up the states of the air entering and leaving a cooling tower does not have any portion of it lying above the saturation curve (e.g. line 1c-2 in Figure 6.26c), no white plume will appear. For a given discharge air state (point 2), the straight line that tangents with the saturation curve at point 2 will not have any point on it that lies above the saturation curve, but there will be for any straight line to its left.

ii) The critical outdoor air state curve

For a cooling tower with a fixed air mass flow rate (m_a) and is handling a given heat rejection rate (Q), the rise in enthalpy of the air from entering to leaving the cooling tower ($h_{a2} - h_{a1}$) is fixed no matter from which state (with the same specific enthalpy) the air enters the cooling tower:

$$Q = m_a(h_{a2} - h_{a1}) \tag{6.27}$$

If point 2 represents the leaving air state, point 1c (Figure 6.26c) will be the critical air entering state; if the air entering state is to its left, white plume will arise, and there will not be white plume if the air entering state is to its right.

By starting from different points along the saturation curve as the leaving air state, the critical entering air state corresponding to each leaving air state can be found from the intersecting point of:

- The straight line that tangents with the saturation curve at the leaving air state in question; and
- The constant enthalpy line corresponding to an enthalpy value that is below that of the air leaving state by the amount corresponding to the given values of m_a and Q (Equation 6.27).

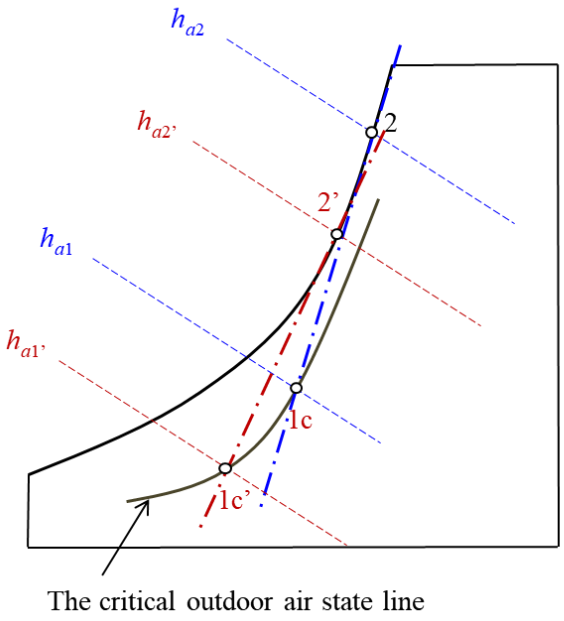

Figure 6.27 Critical outdoor air state curve for white plume control

By joining the critical entering air state points so obtained, a curve that represent the critical outdoor air state can be constructed (Figure 6.27). The critical outdoor air state curve can then be used to check against a particular or a set of outdoor air state(s) to see which outdoor air state would give rise to white plume and which would not.

As can be seen from Equation 6.26, for a given entering air state (point 1 with h_{a1}), the value of h_{a2} will increase (say to h_{a2}* as shown in Figure 6.28) with increase in the heat rejection rate Q or reduction in the air mass flow rate m_a. For the case shown in Figure 6.28, there should not be white plume in the original operating condition with leaving air specific enthalpy being h_{a2}. However, white plume will appear after the heat rejection rate (Q) has been increased or the air mass flow rate (m_a) is reduced. Therefore, besides the entering air state (point 1), Q & m_a, are the key factors that affect whether white plume will arise from a cooling tower.

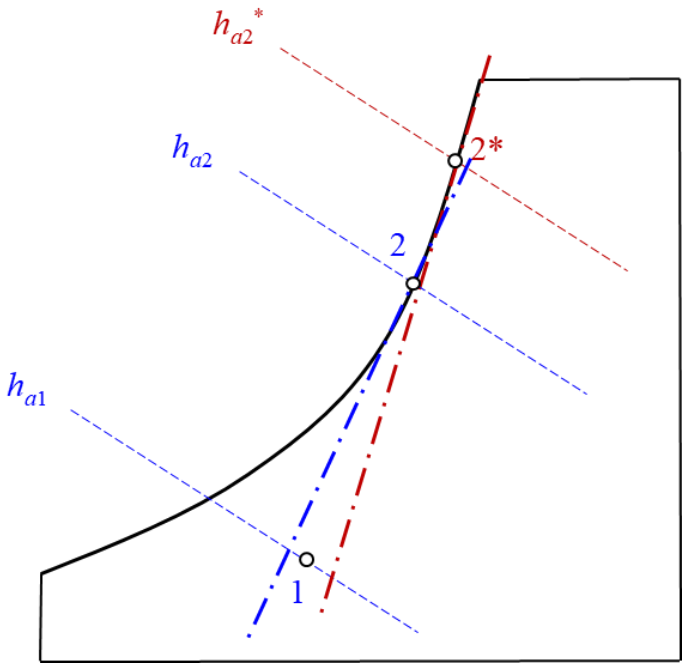

Figure 6.28 Effect of increasing heat rejection rate or reduction in air mass flow rate leading to an increase in the enthalpy difference between the incoming and leaving air of a cooling tower and the risk of white plume emission

Figure 6.29 shows the highly significant impact on the critical outdoor air state curve when the air flow rate is reduced; the lower the air flow rate, the greater the chance that white plume would appear.

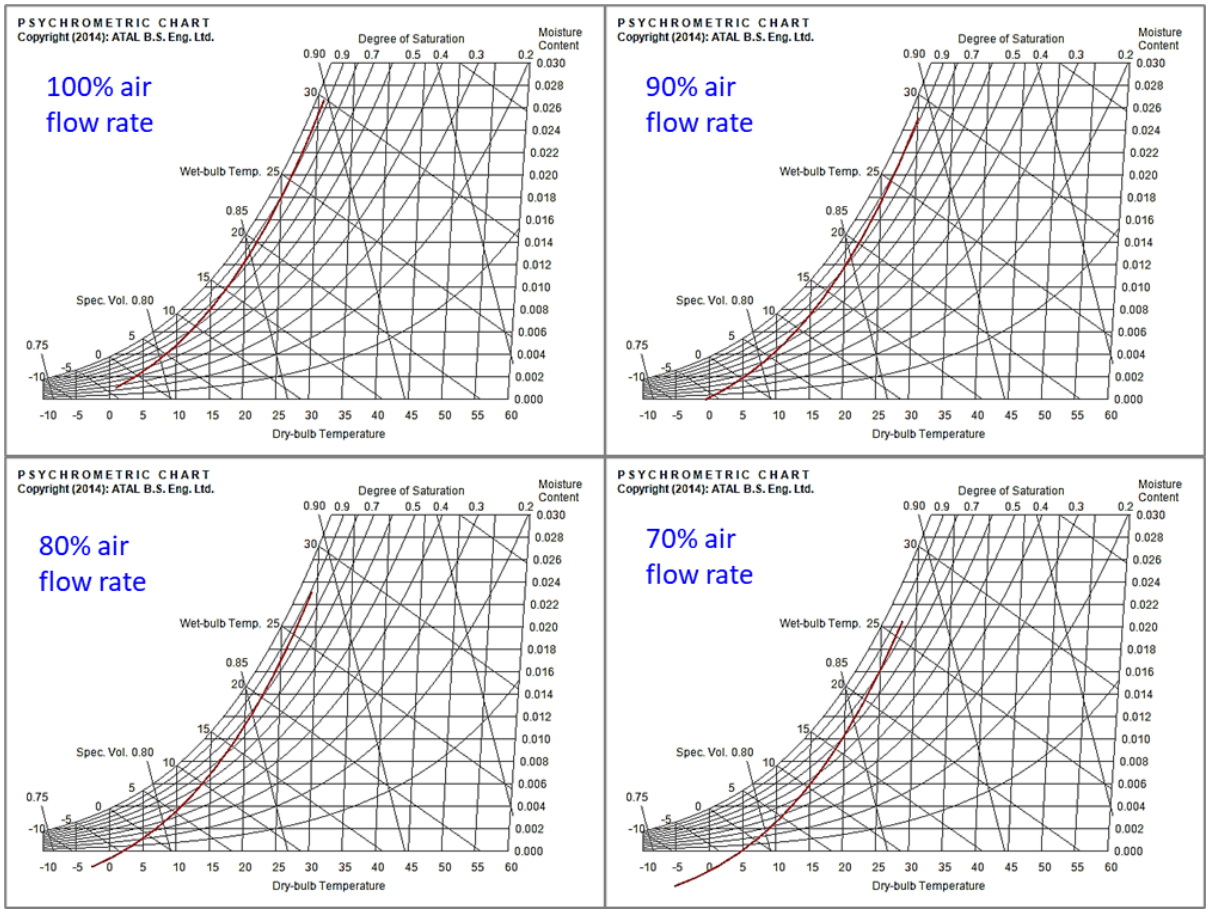

Figure 6.29 Critical outdoor air state curves for 100% load and air flow from 100% to 70%

iii) Plume abatement methods

As discussed above, a cooling tower may emit white plume wherever the outdoor air state is at an unfavourable condition. The outdoor air state, however, is a given condition and is not subject to our control.

When white plume occurs, we may try to eliminate the white plume by:

- Increasing the air flow rate, if possible (as when the fan speed of the cooling tower has been reduced for energy saving; or allowance has been made for running the fan at a speed above the rated condition).

- Operating more cooling towers, if possible (this will have the effect of reducing Q to be handled by each cooling tower but is possible only when there is/are idling cooling tower(s), at the moment white plume arises).

If the above measures are found insufficient, we may minimize occurrence of white plume by installing a heating stage at the exit side of a cooling tower, which may be:

- A water coil with condenser water passing through this coil before being fed to the cooling tower nozzles (Figure 6.30).

- A separate heating coil or heater.

- A gas burner.

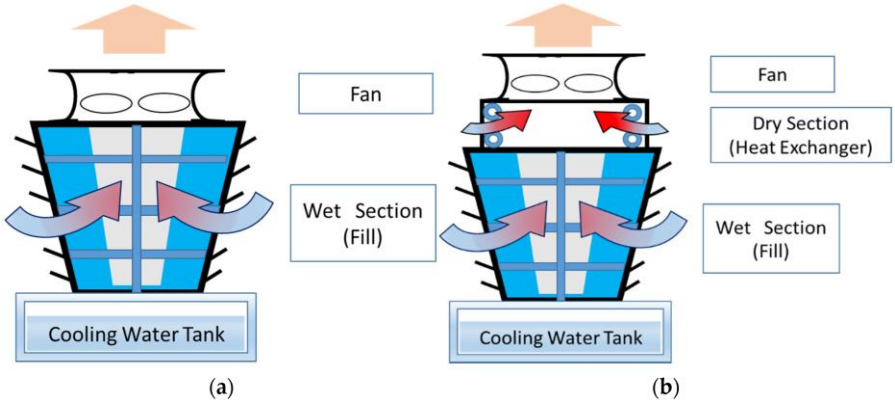

Figure 6.30 Heat exchanger section at exit for elimination of white plume: a) without the heat exchanger; and b) with the heat exchanger

It should be noted that white plume may not be totally eliminated. Impact of occurrence of white plume should be minimized by giving due consideration to cooling tower selection, especially the air flow rate. Installing cooling towers below occupied floors should be avoided if at all possible. Such limits of operation should be clearly conveyed to the client and tenants who may potentially be affected.

6.6 Heat exchangers

6.6.1 Heat exchangers in central air-conditioning systems

As pointed out above, the evaporator and condenser of a chiller are basically heat exchangers (involving a phase changing fluid), which may be shell-and-tube type or finned-coil type heat exchangers. In fact, heating and cooling & dehumidifying coils, cooling towers, air-to-air heat wheels, desiccant dehumidifiers and heat pipes are all heat exchangers. These heat exchangers, however, are not the focus of this section. What we shall examine here are those heat exchanges used for separation of the chilled or condenser water circuit for protection of the chillers from corrosion or excessive pressure, or for enabling supply of chilled water at different temperatures.

Plate-type heat exchangers (Figure 6.10d) can often be found in central air-conditioning installations that utilize seawater for heat rejection, in order that the chillers can work with fresh water rather than the erosive and corrosive seawater (Figure 6.11d). Plate-type heat exchangers are preferred because they are compact in physical size compared to conventional shell-and-tube heat exchangers for the same rate of heat transfer and can provide large heat transfer surfaces such that the required log mean temperature

difference (LMTD, see later discussions) may be as small as 1°C. They are also easier to clean, as they can be conveniently disassembled and re-assembled (Figure 6.31), which is a great advantage to maintenance work.

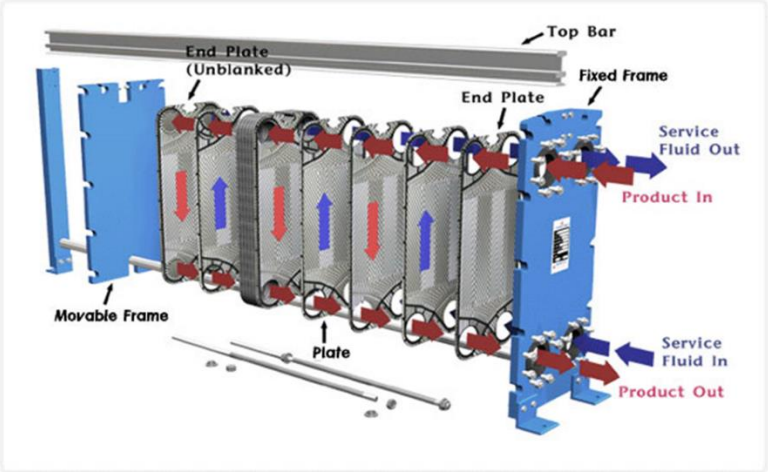

Figure 6.31 Plate-type heat exchanger assembly

In tall buildings, plate-type heat exchangers may also be used as a pressure break (Figure 6.32) such that air-handling equipment serving floors in the high zone can still be supplied with chilled water from a central chiller plant on a floor down below while equipment on lower floors, including the chillers in the central plant, may be subjected to a working pressure much lower than if a system without the pressure break is used. This is especially important to chilled water plants that may utilize seawater for heat rejection, as the use of heat exchangers allows the use of the most efficient chillers to serve the entire building, rather than having to adopt two separate plants for the high and low zone, with the plant serving the high zone comprised of air-cooled chillers or water-cooled chillers in conjunction with cooling towers.

Where different chilled water supply temperatures are needed by the air-side systems, such as chilled ceilings / beams and primary air systems, but only one chiller plant is installed, the chilled water circuit may be split into two circuits through the use of plate-type heat exchangers. The supply chilled water temperature from the chillers can be set to the lower temperature to meet the need of one group of equipment (e.g. the primary air systems) while chilled water at a higher temperature may be obtained through the use of plate-type heat exchangers.

In district cooling systems (DCS), the distribution circuit of the DCS and the chilled water circuits in individual buildings may adopt different chilled water temperatures and may operate at difference working pressures. The different requirements on operating conditions are typically met by using heat exchangers to hydraulically separate the building circuits from the distribution circuit and to facilitate adjustment of chilled water temperature through regulation of flow rates.

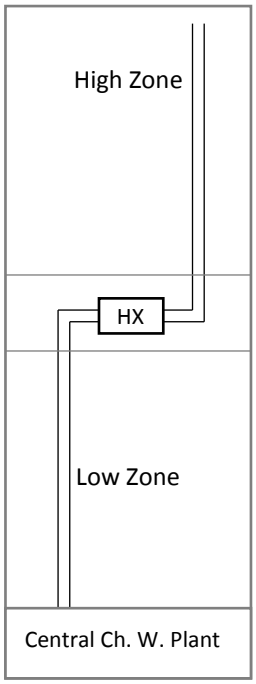

Figure 6.32 Heat exchanger used as a pressure break in a chilled water system serving a tall building

6.6.2 Heat exchanger performance analysis

The analysis below is limited to basic heat exchangers that handle fluids without phase change in the heat exchange process. Depending on the relative flow directions of the two working fluids, heat exchangers may be classified into counter-flow, parallel-flow and cross-flow heat exchangers (Figure 6.33). The counter-flow configuration is preferred due to the better heat transfer performance compared to the other configurations.

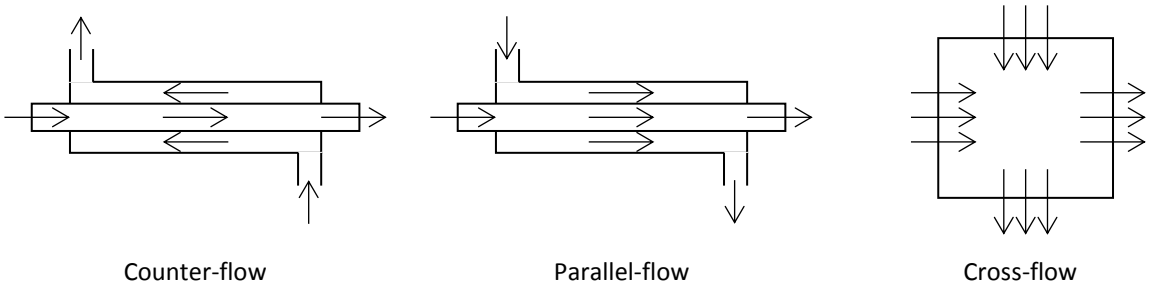

Figure 6.33 Counter-flow, parallel-flow and cross-flow heat exchangers

Consider a single tube, counter-flow heat exchange, with the cross section of the tube as shown in Figure 6.34.

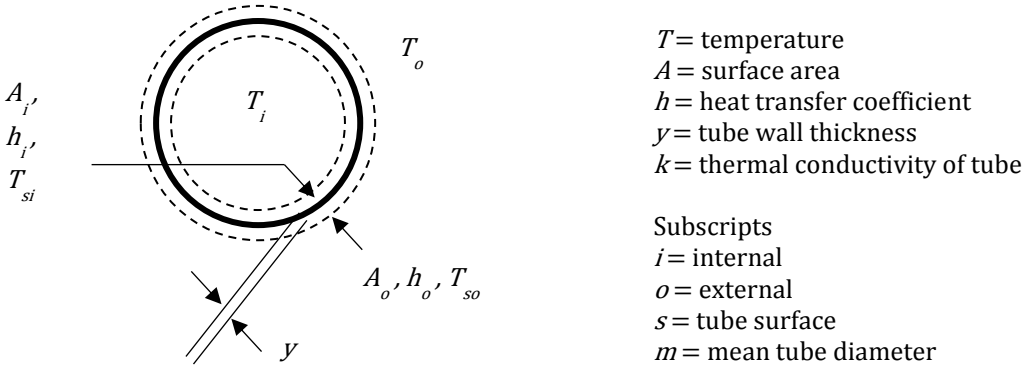

Figure 6.34 Cross-section of a tube in a counter-flow heat exchanger

The heat transfer rate at the internal tube surface, q_i, is given by:

$$q_i = h_i A_i (T_i - T_{si}) \tag{6.28}$$

The heat transfer rate through the tube wall, q_m, is:

$$q_m = kA_m (T_{si} - T_{so})/y \tag{6.29}$$

The heat transfer rate at the external tube surface, q_o, is:

$$q_o = h_o A_o (T_{so} - T_o) \tag{6.30}$$

In the steady state, $q = q_i = q_m = q_o$.

From Equations (6.28) to (6.30),

$$T_i - T_{si} = \frac{q_i}{h_i A_i} \tag{6.31}$$

$$T_{si} - T_{so} = \frac{q_m}{(k/y)A_m} \tag{6.32}$$

$$T_{so} - T_o = \frac{q_o}{h_o A_o} \tag{6.33}$$

Summing up the above equations and using q to denote the heat transfer rate,

$$T_i - T_o = q\left\{\frac{1}{h_i A_i} + \frac{y}{kA_m} + \frac{1}{h_o A_o}\right\}$$

$$T_i - T_o = \frac{q}{A_o}\left\{\frac{1}{h_o} + \frac{yA_o}{kA_m} + \frac{A_o}{h_i A_i}\right\} \tag{6.34}$$

Defining overall heat transfer coefficient, U, as:

$$U = \frac{1}{\frac{1}{h_o}+\frac{yA_o}{kA_m}+\frac{A_o}{h_iA_i}} \tag{6.35}$$

The heat transfer rate through a heat exchanger can be expressed as:

$$q = A_o U(T_i - T_o) \tag{6.36}$$

The area A_o is regarded as the heat transfer area of the heat exchanger.

Under constant mass flow rates of the two fluids, the U value of a heat exchanger may be regarded as a constant. When a heat exchanger has been in use for some time, fouling will occur upon both the inner and outer surfaces of the tubes, due to deposition of minerals and dirt contained in the water. Fouling, once present, will increase the thermal resistance leading to degradation of the heat transfer performance of the heat exchanger. Since fouling is inevitable, allowance is made in design of heat exchangers by including the additional thermal resistances that will arise due to fouling (denoted by R_i and R_o for fouling resistances at both sides) in determining the U-value.

The expression for the U-value, with the fouling resistances included, is as follows:

$$U = 1/\left(\frac{1}{h_o} + R_o + \frac{yA_o}{kA_m} + \frac{A_o}{h_iA_i} + R_i\frac{A_o}{A_i}\right) \tag{6.37}$$

Equation (6.36), however, applies only to a special condition where the temperature difference between the two working fluids in a heat exchanger stays at a constant level of ($T_i - T_o$). This condition, however, is valid only when the same kind of fluid is used both as the hot and the cold fluids, and the mass flow rates of the two are identical. We, therefore, need a more general model for estimation of heat exchanger performance to cater for different kinds of fluid at the two sides of a heat exchanger, and the fluids may flow through the heat exchanger at different flow rates.

Here, our focus is put on the counter-flow heat exchanger model as shown in Figure 6.35. In this model, the two working fluids are denoted as the hot fluid, which is at higher temperatures, and the cold fluid, which is at lower temperatures. At every cross-section of the heat exchanger, heat transfer takes place from the hot fluid through the tube wall to the cold fluid. As a result, the hot fluid temperature will drop while the cold fluid temperature will rise as they flow through the heat exchanger steadily in opposite directions.

With respect to each working fluid, we can write:

$$Q = m_h C_h(T_{h1} - T_{h2}) \tag{6.38}$$

$$Q = m_c C_c(T_{c1} - T_{c2}) \tag{6.39}$$

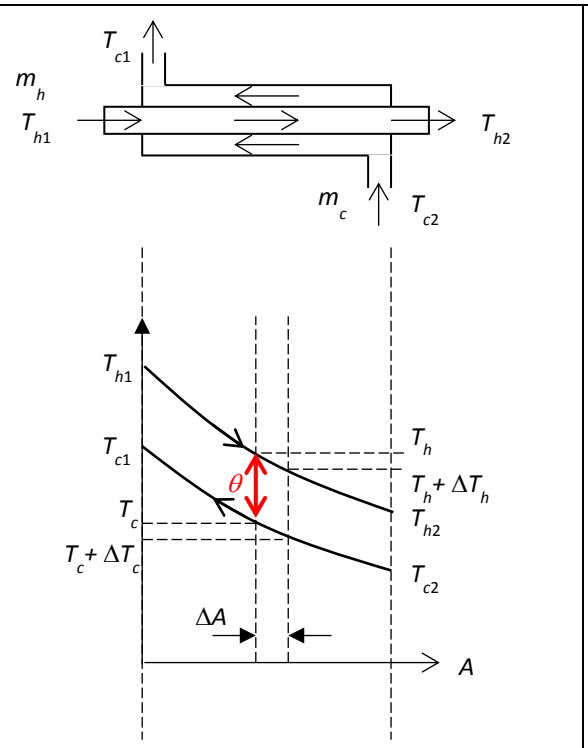

Legend

T_h & T_c = the temperatures of the hot and cold fluids

m_h & m_c = the mass flow rates of the hot and cold fluids

C_h & C_c = the specific heat of the hot and cold fluids

A = the overall heat transfer area of the heat exchanger

U = the overall heat transfer coefficient of the heat exchanger

Q = the overall heat exchange rate between the hot and cold fluids

Figure 6.35 Temperature distribution of the working fluids in a counter-flow heat exchanger

Over an elemental section of the heat exchanger (ΔA) (Figure 6.35),

$$\Delta Q = -m_h C_h \Delta T_h \tag{6.40}$$

$$\Delta Q = -m_c C_c \Delta T_c \tag{6.41}$$

As a result of the definition of Q in Equations (6.38) & (6.39), both equations above have a negative sign at their right-hand side.

The heat loss of the hot fluid and the heat gain of the cold fluid in the elemental section are equal, and each equals the heat transfer from the hot to the cold fluid, given by:

$$\Delta Q = U(T_h - T_c)\Delta A \tag{6.42}$$

Further, let (Figure 6.35):

$$\theta = T_h - T_c \tag{6.43}$$

Then,

$$\Delta\theta = \Delta T_h - \Delta T_c$$

From Equations (6.40) & (6.41),

$$\Delta\theta = -\Delta Q\left\{\frac{1}{m_h C_h} - \frac{1}{m_c C_c}\right\} \tag{6.44}$$

Let,

$$M_c = \frac{1}{1/(m_h C_h) - 1/(m_c C_c)} \tag{6.45}$$

Equation (6.44) can be re-written as:

$$\Delta Q = -M_c \Delta\theta \tag{6.46}$$

Equating the right-hand sides of Equations (6.42) & (6.46), also using Equation (6.43),

$$-M_c \Delta\theta = U\theta\Delta A$$

$$-M_c \frac{\Delta\theta}{\theta} = U\Delta A$$

$$-M_c \int_{\theta_1}^{\theta_2} \frac{d\theta}{\theta} = U \int_0^A dA$$

$$M_c \ln\left(\frac{\theta_1}{\theta_2}\right) = UA \tag{6.47}$$

Returning to Equations (6.38) and (6.39), we can write:

$$Q\left\{\frac{1}{m_h C_h} - \frac{1}{m_c C_c}\right\} = (T_{h1} - T_{h2}) - (T_{c1} - T_{c2})$$

Therefore,

$$M_c = \frac{1}{1/(m_h C_h) - 1/(m_c C_c)} = \frac{Q}{(T_{h1} - T_{h2}) - (T_{c1} - T_{c2})} \tag{6.48}$$

Substituting Equation (6.48) into (6.47),

$$\frac{Q}{(T_{h1} - T_{h2}) - (T_{c1} - T_{c2})} \ln\left(\frac{\theta_1}{\theta_2}\right) = UA$$

Rearranging, we get:

$$Q = AU \cdot \frac{(T_{h1} - T_{h2}) - (T_{c1} - T_{c2})}{\ln\left(\frac{\theta_1}{\theta_2}\right)}$$

Further rearranging the terms at the numerator of the fractional term,

$$Q = AU \cdot \frac{(T_{h1} - T_{c1}) - (T_{h2} - T_{c2})}{\ln\left(\frac{T_{h1} - T_{c1}}{T_{h2} - T_{c2}}\right)} \tag{6.49}$$

Defining log mean temperature difference (*LMTD*) as:

$$LMTD = \frac{(T_{h1} - T_{c1}) - (T_{h2} - T_{c2})}{\ln\left(\frac{T_{h1} - T_{c1}}{T_{h2} - T_{c2}}\right)} \tag{6.50}$$

We get

$$Q = AU \cdot LMTD \tag{6.51}$$

It can be seen from Equation (6.50) that the $LMTD$ of a heat exchange cannot be evaluated using this equation if:

$$(T_{h1} - T_{c1}) = (T_{h2} - T_{c2}) \text{ or } \theta_1 = \theta_2$$

However, using the L' Hospital's rule, the LMTD in this case is given by:

$$LMTD = \lim_{\theta_1 \to \theta_2} \left\{ \frac{\theta_1 - \theta_2}{\ln(\frac{\theta_1}{\theta_2})} \right\} = \lim_{\theta_1 \to \theta_2} \left\{ \frac{1}{\frac{\theta_2}{\theta_1} \cdot \frac{1}{\theta_2}} \right\} = \theta_1 \tag{6.52}$$

Equation (6.51) above is call a Log Mean Temperature Difference (LMTD) model for a heat exchanger. The LMTD model, however, is an implicit model, as it requires the entering and leaving temperatures of both working fluids to be known before the heat transfer rate can be determined. However, if all the four temperatures are already known, we can calculate the heat transfer rate right away from the heat gain or loss of either fluid. Use of the LMTD model, therefore, involves the use of an iterative procedure.

An alternative approach, which is called the effectiveness-number of transfer units (ε-NTU) method / model, allows the heat transfer rate to be determined in an explicit manner.

The definition of the effectiveness (ε) and NTU are as follows:

$$\varepsilon = \frac{Q}{Q_{max}} \tag{6.53}$$

$$Q_{max} = (mC)_{min}(T_{h1} - T_{c2}) \tag{6.54}$$

$$(mC)_{min} = \begin{cases} m_h C_h \text{ if } m_h C_h < m_c C_c \\ m_c C_c \text{ if } m_c C_c < m_h C_h \end{cases} \tag{6.55}$$

$$NTU = \frac{AU}{(mC)_{min}} \tag{6.56}$$

For a counter-flow heat exchanger:

$$\varepsilon = \frac{1 - \exp\left\{-NTU\left[1 - \frac{(mC)_{min}}{(mC)_{max}}\right]\right\}}{1 - \frac{(mC)_{min}}{(mC)_{max}} \exp\left\{-NTU\left[1 - \frac{(mC)_{min}}{(mC)_{max}}\right]\right\}} \tag{6.57}$$

References

[1] ASHRAE Handbook Fundamentals, American Society of Heating, Refrigerating and Air-conditioning Engineers, Inc., 2017.

[2] ASHRAE Handbook Refrigeration, American Society of Heating, Refrigerating and Air-conditioning Engineers, Inc., 2019.

[3] ASHRAE Handbook HVAC Systems and Equipment, American Society of Heating, Refrigerating and Air-conditioning Engineers, Inc., 2020.

[4] Stoeker, W.F., Jones, J.W., Refrigeration and Air Conditioning, 2nd Ed., McGraw-Hill, 1982.

[5] Wang S. K., Handbook of Air Conditioning and Refrigeration, 2nd Ed., McGraw Hill, 2001.

[6] Code of Practice for Energy Efficiency of Building Services Installation, Electrical and Mechanical Services Department, Government of the Hong Kong SAR, 2018.

[7] Threlkeld J. L., Thermal Environmental Engineering, 2nd Ed., Prentice-Hall, Englewood Cliffs, 1970.

[8] McQuiston F. C., Parker J. D., and Spitler J. D., Heating, Ventilating and Air Conditioning Analysis and Design, 5th Ed., John Wiley & Sons, Inc.

[9] Code of Practice for Water-cooled Air Conditioning Systems, Parts 1-3, Electrical and Mechanical Services Department, Government of the Hong Kong SAR, 2006.

Chapter 7 Water-side Systems and Control

As mentioned in the preceding chapter, the chilled water in a central air-conditioning system is the medium for transport of the heat extracted by the air-handling equipment from the air-conditioned spaces to the chillers in the central plant. After the chilled water has been cooled down by the chillers, it will be distributed to the air-handling equipment again for another cycle of heat transport. A piping network provides the flow channels for the chilled water to flow back and forth between the air-handling equipment and the chillers. With power input to their motors, the chilled water pumps will raise the pressure of the chilled water they discharge to a high enough level for overcoming the pressure losses incurred as the water flows through the pipes and fittings in the piping network, and through the chillers and air-handling equipment, until the water returns to the pumps.

The above is just a grossly simplified picture of the chilled water distribution system in a central air-conditioning system. The circuit design of the chilled water distribution system may vary from one building to another to meet the characteristics of individual buildings, such as building geometric configuration and occupation characteristics, load intensity and distribution, etc., and cost considerations. In the first part of this chapter, the most widely adopted types of chilled water pumping system are described and discussed in detail, especially their operating principles and characteristics, which will provide a reference for designers to choose a system design that suits best any project they handle. Annex 7A describes the modifications that can be made to the circuit designs of the chilled water pumping systems to facilitate performance measurement of chillers.

The chilled water pipework is assembled piece-by-piece manually on site, typically by welding or tightening them together using screwed sockets or flanges in conjunction with bolts & nuts. Therefore, testing is needed before they are put into operation to ensure no water leakage which will be disastrous if it does happen. Furthermore, we should ensure the chilled water can be properly distributed to individual branches and individual air-handling equipment to meet their flow demand, which would not happen without fine tuning due to the differences in the pressure drops incurred by the pipes, fittings and equipment in different flow circuits. If the adjustment work is not done, the imbalance in flow rates will become a burden on the control valves at the air-side systems, which may overburden some control valves leading to poor control performance.

Therefore, leakage test and flow balancing are essential parts of commissioning work that should be done properly before a new installation would be accepted and put into normal operation. Although the level of details and scope of coverage are far from sufficient to enable one to become a commissioning specialist, the methods for leakage test and flow balancing are covered in the second part of this chapter to draw the attention of system designers to such works while they do their designs and write the specifications, and of operation and maintenance (O&M) personnel in their routine maintenance, and addition and alteration (A&A) works.

7.1 Single-loop pumping system with differential pressure bypass control

The chilled water system shown schematically in Figure 7.1 is a single-loop pumping system, which is widely adopted in small to medium size buildings. In this system, there is only one group of chilled water pumps, which are constant speed pumps operating in parallel with each other. The air-handling equipment are equipped with two-way (two-port) control valves for regulation of the chilled water flow rate through the cooling coils in the respective air-handling equipment so as to adjust the cooling output of the equipment.

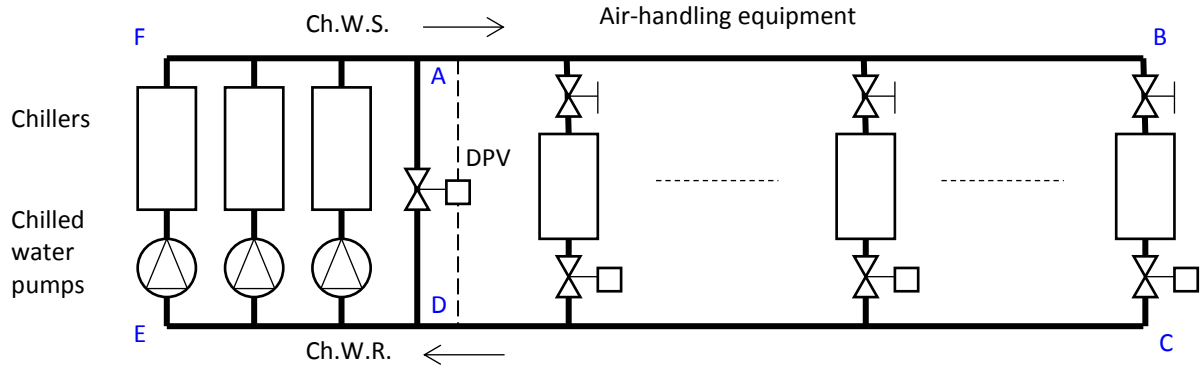

Figure 7.1 A single-loop chilled water pumping system

Two-way control valve refers to the type of control valve that has one ingress port and one egress port for water to flow into and out of the valve and, in between, through the adjustable gap between the valve plug and the valve seat inside the control valve (see Figure 7.2 and later discussions on control valves). Varying the plug position, and thus the area of the gap for water flow inside the control valve, will change the flow rate of chilled water and, in turn, the cooling output of an air-handling equipment.

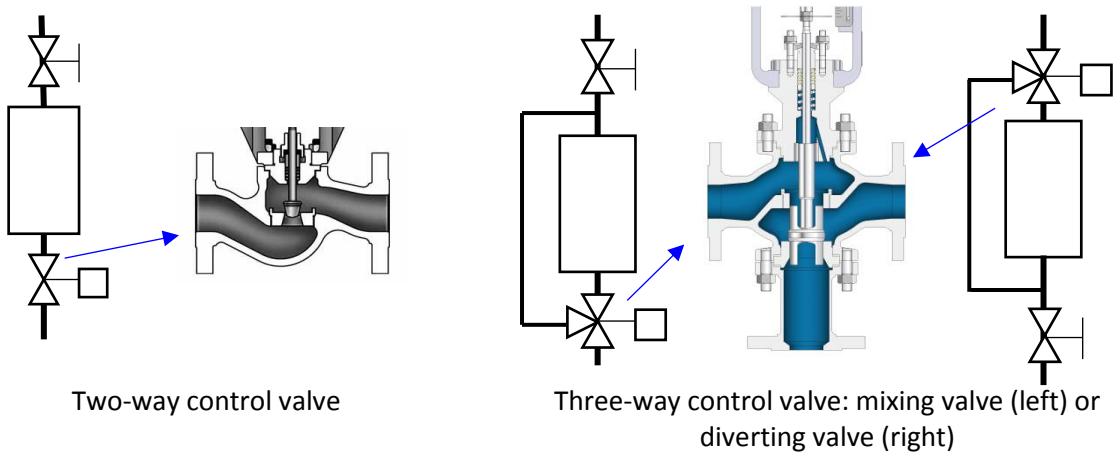

Figure 7.2 Two-way and three-way control valves

Three-way control valves (Figure 7.2) are another type of control valve that may be used for water flow regulation. In a three-way valve, there may be one ingress and two egress ports, in which case it is a diverging valve, or two ingress and one egress ports if it is a converging or mixing valve. Obviously, a three-way valve is more costly than a two-way valve of the same flow capacity due to its more complex design.

Until recently (see later discussions on variable primary flow (VPF) systems), a basic design requirement for chilled water pumping systems is to make sure the chilled water flow rates through individual operating chillers will be maintained steadily at their respective design flow rates. Besides ensuring no deterioration in heat transfer performance of the evaporator under variable load condition, fulfilling this 'constant flow' requirement allows the use of a single measurement, viz. the chilled water supply or return temperature, for chiller output control.

For the system shown in Figure 7.1, consequent upon the use of two-way control valves, the total chilled water flow rate demanded by the air-handling equipment will vary with the cooling load on the equipment. For ensuring each running chiller will have 'constant flow', a differential pressure bypass pipe and, at a suitable point along the bypass pipe, a differential pressure control valve (DPV) have to be installed. The degree of opening of the DPV, and hence the chilled water flow rate through the bypass pipe, will be regulated under the dictate of a differential pressure transmitter that measures the pressure difference across the main supply and return pipes of the system (ΔP_{SR}), e.g. between points A & D shown in Figure 7.1.

When the two-way control valves at the air-handling equipment are being closed for reducing the chilled water flow rates through them, the increase in flow resistance through the control valves will cause the pumping pressure discharged by the constant speed pump(s), ΔP_{SR}, to rise. In response, the DPV will start to open allowing the surplus flow rate to flow through the bypass pipe until ΔP_{SR} returns to the set point level (ΔP_{SRSP}). The DPV will close to reduce the bypass flow if ΔP_{SR} drops instead, until ΔP_{SR} rises back to ΔP_{SRSP} or the DPV is fully closed.

By regulating the bypass flow rate, ΔP_{SR} can be controlled at a nearly constant level (ΔP_{SRSP}), which will also keep the pumping pressure delivered by the chilled water pumps at a nearly constant level. As the chilled water pumps are constant speed pumps, the pumping pressure and flow rate have a fixed relationship, as expressed by the pump curve. Hence, once the pumping pressure is kept nearly constant, so will be the flow rate. As a result, each running chiller would have the chilled water flow rate through its evaporator maintained at a nearly constant level.

The above discussion highlights the key functions served by the differential pressure bypass control system in the single-loop pumping system shown in Figure 7.1: it allows the objective of maintaining constant flows for the chillers while at the same time allows the air-side systems to use two-way valves to adjust cooling output by varying their chilled water flow rates. This will be an economically viable design as long as the cost of the differential pressure bypass control system is lower than the overall cost saving due to using two-way valves in lieu of three-way valves. See also later discussions on the limitations of using three-way valves to ensure constant flows through chillers.

To take the subject a step further, let us analyse in greater detail the operation of the single-loop pumping system with differential pressure bypass control and two-way control valves at air-side systems. Consider first the parallel operation of the chilled water pumps. Assuming the pressure losses due to water flow in the header pipes between points F-A and D-E (Figure 7.1) are negligible, the differential pressures across the parallel chiller branches, each including a chiller and its dedicated pump, are equal. We can construct the combined pressure-flow (P-V) characteristic curve for the chiller branches by first deducting the pressure drop incurred by water flow through a branch, including the chiller, and the pipe and fittings in the branch, from the P-V curve of the pump, as shown in Figure 7.3. The resulting curve may also be called a 'net pump characteristic curve'.

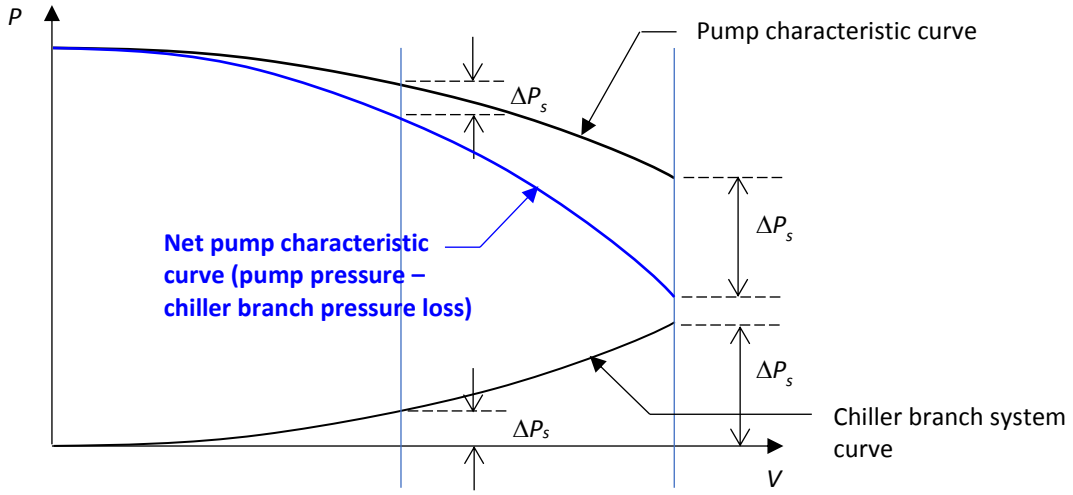

Figure 7.3 Net pump characteristic curve for a pump in a chiller branch

The net pump characteristic curves of the pumps in the system (which may or may not be identical depending on the design of the system under concern) can be combined by summing up the flow rates of all operating pumps at each of a range of pressures along the curves to yield a combined net pump characteristic curve for the system, as shown in Figure 7.4. The operating point of the single-loop pumping system (Figure 7.1) can then be determined, which is the intersection of the combined net pump characteristic curve and the system pressure loss curve (with chiller branch loss discounted).

With the bypass pipe and the differential pressure bypass control system in place, the pumps in a single-loop pumping system may be taken as operating against a special system which comprises two branches in parallel (denoted as the A-B-C-D branch and the A-D branch in Figure 7.1). This special system has the characteristic that it would always incur a constant pressure drop that equals the set-point of the differential pressure bypass control (ΔP_{SRSP}) and, because the pumps are all constant speed pumps, the total flow rate through the two branches, and the pumps (V_{Pump}), is also kept constant by the differential pressure bypass control (Figure 7.5).

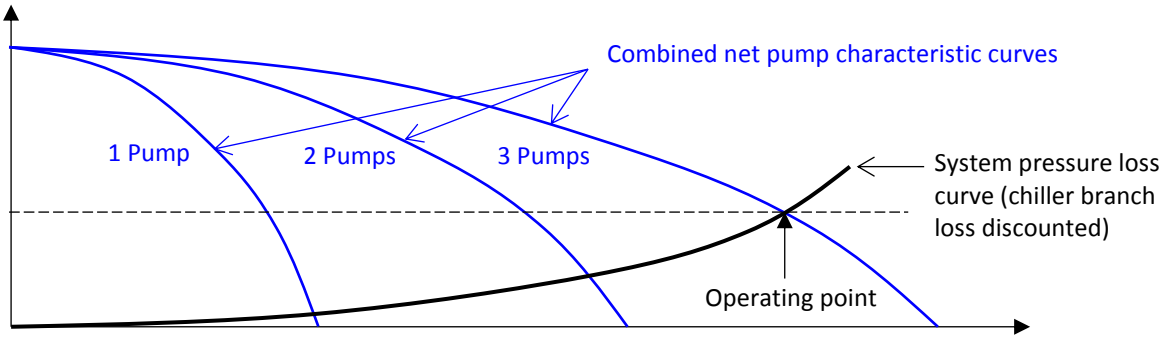

Figure 7.4 Combined net pump characteristic curve

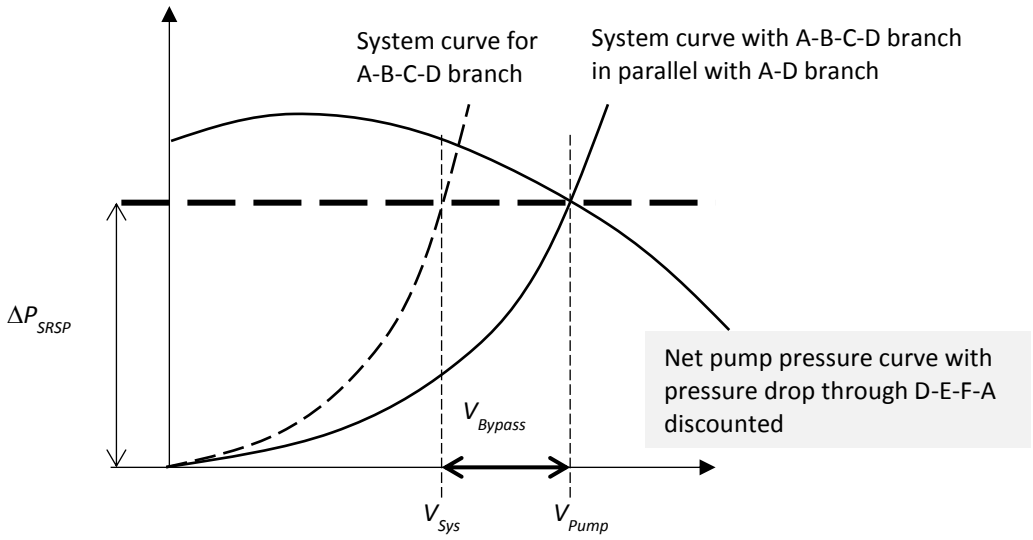

Figure 7.5 Pump and system curves for a single-loop pumping system with differential pressure bypass control under part-load (A, B, ..., F are points in the piping system as shown in Figure 7.1)

However, as far as the distribution circuit connected to the air-side equipment is concerned (the A-B-C-D branch), its system curve will be shifted upward when the control valves of the air-side equipment close to reduce output. If the flow rate through the distribution circuit is V_{Sys}, the bypass flow rate will then be V_{Bypass}, which equals the difference between V_{Pump} and V_{Sys} (Figure 7.5), and V_{Pump} ($= V_{Bypass} + V_{Sys}$) is a constant for each operating condition involving the same number of running chillers and chilled water pumps. Since the flow rate and pumping pressure are held constant, the power demand of each operating chilled water pump will remain the same regardless of the cooling load on its associated chiller. The overall chilled water flow rate in the system will only change in steps according to the total number of chiller/pump groups being put into operation.

Since there is only one group of pumps operating in parallel in the system, the pumping pressure of each pump in a single-loop pumping system has to be sufficient to overcome the total pressure drop round the entire chilled water piping system. The constant flow

characteristic of this system, which is the key reason for using this circuit design, means that each pump will draw the same power whenever it is operating. For larger chilled water systems, the pumping energy use becomes substantial and ways to lower this energy use should be explored, including use of another circuit design.

7.2 Single-loop pumping system with three-way control valves

If the air-handling equipment in a central air-conditioning system are equipped with three-way control valves, the control valve will moderate the chilled water flow rate passing through and bypassing the cooling coil of each air-handling equipment (Figure 7.2) while the air-side control system modulates the cooling output of the equipment. In selection of three-way control valves, a key consideration is to select valves that will provide a relatively stable total flow rate through the two paths over the entire range of the valve plug position (Figure 7.6). This helps ensure the total chilled water flow rate in the system will not vary by a large extent under various load conditions [1] and, therefore, there is no need for differential pressure bypass control. In small systems, the saving of omitting the differential pressure bypass control system may be more than the increase in cost of using three-way valves in lieu of two-way valves.

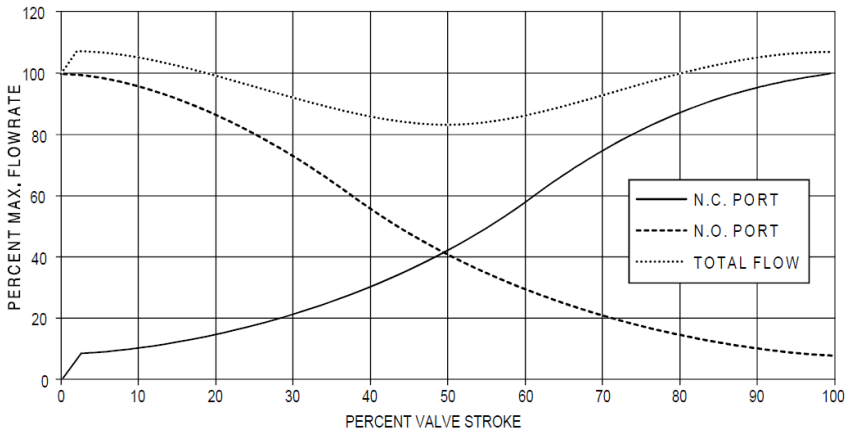

Figure 7.6 Total flow rate through a three-way bypass valve under installed conditions [1]

However, if there are multiple chillers and chilled water pumps in the chilled water system, there will be a serious limitation in operational control of the chillers and chilled water pumps when three-way control valves are installed for the air-handling equipment, as in the case of the system shown in Figure 7.7. The ability of the three-way valve in maintaining a relatively constant total flow rate through the two paths in the air-handling equipment branch implies that the flow resistance of each branch will be kept more or less constant. The same system P-V curve, therefore, can cover both full and part load operations of the system (Figure 7.7).

Under operating conditions where the load on the system has dropped by an extent that one of the chillers and chilled water pumps may be switched-off, when this is done, the total flow rate in the system will drop by a step as shown in Figure 7.7. The reduction in

chilled water flow rate, however, will be evenly shared among all the air-side equipment branches. Therefore, the system operation can still meet with the load provide only that the loads on the air-side systems will all rise and fall by the same proportion. If this is not the case, all chillers and pumps will have to be run to ensure any branch will be able to output the maximum cooling capacity whenever the need arises, but this would mean the chiller plant would be run at low energy efficiency, which is undesirable. Due to this limitation, this system design is only suitable for small buildings with only one or two chillers and a small number of air-handling systems.

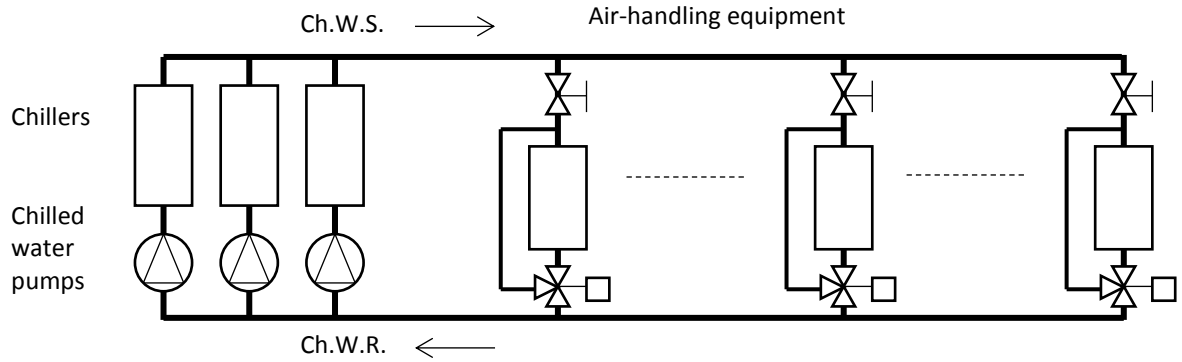

a) Schematic diagram

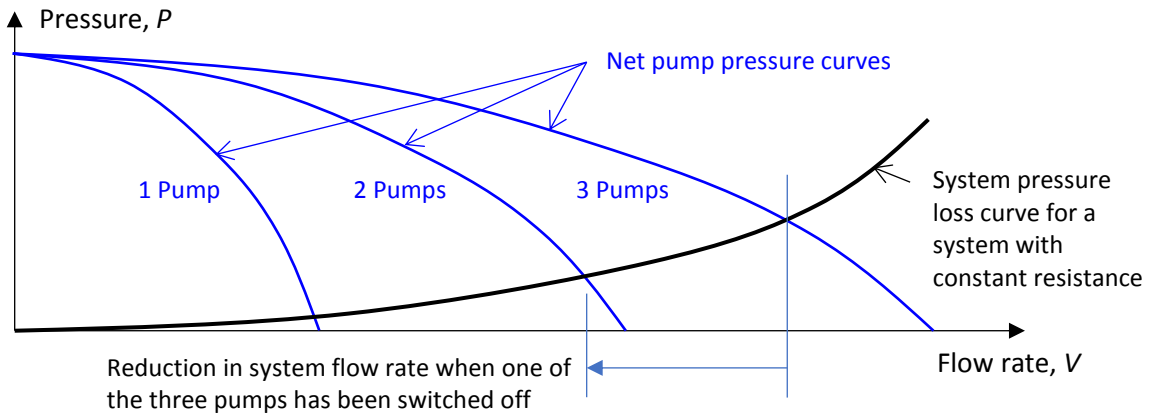

b) Pump and system curves

Figure 7.7 Single-loop pumping system with 3-way control valves

7.3 Two-loop pumping system

For a large size building development, a two-loop chilled water pumping system is preferable to a single-loop pumping system for its energy saving potential under part-load operations. As shown in Figure 7.8a, a two-loop pumping system comprises two circulation loops, referred to as the primary loop (with the chillers in the loop) and the secondary loop (with the air-handling equipment in the loop). There is a bypass pipe linking up the main supply and return pipes (between points A & B in Figure 7.8a) which is a common part of, and the inter-connection between, the two loops.

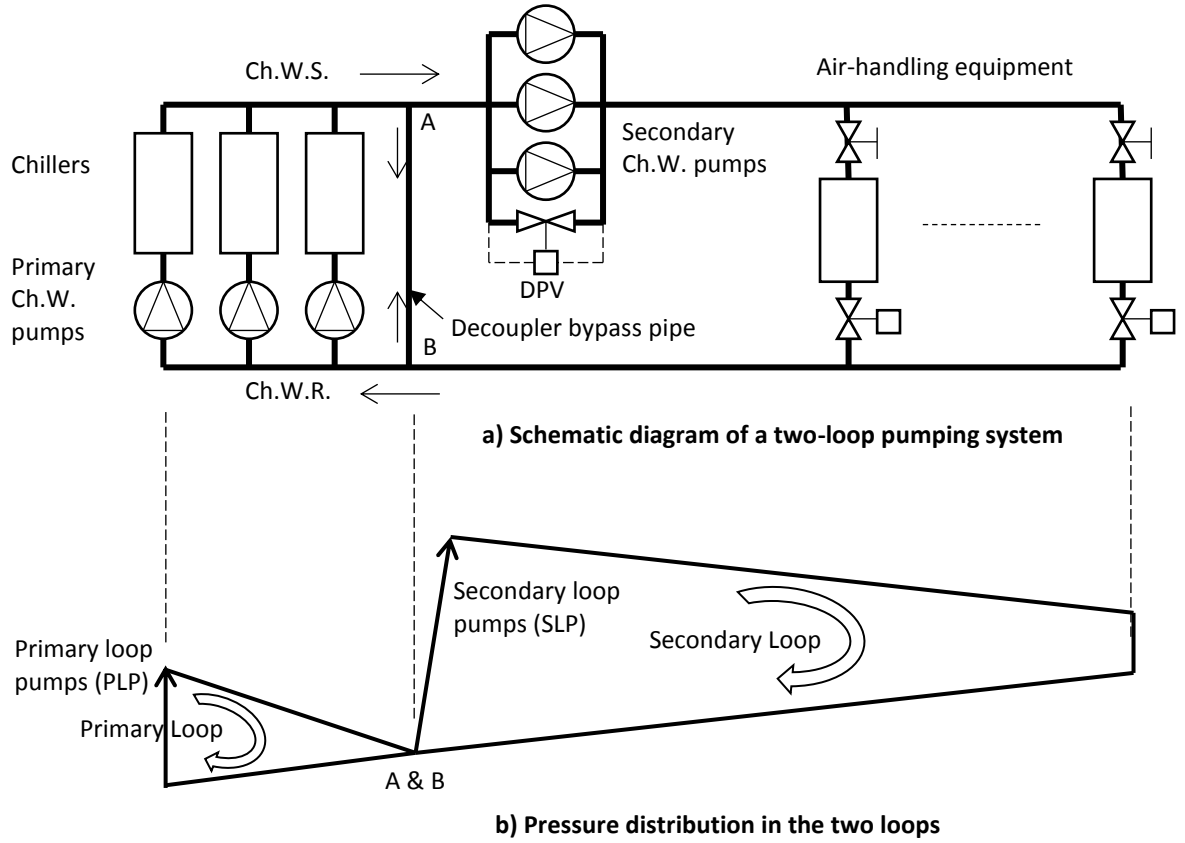

Figure 7.8 Two-loop chilled water pumping system

The bypass pipe plays a crucial role in the two-loop chilled water pumping system in that it hydraulically decouples the two loops. The effect of hydraulic decoupling of the two loops is that any variation in the flow rate in one loop will not affect the flow rate in the other loop. Hydraulic decoupling will arise if the pressure drop across the bypass pipe is minimal, which can be achieved by using a generously sized pipe for the bypass pipe, e.g. at least one standard pipe size above what is required to handle the expected peak flow rate through the pipe. Since the two loops are hydraulically decoupled, there must be a group of pumps for circulating chilled water round each loop.

The reason behind the hydraulic decoupling effect can be more clearly seen from the pressure-distance diagram of the system as shown in Figure 7.8b, which is a plot of the pressure distribution along the flow paths in the two-loop pumping system. Since there is minimal pressure difference across the decoupler bypass pipe (between points A & B in Figure 7.8a), the pressures at these two points are nearly equal and, therefore, they merge into one point when shown in the pressure-distance diagram. Note should be taken that in plotting the pressure-distance diagram (Figure 7.8b), the pressure drop from point A to the suction header of the secondary-loop pumps had been ignored.

With the pressure drop across the decoupler bypass pipe staying at minimal level irrespective of the flow rate it passes, the pressure losses to be overcome by the primary-loop chilled water pumps are limited to those losses incurred by water flow

round the primary-loop (Figure 7.8b), which applies to all possible flow rates round the loop corresponding to various patterns of operation of the chillers and primary-loop pumps. Since the pressure loss across a chiller branch is the dominant pressure loss in the primary-loop, and the branches are in parallel, with the use of constant speed pumps for the primary-loop pumps, each chiller would be fed with a fairly constant flow rate and variation in this flow rate due to changes in number of chillers and primary-loop pumps being run would be small. This characteristics of the primary-loop in a two-loop pumping system, therefore, satisfies the need to ensure constant flows for the chillers.

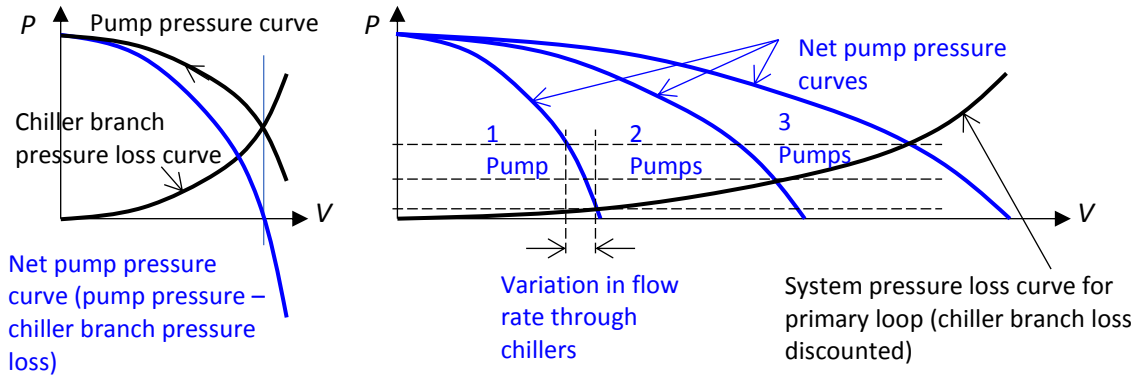

Figure 7.9 Variation in flow rate through a chiller in the primary-loop of a two-loop pumping system

Figure 7.9 shows an analysis of the possible variation in chilled water flow rate through each pump, and chiller, in a system with three identical groups of chiller and primary-loop-pump as shown in Figure 7.8a. As this analysis shows, the flatter the system pressure loss curve, i.e. the smaller the pressure loss of the pipes in the primary-loop (with the pressure loss of the chiller branches discounted), and the steeper the pumping curve nearby the region of the design operating point, the smaller this flow variation.

As shown in Figure 7.8b, the pressure distribution round the secondary-loop forms a loop that is anchored at the point representing the pressure at the decoupler bypass pipe. This means that any change in pressure at the anchor point would have the same effect on all locations in the secondary-loop, i.e. their pressures would rise and drop together by the same amount. Other than this, it would have no effect on the pressures in the secondary-loop, including the pressure drop to be overcome by the secondary-loop pumps; their pumping duty is always to overcome the pressure losses due to chilled water flow round the secondary-loop and this applies to any flow rate that the air-handling equipment may demand for. Therefore, two-way valves can be used for all air-side systems without affecting the flow rate in the primary-loop and without upsetting the constant flow requirement of the operating chillers.

The other important implication is that the flow rate of the secondary-loop pumps can be varied and, when handling a reduced flow rate, the required pump power input will

drop even if constant speed pumps are used. Notwithstanding this, variable speed pumps are preferred nowadays for the greater energy saving that can be achieved.

If the secondary-loop pumps are constant speed pumps, their operating point will ride on the pump pressure curve as the flow rate demand drops due to closing of control valves at the air-handling systems, as shown in the graph at the left side in Figure 7.10. At the same time, the power demand of the secondary-loop pumps will drop, leading to a reduction in pumping energy consumption.

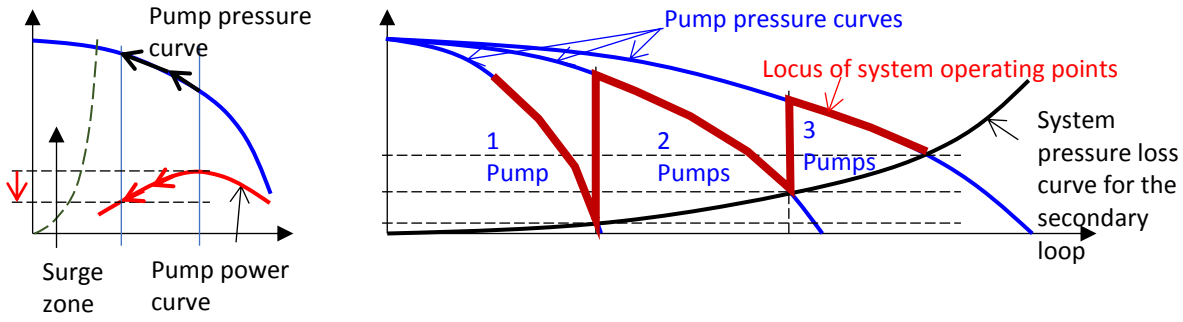

Figure 7.10 Pump pressure and power curves of constant speed secondary-loop chilled water pumps in a two-loop pumping system

Figure 7.10 highlights the variation in pumping pressure of the constant speed secondary-loop chilled water pumps as the load reduces from the design level and the number of pumps in operation is reduced in steps accordingly. The difference between the pumping pressure and the pressure loss of the piping system is the excessive pressure that needs to be throttled off by the control valves, by reducing their degree of opening. As Figure 7.10 shows, this pressure difference will increase when less secondary-loop pumps are running. Since excessively high pressure across an air-handling equipment branch is unfavourable to good performance of the control valve (this will be further discussed later), pumps with flatter pressure-flow characteristics are preferred for use as secondary-loop pumps.

If the flow rate demand of the air-side systems drops to a very low level, in which case there should only be one secondary-loop pump left running, the operating point of the pump may move into the surge zone (Figure 7.10), which will incur excessive noise and vibration that may damage the pipe and the pump. To guard against this from happening, a differential pressure bypass system comprising a bypass pipe installed with a differential pressure control valve (DPV), a differential pressure transmitter and a controller, is installed across the pumps (Figure 7.8a). When the differential pressure across the pump suction and discharge header pipes is found to exceed a pre-set limit, the DPV will open and bypass chilled water, keeping the pump flow rate at a minimum level such that the operating point will lie outside the surge zone. Under this condition, any surplus flow above the flow rate demanded by the air-side system will bypass the distribution circuit and return directly back to the suction side of the pumps.

Compared to constant speed pumps, much greater pumping energy saving can be realized by using variable speed pumps as the secondary-loop pumps in a two-loop pumping system. For pump speed control, a differential pressure transmitter needs to be installed across the critical branch in the chilled water distribution system (Figure 7.11) and the speed control over the secondary-loop pumps shall target to maintain the differential pressure across the critical branch at the set-point level (ΔP_c). Once the differential pressure required across the critical branch is satisfied, all other branches will have a differential pressure exceeding the minimum level required for driving the design flow rate through the branch, even when the pump speed and thus the discharged pressure is reduced to meet a reduction in the total flow rate demand for chilled water.

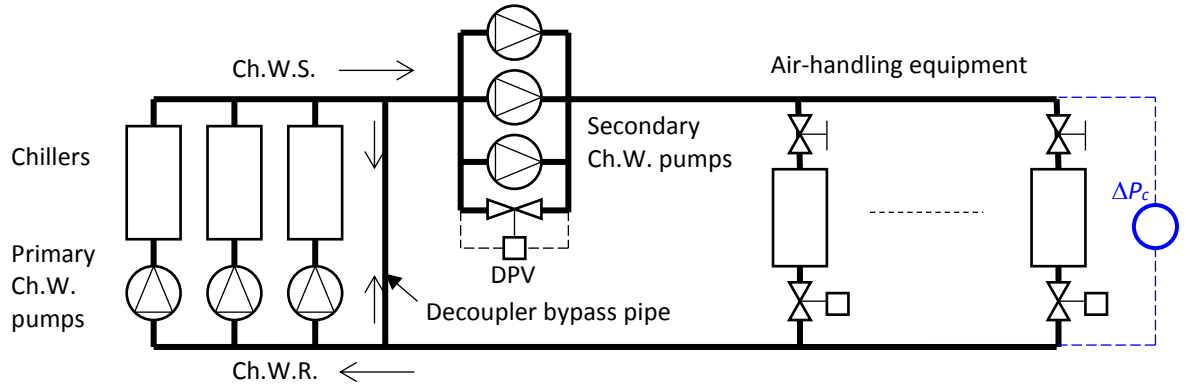

Figure 7.11 A two-loop pumping system with variable speed secondary-loop chilled water pumps and differential pressure transmitter for pump speed control

A reduction in chilled water demand arises as the two-way control valves at the air-handling equipment are closing to reduce cooling output, which will cause a rise in the differential pressure across the critical branch. In response to the feedback signal from the differential pressure transmitter, the pump speed controller will reduce the running speed of the pumps, resulting in reductions in both the pumping pressure and flow rate. This control action will continue until the differential pressure across the critical branch returns to the set point value (ΔP_c). If the chilled water demand is increased later, reflected by opening of the air-side system control valves, the differential pressure across the critical branch, as measured by the differential pressure transmitter, will fall below the set point (ΔP_c) and, in response, the pump speed, and hence the pressure and flow rate discharged, will be increased to restore the differential pressure.

Figure 7.12 shows the changes in the characteristic curves of the system and the pumps when the chilled water demand is reduced from the design level. Closing of control valves means an increase in the overall flow resistance of the system and, hence, its system characteristic curve will be bent upward, as shown by the dotted line above the original curve. The operating point of the system, after any transient variations due to adjustment of the control system have subsided, will be the intersection point of the new system characteristic curve and a new pump characteristic curve corresponding to

the reduced pump running speed, as shown by the dotted line below the original pump characteristic curve at full speed.

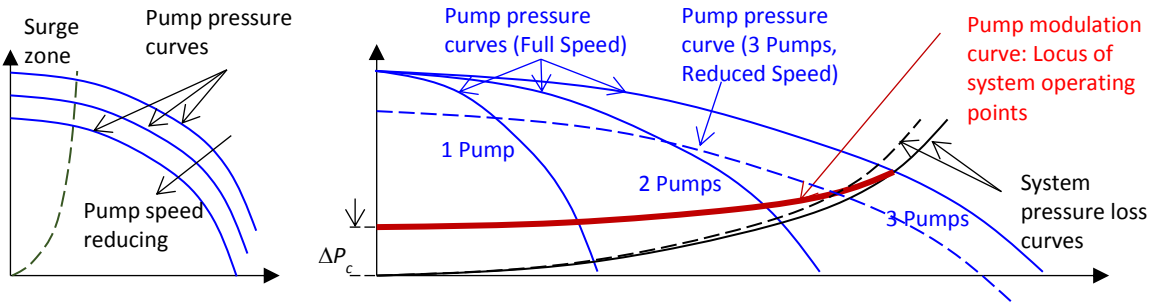

Figure 7.12 Part-load operation and pump modulation curve of a two-loop pumping system with variable speed secondary-loop chilled water pumps

If we can trace the operating points for further steps of flow reduction, we can plot a curve to represent the locus of the system operating points, and such a curve is referred to as the 'pump modulation curve' (Figure 7.12). The pump modulation curve starts from zero flow at a pressure that equals the set point pressure (ΔP_c) across the critical branch for pump speed control, which is the pressure that the control system will try to maintain even if the flow rate demand drops to zero. Ideally, for a well-commissioned system, the curve should stop at the design operating point at the other end.

In reality, a clear pump modulation curve between the two end points may not be traceable, because the air-side equipment may change their flow rate demands to different proportions at different times, which will lead to many possible operating points involving different combinations of flow rate and pumping pressure. Nevertheless, the concept of pump modulation curve is useful to estimation of the pumping energy consumption for chilled water systems with variable speed secondary-loop pumps (we shall return to this topic later).

In the following, a detailed analysis of the possible variations in the chilled water flow rates and temperatures in the primary- and secondary-loops of the two-loop pumping system is given, which provides a basis for the decoupler bypass control for chiller sequencing. Although this sequencing control method is considered old-fashioned and seldom employed nowadays, the analysis is considered worth including here as it can deepen our understanding of the operation of the two-loop pumping system. To facilitate the discussion, a schematic of a two-loop pumping system is shown in Figure 7.13, with the variables involved included.

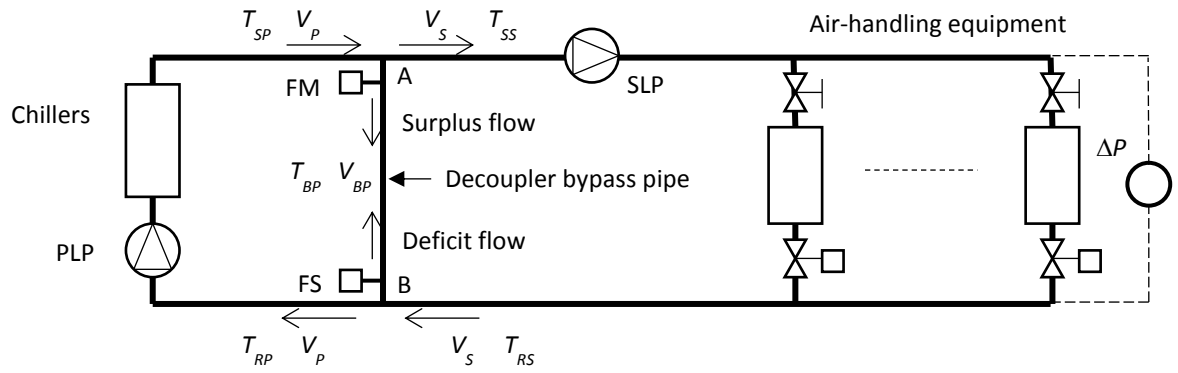

Figure 7.13 Flow rate, temperature, and flow direction of chilled water in the two-loop pumping system

Due to the hydraulic decoupling effect of the bypass pipe, the chilled water flow rates through the primary-loop (V_P) and the secondary-loop (V_S) may vary independently without affecting each other (Figure 7.13). When $V_P > V_S$, a flow rate of V_{BP} ($= V_P - V_S$) will arise in the bypass pipe from junction A at the main supply pipe to junction B at the main return pipe. Bypass flow rate in this direction (from A to B) is called surplus flow because the primary-loop has the capacity to supply a flow rate of chilled water in excess of the demand of the air-handling equipment in the secondary-loop.

With surplus flow,

i) The temperature of chilled water supplied to the air-handling equipment in the secondary-loop (T_{SS}) equals the temperature of the chilled water leaving the chillers in the primary-loop (T_{SP}) and flowing through the bypass pipe (T_{BP}).

ii) The chilled water returning from the air-handling equipment at temperature (T_{RS}) will mix with the chilled water flowing through the bypass pipe at temperature (T_{BP}). Hence, the temperature of chilled water returning to the chillers in the primary loop (T_{RP}) is given by:

$$T_{RP} = (V_S T_{RS} + V_{BP} T_{BP})/V_P \qquad (7.1)$$

However, if $V_P < V_S$, the bypass flow rate V_{BP} ($= V_P - V_S$) flowing through the bypass pipe will be negative in value, meaning that the bypass flow direction will be reversed: this time from junction B at the main return pipe to junction A at the main supply pipe (Figure 7.13). Bypass flow rate in this direction (from B to A) is called deficit flow, which will arise when the chilled water flow rate that the air-handling equipment call for is greater than the total flow rate through the operating chillers and primary-loop pumps (PLP).

With deficit flow:

i) The temperature of both the chilled water returning to the chillers in the primary-loop (T_{RP}) and the chilled water flowing through the bypass pipe (T_{BP})

are equal to the temperature of chilled water returning from the air-handling equipment in the secondary loop (T_{RS}).

ii) The chilled water leaving the chillers at temperature (T_{SP}) will mix with the chilled water flowing through the bypass pipe at temperature (T_{BP}). Hence, the temperature of the chilled water supplied to the air-handling equipment (T_{SS}), as given below, is higher than T_{SP}.

$$T_{SS} = (V_P T_{SP} + |V_{BP}| T_{BP})/V_S \quad (7.2)$$

Deficit flow is undesirable because the elevated chilled water supply temperature ($T_{SS} > T_{SP}$) will degrade the cooling and dehumidifying capacities of the air-handling equipment. Its occurrence, reflected by a reversal in flow direction in the bypass pipe, signifies that the cooling capacity of the operating chillers is insufficient to meet the cooling demand. Therefore, more chiller should be run to cope.

Since the chilled water flow rate round the primary loop may only change in steps, surplus flow will occur under normal operating conditions where the chillers in operation have a total cooling capacity exceeding the cooling demand. However, when the surplus flow exceeds the rated chilled water flow rate of one of the running chillers, the total cooling capacity of the running chillers will remain sufficient when that chiller is stopped.

The reversal in direction of chilled water flow and the surplus flow rate through the decoupler bypass pipe, as outlined above, are sufficient signals for determination of whether the number of operating chillers should be adjusted to cope with load changes and, therefore, may be utilized to sequence on and off chillers. These conditions can be detected by installing a flow switch (FS) and a flow meter (FM) at the decoupler bypass pipe (Figure 7.13). This chiller sequencing control method is called decoupler bypass control which, although usable and in fact had been widely adopted before digital control systems are available, is not the best method for chiller sequencing control from the perspective of energy efficiency of chiller plant operation.

With the hydraulic decoupling effect of the bypass pipe, the primary (production) loop may be coupled to multiple secondary (distribution) loops, each with its own secondary-loop pumps (SLP) and pump speed control (Figure 7.14). The circuit arrangement is most suitable to applications where there are air-handling equipment that belong to different groups / zones (e.g. AHUs in different building towers on a common podium).

Where the routing of the main supply and return pipes spans a long distance (e.g. the riser pipes in a tall building), consideration may be given to using the reverse return arrangement (Figure 7.15). The reverse return circuit narrows down the differences in pressure drop round different branches in the system, thus making balancing an easier task, or even not necessary.

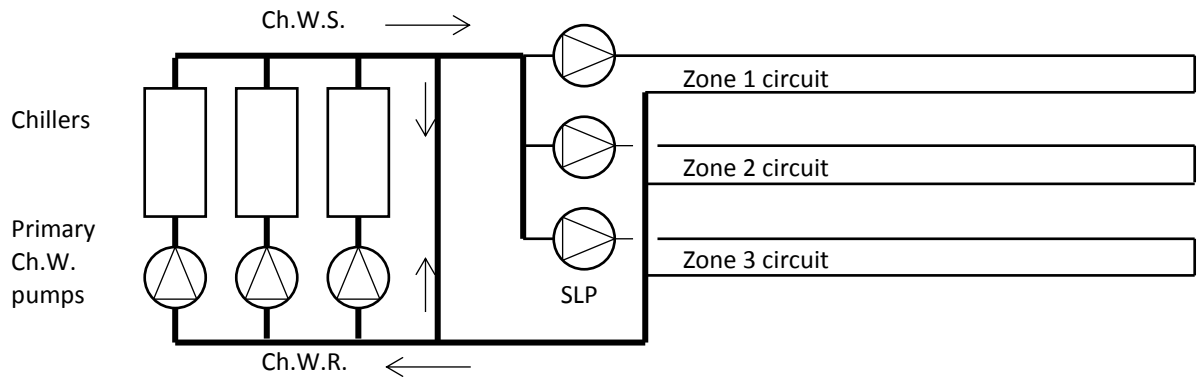

Figure 7.14 A chilled water system comprising one primary-loop and multiple secondary-loops

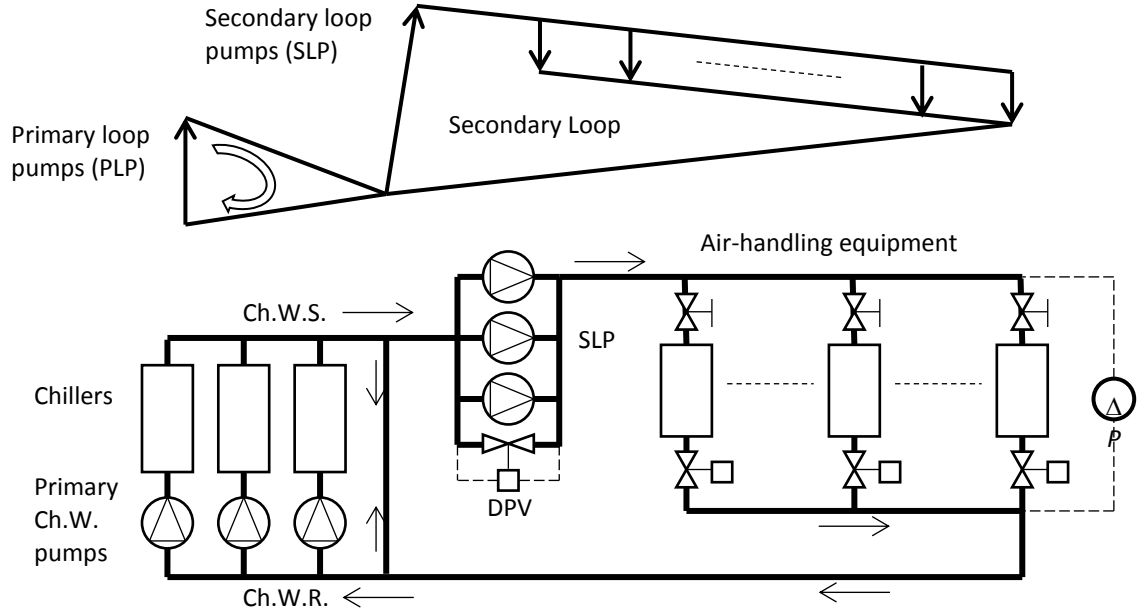

Figure 7.15 A two-loop pumping system with reverse return arrangement

Use of reverse return arrangement for the riser pipes involves one more riser to be installed, and hence requires more pipe shaft space and is more costly. For horizontal distribution of chilled water to air-side equipment, however, reverse return arrangement can be achieved without increasing the space for installation as well as piping cost, as shown in Figure 7.16.

As an extension to the discussions on the single- and two-loop pumping systems described above, Annex 7A describes modifications to these circuit designs to facilitate performance measurements of the chillers, which was the first part a paper published by the author [2]. The second part on empirical verification was omitted for the sake of brevity and interested readers may refer to the paper for the full picture.

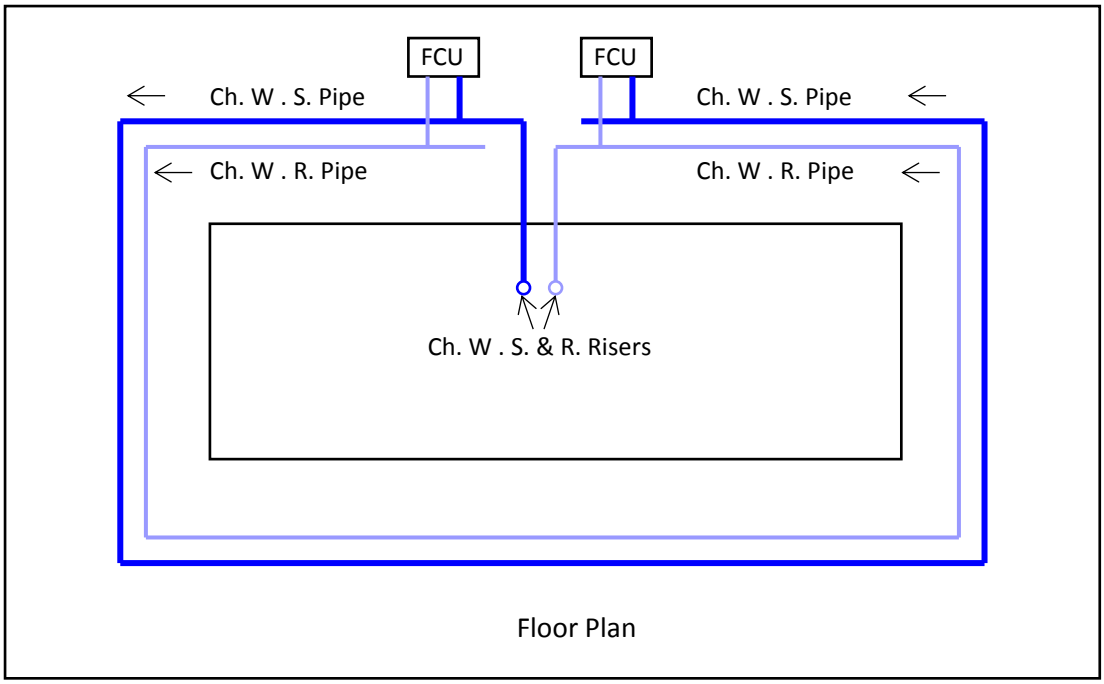

Figure 7.16 Reverse return arrangement for horizontal distribution of chilled water

7.4 Variable primary flow (VPF) systems

The two major chilled water system designs discussed above, namely the single-loop pumping system with differential pressure bypass control and the two-loop pumping system, are both capable of ensuring a nearly constant flow rate through the operating chillers while allowing two-way valves to be used for air-side system control. The single-loop pumping system is simpler and cheaper to own but requires more pumping energy input to run whereas the two-loop pumping system is more complex and costly but saving in pumping energy use can be achieved under part-load operation, especially when variable speed pumps are used as the secondary-loop pumps.

Starting from around year 2000, variable primary flow (VPF) system (Figure 7.17) emerged [3] and has become increasingly common. The VPF system design takes advantage of the simplicity in system configuration (with only one group of pumps) of a single-loop pumping system with constant speed pumps and the energy saving potential with reduction in flow rate under part-load conditions as in the secondary loop of a two-loop pumping system.

In a VPF system, the total chilled water flow rate through the running chillers will vary with the chilled water flow rate demanded by the air-handling equipment. Like secondary-loop pumps (SLPs) in a two-loop pumping system, the running speed of the variable speed (VS) primary-loop pumps (PLPs) is moderated such that the differential pressure across the critical air-handling equipment branch is maintained at the set-point level, thus ensuring all branches in the circuit can be fed with chilled water at the required flow rates.

Unlike pumps in a single-loop system or in the primary loop of a two-loop system, the VS PLPs need not be staged on and off, each together with one dedicated chiller. However, the chilled water flow rate through each chiller must not fall below a minimum level, to ensure proper chiller operation. This is catered for by a bypass control system comprising a flow meter and a bypass pipe across the main supply and return pipes, with a control valve in the pipeline (Figure 7.17).

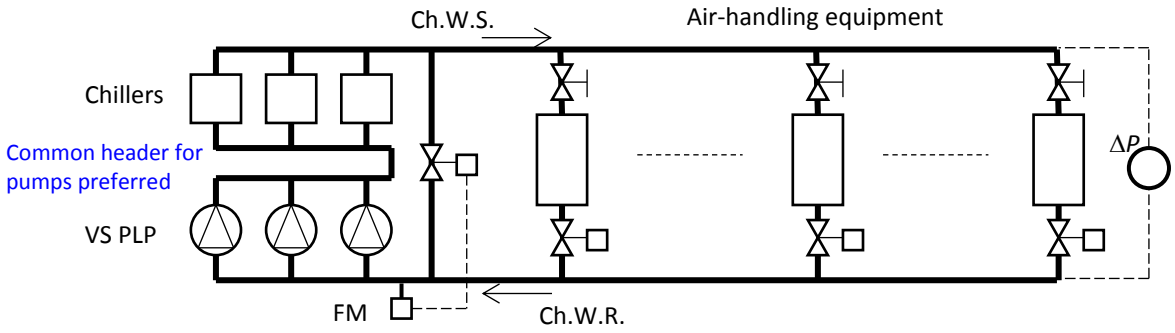

Figure 7.17 A variable primary flow chilled water pumping system

The flow meter of the bypass control system will monitor the flow rate consistently. Once the chilled water flow rate starts to drop below the minimum flow rate required by the last running chiller, the flow meter will command the bypass control valve to open and bypass chilled water to keep the minimum flow rate through the chiller. Alternatively, a low speed limit may be set to the pump speed control such that the pump would stay at the minimum speed even if the differential pressure signal still calls for a reduction in pump speed. The system will be installed with a differential pressure bypass control system (Figure 7.18) which will start to operate when the last pump is running at the minimum speed, thus maintaining a steady minimum flow through the last running chiller.

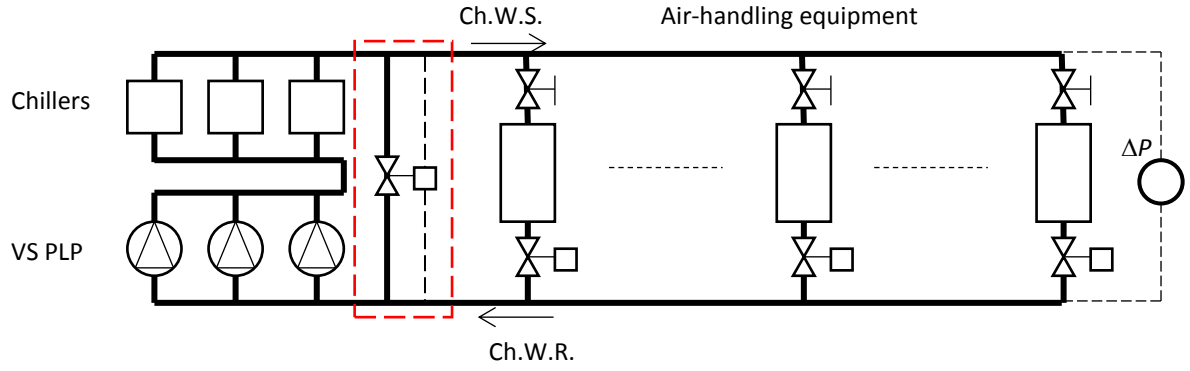

Figure 7.18 A variable primary flow chilled water pumping system with differential pressure bypass control

Although modern chillers allow chilled water flow rate to vary, variation of the water flow rate through each chiller should take place gradually and should stay within the maximum and minimum limits. A recommendation is to limit the flow velocity through the tubes within the range from 0.9 to 3.4m/s [3], i.e. the minimum flow rate to be no less than 26% of the maximum flow (note that the velocity may be below 3.4m/s at rated condition and thus the minimum % flow would be higher than 26%). Many plant operators prefer to limit the minimum flow not to fall below 50% of the rated flow rate of the chiller. In any case, chiller manufacturer's requirement on the minimum flow rate should be checked.

Care should be taken in operational control of the chillers and pumps, especially when staging them on and off [3]:

- The rate of increase and reduction in the chilled water flow rate per unit time should be kept within limits (e.g. less than 10% of design flow per minute) to avoid tripping or stoppage of running chillers.

- Slow acting valves at chiller inlet or outlet need to be used to facilitate sequencing on and off of chiller and pump.

- Lock the pumps at their current speed while staging chillers on and off.

- Before staging on next chiller, raise the chilled water supply temperature set point of the running chillers a few minutes before allowing chilled water flow through the next chiller. This will pre-unload the operating units in preparation of the next chiller to come on stream.

- After the next chiller is staged on for a several minutes, start resetting the chilled water supply temperature set point of the other running chillers back to the desired level.

Furthermore, the valve actuator for the bypass control valve should be fast acting and with PID control to cater for sudden changes in flow demand.

Table 7.1 The advantages and disadvantages of VPF system

Advantages	Disadvantages
Lower first cost	Complexity of bypass control
Less plant space required	Complexity of staging chillers
Reduced pump peak power	
Lower pump annual energy use	

Table 7.1 summarizes the key advantages and disadvantages of using a VPF system compared to the conventional two-loop pumping system. Besides energy saving potential, a major reason for proposing the use of VPF system is its ability to mitigate the low delta-T syndrome. The low delta-T syndrome refers to the operating condition of chilled water systems where the temperature difference between the supply and

return chilled water falls significantly below the design value, which often happens under low load conditions.

Causes of low delta-T syndrome include:

- Improper set point or controls calibration (giving rise to drop in return temp.)
- Use of three-way valves
- Improper coil selection (coil sized for a smaller delta-T; oversized FCUs)
- Improperly selected control valves
- No control valve interlock (control valve still operating when AHU is shut-down)
- Uncontrolled process (coil run wild)
- Leaky valve
- Laminar flow (not too significant)
- Chilled water temperature reset (causes reduced performance of coil)
- Reduced coil effectiveness (fouling)

When low delta-T occurs, the air-side systems would be demanding for a higher than required chilled water flow rate which is out of proportion with the cooling load. With the primary-secondary chilled water pumping system design, low delta-T will lead to either more than required number of chillers to be run, which will cause excessive use of energy, or elevation in supply chilled water temperature due to presence of deficit flow.

Mitigation measures for low delta-T syndrome include:

- Variable speed chillers, which can run efficiently under low PLR
- Check valve in decoupler bypass pipe, avoiding elevation in supply chilled water temperature due to deficit flow
- Over pumping with unequally sized chillers/pumps, avoiding running more than enough chillers
- Low delta-T in primary loop, which can operate normally when low-delta T at secondary side occurs
- Use VPF system, avoiding elevation in supply chilled water temperature due to deficit flow

7.5 Water pressure and pressure test

The hydrostatic pressure at the lowest point of a water piping system is proportional to the vertical distance between the lowest point to the free surface in the expansion tank connected to the water piping system (Figure 7.19). This hydrostatic pressure may well exceed 30 bars in a 100-storey building (see Annex 5A of Chapter 5) and, no matter how high, the equipment, pipes, and fittings must all be able to sustain a working pressure that equals or exceeds the maximum working pressure that may arise.

With few exceptions, the water pressure ratings of system components, including equipment, water pipes, valves, and fittings, in a central air-conditioning system are in the range of PN10, PN16 & PN25, meaning that they can withstand a working pressure of 10, 16 and 25 bars, respectively. Rather than using system components of a high

pressure rating, heat exchangers may be used to break the pressure if an excessively high working pressure would arise without the pressure break (see Section 6.6).

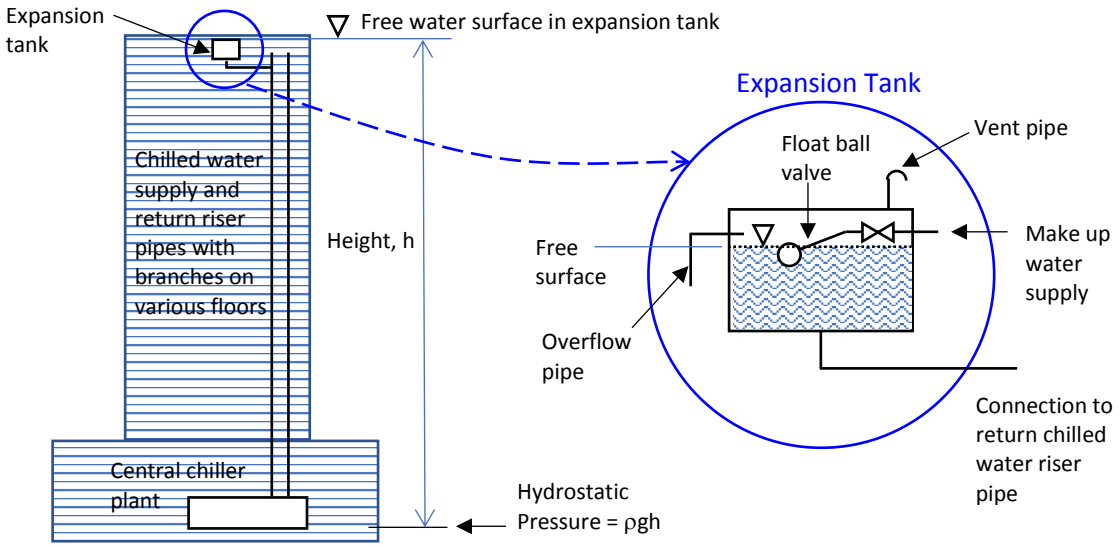

Figure 7.19 Hydrostatic pressure in a chilled water system serving a high rise building

Burst of pipe can endanger building occupants and operation and maintenance (O&M) personnel, and water leakage can lead to serious damages, including direct damages to equipment and accessories, and electrical and other hazards. Such risk exists because water piping systems are assembled on site manually by welding or tightening pipes and fittings together by screwed unions or flanges in conjunction with bolts & nuts. Therefore, a piping installation work will not be complete without carrying out pressure tests to ensure the water piping systems can withstand a sufficiently high pressure without leakage.

Besides the hydrostatic pressure, sudden starting or stoppage of water flow can lead to surge in pressure, which is called 'water hammer'. The pressure rise resulting from water hammer, ΔP_H, is given by:

$$\Delta P_H = \rho c_s \Delta v \qquad (7.3)$$

Where ρ is water density, c_s the velocity of sound propagation in water and, Δv the reduction in velocity of water flow. Note that the reduction in velocity in Equation (7.3) is assumed to be instantaneous. Otherwise, the pressure rise will be lower.

With reference to the typical values of ρ (= 1,000kg/m^3) and c_s (= 1,439m/s) for water, and let v be 3m/s which is suddenly brought to zero, the corresponding rise in pressure is:

ΔP_H = 4,317kPa, or 42.6bar, or 440mH_2O

This is indeed a remarkably high pressure well exceeding the normal range of pressure rating of components and accessories of a water-side air-conditioning system. In reality, however, the observable pressure surge will only reach a peak value significantly lower than the above estimate. This is because it would take a finite time for stopping the water flow, e.g. time for closing a control valve, and, meanwhile, the pressure will be relieved due to expansion of the pipe walls consequent upon the high water pressure present, and by flexible devises in the piping system, such as flexible pipe connections. Where there is such a need, water hammer arrestors may be installed to alleviate the problem.

In practice, the most commonly used criterion for water pipe pressure tests is the higher of 1.5 times the nominal maximum working pressure or 1,000kPa. Pressure test for the entire system is typically split into separate tests on different parts of the system to limit the scale of the test work as well as to cope with the progress of installation, especially for pipes that may become inaccessible when building and other works are constructed or installed later.

Prior to the test, the part of the piping system to be tested should be isolated from the other parts of the system and, where applicable, from various types of major equipment and any pressure sensitive instrument that are normally connected to the pipes in the part of the system under test, and such connection points that would become open should be sealed properly. After charging water into the pipes to boost the internal pressure to the test level by a hand or motorized pump, a valve in the pipe temporarily connecting the pump to the pipes under test will be shut to seal off the pipes completely. The test pressure in the pipes will typically be sustained for 24 hours, during which any drop in pressure due to drop in temperature will be restored, if observed. Otherwise, there should not be any noticeable drop in pressure throughout the test period.

7.6 System balancing

7.6.1 Basic system configuration and the need for balancing

In a piping network, there may be one or more pairs of main supply and return pipes (Figure 7.14) extending from the header pipes in the central chiller plant for distribution of chilled water to air-side systems within the same building or different zones in the same building or different buildings in the same development. Along their run paths, each pair of these main supply and return pipes will be connected to multiple branches, each connected to an air-handling equipment or a sub-branch comprising a pair of supply and return pipes. The supply and return pipes in a sub-branch will be connected to a number of branches, and each of these branches may, in turn, be connected to an air-handling equipment, or a lower tier sub-branch. Air ducting networks are typically less complex but may still comprise branches, sub-branches, sub-sub-branches, and so on.

For simplicity in the following discussion, we would limit our consideration to a piping network that comprise just one pair of supply and return pipes and each branch from these supply and return pipes is connected to an air-handling equipment, as shown in Figure 7.20. Furthermore, our discussion will focus on the design condition where all branches would require a flow rate that equals their respective design flow rate and, for

achieving this, all control valves in the branches would be fully open. The analysis and methods covered below, though discussed in the context of a water piping network, would be applicable to a similar ducting network that is formed by a number of branches, each supplying air into a room with or with passing through a terminal devise, as shown also in Figure 7.20.

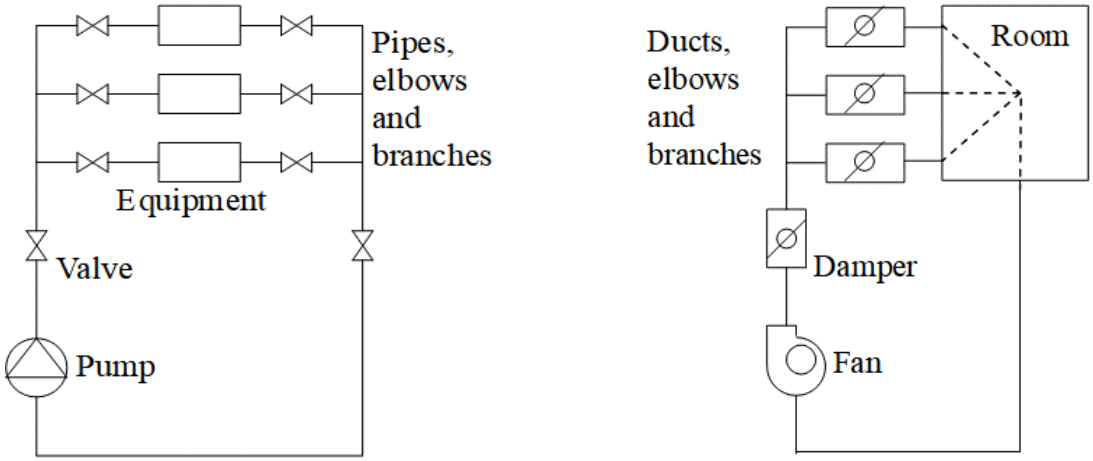

Figure 7.20 A piping network (left) and a ducting network (right)

As can be seen from the piping network shown in Figure 7.20, for a network comprising multiple branches along the run of the main supply and return pipe, there will be branches that are closer to the pump and others further away. Because the pressure will drop as the chilled water flows along the supply and return pipes, the difference in pressure across the connection points of a branch to the supply and return pipes will be higher if the branch is closer to the pump, and lower if further away. This explains for the shape of the pressure-distance diagrams introduced in earlier sections (see Figures 7.8 & 7.15).

The available differential pressure across each branch, however, may not match with the pressure required to drive the design flow rate of the branch to flow through the pipes, fittings, and air-handling equipment in the branch without the intervention of the control valves in the branches. Even though the pump is capable of delivering the total design flow rate at the design pumping pressure, and all pipes and fittings and control valves in the system are properly sized, the piping network, as installed, would not allow each branch to have its design flow rate until the control valves of those branches overfed with chilled water are partially closed to reduce flow rate allowing those in deficit to have their flow rate increased. As will be discussed later in Chapter 8, requiring the control valves to regulate the flow rates to correct imbalance in flow distribution is at the expense of the control performance of the control valves.

Fine tuning is required to correct the flow imbalance before each branch can have its design flow rate without adjustment by the control valve. This tuning is called flow balancing, which could only be carried out if a regulating valve, which at least should be a ball valve but preferably a valve purposely designed for water balancing is installed in each branch (Figure 7.21). The method most widely used is called ‘proportional

balancing', which will be explained and discussed below. The procedures of proportional balancing will then be introduced.

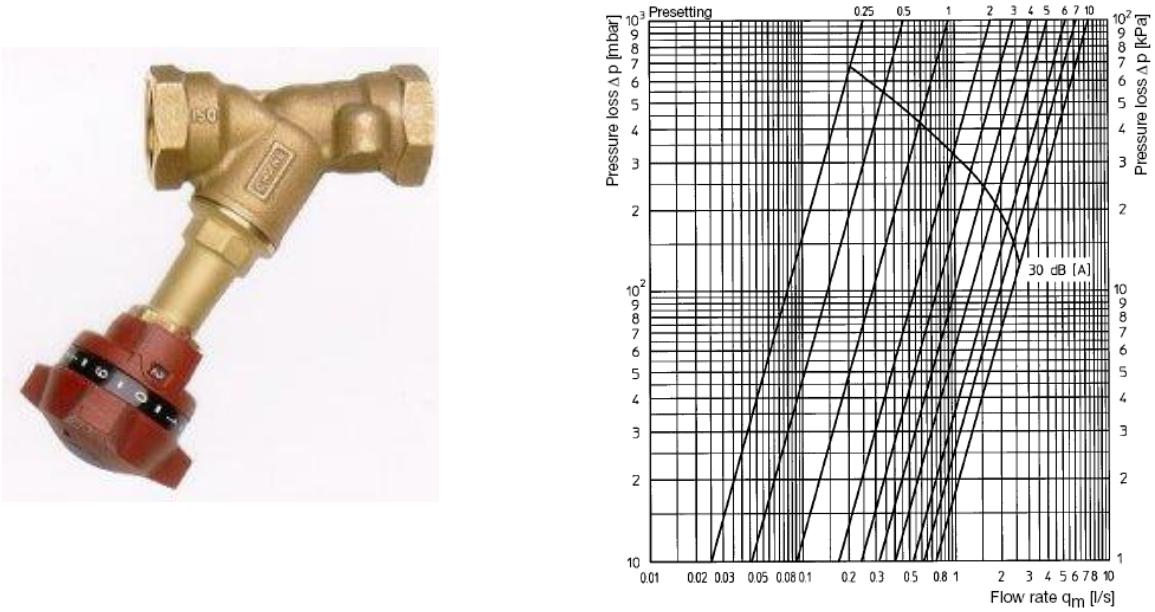

Figure 7.21 Balancing valve and characteristic curves relating pressure drop to flow rate at various number of turns of the valve

7.6.2 Basic principles behind proportional balancing

The pressure drops that components in a ducting system would incur when air is flowing through them have been discussed in Section 5.4.2, including their combined characteristics when the components are connected in series and parallel, which will allow a complex ductwork to be condensed into an equivalent single element to facilitate fan-duct system analyses. Similar principles apply to a piping system.

For a component in a piping system, the relation between the pressure drop, Δp, and the flow rate of chilled water it passes, Q, can be described as:

$$\Delta p = K \cdot Q^n \tag{7.4}$$

Where K is the flow resistance of the component; and n is the flow exponent, which has a value between 1 and 2 for water flow from laminar to fully turbulent conditions. The flow resistance or K value of a component may be a constant (e.g. a pipe or duct section, an elbow, or a branch) or a variable (e.g. a valve but will stay constant as long as its degree of opening is fixed). Recall discussions in Section 5.4.2, for two components in series, the equivalent element representing them will have a flow resistance, K, that equals the sum of the flow resistances of the components, K_1 & K_2.

$$K = K_1 + K_2 \tag{7.5}$$

If they are in parallel instead, the equivalent element representing them will have a flow resistance, K, as given below:

$$\frac{1}{K^{1/n}} = \frac{1}{K_1^{1/n}} + \frac{1}{K_2^{1/n}} \tag{7.6}$$

Now, consider the simple fluid flow network shown in Figure 7.22. It comprises four elements connected to form a loop, with K_1 and K_2 being the flow resistances of the branches from a supply and a return pipe. The pipe sections between the two branches are represented by the flow resistances K_3 & K_4. Water is fed from the supply pipe connected to K_3, and flows through K_3, K_2, and K_4 in one path, and through K_1 in the second path, and back to the central plant through the return pipe connected to K_4. Elements K_3, K_2, and K_4 are in series and the flow path they form is in parallel with K_1. As they are in parallel, both flow paths are subject to the same pressure difference Δp.

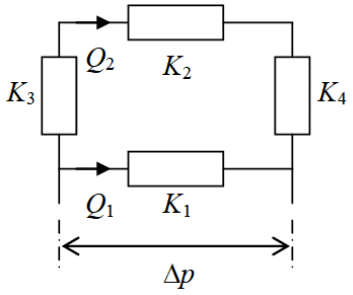

Figure 7.22 A simple flow network with four elements in a loop

Therefore,

$$Q_1 = \left(\frac{\Delta p}{K_1}\right)^{1/n} \tag{7.7}$$

$$Q_2 = \left(\frac{\Delta p}{K_3+K_2+K_4}\right)^{1/n} \tag{7.8}$$

Note also that

$$Q_2 = \left(\frac{\Delta p_3}{K_3}\right)^{1/n} = \left(\frac{\Delta p_2}{K_2}\right)^{1/n} = \left(\frac{\Delta p_4}{K_4}\right)^{1/n} \tag{7.9}$$

Where Δp_2, Δp_3, and Δp_4, are the pressure drops across elements K_2, K_3 and K_4, respectively.

If the differential pressure across the network is changed from Δp to Δp^*, the flow rates through the elements and the pressure drops across them will change to as follows:

$$Q_1^* = \left(\frac{\Delta p^*}{K_1}\right)^{1/n} \tag{7.10}$$

$$Q_2^* = \left(\frac{\Delta p*}{K_3+K_2+K_4}\right)^{1/n} = \left(\frac{\Delta p_3^*}{K_3}\right)^{1/n} = \left(\frac{\Delta p_2^*}{K_2}\right)^{1/n} = \left(\frac{\Delta p_4^*}{K_4}\right)^{1/n} \tag{7.11}$$

Dividing Equation (7.10) by Equation (7.7),

$$\frac{Q_1^*}{Q_1} = \left(\frac{\Delta p*}{\Delta p}\right)^{1/n} \tag{7.12}$$

Similarly, we can write

$$\frac{Q_2^*}{Q_2} = \left(\frac{\Delta p*}{\Delta p}\right)^{1/n} = \left(\frac{\Delta p_3^*}{\Delta p_3}\right)^{1/n} = \left(\frac{\Delta p_2^*}{\Delta p_2}\right)^{1/n} = \left(\frac{\Delta p_4^*}{\Delta p_4}\right)^{1/n} \tag{7.13}$$

It can be observed from the above results that when the differential pressure across the network is changed, the differential pressure across all elements in the network will change by the same proportion, viz., $\Delta p^*/\Delta p$. Furthermore, the flow rates through the elements in the network will all change by the same proportion, viz., Q_i^*/Q_i.

The above observation may be generalized by considering the circuit shown in Figure 7.23. If element K_2 was actually the equivalent element representing four elements, K_5 to K_8, the observations made above on the changes in differential pressures and flow rates of the elements can be extended to the circuit represented by K_2, i.e.:

$$\frac{Q_2^*}{Q_2} = \left(\frac{\Delta p*}{\Delta p}\right)^{1/n} = \frac{Q_5^*}{Q_5} = \left(\frac{\Delta p_5^*}{\Delta p_5}\right)^{1/n} = \frac{Q_6^*}{Q_6} = \left(\frac{\Delta p_6^*}{\Delta p_6}\right)^{1/n} = \left(\frac{\Delta p_7^*}{\Delta p_7}\right)^{1/n} = \left(\frac{\Delta p_8^*}{\Delta p_8}\right)^{1/n} \tag{7.14}$$

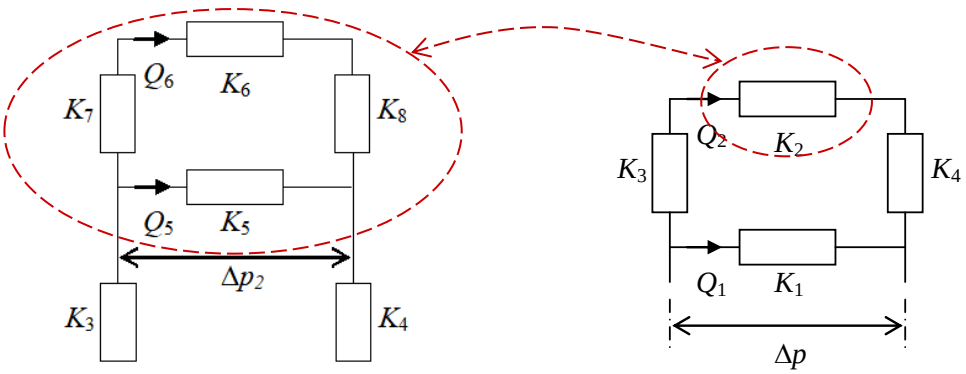

Figure 7.23 A network with fours element represented by an equivalent element

The above observation can be further extended by considering K_6 as an equivalent element representing another simple circuit, and so on, until all elements in a complex circuit are all covered. Therefore, the proportional changes in the differential pressures and flow rates of elements as highlighted above can be applied globally to all elements in the entire network. This is the theoretical basis of the proportional balancing method, as discussed in the next section, which is widely adopted in balancing air ducting and water piping systems.

7.6.3 Procedures of proportional balancing

In the proportional balancing method, the actual flow rate through each branch in a network, Q_i, is first measured and the ratio of the actual flow rate to the design flow rate of the branch, Q_i / Q_{di}, is determined. The lowest actual to design flow rate ratio among the branches is taken as the reference ratio.

$$\left(\frac{Q}{Q_d}\right)_{ref} = Min\left(\frac{Q_1}{Q_{d1}}, \frac{Q_2}{Q_{d2}}, \ldots, \frac{Q_N}{Q_{dN}}\right) \tag{7.15}$$

For each branch in the network that has an actual to design flow rate ratio greater than the reference ratio, the resistance of the branch is increased by adjusting the balancing valve in the branch. The same is done on other branches until the actual to design flow rate ratios of all the branches are nearly the same as the reference ratio.

$$\left(\frac{Q}{Q_d}\right)_{ref} \approx \frac{Q_1}{Q_{d1}} \approx \frac{Q_2}{Q_{d2}} \approx \cdots \approx \frac{Q_N}{Q_{dN}} \tag{7.16}$$

When this is done, the flow rates in all the branches can be adjusted to their respective design flow rates in one go, by adjusting the valve at the discharge side of the pump or by changing the pump impeller to one with the appropriate size.

The flow rate adjustment, however, may take several rounds to complete, as reducing the flow rate in a branch will change the flow rates in all other branches as well. One method to minimize over-balancing is to reduce design to actual flow rate ratio to 110% rather than 100% of the reference ratio.

Annex 7A Chilled water circuit designs for in-situ chiller performance measurement[3]

7A.1 Introduction

As a contractual requirement, in-situ measurement of chiller performance has to be conducted during the testing and commissioning stage of the installation of a new air-conditioning system, to verify whether the performance of the newly installed chillers can meet the specified performance [5]. For up-keeping the energy efficiency of air-conditioning systems in existing buildings, the performance of chillers should also be evaluated from time to time for detection of any performance deterioration due to slowly developing faults, such as tube fouling, accumulation of non-condensable gases or refrigerant leakage, etc. [6-10]

Complicated arrangements are needed in order that a chiller can be tested over its entire capacity range within a short measurement period. Before a new building is occupied, the load on the chillers can be adjusted by turning on an appropriate amount of air-side equipment but the load may fluctuate within the test period, and the process can be rather laborious. In many cases, verification of chiller performance may simply be based on a certain part-load condition achievable during the test. The measured performance will then be compared against the corresponding part-load performance data given by the chiller manufacturer while the full-load test will be deferred until the weather and the building operating conditions permit [11]. Some developers may relax the requirement on in-situ full-load tests but may require ex-factory tests to be witnessed by representatives of the developer, the consulting engineer, and the contractor.

For chillers in existing buildings that are unoccupied on weekends and public holidays, the chillers may be tested on those days such that the cooling load on chillers can be adjusted by switching on and off air-side equipment. This, however, is nearly impossible for commercial buildings in most Asian cities, including Hong Kong. As computer-based building management system (BMS) is widely used nowadays, the performance of chillers in many buildings is continuously monitored and logged by a BMS, which can provide the required data for chiller performance evaluation. However, a long measurement period (up to half a year) is required for accumulating sufficient data for full- and part-load performance evaluation.

In this paper, chilled water circuit designs that can facilitate expeditious evaluation of the full- and part-load performance of chillers are presented. The differences in the chiller operating conditions between using the proposed and the conventional circuit designs are elucidated. The proposed chilled water circuits may be operated in the 'normal' or the 'measurement' mode without interrupting air-conditioning provision in the building. Measures for controlling the temperature of the air or water entering chiller condensers are also discussed. For a demonstration of the effectiveness of the proposed circuit designs, the operating conditions that would arise with and without

[3] Extracted from Yik FWH, Chilled water circuit designs for in situ chiller performance measurement, Building Services Engineering Research and Technology 2008, 29(2): 107-118.

the proposed circuit designs have been analysed, based on the hourly building cooling loads predicted by computer simulation for an office building model in Hong Kong.

7A.2 Alternative chilled water circuit designs

In the forthcoming discussions, and in the chilled water circuits shown in the figures to which the discussions refer, each chiller plant is taken as comprising only two chillers, but situations that will arise when there are more chillers will also be discussed. Furthermore, the assumptions are made that the chilled water leaving different operating chillers are at the same temperature at all times, and that when the chiller in a chiller branch is shut-down, there will be no chilled water flowing through the chiller branch. The former assumed condition is invariably taken as a criterion in setting the controls of chillers, for avoiding the energy penalty due to mixing of chilled water at different temperatures. The latter is achievable when there is a non-return valve at the exit of the primary chilled water pump associated with each of the chillers, which is a basic provision in chiller plants with chillers in parallel.

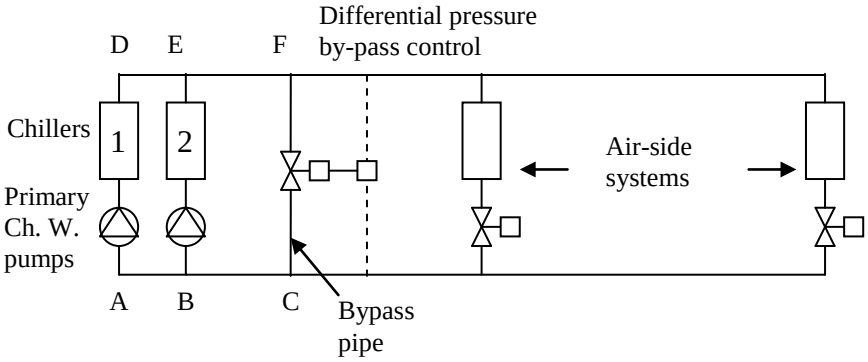

Figure 7A.1 Single-loop pumping system

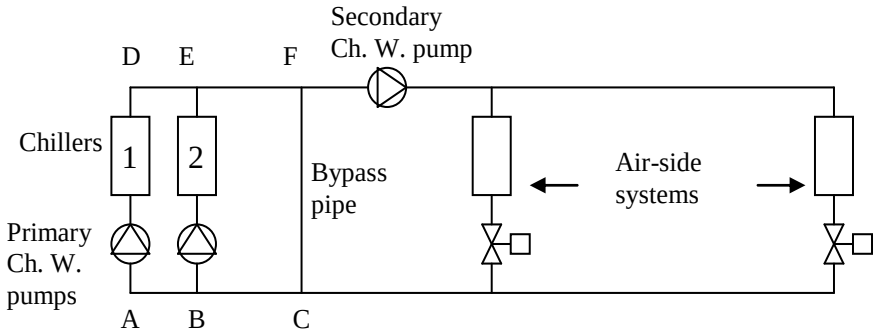

Figure 7A.2 Two-loop pumping system

Figures 7A.1 & 7A.2 show the conventional circuit designs of single- and two-loop chilled water pumping systems in central air-conditioning plants in buildings. Based on the abovementioned assumptions, the share of the total cooling load of each operating chiller is proportional to the ratio of the chilled water flow rate through the chiller (which should be approximately constant) to the total chilled water flow rate through all the operating chillers (which would vary in steps according to the number of chillers and primary chilled water pumps being run), as depicted by Equation (7A.1).

$$\frac{q_i}{\sum_{i=1}^{N} q_i} = \frac{q_{i,Rated}}{\sum_{i=1}^{N} q_{i,Rated}} = \frac{m_i}{\sum_{i=1}^{N} m_i} \qquad (7A.1)$$

Where

q_i = the cooling load on the i^{th} operating chiller, for $i = 1, 2, ..., N$
$q_{i,Rated}$ = the rated cooling capacity of the i^{th} operating chiller
m_i = the chilled water flow rate through the i^{th} operating chiller
N = total number of operating chillers in the plant

With the conventional circuit designs, a chiller will be fully loaded only when the cooling load on the chiller plant equals the total cooling capacity of all operating chillers, i.e. when all the running chillers in the plant are fully loaded, as depicted by Equation (7A.2). Therefore, if chiller performance evaluation is to be based on operating data measured and trend-logged through the use of a BMS, the full-load performance of chillers can be captured only occasionally.

$$\frac{q_i}{q_{i,Rated}} = \frac{\sum_{i=1}^{N} q_i}{\sum_{i=1}^{N} q_{i,Rated}} = 1 \text{ if and only if } q_i = q_{i,Rated} \text{ for i} = 1, 2, ..., N \qquad (7A.2)$$

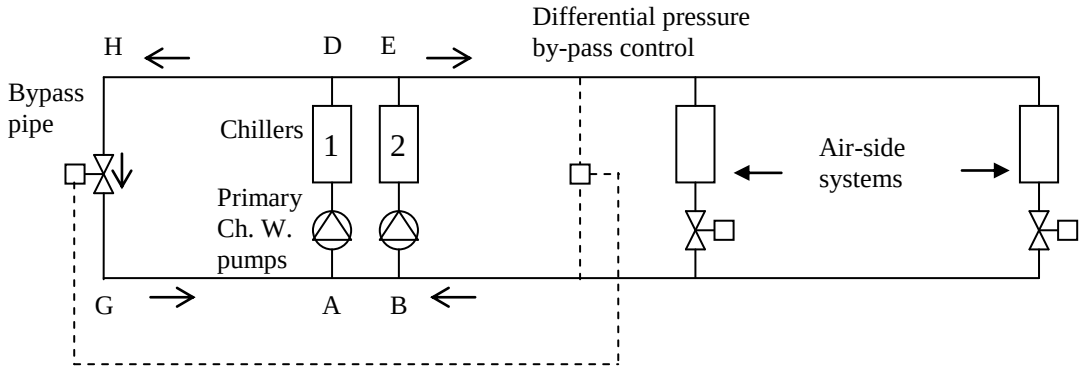

Figure 7A.3 Alternative single-loop pumping system

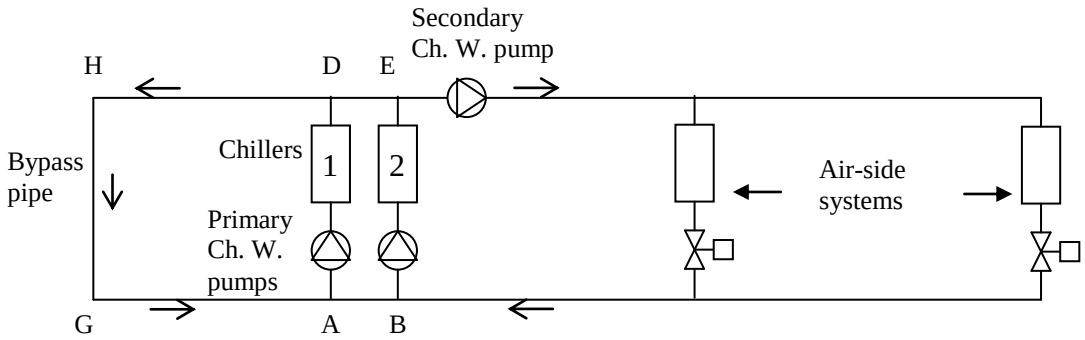

Figure 7A.4 Alternative two-loop pumping system

The single- and two-loop pumping circuits shown in Figures 7A.1 & 7A.2 may be modified to as shown in Figures 7A.3 & 7A.4, respectively. They differ from those shown in Figures 7A.1 & 7A.2 in that the location of the bypass pipe has been relocated to the

left-hand side of the chillers. These chilled water circuit designs have been described by McQuiston et al [12] as a method of distributing cooling load among chillers for achieving higher operating efficiency. The ASHRAE System and Equipment Handbook [13] has also briefly described the differences in load distribution among chillers when the bypass pipe in a two-loop pumping system is located at the left or at the right hand side of the chillers. In the following, the chilled water flow pattern and the load distribution among chillers in systems with these circuit designs, and the practical problem, are discussed, and a method for overcoming the problem is proposed. In particular, how the characteristics of water flow and load distribution in chilled water circuits as shown in Figures 7A.3 & 7A.4 can be beneficially utilized for in-situ measurement of chiller performance is discussed.

7A.3 Water flow pattern and chiller load distribution

With the conventional circuit designs (Figures 7A.1 & 7A.2), the chilled water entering each operating chiller will be at the same temperature. However, with the modified circuit designs (Figures 7A.3 & 7A.4), the operating chillers may be fed with chilled water at different temperatures under certain ranges of cooling load on the chiller plant. If only one of the chillers is running to cope with a total cooling load which is lower than the cooling capacity of the running chiller, the chilled water flow rate that will be delivered to the air-side equipment will be lower than the chilled water flow rate through the running chiller. The surplus chilled water will first flow through the bypass pipe (branch H-G at the left hand side of the chillers) and then mix with the chilled water returning from the air-side equipment before the mixed chilled water enters the running chiller. Under this condition, the running chiller in the plant with the modified chilled water circuit design (Figures 7A.3 & 7A.4) will operate in exactly the same manner as in the plant with the corresponding conventional circuit design (Figures 7A.1 & 7A.2).

When the cooling load on the chiller plant rises beyond the cooling capacity of the running chiller, one more chiller will have to be run to cope with the load. In this case, the flow rate of chilled water returning from the air-side equipment may exceed the flow rate through the rightmost unit (at branch B-E in Figures 7A.3 & 7A.4) among the running chillers, although this is not necessarily the case when the operating characteristics of cooling coils in the air-side equipment are taken into consideration (see further discussions below). As long as the return chilled water flow rate is lower than the total chilled water flow rate through all the running chillers, there will be surplus flow which will flow through the bypass pipe (branch H-G), but the bypassing chilled water, which is at the supply chilled water temperature, will mix with the returning chilled water from the air-side equipment only at the entering point of the leftmost running chiller (point A in Figures 7A.3 & 7A.4).

Under this operating condition, the chilled water entering the rightmost running chiller (at point B in Figures 7A.3 & 7A.4) will be at the temperature of the chilled water returning from the air-side equipment and thus the chiller will be loaded to its full capacity (could be beyond). The remainder of the cooling demand will be coped with by the other running chiller at the left hand side (branch A-D in Figures 7A.3 & 7A.4), while the temperature of the chilled water entering this chiller will be between the temperatures of the chilled water bypassing and returning from the air-side equipment.

For a plant with more chillers and when the cooling load on the plant is rising, the chillers will be loaded to their full capacity one after another in sequence following the direction of the return chilled water flow. Furthermore, the load on a running chiller will start to rise only when all running chillers to its right-hand side have been fully loaded. It follows that, with the circuit designs as shown in Figures 7A.3 & 7A.4, chillers in the plant will have much more chances of being fully loaded.

The operating conditions of chillers in plants with the alternative chilled water circuit designs (Figures 7A.3 & 7A.4) may not be preferable, because the coefficient of performance (COP) of a chiller may not be the highest when it is fully loaded. These circuit designs, however, can make individual chillers run through its entire capacity range as the cooling demand increases or reduces, permitting full- and part-load performance of chillers to be measured within the shortest possible time.

7A.4 Modifications to the alternative water circuit designs

There are practical problems with the alternative circuit designs (Figures 7A.3 & 7A.4) in that chillers can be overloaded. This is because the chilled water temperature difference across a cooling coil will increase as its cooling output is reduced by reducing the flow rate of chilled water fed through the coil, as shown in Figure 7A.5 [14]. Therefore, if the chilled water returning from the cooling coils is allowed to enter a chiller directly, the temperature of the chilled water entering the chiller may exceed the rated entering chilled water temperature of the chiller, which will cause the chiller to be overloaded. With the conventional circuit designs (Figures 7A.1 & 7A.2), this will not happen as the entering chilled water temperature will be lowered due to mixing of the chilled water bypassing and returning from the air-side equipment.

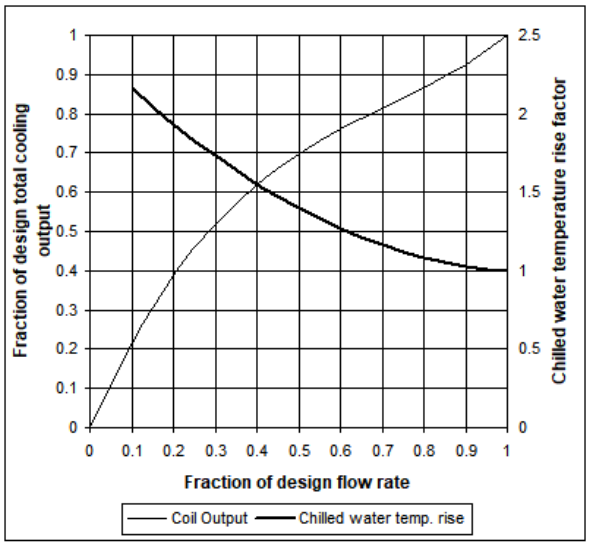

Figure 7A.5 Output and chilled water temperature rise of a cooling coil at reduced chilled water flow rates (Source: Ref. [14])

To overcome the abovementioned problem with the alternative circuit designs, the circuits are further modified to as shown in Figures 7A.6 & 7A.7, respectively. For the single-loop pumping system shown in Figure 7A.6, the differential pressure bypass pipe at the right hand side of the chillers (branch F-C) in the conventional circuit design (Figure 7A.1) together with the differential pressure transmitter for bypass flow rate control are retained, and will be used during normal operation. An additional bypass pipe is installed at the left-hand side of the chillers (branch H-G) for use while chiller performance measurement is being conducted. A chilled water temperature sensor is also installed (between points B & C) downstream of the bypass pipe (branch F-C), for use under the measurement mode. Under normal operation, the differential pressure bypass pipe at the left-hand side of the chillers (branch H-G) should be tightly shut-off and operation of the plant should be exactly the same as the conventional system.

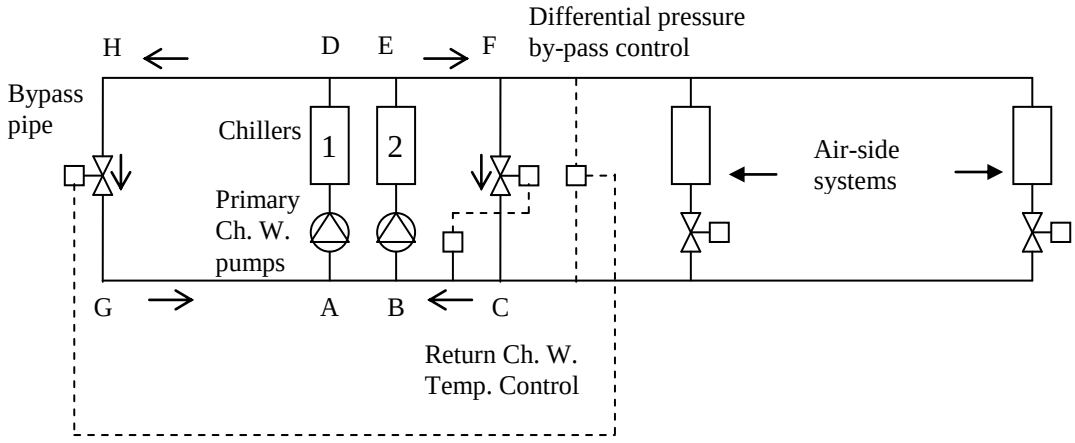

Figure 7A.6 Proposed single-loop pumping system in chiller performance measurement mode

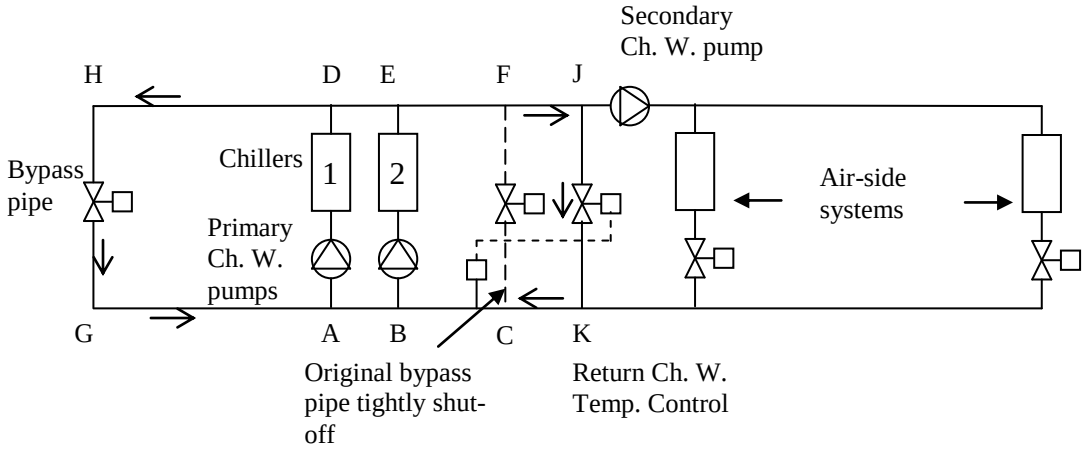

Figure 7A.7 Proposed two-loop pumping system in chiller performance measurement mode

When measurement of full- and part-load performance of chillers is conducted, the differential pressure bypass pipe at the left hand side of the chillers (branch H-G) will be activated, with the bypass control valve in it working under the dictate of the differential pressure signal across the main supply and return pipes, as shown in Figure 7A.6. The original differential pressure bypass control valve at the right hand side of the

chillers (branch F-C) will now be used to control the flow rate of chilled water that will bypass the air-side equipment such that the mixed temperature of the chilled water bypassing and returning from the air-side equipment, as measured by the chilled water temperature sensor (between points B & C), will be kept at the rated entering temperature of the chillers. This helps avoid overloading those chillers that will be fed mainly or entirely with chilled water returning from the air-side equipment.

The modifications to the circuit arrangement for a two-loop pumping system are as shown in Figure 7A.7. The de-coupler bypass pipe of the conventional design (branch F-C in Figure 7A.2) is retained for use during the normal operating mode, while an additional de-coupler bypass pipe is installed at the left hand side of the chillers (branch H-G), for use during the measurement mode. A gate valve (may be motorized) is installed in each of the two de-coupler bypass pipes (branches F-C and H-G) such that only one will be active under either the normal or the measurement mode.

Considering that the pressure drop across a control valve will be quite substantial even when it is fully open but the pressure drop across a de-coupler bypass pipe should be kept at the minimal, an additional bypass pipe (branch J-K), with a control valve in it, is installed for controlling the temperature of chilled water that will enter chillers. This control valve will operate only under the measurement mode, and will open to bypass chilled water according to the mixed chilled water temperature measured by the additional chilled water temperature sensor (between points B & C in Figure 7A.7) downstream of the mixing point of bypass and return chilled water (point K in Figure 7A.7). Similar to the single-loop circuit, the set point for this control system is the rated chilled water entering temperature of the chillers, for avoiding overloading the chillers.

With the proposed circuit designs (Figures 7A.6 & 7A.7), only the leftmost unit among the running chillers will undergo a wide range of load changes, which is needed for testing part-load performance. When a particular chiller is to be tested while the total cooling load is insufficient to load all those chillers at its right-hand side (closer to the air-side equipment) to their full capacity, some of the chillers may be turned-off, to ensure there will be cooling load on the chiller being tested. However, chillers at the right-hand side will have much less chances of being partially loaded. This problem can be overcome by using the supplementary piping circuit shown in Figure 7A.8, which will allow any chiller to be selected as the leftmost unit for a part-load test.

As all running chillers except the leftmost unit will be loaded steadily while the cooling load on those chillers is dependent on the return chilled water temperature, which is under the control of the temperature sensor between points B and C in Figures 7A.6 & 7A.7, when the load on the chiller plant is significantly below the installed capacity of the plant, more chillers can be turned-on and the return chilled water temperature set-point can be re-set upward. This method provides an extra handle for controlling loads on the running chillers for part-load performance tests: it will allow a stable part-load on the running chillers (except the leftmost unit) to be maintained or a specific load on the leftmost unit to be achieved for performance testing.

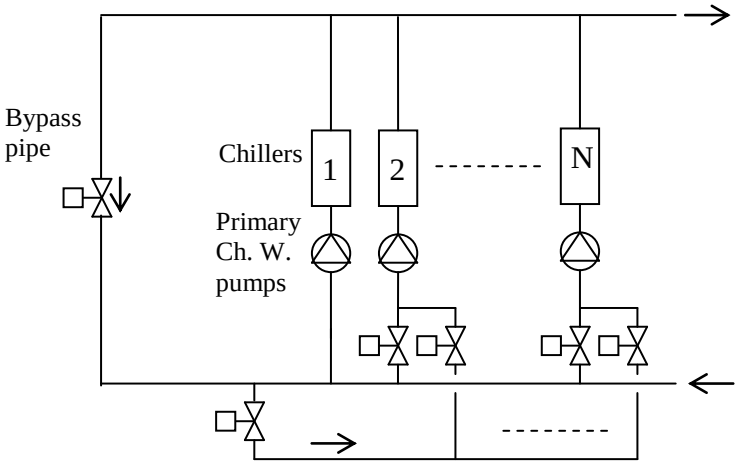

Figure 7A.8 Circuit arrangement that allows any chiller to be switched to become the leftmost chiller from the air-side equipment

7A.5 Condenser air or water entering temperature control

When chiller performance is to be tested under a constant condenser cooling medium entering temperature, additional control devices are needed for controlling the temperature of the condenser water or air, depending on whether the plant is water-cooled or air-cooled. For water cooled chiller plants, a condenser water bypass system, as shown in Figure 7A.9, can be used for this purpose. In fact, such condenser water temperature control systems are standard provisions in water-cooled chiller plants that use cooling towers for heat rejection, to protect the chillers from unstable operation when the entering condenser water temperature becomes too low.

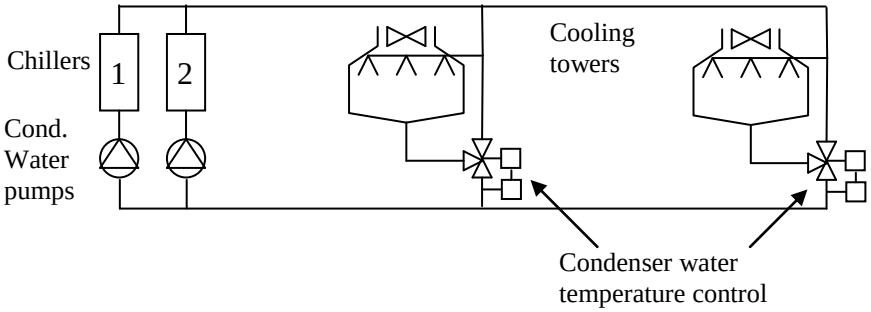

Figure 7A.9 Condenser water temperature control systems for a plant with cooling towers

For an indirect seawater cooled chiller plant with heat exchangers that separate the condenser water circuit from the seawater circuit, condenser water temperature control systems similar to those shown in Figure 7A.9 can be used to control the condenser water flow rates through and bypassing the heat exchangers, such that condenser water at the required temperature can be obtained. For a direct seawater cooled chiller plant, a bypass control system will need to be installed such that a fraction of the warm seawater leaving chiller condensers can be re-circulated and mixed with

the seawater from the supply main pipe such that the temperature of seawater entering condensers of the chillers can be controlled at the required level through regulating the bypass flow rate.

For air-cooled chillers, controlling the entering condenser air temperature will be much more difficult. Testing of air-cooled chillers, therefore, may have to be based on the ambient air temperature available. Alternatively, the number or speed of condenser fans may be regulated such that condensing pressure at the rated level, or at other levels as may be required, can be achieved.

References

[1] Johnson Controls, Application Considerations: Three-way Equal Percentage Flow Characteristic, Valve and Actuator Manual, Johnson Controls, Inc., 1992.

[2] Yik FWH, Chilled water circuit designs for in situ chiller performance measurement, Building Services Engineering Research and Technology 2008, 29(2): 107-118.

[3] Trane, Variable-Primary-Flow Systems Revisited, Engineers Newsletter, American Standard Inc., 2002, Vol. 31, No.4.

[4] CIBSE Commissioning Code W: Water distribution systems, Chartered Institution of Building Services Engineers, 2010.

[5] ASHRAE Guideline 1-1996: The HVAC Commissioning Process. American Society of Heating, Refrigerating and Air-conditioning Engineers, Inc., 1996.

[6] Piper JE. Operations and Maintenance Manual for Energy Management. New York: Sharpe Professional, 1999.

[7] Gordon J, Ng KC. Centrifugal chillers: thermodynamic modelling and a diagnostic case study. International Journal of Refrigeration 1995; 18(1):31-41.

[8] Katipamula S, Brambley MR. Methods for fault detection, diagnostics and prognostics for building systems – A review, Part I. International Journal of heating, Ventilating, Air Conditioning and Refrigerating Research 2005; 11(1): 3-25.

[9] Katipamula S, Brambley MR. Methods for fault detection, diagnostics and prognostics for building Systems – A review, Part II. International Journal of heating, Ventilating, Air Conditioning and Refrigerating Research 2005; 11(2): 169-187.

[10] Cui J, Wang SW. A model-based online fault detection and diagnosis strategy for centrifugal chiller systems. International Journal of Thermal Science 2005; 44(10): 986-999.

[11] ASHRAE Guideline 14-2002: Measurement of Energy and Demand Savings. American Society of Heating, Refrigerating and Air-conditioning Engineers, Inc., 2002.

[12] McQuiston FC, Parker JD, Spitler JD. Heating, Ventilating and Air Conditioning Analysis and Design, 5th Ed. John Wiley & Sons, Inc. 2000; p.336.

[13] ASHRAE Handbook, Systems and Equipment, Ch.12, p.12.12. American Society of Heating, Refrigerating and Air-conditioning Engineers, Inc., 2000.

[14] Yik FWH. Analyses of operations of control valves in air-conditioning systems comprising multiple chillers and chilled water pumps. Transactions, The Hong Kong Institution of Engineers 2001; 8(3): 51-57.

Chapter 8 Water-side System Pipe Sizing and Control Valve Selection

8.1 Design process for the water-side system

Based on the estimated design cooling loads of air-conditioned spaces in a building, we can determine the requirements on the cooling capacity, supply air flow rate and chilled water flow rate of individual air-handling equipment serving those spaces. Rather than summing up the chilled water flow rate requirements of all the air-handling equipment, the total chilled water supply flow rate that the central chiller plant should be able to deliver should be determined from the estimated design block cooling load of the building. As explained in Chapter 3, the diversity in occurrence of peak cooling demands of the spaces is accounted for in estimation of the block cooling load. It, therefore, is a more realistic basis for determination of the central plant capacity.

Following design cooling load estimation, design decisions would need to be made regarding the type of heat rejection system, the type of chilled water pumping system, the number of chillers and pumps and, where required, other chiller plant equipment, e.g. seawater pumps, condenser water pumps and cooling towers, to be adopted. Decisions would need to be made also on the locations of the air-handling equipment, e.g. in AHU rooms preserved for their accommodation or within the air-conditioned space, as well as the location of the chiller plant and, where applicable, the locations of the other major equipment, in the building.

Multiple chiller units would typically be adopted to allow adjustment of cooling capacity to meet the varying cooling load by turning chillers on and off, which will help uphold the operating efficiency of the chillers. The reliability of the chiller plant would also be enhanced with multiple units because a large percentage of the installed cooling capacity would remain available when one of the chillers is out of order or needs to be set aside for maintenance. Each chiller would typically be equipped with a chilled water pump or primary-loop pump of matching design water flow rate, and one more unit would typically be added as standby. Similar consideration would be given to condenser water pumps and cooling towers, which would ease operational control.

When the above design work has been done, we may proceed to determining the pipe routing for distribution of the chilled water supply from the chiller plant to individual air-handling equipment, and the chilled water flow rates to be carried by individual supply and return pipe sections in the piping network. The required pipe routing is dependent on the locations of the main chiller plant room, the air-handling equipment or their plant rooms, and locations of pipe ducts available for installation of riser pipes. Whilst the routing of chilled water pipes from the chiller plant to the air-handling equipment would be the same, the pipe routing within the chiller plant room would depend on which chilled water pumping system is chosen for the building.

The next step would then be determination of the required sizes of the pipes and the pressure drops that would be incurred by chilled water flowing through the pipe sections at the estimated flow rates. With this result, we may proceed to selection of control valves for the air-handling equipment and then selection of chilled water pumps. Besides the considerations to be given to pipe sizing and control valve selection, detailed explanation on why control valves would need to be selected before pump

selection will be given in this chapter. Where applicable, similar considerations as outlined above are to be given to the condenser and/or seawater circulation systems.

Good planning would help avoid unnecessary pipe runs and bends, leading to optimal use of pipe and insulation materials and minimum possible pressure losses and pumping energy use. Additionally, the architect should be made aware of the space and building work requirements of the air-side and water-side systems at an early stage of the building design process to ensure the system can be installed as planned.

8.2 Pressure loss estimation and pipe sizing

Pipe sizing, i.e. selection of a pipe of a certain diameter for conveying a given water flow rate, involves a compromise between the first cost and the running cost of the system. A pipe of a larger diameter is more expensive than a smaller pipe but the pressure loss that the water flow would incur is smaller with the larger pipe, which means less pumping energy would be needed to drive water flow at the required flow rate. Pipe sizing is typically guided by an allowable pressure drop per unit pipe length. Other considerations include the flow generated noise which should be kept low by limiting the flow velocity inside a pipe below a maximum tolerable level.

To inform pipe sizing, we need to know the relation between flow rate or velocity inside a pipe of a given diameter and the corresponding pressure drop that would be incurred. The fundamental principles governing air flow through ducts and fittings, which are covered in Chapter 5, apply equally to water flow through pipes and fittings. The major fluid mechanics relations that we need to use for pipe sizing include:

i) The Bernoulli's equation applicable to fluid flow along a pipeline:

$$p_1 + \rho\frac{u_1^2}{2} + \rho g z_1 = p_2 + \rho\frac{u_2^2}{2} + \rho g z_2 + \Delta p_l \qquad (8.1)$$

Where p is static pressure, ρ fluid density, u flow velocity, g the gravitational acceleration, z height above a datum level, and Δp_l pressure loss. The subscripts 1 & 2 denote two locations along the streamline over which the pressure loss is incurred.

ii) The Darcy–Weisbach equation for fluid flow inside a duct or pipe of uniform internal diameter, for evaluation of the pressure loss term in the Bernoulli's equation:

$$\Delta p_l = f \cdot \frac{L}{D} \cdot \rho\frac{u^2}{2} \qquad (8.2)$$

Where f is the friction factor, L the pipe length and D the pipe diameter.

iii) The Colebrook's equation, for evaluation of the friction factor in the Darcy-Weisbach equation:

$$\frac{1}{\sqrt{f}} = -2\log\left(\frac{k}{3.7D} + \frac{2.51}{Re\sqrt{f}}\right) \qquad (8.3)$$

Where Re is Reynold's Number, defined as:

$$Re = \frac{\rho \cdot u \cdot D}{\mu} \tag{8.4}$$

And k is the surface roughness of the internal pipe wall, and μ the viscosity of the fluid.

Equation (8.3) is used mainly in calculation routines implemented in a computer but is seldom used in manual calculations because it is an implicit equation involving the unknown f on both sides which requires the use of an iterative procedure to solve. Alternatively, a graph showing how the friction factor will vary with surface roughness and diameter of a pipe and with the Reynold number (proportional to the flow rate), typically called a Moody diagram as shown in Figure 8.1, can be used for evaluation of the friction factor.

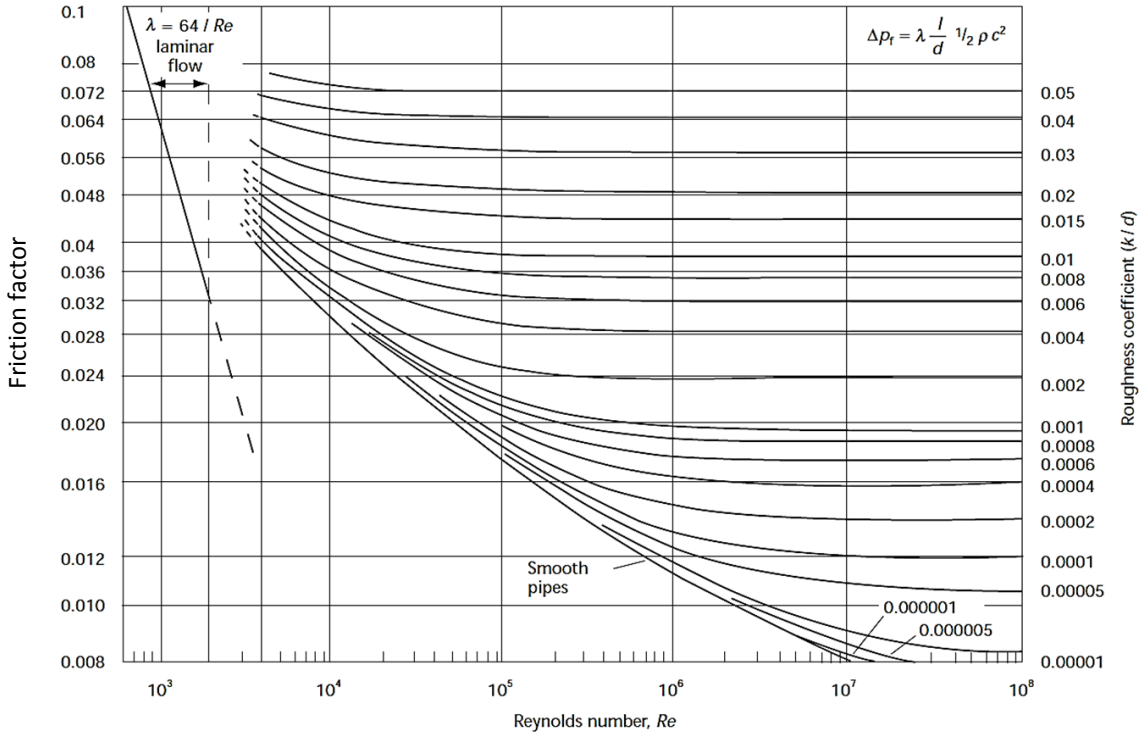

Figure 8.1 Moody diagram (friction factor denoted as λ in this diagram)

For a specific fluid, e.g. water, and a specific type of pipe, e.g. galvanized iron (GI) pipe or black steel pipe, graphs or tables showing the pressure loss per unit length and flow velocity for pipes of different nominal sizes when applied to convey a given range of flow rate may be constructed to facilitate pipe sizing. Such graphs and tables may be found in handbooks, e.g. [1, 2], and textbooks, e.g. [3, 4], in the air-conditioning field. Figure 8.2 shows an example of pipe frictional loss chart for pipe sizing.

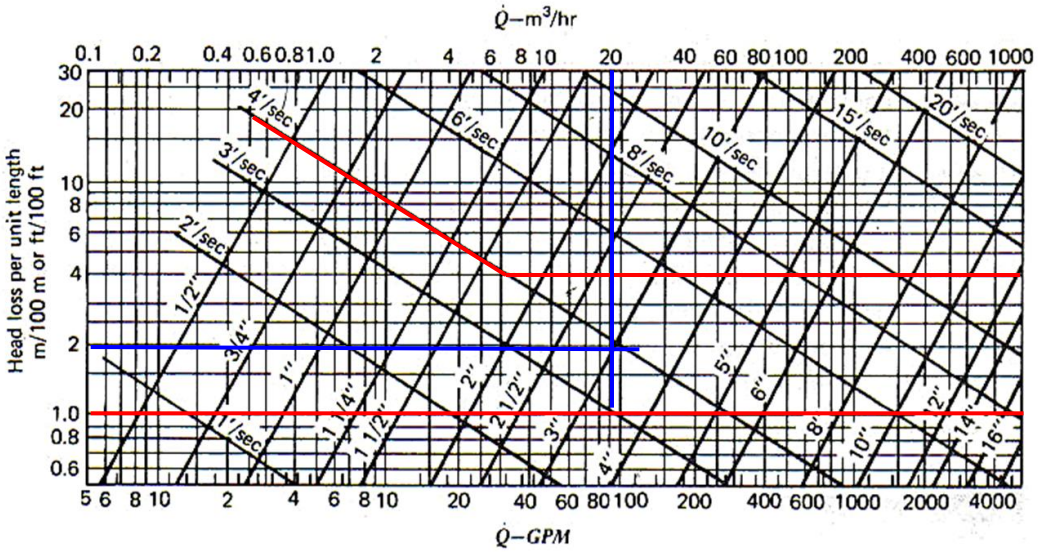

Figure 8.2 Pipe frictional loss chart for sizing steel pipes conveying water

The recommended pipe sizing criteria [1] are that for pipe size < 50mm, flow velocity should not exceed 1.2m/s and, for larger pipes, the pressure drop should not exceed 400 Pa/m. Pipes sized may have pressure drop per unit length ranging from 100 to 400 Pa/m, averaged at around 250 Pa/m. These thresholds have been shown in Figure 8.2 as lines for an upper limit and a lower limit and operating conditions between these two lines are considered adequate. For example, for a flow rate of 20m^3/h, we may use a pipe of 75mm diameter in which case the flow velocity would be slightly below 1.2m/s ($\approx$ 4 ft/s) and the pressure loss slightly lower than 200 Pa/m ($\approx$ 2 mH_2O/100m pipe run) (Figure 8.2).

For pipe fittings, such as bends, tees and joints, and other system components, such as coils, valves, strainers, etc., local loss coefficient and velocity pressure are also used for quantification of pressure loss.

$$\Delta p = C \cdot \frac{1}{2}\rho u^2 \tag{8.5}$$

Unlike air ducts, water pipes are typically circular in cross-section and, therefore, there is no need for the concepts of hydraulic mean diameter and equivalent diameter in quantification of pipe pressure losses. Nevertheless, similar approach can be used to determine the overall pressure drop of a piping system from the pressure loss characteristics of components in the system, including components in series and parallel configurations. Tables and charts that provide pressure loss characteristics of pipe fittings are also available in relevant handbooks and guides, such as the ASHRAE Handbook, Fundamentals [1] and CIBSE Guide C [2].

An alternative method for quantification of the pressure loss characteristics of fittings and system components is to express the loss of a fitting or system component in terms of the length of a straight pipe of the same material and diameter which will incur the same pressure drop as the fitting or system component while passing the same fluid at

the same flow rate. This measure is called equivalent length, which is a convenient method for pipe loss calculations: the equivalent lengths of the fittings and system components may simply be added to the physical lengths of the pipe run to get the total equivalent length and this may be multiplied by an average pressure drop per unit length to yield the overall pressure drop through a pipeline or an entire system.

At an early stage of design development, a rule of thumb may be used for making allowances for fitting pressure losses. A common practice is to assume that fitting pressure losses would be about 50 to 100% of the total loss of the pipes along the pipe run. However, such results should be checked and corrected when more details of the design become available.

8.3 Control valves

As highlighted in the discussion on chilled water pumping systems given in Chapter 7, the key functions of control valves, including two-way and three-way valves, are to:

- Modulate the output of a heating or cooling coil for maintaining the temperature of the supply air or indoor space at the set point level.

- Keep the pressure difference across two points in a piping network at the set point level, e.g. in differential pressure bypass control for ensuring constant chilled water flows through chillers in a single-loop pumping system.

- Control water flow rate, e.g. in differential pressure bypass control for ensuring the secondary loop pumps in a two-loop pumping system will not run into the surge zone, and in minimum flow rate control for protecting chillers in a variable primary flow (VPF) system.

Control valves in air-conditioning systems may also be used to control water temperature, through regulation of water flow rates from two streams that would mix with each other, e.g. for cooling tower water leaving temperature low limit control, or that would exchange heat via a heat exchanger, e.g. for control of leaving chilled water temperature at the secondary-side of a heat exchanger that serve as a pressure break in a super-tall building.

Properly functioning control valves are crucial to satisfactory performance of air-conditioning systems. Unfortunately, the principles behind proper control valve selection are often not well understood, resulting in improper valve selection which is undesirable. Undersized control valves will give rise to degraded system output or excessive pumping energy use whilst oversized control valves will lead to poor control performance, such as hunting.

In the following, the key characteristics of control valves and proper selection criteria will be elucidated. Problems with inadequate control valves will be explained and discussed. Common causes of confusion and misconceptions will also be highlighted.

8.3.1 Control valve characteristics

A control valve is basically a flow restriction with variable flow resistance. Figure 8.3 shows the internal parts of a two-way control valve. Its flow resistance can be adjusted by varying the degree of opening of the valve, quantified by the valve lift, *Z*, also called valve stroke or travel, which is the linear displacement of the valve plug measured from the fully closed position (Figure 8.4). Its flow resistance is the lowest when the valve is fully open and reaches an extremely high value when the valve is fully closed. The movement of the valve plug is driven by a valve actuator, which may be a pneumatic actuator (Figure 8.3) or an electric actuator. Nowadays, pneumatic actuators are used mainly for large valves and electric actuators are more commonly used in air-conditioning systems in commercial buildings.

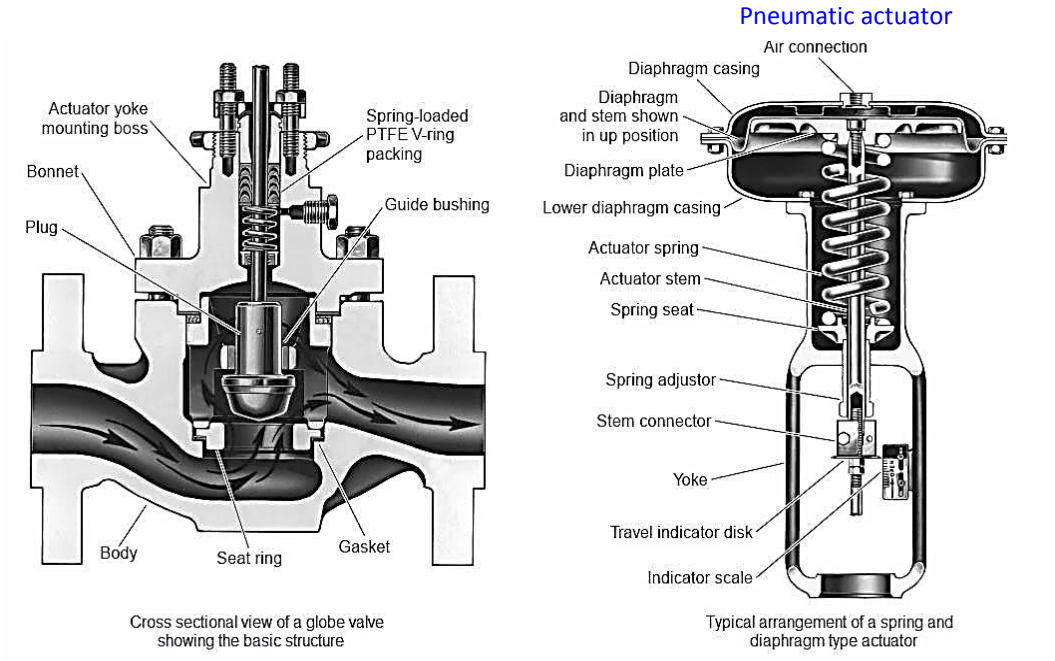

Figure 8.3 Cross-sectional views of a control valve and valve actuator

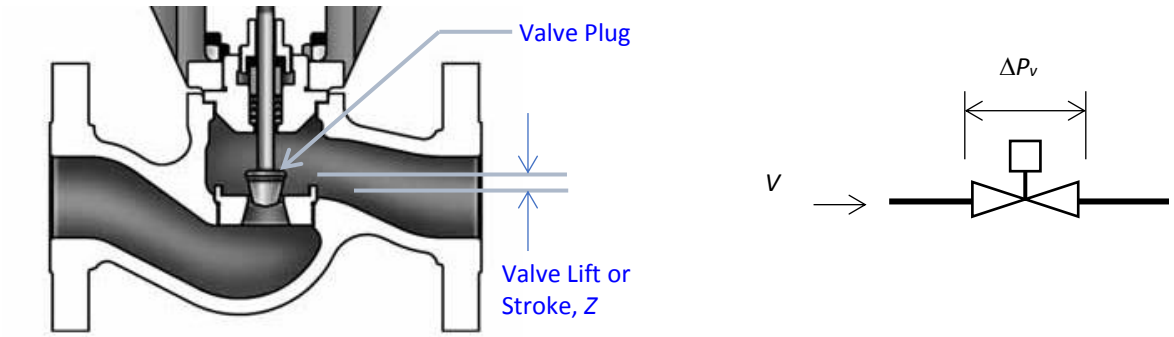

Figure 8.4 The valve plug position, quantified by the lift or stroke (left), and typical symbol used to denote a control valve (right)

i) Flow coefficient of control valve

When an incompressible fluid is flowing steadily, under fully turbulent condition, through a flow restriction with a fixed resistance, such as a control valve with its valve lift fixed, the relation between the pressure drop across the flow restriction and the flow rate through it can be written, according to Equation (8.5), as:

$$\Delta P = k\frac{1}{2}\rho u^2 = k\frac{1}{2}\rho\left(\frac{V}{A}\right)^2 \tag{8.6}$$

Where

ΔP = pressure drop across the flow restriction
k = proportionality constant
ρ = density of fluid
V = volume flow rate of fluid
A = flow cross-sectional area of flow restriction

For a particular control valve at a given valve lift (Z), the above equation may be re-arranged to:

$$\sqrt{\frac{\Delta P_v}{\rho}} = \frac{\sqrt{k}}{\sqrt{2}\cdot A}V$$

$$V = C\sqrt{\frac{\Delta P_v}{\rho}} \tag{8.7}$$

where ΔP_v is the differential pressure across the control valve (Figure 8.4).

Since the flow resistance of a control valve will change with the valve lift, Z, the value of the coefficient, C, in the above equation is a function of Z. This implies that, for each modular size of control valve of a particular design, a set of C values corresponding to a range of Z values, or a curve or an equation relating the two, is needed to represent its characteristics, which is rather cumbersome.

It is a conventional practice to specify the performance of a control valve separately for the fully-open characteristic, which is related to its flow capacity, and the characteristics at different degrees of valve opening, which affects its control performance. The following equation is commonly used to describe the relationship between the flow rate and pressure drop across a fully open control valve:

$$V = C_v\sqrt{\Delta P_v} \tag{8.8}$$

With the understanding that the fluid under concern is always water, the density term in the equation has been dropped. The coefficient C_v in the equation is called the 'flow coefficient', which is a measure of the valve capacity (or size), and thus a key parameter for valve sizing.

A closer look at this equation unveils that the flow coefficient (C_v) carries dimension, which is in the unit derived from the unit of flow rate divided by the square root of the unit of pressure. Its value, therefore, is dependent on the units used to quantify flow rate and pressure. Conventionally, flow rate and pressure are measured, respectively, in (UK or US) GPM (gallon per minute) and PSI (pounds per square inch). Corresponding to these units (but often not explicitly mentioned), C_v is used as the symbol for flow coefficient, and referred to directly as 'Cee-Vee'.

Alternative forms of the flow-pressure drop relationship (Equation (8.8)) for metric / SI units include:

The metric version:

$$V = K_v\sqrt{\Delta P_v/\rho} \tag{8.9a}$$

where K_v is the flow coefficient, and V is in m^3/h, ΔP_v in bar & ρ in kg/m^3.

A simplified version commonly used (for water):

$$V = K_v\sqrt{\Delta P_v} \tag{8.9b}$$

where K_v is the flow coefficient, and V is in m^3/h & ΔP_v in bar.

The SI version adopted in BS4740:

$$V = A_v\sqrt{\Delta P_v/\rho} \tag{8.9c}$$

where A_v is the flow coefficient, and V is in m^3/s, ΔP_v in Pa & ρ in kg/m^3.

Multiplying factors for conversion of flow coefficient in one unit to another are as summarized in Table 8.1.

Table 8.1 Multiplying factors for conversion between flow coefficients (ρ = 1000kg/m³)

From ↓ To →	C_v (US)	C_v (UK)	K_v (Eq. 8.9a)	K_v (Eq. 8.9b)	A_v
C_v (US)	1	0.8327	27.35	0.8650	24.03×10^{-6}
C_v (UK)	1.201	1	32.85	1.039	28.86×10^{-6}
K_v (Eq. 8.9a)	0.03656	0.03044	1	0.03162	0.8784×10^{-6}
K_v (Eq. 8.9b)	1.156	0.9626	31.62	1	27.78×10^{-6}
A_v	41.62×10^3	34.65×10^3	$1{,}138 \times 10^3$	36.00×10^3	1

ii) Inherent characteristics of control valve

With the capacity of a fully-open control valve quantified by the flow coefficient, a normalized characteristic curve may then be used to show the change in flow rate with valve lift, or vice versa, for a series of control valves designed to exhibit that flow-lift characteristic. Such a curve is called the 'inherent characteristic' of a control valve, denoted by:

$$v = f(z) \quad \text{or} \quad z = g(v) \tag{8.10}$$

Where v and z are, respectively, normalized flow rate and normalized valve lift, defined as follows:

$$v = V/V_O \tag{8.11}$$

$$z = Z/Z_O \tag{8.12}$$

In the above equations, V is the flow rate when the valve lift is Z and V_O & Z_O are the fully-open flow rate and maximum valve lift. Since, at a fixed valve lift, the flow rate will still vary with the differential pressure (ΔP_v) across the control valve, an inherent characteristic curve can only be defined under a constant ΔP_v across a control valve when the valve lift is varied. Figure 8.5 shows some inherent characteristic curves of control valves.

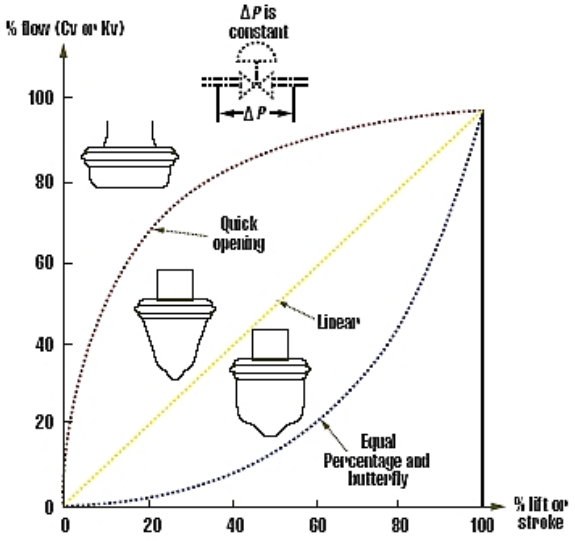

Specific inherent characteristics can be achieved through varying valve plug design.

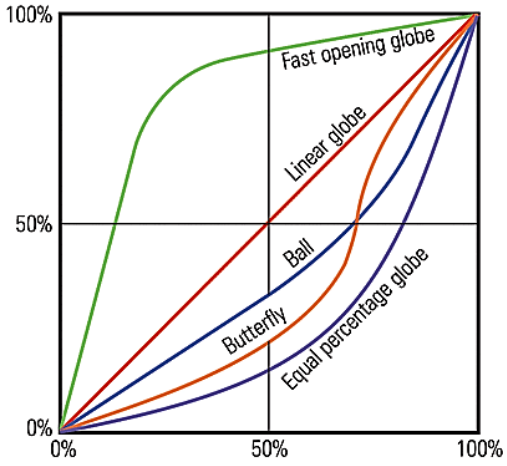

Inherent characteristics of typical types of control valve.

Figure 8.5 Inherent characteristics of control valves

As the inherent characteristic curves show (Figure 8.5):

1) A quick opening valve will allow the flow rate to rise from zero to a high percentage of the full-flow rate when the valve is opened from the fully closed

position to a small valve lift. Such valves are suitable for equipment that are expected to deliver a large output within a short duration after being put into operation.

2) For a linear valve, the change in flow rate would be directly proportional to the valve lift, which should provide good control characteristic, but this would be the case only if the differential pressure across the control valve would remain relatively stable.

3) For an equal percentage valve, the change in the flow rate per unit change in the valve lift is proportional to the current flow rate (see equation below), i.e. the change in flow rate will be large if the current flow rate is large, and vice versa:

$$\frac{dv}{dz} = K \cdot v \qquad (8.13)$$

where K is the proportionality constant. Note that Equation (8.13) is undefined when v approaches zero, which can be clearly seen when it is integrated:

$$\frac{dv}{v} = K \cdot dz$$

$$\ln v = K \cdot z + A \qquad \text{where } A \text{ is an integral constant}$$

The boundary condition $z = 0$ & $v = 0$ should allow us to evaluate A but the result is $-\infty$. This, however, is not a serious restriction to the application of Equation (8.13) to equal percentage valves as long as it is not applied to a valve lift too close to zero.

Using the boundary condition $z = 1$ & $v = 1$, we get

$$0 = K + A \qquad \text{or} \qquad A = -K$$

$$\ln v = K(z - 1) \qquad \text{or} \qquad v = \exp[K(z - 1)]$$

The value of K can be determined by curve fitting the inherent characteristic curve of a given equal percentage valve.

As will be shown in later discussions, equal percentage valves are preferred in many applications to HVAC systems for the better overall control performance that they can offer.

iii) Installed characteristics

The flow coefficient (K_v) in conjunction with the inherent characteristic curve ($v = f(z)$) will allow the flow rate (V) that the control valve will let pass at a particular valve lift (Z) and under a given differential pressure (ΔP_v) to be determined by following the calculation steps given below:

1) $V_O = K_v\sqrt{\Delta P_v}$

2) $z = Z/Z_O$

3) $v = f(z)$

4) $V = v \cdot V_O$

Note that V_O above denotes the flow rate when the control valve is fully open while the pressure difference across it is at the SAME ΔP_v value as in the case being evaluated. Here, V_O is most likely different from the design flow rate of the control valve.

Alternatively, we may need to determine the valve lift (Z) for achieving a particular flow rate (V) under a given differential pressure (ΔP_v) for a control valve with known flow coefficient (K_v) and inherent characteristic ($z = g(v)$). The steps for this evaluation are:

1) $V_O = K_v\sqrt{\Delta P_v}$

2) $v = V/V_O$

3) $z = g(v)$

4) $Z = z \cdot Z_O$

In both examples above, the differential pressure across the control valve (ΔP_v) is a known quantity. However, in practice, this would often not be the case, which can be seen if the last example is applied to a pumped piping circuit with a constant speed pump (Figure 8.6). For this system, the design operating point is shown as the intersection point of the pump curve and the system curve with the control valve fully-open and passing a flow rate of V_D. A system curve with the pressure loss incurred by the control valve that is kept at the fully-open state discounted can be plotted, as shown by the broken line curve in Figure 8.6. Therefore, the vertical distance between this system (broken line) curve and the pump curve represents the pressure drop to be throttled off by the control valve.

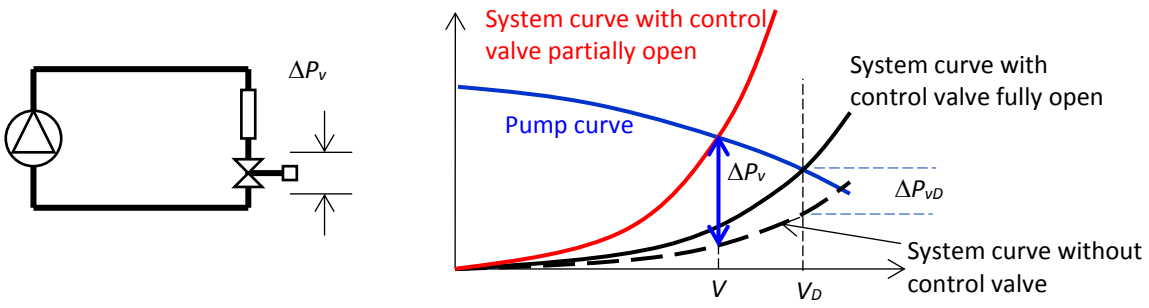

Figure 8.6 The pressure across the control valve in a pumped circuit

As shown in Figure 8.6, the differential pressure across the control valve will increase from ΔP_{vD} to ΔP_v when it is required to reduce the flow rate passing through it by reducing its valve lift from Z_O to Z. Since the inherent characteristic of a control valve will be valid only if the differential pressure across the control valve is held constant, the first task to be done in this example would be to evaluate ΔP_v when the flow rate through the system is V, e.g. by a graphical analysis similar to Figure 8.6.

The rise in differential pressure across the control valve implies that the valve lift will need to be reduced to a value (z) that is smaller than what can be found from the inherent characteristic curve for the same flow rate (z_D) as shown in Figure 8.7, where the control valve is assumed to have a linear inherent characteristic, viz. $g(v_D)$.

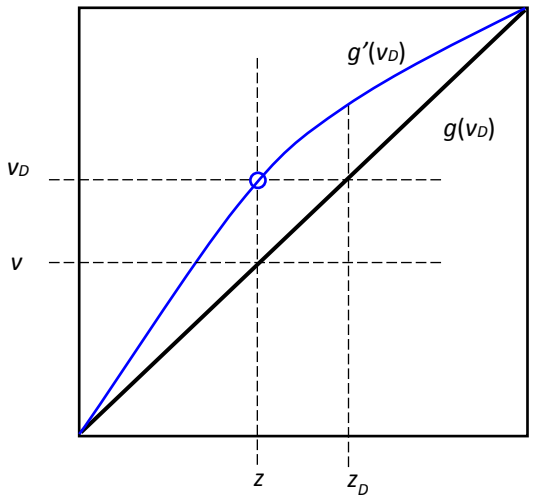

$$V_O = K_v\sqrt{\Delta P_v}; \qquad V_{OD} = K_v\sqrt{\Delta P_{vD}}$$

$$V_O > V_{OD}$$

$$v = V/V_O; \qquad v_D = V/V_{OD}$$

$$v < v_D$$

$$z = g(v); \qquad z_D = g(v_D)$$

$$z = g'(v_D)$$

Actual valve lift required $= Z = z \cdot Z_O$

Figure 8.7 The inherent and installed characteristics curves of a control valve

By using the fully open flow rate (V_{OD}) under the design pressure difference (ΔP_{vD}) as the basis for normalization of the actual flow rate (V), the normalized flow rate (denoted by v_D) would be greater than v obtained by normalizing V by the flow rate that would result when the control valve is fully open under the actual differential pressure across the control valve (ΔP_v) (Figure 8.7). The point representing the combination of v_D and z can be plotted side by side with the inherent characteristic curve of the control valve ($g(z)$) (Figure 8.7). Repeating the process for a range of operating conditions will allow a response curve ($z = g'(v_D)$) for the system to be constructed. Such a curve is called the 'installed characteristic'.

Compared to its inherent characteristic, the installed characteristic of a control valve will look like a distorted version of the inherent characteristic toward the upper left direction. The distortion will be severer the greater the increase in the differential pressure across the control valve when it closes so as to reduce flow rate. Control performance will become poor if the installed characteristic becomes too steep (Figure 8.8). Use of equal percentage valve, therefore, will help alleviate this problem.

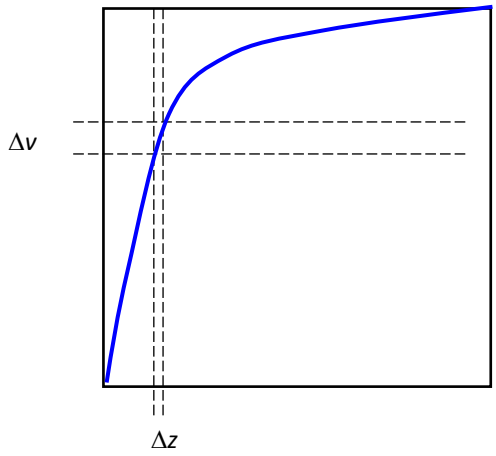

The steep slope of the installed characteristics curve means a small change in valve lift would result in a large change in flow rate. If the required precision in positioning the valve lift to get the right flow rate cannot be met, more than the required reduction in flow rate may result when the valve is slightly closed. The valve will soon be required to open wider as the flow rate is less than that required but the correction may also be more than required. Such repeated corrective actions would lead to hunting.

Figure 8.8 A steep installed characteristics curve of a control valve

8.3.2 Control valve selection

In selecting a control valve for an application, attention should be given to ensure:

1) The size of the control valve is appropriate such that it can pass the design flow rate when subject to the differential pressure that will be available under the design operating condition without incurring too high a pumping pressure requirement on the chilled water pumps.

2) The control valve can provide adequate control performance, with respect to regulation of system output rather than flow rate, under part-load conditions without hunting.

3) The control valve can stop water flow completely when fully closed, i.e. remain tightly shut-off, or will let by a small flow rate, which is a design feature for prevention of water freezing into ice in hot water systems.

From the above discussion on installed characteristics of a control valve in a system, we can also see that the choice of the design differential pressure across a fully-open control valve when the valve is passing the design flow rate (ΔP_{vD}) can affect the flow control performance of control valves (Figure 8.7). The installed characteristic curve would be curved toward the left upper corner of the graph by a greater extent if the value of ΔP_{vD} is reduced, and a steep installed characteristic curve at the low flow rate region would lead to poor control performance (Figure 8.8). This can be alleviated by selecting a smaller control valve which will incur a larger ΔP_{vD}, but this implies the need for a higher pumping pressure.

Therefore, a proper balance needs to be struck between pumping pressure, and hence pumping energy consumption, and flow control performance. The most widely used design parameter to guide control valve selection is the valve authority, N, as defined below:

$$N = \frac{\Delta P_v}{\Delta P_v + \Delta P_R} \tag{8.14}$$

Where ΔP_v is the pressure drop across the control valve in the fully open state and ΔP_R the pressure drop of the remainder of the circuit, both evaluated when the flow rates of all involved components in the circuit are at their respective design values. Note that:

$$\Delta P_P = \Delta P_v + \Delta P_R \tag{8.15}$$

Where ΔP_P is the design pump pressure. Therefore, Equation (8.14) may also be written as:

$$N = \frac{\Delta P_v}{\Delta P_P} \tag{8.16}$$

Figure 8.9 shows the relation among these pressures.

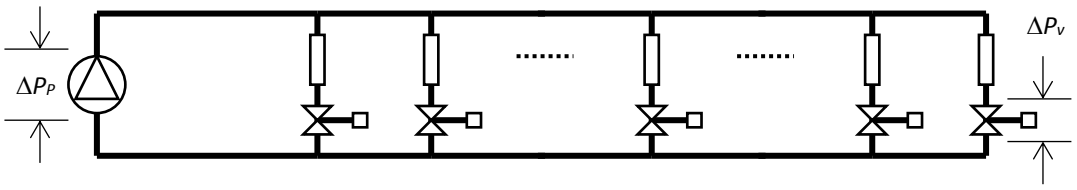

Figure 8.9 Pump pressure and pressure drop across control valve

In a water pumping system with multiple branches as shown in Figure 8.9, water flow through each branch will undergo a complete loop, referred to as a circuit. Note that ΔP_R, the pressure drop of the remainder of the circuit, includes the pressure drops incurred by all components in a circuit except that of the control valve. This means that the pressure losses through the main supply and return pipes, the branch pipe, the coil, and the fittings in the circuit are all included.

With the same pump in each of the branch circuits, the pump pressure is the same for all the branches. This implies that the sum of ΔP_v & ΔP_R is the same among all branches in a pumped water network with a single pump or a single group of pumps in parallel. Hence, if all branches in the system are identical in terms of their design flow rates and are installed with control valve of the same model and size, they would have the same ΔP_v value while passing the same design flow rate provided their ΔP_R values are adjusted to the same value, such as by balancing [5].

In designing a chilled water pumping system, ΔP_R can be evaluated based on design information, including pressure drop per unit length and pipe run of individual pipe sections, pressure drops across equipment components and fittings involved, etc. This calculation needs to be done for circuits that have the potential to be the critical circuit, i.e. the circuit with the highest ΔP_R value. With the critical circuit identified and its ΔP_R evaluated, and a minimum valve authority value (N_m) chosen, we may proceed to determine the minimum fully-open pressure drop of the control valve (ΔP_v) for the critical circuit when it is passing the design flow rate, using Equation (8.17) obtained by solving for ΔP_v from Equation (8.14).

$$\Delta P_v = \frac{N_m}{1-N_m}\Delta P_R \tag{8.17}$$

The above result would be the minimum pressure drop of the control valve to be selected when it is fully-open while passing the design flow rate, but, in practice, a control valve that would lead to a ΔP_V value slightly higher than the minimum may have to be adopted. The required pump pressure can then be determined from the sum of ΔP_V and ΔP_R (Equation (8.15)). The actual valve authority will then be:

$$N = \frac{\Delta P_v}{\Delta P_P} \tag{8.18}$$

As illustrated above, pump selection can only be done after selection of control valve for the critical circuit. For all other branches, the minimum ΔP_V value is given by:

$$\Delta P_v = N_m \Delta P_P \tag{8.19}$$

Control valves for all branches except the critical branch should be selected to meet as close as possible this minimum ΔP_V value, and always subject to the condition that:

$$N_m \Delta P_P \leq \Delta P_v \leq (\Delta P_P - \Delta P_R) \tag{8.20}$$

Figure 8.10 shows the ways in which the pressure drop of the remainder of the circuit, which is split into the pressure drop of the supply side (ΔP_{rs}) and the pressure drop of the return side (ΔP_{rr}) of the remainder of the circuit ($\Delta P_R = \Delta P_{rs} + \Delta P_{rr}$), may be defined for valve authority calculation for different types of chilled water pumping systems, using Equation (8.14). For the secondary-loop of a two-loop pumping system (Figure 8.10a), this definition is same as the general definition discussed above.

For the single-loop pumping system with differential pressure bypass control (Figure 8.10b), since the differential pressure bypass control can maintain the pressure difference across the bypass path at a stable level, this stable pressure differential may be taken as the 'effective pump pressure' and thus the remainder of the circuit may start from and end at the connection points of the bypass pipe to the main supply and return pipes. For a single-loop pumping system with three-way valves (Figure 8.10c), given that the control valve operation will not affect significantly the total flow rate and pressure drop through each branch, only the pressure drops within the branch need to be considered.

As mentioned above, trade-off is needed between good control performance, which requires a larger valve authority value, and pumping energy use conservation, which requires a smaller valve authority value. Most handbooks recommend the use of a minimum valve authority value of 0.5 but in practice, reasonably good performance can be achieved when the valve authority value is greater than 0.3 provided equal percentage valves are used [6]. Besides compensating for the curvature of the installed characteristic, the inherent characteristic of an equal percentage valve can also compensate for the relation between output of heating and cooling coils and the hot or chilled water flow rates through the coils, as illustrated in Figure 8.11. A case study that illustrates the effects of choosing different valve authority values in selection of control valves is given in Annex 8A for reference.

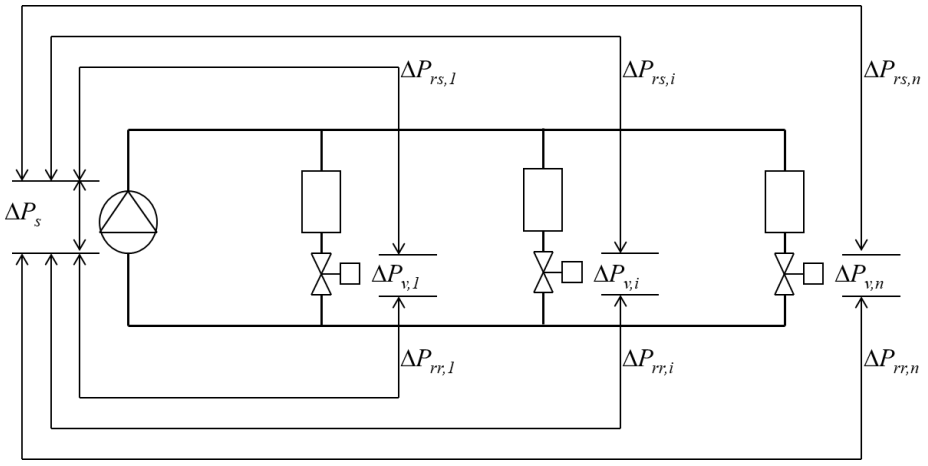

a) Secondary-loop in a two-loop pumping system

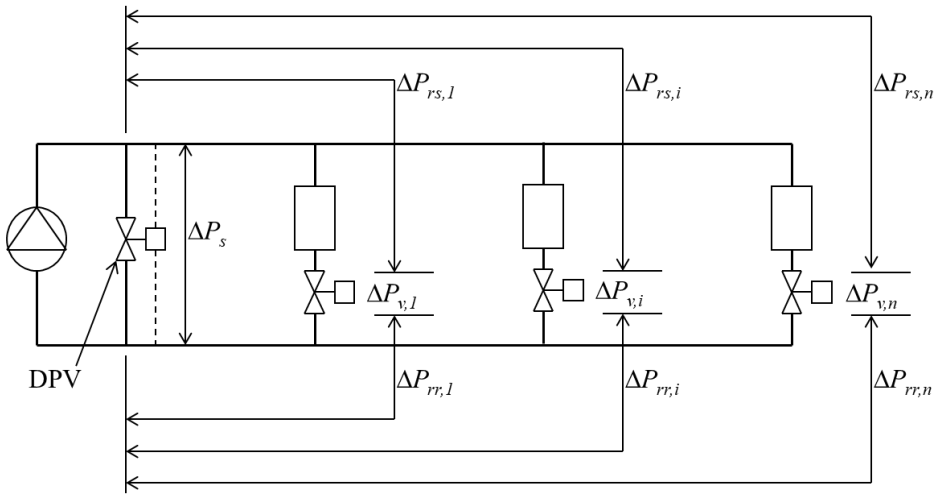

b) A single-loop pumping system

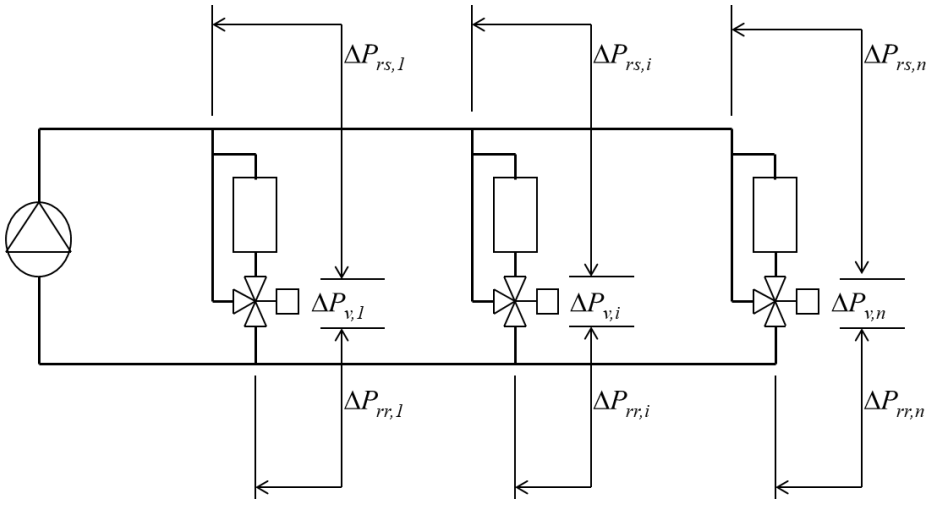

c) A pumping system with three-way valves

Figure 8.10 Pressure drops of the remainder of the circuit for various branches

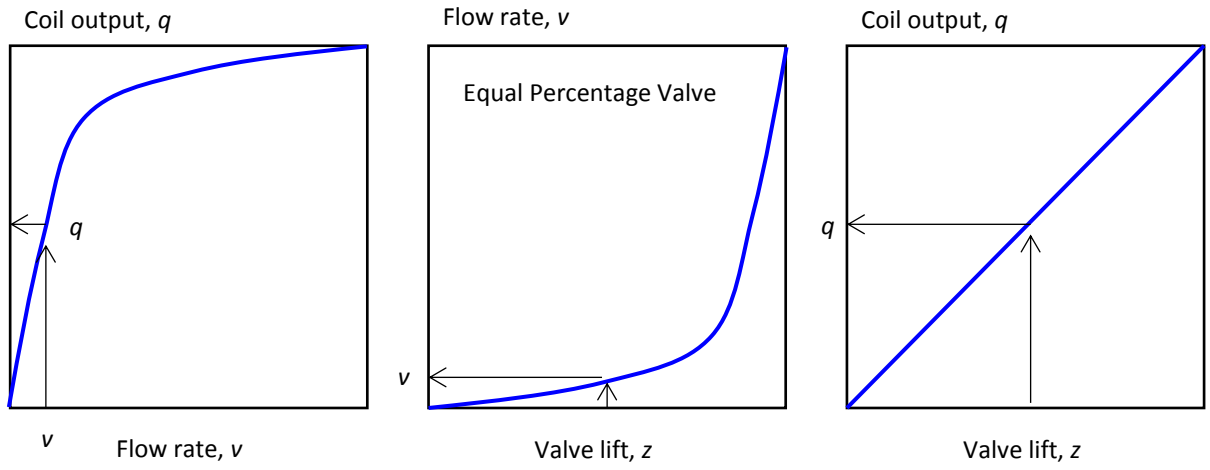

Figure 8.11 Compensation for coil output characteristics by using an equal percentage valve

8.3.3 Control valve and system balancing

As discussed above, a large differential pressure across a control valve has negative impact on the control performance of the control valve. For a system with constant speed pumps and multiple branches, the differential pressure across a branch (ΔP_B) will increase as the control valve closes to reduce the chilled water flow rate through the branch for cooling output regulation. Furthermore, branches closer to the pump will be subjected to higher ΔP_B values than branches further away (see more detailed discussions on this issue later). Although the increase in ΔP_B, due to increase in ΔP_V for output regulation, is inevitable, the effect due to positions of branches in a piping system may be alleviated by water balancing, which is widely considered to be a necessary commissioning process (see Section 7.6).

To facilitate balancing, each branch in a piping network is installed with a balancing valve, which may simply be a globe valve, or a type of valve specifically designed for water balancing (Figure 7.21) [5]. The objective of balancing is to adjust the balancing valve installed in each branch such that the control valve may stay at fully-open position when the branch is passing the design flow rate, with the excessive pressure throttled off by the balancing valve rather than having the control valve to also handle the excessive pressure. This preserves the full-range of valve lift for flow adjustment under part-load conditions and, hence, balancing is generally considered to be useful in improving flow control performance in water pumping systems.

However, whether or not to carry out water balancing is a controversial topic for systems employing variable speed pumps where pump speed is regulated with reference to the differential pressure across the furthermost or critical branch in the system [6]. In the following, the effect of balancing on a single-loop pumping system and on a two-loop pumping system with and without variable speed secondary-loop pumps are analyzed and discussed in detail to unveil the problems that may arise with and without water balancing. For simplicity, the assumptions are made in the following

discussions that the system under concern has identical branches and the chilled water flow rate demands of the branches would increase or reduce together by the same proportion unless otherwise stated in individual cases.

i) Single-loop pumping system with differential pressure bypass control

Figure 8.12 shows the pressure-distance diagrams of the single-loop pumping system under the design (in black) and a part-load (in blue) condition. Because, in this system, the differential pressure across the bypass pipe will be controlled by the differential pressure bypass control system to always stay within a narrow region about the set point (ΔP_{DPC}), our analysis here simply assumes the differential pressure across the bypass pipe is a constant that equals ΔP_{DPC} and thus the pumps in the system may be ignored.

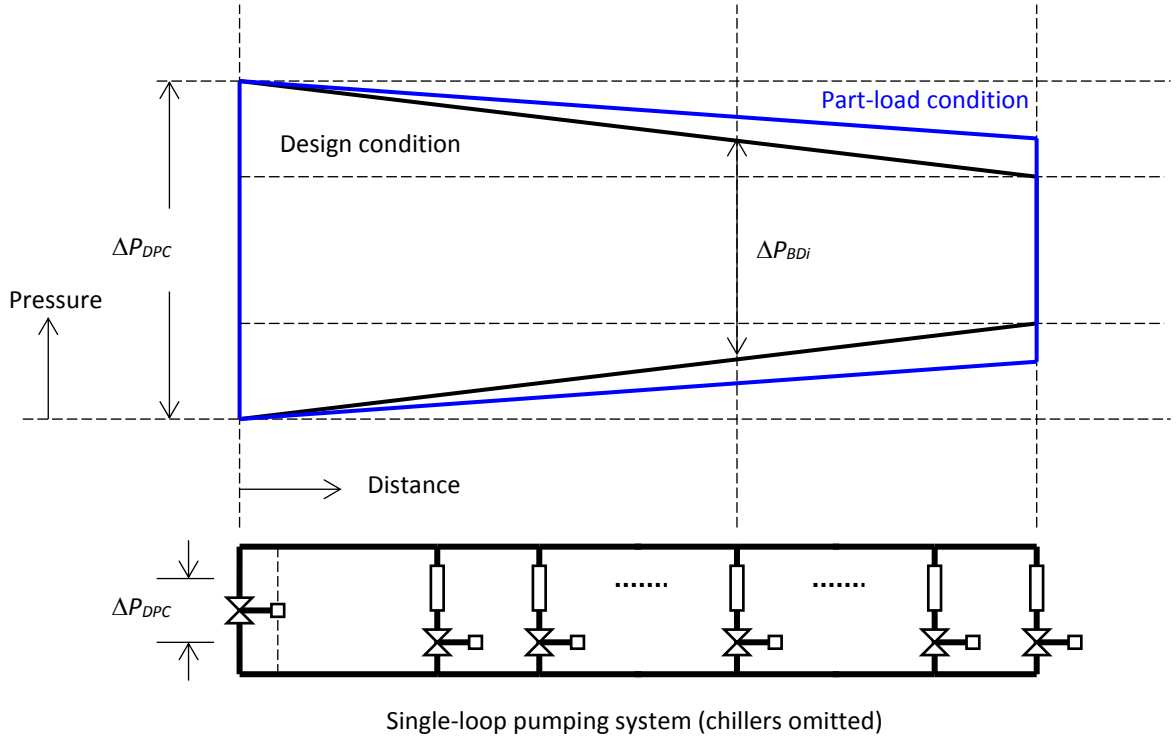

Figure 8.12 Circuit and pressure-distance diagrams for a single-loop pumping system

With the part of the pumping system from the pumps to the bypass pipe ignored, the water pressure in this system will be the highest at the point of connection of the supply pipe and the bypass pipe. As pressure drop will be incurred when there is water flow, water pressure will start to drop in the direction of water flow, along the supply pipe, through a branch, and along the return pipe until the pressure reaches the lowest level at the connection point to the bypass pipe. This explains why the differential pressure across those branches closer to the pump side will be higher than across those branches further away.

Furthermore, under the design condition, the differential pressure across the furthermost branch will be the lowest but should still be sufficient to drive its design flow rate through the branch, whereas the differential pressure across all other branches will be higher than required for driving the design flow rates through the respective branches. Without balancing, all branches will have a flow rate that deviates from their respective design flow rate, which will need to be corrected by partially closing the control valves at branches with excessive differential pressure. This means that the range of valve lift available for further adjustment of the branch flow rate is reduced.

When the total chilled water flow rate demand drops under part-load condition, the differential pressure across all branches will rise further (Figure 8.12) because the pressure drop per unit length of pipe run in the main supply and return pipes will become smaller compared to the design condition. Therefore, the control valves will have to reduce their valve lifts further to throttled off the excessive pressures in order to achieve the required flow rates.

It can be seen from the above discussions that, for a single-loop pumping system with bypass control, balancing will indeed be a useful measure for improving control valve performance.

ii) Two-loop pumping system with constant speed secondary-loop pumps

As shown by the pressure-distance diagrams in Figure 8.13 for the secondary-loop of a two-loop pumping system under the design and a part-load condition, the situations under both conditions will be similar to the case with single-loop pumping discussed above, except that there will also be a rise in pumping pressure under part-load condition. The excessive pressure that needs to be throttled off by the control valve at an intermediate branch, therefore, will be even greater.

Therefore, balancing will help improve the performance of flow control at the branches but, because the effect would be limited to the excessive pressure due to the gradients of pressure drop along the main supply and return pipes, the effect of balancing will be less significant compared to the single-loop pumping system discussed above. The right choice of control valves, e.g. use of equal percentage valves, may have a greater contribution than water balancing.

iii) Two-loop pumping system with variable speed secondary-loop pumps

Consider the case where the secondary-loop pumps in the system discussed above are replaced by variable speed pumps and a differential pressure transmitter is installed across the furthermost branch for pump speed control (Figure 8.14). The setpoint of the differential pressure across the furthermost branch is ΔP_C, which equals the pressure difference required to drive the design flow rate through the furthermost branch when the control valve in the branch is fully open. Under the design condition, the differential pressure across all branches except the furthermost branch will be higher than required for driving the design flow rates through the respective branches, as shown in the pressure-distance diagram in Figure 8.14 for this operating condition.

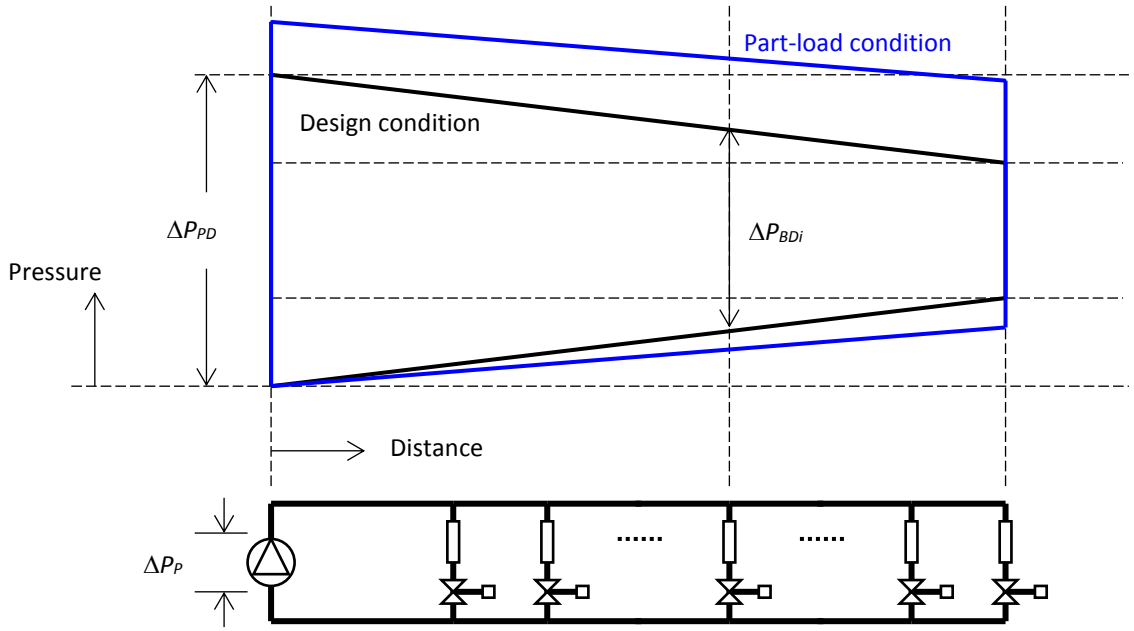

Figure 8.13 Circuit and pressure-distance diagrams for the secondary-loop of a two-loop pumping system with constant speed secondary-loop pumps

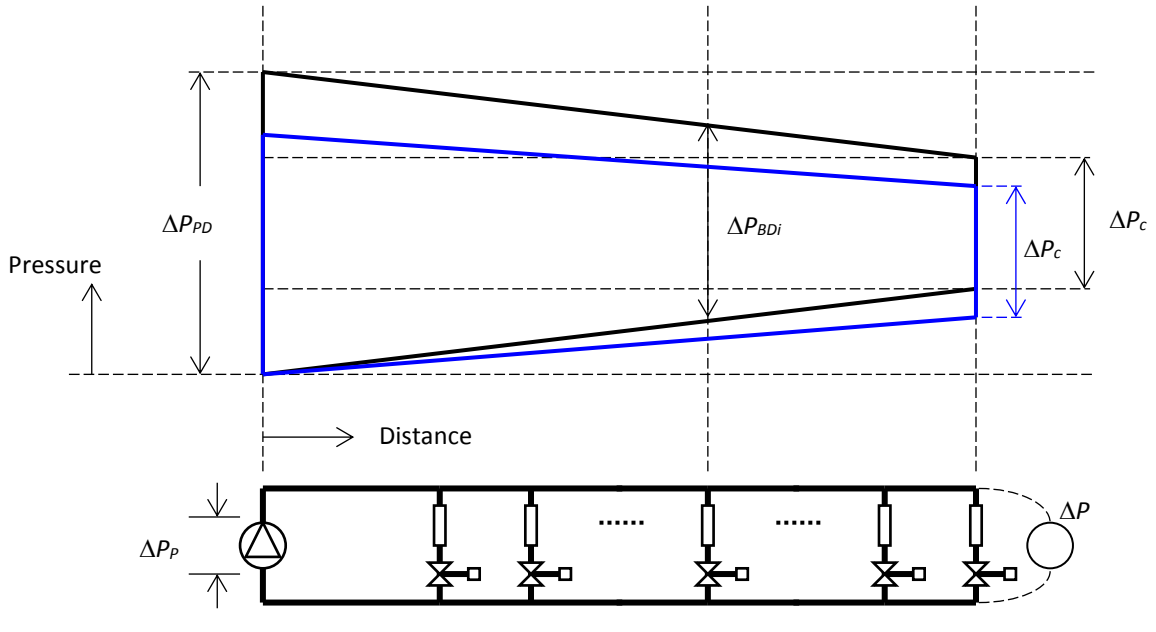

Figure 8.14 Circuit and pressure-distance diagrams for the secondary-loop of a two-loop pumping system with variable speed secondary-loop pumps

This means that if without balancing, all branches will have a flow rate that deviates from their respective design flow rate, which will need to be corrected by partially

closing the control valves at branches with excessive differential pressure. Therefore, the range of valve lift available for further adjustment of the branch flow rate is reduced.

When the system is operating under part-load where the total chilled water flow rate demand drops, the differential pressure across the furthermost branch will be maintained at ΔP_C by a reduction in running speed of the pumps. As shown by the pressure-distance diagram in Figure 8.14 for the part-load condition, the differential pressure across all branches except the furthermost branch will drop as the speed of the secondary-loop pumps is reduced.

Therefore, it is possible that if balancing is done, some branches may not be able to get the required flow rate due to the reduced differential pressure across the branches. The case would be even worse if a group of branches at the far side are all shut-down, which could happen in a composite building with commercial tenants on lower levels and office tenants on upper floors during after-office hours (Figure 8.15). These discussions support those who consider balancing not necessary for systems with variable speed pumping.

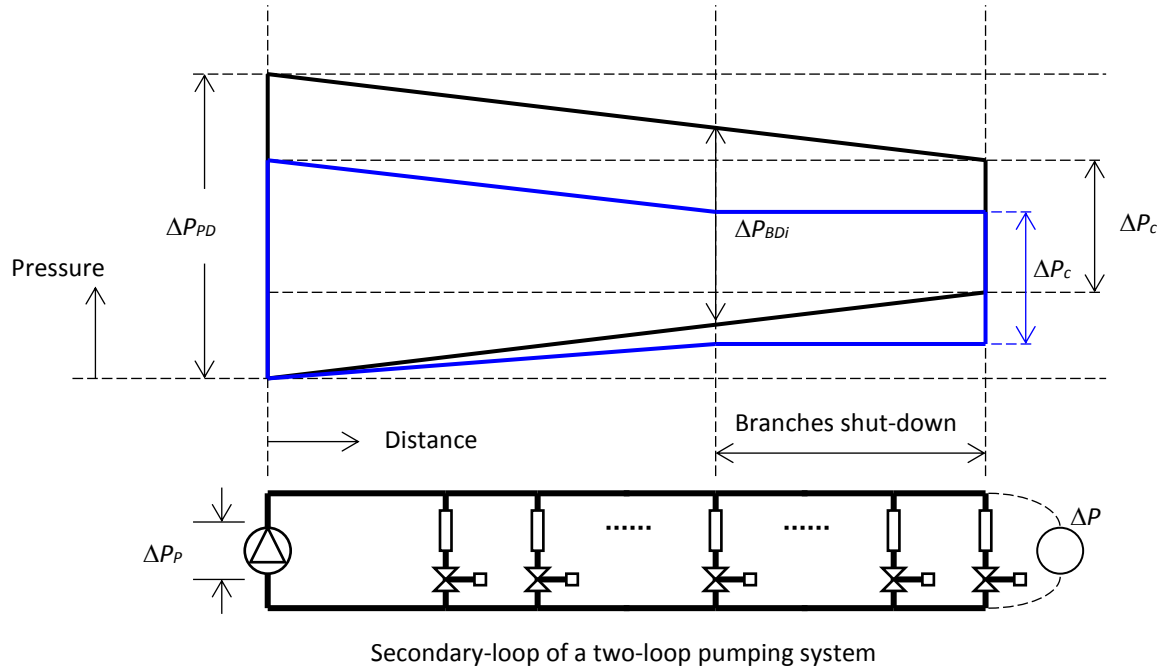

Figure 8.15 Circuit and pressure-distance diagrams for the secondary-loop of a two-loop pumping system with variable speed secondary-loop pumps when a group of branches are shut-down

8.3.4 Pressure independent control valves

At the beginning of the 21st century, a new design of control valve, commonly called pressure independent control valve (PICV), comprising a differential pressure control valve and a flow control valve, emerged in the HVAC market. In essence, the differential pressure control valve in the PICV would try to keep the differential pressure across the flow control valve at a constant level such that the flow control valve would be free from

the adverse impacts of variations in the differential pressure across it, which may arise as control systems for air-handling equipment connected to the same piping system adjust their flow demands to cope with load changes (see discussions in preceding sections).

Figure 8.16 shows the relationship between the flow control valve (V1) and the differential pressure control valve (V2) in a PICV. When the difference between P1 and P2, which are the pressures upstream and downstream of V1, varies, V2 will adjust its lift to compensate such that the difference between P1 & P2 will be brought back to the preset level. Therefore, V1 would be operating under a relatively stable differential pressure. With air-handling equipment equipped with PICV's, there should be no need for water balancing and thus no balancing valves need to be installed.

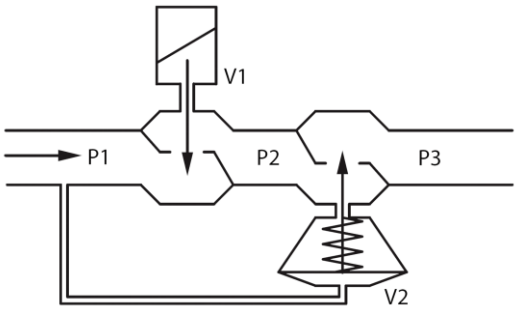

Figure 8.16 Schematic for a pressure independent control valve

For selection of PICV, a valve authority similar to that defined in Equation (8.14) may be used:

$$N = \frac{\Delta P_{PICV}}{\Delta P_{PICV} + \Delta P_R} \tag{8.21}$$

Where ΔP_{PICV} is the overall differential pressure across the PICV (ΔP_{PICV} = P1 – P3) and ΔP_R is the pressure drop of the remainder of the circuit. For reasonably good control performance, N should be between 0.25 to 0.5.

Most designs of PICV would seek to equalize the pressure drop across the control valve, ΔP_V (= P1 – P2), and that across the differential pressure control valve, ΔP_{DP} (= P2 – P3). Since $\Delta P_{PICV} = \Delta P_V + \Delta P_{DP}$, ΔP_V would be equal to half of ΔP_{PICV}, and also to half of the pressure drop of a conventional control valve selected based on the same valve authority.

As far as just the flow control valve inside the PICV is concerned, one may argue that its valve authority equals 1, but this is not meaningful. Yet, some would, based on this argument, claim that there is no need to concern about valve authority if PICV is used. This practice, however, could lead to unsatisfactory performance of the differential pressure control valve which would in turn affect the performance of the flow control valve in the PICV.

Annex 8A Case study on control valve selection

8A.1 Introduction

This case study, which had been included in a paper published in 1999 [6], was intended to illustrate the effects of using control valves sized for different valve authorities. A hypothetical system was devised to provide a basis for the case study. This system comprises a secondary-loop pump distributing the total chilled water flow rate evenly to 40 equal-spaced identical branches connected to the main supply and return pipes in parallel, with each branch comprising a cooling coil and a two-way control valve (Figure 8A.1).

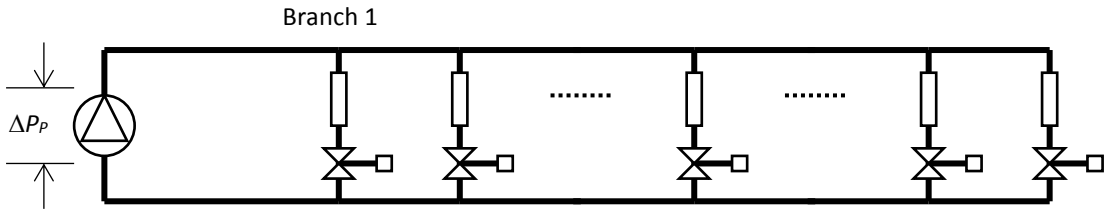

Figure 8A.1 Circuit of the secondary-loop of a two-loop pumping system

The total pipe-runs of the main supply and return pipes are each 160m, with the pipes sized for a rate of pressure drop of 250Pa/m. A factor of 1.75 had been applied to the pipe pressure drop calculated based on the pipe run and pressure drop per meter pipe run, to account for the pressure drops incurred by various pipe fittings, such as bends, tees, and branches. The total pressure drop across each branch, with that incurred by the control valve discounted, was assumed to be 45kPa.

Each of the control valves in the branches was assumed to be an equal percentage valve with inherent characteristic as described by the following model[4]:

$$v = 0.02 \exp(3.912 \cdot z) \qquad (8A.1)$$

The model for relating the normalized flow rate, v, and the normalized cooling output, q, of each of the cooling coils is as given below:

$$q = 1.2709v^3 - 2.6609v^2 + 2.4169v \qquad (8A.2)$$

The basis for normalization of flow rate was the design flow rate of the cooling coil and that for normalization of cooling output was the design output of the coil. It can be seen from Equation (8A.2) that substituting $v = 1$ into the model would yield a q value that is slightly greater than 1 (by about 3%), which can be attributed to inaccuracy introduced in the process of curve-fitting operating data of a coil as given by its manufacturer. This error was considered negligible and thus Equation (8A.2) was used without correction.

[4] This is equivalent to $v = \exp(3.912(z - 1))$, a model of the form of the equation given in section 8.3.1 ii) 3) of this chapter.

8A.2 Simulation results

Simulation calculations were carried out to find the relationship between q and z for branch 1 in the system (Figure 8A.1) for a range of system features, including the use of linear or equal percentage valves in the branches, valves with authorities ranging from 0.1 to 0.5, the use of constant or variable speed pumps, and with system balancing for the cases with constant speed pumps and no balancing for the cases with variable speed pumps. Branch 1 was selected to unveil the impacts of these system parameters on the control performance of the control valve in regulating system output because it is the branch that would experience the greatest change in differential pressure across the branch, and hence it can represent the worst scenario.

i) With constant speed pumps; system balanced

The simulation results shown in Figure 8A.2 unveil that when linear control valves were used, the relationship between the coil output and the valve lift would be far from linear. Increasing the valve authority would help improve this but poor control performance could still be expected at the low output, low valve lift region even if a valve authority of 0.5 was used.

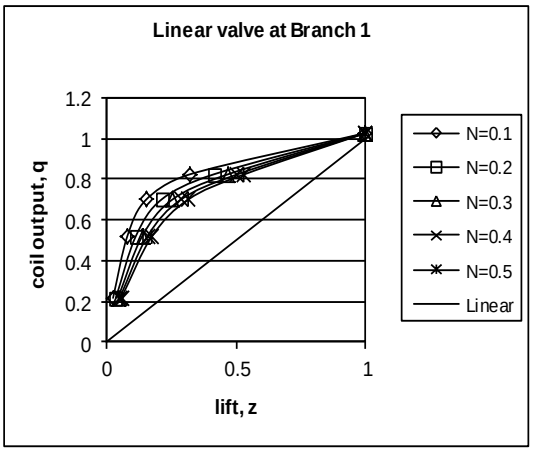

Figure 8A.2 Results for the case with constant speed pump, linear control valves and balanced system branches

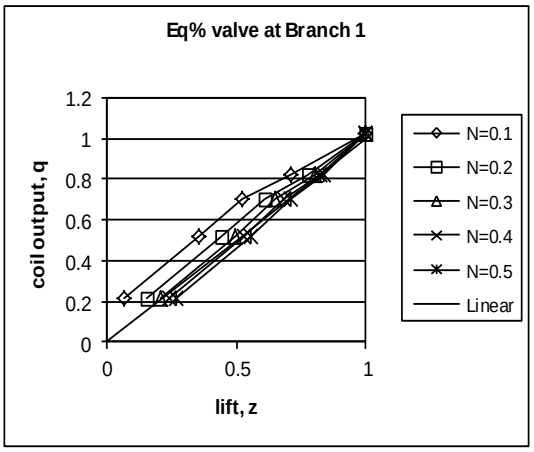

Figure 8A.3 Results for the case with constant speed pump, equal percentage control valves and balanced system branches

As Figure 8A.3 shows, if all control valves were replaced by equal percentage valves, a close to linear relationship between the coil output and valve lift can be achieved, even for the relatively low valve authority of 0.1. The improvement achievable by raising the authority value beyond 0.3 is marginal.

ii) With variable speed pumps; system not balanced

As shown in Figure 8A.4, with linear valves and no balancing, a substantial portion of the full valve stroke would be used to offset the excessive pressure difference across the branch before the valve could effectively reduce the coil output by reducing its lift. At

the valve authority of 0.5, the effective portion might be considered acceptable, but valves selected for a lower authority would leave too narrow an effective range of valve lift for output control.

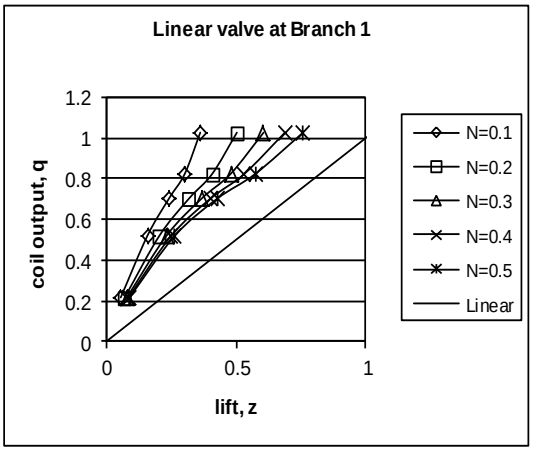

Figure 8A.4 Results for the case with variable speed pump, linear control valves and system not balanced

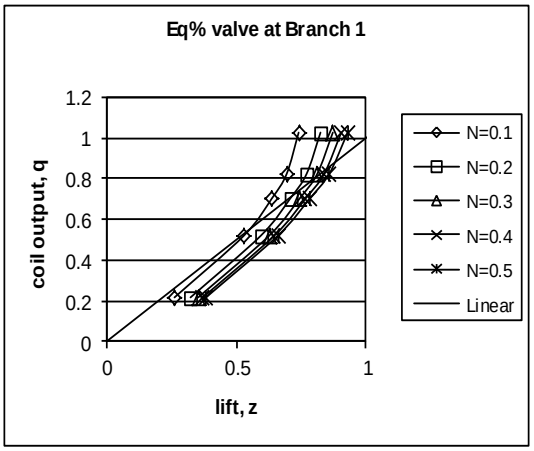

Figure 8A.5 Results for the case with variable speed pump, equal percentage control valves and system not balanced

If equal percentage valves were used instead, see Figure 8A.5, a near linear coil output – valve lift relationship could be achieved for valves sized for an authority down to 0.2. Furthermore, the loss in the effective valve stroke was significantly lower than when linear valves were used.

8A.3 Conclusion

It may be concluded from the case studies reported above that a close to linear relationship between coil output and valve lift could be achieved with the use of equal percentage valves sized for a valve authority of 0.2 – 0.3. Further improvement would be marginal if a valve authority of greater than 0.3 was used. The corresponding requirement on pumping pressure, and power, however, will increase very significantly. For the system studied above, the pumping pressure required would be raised from 264kPa for $N = 0.3$ to 370kPa for $N = 0.5$.

However, if linear valves are used, poor performance may still result even if the valves are sized for a valve authority of 0.5 or above. Equal percentage valve with $N = 0.3$ should be good enough.

References

[1] ASHRAE Handbook – Fundamentals, American Society of Heating, Ventilating and Air-conditioning Engineers, Inc., 2017.

[2] CIBSE Guide C Reference Data, The Chartered Institution of Building Services Engineers, UK 2007.

[3] Jones, W.P., Air-conditioning Engineering, 3rd Ed., Edward Arnold, 1985.

[4] McQuiston, F.C., Parker, J.D., Spitler, J.D., Heating, Ventilating, and Air Conditioning Analysis and Design, 5th Ed., John Wiley & Sons, Inc., 2000.

[5] CIBSE Commissioning Code W, Water Distribution Systems, The Chartered Institution of Building Services Engineers, 2010.

[6] Yik, F.W.H., Selection control valves for air-conditioning systems, HKIE Transactions 1999, 6(2): 11-18.

[7] Yik, F.W.H., Analyses of operations of control valves in air-conditioning systems comprising multiple chillers and chilled water pumps, HKIE Transactions 2001, 8(3): 51-57.

Chapter 9 System Performance and Control Optimization

9.1 Introduction

As highlighted in Chapter 1, air-conditioning systems are intensive energy consumers and, for that reason, are responsible for a significant portion of the global greenhouse gas emissions. Therefore, air-conditioning system designers have the duty to ensure their designs are not only workable but also energy efficient. System operators, in turn, should ensure their plants are run in the most efficient manner and adequate operation and maintenance (O&M) measures are implemented to upkeep the energy efficiency of the major equipment.

In Chapters 6 & 7, various water-side system designs that may be adopted for a central air-conditioning system, the associated equipment and control systems, and their operating principles and characteristics, have been elucidated. As pointed out in the discussions in these chapters, the design decisions that have the greatest impact on the energy performance of the central chiller plant include the choice of medium for chiller condenser heat rejection and the type of pumping system selected for chilled water distribution. Sizing of water pipes and selection of control valves covered in Chapter 8, which are important tasks in the design process, can also impact significantly on the energy use of the water-side system.

The materials covered in the last three chapters are essential knowledge to designers for them to carry out the design of a central air-conditioning system and ensure the system would operate with acceptable functional and energy performance. In this chapter, our attention will focus on the operational control of a central chiller plant, especially on how a chiller plant can be run at the highest possible energy efficiency. This requires quantification of the operating performance of all major equipment in the system and determination of the combination of equipment to be run under a given cooling demand and other operating conditions such that the energy consumption of the plant would be kept to the lowest possible.

To begin with, how an optimal chiller sequencing control strategy can be developed to enhance the operating efficiency of a chiller plant by taking advantage of the part-load characteristics of the chillers will be discussed and illustrated graphically. Analyses of results of applying this method suggested that the traditional operational control strategy, which focused on meeting the cooling demand by running just the required minimum number of equipment, could be justified for older system designs where modern equipment like variable flow chillers and variable speed drives for chillers, pumps, and cooling tower fans were absent.

We shall then move on to explore methods for enhancing the performance of major equipment in a modern chiller plant and for predicting the energy consumption of the equipment and the entire chiller plant. A model for predicting the performance of a chiller operating under variable chilled and condenser water temperatures and flow rates, and a cooling tower model that can handle variable air and condenser water flow rates, will be introduced. Derivation of a method for prediction of pumping energy use for variable speed pumps in a pumping network will also be presented.

For a modern chiller plant, the key means that may be employed to optimize the energy use of the plant include resetting the supply chilled water temperature set point of chillers, varying the flow rates of chilled water and, for systems with water-cooled chillers, also the condenser water, through the chillers by varying the running speeds of the associated pumps, and selecting the optimal combination of equipment to be run. For systems employing cooling towers for heat rejection, varying the temperature of condenser water leaving the cooling towers and entering chillers and varying the running speed of cooling tower fans are also possible means for plant energy use reduction.

This considerable number of parameters that may be adjusted to enhance performance implies that there are many opportunities to minimize the energy use of a chiller plant. On the other hand, these means may impact the performance of different equipment in different ways, e.g. when one means is used to reduce the energy use of a piece of equipment, the energy use of another equipment may increase as a result. Therefore, a thorough and comprehensive analysis would be needed to evaluate and compare the overall result of each possible option before a decision can be made on how to operate the plant for the best possible efficiency, which would be impossible unless a computer is used to handle the calculations involved.

With the ability to predict equipment performance, optimization search algorithms can be developed for identification of the optimal combination of equipment and control settings that would lead to the least possible energy use for meeting a given cooling demand under the given operating conditions. An example search method will be presented to illustrate how control optimization for a chiller plant may be implemented.

Up to this point, attention has been put on chiller plant control optimization. Before this chapter closes, extension of the scope of optimization to also cover the air-side systems, thus enabling whole air-conditioning system control optimization, will be discussed.

9.2 Sequencing control of chiller plant equipment

In most central air-conditioning systems, there are multiple units of the same type of equipment, including chillers, pumps, cooling towers, etc., which can provide the following benefits:

1) When the load on the plant drops, some of the units may be turned-off for energy saving.

2) The smaller unit sizes can provide greater flexibility with respect to space for installation and access for maintenance, repair, and replacement.

3) A greater number of equipment enhances availability of service as there are still equipment that are operational when one or two equipment break down.

4) When a piece of equipment is redundant, it can be set-aside for maintenance such that its efficiency and reliability will be enhanced when put back into operation.

Point 1) above is a key means for minimizing the energy use of a central chiller plant. However, it implies that the cooling load on the plant needs to be consistently monitored and appropriate actions need to be taken whenever there are significant changes in the load. This, of course, may be done manually by the plant operators, but the control would then be subject to human errors that could arise from time to time, resulting in sluggish response, imprecise control, inefficient operation, and possibly inadvertent damage to the equipment.

Nowadays, a certain kind of automatic sequencing control would be implemented to start and stop the plant equipment according to pre-set schedules and the cooling demand, which would typically be one of the key functions of the building management system (BMS) that controls not only the operation of the air-conditioning system but also other building services systems in the same building. With automatic sequencing control, unnecessary operation of equipment can be avoided, equalization of wear & tear of equipment can be achieved by operating equipment in rotation (also known as duty cycling), and the overall energy performance of the plant can be enhanced by implementing appropriate optimized sequencing control strategies.

9.2.1 Primitive chiller plant sequencing control methods

For chiller plants with the single-loop chilled water pumping design, the classical sequencing control for the chillers was based on the chilled water return temperature. A sensor used to provide feedback about this temperature would be connected to a cam-type controller which would, according to the pre-set on- and off-settings, determine whether to start or stop a chiller. The algorithm employed for this sequencing control is called floating-point control (Figures 9.1 & 9.2).

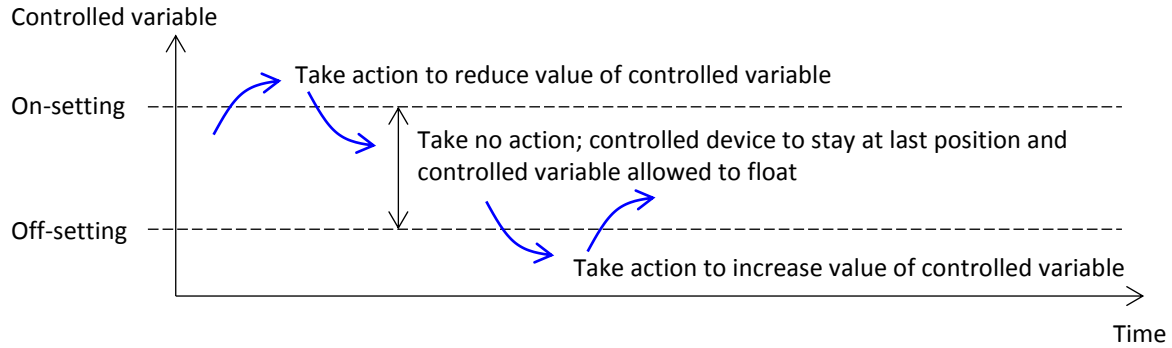

Figure 9.1 Floating-point control algorithm

With floating-point control (Figure 9.1), when the chilled water return temperature overshoots the on-setting signifying the cooling output of the running chillers is insufficient to cope with the load, one more set of chiller, together with its associated chilled water pump and, where applicable, seawater / condenser water pump and cooling tower, will be turned-on. More groups of chiller and associated equipment will be turned-on, one after another with a sufficient time delay in between, until the chilled water return temperature stays below the on-setting again or all chillers in the plant are already running (Figure 9.2). The actions will be reversed when the chilled water return

temperature falls below the off-setting, to sequence off the chillers and associated equipment.

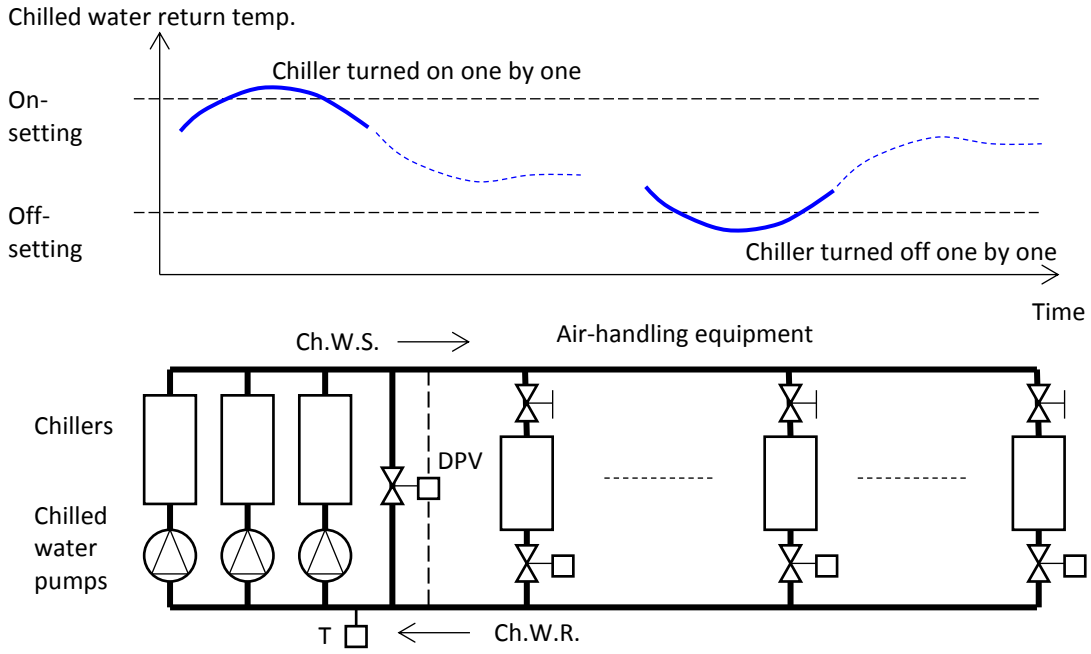

Figure 9.2 Chilled water return temperature of a chiller plant with single-loop pumping under a floating-point control algorithm

This simple control strategy is possible provided the chilled water flow rate through each operating chiller stays at a constant level such that the return temperature alone can fully reflect the cooling load on the chillers, which was a key design requirement for chillers in the past (see also discussions in Chapter 7). On and off of the water pumps and other associated equipment are controlled according to a simple interlocking relation with the chillers that each pump and other associated equipment is dedicated to serve.

Though simple and workable, this method of chiller sequencing control would tend to run more chillers than required and thus could not ensure the chiller plant would operate in the most energy efficient manner at all times. This is mainly due to the use of a pair of fixed on-setting and off-setting for chiller on-off control. Indeed, over-shooting of the on-setting does mean more chiller unit(s) should be put into operation to meet the increased cooling demand. However, the use of a single off-setting would mean that the setting would have to be set at a level corresponding to below 50% of the cooling capacity of the running chillers. In other words, if the design chilled water supply and return temperatures are 7 and 12°C, the on-setting can be set at 12°C, but the off-setting would need to be set at or below 9.5°C.

The abovementioned off-setting is needed to ensure when only two chillers are running, one of the chillers would be turned-off only if the load falls below 50% of the total capacity of the two chillers. An off-setting that is higher than this setting would cause

the second chiller that remains running to be switched off pre-maturely, leading to unstable operation as the last chiller becomes over-loaded and a call will arise for turning on one more set of chiller. However, if a chiller plant has more chiller units, say 6 chillers, of the same capacity and all have been running to cope with the load, the control system will not attempt to switch off one chiller unless and until the cooling load has dropped to a level lower than the total capacity of half the total number of chillers, which is 3 in the example here. Thereafter, the control system would keep 5 chillers running unless and until the cooling demand falls further to a level below the total capacity of 2.5 chillers. The situation would be even worse if the chiller plant comprises a mix of chillers of different capacities.

For chiller plants with the two-loop pumping system design, the classical decoupler bypass control method, as introduced and discussed in detail in Chapter 7, was widely used for chiller sequencing control before the emergence of more sophisticated control devices, such as software based control algorithms implemented through direct digital controllers (DDCs) or programmable logic controllers (PLCs), and it may still be in use in some older plants. Sequencing control over the secondary-loop chilled water pumps in the plant may also be done through interlocking with the chillers but this is not a necessary approach.

Though is free from the abovementioned limitation of the floating-point control method, the decoupler bypass control method, which utilizes chilled water flow rate as a proxy of cooling load, may mislead the decision of whether more or less chillers are to be run. For example, due to the non-linear response of cooling coils, they may reduce chilled water flow rate demand by a greater proportion than the reduction in cooling load while maintaining a higher rise in chilled water temperature across the coils (see Figure 8.11). In this case, the surplus flow rate through the bypass pipe may signal to switch off a chiller, but this action could reduce the cooling capacity to below the demand.

On the other hand, for chiller plants that suffer from the low delta-T syndrome (see Section 7.4), the air-side systems would be demanding more chilled water flow rate than they should, thus giving rise to a smaller than normal temperature differential between the supply and return chilled water. As a result, more chillers than required would be run when the decoupler bypass control method is used.

9.2.2 A simple approach for optimizing chiller plant sequencing control

Since the 1980's, more and more measuring instruments and intelligent control devices have been used to control chiller plant equipment operation for greater accuracy and higher efficiency. Rather than relying on indirect indications of the demand for output of the chiller plant, the chilled water flow rate and supply and return temperatures can be measured such that the cooling load can be computed based on these measurements (Figure 9.3). Sequencing on and off of chillers and pumps can then be done based on the cooling load and chilled water flow rate demand directly. The cooling load levels that would trigger starting and stopping of chiller / pump groups may also be set such that the set of equipment that will be put into operation would be the optimal set that would led to the minimum energy consumption.

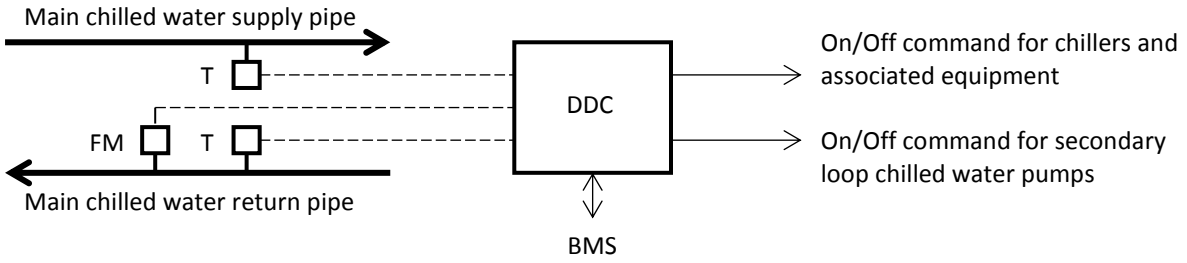

Figure 9.3 Cooling load and chilled water flow measurements for chiller and pump sequencing control

An example of exploring whether energy saving could be achieved by using a set of optimized change-over points for chiller sequencing is given below, with the aid of Figure 9.4. The focus of the discussion is put, for the moment, only on the chiller performance characteristics.

Figure 9.4 a) shows the part-load performance curves of an air-cooled centrifugal chiller, an air-cooled screw chiller and an air-cooled oil-free chiller (see Section 6.2.3 i about this type of chiller), which were established by curve-fitting data obtained from the manufacturers. In these graphs, the chiller power demands were plotted against the cooling outputs, after normalization by the rated power demand and the rated cooling capacity, respectively, for several selected outdoor air temperatures (denoted by 'y' in the figure), including the outdoor air temperature (35°C) at which the chillers were rated and three more temperatures below this, in intervals of five degrees.

For this analysis, we may focus on the chiller performance curves for a chosen outdoor air temperature and, for simplicity, let us pick 35°C, the outdoor air temperature at which the chillers were rated. For all cases discussed below, the chillers are assumed to be running under this outdoor air temperature. From this set of curves, the power demands of the chillers, when they are outputting 50% of their rated cooling capacities, can be determined, as shown in Figure 9.4 b). By doubling this power demand of each unit, we get the total power demand of running two identical chillers, each outputting 50% of their rated cooling capacity. This total power demand can then be compared with the power demand of running just one chiller at 100% of its capacity to determine which would be a more energy efficient way to deploy the chillers.

It can be seen from Figure 9.4 b) that whether running two chillers each at 50% capacity would consume more power than running just one chiller at full capacity is dependent on the part-load performance characteristics of the chillers under concern. This is true for the centrifugal and screw chillers, but the opposite is true for the oil-free chillers, i.e. less energy would be consumed by running two oil-free chillers than running just one unit. As can be observed from these graphs, the condition that determines if more or less energy would be consumed by running one more chiller is whether the point on the performance curve that represents the power demand of the chiller under the load it would share, after one more chiller is run, is above or below the diagonal straight-line joining the origin and the full-load operating point of the curve corresponding to the condenser cooling medium temperature under concern.

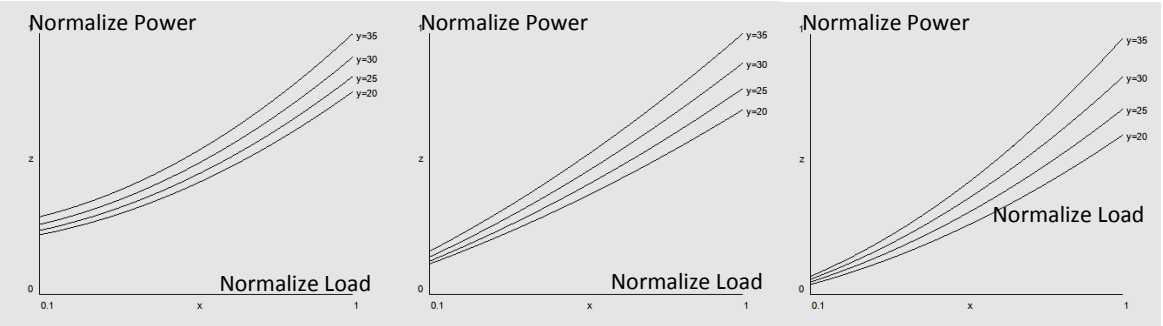

Air-cool centrifugal | Air-cool screw | Air-cool oil-free

a) Part-load performance curves of chillers

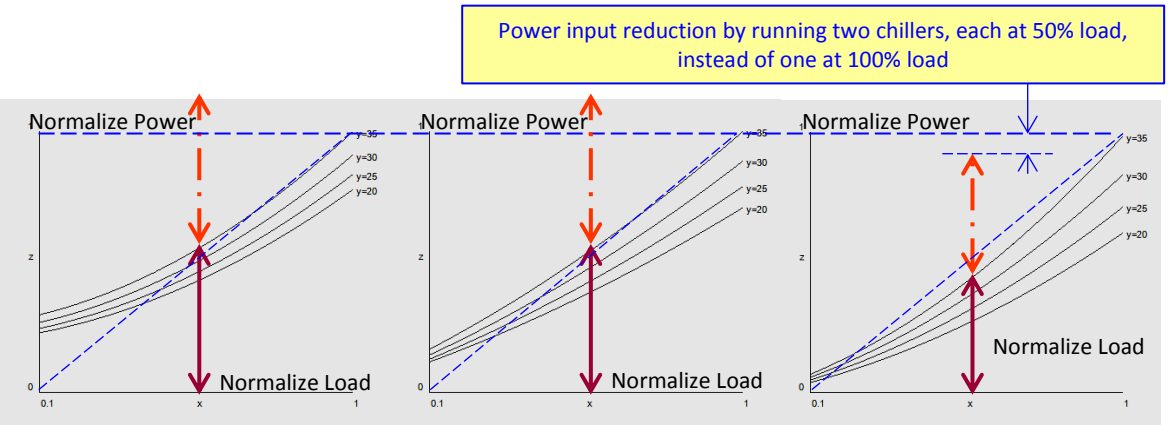

Air-cool centrifugal | Air-cool screw | Air-cool oil-free

b) Potential energy saving by running more chillers than required

Note: y = condenser air inlet temperature, °C
Normalized load and power based on rated capacity and power

Figure 9.4 Analysis of potential energy saving by running more chillers than required

Similar analyses can be done for a plant with multiple chillers to explore the energy saving potential of optimization of chiller deployment to cope with the cooling demand from time to time. Figure 9.5 shows an example for a plant comprising 4 identical chillers. As can be seen in this figure, the power demand curves used in this analysis represent the total power demand of the number of chillers being run together with other equipment that must also be run, which should not be ignored in the analysis. For the case shown in Figure 9.5, the overall power demand of the plant could be minimized by following the lowest curve in the graph as the load on the plant varies. Optimized switch over points may also be determined from the graph as shown in Figure 9.5 b).

The favourable case shown in Figure 9.5 would be possible provided only that the chiller power curve stays below the diagonal line by a margin sufficient to compensate for the power demand of running an extra group of equipment associated with the

chiller. In many cases, the situation shown in Figure 9.6 may result, in which case the optimal way of deployment of the chillers and associated equipment would be to let the chillers to run up to their full capacity before switching on one more chiller.

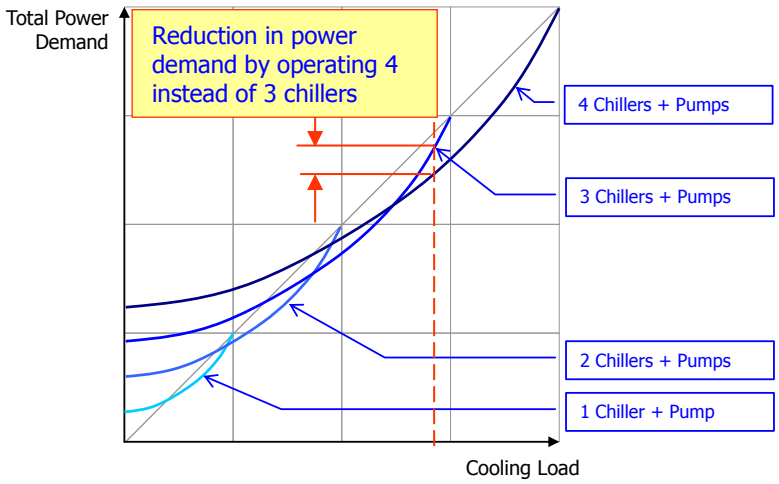

a) Power demand reduction potential

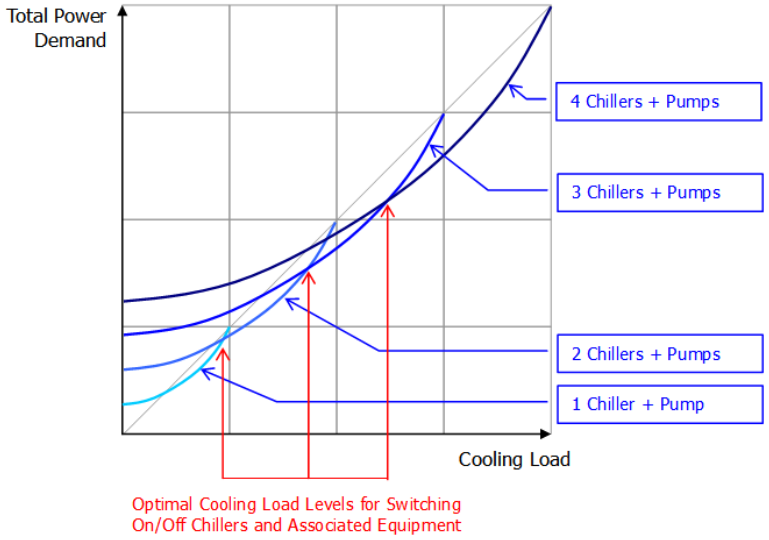

b) Optimal switching over points

Figure 9.5 Determination of optimal switch-over points for sequencing control of a chiller plant with four identical chillers

If identical chillers are employed, the chiller plant power–cooling load curves needed in the analysis, as exemplified by the cases discussed above, can be constructed simply by scaling up the total power curve of one chiller and its associated equipment. For each point on this graph, doubling up the power and the load would yield a point for the total power of two chillers and their associated equipment, as shown in Figure 9.7. Repeating the same steps for all operating points on the curve for one chiller and scaling up the power and load by increasing number of chillers involved would yield a family of curves

for different number of groups of chiller and associate equipment such as those shown in Figure 9.5. For a mix of chillers of different sizes, the curves can be constructed by considering each possible combination, one-by-one.

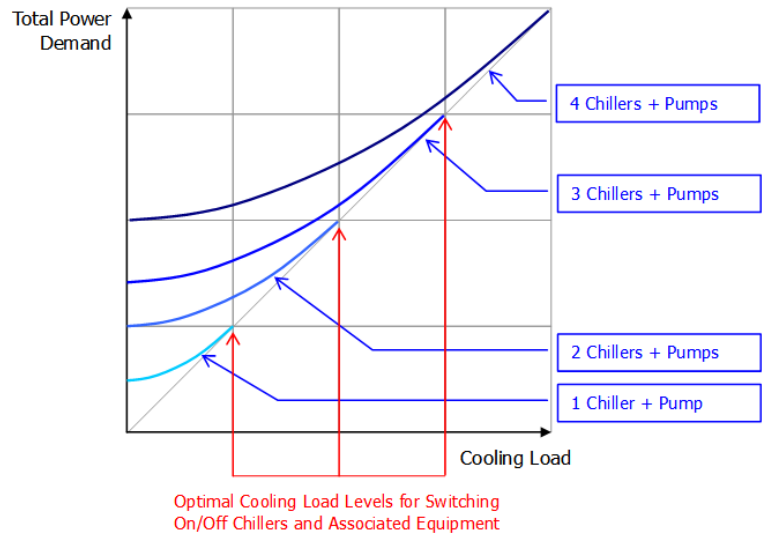

Figure 9.6 Analysis of potential energy saving for a chiller plant with four chillers (without overlaps among the power curves)

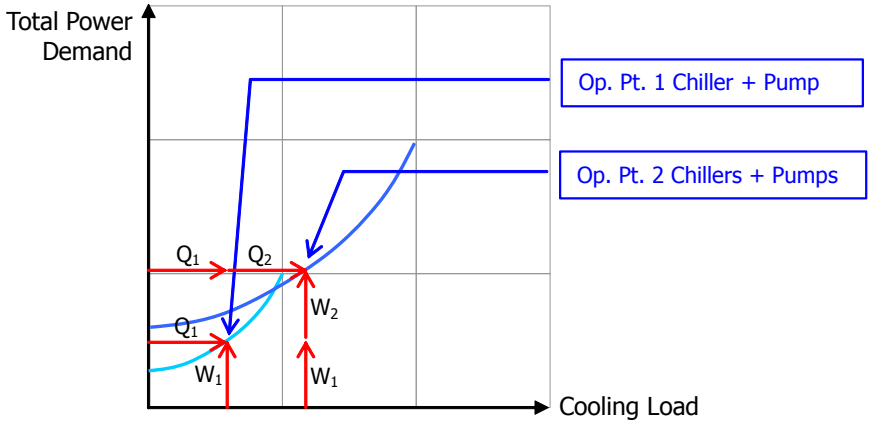

Figure 9.7 Construction of combined power–load curves for chillers and associated equipment in a chiller plant

In carrying out the analysis for finding the optimal chiller sequencing control strategy for a chiller plant, note should be taken of the following:

- The power demands of all other equipment that will be turned-on and -off together with their associated chillers must be included.
- In the analysis, chiller part-load performance curves for the same cooling medium temperature must be used.

- The analysis should be repeated for a range of condenser cooling medium inlet temperatures, one-by-one, to guide operation of the chiller plant under any of the conditions covered.

- The above analysis cannot be replaced by a single-round of analysis using the performance curve rated according to the AHRI Standard 550/590 [1], which allows for a condenser water temperature relief of 4°F per 10% drop in load and thus giving erroneous results.

- The more chillers are installed in a plant to cope with a given total cooling demand, the greater the chance to reduce total chiller energy use by running more than enough number of chillers, but the benefit could be offset by having to adopt smaller chillers of lower COP.

The method discussed above for developing a chiller sequencing control strategy does not take into account the effects of other possible means that may lead to reduction in the overall power demand of the chiller plant, such as reset of chilled water supply temperature, varying the chilled water flow rate and, if applicable, condenser water flow rate, etc. It, therefore, can only be applied to a relatively simple chiller plant with constant flow chillers and fixed chilled water supply temperature. A convenient way of implementing this control strategy is to establish a matrix of optimal switch-over points for a range of condenser cooling medium inlet temperatures to which the sequencing control algorithm may refer in deciding the combination of chillers and associated equipment to deploy.

9.3 Equipment performance prediction

A key task that needs to be performed repeatedly in searching for the optimal pattern of operation of a chiller plant, including the combination of equipment to be deployed and the control settings for the equipment, is prediction of the overall power demand of the chiller plant corresponding to each possible operation pattern under consideration. Therefore, the optimization algorithm must have access to simulation models for prediction of the performance of the major equipment. Models that can embrace all major influential system variables and are suitable for application to modern chiller plants are described below.

9.3.1 Chiller model

For supporting chiller plant control optimization, the chiller model needed should allow either the power demand (W_{ch}) or the coefficient of performance (COP) of a chiller to be predicted when given the cooling load on the chiller (Q_{ch}), the chilled water supply temperature (T_{cho}), the chilled water flow rate ($(\rho V)_{ch}$), and the condenser water or air inlet temperature (T_{cdi}) and flow rate ($(\rho V)_{cd}$). The relationship may be expressed as a mathematical function as given below:

$$W_{ch} = W_{ch}(Q_{ch}, T_{cho}, (\rho V)_{ch}, T_{cdi}, (\rho V)_{cd}) \quad (9.1a)$$

Or

$$COP = COP(Q_{ch}, T_{cho}, (\rho V)_{ch}, T_{cdi}, (\rho V)_{cd}) \quad (9.1b)$$

Different mathematical models may be used and, amongst them, black-box models in the form of a multiple linear equation derived by curve-fitting empirical data, or grey-box models derived from fundamental principles in conjunction with empirical data, are the most widely used types of model for this purpose. For a simple case with constant flow chillers and constant chilled water supply temperature, the model may be simplified to:

$$W_{ch} = W_{ch}(Q_{ch}, T_{cdi}) \quad (9.2)$$

For this case, a bi-quadratic equation as shown below would suffice [2]:

$$\begin{aligned} w_{ch} = {} & a_0 + a_1 PLR + a_2 PLR^2 + a_3 T_{cdi} + a_4 T_{cdi}^2 + a_5 PLR \cdot T_{cdi} \\ & + a_6 PLR^2 \cdot T_{cdi} + a_7 PLR \cdot T_{cdi}^2 + a_8 PLR^2 \cdot T_{cdi}^2 \end{aligned} \quad (9.3)$$

In Equation (9.3), the chiller power demand, W_{ch}, is expressed in normalized form, w_{ch}, which equals:

$$w_{ch} = W_{ch}/W_{ch,rated} \quad (9.4a)$$

And the cooling load on the chiller, Q_{ch}, is expressed in part-load ratio, PLR, which is defined as:

$$PLR = Q_{ch}/Q_{ch,rated} \quad (9.4b)$$

Where $W_{ch,rated}$ and $Q_{ch,rated}$ are the rated power and cooling capacity of the chiller, respectively.

For use in more sophisticated control optimization that will embrace all system variables that may affect chiller performance, the grey-box model proposed by Gordon & Ng [3], which is a versatile model and a version of this model [4] that can embrace all key independent variables, as shown in Equation (9.1), is considered a good option. Detailed derivation of this version of the Gordon & Ng model, shown as Equation (9.5) below, is given in Annex 9A at end of this chapter such that readers may understand the assumptions behind and the limitations of the model.

$$y = a_1 x_1 + a_2 x_2 + a_3 x_3 \quad (9.5)$$

Where

$$y = \left(1 + \frac{1}{COP}\right)\frac{T_{cho}}{T_{cdi}} - 1 - \frac{1}{(\rho V c)_{cd}}\frac{Q_{ch}}{T_{cdi}}\left(1 + \frac{1}{COP}\right) \quad (9.6a)$$

$$x_1 = \frac{T_{cho}}{Q_{ch}} \quad (9.6b)$$

$$x_2 = \frac{T_{cdi} - T_{cho}}{Q_{ch} T_{cdi}} \quad (9.6c)$$

$$x_3 = \frac{Q_{ch}}{T_{cdi}}\left(1 + \frac{1}{COP}\right) \tag{9.6d}$$

$$a_1 = \Delta S_{Int} \tag{9.7a}$$

$$a_2 = Q_L \tag{9.7b}$$

$$a_3 = \frac{1-\varepsilon_{cd}}{(\rho Vc\cdot\varepsilon)_{cd}} + \frac{1-\varepsilon_{ch}}{(\rho Vc\cdot\varepsilon)_{ch}} \tag{9.7c}$$

In Equations (9.7a, b & c), ΔS_{Int} is the entropy generation terms that represent the irreversibilities resulting from the energy transfers into, within and out of the chiller, Q_L is the heat leakage, and ε is the effectiveness of the condenser or the evaporator as denoted by the subscript used (*cd* or *ch*). These are typically unknown parameters, and thus are included in the undetermined coefficients a_1 to a_3 of the model (Equation 9.5), which are to be evaluated based on empirical data that allow y, and x_1 to x_3 to be computed for a regression analysis.

It can be seen from the Gordon & Ng model, expressed by Equations (9.5) to (9.7), that the model can explicitly cater for the effects of variations in the condenser water flow rate (see Equation (9.6a)) but cannot do so for the chilled water flow rate. This term does appear in Equation (9.7c) but its effects cannot be explicitly accounted for. Nevertheless, as explained in Annex 9A, the effect of variations in the chilled water flow rate is not significant and, therefore, this model can be applied to chillers with variable chilled and condenser water flow rates.

Equation (9.5) is in a form suitable for evaluation of the undetermined coefficients (a_1 to a_3) by regression with operating data of a chiller. Once the coefficients have been evaluated, the model for the chiller may be re-arranged to the following form to facilitate chiller performance prediction calculations.

$$COP = \frac{\left\{\frac{T_{cho}}{T_{cdi}} - \frac{1}{(\rho Vc)_{cd}}\frac{Q_{ch}}{T_{cdi}} - a_3\frac{Q_{ch}}{T_{cdi}}\right\}}{1 + a_1\frac{T_{cho}}{Q_{ch}} + a_2\left(\frac{T_{cdi}-T_{cho}}{Q_{ch}T_{cdi}}\right) - \left\{\frac{T_{cho}}{T_{cdi}} - \frac{1}{(\rho Vc)_{cd}}\frac{Q_{ch}}{T_{cdi}} - a_3\frac{Q_{ch}}{T_{cdi}}\right\}} \tag{9.8}$$

One crucial point that users of the model should take note of is that since the Gordon & Ng chiller model was derived from the first and second laws of thermodynamics, all the temperature terms in the model are absolute temperatures, in degree Kelvin.

9.3.2 Cooling tower model

For cooling towers that operate with constant air and water flow rates, their performance can be expressed as a function relating three key variables, namely, the outdoor air wet-bulb temperature and the entering and leaving water temperatures. For convenience in application, a model for such cooling towers may be expressed as a bi-quadratic equation [2], as follows:

$$T_{w2} = T_{w2}(T_{wb}, R)$$

$$T_{w2} = c_0 + c_1 R + c_2 R^2 + c_3 T_{wb} + c_4 T_{wb}^2 + c_5 R T_{wb} + c_6 R^2 T_{wb} + c_7 R T_{wb}^2 + c_8 R^2 T_{wb}^2 \quad (9.9)$$

Where

T_{w1} & T_{w2} = entering and leaving water temperatures, respectively, °C
$R = T_{w1} - T_{w2}$, called range of a cooling tower, °C
T_{wb} = wet bulb temperature of ambient air, °C
c_0 to c_8 are the coefficients

The coefficients c_0 to c_8 are typically evaluated for a specific cooling tower based on performance data provided by the manufacturer.

For cooling towers that operate with variable flow rates of air and water, a more versatile model is needed. In Chapter 6, the following equation (Equation (6.20)) was derived and based on which the number of transfer unit (*NTU*) of a cooling tower was defined.

$$NTU = \frac{h_d a}{m_w} V_T = C_w \sum_{T_{w1}}^{T_{w2}} \frac{\Delta T_w}{h_{sw} - h_a} \quad (9.10)$$

With reference to the given outdoor air state, air and water mass flow rates, and entering water temperature, and the required leaving water temperature, we can evaluate the required NTU, denoted by NTU_R, by using the right-hand side of Equation (9.10) for meeting the corresponding heat rejection duty. In actual operation, the NTU_R should match with the available NTU of the cooling tower, denoted by NTU_A, which may be estimated by using the following model [5]:

$$NTU_A = C_{ctr}(m_a/m_w)^{0.6} \quad (9.11)$$

Where m_a & m_w are the mass flow rates of air and water through the cooling tower and C_{ctr} is the model coefficient.

We, however, may not be able to obtain the value of the model coefficient from a cooling tower manufacturer. Instead, we may evaluate the coefficient by first evaluating the NTU_R based on the design operating conditions of a cooling tower and regard the result as the NTU_A of the cooling tower selected for this design duty. We can then determine the value of the coefficient using Equation (9.12) and assume that this coefficient is a constant for the selected cooling tower applicable to all operating conditions.

$$C_{ctr} = NTU_A \cdot (m_a/m_w)^{-0.6} \quad (9.12)$$

With the model coefficient C_{ctr} evaluated, we may determine NTU_A when the mass flow rates of air and water are known or assigned with assumed values, using Equation (9.11). A trial and error procedure may then be used to determine NTU_R for an assumed value of the unknown leaving water temperature and continue to adjust this assumed value until the NTU_R calculated matches with NTU_A. The numerical integration method described in Chapter 6, as denoted by Equation (9.10), may be used for evaluation of NTU_R in this process.

9.3.3 Variable speed pump or fan model and power input prediction

Pump or fan power demand, W, is a function of the water or air flow rate, V, and the rise in pressure, ΔP, delivered by the pump or fan.

$$W = \frac{\Delta P \cdot V}{\eta} \tag{9.13}$$

In the above equation, η is the efficiency of the pump or fan. At a given running speed, N, the relation between ΔP and V is fixed, as shown by the pump or fan characteristic curve provided by the manufacturer. The curve showing ΔP as a function of V, $\Delta P(V)$, at the design speed, N_0, may be modelled by a polynomial as shown below:

$$\Delta P = a_0 + a_1 V + a_2 V^2 + a_3 V^3 + a_4 V^4 \qquad (\text{at } N = N_0) \tag{9.14}$$

Likewise, the corresponding relation between pump or fan power, W, and flow rate, V, at the design speed may be modelled by a polynomial:

$$W = b_0 + b_1 V + b_2 V^2 + b_3 V^3 + b_4 V^4 \qquad (\text{at } N = N_0) \tag{9.15}$$

For most pumps and fans, a polynomial of order 3 or 4 should be good enough to provide an accurate relation between ΔP or W and V at a given speed. If sufficient operating data are available, we may establish mathematical models for the performance curves of a variable speed pump or fan with running speed included as an independent variable. Such mathematical models, however, could involve many terms and thus are cumbersome to use, and they may even lead to numerical problems in processes that involve solving for an independent variable in the equation by iteration. However, if less terms are used, the accuracy of the predictions may not be acceptable.

Alternatively, we may make use of the pump/fan affinity laws, as shown below, in conjunction with the pressure and power models for the design speed, as shown in Equations (9.14) & (9.15), to find pump or fan performance at any speed below the design speed.

$$\frac{V_1}{V_0} = \frac{N_1}{N_0} \tag{9.16a}$$

$$\frac{\Delta P_1}{\Delta P_0} = \left(\frac{N_1}{N_0}\right)^2 = \left(\frac{V_1}{V_0}\right)^2 \tag{9.16b}$$

$$\frac{W_1}{W_0} = \left(\frac{N_1}{N_0}\right)^3 = \left(\frac{V_1}{V_0}\right)^3 \tag{9.16c}$$

In the above set of pump/fan affinity laws, the subscripts 0 & 1 denote not any two arbitrary operating conditions but two operating conditions that are dynamically similar (Figure 9.8).

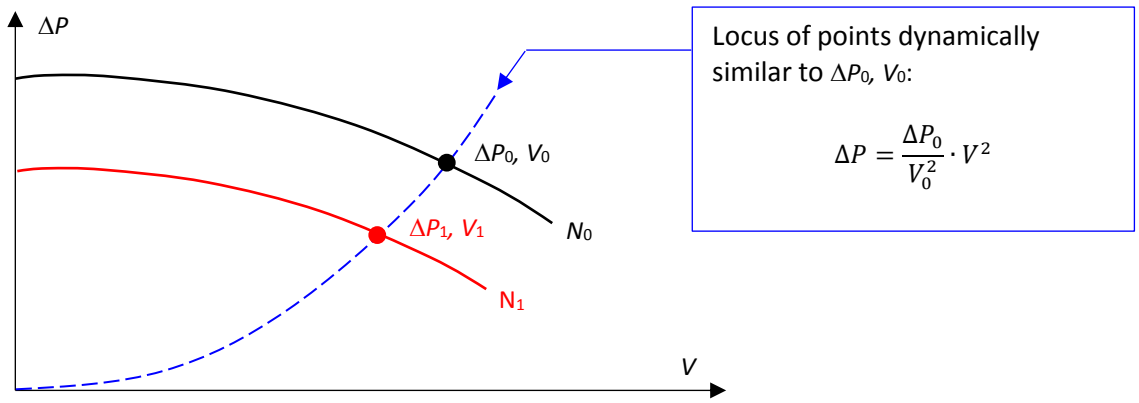

Figure 9.8 Dynamically similar operating points of a pump or fan

According to Equation (9.16b), points that are dynamically similar to a given point, say $(\Delta P_0,\ V_0)$, are any point along a parabola that passes through the origin and the given point, and the relation between ΔP and V for any point on this curve is as given by:

$$\Delta P = \frac{\Delta P_0}{V_0^2} \cdot V^2 \tag{9.17}$$

If $(\Delta P_0,\ V_0)$ is the design operating point of a pump or fan and N_0 is its design running speed, when the pump or fan is running at N_1 at the operating point $(\Delta P_1,\ V_1)$, as shown in Figure 9.9, the operating point at the design running speed (N_0) that is dynamically similar to $(\Delta P_1,\ V_1)$ is $(\Delta P_0',\ V_0')$, which may be different from $(\Delta P_0,\ V_0)$. This is a point that should be borne in mind when we apply the pump/fan affinity laws to find the performance of a pump or fan when it is operating at a speed different from its design speed.

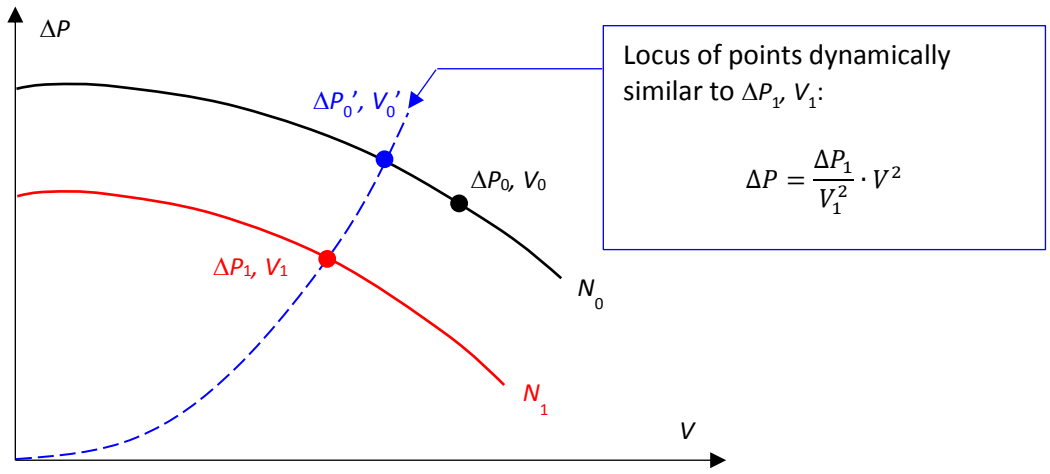

Figure 9.9 Operating point dynamically similar to $\Delta P_1,\ V_1$

In a piping or ducting system with variable speed pump or fan, the operating point that would arise when the running speed of the pump or fan is varied is dependent on the characteristics of the piping or ducting system as well as the way in which pump or fan speed control is implemented. Assuming that what we need to evaluate is the pump or fan power, W_1, when the pump or fan is required to deliver a flow rate of V_1, this can be determined only if the pump or fan pressure required, ΔP_1, is known. Therefore, an additional model is needed for us to determine the required pump or fan pressure, ΔP, for the given flow rate, V, in the piping or ducting system.

As discussed in Chapter 7 and shown in Figure 7.12, for a pumping system with the pump speed controlled to achieve a steady differential pressure across the critical branch, we may use a pump modulation curve to represent the pumping pressure required at various flow rates. Likewise, a fan modulate curve may also be defined for a VAV system with duct static pressure control that keeps the duct static pressure at a selected position in the ducting system at its set-point level by varying the fan speed. The pump or fan modulation curve is an idealized representation of the pump or fan operating points under the full- and part-load conditions of a system.

In reality, the operating points may deviate from the modulation curve depending on the pattern of operating of the branch control valves or VAV terminals. However, there are two operating conditions on a pump or fan modulation curve that are certain:

When $V = V_0$; $\Delta P = \Delta P_0$
When $V = 0$; $\Delta P = \Delta P_c$

Where ΔP_c is the set point differential pressure across the critical branch of a piping system or at the location along the main supply air duct that is kept under control. For our application, the pump modulation curve may be approximated by (Figure 9.10):

$$\Delta P = \Delta P_c + K \cdot V^2 \tag{9.18}$$

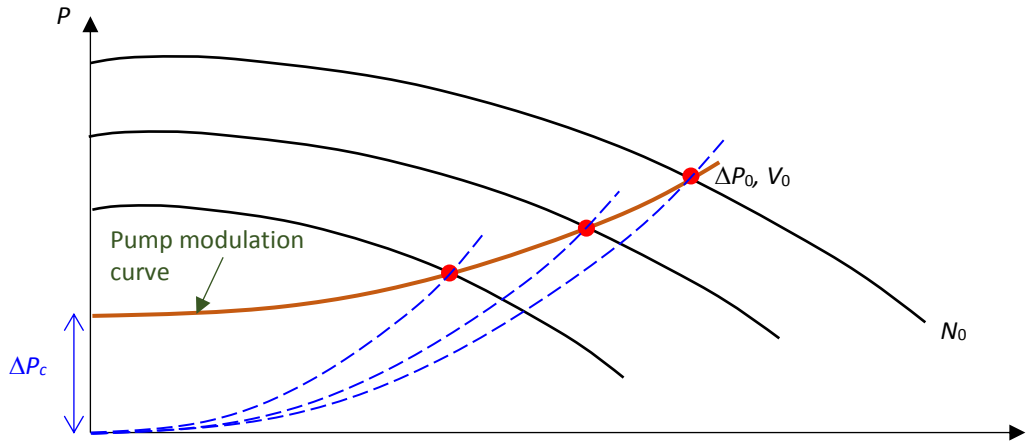

Figure 9.10 Pump or fan modulation curve

Applying the above model to the design operating point (ΔP_0, V_0) allows the coefficient K in the model to be evaluated as follows:

$$K = (\Delta P_0 - \Delta P_c)/V_0^2 \tag{9.19}$$

The relations between the design and part-load operating points (points denoted by subscripts 0 & 1) and between the part-load operating point and the point at the rated pump speed that is dynamically similar to it (denoted by subscript 2) are as shown in Figure 9.11.

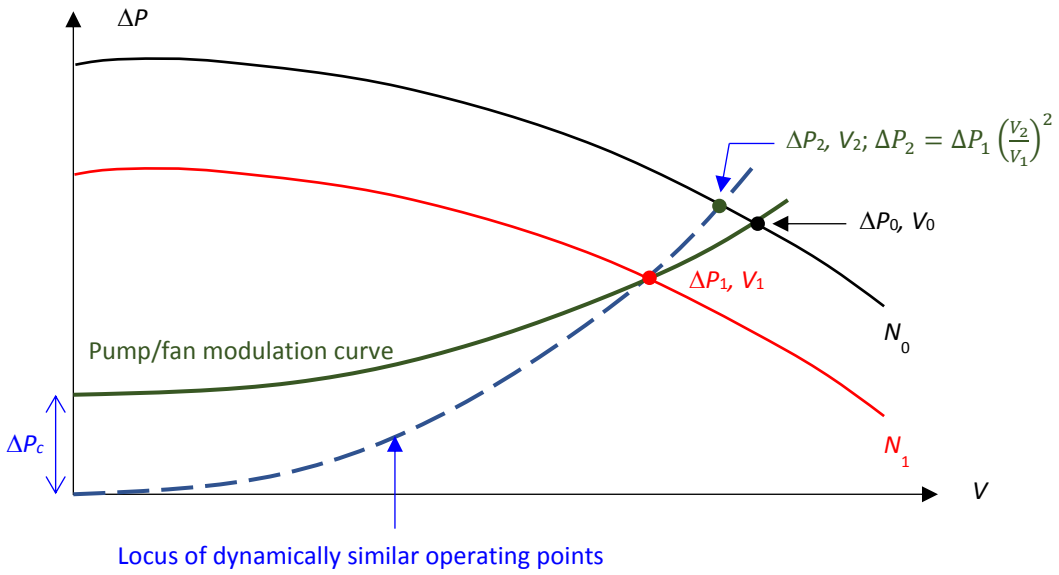

Figure 9.11 Pump or fan modulation curve

With reference to Figure 9.11, the following steps may be used to determine part-load pump or fan power:

1. Based on given value of V_1 at the part-load condition, evaluate ΔP_1 using the pump or fan modulation curve (Equation (9.18)).

2. Evaluate ΔP_2 & V_2 based on ΔP_1 & V_1 using the relation between dynamically similar points (Equation (9.16)).

3. Find W_2 corresponding to point (ΔP_2, V_2) at the design pump or fan speed (N_0) (Equation (9.15))

4. Evaluate W_1 and N_1 from:

$$W_1 = W_2 \left(\frac{V_1}{V_2}\right)^3 \tag{9.20}$$

$$N_1 = N_0 \left(\frac{V_1}{V_2}\right) \tag{9.21}$$

As shown in Equation (9.22) below, the efficiencies of the pump or fan at dynamically similar operating points are equal.

$$\eta_1 = \frac{\Delta P_1 V_1}{W_1} = \Delta P_2 \left(\frac{V_1}{V_2}\right)^2 \cdot V_1 \cdot \frac{1}{W_2} \left(\frac{V_2}{V_1}\right)^3 = \frac{\Delta P_2 V_2}{W_2} = \eta_2 \tag{9.22}$$

The accuracy of the estimates made by using the method discussed above is dependent mainly on how well the pump/fan modulation curve model is able to predict the pump/fan pressure corresponding to the flow rate in demand. For an application where the pump/fan pressure is consistently measured by the BMS, the measured pressure value may be used instead of using the modulation curve model to predict the pump/fan pressure. Nevertheless, a model would still be needed for prediction of the change in pump/fan pressure corresponding to the change in air or chilled water flow rate demand that may result from changes that may be made to the operating condition or control settings for optimization of energy performance.

9.4 Control optimization for a chiller plant

Having introduced the models for the major equipment in a chiller plant, we can now proceed to discuss control optimization for a chiller plant. Owning to the complex calculations involved, chiller plant control optimization is typically implemented through a computer program written specifically for this purpose. The key function of this program is to determine, given the current operating conditions, including the cooling demand, chilled water flow rate demand, and the conditions of the weather and/or cooling medium, and certain constraints to be observed, the combination of equipment to be deployed and the control settings to be adopted such that, while the cooling and chilled water flow rate demands, and the applicable constraints, can be satisfied, the total power demand of the chiller plant will be minimized.

The calculations to be undertaken by the chiller plant control optimization program are not only complex, they also need to be completed very quickly. The bottom line is that, by the time the optimal pattern of equipment deployment and control settings are determined, there should not be significant changes in the general operating conditions of the chiller plant that may invalidate the output of the optimization program. Since such computational demand would far exceed the capability of a typical building management system (BMS), the control optimization program needs to be run on a platform, which may be called a building energy management system (BEMS), that is separate from but is consistently communicating with the BMS. The BEMS may reside in a cloud server or a computer dedicated for this application. It will consistently acquire data of relevant operating parameters from the BMS server, carry out the computations and optimization search function, and send command signals on the optimal operation pattern and control settings for the chiller plant equipment to the BMS for execution.

To provide a focus for the ensuing elaborations on the key function of a chiller plant control optimization program, reference is made to the characteristics of a hypothetical chiller plant. For simplicity, the assumptions are made that the chiller plant has cooling towers for heat rejection, uses the variable primary flow (VPF) design for chilled water

distribution, is composed of a number of identical units of water-cooled chillers and each chiller is equipped with a variable speed chilled water pump, a variable speed condenser water pump, and a variable speed cooling tower, all with capacities matching with the chiller they serve (Figure 9.12).

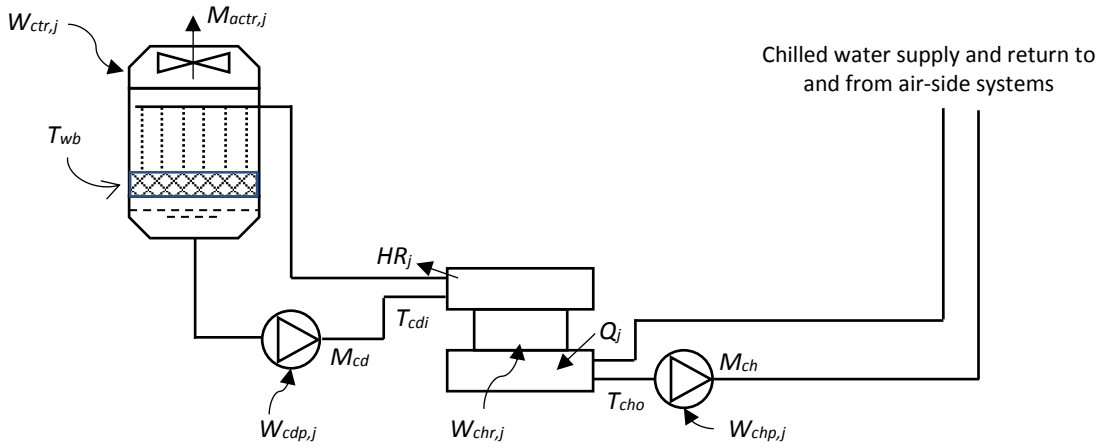

Figure 9.12 Schematic diagram of reference chiller plant

9.4.1 Required system and equipment models

The total power demand of the chiller plant, W_{plt}, is dependent on a number of system variables as shown in Equation (9.23), which is the objective function to be minimized at every time step the control optimization program is called to provide a solution.

$$W_{plt} = f(Q, N_{chr}, T_{cho}, M_{ch}, N_{chp}, T_{cdi}, M_{cd}, N_{cdp}, N_{ctr}, T_{wb}) \tag{9.23}$$

Where

Q = cooling load on the plant
N_{chr} = number of chillers to be run
T_{cho} = supply chilled water temperature
M_{ch} = chilled water mass flow rate
N_{chp} = number of chilled water pumps to be run
T_{cdi} = condenser water temperature entering chillers
M_{cd} = condenser water flow rate
N_{cdp} = number of condenser water pumps to be run
N_{ctr} = number of cooling towers to be run
T_{wb} = wet bulb temperature of outdoor air

The total power demand of the chiller plant, W_{plt}, may alternatively be expressed as the sum of power demands of the operating equipment, as shown below.

$$W_{plt} = \sum_{j=1}^{N_{chr}} W_{chr,j} + \sum_{j=1}^{N_{chp}} W_{chp,j} + \sum_{j=1}^{N_{cdp}} W_{cdp,j} + \sum_{j=1}^{N_{ctr}} W_{ctr,j} \tag{9.24}$$

For our case where the units of equipment of each type are identical, the above may be simplified to:

$$W_{plt} = N_{chr}W_{chr,j} + N_{chp}W_{chp,j} + N_{cdp}W_{cdp,j} + N_{ctr}W_{ctr,j} \quad (9.25)$$

The power demand of each equipment, in turn, is dependent on the respective influencing variables as shown below.

i) For a running chiller:

$$W_{chr,j} = W_{chr,j}(Q_j, T_{cho}, M_{ch,j}, T_{cdi}, M_{cd,j}) \quad (9.26)$$

Where

$$Q_j = \frac{Q}{N_{chr}} \quad (9.27a)$$

$$M_{ch,j} = \frac{M_{ch}}{N_{chr}} \quad (9.27b)$$

$$M_{cd,j} = \frac{M_{cd}}{N_{chr}} \quad (9.27c)$$

ii) For a chilled water pump or a condenser water pump:

$$W_{chp,j} = W_{chp,j}(M_{chp,j}, \Delta P_{ch}) \quad (9.28)$$

$$W_{cdp,j} = W_{cdp,j}(M_{cdp,j}, \Delta P_{cd}) \quad (9.29)$$

Where

$$M_{chp,j} = \frac{M_{ch}}{N_{chp}} \quad (9.30)$$

$$M_{cdp,j} = \frac{M_{cd}}{N_{cdp}} \quad (9.31)$$

The chilled water pump pressure, ΔP_{ch}, may be determined from the pump modulation curve model for the system:

$$\Delta P_{ch} = \Delta P_{chc} + K_{ch}M_{ch}^2 \quad (9.32)$$

However, the condenser water pump pressure, ΔP_{cd}, needs to be evaluated from the pressure drop across the condenser of a chiller, $\Delta P_{cd,j}$, the pressure drop across a cooling tower, $\Delta P_{ctr,j}$, and the pressure drop round the piping system of the condenser water circuit ($= K_{cd}M_{cd}^2$):

$$\Delta P_{cd} = \Delta P_{cd,j} + \Delta P_{ctr,j} + K_{cd}M_{cd}^2 \quad (9.33)$$

Note that $\Delta P_{cd,j}$ & $\Delta P_{ctr,j}$ may be assumed to be proportional to the square of the respective flow rate of condenser water through the chiller condenser and the cooling tower.

iii) For a cooling tower, the power demand of its fan may be taken as dependent solely on its running speed ($S_{ctr,j}$):

$$W_{ctr,j} = W_{ctr,j}(S_{ctr,j}) \tag{9.34}$$

The cooling tower fan speed, $S_{ctr,j}$, affects the air flow rate through the cooling tower, $M_{actr,j}$, and, in turn, the heat transfer performance of the cooling tower and, therefore, it is one of the control settings to be determined in the optimization search process.

Whereas the real-time measurements of the total cooling output, Q, and chilled water flow rate, M_{ch}, are inputs to the optimization process, the number of chillers to be run, N_{chr}, and the chilled water supply temperature, T_{cho}, may be varied, together with other variables that may also be varied in the optimization search. However, as a result of the characteristics of cooling coils in the air-side systems, varying T_{cho} by ΔT_{cho}, would lead to a change in M_{ch}, say from $M_{ch,Last}$ to M_{ch}, which should be accounted for in the process:

$$M_{ch} = M_{ch,Last} + \frac{\partial M_{ch}}{\partial T_{cho}} \Delta T_{cho} \tag{9.35}$$

There is, therefore, a need for a model that relates the chilled water flow rate demand of the air-side systems to the cooling load and supply chilled water temperature:

$$M_{ch} = f(Q, T_{cho}) \tag{9.36}$$

This model may be established from an analysis of the plant operating data. If such empirical model is unavailable, the following model, derived from simulation of the response of a typical cooling coil to rises in the supply chilled water temperature from the design set point temperature, $T_{cho,sp}$, may be used:

$$M_{ch} = F \cdot \frac{Q}{C_w \cdot DT_{cho,sp}} \tag{9.37a}$$

Where

$$F = 1 + 0.1098 \cdot \theta - 0.0366 \cdot \theta^2 + 0.0488 \cdot \theta^3 \tag{9.37b}$$

$$\theta = T_{cho} - T_{cho,sp} \tag{9.37c}$$

C_w is the specific heat of water and $DT_{cho,sp}$ the difference between the design supply and return chilled water temperatures.

9.4.2 Evaluation of the plant total power demand for one set of defined conditions

When Q, T_{wb}, N_{chr}, M_{ch}, T_{cho}, M_{cd}, and T_{chi} are defined, we can determine $W_{chr,j}$ using the chiller model (e.g. the Gordon & Ng model given above). The condenser heat rejection rate of a chiller, HR_j, and of the entire plant, HR, may then be evaluated, as follows:

$$HR_j = Q_j + W_{chr,j} \tag{9.38a}$$

$$HR = N_{chr} \cdot HR_i \tag{9.38b}$$

The condenser water temperature returning to the cooling towers, T_{cdo}, would then be:

$$T_{cdo} = T_{cdi} + \frac{HR}{C_w M_{cd}} \tag{9.39}$$

Where C_w is the specific heat of water.

For simplicity, the number of chilled water pumps, N_{chp}, and condenser water pumps, N_{cdp}, that will be run are assumed here to be equal to the number of chillers, N_{chr}, that will be put into operation. This is often a choice preferred by plant operators to simplify the operational procedures involved in turning on and off chillers and pumps, especially in the case of a variable primary flow (VPF) system. However, the number of cooling towers to be run should be made an independent variable for which an optimal value will be sought in the optimization search process. This is because running more cooling towers than the required minimum can often lead to significant reduction in the overall power demand of a chiller plant.

When N_{chp}, N_{cdp} & N_{ctr}, and hence the water flow rate through individual pumps, are also defined, the running speed and power demand of the chilled and condenser water pumps can be evaluated using the pumping pressure models (e.g. Equations (9.32) & (9.33)) and the pump models (see Section 9.3.3) available. The solution process will involve the use of an iterative process to solve for the flow rate, V_2, at the operating point along the pump curve for the rated speed, N_0, that is dynamically similar to the actual pump operating point (Figure 9.11), from a polynomial resulting from substituting $\Delta P_1 \cdot (V_2/V_1)^2$ for ΔP_2 in Equation (9.14):

$$\frac{\Delta P_1}{V_1^2} V_2^2 = a_0 + a_1 V_2 + a_2 V_2^2 + a_3 V_2^3 + a_4 V_2^4$$

$$0 = a_0 + a_1 V_2 + \left(a_2 - \frac{\Delta P_1}{V_1^2}\right) V_2^2 + a_3 V_2^3 + a_4 V_2^4 = f(V_2) \tag{9.40}$$

The well-known Newton-Raphson method is an efficient numerical scheme for this purpose. In this method, from an initial estimate of V_2, denoted by $V_{2,0}$, a better estimate, $V_{2,1}$, can be evaluated from:

$$V_{2,1} = V_{2,0} - f(V_{2,0})/f'(V_{2,0}) \tag{9.41}$$

Where

$$f'(V_2) = df(V_2)/dV_2 \tag{9.42}$$

The cooling tower model (see Section 9.3.2) may now be used to determine the air mass flow rate required, $M_{actr,j}$, for the cooling towers to cool the condenser water at the flow rate of $M_{cd,j}$, from T_{cdo} down to T_{cdi}. This requires the use of an iterative process involving evaluation of NTU_R from an assumed value for $M_{actr,j}$, together with the current values for the condenser water flow rate, $M_{wctr,j}$, and the return and supply condenser water temperatures, T_{cdo} & T_{cdi}, by a numerical integration process (see Equation 9.10). The NTU_A should also be evaluated from the ratio of $M_{actr,j}$ to $M_{wctr,j}$ (see Equation 9.11). If the values of NTU_R and NTU_A are not close enough to each other, a new estimate for $M_{actr,j}$ is to be made and the calculations should be repeated, until the two are more or less equal.

Based on the converged solution for the air mass flow rate, $M_{actr,j}$, obtained, the cooling tower fan speed, $S_{ctr,j}$, and hence the fan power, $W_{ctr,j}$, can be evaluated. For a cooling tower fan, we may simply apply the fan laws, i.e. the flow rate is proportion to the fan speed, and the fan power is proportional to the cube of the fan speed. Therefore, the ratio of the actual fan power to the rated power is proportional to the cube of the ratio of the actual air flow rate to the rated air flow rate.

The calculation steps discussed in this sub-section may be written into a subroutine for prediction of the plant total power demand under a given set of values for all the operating parameters that may be varied for plant power demand minimization. This subroutine, which serves the function of Equation (9.23), may be called repeatedly in the optimization search program to determine the impact of adjusting the value of each of the variable operating parameters on the plant total power demand.

9.4.3 Optimization search

Figure 9.13 shows the hierarchical arrangement in an optimization search algorithm that may be used for determining the optimal combination of equipment to be run and the control settings to be used, under a given set of external inputs, including Q, M_{ch}, and T_{wb}, for the reference chiller plant defined at the beginning of Section 9.4.

As shown in Figure 9.13, the search for the optimal chilled water supply temperature (T_{cho}) is put at the top level. The optimization search at this level involves evaluating and comparing the overall plant energy use (W_{plt}) when a particular value of T_{cho} (called the current value) and when a value of T_{cho} that is higher than the current value by a pre-set incremental step (e.g. 0.5 ^{o}C) were used in turn as the set point temperature. As discussed in Sub-section 9.4.1, the total chilled water flow rate, M_{ch}, must be re-evaluated to reflect the impact of a change in T_{cho} on M_{ch}. This will be further discussed later when consideration is given to control optimization for the air-side systems as well.

If the lowest overall plant energy use is found to be associated with the T_{cho} value that is higher than the current value, this T_{cho} value will replace the current value. The overall plant energy use will then be evaluated for a further increased T_{cho} value next to the new current value, and the plant energy use values will be compared once again. This process will start from the design chilled water temperature and will be repeated until

the minimum overall plant energy use corresponds to the current T_{cho} value, which is then the optimal T_{cho} value, or when the maximum allowable chilled water temperature is reached.

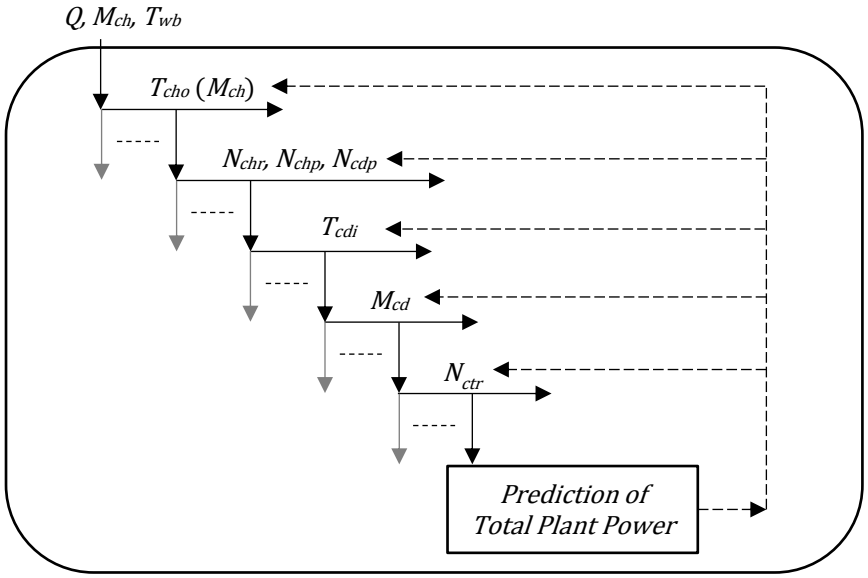

Figure 9.13 Schematic diagram of a search algorithm with multiple loops of optimization search for different system variables

Figure 9.14 provides an illustration for this search process. Assuming the T_{cho} value of point 0 in the figure was the design value and thus the starting current value, and the plant overall power demand (W_{Plt}) corresponding to the T_{cho} values at points 0 & 1 were evaluated and compared. This will lead to the T_{cho} value of point 1 to be taken as the current value for the lower W_{Plt} value it is associated with, and the search algorithm will proceed to consider point 2. In the following steps, the T_{cho} values of point 2 and point 3 will be taken in turn as the current value and, when point 4 is evaluated, the overall plant power demand corresponding to the T_{cho} value of point 3 will be found to be the optimal value.

A starting point of an optimization search that differs from that selected above (the design point), e.g. the point adopted in the last time step, may be used. In this case, the plant total power demands for the starting point and the points adjacent to it at both sides would need to be evaluated to determine the direction of search, which should be the direction that the plant total power demand would drop by the greatest amount. The search would stop when the plant total power demand corresponding to the central point is lower than those corresponding to the adjacent points at both sides, or when the limit of the variable range of the concerned parameter is reached.

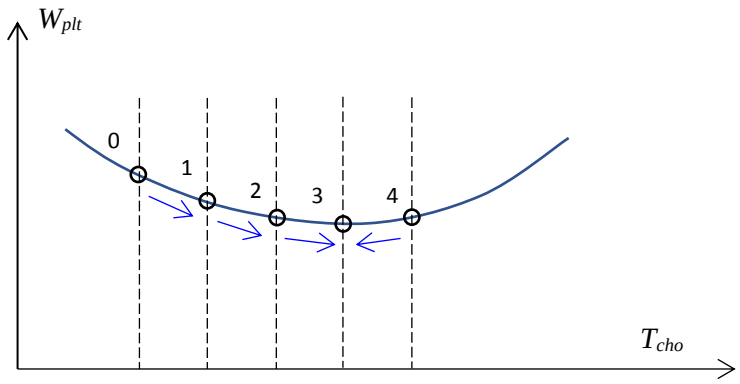

Figure 9.14 Optimization search for a system variable T_{cho}

For each T_{cho} value under consideration in the search process discussed above, a lower tier optimization search module will be called to determine the optimal combination of chillers and chilled and condenser water pumps to be run such that, under the given Q, T_{wb} and T_{cho} values, the overall plant energy use will be the lowest. For each combination of chillers, chilled water pumps and condenser water pumps being considered, the lower tier module will be called to search for the optimal condenser water supply temperature to be used in the system for achieving the lowest overall chiller plant power demand. For each temperature under consideration, optimization search for the optimal condenser water flow rate will be carried out. In turn, the module for determining the combination of cooling towers to be run, and their fan speed, for minimization of the overall plant power consumption under a given combination of running chillers and pumps and condenser water temperature and flow rate will also be called by the condenser flow rate optimization search module.

In each of the search modules discussed above, adequate limit checks are incorporated to ensure no violation of any constraints, e.g. chilled water flow rate through each chiller not to exceed it rated value nor falling below the minimum allowable level; the speeds of all pumps and cooling tower fans not to fall outside their respective low and high limits, etc. Since all the system operating parameters are optimized when an optimal value of T_{cho} is found, the corresponding overall plant power demand will already be the result of operating the optimal combination of equipment and using the optimal combination of control settings.

Programs developed according to the search method discussed above have been found to be performing reasonably well in practice. This search method is certainly not the most efficient method in respect of the computational efforts required but it is easy to be coded into a control optimization program. The workable limits on the ranges of the adjustable parameters, the small change in operating condition that would arise within a time step, and the significant impacts of some changes, can help limit the extend of search to be undertaken in each time step. Of course, more advanced search algorithms [6], such as the slope of the steepest descent method, may be employed, if preferred.

9.5 Control optimization for air-side systems and whole system optimization

In this section, control optimization of air-side systems will be discussed, including discrete measures that may be applied irrespective of whether other measures will be implemented simultaneously, and measures that would impact other measures, including the central chiller plant control optimization discussed above. How air-side system control optimization may be integrated with the central chiller plant control optimization to achieve overall control optimization for the entire central air-conditioned system will also be discussed.

9.5.1 Air-side system control optimization

For a constant air volume (CAV) or primary air fan-coil system, there is little scope for control optimization that would yield significant energy saving. Optimization of the chilled water supply temperature and flow rate is one issue that may be considered, which has already been covered in Section 9.4.1 where the strategy of resetting chilled water supply temperature and its impact on the chilled water flow rate demand of the air-side systems are discussed.

Resetting the set-point temperature of the air-conditioned space with reference to the outdoor temperature may be another option but once a re-set schedule for determining the set-point from the measured outdoor temperature has been determined, the control is straightforward to implement without the need for complex calculations from time to time. The margin of reset, however, is typically quite narrow as, to most commercial buildings, thermal comfort of the occupants is usually an issue of higher priority than energy saving.

Optimal start/stop control over the air-side system equipment, which involves determining when to start the air-side equipment before commencement of the occupied period of the air-conditioned spaces, and when to stop the equipment towards the end of the occupied period, may involve determination of the optimal lead time for the start/stop control. However, the major purpose of implementing this control is more often for curbing rise in maximum current demand of the central chiller plant rather than for the potential energy saving, which would not be substantial after all. Furthermore, such optimization control may be implemented according to a pre-determined schedule devised through a detailed analysis of the response of the air-conditioned space to starting and stopping of the air-conditioning system, and carried out separately from the continued control optimization for the central chiller plant and other systems.

For a fresh air (FA) or primary air (PA) supply system, demand controlled ventilation (DCV), which involves regulation of the supply FA/PA flow rate according to the demand, as reflected by measurements of the occupancy or carbon dioxide concentration in the air-conditioned spaces, is the major strategy of energy conservation. This will also be a straightforward control issue and there is no need for run-time optimization, although the associated cooling load and chilled water demand for FA/PA treatment may affect the optimal pattern of equipment and control settings that the optimization search process will find.

For a variable air volume (VAV) system that serves multiple zones where each zone is served by one or more VAV boxes (or terminals) that receive supply air (SA) from an air-handling unit (AHU) via a SA ductwork (Figure 9.15), duct static pressure reset (DSPR) control can be a highly effective measure that can lead to very substantial energy saving. Besides this, other measures may be implemented, which would have significant impacts on the continued control optimization for the central chiller plant. The next sub-section is dedicated to more detailed discussions on control optimization for a VAV system.

9.5.2 VAV system control optimization

In a multi-zone VAV system (Figure 9.15), there are two control loops: one for controlling the temperature of the supply air (SA) discharged by the air-handling unit (AHU), which is done through regulating the chilled water flow rate through the cooling coil in the AHU; and the other for controlling the SA flow rate according to the static pressure in the ductwork, at the position where the duct static pressure sensor is installed. Traditionally, the SA flow rate would be regulated by using an inlet guide vane but, nowadays, most VAV AHUs are equipped with a variable frequency drive such that SA flow rate regulation can be done by varying the fan speed, which is more energy efficient than using an inlet guide vane. In the following discussion, fan speed regulation is assumed to be the mechanism for SA flow rate control.

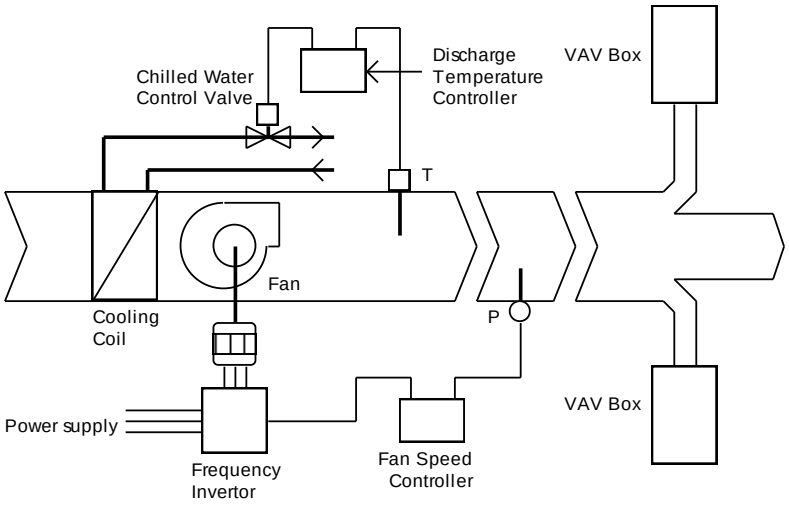

Figure 9.15 VAV system for multiply zones

On top of the abovementioned basic control functions, the following control strategies may be employed to optimize the energy efficiency of the system:

1. Duct static pressure reset (DSPR) control
2. Fresh air (FA) flow rate regulation, also known as demand control ventilation, typically based on indoor CO_2 concentration
3. SA temperature (T_{sa}) reset control
4. Chilled water supply temperature (T_{cho}) reset control

a) DSPR control

The DSPR control tries to lower the duct static pressure setpoint step-by-step until the allowable maximum number of VAV boxes that need to fully open their dampers in order to get the required SA flow rate is reached; the duct static pressure will be reset upward instead if this allowable maximum number is exceeded by a pre-set margin. With this control, the SA fan will be kept running at the lowest possible speed, and hence it will only consume the lowest possible amount of electricity, and yet without starving any VAV box for SA.

Since there are no operational conflicts between the DSPR control and any of the other control strategies listed above, it can be implemented with or without implementing, in parallel, any of the other control strategies. It can also be implemented independently no matter whether chiller plant control optimization is implemented simultaneously. However, the operating conditions of the VAV system under DSPR control may affect the effect of implementing the other control strategy (e.g. T_{sa} reset) and, therefore, evaluation of the achievable energy saving of the control strategy under concern must account for the conditions of the system with the DSPR control in operation.

b) FA flow rate regulation

Similar to the DSPR control, the CO_2 based FA flow rate regulation method may be implemented to reduce energy use for air-conditioning with or without also implementing any of the other control strategies on the list. For implementing this control, sensors will be installed to measure the CO_2 concentrations in the occupied zones, as a surrogate measurement of the occupancy level in each zone. With the FA supply into individual occupied zones regulated with reference to the CO_2 concentration in the zone, the cooling load for FA treatment can be reduced whenever the demand for FA supply can be reduced, which would be possible at times of low occupancy.

A low limit has to be set in this control to ensure there would at least be a certain FA supply into the occupied spaces even though the occupancy level is low or even zero. This is especially important if part of the general exhaust from the air-conditioned spaces is used for making up the air that will be extracted from the toilets, which will be disposed of as exhaust air, while allowing the toilets to enjoy a limited degree of cooling as a by-product of ventilation provision. As long as the effect of FA flow rate regulation on the air-conditioning system is accounted for in determining the impact of the other control strategies, no additional consideration would need to be given to it in air- and water-side system control optimization.

However, if total heat recovery wheels are adopted where the general exhaust air is used to pre-treat the hot and humid outdoor air before the outdoor air is drawn through the FA AHUs, a balance needs to be struck between the energy saving due to reduction of FA flow rate and the lowering in the effectiveness of the heat recovery wheels due to the corresponding reduction in the exhaust air flow rate. This optimization, however, would remain a standalone function with little relation to the operation of other energy conservation or optimization measures.

c) T_{sa} reset control

By lowering the set point value for the supply air temperature for a particular air-side system, $T_{sa,i}$, the required SA flow rate ($V_{sa,i}$) for handling the same room sensible cooling load ($q_{rs,i}$) can be reduced, and hence the fan power ($W_{saf,i}$) will drop. However, the cooling coil will need a higher flow rate of chilled water ($M_{ch,i}$) (assuming T_{cho} is unchanged) to cool the SA down to the lower temperature set point, which, in turn, will incur an increase in the chilled water pump power (W_{chp}). The following equations describe the changes in fan and pump power resulting from a change in $T_{sa,i}$:

$$\delta W_{saf,i} = \frac{\partial W_{saf,i}}{\partial V_{sa,i}} \cdot \frac{\partial V_{sa,i}}{\partial T_{sa,i}} \cdot \delta T_{sa,i} \tag{9.43}$$

$$\delta W_{chp} = \frac{\partial W_{chp}}{\partial M_{ch,i}} \cdot \frac{\partial M_{ch,i}}{\partial T_{sa,i}} \cdot \delta T_{sa,i} \tag{9.44}$$

Since $V_{sa,i}$ is determined by the difference between the indoor air temperature set point ($T_{r,i}$) and $T_{sa,i}$,

$$V_{sa,i} = \frac{q_{rs,i}}{\rho_a Cp_a (T_{r,i} - T_{sa,i})} \tag{9.45}$$

$$\frac{\partial V_{sa,i}}{\partial T_{sa,i}} = \frac{q_{rs,i}}{\rho_a Cp_a (T_{r,i} - T_{sa,i})^2} \tag{9.46}$$

As Equation (9.46) unveils, the reduction in $V_{sa,i}$ will become smaller for each further drop in $T_{sa,i}$, i.e. there will be a diminishing return in reducing $V_{sa,i}$ by lowering $T_{sa,i}$.

The change in fan power per unit change in SA flow rate ($\partial W_{saf,i}/\partial V_{sa,i}$) is a characteristic of the fan (which can be evaluated from fan curves that relate fan power to flow rate at given fan speeds) and is dependent on the operating point at which the change occurs. Therefore, the potential fan energy saving is dependent on the current system flow rate and fan pressure and, hence, it may be affected by the DSPR control.

On the other hand, the change in $M_{ch,i}$ per unit change in $T_{sa,i}$ ($\partial M_{ch,i}/\partial T_{sa,i}$) is a characteristic of the cooling coil in the AHU and is dependent on the temperature of the chilled water supply, T_{cho}. With T_{cho} held constant, $M_{ch,i}$ will increase by a greater and greater extent as $T_{sa,i}$ is reduced step-by-step but there is a limit to increasing $M_{ch,i}$ through a cooling coil, e.g. when the control valve is already fully open.

The change in chilled water pump power per unit change in chilled water flow rate ($\partial W_{chp}/\partial M_{ch,i}$) is a characteristic of the pump and is dependent on the pumping pressure and total chilled water flow rate being handled by the pump. Therefore, the change in chilled water pump power may be affected by the operating conditions of other AHUs and the current T_{cho} setpoint being set for chiller plant control optimization.

A downward adjustment of the SA temperature setpoint will be worthwhile provided that:

$$\delta W_{saf,i} + \delta W_{chp} \leq 0 \tag{9.47}$$

The optimal condition is reached when the sum of the changes in fan and pump power demands, i.e. the LHS of Equation (9.47), equals zero. This is also a local optimization process for the air-side system under concern, with T_{cho}, M_{ch}, and W_{chp} being the links to the chiller plant control optimization process.

d) T_{cho} reset control

The chilled water supply temperature (T_{cho}) reset control is one of the component strategies of the overall chiller plant control optimization strategy discussed earlier. By raising the setpoint for T_{cho}, the chillers will require less power input for the same total cooling output. As a consequence, however, the air-side systems would require more chilled water for coping with the room cooling loads and the increased chilled water flow rate (M_{ch}) will lead to a corresponding increase in the chilled water pump power (W_{chp}), as depicted by Equation (9.48).

$$\delta W_{chp} = \frac{\partial W_{chp}}{\partial M_{ch}} \cdot \frac{\partial M_{ch}}{\partial T_{cho}} \cdot \delta T_{cho} \tag{9.48}$$

The rate of change in M_{ch} with respect to T_{cho} ($\partial M_{ch}/\partial T_{cho}$) is an aggregate response of all the cooling coils connected to the chilled water circuit, as shown below.

$$\frac{\partial M_{ch}}{\partial T_{cho}} = \sum \frac{\partial M_{ch,i}}{\partial T_{cho}} \qquad \text{for } i = 1, 2, \ldots, n \text{ and } n = \text{no. of air-side systems} \tag{9.49}$$

Compared with Equations (9.36) or (9.37), which is an aggregated model relating chilled water flow rate demand, M_{ch}, to the chilled water supply temperature, T_{cho}, Equation (9.49) above is a refinement of this model that uses a similar model for each air-side system. This refined method can only be employed if the air-side systems have their own control optimization programs which are linked to the chiller plant control optimization program.

As noted above, the increase in pump power due to the increase in chilled water flow rate, $\partial W_{chp}/\partial M_{ch}$, is a characteristic of the pump and is dependent on the pumping pressure and total chilled water flow rate being handled by the pump. Raising the T_{cho} set point is worthwhile provided the reduction in chiller power demand (δW_{chr}) can more than compensate the corresponding increase in chilled water pump power (δW_{chp}), i.e.:

$$\delta W_{chr} + \delta W_{chp} \leq 0 \tag{9.50}$$

The optimal condition is reached when the sum of the changes in chiller and pump power demands, i.e. the LHS of Equation (9.50), equals zero.

9.5.3 Air-side and water-side system control optimization

As discussed above, each air-side system may need to be supported by a control optimization program to minimize the energy use of the system. Given that all air-side systems served by a central chilled water supply system will receive chilled water

supply at a single T_{cho}, and a change in T_{cho} will affect the $M_{ch,i}$ through each of the air-side systems, optimization of the water-side system control has to take due account of the impacts of changing T_{cho} on all the air-side systems. Conversely, the extent to which T_{cho} should be adjusted to optimize the energy performance of the entire system due to a change in operating condition of a single air-side system should be much smaller.

Despite that control optimization for the air-side systems and the central chiller plant are inter-related, they may be segregated in operation. Whereas each of the air-side control optimization program and the central chiller plant optimization program are running in parallel, all of them would tap into the same database that is being kept updated for data. This will avoid the need for a single, all embracing optimization program to handle the operations of the entire air-conditioning system, which would be computationally burdensome to use.

Therefore, when considering whether to reset the setpoint for the $T_{sa,i}$ of a particular air-side system, it is logical to consider T_{cho} as given, i.e. it will stay at the current value. When chiller plant control optimization is considered, the operating condition of each air-side system, including the sensible and latent cooling coil load and $T_{sa,i}$, should be regarded as fixed at their current values when the change in the M_{ch} due to a change in T_{cho} is evaluated. Equation (9.47) provides the guiding principle for the air-side system control optimization while Equation (9.50) should be observed in the chiller plant control optimization.

Annex 9A Gordon-Ng Chiller Model

As introduced in Section 9.3.1, the chiller model developed by Gordon and Ng [3] was derived from fundamental thermodynamics principles, with undetermined coefficients that need to be evaluated from empirical data, and hence it is a grey-box model. In this annex, the model will be derived from scratch such that every step taken, and assumptions made in the process are stated and discussed to deepen readers' understanding of the model.

9A.1 Derivation of the model

Regarding the chiller as a reversed heat engine, from 1st and 2nd laws of thermodynamics, we can write

$$\Delta E = \sum Q - \sum W = 0 = Q_{ch} + Q_{ch}^{Leak} - Q_{cd} - Q_{cd}^{Leak} - Q_{cp}^{Leak} + W_{in} \tag{9A.1}$$

$$\Delta S = \sum \frac{Q}{T} = 0 = \frac{Q_{ch}+Q_{ch}^{Leak}}{T_{ch}} - \frac{Q_{cd}+Q_{cd}^{Leak}}{T_{cd}} + \Delta S_{Int} \tag{9A.2}$$

Where E denotes internal energy, S entropy, Q heat input, W work output, and T temperature. Subscripts ch denotes chiller (or evaporator), cd condenser, cp compressor, in input, and Int internal. Superscript $Leak$ denotes leakage. Note that T_{cd} and T_{ch} denote the condensing and evaporating temperatures of the refrigerant in the condenser and evaporator, respectively.

From Equation (9A.1),

$$Q_{cd} + Q_{cd}^{Leak} = Q_{ch} + Q_{ch}^{Leak} - Q_{cp}^{Leak} + W_{in} \tag{9A.3}$$

Sub. Equation (9A.3) into Equation (9A.2),

$$\frac{Q_{ch}+Q_{ch}^{Leak}}{T_{ch}} - \frac{Q_{ch}+Q_{ch}^{Leak}-Q_{cp}^{Leak}+W_{in}}{T_{cd}} + \Delta S_{Int} = 0$$

$$\frac{W_{in}}{T_{cd}} = \frac{Q_{ch}+Q_{ch}^{Leak}}{T_{ch}} - \frac{Q_{ch}+Q_{ch}^{Leak}}{T_{cd}} + \frac{Q_{cp}^{Leak}}{T_{cd}} + \Delta S_{Int}$$

$$W_{in} = \left(Q_{ch} + Q_{ch}^{Leak}\right)\left(\frac{T_{cd}}{T_{ch}} - 1\right) + Q_{cp}^{Leak} + T_{cd}\Delta S_{Int} \tag{9A.4}$$

Note that

$$COP = \frac{Q_{ch}}{W_{in}}$$

$$W_{in} = \frac{Q_{ch}}{COP}$$

It follows that

$$\frac{1}{COP} = \left(1 + \frac{Q_{ch}^{Leak}}{Q_{ch}}\right)\left(\frac{T_{cd}}{T_{ch}} - 1\right) + \frac{Q_{cp}^{Leak}}{Q_{ch}} + \frac{T_{cd}}{Q_{ch}}\Delta S_{Int}$$

$$\frac{1}{COP} = \frac{T_{cd}}{T_{ch}} - 1 + \frac{Q_{ch}^{Leak}}{Q_{ch}}\left(\frac{T_{cd}}{T_{ch}} - 1\right) + \frac{Q_{cp}^{Leak}}{Q_{ch}} + \frac{T_{cd}}{Q_{ch}}\Delta S_{Int}$$

$$1 + \frac{1}{COP} = \frac{T_{cd}}{T_{ch}} + \frac{Q_{ch}^{Leak}}{Q_{ch}}\left(\frac{T_{cd}}{T_{ch}} - 1\right) + \frac{Q_{cp}^{Leak}}{Q_{ch}} + \frac{T_{cd}}{Q_{ch}}\Delta S_{Int} \quad (9A.5)$$

Multiplying (T_{ch}) to all terms in Equation (9A.5) and putting (T_{cd}) to the LHS, we get

$$\left(1 + \frac{1}{COP}\right)T_{ch} - T_{cd} = \frac{Q_{ch}^{Leak}}{Q_{ch}}(T_{cd} - T_{ch}) + T_{ch}\frac{Q_{cp}^{Leak}}{Q_{ch}} + \frac{T_{cd}T_{ch}}{Q_{ch}}\Delta S_{Int} \quad (9A.6)$$

By regarding the condenser and evaporator of the chiller as heat exchangers and applying the ε-NTU model to the heat exchangers, and ignoring heat transfers in the desuperheating and subcooling processes in the condenser and in the superheating process in the evaporator, we can write:

$$Q_{cd} = (\rho Vc \cdot \varepsilon)_{cd}(T_{cd} - T_{cdi}) \quad (9A.7)$$

$$Q_{ch} = (\rho Vc \cdot \varepsilon)_{ch}(T_{chi} - T_{ch}) \quad (9A.8)$$

In the above equations, the additional subscripts i and o denote the states of chilled (ch) or condenser (cd) water at the inlet and outlet of the evaporator and condenser, respectively. Mass flow rate of water is given by the product of its density, ρ, and volume flow rate, V, and c denotes specific heat of water.

Note that

$$Q_{ch} = (\rho Vc)_{ch}(T_{chi} - T_{cho})$$

$$T_{chi} = T_{cho} + \frac{Q_{ch}}{(\rho Vc)_{ch}} \quad (9A.9)$$

Sub. Equation (9A.9) into Equation (9A.8),

$$Q_{ch} = (\rho Vc \cdot \varepsilon)_{ch}\left(T_{cho} + \frac{Q_{ch}}{(\rho Vc)_{ch}} - T_{ch}\right)$$

$$Q_{ch}(1 - \varepsilon) = (\rho Vc \cdot \varepsilon)_{ch}(T_{cho} - T_{ch})$$

$$Q_{ch} = \left(\rho Vc \cdot \frac{\varepsilon}{1-\varepsilon}\right)_{ch}(T_{cho} - T_{ch}) \quad (9A.10)$$

Defining

$$R_{cd} = \frac{1}{(\rho Vc \cdot \varepsilon)_{cd}} \quad (9A.11)$$

$$R_{ch} = \frac{1}{(\rho Vc \cdot \varepsilon/(1-\varepsilon))_{ch}} \quad (9A.12)$$

From Equations (9A.7), (9A.10), (9A.11) & (9A.12), we get

$$T_{cd} = T_{cdi} + R_{cd}Q_{cd} \tag{9A.13}$$

$$T_{ch} = T_{cho} - R_{ch}Q_{ch} \tag{9A.14}$$

From Equation (9A.1),

$$Q_{cd} = Q_{ch} + Q_{ch}^{Leak} - Q_{cd}^{Leak} + W_{in} - Q_{cp}^{Leak}$$

$$Q_{cd} = Q_{ch} + W_{in} + \left(Q_{ch}^{Leak} - Q_{cd}^{Leak} - Q_{cp}^{Leak}\right)$$

$$Q_{cd} = Q_{ch}\left(1 + \frac{1}{COP}\right) + \left(Q_{ch}^{Leak} - Q_{cd}^{Leak} - Q_{cp}^{Leak}\right) \tag{9A.15}$$

Ignoring the leak terms,

$$Q_{cd} = Q_{ch}\left(1 + \frac{1}{COP}\right) \tag{9A.16}$$

Using Equations (9A.13), (9A.14) & (9A.16), the LHS of Equation (9A.6) becomes:

$$\left(1 + \frac{1}{COP}\right)T_{ch} - T_{cd} = \left(1 + \frac{1}{COP}\right)(T_{cho} - R_{ch}Q_{ch}) - T_{cdi} - R_{cd}Q_{ch}\left(1 + \frac{1}{COP}\right)$$

$$\left(1 + \frac{1}{COP}\right)T_{ch} - T_{cd} = \left(1 + \frac{1}{COP}\right)T_{cho} - T_{cdi} - Q_{ch}\left(1 + \frac{1}{COP}\right)(R_{cd} + R_{ch}) \tag{9A.17}$$

Sub. Equation (9A.17) back into Equation (9A.6), we get

$$\left(1 + \frac{1}{COP}\right)T_{cho} - T_{cdi} - Q_{ch}\left(1 + \frac{1}{COP}\right)(R_{cd} + R_{ch})$$

$$= \frac{Q_{ch}^{Leak}}{Q_{ch}}(T_{cd} - T_{ch}) + T_{ch}\frac{Q_{cp}^{Leak}}{Q_{ch}} + \frac{T_{cd}T_{ch}}{Q_{ch}}\Delta S_{Int}$$

It can be seen from the above equation that its right-hand side, comprising the heat leakage and entropy generation terms, represents the irreversibilities resulting from the energy transfers into, within and out of the chiller, which would be equal to zero if the chiller is an ideal one. Replacing the T_{cd} at the right-hand side of the equation by T_{cdi}, and T_{ch} by T_{cho}, and combining the compressor leakage term with the evaporator leakage term, denoted by Q_L, and re-arranging, we get:

$$\left(1 + \frac{1}{COP}\right)T_{cho} = T_{cdi} + Q_{ch}\left(1 + \frac{1}{COP}\right)(R_{cd} + R_{ch}) + \frac{Q_L}{Q_{ch}}(T_{cdi} - T_{cho})$$

$$+ \frac{T_{cdi}T_{cho}}{Q_{ch}}\Delta S_{Int}$$

Apparently, the substitutions of the refrigerant temperatures by water temperatures as described above would lead to a reduction in the evaporator leakage term (but an

increase in the compressor leakage term), and either a reduction or an increase in the internal entropy generation term. However, this should not lead to significant errors because, as will be discussed later, these temperature terms are the predictor variables for evaluation of the thermal resistance, the leakage and the entropy generation terms from actual chiller operating data. Given that T_{cd} is closely related to T_{cdi} and T_{ch} to T_{cho}, the regression process will adjust the values of the unknowns to compensate for the changes in the predictor variables used.

Dividing all the terms in the above equation throughout by T_{cdi}, we get,

$$\left(1+\frac{1}{COP}\right)\frac{T_{cho}}{T_{cdi}} = 1 + \frac{T_{cho}}{Q_{ch}}\Delta S_{Int} + \frac{Q_L}{Q_{ch}}\left(\frac{T_{cdi}-T_{cho}}{T_{cdi}}\right) + \frac{Q_{ch}}{T_{cdi}}\left(1+\frac{1}{COP}\right)(R_{cd}+R_{ch}) \quad (9A.18)$$

To account for the effect of varying chilled and condenser water flow rates, Equations (9A.11) & (9A.12) are substituted into the above to yield:

$$\left(1+\frac{1}{COP}\right)\frac{T_{cho}}{T_{cdi}} = 1 + \frac{T_{cho}}{Q_{ch}}\Delta S_{Int} + \frac{Q_L}{Q_{ch}}\left(\frac{T_{cdi}-T_{cho}}{T_{cdi}}\right) + \frac{Q_{ch}}{T_{cdi}}\left(1+\frac{1}{COP}\right)\left(\frac{1}{(\rho Vc\cdot\varepsilon)_{cd}} + \frac{1}{(\rho Vc\cdot\varepsilon/(1-\varepsilon))_{ch}}\right) \quad (9A.19)$$

For modelling a given chiller, values of ΔS_{Int}, Q_L, ε_{cd} and ε_{ch} are unknowns that need to be evaluated based on operating records of the other system variables in the equation.

By defining:

$$y = \left(1+\frac{1}{COP}\right)\frac{T_{cho}}{T_{cdi}} - 1 \quad (9A.20)$$

$$x_1 = \frac{T_{cho}}{Q_{ch}} \quad (9A.21)$$

$$x_2 = \frac{T_{cdi}-T_{cho}}{Q_{ch}T_{cdi}} \quad (9A.22)$$

$$x_3 = \frac{Q_{ch}}{T_{cdi}}\left(1+\frac{1}{COP}\right)\left(\frac{1}{(\rho Vc)_{cd}}\right) \quad (9A.23)$$

$$x_4 = \frac{Q_{ch}}{T_{cdi}}\left(1+\frac{1}{COP}\right)\left(\frac{1}{(\rho Vc)_{ch}}\right) \quad (9A.24)$$

Equation (9A.19) may be written as:

$$y = a_1x_1 + a_2x_2 + a_3x_3 + a_4x_4 \quad (9A.25)$$

Where

$$a_1 = \Delta S_{Int} \quad (9A.26)$$

$$a_2 = Q_L \tag{9A.27}$$

$$a_3 = \frac{1}{\varepsilon_{cd}} \tag{9A.28}$$

$$a_4 = \frac{1-\varepsilon_{ch}}{\varepsilon_{ch}} \tag{9A.29}$$

The coefficients a_1 to a_4 can be evaluated by multiple linear regression with operating records of the relevant parameters of the chiller under concern.

9A.2 Observations and avoidance of co-linearity

As can be seen from the expressions for x_3, x_4, a_3 and a_4 in Equations (9A.23), (9A.24) (9A.28) & (9A.29), with the values of the effectiveness terms (ε) being a fraction not too far below 1.0, the impact of varying the chilled water flow rate will be much less significant than varying the condenser water flow rate. From physical considerations, variations in the condenser water flow rate will directly affect the condensing temperature of the refrigerant, and thus the compressor power demand, with relatively minor effect on the refrigerant flow rate and the cooling output. The condenser water flow rate, therefore, must be a significant term in a model for prediction of chiller *COP* or power demand, and the Gordon & Ng model (shown as Equation (9A.19) or (9A.25)) can reflect well this phenomenon.

The effect of varying the chilled water flow rate, however, will cause the internal capacity control system in the chiller to make adjustment to the refrigerant flow rate in order to keep the chilled water leaving temperature at the set point level, thereby restraining the change in the evaporating temperature that will arise. As a matter of course, the compressor power demand will change, but this can be attributed largely to the change in the cooling load, and hence the refrigerant flow rate, resulting from the change in the chilled water flow rate. Therefore, with cooling output already present as an independent variable, the chilled water flow rate should play a much less significant role in the model, which is indeed the case in the Gordon & Ng model.

Note also that x_3 and x_4 are rather similar and, under actual operating conditions, V_{cd} and V_{ch} may vary nearly in proportion to each other. In other words, co-linearity problems may arise with the use of the Gordon & Ng model shown as Equation (9A.25).

Following the above arguments on the relative effects of changes in the chilled and condenser water flow rates, Equation (9A.19) was re-arranged, as shown below:

$$\left(1+\frac{1}{COP}\right)\frac{T_{cho}}{T_{cdi}} = 1 + \frac{T_{cho}}{Q_{ch}}\Delta S_{Int} + \frac{Q_L}{Q_{ch}}\left(\frac{T_{cdi}-T_{cho}}{T_{cdi}}\right) + \frac{Q_{ch}}{T_{cdi}}\left(1+\frac{1}{COP}\right)\left(\frac{1}{(\rho Vc\cdot\varepsilon)_{cd}} + \frac{1}{(\rho Vc\cdot\varepsilon/(1-\varepsilon))_{ch}}\right)$$

$$\left(1+\frac{1}{COP}\right)\frac{T_{cho}}{T_{cdi}} = 1 + \frac{T_{cho}}{Q_{ch}}\Delta S_{Int} + \frac{Q_L}{Q_{ch}}\left(\frac{T_{cdi}-T_{cho}}{T_{cdi}}\right)$$

$$+\frac{Q_{ch}}{T_{cdi}}\left(1+\frac{1}{COP}\right)\left(\frac{1}{(\rho Vc\cdot\varepsilon)_{cd}}-\frac{1}{(\rho Vc)_{cd}}+\frac{1}{\left(\rho Vc\cdot\frac{\varepsilon}{1-\varepsilon}\right)_{ch}}\right)$$

$$+\frac{1}{(\rho Vc)_{cd}}\frac{Q_{ch}}{T_{cdi}}\left(1+\frac{1}{COP}\right)$$

$$\left(1+\frac{1}{COP}\right)\frac{T_{cho}}{T_{cdi}}-1-\frac{1}{(\rho Vc)_{cd}}\frac{Q_{ch}}{T_{cdi}}\left(1+\frac{1}{COP}\right)=\frac{T_{cho}}{Q_{ch}}\Delta S_{Int}+Q_L\left(\frac{T_{cdi}-T_{cho}}{Q_{ch}T_{cdi}}\right)$$
$$+\frac{Q_{ch}}{T_{cdi}}\left(1+\frac{1}{COP}\right)\left(\frac{1-\varepsilon_{cd}}{(\rho Vc\cdot\varepsilon)_{cd}}+\frac{1-\varepsilon_{ch}}{(\rho Vc\cdot\varepsilon)_{ch}}\right) \quad (9A.30)$$

Equation (9A.30) may also be written, in abbreviated form, as follows:

$$y=a_1x_1+a_2x_2+a_3x_3 \quad (9A.31)$$

Where,

$$y=\left(1+\frac{1}{COP}\right)\frac{T_{cho}}{T_{cdi}}-1-\frac{1}{(\rho Vc)_{cd}}\frac{Q_{ch}}{T_{cdi}}\left(1+\frac{1}{COP}\right)$$

$$x_1=\frac{T_{cho}}{Q_{ch}}$$

$$x_2=\frac{T_{cdi}-T_{cho}}{Q_{ch}T_{cdi}}$$

$$x_3=\frac{Q_{ch}}{T_{cdi}}\left(1+\frac{1}{COP}\right)$$

$$a_1=\Delta S_{Int}$$

$$a_2=Q_L$$

$$a_3=\frac{1-\varepsilon_{cd}}{(\rho Vc\cdot\varepsilon)_{cd}}+\frac{1-\varepsilon_{ch}}{(\rho Vc\cdot\varepsilon)_{ch}}$$

The coefficient a_3 in Equation (9A.31) would be relatively small in value; the closer ε_{cd} and ε_{ch} to unity the smaller. Therefore, even though a_3 is, in fact, dependent on the condenser and chilled water flow rates, which are variables in the case under concern, regarding it as a constant and having it evaluated from operating records of a chiller through regression should lead to limited inaccuracies of the model predictions. The version of the Gordon & Ng model presented as Equation (9A.31) can be applied to chillers with variable chilled and condenser water flow rates.

References

[1] AHRI, Standard for Performance Rating of Water-chilling and Heat Pump Water-heating Packages Using the Vapor Compression Cycle, Air-Conditioning, Heating, and Refrigeration Institute, 2015.

[2] Underwood CP, Yik FWH, Modelling Methods for Energy in Buildings, Blackwell, 2004.

[3] Gordon, J.M., & Ng, K.C., Thermodynamic modeling of reciprocating chillers, Journal of Applied Physics 75 (1994): 2769 – 2774.

[4] Gordon, J.M., Ng, K.C., Chua, H.T., & Lim, C.K., How varying condenser coolant flow rate affects chiller performance: thermodynamic modeling and experimental confirmation, Applied Thermal Engineering 20 (2000): 1149 – 1159.

[5] ASHRAE, Handbook – HVAC Systems and Equipment, Chapter 40, American Society of Heating, Refrigerating and Air-conditioning Engineers, 2020.

[6] Press, W.H., Flannery, B.P., Teukolsky, S.A., Vetterling, W.T., Numerical Recipes, The Art of Scientific Computing (Fortran Version), Cambridge University Press, 1999.

Chapter 10 Heating Systems, Heat Recovery Chillers, Heat Pumps and Absorption Chillers

10.1 Heating load calculation

Prior to the discussions in Chapter 3 on the method for design cooling load calculation, the related heat transfer fundamentals are covered, which are applicable to heating load calculations to be discussed below. For design heating load estimation, we may focus on the steady state heat losses to the outdoors through the building envelop, as well as to the air drawn in for ventilation and the air that enters the building by infiltration, i.e. through unintended openings and window/door cracks, all of which need to be compensated by heating. On the other hand, solar and internal heat gains, and the thermal storage effects of the building fabric, may be ignored.

Once the design indoor and outdoor temperatures are defined, the steady state heat loss through a building envelop element (e.g. a wall or window) may be determined by:

$$Q_{w,j} = A_{w,j} U_{w,j} (T_{i,j} - T_o) \tag{10.1}$$

Where

$Q_{w,j}$ = heat loss through the j^{th} component in the building envelop
$A_{w,j}$ = heat transfer area of the j^{th} component in the building envelop
$U_{w,j}$ = U-value of the j^{th} component in the building envelop
$T_{i,j}$ = design indoor temperature of the room that is enclosed by the j^{th} component in the building envelop
T_o = design outdoor temperature

The part of the design heating load of a room in a building due to heat losses through the building envelop may be estimated by summing the heat losses through individual external walls, windows, and roofs enclosing the room:

$$Q_W = \sum_{j=1}^{N} A_{w,j} U_{w,j} (T_{i,j} - T_o) \tag{10.2}$$

The heating load for raising the temperature of the ventilation and infiltration air can be estimated by:

$$Q_{FA} = \rho_a V_{FA} Cp_a (T_{i,j} - T_o) \tag{10.3}$$

$$Q_{Inf} = \rho_a V_{Inf} Cp_a (T_{i,j} - T_o) \tag{10.4}$$

Where

Q_{FA} = load for heating fresh air for ventilation for the room
Q_{Inf} = load for heating infiltration for the room
V_{FA} = total volume flow rate of fresh air for ventilation for the room
V_{Inf} = total rate of infiltration for the room
ρ_a = density of air
Cp_a = specific heat of air

The sum of the above three heating load components equals the design heating load of a room in a building:

$$Q_H = Q_W + Q_{FA} + Q_{Inf} \tag{10.5}$$

The design heating loads of individual rooms in a building are the basis for selection and sizing of the space heating equipment serving the rooms, such as radiators, and the pipes that supply hot water to them.

Since design heating loads are assumed to be results of steady state heat transfers, the block design heating load can be determined simply by summing up the design heating loads of all heated rooms in the building without the need to consider diversity among the loads. The block design heating load determines the sizes required of the equipment and components of the central heating plant, e.g. the boilers used to raise the required amount of heat with input of fuel or electricity. Allowance for the pick-up loss, i.e. heat taken up by the piping system and equipment to pick up temperature after shutdown, needs to be made in sizing the capacity required of the central heating plant.

10.2 Heating systems and equipment

For providing central heating to a building, one or more boilers may be used to heat up water and the hot water from the boiler may then be distributed to space heating equipment serving various rooms in the building. Because domestic hot water supply would also be an essential building services provision for buildings in cold climate regions, the boiler will normally be used to serve both spacing heating and domestic hot water supply. The system shown in Figure 10.1 is an example where a boiler is used to provide both space heating and hot water supply for a house.

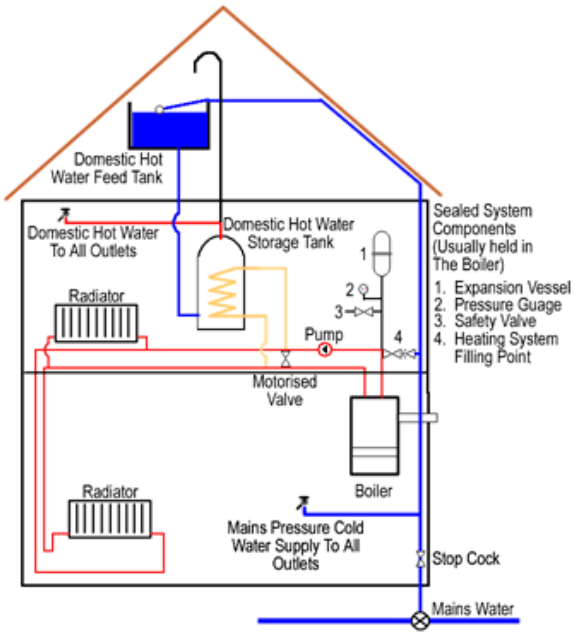

Figure 10.1 A domestic hot water system for space heating and hot water supply

In the system shown in Figure 10.1, the domestic hot water circuit is separated from the spacing heating circuit through the use of a hot water storage tank, which serves the functions of both a calorifier and a storage tank. This arrangement, which is also used in larger systems serving commercial buildings, safeguards the hygienic condition of, and can cope with the variable demand for, domestic hot water supply. Unlike the domestic hot water supply circuit, which is a once-through circuit, the hot water for space heating is recirculated round the heating circuit to which the radiators that provide space heating are connected.

10.2.1 Boilers

Boilers are often used for raising heat for space heating and domestic hot water supply and boiler units, large and small, are available to meet the needs of different applications (Figure 10.2). Boilers may be used to produce steam but for space heating and domestic hot water supply, boilers that output hot water are a simpler solution that can serve well the purpose. For commercial and domestic buildings in cities, gas and electricity are the most common fuel/energy input for raising heat as their use will not give rise to dark smoke or will emit no flue gas at all.

Domestic type boiler

Boilers in a central heating plant

Figure 10.2 Boilers of different sizes

The criteria for gauging the efficiency of boilers include combustion efficiency and overall efficiency. Combustion efficiency, η_C, is defined as:

$$\eta_C = \frac{\text{Gross Heat in Fuel - Residual Heat in Flue Gas}}{\text{Gross Heat in Fuel}} \tag{10.6}$$

Typical values of η_C is 75-86% for well-maintained non-condensing boilers and 88-95% for condensing boilers.

Overall efficiency, η_T, is defined as:

$$\eta_T = \frac{\text{Heat Delivered to Heating System}}{\text{Gross Heat in Fuel}} \tag{10.7}$$

The difference between the two efficiencies is given rise by radiation and convection heat losses from the boiler casing and amounts, typically, to 3-5%

Condensing boilers mentioned above have extended heat exchange area and operate with low system water temperature. This causes flue products to condense, leading to increased efficiency. Figure 10.3 shows the overall efficiency of a condensing boiler, highlighting the limit of flue gas dew point (above which no condensation would occur), which is the limit for the condensing mode of operation.

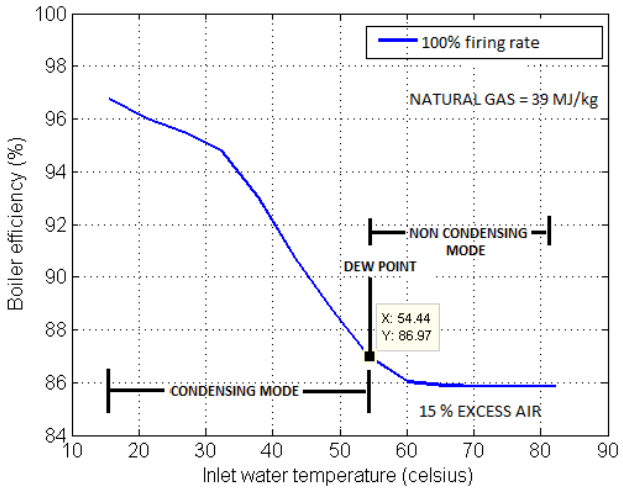

Figure 10.3 Boiler efficiency of a condensing boiler

Unlike chillers, boilers are more tolerant in respect of the flow rate of water passing through them. Therefore, small systems may simply adopt a constant flow design, but larger hot water circulation systems may have multiple circulation pumps which may be staged in steps according to the demand.

Malfunctioning of hot water systems, especially the boilers, is hazardous and could cause serious injury and damage. Therefore, boilers are equipped with safety bleed-off valves, high temperature cut-outs, etc., and the domestic hot water circuit should include a vent pipe extended above the make-up tank, etc. These are typically parts of the regulatory requirements in codes that govern the design, operation and maintenance of boilers and hot water systems in buildings.

10.2.2 Radiators

Air-side equipment for space cooling rely mainly on convective heat transfer (but chilled ceiling is an exception), and such equipment may also be used for space heating. However, greater use of radiant heat transfer is possible in space heating due to the considerably larger difference between the indoor air temperature and the water temperature in the space heating equipment. Since convective type air-side equipment

are already covered in Chapter 4, focus is put in the following on the type of air-side equipment for space heating, which are called radiators (Figure 10.4). Floor panels embedded with hot water pipes will be briefly discussed as the next topic.

Radiators are a very commonly used low cost solution for space heating provision. They require wall or floor spaces for mounting, and are often installed below the sill of windows, which would counteract with the cold air that tend to flow downward along the cold glass surface, ensuring good temperature distribution inside the room. They are easy to clean (especially column type radiators which explains why they are favoured in hospitals), are adaptable to various automatic control methods, but are not suitable for operating with a high temperature medium due to safety.

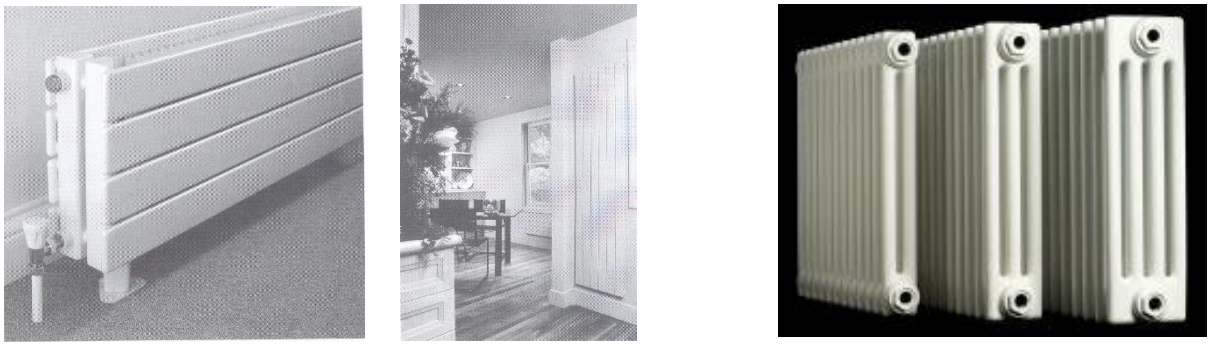

Panel type Column type

Figure 10.4 Panel and column type radiators for space heating

In spite of their name, heat transfer from a radiator to the indoor space typically involves 30% radiant emission and 70% convection. The mixed emission mode reduces room temperature gradient and leads to reasonably good comfort characteristic.

The output of radiators and convectors is given by:

$$q = K(T_{wm} - T_a)^n \tag{10.8}$$

Where

$q =$ heat emission rate, W
$K =$ emitter specific constant, W K^{-n}
$T_{wm} =$ mean water temperature in emitter, ^{o}C
$T_a =$ air temperature in heated room, ^{o}C
$n =$ exponent = 1.3 for panel and column radiators, and 1.4 -1.5 for natural convectors

By energy conservation, the heat emission rate, q, is equal to the heat loss of the hot water flowing through the emitter:

$$q = m_w C_w (T_{ws} - T_{wr}) \tag{10.9}$$

Where

$m_w =$ water mass flow rate, kg/s
$C_w =$ specific heat of water, kJ/kgK
$T_{ws} =$ supply hot water temperature, °C
$T_{wr} =$ return hot water temperature, °C

The mean water temperature, T_{wm}, in Equation (10.8) is given by:

$$T_{wm} = \frac{1}{2}(T_{ws} + T_{wr}) \tag{10.10}$$

If the heat emission rate of the radiator is for compensating the heat losses of a room, we may also write:

$$q = C(T_a - T_o) \tag{10.11}$$

Where

$T_o =$ outdoor temperature, °C
$C =$ total heat loss coefficient for the room W/K

From Equations (10.8), (10.9) & (10.11), the relation between a part-load condition (denoted by a prime notation) and the design condition can be written as:

$$\frac{q'}{q} = \left(\frac{T'_{wm} - T_a}{T_{wm} - T_a}\right)^n = \frac{m'_w}{m_w}\frac{(T'_{ws} - T'_{wr})}{(T_{ws} - T_{wr})} = \frac{T_a - T'_o}{T_a - T_o} \tag{10.12}$$

Example 10.1

Figure 10.5 shows the layout of an office floor in a commercial building in a cold climate region. The layout of the space heating system and the heating loads of the six rooms on the floor are as shown in the figure. The heating system comprises a hot water heater, a constant flow hot water pump, cast iron column radiators in individual rooms and a piping system that connects, in series (see Figure 10.7), the radiators to the water heater. Each radiator may comprise a number of sections and the heat emission rate of each section (Q_s) can be determined using the following equation where k may be regarded as a constant; t_m is the mean water temperature in the radiator; and t_r is the room air temperature.

$$Q_s = k(t_m - t_r)^{1.3}$$

The system was designed based on the conditions where the design room air temperature is 20°C; the system hot water flow rate is constant; the temperature of hot water from the water heater is 95°C; and the overall water temperature drop in the system is 25°C. Each radiator section can emit 100W of heat under the condition where the difference between the mean water temperature in the radiator and the room air temperature is 64.5K.

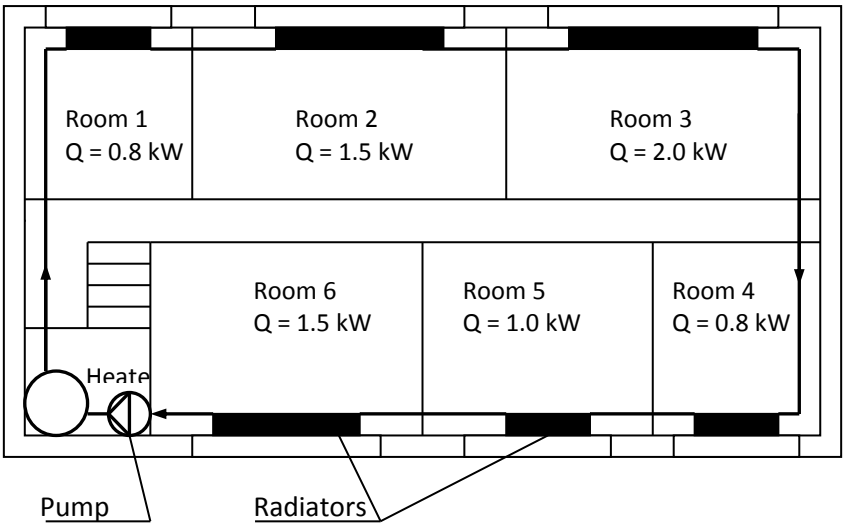

Figure 10.5 Floor plan of an office building and layout of its heating system

Determine the number of sections required in the radiator for each room. Use 4.18kJ/kgK as the value of the specific heat of water in the calculations.

Solution to Example 10.1

The total design heating load (Q_T) is calculated from the loads of individual rooms as shown below.

Design heating load	
Room 1	0.8 kW
Room 2	1.5 kW
Room 3	2.0 kW
Room 4	0.8 kW
Room 5	1.0 kW
Room 6	1.5 kW
Total	7.6 kW

The hot water supply flow rate required (m_w) can be determined from the given water temperature rise in the system ($\Delta t_w = t_{ws} - t_{wr} = 25$) and the specific heat of water (C_w, taken as 4.18 kJ/kgK) as follows:

$$m_w = \frac{Q_T}{C_w \Delta t_w} = \frac{7.6}{4.18 \times 25} = 0.0727 \text{kg/s}$$

The water temperature drop across the radiator in each room (Δt_{wi}) can be determined based on the heating load of the room (Q_i) as follows:

$$\Delta t_{wi} = \frac{Q_i}{m_w C_w}$$

Therefore, the inlet water temperature for the radiator in the i^{th} room (t_{wsi}) can be found from the total temperature drop across all upstream radiators:

$$t_{wsi} = t_{ws} - \sum_{j=1}^{i-1} \Delta t_{wj}$$

The leaving water temperature from the i^{th} radiator (t_{wri}) will become the inlet temperature of the radiator downstream of it, i.e.

$$t_{ws(i+1)} = t_{wri}$$

The mean water temperature in the i^{th} radiator (t_{mi}) is:

$$t_{mi} = \frac{t_{wsi}+t_{wri}}{2}$$

Therefore, the heat emission that a radiator section in the i^{th} radiator can output (Q_{si}) is:

$$Q_{si} = k(t_{mi} - t_r)^{1.3}$$

Where t_r is the room temperature.

The value of k can be evaluated from the given data as follows:

$$k = \frac{100}{64.5^{1.3}} = 0.4442 \text{W/K}^{1.3}$$

Based on the above, the output per radiator section in the radiator in each room and the number of sections required for each radiator can be determined as summarized below:

Room No. (i)	t_{wsi}	Δt_{wi}	t_{wri}	t_{mi}	t_{mi} - t_r	Q_{si}	No. of Sections	
1	95.00	2.63	92.37	93.68	73.68	118.89	6.73	7
2	92.37	4.93	87.43	89.90	69.90	111.02	13.51	14
3	87.43	6.58	80.86	84.14	64.14	99.28	20.14	21
4	80.86	2.63	78.22	79.54	59.54	90.12	8.88	9
5	78.22	3.29	74.93	76.58	56.58	84.34	11.86	12
6	74.93	4.93	70.00	72.47	52.47	76.46	19.62	20

10.2.3 Embedded floor heating panels

An alternative arrangement for space heating is to embed either hot water pipes or electric heaters within the floor slab (Figure 10.6), which is suitable for residential and office developments. The heated floor slab will emit heat uniformly, typically with 60% radiant emission [1], which can provide a comfortable indoor environment. Since the pipes or cables are concealed, no routine maintenance is required. However, control can be difficult due to the high thermal capacity and the low temperature media used. On the other hand, the low operating temperature allows efficient use of heat pumps or condensing boilers.

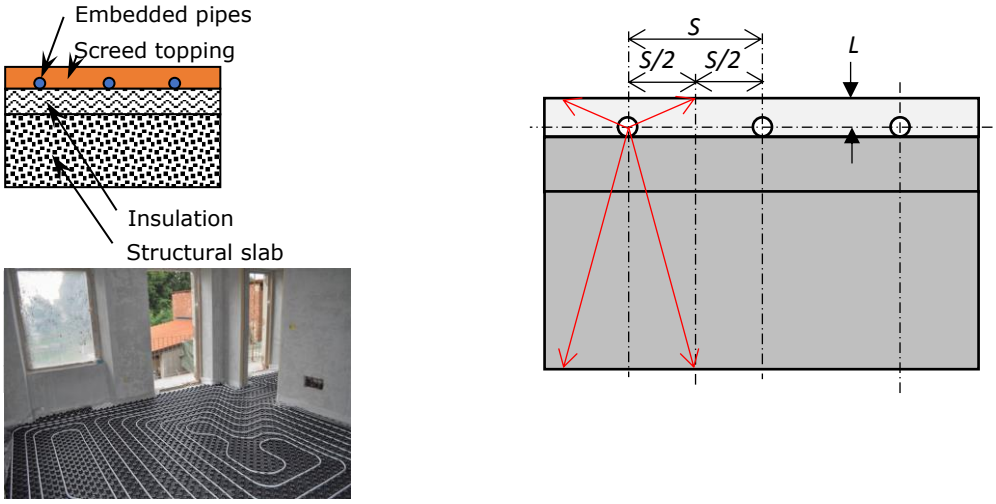

Figure 10.6 Embedded floor heating system

The method for sizing of embedded panel systems described below is based on mean heat flow paths defined with reference to the pipe spacing, S, and the "topping" depth from the pipe centre-line, L (Figure 10.6). Typical values for S is 150-400mm and L 25-40mm (usually a cement screed is used as "topping"). The embedded pipework is a high-density plastic (15mm nominal diameter), usually polybutylene. Insulation consisting of 50mm (max. thickness) rigid foam-based material is appropriate.

The typical design procedures for the floor heating system are briefly listed below and exemplified in Example 10.2:

- Assume a suitable spacing, S.
- Set the floor surface temperature to meet the required heat load (max. 25°C for extended occupancy or 27°C for casual occupancy).
- Use Fourier's equation ($q = -k\, dT/dx$) to find the required mean water temperature based on the mean path, L', and the required upward emission.
- Calculate the downward loss based on mean path, L'_d, and add this to the design load to form the required system duty.

Example 10.2

The indoor temperature of a room is to be maintained at 19°C using underfloor hot water pipes. The floor area of the room is 50m² and the 15mm diameter pipes are to be uniformly distributed over the entire floor area with a pipe spacing, S, of 200mm. If the room design heating load is 2,500W, use the data given below to determine the required overall heating load and water flow temperature.

Data:

Insulation thickness and conductivity: 50mm, 0.035W/m-K
Slab thickness and conductivity: 200mm, 1.6W/m-K
Slab bottom surface temperature: 18.5°C
Screed topping thickness (above pipe centreline): 32.5mm
Screed topping thermal conductivity: 1.4W/m-K
Maximum floor surface temperature: ≤ 26°C
Overall floor surface resistance: 0.12m²/KW
Water circuit temperature difference: 10K

Solution to Example 10.2

The design heat load of 2,500W represents the required upward emission from the floor. The upward floor emission can be obtained from the following in which R_s is the floor surface resistance (m²/kW), A_s the floor (heated) surface area (m²), T_s the floor surface temperature (°C), T_{ai} the internal air temperature (°C) and q_u the upward emission from the floor (W):

$$q_u = 2500 = \frac{A_s}{R_s}(T_s - T_{ai}) = \frac{50}{0.12}(T_s - 19)$$

Solving for T_s,

$$T_s = 19 + 2500 \times \frac{0.12}{50} = 25^oC$$

The design floor surface temperature of 25°C is lower than the maximum allowable temperature of 26°C and is thus acceptable.

The mean upward heat conduction path, L', is obtained from the following in which L is the screed topping thickness above the pipe centre-line (= 32.5mm) and S is the pipe spacing (= 200mm):

$$L' = \frac{1}{2}\left[L + \sqrt{L^2 + (S/2)^2}\right] = \frac{1}{2}\left[32.5 + \sqrt{32.5^2 + (200/2)^2}\right] = 68.8\text{mm}$$

Now express the upward conduction between the mean centre-line temperature (which is taken to be the required mean water temperature, T_{wm}, and the floor surface which will be the same as the required floor surface emission (i.e. 2500W). Using the Fourier equation with a screed conductivity, k_t (Wm^{-1}K^{-1}):

$$q_u = 2500 = \frac{k_t A_s}{L'}(T_{wm} - T_s) = \frac{1.4 \times 50}{0.0688}(T_{wm} - 25)$$

Solving for T_{wm} from the above, we get:

$$T_{mw} = 25 + \frac{2500 \times 0.0688}{1.4 \times 50} = 27.46^oC$$

For a required water circuit temperature differential of 10K, the required flow and return temperatures will be:

$$T_{wf} = 27.46 + \frac{10}{2} = 32.46^{o}\text{C}$$

$$T_{wr} = 27.46 - \frac{10}{2} = 22.46^{o}\text{C}$$

For the downward loss component, the mean downward path length, L'_d, is calculated as follows:

The vertical distance between the centre of the pipe to the bottom surface of the slab = (15/2) +50 + 200 = 257.5mm

$$L'_d = \frac{1}{2}\left[257.5 + \sqrt{257.5^2 + (200/2)^2}\right] = 266.9\text{mm}$$

The mean path length from the pipe centre to the interface between the insulation and concrete slab, L''_d, is:

$$L''_d = \frac{1}{2}\left[57.5 + \sqrt{57.5^2 + (200/2)^2}\right] = 86.4\text{mm}$$

Therefore, the overall U-value from the pipe centre-line to the under surface of the concrete slab (which is at 18.5°C) will be:

$$U_d = \frac{1}{\frac{L''_d}{k_{insulation}} + \frac{L'_d - L''_d}{k_{slab}}} = \frac{1}{\frac{0.0864}{0.035} + \frac{0.267 - 0.0864}{1.6}} = 0.387\text{W/m}^2\text{-K}$$

Thus, the required overall capacity of the under-floor heating coil will be:

$$q_{tot} = q_u + q_d = 2500 + 0.387 \times 50 \times (27.6 - 18.5) = 2673.4\text{W}$$

10.2.4 Hot water piping system

The water supply temperature and pressure in a heating system may vary to cope with the characteristics of the applications. Table 10.1 below shows the range of temperature and pressure used for plants of different scales [2].

Table 10.1 Water supply temperature and pressure of heating systems (source: Chapter 12 ASHRAE System and Equipment Handbook 2000 [2])

	Low temperature system	Medium temperature system	High temperature system
Water temperature, °C	< 120, typically 90-100	120 – 175	>175
Working pressure, kPa	Up to 200	Up to 1100	About 2000
Capacity, MW	≤ 1.5	1.5 to 3	3 to 6

Several circuit designs, including series loop, one-pipe, two-pipe direct-return, and two-pipe reverse-return circuits, may be employed for the hot water piping system for space heating (Figure 10.7). Table 10.2 summarizes the advantages and disadvantages of these circuit designs.

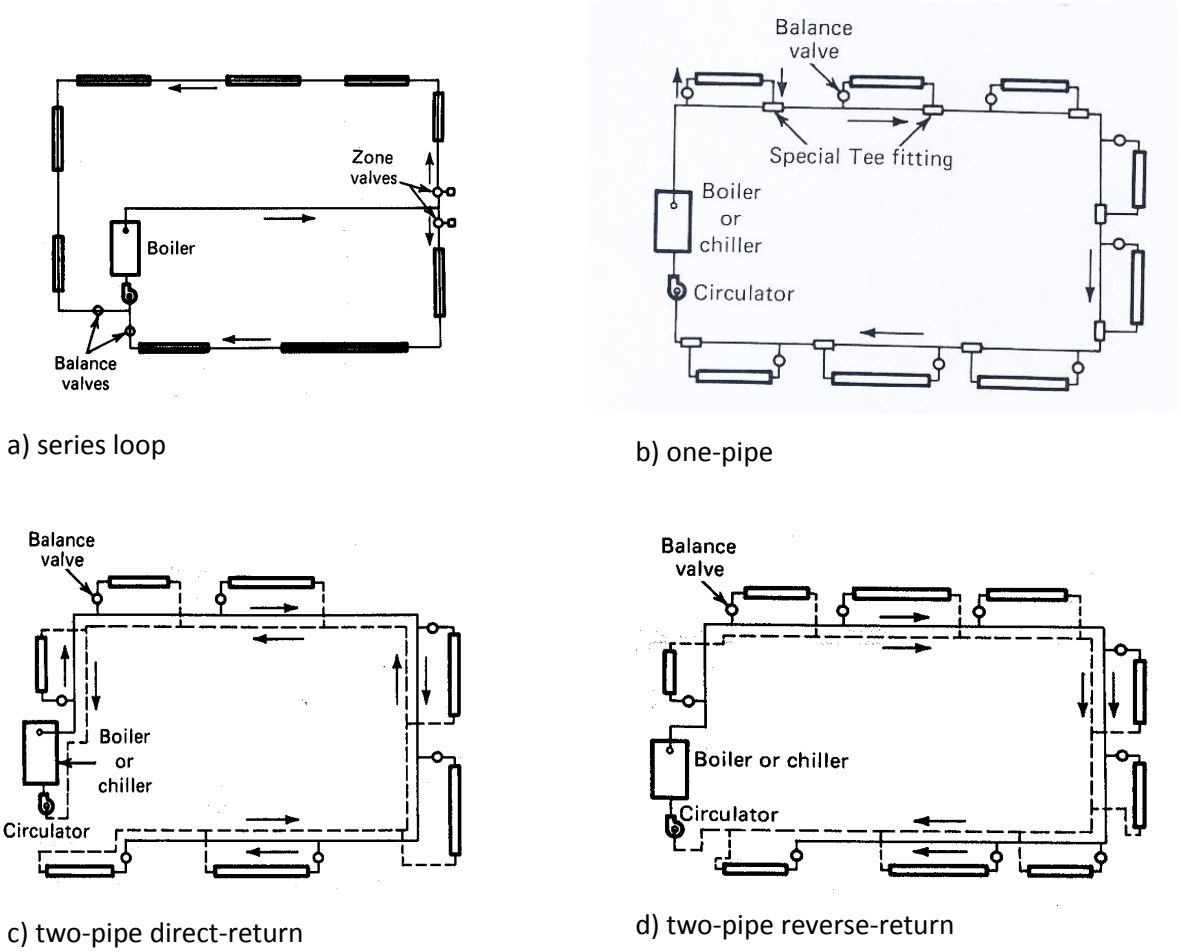

a) series loop

b) one-pipe

c) two-pipe direct-return

d) two-pipe reverse-return

Figure 10.7 Hot water piping circuits

Although the methods for designing chilled water piping systems, covered in Chapters 7 & 8, are applicable to designing hot water piping systems, there are extra considerations that need to be taken. For a hot water piping system, a closed expansion tank is often used such that the pressure in the hot water piping system can be adjusted, through varying the pressure of the gas, typically nitrogen (N_2), in the expansion tank. This is needed to prevent flash over of hot water into steam in the piping system at locations where the pressure is low, which will block water circulation and thus interruption to normal operation. The calculations involved for checking the system pressure and determining the charge pressure of the expansion tank are illustrated in the following example.

Table 10.2 Comparison of hot water piping circuits for space heating

Circuit	Advantages	Disadvantages
Series loop	Simple and low cost.	Inflexible (simultaneous) operation. Heating temperature not constant.
One-pipe (with bypass at each emitter)	Able to operate individually and more flexibly. More suitable for connecting up a large number of radiators. Larger heat transfer areas required (smaller water flow rate through individual radiator).	Heating temperature not constant.
Two-pipe direct-return	Water supply temperature to an emitter not affected by upstream emitters. Smaller heat transfer areas needed as compared to the previous two (due to higher supply water temperature available).	Balancing a problem for a large system. Higher pumping cost.
Two-pipe reverse-return	Same as two-pipe, direct return plus easy balancing.	May need larger pipes as compared to direct-return.

Example 10.3

The system shown in Figure 10.8 uses a closed expansion tank with pressurized nitrogen (N_2) at 8bar. With reference to the data given below, find the maximum flow water temperature that should be used if i) the pump is located at 'A'; and ii) the pump is located at 'B'.

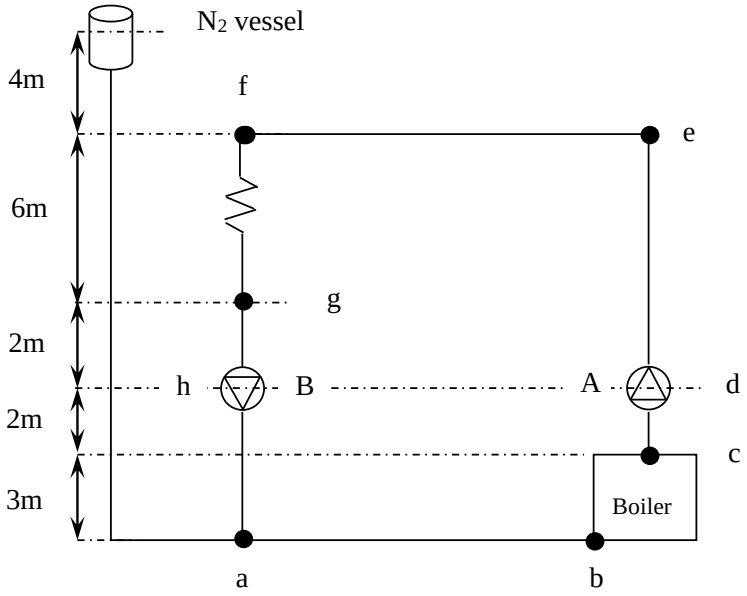

Figure 10.8 Schematic of a hot water circulation circuit

Data: Anti-flash margin: 10K
Density – water at system temperature: 900kg/m^3

Density – water in feed/expansion line: 1000kg/m^3
Section pressure losses (kPa):

a-b 25	b-c 18	c-d 18	d-e 25
e-f 35	f-g 180	g-h 12	h-a 12

Solution for Example 10.3

The pressure in the expansion tank is 8 bar, as given, which equals 810.6 kPa.

Taking the level at point 'a' as the datum for elevation and system pressure calculations, the overall height from point 'a' to the free surface in the expansion tank equals:

$4 + 6 + 2 + 2 + 3 = 17\text{m}$

At the bottom of the cold water column in the expansion pipe connecting the expansion tank to point 'a', the pressure is:

$810.6 + 1000 \times 9.81 \times 17 / 1000 = 977.4$ kPa

From the given pressure drop values for various pipe sections, the required pump head for the circulation pump is 325 kPa as shown in the following table.

		Pipe sections								
	Unit	a-b	b-c	c-d	d-e	e-f	f-g	g-h	h-a	Pump Head
Press loss	kPa	25	18	18	25	35	180	12	12	325

With the pump at A

The pressures at various points in the system were determined, with reference to point 'a'. For example, the pressure at point 'b' is given by:

977.4 – 0 (pressure change due to elevation) – 25 (pressure loss along the pipe section) = 952.4 kPa.

The pressure at point 'c' is given by:

977.4 – $3 \times 9.81 \times 900 / 1000$ (pressure change due to elevation) – (25 + 18) (pressure loss along the pipe section) = 907.9 kPa.

The pressure at the suction side of the pump (denoted by point d(ps)) was likewise calculated to be 872 kPa.

The pumping pressure was then added to yield the pressure at the discharge side (point d(pd)) which is 1197 kPa.

The pressures at points 'e' to 'h' were likewise determined as summarized below.

With pump at A		Points in system									
		a	b	c	d (ps)	d (pd)	e	f	g	h	
Altitude	m	0	0	3	5	5	13	13	7	5	
SP	kPa	977	977	951	933	933	863	863	916	933	
DP	kPa	0	-25	-43	-61	264	239	204	24	12	Min
TP	kPa	977	952	908	872	1197	1102	1067	940	945	872
	bar										8.61

Among various points in the system, it was found that the minimum pressure was 872 kPa, or 8.61 bar, at the suction side of the point, i.e. at point d(ps). The saturation temperature of water at 8.61 bar was determined by interpolation between the values for 8 & 9 bar to be 173.4°C, as shown below. Taking into consideration the requirement for 10K anti-flash margin, the maximum water temperature that may be used is 163.4 °C.

Pressure	bar	8	9	8.61
Sat Water Temp	C	170.4	175.4	173.4
Max temp	C			163.4

With the pump at B

The calculation results for this case were as summarized in the table below.

		Points in system									
		a	b	c	d	e	f	g	h (ps)	h(pd)	
Altitude	m	0	0	3	5	13	13	7	5	5	
SP	KPa	977	977	951	933	863	863	916	933	933	
DP	KPa	0	-25	-43	-61	-86	-121	-301	-313	12	Min
TP	KPa	977	952	908	872	777	742	615	620	945	615
	bar										6.07
Press	bar	6	7								6.07
Sat Water Temp	C	158.8	165								159.2
Max temp	C										149.2

10.3 Heat recovery chillers and heat pumps

As outlined in Section 6.2.2, a reversed heat engine may be used as a chiller for outputting cooling, or as a heat pump for supplying heat, or both. Similar to a chiller that extracts heat from the chilled water, a heat pump obtains heat from a source and brings the heat to a higher temperature before the heat is output for space or water heating.

Compared to a boiler, which will always have an efficiency below 1, a heat pump can output an amount of heat that is several times the required work input. However, this will be a fair comparison only if a motor driven, vapour compression heat pump is compared against an electric water heater. For gas or oil boilers, a simplistic comparison of a fuel input with electricity input may not provide a sound basis for decision making.

When different fuel/energy inputs are involved, besides thermal efficiency, the comparison may need to consider differences in owning and operating costs, air and

water pollution incurred to the local environment, greenhouse gas emissions and other global environmental burdens incurred, etc. Nevertheless, the ratio of heat output to work input, which is called the coefficient of performance of a heat pump, COP_{HP}, is widely used as a metric for gauging the performance of heat pumps.

While being used to supply cooling, a chiller can also function as a heat pump to provide heating simultaneously, e.g. using its condenser heat rejection for hot water heating, in which case the chiller is called a heat recovery chiller (Figure 10.9).

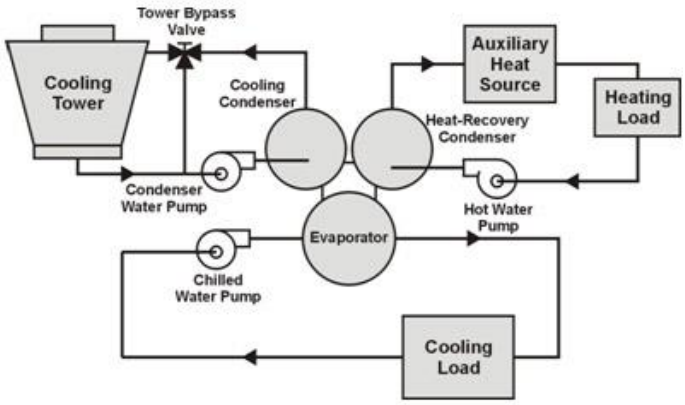

Figure 10.9 A double bundle heat recovery chiller

In a heat recovery chiller, there are two bundles of condenser tubes that are compartmentalized from each other within one condenser cell, or in separate cells (Figure 10.9). The hot gas from the compressor will be cooled firstly by the tube bundle for heat recovery. The water leaving the heat recovery tube bundle, if not high enough in temperature to meet the usage requirement, will be heated up further by a calorifier (with steam or hot water supply from a boiler) or a water heater. Where the heat rejection rate corresponding to the required cooling output is greater than the amount removed by the heat recovery tube bundle, rejection of condensation heat of the gas refrigerant will continue through the second bundle, and the heat will be carried away by the condenser water to a cooling tower or heat exchanger for rejection to the atmosphere or a river or lake, or the sea.

As the above discussion implies, the amount of heat recoverable from a heat recovery chiller is dependent on the cooling demand while coping with the latter is the priority of the chiller. Therefore, heating equipment, such as water heaters or boilers or heat pumps, that can cope with the heating demand without the heat recovery chillers are still required. Such central heating and cooling plants are suitable for buildings that would have simultaneous demands for heating and cooling, such as large commercial/ office buildings, hotels, hospitals, complex developments, etc.

Contrary to heat recovery chillers, heat pumps are meant primarily to supply heat whilst supplying cooling simultaneously is a bonus, and the amount of cooling available is dependent on the heating demand. Rather than from a cooling load, most heat pumps obtain heat supply from a heat source, such as the outdoor air directly, or indirectly

through cooling air in a cooling tower by the water being circulated between the heat pump and the cooling tower. However, as the water in the system must stay above the freezing temperature, the system may work only if the outdoor air temperature is well above 0°C. Water from a river or lake or the harbour can also serve as a heat source for heat pumps and in such systems, heat exchangers would be used to separate the water through the heat pump and the water in the heat source, and glycol may be added to the water in the heat pump circuit to reduce its freezing temperature. Another heat source is from the ground and heat is extracted from the ground by circulating water through pipes buried underground (Figure 10.10). According to their heat sources, heat pumps may be called air source, water source or ground source heat pumps.

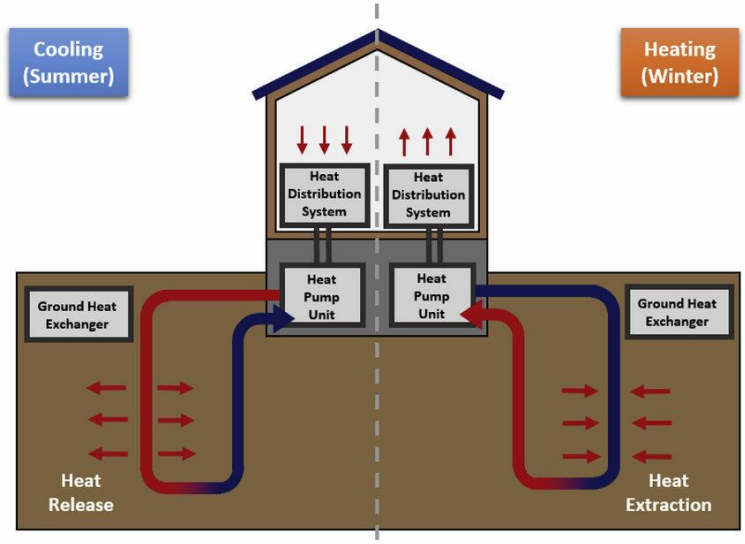

Figure 10.10 Ground source heat pump

As shown in Figure 10.10, a ground source heat pump may function as a heating equipment in winter and a cooling equipment in summer. The ground plays the role of a huge heat storage, allowing the heat rejected into the ground by the system in summer as well as heat gains from solar radiation and the ambient air, to be stored and retrieved for use in winter. Balance between the heat stored in the ground in summer and the heat retrieved from the ground in winter is essential to sustainability of the ground source heat pump system. Otherwise, the ground temperature may rise or drop, which will affect the amount of heat that can be extracted from, or the heat that can be rejected into, the ground.

The thermodynamic performance of heat pumps is dependent on the temperature of the heat source, as well as the temperature at which heat is to be supplied. Table 10.3 provides a summary of heat pump performance over a range of heat source temperature and heat output temperature. The data in the table show that high heat supply temperatures (e.g. above 65°C) cannot be achieved unless the heat source temperature is also high (above 0°C). Compared to boilers and water heaters, the temperature of heat supply that heat pumps can provide is lower, which is a limitation of the application of heat pumps.

Table 10.3 The COP of heat pumps at different output temperatures (source: https://en.wikipedia.org/wiki/Heat_pump)

Pump type and source	**Typical use**	**35 °C (e.g. heated screed floor)**	**45 °C (e.g. heated screed floor)**	**55 °C (e.g. heated timber floor)**	**65 °C (e.g. radiator or DHW)**	**75 °C (e.g. radiator and DHW)**	**85 °C (e.g. radiator and DHW)**
High-efficiency air source heat pump (ASHP), air at −20 °C		2.2	2.0	-	-	-	-
Two-stage ASHP, air at −20 °C	Low source temperature	*2.4*	2.2	1.9	-	-	-
High efficiency ASHP, air at 0 °C	Low output temperature	*3.8*	2.8	2.2	2.0	-	-
Prototype transcritical CO_2 (R744) heat pump with tripartite gas cooler, source at 0 °C	High output temperature	3.3	-	-	*4.2*	-	3.0
Ground source heat pump (GSHP), water at 0 °C		5.0	3.7	2.9	2.4	-	-
GSHP, ground at 10 °C	Low output temperature	*7.2*	5.0	3.7	2.9	2.4	-
Theoretical Carnot cycle limit, source −20 °C		5.6	4.9	4.4	4.0	3.7	3.4
Theoretical Carnot cycle limit, source 0 °C		8.8	7.1	6.0	5.2	4.6	4.2
Theoretical Lorentzen cycle limit (CO_2 pump), return fluid 25 °C, source 0 °C		10.1	8.8	7.9	7.1	6.5	6.1
Theoretical Carnot cycle limit, source 10 °C		12.3	9.1	7.3	6.1	5.4	4.8

There are district energy systems that are equipped with tri-generation plants for supplying cooling, heating, and electricity to consumers in a geographical region (Figure 10.11). A tri-generation plant comprises generators that convert a fuel input into electricity output while generating heat as a by-product in the process. The heat may be used for heating supply directly or to drive an absorption chiller (see next section) to provide chilled water for cooling. Alternatively, more electricity than the demand may be generated and the surplus is used to run vapour compression chillers for chilled water supply. The heat rejection of the absorption or vapour compression chillers may also be used to pre-heat water. The different possible modes of operation for a tri-generation plant allow the operators to choose the most efficient way of meeting the demands for heating, cooling, and electricity.

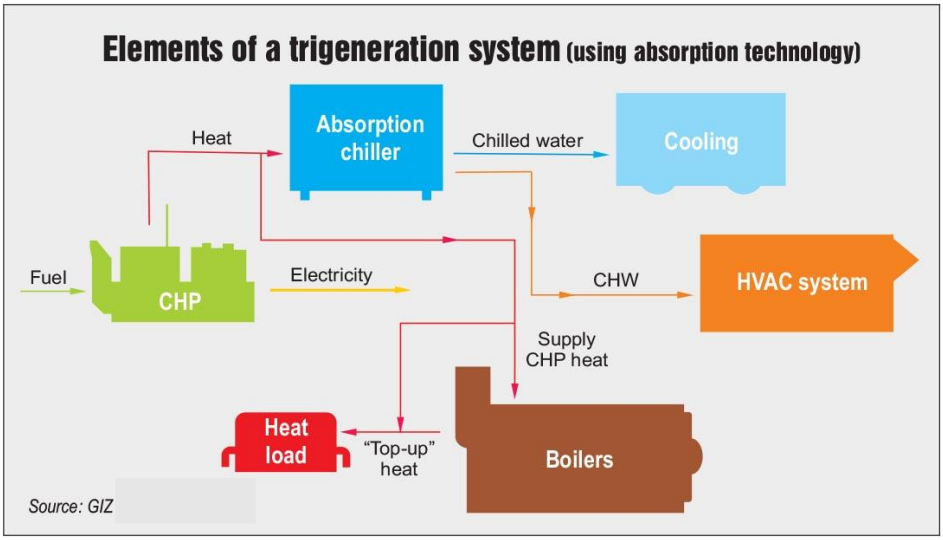

Figure 10.11 Tri-generation plant

10.4 Absorption refrigeration

10.4.1 System configuration and processes

The vapour compression refrigeration machine introduced in Chapter 6 requires work input for it to output cooling. Instead of a refrigerant compressor, raising the pressure and temperature of the vapour refrigeration from the state it leaves the evaporator to the state it enters the condenser can be performed by a chemical method, which requires the input of heat, and chillers that work on this principle are called absorption chillers [3]. In an absorption chiller (Figure 10.12), the following components act together to replace the compressor in a vapour compression system:

- Absorber
- Pump
- Generator
- Throttling device

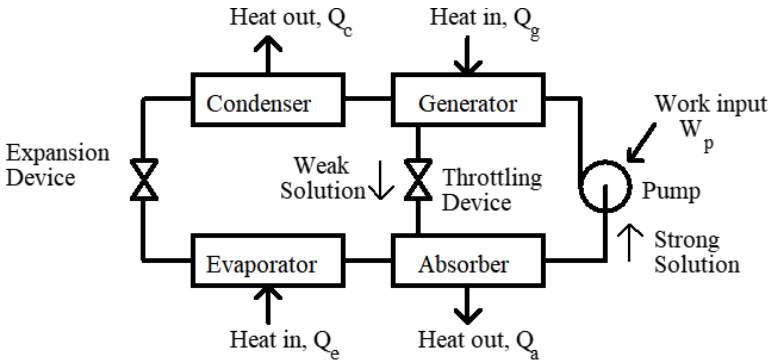

Figure 10.12 An absorption chiller

In an absorption chiller, a medium, called the absorbent, is used in addition to the refrigerant. The absorbent should ideally circulate round only the above four components without going into the other components (e.g. the condenser and evaporator) of the refrigeration system. The processes taking place in an absorption chiller include:

1. The vapour refrigerant coming out of the evaporator is absorbed by the absorbent (weak solution) in the absorber. In this process, the refrigerant dissolves into the absorbent and the concentration of refrigerant in the mixture increases (and the absorbent then becomes strong solution). To maintain the solubility, the condensation heat of the refrigerant and the heat of dilution of the absorbent (call the heat of absorption) must be removed from the absorber.

2. The pressure of the strong solution is raised by the pump and the solution then enters the generator. In some small systems, the pump can be omitted, with the pressure difference maintained by gravitational force.

3. In the generator, heat is supplied to drive the refrigerant out of the strong solution. As a result, the concentration of refrigerant in the absorbent/ refrigerant mixture decreases and the absorbent becomes weak solution again.

4. The vapour refrigerant from the generator will then enter the condenser and go on with the conventional refrigeration cycle, i.e. condense into liquid, be throttled through the expansion device to the evaporator pressure, and evaporate in the evaporator to produce refrigeration effect for cooling the chilled water.

5. The weak solution, at the generator pressure, will pass through a throttling device for lowering its pressure before it enters the absorber again to absorb refrigerant vapour from the evaporator.

With this system, the major input of energy is heat at the generator. The work input to the pump is relatively small and may be neglected in the analysis.

10.4.2 Evaporation and condensation characteristics of a homogeneous binary mixture

The absorption refrigeration process can be understood by analysing the relations among the concentration, temperature, and pressure of a mixture in a hypothetical experiment as shown in Figure 10.13 and discussed below.

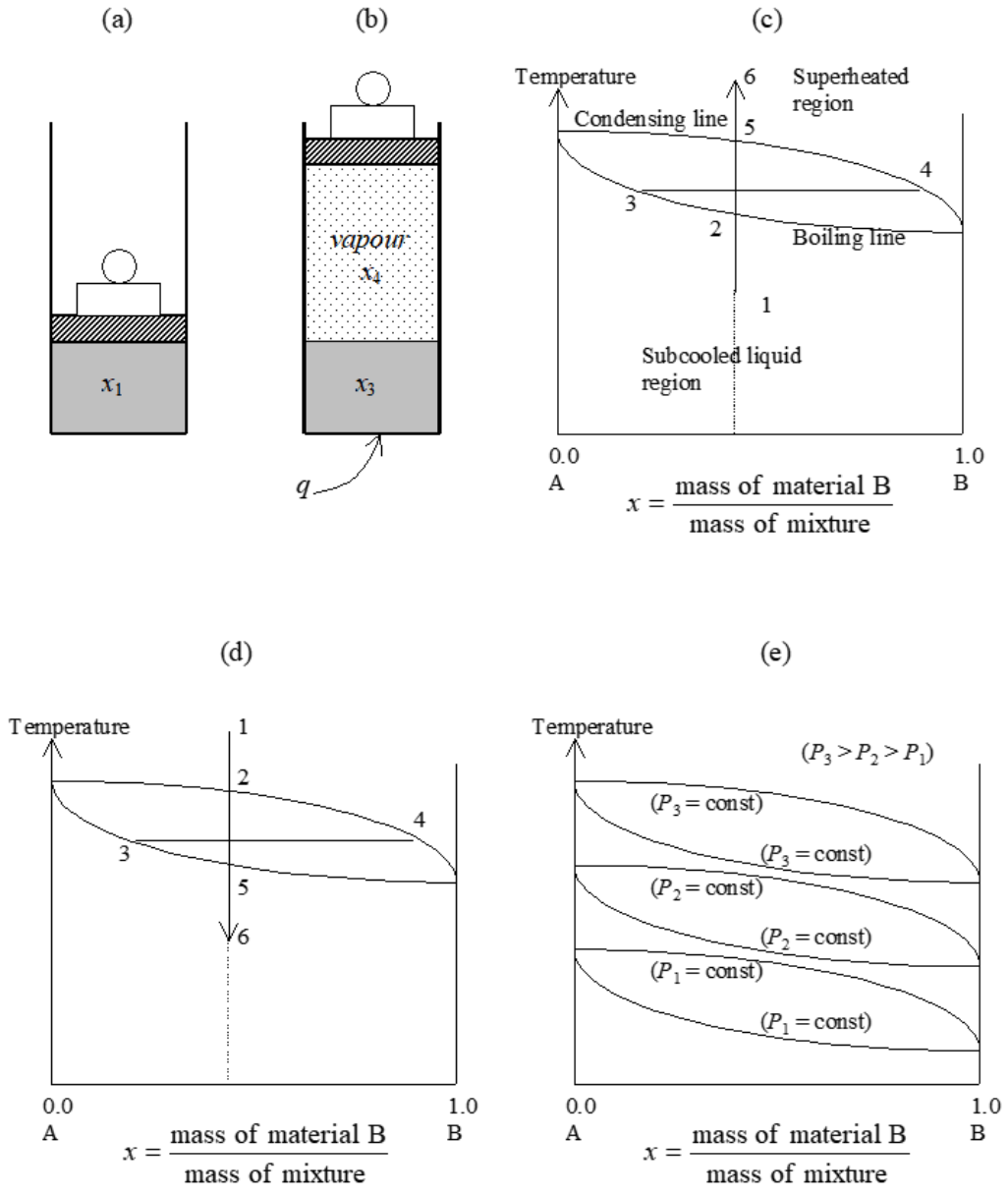

Figure 10.13 Evaporation and condensation characteristics for a homogeneous binary mixture

The mixture we are looking at is called a binary mixture because it comprises two substances, namely the refrigerant and the absorbent. Accordingly, we need to specify three properties for defining the state of the mixture, and this often involves the use of the temperature, pressure, and concentration of the mixture. The concentration is

quantified by the mass of one constituent substance in the mixture per unit mass of the mixture. Unlike in psychrometry, we do not have one of the properties (total pressure in psychrometry) that may be assumed to be the same at all times and, instead of the mass of a selected substance of the mixture (dry air in psychrometry), we use here the total mass of the mixture as the base for quantifying concentration (moisture content in psychrometry).

Consider two pure substances A and B which are mutually miscible to become a homogeneous mixture. Assume that the boiling temperatures of the two substances are different, and that of substance A is higher than that of substance B. Starting from a homogeneous liquid solution under a given pressure, with x kg of B in each kg of the mixture (Figure 10.13.a), if the mixture is heated while the pressure is held constant, up to a certain temperature, vapour mixture will start to appear and the concentrations of B in the liquid and in the vapour will deviate from the original concentration (x) (Figure 10.13.b & c). Since substance B has a lower boiling point, there will be more B in the vapour mixture than in the liquid. The proportion of liquid and vapour, and their respective concentrations, will change with their temperature.

If the experiment of heating up a mixture of the two substances is repeated for liquid mixtures with different initial concentrations ranging from 0 (only A) to 1 (only B), and the equilibrium temperature and the concentrations of B in the liquid and vapour found in the experiment are plotted on a temperature-concentration chart, two lines can be traced. The lower line represents the boiling line and the upper line the condensing line (Figure 10.13.c).

Continued heating of the mixture will eventually cause all the liquid to vaporize and, at this stage, the concentration of the vapour mixture is identical to the concentration of the original liquid (x) (Figure 10.13.c). The range of saturation temperatures of the mixture (corresponding to the boiling and condensing lines) will change with concentration of the components as well as the pressure maintained in the process (Figure 10.13.e). The process can be reversed starting from a vapour mixture and gradually cooling the vapour into a liquid mixture (Figure 10.13.d).

Alternative to a temperature-concentration diagram, the saturation curves of a binary mixture can be more usefully represented in the form of an enthalpy-concentration diagram in which the condensing line and the boiling line are separated by a distance that equals the latent heat of vaporization (Figure 10.14). In this diagram, constant temperature lines are also shown in the sub-cooled liquid (below the boiling line) and superheated vapour (above the condensing line) regions.

10.4.3 Theoretical coefficient of performance of an absorption refrigeration cycle

Based on the 1st law of thermodynamics, energy (heat and work) balance on the absorption refrigeration system (Figure 10.15) can be written as:

$$\sum Q - \sum W = 0$$

$$Q_g + Q_e - Q_a - Q_c + W_p = 0 \qquad (10.13)$$

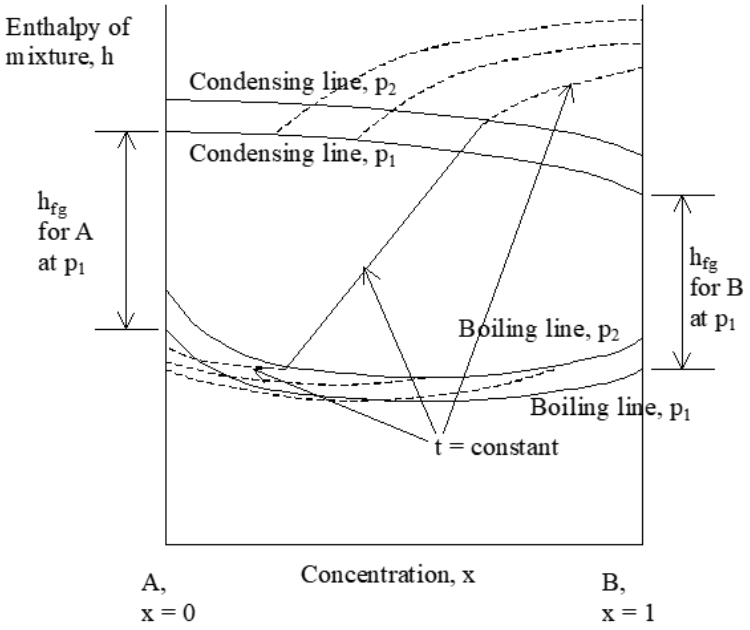

Figure 10.14 Enthalpy-concentration diagram for liquid and vapour regions for a homogeneous binary mixture

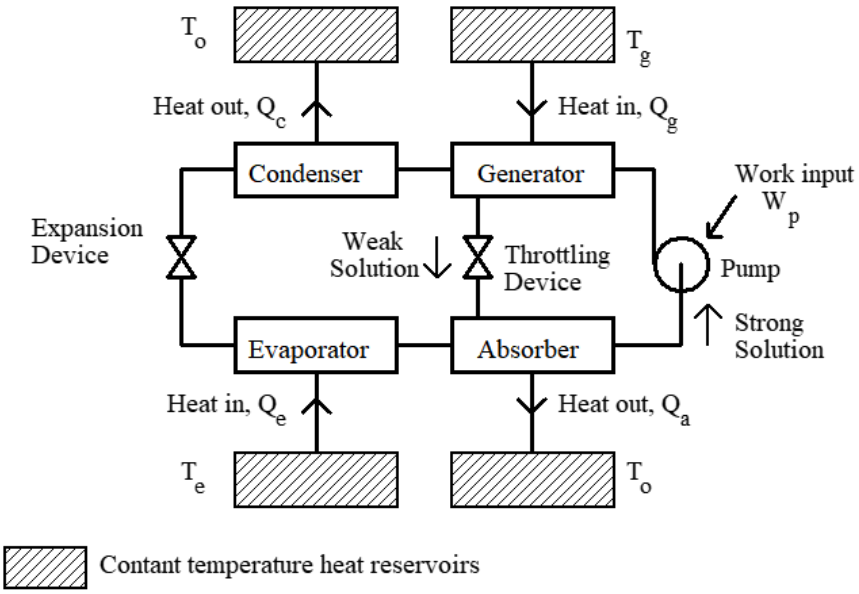

Figure 10.15 Heat and work flow between an absorption refrigeration machine and the surrounding

Where the waste heat, Q_o, is:

$$Q_o = Q_a + Q_c \tag{10.14}$$

In the above equations, Q denote heat exchanges of components of the absorption chiller with the surrounding heat reservoirs, and the subscripts g, e, a, & c denote, respectively, the generator, evaporator, absorber, and the condenser that are exchanging heat with these surrounding heat reservoirs. The sign of the Q terms in Equation (10.13) follow the thermodynamic convention, i.e. heat input to a system is positive, and vice versa. W_p denotes the work input to the pump. Since work output is positive, the sign of W_p becomes positive in Equation (10.13).

Furthermore, the assumption is made that the absorber and the condenser would both be cooled by cooling water from the same source. Therefore, a single heat reservoir, denoted by the subscript o, is used to represent the surrounding that exchanges heat with them.

According to the 2nd law of thermodynamics, the net change in entropy for the system plus the surroundings must be greater than or equal to zero. Since the working fluid within the system undergoes a cycle, the total change in entropy for the system is zero. The overall increase in entropy, ΔS_{tot}, therefore, comprises only the contributions of the heat reservoirs:

$$\Delta S_{tot} = \Delta S_g + \Delta S_e + \Delta S_o \geq 0 \tag{10.15}$$

Assume that the temperature of the environment (T_o) (the cooling medium for the absorber and the condenser), the generator heating medium temperature (T_g), and the temperature of the refrigerated medium at the evaporator (T_e) are all constants, and the reservoirs are internally reversible (thus $dQ = TdS$ applies to each and can be integrated to yield $Q = T\Delta S$).

Hence, the enthalpy changes at the right-hand side of Equation (10.15) may be calculated as:

$$\Delta S_g = -\frac{Q_g}{T_g};\ \Delta S_e = -\frac{Q_e}{T_e};\ \Delta S_o = \frac{Q_o}{T_o} \tag{10.16}$$

It follows that:

$$\Delta S_{tot} = -\frac{Q_g}{T_g} - \frac{Q_e}{T_e} + \frac{Q_o}{T_o} \geq 0 \tag{10.17}$$

Expressing Q_o in Equation (10.17) in terms of Q_g, Q_e & W_p through Equations (10.13) & (10.14), we get:

$$-\frac{Q_g}{T_g} - \frac{Q_e}{T_e} + \frac{Q_g + Q_e + W_p}{T_o} \geq 0$$

$$\frac{Q_g}{T_o} - \frac{Q_g}{T_g} + \frac{Q_e}{T_o} - \frac{Q_e}{T_e} + \frac{W_p}{T_o} \geq 0$$

$$Q_g - \frac{T_o Q_g}{T_g} + Q_e - \frac{T_o Q_e}{T_e} + W_p \geq 0$$

$$Q_g\left(\frac{T_g-T_o}{T_g}\right)+Q_e\left(\frac{T_e-T_o}{T_e}\right)+W_p \geq 0$$

$$Q_g\left(\frac{T_g-T_o}{T_g}\right) \geq Q_e\left(\frac{T_o-T_e}{T_e}\right)-W_p \qquad (10.18)$$

If the pump work is neglected,

$$COP=\frac{Q_e}{Q_g} \leq \left\{\frac{T_e(T_g-T_o)}{T_g(T_o-T_e)}\right\} \qquad (10.19)$$

When all the processes are reversible,

$$COP_{Max}=\left\{\frac{T_e(T_g-T_o)}{T_g(T_o-T_e)}\right\} \qquad (10.20)$$

10.4.4 Choice of refrigerant and absorbent combination

For an ideal refrigerant-absorbent combination, the refrigerant should permit boiling at 2-10 ^{o}C and condensation at 37 ^{o}C or above at pressures not far from atmospheric; have a large latent heat of vaporization; and have low heat capacity and molecular weight. The absorbent should have a high boiling point (low volatility); have low viscosity and heat capacity; and stay as a liquid under the possible operating conditions. Furthermore, the absorbent in the combination must have a high affinity for the refrigerant vapour; be chemically stable and non-corrosive, both individually and in combination; give a solution with low heat capacity and viscosity; and yield a solution with a small heat of dilution.

There are two refrigerant-absorbent combinations in common use:

1) Ammonia (refrigerant) - water (absorbent)

   Systems using this combination is often called aqua-ammonia systems. They are widely used in domestic refrigerators and process industries in the past. Limitations of this combination include that ammonia is slightly toxic and the absorbent (water) is quite volatile. Additional devices are required to minimize flow of ammonia into the condenser (e.g. Dephlegmator and Rectifying Column).

2) Water (refrigerant) - Lithium Bromide (absorbent) (LiBr)

   This combination is common for air-conditioning applications. It has the advantages that LiBr is non-volatile, and the system is simpler and offers higher COP than aqua-ammonia systems. The main disadvantages of this combination include that the evaporating temperature is relatively high and the system pressure rather low, and the pair is not mutually soluble under certain conditions (e.g. below 0 ^{o}C)

The table below shows a comparison between these two commonly used refrigerant-absorbent combinations.

Table 10.4 Comparison between two refrigerant-absorbent combinations

Combination	Ammonia-Water	Water-LiBr
COP	about 0.5	about 0.8
Evaporating temperature	can operate below 0 °C	above 3 °C
Operating pressure	above atmospheric	below atmospheric (purge unit needed)

10.4.5 Analysis of thermodynamic processes in absorption refrigeration systems

Analyses of the processes taking place in an adsorption chiller are discussed below, which would enable the performance of an adsorption chiller to be analysed.

a) Adiabatic mixing

Consider two streams of binary mixtures mixing with each other as shown in Figure 10.16. From energy balance:

$$m_1 h_1 + m_2 h_2 = m_3 h_3 \tag{10.21}$$

Overall mass balance:

$$m_1 + m_2 = m_3 \tag{10.22}$$

Mass balance on concentration of one constituent in the mixture:

$$m_1 x_1 + m_2 x_2 = m_3 x_3 \tag{10.23}$$

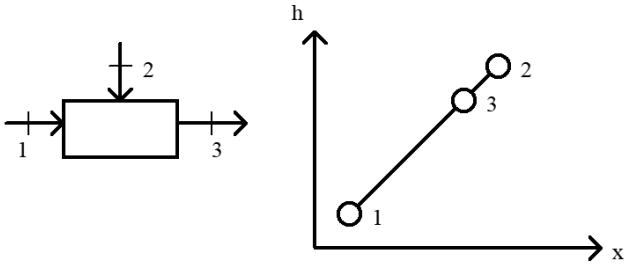

Figure 10.16 Steady-flow adiabatic mixing process

From Equation (10.22),

$$m_1 = m_3 - m_2 \tag{10.24}$$

$$m_2 = m_3 - m_1 \tag{10.25}$$

Substituting Equation (10.24) into Equation (10.21) yields:

$$h_3 = h_1 + \frac{m_2}{m_3}(h_2 - h_1) \qquad (10.26)$$

Substituting Equation (10.25) into Equation (10.23) yields:

$$x_3 = x_1 + \frac{m_2}{m_3}(x_2 - x_1) \qquad (10.26)$$

Note that mixing of two streams of solutions at different temperatures may result in the mixture condition lying inside the saturation region (between the condensing and boiling lines). In this case, a trial and error graphical method based on a properties chart can be used to determine the mixture temperature and concentrations of the liquid and vapour components (see Figure 10.17).

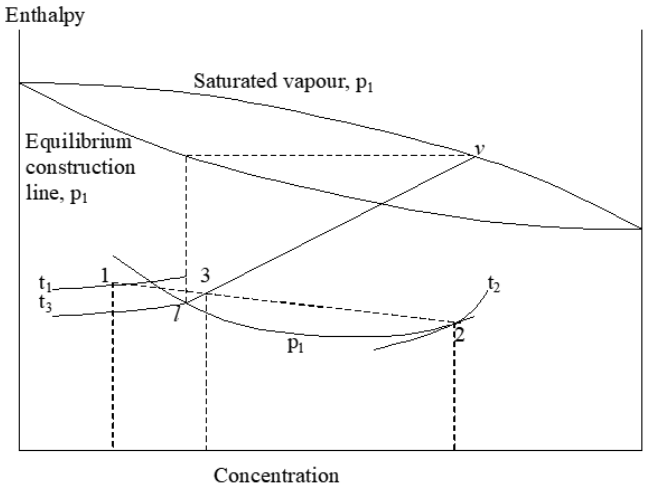

Figure 10.17 Mixture condition in the saturated region

In the example shown in Figure 10.17, point 3 represents the state of the mixture of two mixtures at states represented by points 1 & 2. As point 3 lies in the saturation region, the mixture comprises saturated liquid and vapour components, which are at states denoted by points *l* and *v*, in the chart. The state points *l* and *v* are related by the construction line corresponding to the pressure of the mixture, p_1, in that the vertical line extended from the liquid state point and the horizontal line extended from the vapour state point should cross each other at a point lying on the construction line. Based on this principle, the locations of points *l* and *v* can be found by a graphical trial and error process.

The situation illustrated in Figure 10.17 may happen in an aqua-ammonia system. Similar situation will not happen in a LiBr – water adsorption chiller as the LiBr – water mixture will always be a liquid.

b) Mixing of two streams with heat exchange

This occurs at the absorber of the system. The process is as shown in Figure 10.18.

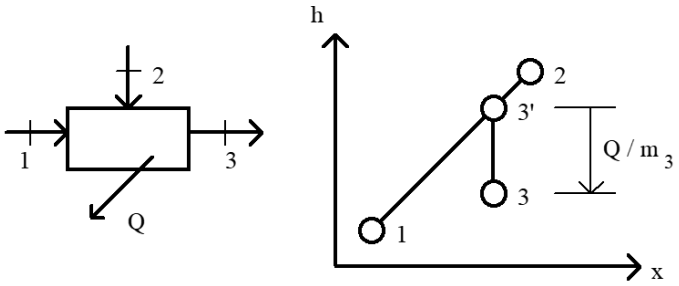

Figure 10.18 Mixing process with heat exchange

Energy balance:

$$m_1 h_1 + m_2 h_2 = m_3 h_3 + Q \tag{10.27}$$

Mass balances are same as the adiabatic mixing process and thus Equations (10.23) & (10.26) are applicable. However, the enthalpy of the mixture becomes:

$$h_3 = h_1 + \frac{m_2}{m_3}(h_2 - h_1) - \frac{Q}{m_3} \tag{10.26}$$

The process in the generator is the reverse of the mixing and cooling process discussed above as it involves heating up a mixture such that the mixture decomposes into a vapour with a high concentration of the refrigerant, and a liquid, the weak solution, with a low concentration of the refrigerant in the mixture.

c) Heating and cooling processes

Alternate heating and cooling processes, with vapour/liquid separation in between, are essential to help produce high purity ammonia vapour in an aqua-ammonia system. The processes are as shown in Figures 10.19.a & 10.19.b.

d) Throttling process

In this process, both the enthalpy and concentration of the mixture remain unchanged. The initial and final state points of the mixture, therefore, coincide on an enthalpy-concentration diagram. It however should be noted that the pressure, and in general the temperature, of the mixture leaving the throttling device are lower and the concentrations of liquid and vapour components would need to be determined by trial and error on the properties diagram (Figure 10.20).

By using the above procedures to analyse the processes involved in an absorption refrigeration system together with the enthalpy-concentration diagram for the refrigerant-absorbent under concern, the overall heat supply and cooling requirements and the refrigeration effect of the system can be calculated.

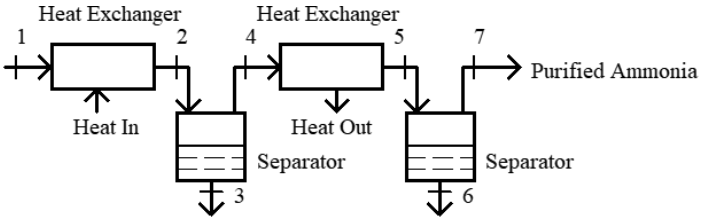

(a)

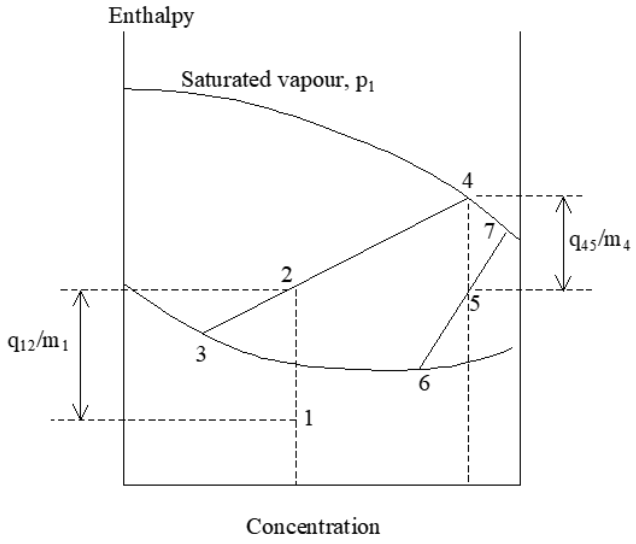

(b)

Figure 10.19 Alternate heating and cooling processes for rectifying ammonia-water mixture

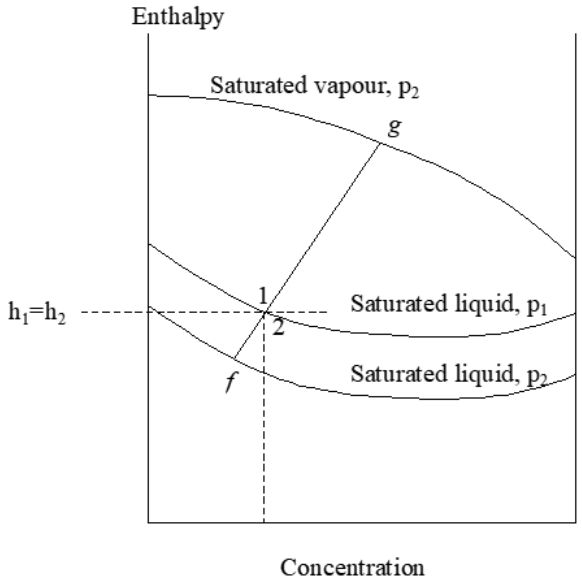

Figure 10.20 Throttling process

10.5 Applications of absorption refrigeration

Because of concerns about depletion of fossil fuel reserves and the environmental burdens and financial costs that consumption of energy will incur, application of absorption systems is attractive where relatively cheap heat energy or waste heat is available. Typical examples are heat rejection from other systems at suitable temperatures (90 - 100 ^{o}C); e.g. steam from power plants, high temperature liquid from chemical and processing plants, etc., or low-grade heat derived from natural resources, e.g. solar heat.

Compared with vapour compression refrigeration systems, the absorption system is

- simpler and less expensive to manufacture
- operates with less noise
- can utilize low grade heat sources
- required minimal electricity input
- has a much lower COP but the differentiation between the inputs for determining COP must be made.

10.6 Adsorption chiller

A new generation of chillers that produces cooling with heat input are now available. Instead of an absorbent, they utilize a hygroscopic material (e.g. silica gel), and such chillers are called adsorption chillers (as contrast to absorption chillers). The working principle of an adsorption chiller, with reference to Figure 10.21, are described briefly below:

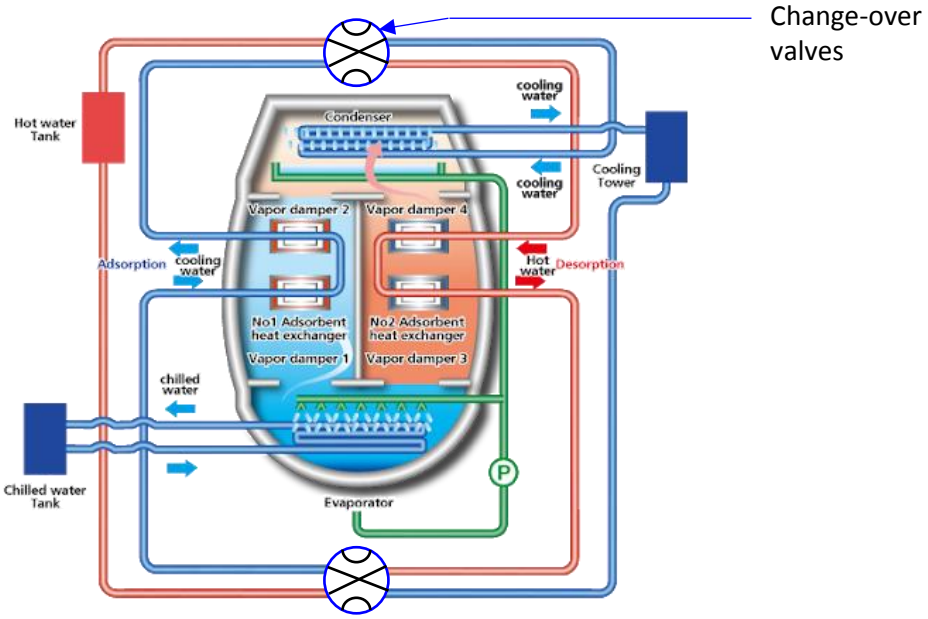

Figure 10.21 Working principle of an adsorption chiller (Source: http://www.tokyo-boeki-machinery.jp/adsorption_chiller/genri.html)

- There are two chambers inside the chiller that house the adsorbents. The two chambers will be used alternately for the adsorption and desorption processes. The flow of hot or cooling water through the heat exchangers inside the chambers is controlled by the change-over valves and the flow of refrigerant vapour by the vapour dampers.

- Chilled water is cooled by vaporization of water (refrigerant) when the water is sprayed onto the chilled water circulation tubes inside the evaporator under a pressure well below atmospheric pressure (i.e. a partial vacuum condition). Vapour damper (1) or (3) will be opened by the pressure of the refrigerant vapour in the evaporator.

- As the adsorbent (silica gel) inside the adsorption heat exchanger adsorbs the refrigerant vapour produced in the evaporator, cooling water is circulated through the tubes surrounded by the adsorbent, to take away the heat of adsorption for sustaining adsorption of refrigerant vapour.

- In the other chamber, hot water flows through the tubes of the adsorption heat exchanger and heats up the adsorbent such that the adsorbed vapour is released (i.e. desorption). Vapor damper (2) or (4) will be opened by the refrigerant vapour pressure.

- The water vapour (refrigerant) released from the adsorption heat exchanger is cooled by the condenser and condenses back into liquid water, which flows into the evaporator and will undergo another cycle of evaporation, adsorption, desorption, and condensation again.

Figure 10.22 shows an adsorption chiller installed in the Zero Carbon Building in Hong Kong.

Figure 10.22 An adsorption chiller

References

[1] Oughton D.R., Hodkinson, S.L., Faber & Kell's Heating and Air-conditioning of Buildings, 10th Ed., Butterworth-Heinemann, 2008.

[2] ASHRAE Handbook, System and Equipment, American Society of Heating, Refrigerating and Air-conditioning Engineers, Inc., 2000.

[3] DETR, Good Practice Guide 256, An introduction to absorption cooling, Department of the Environment, Transport and the Regions, UK, 1999.

Appendix A Developing an Electronic Psychrometric Chart and Property Calculator

A.1 Introduction

Psychrometric calculations are an indispensable part of air-conditioning system design and analysis. The thermodynamic properties of moist air at the entering and leaving air states of air-conditioning processes are either the input or the outcome of psychrometric calculations. Being a graphical representation of the relations among properties of moist air, psychrometric chart is a convenient tool that air-conditioning engineers rely upon to determine moist air properties. Charts published by professional institutions, including the Chartered Institution of Building Services Engineers (CIBSE) in the UK and the American Society of Heating, Refrigerating and Air-conditioning Engineers (ASHRAE) in the US, are the most widely used versions in the field.

Although printed psychrometric charts are reasonably convenient to use, air-conditioning engineers will be able to perform system design and analysis more efficiently and accurately if they are equipped with a computer program that can evaluate moist air properties and create a graphical image of a psychrometric chart. This will also enable great enhancement of the quality of presentation of psychrometric calculation results, especially when a picture of a psychrometric chart together with the processes being analysed can be exported and embedded into reports. Developing such a program will be an interesting and challenging task to students and engineers who are conversant with psychrometry and often perform psychrometric calculations.

This Appendix is intended to portray the basic psychrometric calculation methods required for the development of a psychrometric analysis program that can:

1. Generate a graphical image of psychrometric chart.

2. Perform psychrometric calculations to determine moist air properties from input of two of the properties (total pressure of moist air assumed to be one standard atmospheric pressure).

3. Determine the heat and moisture transfer rates for psychrometric processes.

The basic principles and psychrometric equations underpinning the calculation methods, which are the fundamentals needed for developing such a program, are covered in the following sections of this Appendix while the more complicated numerical solution schemes involved are described in the Annexes.

A computer program that implements the methods to calculate moist air properties and to produce electronic images of psychrometric chart and processes can be developed using an appropriate computer programming language, such as Visual Basic, Visual C#, Python, etc. This has actually been done by the author and hence the methods have been verified to be workable. The methods have also been implemented in an Excel workbook, with the use of Visual Basic for Applications (VBA) for programming the numerical calculation routines.

A.2 Constructing a psychrometric chart

A.2.1 Axes and scales for the chart

Using a computer to construct a psychrometric chart requires representation of all the constant moist air property lines by mathematical equations. In order that changes in the energy and moisture content of moist air in a psychrometric process will be proportional to the linear distance between the start and the end state points of the process when shown on the chart, the two principal axes of the chart shall represent linear scales of the specific enthalpy and moisture content of moist air (see also Section 2.4.2.2). The scales for the two co-ordinates shall be carefully selected such that the chart will fit the size of the screen or paper on which the chart is shown.

Conventionally, the moisture content scale is represented by the vertical axis, and the specific enthalpy scale by an inclined axis. This arrangement helps make the chart more convenient to use, but it gives rise to the need for defining an auxiliary variable, to serve as the variable represented by the horizontal axis. This variable should be linearly dependent on the two principal variables such that the moisture content and this variable will form a pair of orthogonal co-ordinates, as are needed for generating a graphical image in a computer. Figure A.1 shows the relations among the specific enthalpy (along a skewed co-ordinate), moisture content (along the ordinate) and the auxiliary variable, denoted here by x (with a linear scale along the abscissa), in such a chart.

For a state point (h, w), which will appear in the target chart at ($h\,S_h$, $w\,S_w$) (Figure A1),

$$h\,S_h = x\cos\theta + w\,S_w\,\sin\theta \qquad \text{(A.1)}$$

Where h and w are the values of specific enthalpy and moisture content, and S_h and S_w are the scales for showing h & w, respectively, on the chart.

Hence,

$$x = \left(\frac{S_h}{\cos\theta}\right)h - \left(\frac{S_w\sin\theta}{\cos\theta}\right)w \qquad \text{(A.2)}$$

Through using the definitive equation for specific enthalpy (Equation (A.3)), x can also be related to the dry bulb temperature, t, which is more often the known property, as follows:

$$h = Cp_{da}t + w\,(Cp_s t + h_{fg,0}) \qquad \text{(A.3)}$$

Where Cp_{da}, Cp_s, and $h_{fg,0}$ are, respectively, the specific heat of dry air, specific heat of water vapour and latent heat of vaporization of liquid water into vapour at 0°C, and here, all of them are simply regarded as constants.

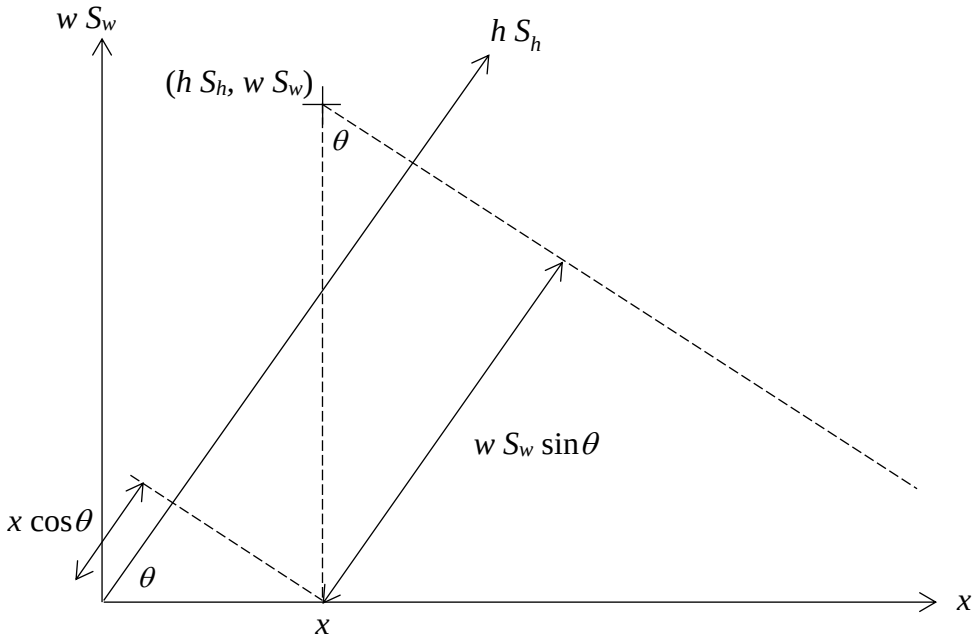

Figure A.1 Axes for plotting a psychrometric chart

Substituting Equation (A.3) into Equation (A.2),

$$x = \left(\frac{S_h}{\cos\theta}\right)\left[Cp_{da}t + w\,(Cp_s t + h_{fg,0})\right] - \left(\frac{S_w \sin\theta}{\cos\theta}\right) w$$

$$x = \left[\left(\frac{S_h}{\cos\theta}\right)\,(Cp_s t + h_{fg,0}) - \left(\frac{S_w \sin\theta}{\cos\theta}\right)\right] w + \left(\frac{S_h}{\cos\theta}\right) Cp_{da} t \qquad \text{(A.4)}$$

From Equation (A.4), w can be expressed in terms of x and t as follows:

$$w = \left[\frac{\cos\theta}{S_h(Cp_s t + h_{fg,0}) - S_w \sin\theta}\right]\left(x - \frac{S_h}{\cos\theta} Cp_{da} t\right) \qquad \text{(A.5)}$$

It can be seen from Equation (A.5) that when t is fixed at a constant value, the line corresponding to this constant temperature ($w(x)$ when t = constant) is a straight line with an inclination angle dependent on the sign and value of the expression within the square bracket. If the constant temperature line for a particular value of t is to be made a vertical straight line, then:

$$\frac{dw}{dx} = \left[\frac{\cos\theta}{S_h(Cp_s t + h_{fg,0}) - S_w \sin\theta}\right] \to \infty \qquad \text{(A.6)}$$

This requires the denominator at the right-hand side of Equation (A.6) to be equal to zero, i.e.,

$$S_h(Cp_s t + h_{fg,0}) - S_w \sin\theta = 0$$

$$\sin\theta = \frac{S_h}{S_w}\left(Cp_s t + h_{fg,0}\right) \qquad \text{(A.7)}$$

If the temperature at which the constant temperature line is vertical is 0°C, then

$$\sin\theta = \frac{S_h}{S_w} h_{fg,0}$$

When a choice has been made on the values of the two scaling factors (S_h and S_w), the inclination angle of the h-axis (θ) can be solved from Equation (A.7).

Equations (A.2) and (A.4) provide the necessary means for determining the coordinates (x, w) for state points represented by (h, w) and (t, w) respectively. Since x and w are along a pair of orthogonal axes, constant property lines that form a psychrometric chart, which are lines connecting the state points of moist air with constant values for that property, can be plotted graphically in the usual manner.

A.2.2 Constant property lines on a psychrometric chart

A.2.2.1 Constant moisture content, specific enthalpy, and temperature lines

Since moisture content is chosen as the variable along the vertical or y axis, constant moisture content lines are simply horizontal lines on a psychrometric chart.

Constant specific enthalpy lines are downward sloping straight lines passing through state points with the same values of h they represent. For each h value, the x & w relationship is described by Equation (A.2). However, as mentioned in Section 2.4.2.1, constant specific enthalpy lines are conventionally omitted on a psychrometric chart to avoid confusion, as they nearly overlap with constant wet-bulb lines.

Equation (A.4) or (A.5) can be used to determine the coordinates (x, w) for any constant temperature lines on the chart. Equations for other constant property lines can also be derived as described in the following sections.

A.2.2.2 The saturation curve

An equation for representing the saturation curve, which is the upper boundary of the chart, can be derived based on the following model given in the ASHRAE Handbook (also given as Equation (2.13) in the main text of this book):

$$\ln(P_{ws}) = \frac{C_8}{T} + C_9 + C_{10}T + C_{11}T^2 + C_{12}T^3 + C_{13}\ln(T) \qquad \text{(A.8)}$$

where

P_{ws} = saturation vapour pressure, Pa
T = absolute temperature, K (= 273.15 + t in °C)
$C_8 = -5.8002206 \times 10^3$
$C_9 = 1.3914993$
$C_{10} = 4.8640239 \times 10^{-2}$

$C_{11} = 4.1764768 \times 10^{-5}$
$C_{12} = -1.4452093 \times 10^{-8}$
$C_{13} = 6.5459673$

With Equation (A.8), the saturation vapour pressure for various temperatures can be determined, which will then allow the saturation moisture content, w_s, to be determined as follows:

$$w_s = 0.622 \frac{P_{ws}}{P_{atm} - P_{ws}} \tag{A.9}$$

Knowing w_s for a range of values of temperature t, the corresponding x values can be calculated using Equation (A.4), which will then allow the saturation curve ($w_s = w_s(x)$) to be plotted.

A.2.2.3 Constant degree of saturation lines

The degree of saturation, μ, of moist air at a specific state is the ratio of the moisture content of the moist air (w) to the saturation moisture content at the same temperature (w_s), as shown below:

$$\mu = \frac{w}{w_s}$$

And hence,

$$w = \mu \cdot w_s \tag{A.10}$$

The saturation moisture content for moist air at various temperatures can be determined using Equations (A.8) and (A.9) above, which can be combined and regarded as a function that relates w_s to t, as expressed below:

$$w_s = w_s(t)$$

For a given value of μ, the moisture content (w) corresponding to each temperature within the range of temperature to be shown on the chart can be determined using Equation (A.10). Knowing the data pair (t, w), the coordinates for the corresponding state point on the chart, i.e. (x, w), can be determined using Equation (A.4), and thus the constant degree of saturation line can be plotted.

A.2.2.4 Constant wet bulb temperature lines

Notwithstanding that the wet bulb temperature of moist air is often measured using a hygrometer, the wet bulb temperature so measured is not a thermodynamic property of the moist air, but just an approximation of the thermodynamic wet bulb temperature. The latter, derived based on a theoretical adiabatic saturation process (see Section 2.2.10 in the main text of this book), is indeed a thermodynamic property of moist air, and is therefore used here to construct a psychrometric chart.

Through heat and mass balances on an adiabatic saturation process, it can be shown that the properties of moist air (h, w) at a given thermodynamic wet bulb temperature t_{wb} (hereinafter referred to simply as wet bulb temperature), are related by the following equation (See Equation (2.42) in the main text):

$$h_{wb} = h + (w_{wb} - w)h_{f,wb} \tag{A.11}$$

Where:

w_{wb} = saturation moisture content at t_{wb}, to be evaluated using Equations (A.8) & (A.9)
h_{wb} = enthalpy of moist air saturated at t_{wb}, to be evaluated using Equation (A.3)
$h_{f,wb}$ = enthalpy of saturated liquid water at t_{wb}, = $C_f \times t_{wb}$
C_f = specific heat of water ≈ 4.18kJ/kgK.

For saturated moist air at a given value of t_{wb}, the values of w_{wb} and h_{wb} of the saturated moist air will be fixed and can be evaluated, as shown above. Equation (A.11) then provides the relation between h and w of any unsaturated air state with the wet bulb temperature t_{wb}. Together with Equation (A.2), the values of (x, w) can be evaluated for a range of w values for plotting the constant wet-bulb line on the psychrometric chart.

Alternatively, Equation (A.11) can be expanded and rearranged to as follows, such that the moist air state can be defined by t, in lieu of h, and w:

$$h_{wb} = Cp_{da}t + w(Cp_s t + h_{fg,0}) + (w_{wb} - w)h_{f,wb}$$

Solving for w from the above,

$$w = \frac{h_{wb} - Cp_{da}t - w_{wb}h_{f,wb}}{Cp_s t + h_{fg,0} - h_{f,wb}} \tag{A.12}$$

According the above explanations, w is related to t by Equation (A.12) when t_{wb} is fixed, and hence, w_{wb}, h_{wb} and $h_{f,wb}$ are all fixed. With this equation and by using a suitable range of values for t, the corresponding values of w for moist air states with wet-bulb temperature at t_{wb} can be evaluated. Based on this set of (t, w) values, one for each state of air on the constant wet-bulb temperature line for t_{wb}, Equation (A.4) can be used to construct constant web-bulb temperature lines on a psychrometric chart. By re-arranging Equation (A.11) to as follows, it becomes apparent that a constant wet-bulb line is a straight-line on a psychrometric chart.

$$h = (h_{f,wb})w - (h_{wb} - w_{wb}h_{f,wb}) \tag{A.13}$$

A.2.2.5 Constant specific volume lines

Constant specific volume (v) lines refer to lines linking up state points that have the same volume of dry air per unit mass of dry air, as shown below:

$$v = V/m_{da}$$

For a given volume, V, the mass of dry air, m_{da}, is related to this volume and other properties by the perfect gas law as follows:

$$P_{da}V = m_{da}R_{da}T$$

Where

P_{da} = partial pressure of dry air in the moist air, Pa
R_{da} = gas constant of air = 287.1 J/kgK
T = temperature in absolute scale, K

It follows that

$$v = V/m_{da} = \frac{R_{da}T}{P_{da}} \quad \text{(A.14)}$$

The partial pressure of dry air in moist air is related to the partial vapour pressure (P_w) and moisture content (w) as shown below:

$$P_{da} = P_{atm} - P_w \quad \text{(A.15)}$$

$$w = 0.622\frac{P_w}{P_{atm}-P_w} \quad \text{(A.16)}$$

Given a moisture content value, the partial vapour pressure can be solved from Equation (A.16), as follows:

$$P_w = \frac{wP_{atm}}{0.622+w} \quad \text{(A.17)}$$

Using Equation (A.15),

$$P_{da} = \frac{0.622P_{atm}}{0.622+w} \quad \text{(A.18)}$$

Substituting Equation (A.18) into (A.14),

$$v = \frac{0.622+w}{0.622P_{atm}}R_{da}(t + 273.15)$$

Solving for t from above,

$$t = \frac{0.622P_{atm}v}{(0.622+w)R_{da}} - 273.15 \quad \text{(A.19)}$$

With Equations (A.19) and (A.4), constant specific volume lines can be constructed on a psychrometric chart.

The constant specific volume lines are, in fact, non-linear, although they appear to be straight lines on a psychrometric chart, as shown below.

Let

$$H = \frac{S_h}{cos\theta}$$

$$W = \frac{S_w sin\theta}{cos\theta}$$

Equation (A.4), can be re-written to as follows:

$$x = \left[HCp_s t + Hh_{fg,0} - W\right]w + HCp_{da}t$$

Recognizing that H & W are constants and Cp_s, $h_{fg,0}$ and Cp_{da} may also be regarded as constants, the above equation is further simplified by the use of three constant terms, H_1, H_2 & H_3, as follows:

$$x = [H_1 t + H_2]w + H_3 t \qquad \text{(A.20)}$$

Also let

$$Q = \frac{0.622 P_{atm} v}{R_{da}}$$

And Q is also a constant when v is fixed. Equation (A.19), can be re-written to as follows:

$$t = \frac{Q}{(0.622+w)} - 273.15$$

Substituting the above into Equation (A.20),

$$x = \left[H_1\left(\frac{Q}{(0.622+w)} - 273.15\right) + H_2\right] w + H_3\left(\frac{Q}{(0.622+w)} - 273.15\right) \qquad \text{(A.21)}$$

If we express Equation (A.21) as:

$$x = a\, w + b$$

The constant specific volume lines would have been straight lines if both a and b in the above equation are constants. However, by inspecting the terms in Equation (A.21) that are represented by a and b, it can be seen that both of them will vary with w, and therefore, the constant specific volume lines are in fact non-linear. Nevertheless, numerical calculations show that over the range of moisture content from 0 to 0.03 kg/kg, the constant specific volume lines may, for practical applications, be regarded as near to linear.

A.2.3 Example chart

On the basis of the equations summarised above, a sample psychrometric chart has been plotted using an Excel Workbook, as shown in Figure A.2.

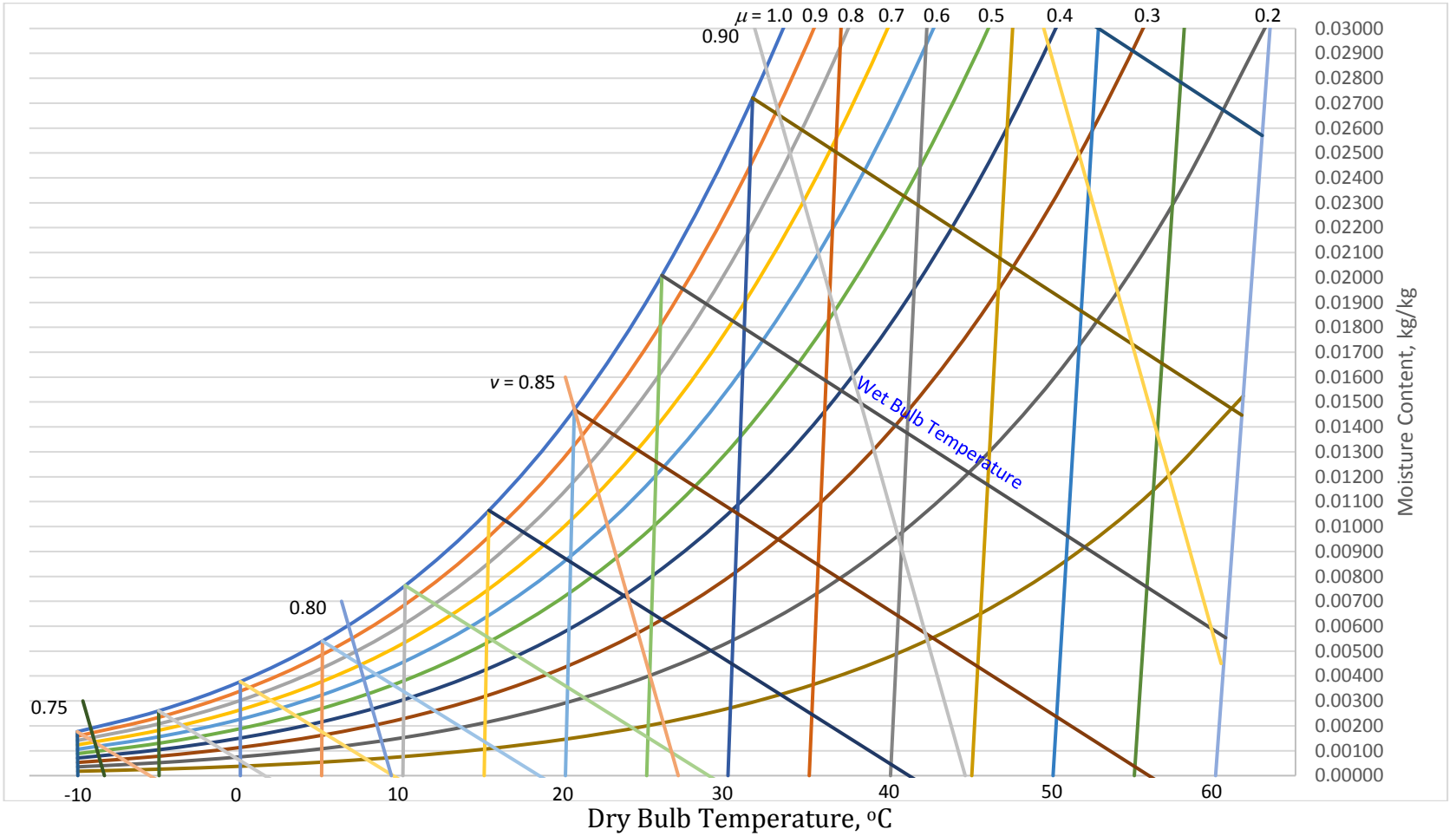

Figure A.2 Example Psychrometric Chart Plotted Using an Excel Workbook

The constant dry bulb, constant wet bulb, constant degree of saturation and constant specific volume lines that make up the psychrometric chart in Figure A.2 were plotted based on the following length scales for representing specific enthalpy and moisture content values in the chart, and with the constant temperature line at zero degree centigrade made a vertical straight-line:

S_h	0.01
S_w	33
θ (Deg)	49.278
Sin θ	0.758
Cos θ	0.652

The constant property lines were plotted in the chart at constant values at intervals within the ranges as summarized below:

- Constant temperature lines from -10°C to 60°C, at 5-degree intervals;
- Constant degree of saturation lines from 10 to 100%, at 10% intervals;
- Constant wet bulb temperature lines from -10°C to 35°C, at 5-degree intervals; and
- Constant specific volume lines from 0.75 to 0.95 m^3/kg, at 0.05 m^3/kg intervals.

A.3 Psychrometric property calculations

It can be seen that the psychrometric chart constructed, as described above and shown in Figure A.2, is with such coarse subdivisions that it cannot provide accurate enough values for moist air properties as could a standard chart from either CIBSE or ASHRAE. Furthermore, no scales for specific enthalpy have been plotted on the chart.

Although the subdivisions can be refined, and scales for specific enthalpy may be added, the chart can serve at best just the same function as a printed chart. Alternatively, routines can be developed for evaluating psychrometric properties of moist air at a given state point, as defined by two of its properties, and the routines can be made available in conjunction with the chart. The methods and equations involved are discussed in detail in the following.

A.3.1 Known properties for calculation of other properties

The following lists the moist air properties that may be encountered in psychrometric analyses:

1. Specific enthalpy, h (kJ/kg)
2. Moisture content, w (kg/kg)
3. Dry bulb temperature, t (°C)
4. Wet bulb temperature, t_{wb} (°C)
5. Dew point temperature, t_{dp} (°C)
6. Relative humidity, ϕ
7. Degree of saturation, μ
8. Specific volume, v (m^3/kg)

9. Water vapour pressure, P_w (Pa)

A psychrometric property calculation tool should be capable of evaluating all properties of moist air when values are given for any two of the properties that can define the state of the moist air (assuming the total pressure of moist air is fixed at one standard atmospheric pressure, i.e. $P_a = P_{atm}$). However, not all possible combinations of any two among the properties listed above need to be catered for, because some combinations may be ruled out as explained below:

1. Moisture content w, dew point temperature t_{dp} and water vapour pressure P_w are alternative properties – when any one of them is fixed, the other two will also be fixed even if the moist air state has yet to be defined by an extra property. Therefore, the two known properties for determination of other properties of moist air cannot be both from this set of properties.

2. Although relative humidity ϕ and degree of saturation μ are, strictly speaking, not alternative properties (determination of one from the other requires knowledge about the moist air state), they are typically treated as alternative properties or used as the same property. Hence, the two known properties may comprise either ϕ or μ but not both.

3. In practical applications, water vapour pressure P_w and specific volume v are seldom known properties. More often, they are evaluated as an intermediate result for other calculations (e.g. v is needed in calculations involving volume flow rate of the moist air).

4. Furthermore, specific enthalpy h and wet-bulb temperature t_{wb} are not a good combination of known properties for determination of the other unknown properties because the accuracy of the results is highly sensitive to the accuracy of these properties, as minute changes in the value of one will lead to significant changes in the moist air state and thus in the values of the other properties.

In the light of the above considerations, methods are presented for determination of moist air properties from given values only for the combinations of properties listed in Table A.1.

Furthermore, because specific enthalpy (h) and moisture content (w) are the two properties that are needed for determining the heat and moisture gain or loss in a psychrometric process, and they are also the calculation results from heat and mass balance calculations, h and w are selected as the 'pivotal' variables in the development of psychrometric calculation routines. This means that the program will first evaluate h and/or w when none or only one of them, are with given values, while routines for evaluation of other properties would all start from known values of h and w. Additionally, calculation routines should be made available for conversion of values of t_{dp} and P_w to w, and vice versa. The following describes the methods to be used for the psychrometric calculations.

Table A.1 Combinations of known properties as input for calculation of other properties

No.	Properties	No.	Properties
1 - 3	h, w (or t_{dp} or P_w)	12	t, μ
4	h, t	13 - 15	w (or t_{dp} or P_w), t_{wb}
5	h, ϕ	16 - 18	w (or t_{dp} or P_w), ϕ
6	h, μ	19 - 21	w (or t_{dp} or P_w), μ
7 - 9	t, w (or t_{dp} or P_w)	22.	t_{wb}, ϕ
10	t, t_{wb}	23.	t_{wb}, μ
11	t, ϕ		

A.3.2 Psychrometric calculation methods

A.3.2.1 Evaluation of moisture content, vapour pressure and dew point given the value of anyone

Equations (A.8) and (A.9) can be used to determine moisture content (w) from a known value of water vapour pressure (P_w) or dew point temperature (t_{dp}). When w is known instead, P_w can be evaluated by using Equation (A.17). However, evaluation of t_{dp} from a known value of w is more complicated, as this involves solving for T in Equation (A.8), which is a non-linear equation and needs to be dealt with by using a numerical method. The method devised for this purpose is summarised in Annex A.I.

A.3.2.2 Evaluation of moisture content and/or enthalpy given other properties

The following summarises the methods for evaluation of w or h given different combinations of psychrometric properties.

a) With h being one of the given properties

a.1) When h and t are given, w may be evaluated from the following equation, which can be derived directly from the definition of h (Equation A.3):

$$w = \frac{h - Cp_{da} t}{Cp_s t + h_{fg,0}} \qquad \text{(A.22)}$$

a.2) When h and ϕ are given, evaluation of w requires an iterative procedure as shown in Annex A.II.

a.3) With minor modifications to the method shown in Annex A.II, as described below, it will be applicable to evaluation of w, when h and μ are the given properties.

After evaluating the saturation vapour pressure (P_{wsi}) for a temperature t_i, where $i = 0$, 1 or 2, the corresponding saturation moisture content (w_{si}) is evaluated. The moisture content (w_i) at t_i and μ may then be evaluated as follows:

$$w_i = \mu\, w_{si} \tag{A.23}$$

The specific enthalpy h_i can be determined from t_i and w_i by using the equation that defines specific enthalpy (Equation A.3). The other steps for correcting the temperature estimate will remain the same.

b) With t being one of the given properties

b.1) When t and w are given, h can be determined in a straightforward manner, as

$$h = Cp_{da}t + w(Cp_s t + h_{fg,0}) \tag{A.24}$$

b.2) When t and t_{wb} are given, h and w can be determined as follows:

The saturation vapour pressure (P_{wb}) corresponding to the wet bulb temperature is first calculated, using Equation (A.8). Following this, the corresponding saturation moisture content (w_{wb}), saturation specific enthalpy (h_{wb}) and saturation liquid water enthalpy ($h_{f,wb}$) can be determined as follows:

$$w_{wb} = 0.622\frac{P_{wb}}{P_{atm}-P_{wb}} \tag{A.25}$$

$$h_{wb} = Cp_{da}t_{wb} + w_{wb}(Cp_s t_{wb} + h_{fg,0}) \tag{A.26}$$

$$h_{f,wb} = 4.18 \cdot t_{wb} \tag{A.27}$$

Equation (A.12), shown again as Equation (A.28) below, may then be used to evaluate w.

$$w = \frac{h_{wb}-Cp_{da}t-w_{wb}h_{f,wb}}{Cp_s t+h_{fg,0}-h_{f,wb}} \tag{A.28}$$

Knowing t and w, h can be evaluated by using the definition of specific enthalpy, as shown in Equation (A.24).

b.3) When t and ϕ are given, the saturation vapour pressure (P_{ws}) at t can be calculated first using Equation (A.8). The vapour pressure (P_w) at t and ϕ will then be:

$$P_w = \phi\, P_{ws}$$

Knowing P_w allows w to be calculated, which can then be used in conjunction with t to calculate h.

b.4) When t and μ are given, the saturation vapour pressure (P_{ws}) at t can be calculated first using Equation (A.8). The saturation moisture content (w_s) can

then be determined, which will then allow w to be determined ($w = \mu\, w_s$). The specific enthalpy (h) can also be determined based on w and t (Equation (A.24)).

c) With w being one of the given properties

c.1) When w and t_{wb} are the known properties, h can be determined using the following method.

When the value of t_{wb} is given, the values of h_{wb}, w_{wb} and $h_{f,wb}$ can be determined using Equations (A.25) to (A.27), and P_{wb} in Equations (A.25) can be determined using Equation (A.8).

Since $h_{wb} = h + (w_{wb} - w)h_{f,wb}$,

$$h = h_{wb} - (w_{wb} - w)h_{f,wb} \qquad \text{(A.29)}$$

c.2) When w and ϕ are given, an iterative procedure similar to that shown in Annex A.II is needed for evaluation of h. The procedures include:

i) Assume two temperatures, t_0 and t_1.

ii) Determine the saturation vapour pressures P_{ws0} and P_{ws1} corresponding respectively to the two temperatures.

iii) Evaluate the respective vapour pressures P_{w0} ($= \phi\, P_{ws0}$) and P_{w1} ($= \phi\, P_{ws1}$), and then the moisture contents w_0 and w_1 corresponding to P_{w0} and P_{w1}.

iv) Determine the temperature correction Δt by:

$$\Delta t = \frac{w_1 - w}{w_0 - w_1}(t_0 - t_1) \qquad \text{(A.30)}$$

v) Determine improved estimate of t (t_2) by:

$$t_2 = t_1 - \Delta t$$

vi) Based on t_2, evaluate P_{ws2}, P_{w2} and then w_2

v) Compare the value of w_2 with the given value for w. If the deviation is larger than the tolerable limit, swap the values for the variables as follows:

$t_0 = t_1$ and $w_0 = w_1$

$t_1 = t_2$ and $w_1 = w_2$

vi) Repeat from step iii) until a converged solution for w is found. The resultant values of t can then be used in conjunction with w to determine h.

c.3) When w and μ are given, the above iterative procedure can be modified in the same way as described in b.4) above for evaluation of h.

d) With t_{wb} being one of the given properties

d.1) The methods for evaluating w and h from known values of t_{wb} and ϕ, are shown in Annex A.III.

d.2) The methods for evaluating w and h with t_{wb} and μ being the known inputs are given in Annex A.IV.

A.3.2.3 Evaluation of properties from given specific enthalpy and moisture content values

For given values of specific enthalpy (h) and moisture content (w), the other psychrometric properties of the moist air can be determined using the methods described below.

a) Temperature, t

$$t = \frac{h - w h_{fg,0}}{Cp_d + w Cp_s} \quad \text{(A.31)}$$

b) Vapour pressure, P_w

$$P_w = \frac{w P_{atm}}{0.622 + w} \quad \text{(A.32)}$$

c) Relative humidity, ϕ

First evaluate t using Equation (A.31) and P_w using Equation (A.32). The saturation vapour pressure P_{ws} at t can then be evaluated using Equation (A.8). By definition:

$$\phi = \frac{P_w}{P_{ws}} \quad \text{(A.33)}$$

d) Degree of saturation, μ

First evaluate t using Equation (A.31) and the saturation vapour pressure P_{ws} at t using Equation (A.8). Then evaluate w_s from:

$$w_s = 0.622 \frac{P_{ws}}{P_{atm} - P_{ws}}$$

By definition:

$$\mu = \frac{w}{w_s} \quad \text{(A.34)}$$

e) Wet bulb temperature, t_{wb}

The method is described in Annex A.V.

f) Dew point temperature, t_{dp}

The method is described in Annex A.I.

g) Specific volume, v

First evaluate t using Equation (A.31). Then,

$$v = \frac{0.622+w}{0.622P_{atm}} R_{da}(273.15 + t) \quad \text{(A.35)}$$

A.4 Evaluation of the supply air state in the space air-conditioning processes

Evaluation of the heat and mass transfers involved in the following standard psychrometric processes has been covered in Chapter 2:

Sensible heating
Sensible cooling
Cooling and dehumidification
Heating and humidification (space air-conditioning)
Adiabatic saturation

Here, focus is put on the space air-conditioning process with a given sensible heat ratio, which is a key component of the conventional all air cycle and, in turn, the starting point of air-conditioning system design. A graphical method is described in Chapter 2 for finding the leaving coil and supply air states simultaneously on a psychrometric chart. The following outlines a numerical method for the same purpose.

Let:

(h_R, w_R) be the room air state
(h_{SA}, w_{SA}) be the supply air state
(h_L, w_L) be the leaving coil air state
γ = ratio of room sensible to latent load
μ_L = degree of saturation of leaving coil air (fixed)

Because the process that brings the air from the leaving coil state to the supply air state is a sensible heating process:

$$w_{SA} = w_L$$

$$t_{SA} - t_L = \Delta t_F$$

Where Δt_F is the temperature rise due to fan heat gain, which is assumed to be known and fixed.

Expressing the specific enthalpies of the room air and supply air states in terms of temperature and moisture content:

$$h_R = Cp_{da}t_R + w_R\left(Cp_s t_R + h_{fg,0}\right) \tag{A.36}$$

$$h_{SA} = Cp_{da}t_{SA} + w_{SA}\left(Cp_s t_{SA} + h_{fg,0}\right) \tag{A.37}$$

The total room cooling load is proportional to the difference in specific enthalpy of the room air and the supply air states, as given below:

$$h_R - h_{SA} = Cp_{da}(t_R - t_{SA}) + Cp_s(w_R t_R - w_{SA}t_{SA}) + (w_R - w_{SA})h_{fg,0} \tag{A.38}$$

At the right-hand side of Equation (A.38), the sum of the first and the second term represents the room sensible heat and the last term represents the room latent heat absorbed by each kg/s of the supply air.

It follows that the ratio of room sensible load to the room latent load, γ, is given by:

$$\gamma = \frac{Cp_{da}(t_R - t_{SA}) + Cp_s(w_R t_R - w_{SA}t_{SA})}{(w_R - w_{SA})h_{fg,0}} \tag{A.39}$$

By re-arranging Equation (A.39) and expanding the terms, we get:

$$\gamma h_{fg,0}w_R - \gamma h_{fg,0}w_{SA} = Cp_{da}t_R - Cp_{da}t_{SA} + Cp_s w_R t_R - Cp_s w_{SA}t_{SA}$$

Further manipulation of the above yields

$$Cp_{da}t_{SA} + Cp_s w_{SA}t_{SA} - \gamma h_{fg,0}w_{SA} = Cp_{da}t_R + Cp_s w_R t_R - \gamma h_{fg,0}w_R \tag{A.40}$$

$$Cp_{da}t_{SA} + w_{SA}(Cp_s t_{SA} + h_{fg,0}) - (1+\gamma)h_{fg,0}w_{SA} = Cp_{da}t_R + w_R(Cp_s t_R + h_{fg,0}) - (1+\gamma)h_{fg,0}w_R$$

And finally,

$$h_{SA} - (1+\gamma)h_{fg,0}w_{SA} - \left[h_R - (1+\gamma)h_{fg,0}w_R\right] = 0 \tag{A.41}$$

It can be seen from Equation (A.41) that with either the room air state (h_R, w_R) or the supply air state (h_{SA}, w_{SA}) fixed:

i) the other state point lines on a straight line passing through the fixed state; and

ii) the slope of the line is governed by the room sensible heat ratio γ.

Additional psychrometric relations that need to be employed include Equations (A.8), (A.9) and the following:

$$w = \mu w_s \tag{A.42}$$

For the problem at hand,

$$w_L = w_{SA} = \mu_L w_{s,L} \tag{A.43}$$

Where $w_{s.L}$ is the saturated air moisture content at the leaving coil air temperature. Furthermore,

$$t_{SA} = t_L + \Delta t_F \tag{A.44}$$

From Equation (A.40), replacing w_{SA} by $\mu_L w_{s,L}$, and t_{SA} by $t_L + \Delta t_F$, yields:

$$Cp_{da}(t_L + \Delta t_F) + \mu_L\left[Cp_s w_{s,L}(t_L + \Delta t_F) - \gamma h_{fg,0} w_{s,L}\right] - (Cp_{da} t_R + Cp_s w_R t_R - \gamma h_{fg,0} w_R) = 0 \tag{A.45}$$

Note that the leaving coil temperature, t_L, is the only unknown in Equation (A.45), as all other parameters can either be evaluated from this temperature or have fixed values. The equation is therefore readily solvable using a numerical method.

Denoting Equation (A.45) as:

$$f(t_L) = 0 \tag{A.46}$$

The unknown t_L can be solve by first making two estimates of t_L, denoted by t_{L0} and t_{L1}. The correction, Δt_L, for improving the estimate can be evaluated by:

$$\Delta t_L = \frac{f(t_{L1})}{f(t_{L0}) - f(t_{L1})}(t_{L0} - t_{L1}) \tag{A.47}$$

If Δt_L exceeds the tolerable inaccuracy, the following steps can be taken to further improve the estimate:

$t_{L2} = t_{L1} - \Delta t_L$

$t_{L0} = t_{L1}$ and $t_{L1} = t_{L2}$

Use Equation (A.47) to determine the correction again. The steps are to be repeated until Δt_L approaches zero.

Annex A.I A method for solving saturation temperature from a known value of moisture content

Equation (A.8) in the main text is a mathematical expression that allows the saturation water vapour pressure (P_{ws}) to be evaluated for a given temperature (t), which has been used to construct the saturation curve in the example psychrometric chart shown in Figure A.2. Equation (A.9) can then be used to evaluate the corresponding saturation moisture content (w_s). However, if t is unknown and is to be evaluated from a given value of moisture content, a numerical method is required. The following describes one for this purpose.

The method involves iterative calculations that begin with an initial estimate of the temperature (t_0), as shown in Figure A.I.a. For this temperature, the saturation moisture content (w_0) can be calculated using Equations (A.8) and (A.9).

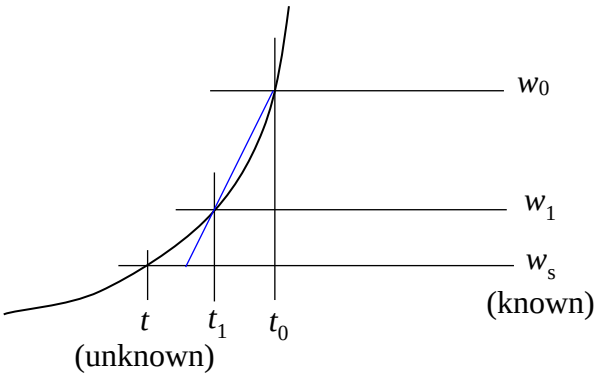

Figure A.I.a Numerical estimation of the temperature corresponding to a given saturation moisture content ($t_0 < t$)

An initial estimate of the correction to be applied to the estimated temperature (Δt) is to be made also, to provide a better estimate of the temperature t, denoted as t_1, as follows:

$$t_1 = t_0 - \Delta t \qquad \text{(A.I.1)}$$

Note that if w_0 is greater than w_s (the given moisture content), the initial value to be assigned to Δt should be a positive value; a negative value is to be used otherwise.

The saturation moisture content, w_1, corresponding to the newly estimated temperature can also be determined using Equations (A.8) and (A.9). If w_1 differs from w_s by an amount (ε; $\varepsilon = w_1 - w_s$) that is beyond the acceptable error limit, a further step of numerical calculation will be needed. For this new step, the temperature correction (Δt; $\Delta t = t_1 - t_2$, where t_2 is a better estimate to be determined in this new step) is to be determined as follows:

$$\frac{\Delta t}{w_1 - w_s} = \frac{t_0 - t_1}{w_0 - w_1}$$

$$\Delta t = \frac{w_1 - w_s}{w_0 - w_1}(t_0 - t_1) \qquad \text{(A.I.2)}$$

Then,

$$t_2 = t_1 - \Delta t \qquad \text{(A.I.3)}$$

The saturation moisture content corresponding to t_2 (w_2) should then be determined and compared with the given value (w_s). If the error (ε; $\varepsilon = w_2 - w_s$) is still beyond acceptable limit, the following change of variables should be made:

$t_0 = t_1$ and $w_0 = w_1$

$t_1 = t_2$ and $w_1 = w_2$

Equation (A.I.2) may then be used again to provide a better estimate of the temperature correction (Δt) required, and the calculation step needs to be repeated. This iterative procedure should continue until the error becomes smaller than the acceptable maximum limit.

Although the initial estimate for t_0 was shown in Figure A.I.a to be higher than the unknown value of t, this is not a necessary condition of the calculation routine. As shown in Figure A.I.b, the algorithm will also work if t_0 is lower than the unknown value of t.

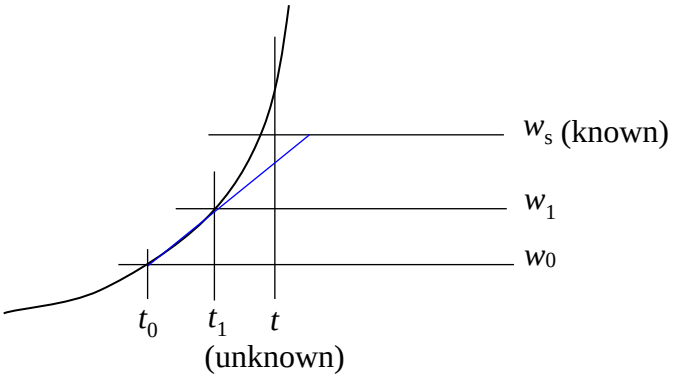

Figure A.I.b Numerical estimation of the temperature corresponding to a given saturation moisture content ($t_0 < t$)

Annex A.II A method for solving w from known values of h & ϕ

The method devised for solving for moisture content from known values of specific enthalpy (h) and relative humidity (ϕ) begins with two assumed temperature values t_0 and t_1. Based on t_0, the saturation vapour pressure at this temperature, P_{ws0}, can be calculated using Equation (A.8). The vapour pressure (P_{w0}) of moist air at t_0 and ϕ, and the corresponding values of moisture content (w_0) and specific enthalpy (h_0), can then be calculated as follows:

$$P_{w0} = \phi\, P_{ws0}$$

$$w_0 = 0.622 \frac{P_{w0}}{P_{atm} - P_{w0}}$$

$$h_0 = Cp_{da} t_0 + w_0 (Cp_s t_0 + h_{fg,0})$$

If h_0 is greater than the known value of h, then, t_1 should be assigned with a value smaller than t_0, and vice versa. The difference between these two temperatures ($t_0 - t_1$) is arbitrary in the first iterative step. The saturation vapour pressure (P_{ws1}) at t_1, and then the moisture content (w_1) and the specific enthalpy (h_1) at t_1 and ϕ, can also be determined in the same manner. Figure A.II shows the relations among these state points on a psychrometric chart.

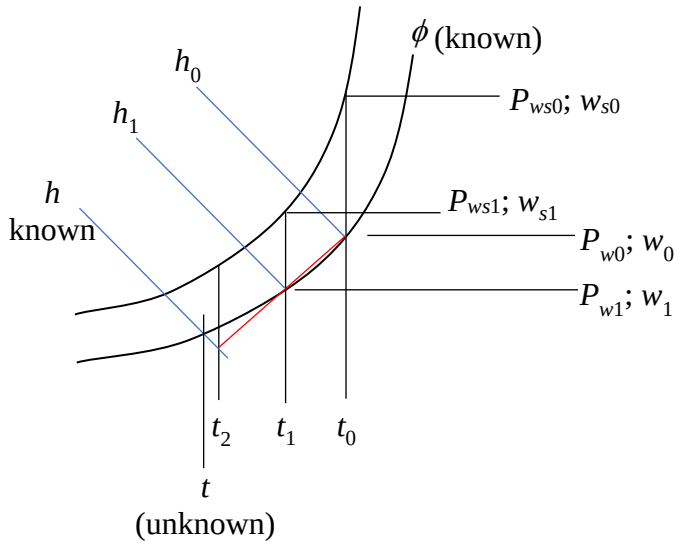

Figure A.II Numerical estimation of the temperature and moisture content of a moist air given its specific enthalpy and relative humidity

The correction to the temperature estimate, Δt, can then be determined as follows:

$$\Delta t = \frac{h_1 - h}{h_0 - h_1}(t_0 - t_1) \qquad \text{(A.II.1)}$$

Then, a better estimate for t (t_2) will be made as follows:

$$t_2 = t_1 - \Delta t \qquad \text{(A.II.2)}$$

The saturation vapour pressure (P_{ws2}) at t_2, and then the moisture content (w_2) and specific enthalpy (h_2) at t_2 and ϕ can be determined using the same method as discussed above. The value of h_2 may now be compared with the given value of h. If the error (ε; $\varepsilon = h_2 - h$) is beyond acceptable limit, the values for the following variables should be swapped:

$t_0 = t_1$ and $h_0 = h_1$

$t_1 = t_2$ and $h_1 = h_2$

Equation (A.II.1) can then be used again to provide a better estimate of the temperature correction (Δt) required, and the calculation step should be repeated. This iterative procedure should continue until the error becomes smaller than the acceptable maximum limit. When a converged solution is obtained, both w and t would have been evaluated for the given h and ϕ values.

Annex A.III A method for solving h & w from known values of t_{wb} & ϕ

Equations (A.8) and (A.25) to (A.27) are to be used first to evaluate the vapour pressure (P_{wb}), moisture content (w_{wb}) and specific enthalpy (h_{wb}) of saturated moist air at the given wet bulb temperature (t_{wb}), and the saturated liquid water specific enthalpy ($h_{f,wb}$) at the same temperature. Equation (A.III.1), adapted from Equation (A.28), can then be used to relate the moisture content (w_i') to the temperature (t_i) of moist air at the same wet bulb temperature (t_{wb}).

$$w_i' = \frac{h_{wb} - cp_{da} t_i - w_{wb} h_{f,wb}}{cp_s t_i + h_{fg,0} - h_{f,wb}} \qquad \text{(A.III.1)}$$

Similar to the numerical solution scheme shown in Annex A.II, this numerical method also begins with using two assumed temperatures t_0 and t_1.

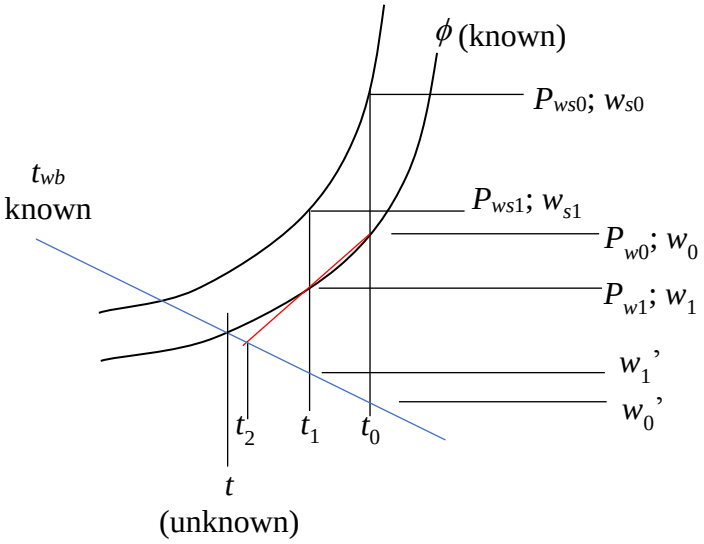

Figure A.III Numerical estimation of the temperature and moisture content of a moist air given its wet bulb temperature and relative humidity

For each of the assumed temperatures, two moisture contents (w_i and w_i'; $i = 0$ and 1) are calculated; w_i from ϕ and P_{wsi} and w_i' from Equation (A.III.1). The two moisture contents for a given temperature should equal each other if the temperature is the temperature of the moist air at the given state. If this is not the case, the temperature correction (Δt) for providing a better estimate will be determined based on the following:

$$\frac{\Delta t}{\Delta t + (t_0 - t_1)} = \frac{w_1 - w_1'}{w_0 - w_0'}$$

It follows that

$$\Delta t = \frac{w_1 - w_1'}{(w_0 - w_{0)}' - (w_1 - w_1')} (t_0 - t_1) \qquad \text{(A.III.2)}$$

The better temperature estimate (t_2) can now be determined from:

$$t_2 = t_1 - \quad t \tag{A.III.3}$$

The following swapping of values for variables should then be performed:

$w_0 = w_1$ and $w_0' = w_1'$

$t_0 = t_1$ and $t_1 = t_2$

The moisture contents w_1 and w_1' should then be re-evaluated, followed by re-evaluation of Δt (using Equation (A.III.2)). If t exceeds zero by more than an acceptable limit, the value swapping and re-evaluation procedures should be repeated until the value of Δt becomes small enough. When this is achieved, the moisture content w and temperature t for the given moist air state are solved, which can then be used to compute h, using the definition of h.

Annex A.IV A method for solving h & w from known values of t_{wb} & μ

Nearly the same procedure as described in Annex A.III can be used for solving h & w from known values of t_{wb} & μ, except that evaluation of w_0 and w_1 are by scaling down the saturation moisture contents at the corresponding temperatures, w_{s0} and w_{s1}, by using the given degree of saturation. Equation (A.III.1) can still be used to relate the moisture content (w_i') to the temperature (t_i) of moist air at the same wet bulb temperature (t_{wb}).

Annex A.V A method for solving t_{wb} from known values of h & w

With given values for h and w, the dry bulb temperature t can be computed first by using Equation (A.31).

The numerical method begins with two estimated values for the wet bulb temperature, t_{wb0} and t_{wb1}. For each assumed value (t_{wbi}; $i = 0$ or 1), Equations (A.8) and (A.25) to (A.27) can be used to evaluate the vapour pressure (P_{wbi}), moisture content (w_{wbi}) and specific enthalpy (h_{wbi}) for moist air saturated at the assumed wet bulb temperature value, and the saturated liquid water specific enthalpy ($h_{f,wbi}$) at the same assumed temperature (see description in Annex A.III).

Equation (A.V.1) can then be used to compute the moisture content (w_i) corresponding to the dry bulb temperature t computed above (for the given combination of h & w), and at the assumed wet bulb temperature (t_{wbi}).

$$w_i = \frac{h_{wbi} - Cp_{da}t - w_{wbi}h_{f,wbi}}{Cp_s t + h_{fg,0} - h_{f,wbi}} \qquad \text{(A.V.1)}$$

The temperature correction, Δt_{wb}, for improving the estimate is computed using:

$$\Delta t_{wb} = \frac{w_1 - w}{w_0 - w_1}(t_{wb0} - t_{wb1}) \qquad \text{(A.V.2)}$$

The better estimate is calculated from:

$$t_{wb2} = t_{wb1} - \Delta t_{wb} \qquad \text{(A.V.3)}$$

If the value of Δt_{wb} so computed deviates from zero by an amount exceeding the tolerable limit, swapping of values for the variables as follows will be made:

$t_{wb0} = t_{wb1}$ and $t_{wb1} = t_{wb2}$

$w_0 = w_1$

The moisture content w_1 will be re-evaluated using Equation (A.V.1) together with values of w_{wb1}, h_{wb1}, and $h_{f,wb1}$ evaluated from the updated wet bulb temperature (= t_{wb1} after swapping). The temperature correction, Δt_{wb}, will be re-evaluated and checked if it is close enough to zero. The steps will be repeated until Δt_{wb} approaches zero at which time the wet bulb temperature is solved.

Appendix B Data for Building Cooling Load Calculation

This appendix comprises a series of tables that provide the necessary data for design cooling load calculations for buildings in Hong Kong. The data include:

B.1 Summary Weather Data of Hong Kong from ASHRAE

B.2 Clear Sky Total Solar Irradiance Upon Vertical and Horizontal Surfaces (Jun. to Dec.)

B.3 Incident Angles (Degree) of Direct Solar Radiation upon Surfaces Facing Principle Directions (Jun. to Dec.)

B.4.1 Solar Heat Gain Factors for Transmitted Solar Heat Gain (Jun. to Dec.)

B.4.2 Solar Heat Gain Factors for Absorbed Solar Heat Gain (Jun. to Dec.)

B.1 Summary Weather Data of Hong Kong from ASHRAE

2009 ASHRAE Handbook - Fundamentals (SI)

HONG KONG OBSERVATO, China WMO#: **450050**

Lat: **22.30N** Long: **114.17E** Elev: **62** StdP: **100.58** Time Zone: **8.00 (CHN)** Period: **82-92** WBAN: **99999**

Annual Heating and Humidification Design Conditions

Coldest Month	Heating DB		Humidification DP/MCDB and HR						Coldest month WS/MCDB				MCWS/PCWD to 99.6% DB	
	99.6%	99%	99.6%			99%			0.4%		1%			
			DP	HR	MCDB	DP	HR	MCDB	WS	MCDB	WS	MCDB	MCWS	PCWD
2	**9.6**	**10.9**	**-1.1**	**3.5**	**13.0**	**1.8**	**4.3**	**14.0**	**9.2**	**15.9**	**8.4**	**15.8**	**2.2**	**10**

Annual Cooling, Dehumidification, and Enthalpy Design Conditions

Hottest Month	Hottest Month DB Range	Cooling DB/MCWB						Evaporation WB/MCDB						MCWS/PCWD to 0.4% DB	
		0.4%		1%		2%		0.4%		1%		2%			
		DB	MCWB	DB	MCWB	DB	MCWB	WB	MCDB	WB	MCDB	WB	MCDB	MCWS	PCWD
7	**3.5**	**32.2**	**26.5**	**31.7**	**26.4**	**31.2**	**26.3**	**27.4**	**30.5**	**27.1**	**30.1**	**26.9**	**29.9**	**3.4**	**270**

Dehumidification DP/MCDB and HR									Enthalpy/MCDB						Hours
0.4%			1%			2%			0.4%		1%		2%		8 to 4 &
DP	HR	MCDB	DP	HR	MCDB	DP	HR	MCDB	Enth	MCDB	Enth	MCDB	Enth	MCDB	12.8/20.6
26.6	**22.3**	**29.3**	**26.2**	**21.8**	**29.1**	**26.1**	**21.6**	**29.0**	**87.5**	**30.6**	**86.4**	**30.3**	**85.3**	**30.1**	**970**

Extreme Annual Design Conditions

Extreme Annual WS			Extreme Max	Extreme Annual DB				n-Year Return Period Values of Extreme DB							
				Mean		Standard deviation		n=5 years		n=10 years		n=20 years		n=50 years	
1%	2.5%	5%	WB	Min	Max	Min	Max	Min	Max	Min	Max	Min	Max	Min	Max
8.6	**7.4**	**6.5**	**28.4**	**7.6**	**33.5**	**1.7**	**0.3**	**6.3**	**33.7**	**5.3**	**33.9**	**4.4**	**34.1**	**3.1**	**34.4**

B.1 Summary Weather Data of Hong Kong from ASHRAE (Cont'd)

Monthly Climatic Design Conditions

			Annual	Jan	Feb	Mar	Apr	May	Jun	Jul	Aug	Sep	Oct	Nov	Dec
Temperatures, Degree-Days and Degree-Hours	Tavg		23.1	16.2	16.1	18.5	21.9	25.8	27.9	29.0	28.8	27.8	25.5	21.7	17.6
	Sd			2.37	2.57	3.33	2.70	2.01	1.70	1.29	1.27	1.50	1.85	2.49	2.85
	HDD10.0		2	1	0	1	0	0	0	0	0	0	0	0	1
	HDD18.3		237	72	71	39	3	0	0	0	0	0	0	4	46
	CDD10.0		4782	192	171	264	357	489	538	588	581	534	481	350	236
	CDD18.3		1976	6	8	46	111	231	288	330	323	284	223	104	23
	CDH23.3		18618	0	1	79	436	1826	3226	4110	3924	3126	1657	228	5
	CDH26.7		5853	0	0	0	31	366	1081	1696	1521	957	200	3	0
Monthly Design Dry Bulb and Mean Coincident Wet Bulb Temperatures	0.4%	DB		22.1	23.1	26.0	28.6	31.2	32.2	33.0	32.9	32.5	30.6	26.9	24.0
		MCWB		18.5	19.8	22.7	24.3	26.2	26.5	26.8	26.6	25.6	25.2	21.9	19.3
	2%	DB		20.9	21.9	25.1	27.6	30.2	31.5	32.2	32.1	31.5	29.3	26.0	22.6
		MCWB		17.5	19.3	22.6	24.2	26.0	26.6	26.7	26.6	25.8	24.6	21.7	18.1
	5%	DB		20.0	20.7	24.3	26.7	29.4	30.9	31.6	31.5	30.8	28.5	25.2	21.7
		MCWB		16.9	18.4	22.2	23.8	25.7	26.5	26.6	26.5	25.7	24.2	21.4	17.6
	10%	DB		19.1	19.6	23.3	26.0	28.6	30.3	31.1	31.0	30.1	27.7	24.7	21.0
		MCWB		16.2	17.4	21.4	23.6	25.4	26.4	26.4	26.4	25.5	23.8	21.1	17.2
Monthly Design Wet Bulb and Mean Coincident Dry Bulb Temperatures	0.4%	WB		19.5	21.1	23.6	25.3	26.9	27.7	27.7	27.7	27.3	26.2	23.9	20.1
		MCDB		21.0	22.4	25.2	27.1	29.8	30.6	30.9	31.1	30.3	28.9	25.6	22.6
	2%	WB		18.5	19.9	23.1	24.6	26.5	27.2	27.3	27.2	26.9	25.6	23.0	19.4
		MCDB		20.2	21.5	24.7	26.6	29.3	30.0	30.4	30.3	29.6	28.1	25.0	21.8
	5%	WB		17.6	18.9	22.5	24.2	26.1	27.0	27.1	27.0	26.6	25.1	22.4	18.6
		MCDB		19.4	20.5	24.1	26.3	28.8	29.8	30.3	30.0	29.3	27.6	24.6	21.0
	10%	WB		16.8	18.0	21.5	23.8	25.7	26.7	26.9	26.7	26.2	24.6	21.8	17.8
		MCDB		18.7	19.2	23.1	25.9	28.2	29.4	30.0	29.6	29.0	27.2	24.2	20.4
Mean Daily Temperature Range		MDBR		3.5	3.1	3.4	3.3	3.3	3.0	3.5	3.5	3.4	3.2	3.5	3.8
	5% DB	MCDBR		4.1	4.6	4.3	4.2	4.0	3.6	4.1	4.3	4.2	3.7	3.6	4.1
		MCWBR		2.7	3.1	2.6	2.2	1.7	1.3	1.3	1.6	1.8	1.9	2.2	2.4
	5% WB	MCDBR		3.5	4.2	4.0	4.0	3.6	3.3	3.6	3.9	3.7	3.2	3.1	3.6
		MCWBR		2.7	3.2	3.0	2.4	1.9	1.4	1.5	1.6	1.6	1.5	2.2	2.6
Clear Sky Solar Irradiance	taub			0.631	0.658	0.766	0.775	0.701	0.659	0.617	0.682	0.741	0.725	0.621	0.604
	taud			1.519	1.499	1.395	1.410	1.530	1.612	1.693	1.568	1.467	1.469	1.591	1.581
	Ebn,noon			636	656	611	617	662	685	714	670	619	599	641	638
	Edh,noon			256	279	324	327	289	264	244	276	297	281	236	233

B.1 Summary Weather Data of Hong Kong from ASHRAE (Cont'd)

CDD*n*	Cooling degree-days base n°C, °C-day	Lat	Latitude, °	Period	Years used to calculate the design conditions
CDH*n*	Cooling degree-hours base n°C, °C-hour	Long	Longitude, °	Sd	Standard deviation of daily average temperature, °C
DB	Dry bulb temperature, °C	MCDB	Mean coincident dry bulb temperature, °C	StdP	Standard pressure at station elevation, kPa
DP	Dew point temperature, °C	MCDBR	Mean coincident dry bulb temp. range, °C	taub	Clear sky optical depth for beam irradiance
Ebn,noon	} Clear sky beam normal and diffuse hori-	MCDP	Mean coincident dew point temperature, °C	taud	Clear sky optical depth for diffuse irradiance
Edh,noon	} zontal irradiances at solar noon, W/m2	MCWB	Mean coincident wet bulb temperature, °C	Tavg	Average temperature, °C
Elev	Elevation, m	MCWBR	Mean coincident wet bulb temp. range, °C	Time Zone	Hours ahead or behind UTC, and time zone code
Enth	Enthalpy, kJ/kg	MCWS	Mean coincident wind speed, m/s	WB	Wet bulb temperature, °C
HDD*n*	Heating degree-days base n°C, °C-day	MDBR	Mean dry bulb temp. range, °C	WBAN	Weather Bureau Army Navy number
Hours 8/4 & 12.8/20.6	Number of hours between 8 a.m. and 4 p.m with DB between 12.8 and 20.6 °C	PCWD	Prevailing coincident wind direction, °, 0 = North, 90 = East	WMO#	World Meteorological Organization number
HR	Humidity ratio, g of moisture per kg of dry air			WS	Wind speed, m/s

B.2 Clear Sky Total Solar Irradiance Upon Vertical and Horizontal Surfaces (W/m^2)

Month	**Jun**								
LST	N	NE	E	SE	S	SW	W	NW	Hori
6	21.7	37.4	36.8	20.5	9.9	9.9	9.9	9.9	18.8
7	168.4	352.2	367.9	202.9	62.4	62.4	62.4	62.4	171.6
8	245.3	541.3	592.5	359.1	114.1	111.2	111.2	111.2	379.9
9	268.7	589.4	666.1	441.1	160.1	151.4	151.4	151.4	585.1
10	268.1	542.7	621.7	448.5	197.5	182.1	182.1	182.1	758.4
11	260.4	438.3	494.1	390.7	223.7	204.4	202.7	208.7	881.3
12	254.8	306.3	318.3	283.6	236.7	229.9	228.4	232.8	942.4
13	255.4	228.8	223.3	225.8	235.4	305.6	351.9	330.8	936.3
14	261.8	203.9	199.8	199.8	219.9	405.3	521.6	459.8	863.6
15	269.1	177.3	177.3	177.3	191.6	452.4	636.8	556.3	730.6
16	266.9	144.9	144.9	144.9	152.5	432.0	662.6	589.0	550.0
17	236.5	103.1	103.1	103.1	105.1	336.3	564.2	519.2	341.6
18	146.0	52.8	52.8	52.8	52.8	168.5	310.4	300.1	137.5
19	6.0	3.4	3.4	3.4	3.4	5.6	9.1	9.3	6.1

B.2 Clear Sky Total Solar Irradiance Upon Vertical and Horizontal Surfaces (W/m^2) (Cont'd)

Month	**Jul**								
LST	N	NE	E	SE	S	SW	W	NW	Hori
6	5.0	8.2	8.4	5.4	3.1	3.1	3.1	3.1	5.6
7	131.7	310.0	340.6	199.2	52.9	52.1	52.1	52.1	141.0
8	200.1	515.5	597.9	384.3	106.1	100.7	100.7	100.7	351.9
9	213.8	565.8	684.5	482.5	153.3	140.9	140.9	140.9	564.8
10	205.3	515.8	643.2	498.0	192.1	171.9	171.9	171.9	747.1
11	213.4	405.8	512.6	442.1	241.1	196.7	193.1	193.8	878.9
12	222.5	267.1	329.2	331.8	273.3	223.2	216.3	216.0	947.7
13	222.5	215.8	216.0	223.0	273.2	333.0	331.1	268.5	947.4
14	213.3	193.6	193.0	196.4	240.7	442.9	514.1	407.0	878.0
15	205.4	171.7	171.7	171.7	191.7	498.2	644.1	516.6	745.6
16	213.9	140.6	140.6	140.6	152.9	482.0	684.4	565.9	562.9
17	199.8	100.3	100.3	100.3	105.6	383.0	596.3	514.4	349.8
18	130.7	51.6	51.6	51.6	52.4	197.1	337.2	307.1	139.2
19	4.6	2.9	2.9	2.9	2.9	4.9	7.6	7.4	5.2

B.2 Clear Sky Total Solar Irradiance Upon Vertical and Horizontal Surfaces (W/m^2) (Cont'd)

Month	**Aug**								
LST	N	NE	E	SE	S	SW	W	NW	Hori
6	0.8	1.3	1.5	1.1	0.6	0.5	0.5	0.5	1.2
7	64.0	189.7	235.6	163.1	45.2	40.9	40.9	40.9	96.4
8	112.6	411.2	546.5	411.7	112.9	97.7	97.7	97.7	305.5
9	157.5	473.2	668.8	553.6	216.0	144.2	144.2	144.2	524.4
10	189.2	427.6	643.7	592.8	312.5	179.5	179.5	179.5	712.8
11	209.7	319.0	517.8	546.4	385.0	217.1	203.1	203.1	848.2
12	219.5	233.4	334.0	435.9	422.8	303.1	229.4	218.3	917.2
13	219.0	216.3	226.2	286.8	420.7	449.5	354.4	234.8	913.4
14	208.1	201.2	201.2	213.3	379.0	554.5	534.1	332.0	837.2
15	186.5	176.4	176.4	176.4	303.5	593.1	651.7	435.9	695.6
16	153.6	139.9	139.9	139.9	205.3	544.0	663.8	472.7	502.9
17	110.1	92.3	92.3	92.3	106.0	390.9	523.7	396.6	282.6
18	55.2	34.7	34.7	34.7	38.2	133.9	194.6	158.0	78.6
19	20.8	10.9	10.9	10.9	11.5	35.0	55.1	48.1	24.3

B.2 Clear Sky Total Solar Irradiance Upon Vertical and Horizontal Surfaces (W/m^2) (Cont'd)

Month	**Sep**								
LST	N	NE	E	SE	S	SW	W	NW	Hori
6	0.0	0.0	0.0	0.0	0.0	0.0	0.0	0.0	0.0
7	32.4	99.6	145.6	120.6	47.2	29.7	29.7	29.7	63.4
8	95.2	292.9	471.5	423.4	188.7	92.3	92.3	92.3	261.7
9	143.5	346.1	612.9	607.5	334.2	143.5	143.5	143.5	475.7
10	181.2	297.5	597.1	668.4	456.5	193.0	181.2	181.2	657.9
11	205.4	226.6	476.1	629.6	541.4	276.2	205.4	205.4	784.4
12	216.0	218.7	298.5	518.9	580.1	438.6	236.6	216.0	841.9
13	212.9	212.9	221.2	366.3	568.7	576.0	383.0	223.2	824.9
14	196.1	196.1	196.1	219.8	508.3	657.8	540.7	244.2	735.1
15	165.8	165.8	165.8	170.2	405.1	654.7	620.3	329.1	581.2
16	123.1	122.0	122.0	122.0	270.1	540.6	571.6	337.7	380.8
17	68.4	64.9	64.9	64.9	121.3	296.6	343.7	222.4	165.2
18	5.6	5.0	5.0	5.0	6.5	13.0	15.9	11.7	9.2
19	0.0	0.0	0.0	0.0	0.0	0.0	0.0	0.0	0.0

B.2 Clear Sky Total Solar Irradiance Upon Vertical and Horizontal Surfaces (W/m^2) (Cont'd)

Month	**Oct**								
LST	N	NE	E	SE	S	SW	W	NW	Hori
6	0.0	0.0	0.0	0.0	0.0	0.0	0.0	0.0	0.0
7	19.1	47.5	80.5	76.6	39.7	19.1	19.1	19.1	38.0
8	79.9	198.6	394.5	408.1	227.9	79.9	79.9	79.9	215.2
9	130.3	233.0	541.0	621.5	409.3	137.8	130.3	130.3	415.7
10	166.9	188.8	530.1	697.7	551.1	204.2	166.9	166.9	585.5
11	189.6	195.2	416.3	666.3	643.4	365.2	190.0	189.6	699.8
12	198.3	198.3	249.3	558.9	680.0	522.4	222.0	198.3	745.8
13	193.2	193.2	198.4	407.8	658.4	644.3	376.1	195.1	718.7
14	174.1	174.1	174.1	244.8	580.3	698.6	508.3	191.7	621.3
15	141.2	141.2	141.2	152.6	450.6	653.5	551.1	225.4	464.2
16	94.4	94.4	94.4	94.7	278.1	478.2	450.8	218.8	268.3
17	35.0	35.0	35.0	35.0	83.4	162.7	167.6	93.9	76.2
18	4.0	3.9	3.9	3.9	6.5	12.3	13.6	8.8	8.8
19	0.0	0.0	0.0	0.0	0.0	0.0	0.0	0.0	0.0

B.2 Clear Sky Total Solar Irradiance Upon Vertical and Horizontal Surfaces (W/m^2) (Cont'd)

Month	**Nov**								
LST	N	NE	E	SE	S	SW	W	NW	Hori
6	0.0	0.0	0.0	0.0	0.0	0.0	0.0	0.0	0.0
7	9.0	16.7	29.2	30.0	18.3	9.0	9.0	9.0	16.7
8	63.3	141.7	341.8	384.1	234.2	65.2	63.3	63.3	168.5
9	109.6	162.6	502.9	629.9	445.0	121.2	109.6	109.6	359.6
10	143.4	155.2	498.4	722.0	602.2	230.3	143.4	143.4	525.2
11	164.6	164.8	388.9	699.6	702.4	395.2	165.3	164.6	638.3
12	173.1	173.1	224.7	597.4	742.8	553.5	192.5	173.1	685.1
13	168.7	168.7	174.2	447.6	721.8	674.3	340.6	168.7	660.7
14	151.5	151.5	151.5	281.5	640.3	725.6	472.4	159.5	567.6
15	121.7	121.7	121.7	138.2	500.9	673.8	516.3	149.2	416.6
16	79.3	79.3	79.3	83.4	306.5	481.1	414.8	160.5	229.3
17	25.6	25.6	25.6	25.6	73.5	127.6	120.8	59.2	53.2
18	0.0	0.0	0.0	0.0	0.0	0.0	0.0	0.0	0.0
19	0.0	0.0	0.0	0.0	0.0	0.0	0.0	0.0	0.0

B.2 Clear Sky Total Solar Irradiance Upon Vertical and Horizontal Surfaces (W/m^2) (Cont'd)

Month	**Dec**								
LST	N	NE	E	SE	S	SW	W	NW	Hori
6	0.0	0.0	0.0	0.0	0.0	0.0	0.0	0.0	0.0
7	1.2	2.0	3.4	3.5	2.2	1.2	1.2	1.2	2.8
8	51.8	116.0	275.7	308.5	187.3	53.2	51.8	51.8	127.5
9	101.1	158.1	483.0	599.9	417.3	111.2	101.1	101.1	318.4
10	137.8	150.7	508.7	724.8	591.2	210.2	137.8	137.8	492.6
11	161.6	163.1	416.4	724.5	706.0	375.0	161.6	161.6	617.9
12	172.7	172.7	259.1	635.8	759.5	538.4	187.9	172.7	678.6
13	170.7	170.7	179.9	492.0	750.2	669.2	309.7	170.7	667.9
14	155.9	155.9	155.9	325.0	678.3	735.3	452.6	160.7	587.1
15	128.3	128.3	128.3	165.7	545.8	702.7	516.1	144.4	445.1
16	87.8	87.8	87.8	94.4	354.6	532.6	443.5	157.7	261.4
17	35.2	35.2	35.2	35.5	113.4	191.5	175.8	79.9	77.4
18	14.2	14.2	14.2	14.2	37.6	69.5	68.7	36.0	31.6
19	0.0	0.0	0.0	0.0	0.0	0.0	0.0	0.0	0.0

B.3 Incident Angles (Degree) of Direct Solar Radiation upon Surfaces Facing Principle Directions

Month	**Jun**								
LST	N	NE	E	SE	S	SW	W	NW	Hori
6	66.2	21.4	24.1	68.9	113.8	158.6	155.9	111.1	86.6
7	71.8	30.4	24.9	65.1	108.2	149.6	155.1	114.9	73.7
8	77.0	41.1	32.9	64.2	103.0	138.9	147.1	115.8	60.4
9	81.5	52.4	44.3	66.3	98.5	127.6	135.7	113.7	46.9
10	85.1	63.7	57.2	71.2	94.9	116.3	122.8	108.8	33.3
11	87.6	74.7	70.6	78.2	92.4	105.3	109.4	101.8	19.5
12	88.9	85.2	84.3	86.8	91.1	94.8	95.7	93.2	5.8
13	88.7	94.8	98.1	96.6	91.3	85.2	81.9	83.4	8.2
14	87.3	103.2	111.8	107.2	92.7	76.8	68.2	72.8	22.0
15	84.6	109.9	125.2	118.3	95.4	70.1	54.8	61.7	35.7
16	80.8	114.2	137.9	129.6	99.2	65.8	42.1	50.4	49.3
17	76.1	115.8	148.9	140.9	103.9	64.2	31.1	39.1	62.8
18	70.8	114.4	155.9	151.4	109.2	65.6	24.1	28.6	76.0
19	65.2	110.2	155.1	159.8	114.8	69.8	24.9	20.2	88.9

B.3 Incident Angles (Degree) of Direct Solar Radiation upon Surfaces Facing Principle Directions (Cont'd)

Month	**Jul**								
LST	N	NE	E	SE	S	SW	W	NW	Hori
6	69.7	24.7	20.3	65.3	110.3	155.3	159.7	114.7	89.4
7	75.3	32.6	20.4	61.1	104.7	147.4	159.6	118.9	76.2
8	80.6	42.9	29.2	59.9	99.4	137.1	150.8	120.1	62.7
9	85.3	54.0	41.4	61.8	94.7	126.0	138.6	118.2	48.9
10	89.1	65.3	54.9	66.7	90.9	114.7	125.1	113.3	35.1
11	91.8	76.5	68.8	73.9	88.2	103.5	111.2	106.1	21.2
12	93.2	87.3	83.0	82.8	86.8	92.7	97.0	97.2	7.7
13	93.1	97.3	97.2	92.8	86.9	82.7	82.8	87.2	7.8
14	91.8	106.2	111.3	103.6	88.2	73.8	68.7	76.4	21.4
15	89.1	113.3	125.2	114.8	90.9	66.7	54.8	65.2	35.2
16	85.3	118.2	138.7	126.1	94.7	61.8	41.3	53.9	49.1
17	80.6	120.1	150.9	137.2	99.4	59.9	29.1	42.8	62.8
18	75.3	118.9	159.7	147.5	104.7	61.1	20.3	32.5	76.3
19	69.6	114.6	159.6	155.4	110.4	65.4	20.4	24.6	89.5

B.3 Incident Angles (Degree) of Direct Solar Radiation upon Surfaces Facing Principle Directions (Cont'd)

Month	**Aug**								
LST	N	NE	E	SE	S	SW	W	NW	Hori
6	79.0	34.1	11.4	56.1	101.0	145.9	168.6	123.9	90.0
7	84.6	40.8	12.3	51.3	95.4	139.2	167.7	128.7	78.9
8	90.0	50.1	24.9	50.1	90.0	129.9	155.1	129.9	65.1
9	94.9	60.8	39.2	52.6	85.1	119.2	140.8	127.4	51.2
10	98.8	72.0	53.8	58.3	81.2	108.0	126.2	121.7	37.6
11	101.6	83.3	68.6	66.4	78.4	96.7	111.4	113.6	24.6
12	103.0	94.4	83.4	76.1	77.0	85.6	96.6	103.9	14.6
13	102.9	105.0	98.2	86.7	77.1	75.0	81.8	93.3	15.3
14	101.4	114.5	113.0	97.9	78.6	65.5	67.0	82.1	25.9
15	98.4	122.4	127.7	109.2	81.6	57.6	52.3	70.8	39.0
16	94.4	127.9	142.3	120.3	85.6	52.1	37.7	59.7	52.7
17	89.5	130.0	156.5	130.9	90.5	50.0	23.5	49.1	66.5
18	84.1	128.3	168.6	140.0	95.9	51.7	11.4	40.0	80.4
19	78.4	123.3	167.7	146.4	101.6	56.7	12.3	33.6	90.0

B.3 Incident Angles (Degree) of Direct Solar Radiation upon Surfaces Facing Principle Directions (Cont'd)

Month	**Sep**								
LST	N	NE	E	SE	S	SW	W	NW	Hori
6	91.5	46.7	5.2	43.8	88.5	133.3	174.8	136.2	90.0
7	97.1	52.7	11.4	38.6	82.9	127.3	168.6	141.4	81.2
8	102.6	61.3	26.1	37.9	77.4	118.7	153.9	142.1	67.6
9	107.5	71.3	41.0	41.7	72.5	108.7	139.0	138.3	54.3
10	111.5	82.1	56.0	49.1	68.5	97.9	124.0	130.9	42.0
11	114.2	93.4	70.9	58.6	65.8	86.6	109.1	121.4	31.7
12	115.5	104.7	85.9	69.2	64.5	75.3	94.1	110.8	25.9
13	115.1	115.7	100.9	80.4	64.9	64.3	79.1	99.6	27.7
14	113.2	125.9	115.8	91.7	66.8	54.1	64.2	88.3	36.0
15	109.8	134.6	130.8	102.9	70.2	45.4	49.2	77.1	47.4
16	105.4	140.5	145.8	113.4	74.6	39.5	34.2	66.6	60.2
17	100.2	142.4	160.6	122.8	79.8	37.6	19.4	57.2	73.7
18	94.6	139.5	174.8	130.4	85.4	40.5	5.2	49.6	87.4
19	88.9	132.8	168.6	135.0	91.1	47.2	11.4	45.0	90.0

B.3 Incident Angles (Degree) of Direct Solar Radiation upon Surfaces Facing Principle Directions (Cont'd)

Month	**Oct**								
LST	N	NE	E	SE	S	SW	W	NW	Hori
6	102.6	58.0	14.6	33.0	77.4	122.0	165.4	147.0	90.0
7	108.3	63.6	19.4	27.3	71.7	116.4	160.6	152.7	83.8
8	113.8	71.4	31.3	27.2	66.2	108.6	148.7	152.8	70.9
9	118.8	80.8	44.9	32.8	61.2	99.2	135.1	147.2	58.9
10	122.9	91.2	59.2	41.8	57.1	88.8	120.8	138.2	48.3
11	125.6	102.2	73.6	52.3	54.4	77.8	106.4	127.7	40.3
12	126.7	113.5	88.1	63.5	53.3	66.5	91.9	116.5	36.8
13	126.1	124.8	102.6	74.8	53.9	55.2	77.4	105.2	38.9
14	123.7	135.6	117.1	86.0	56.3	44.4	62.9	94.0	45.9
15	119.9	145.1	131.4	96.6	60.1	34.9	48.6	83.4	55.9
16	115.2	151.8	145.3	106.3	64.8	28.2	34.7	73.7	67.7
17	109.7	153.4	157.9	114.6	70.3	26.6	22.1	65.4	80.4
18	104.1	148.9	165.4	120.8	75.9	31.1	14.6	59.2	90.0
19	98.5	140.5	160.6	124.2	81.5	39.5	19.4	55.8	90.0

B.3 Incident Angles (Degree) of Direct Solar Radiation upon Surfaces Facing Principle Directions (Cont'd)

Month	**Nov**								
LST	N	NE	E	SE	S	SW	W	NW	Hori
6	109.3	65.0	22.0	27.2	70.7	115.0	158.0	152.8	90.0
7	115.0	70.0	25.1	20.2	65.0	110.0	154.9	159.8	87.4
8	120.5	77.2	34.7	19.8	59.5	102.8	145.3	160.2	75.1
9	125.7	86.0	46.9	26.4	54.3	94.0	133.1	153.6	63.9
10	130.0	95.9	60.2	36.3	50.0	84.1	119.8	143.7	54.3
11	132.9	106.6	73.9	47.3	47.1	73.4	106.1	132.7	47.3
12	134.2	117.7	87.8	58.7	45.8	62.3	92.2	121.3	44.3
13	133.5	129.1	101.7	69.9	46.5	50.9	78.3	110.1	45.9
14	131.1	140.2	115.5	80.8	48.9	39.8	64.5	99.2	51.7
15	127.2	150.6	128.9	91.0	52.8	29.4	51.1	89.0	60.6
16	122.2	158.6	141.6	100.2	57.8	21.4	38.4	79.8	71.4
17	116.8	160.8	152.3	107.9	63.2	19.2	27.7	72.1	83.4
18	111.1	155.5	158.0	113.7	68.9	24.5	22.0	66.3	90.0
19	105.5	146.1	154.9	116.8	74.5	33.9	25.1	63.2	90.0

B.3 Incident Angles (Degree) of Direct Solar Radiation upon Surfaces Facing Principle Directions (Cont'd)

Month	**Dec**								
LST	N	NE	E	SE	S	SW	W	NW	Hori
6	109.4	65.6	23.7	28.1	70.6	114.4	156.3	151.9	90.0
7	115.0	70.0	25.0	20.0	65.0	110.0	155.0	160.0	90.0
8	120.7	76.7	33.4	18.0	59.3	103.3	146.6	162.0	78.1
9	125.9	85.1	45.0	23.8	54.1	94.9	135.0	156.2	66.8
10	130.4	94.8	57.9	33.5	49.6	85.2	122.1	146.5	57.0
11	133.7	105.3	71.4	44.4	46.3	74.7	108.6	135.6	49.6
12	135.3	116.3	85.1	55.8	44.7	63.7	94.9	124.2	45.8
13	135.1	127.6	98.9	67.0	44.9	52.4	81.1	113.0	46.4
14	132.9	138.9	112.6	77.9	47.1	41.1	67.4	102.1	51.4
15	129.2	149.6	126.0	88.2	50.8	30.4	54.0	91.8	59.7
16	124.4	158.5	138.6	97.5	55.6	21.5	41.4	82.5	70.0
17	119.0	162.3	149.6	105.5	61.0	17.7	30.4	74.5	81.6
18	113.3	158.0	156.3	111.6	66.7	22.0	23.7	68.4	90.0
19	107.8	148.9	155.0	115.2	72.2	31.1	25.0	64.8	90.0

B.4.1 Solar Heat Gain Factors for Transmitted Solar Heat Gain

Month	Jun								
	TSHGF	(W/m2)							
LST	N	NE	E	SE	S	SW	W	NW	Hori
6	16.95	30.94	30.44	15.86	7.93	7.93	7.93	7.93	14.43
7	122.28	297.02	311.37	156.91	49.83	49.83	49.83	49.83	123.02
8	167.60	451.20	498.82	279.43	91.14	88.88	88.88	88.88	302.27
9	178.73	481.87	552.39	338.22	127.96	120.99	120.99	120.99	484.89
10	183.13	424.35	501.29	329.66	157.82	145.52	145.52	145.52	641.58
11	188.89	311.01	365.64	268.18	178.75	163.30	161.97	166.75	752.31
12	193.38	211.07	217.17	201.51	189.13	183.70	182.52	186.02	802.12
13	192.88	182.82	178.45	180.38	188.10	210.42	237.54	224.04	797.47
14	187.81	162.93	159.63	159.63	175.73	281.54	394.58	332.92	736.85
15	182.28	141.70	141.70	141.70	153.06	335.83	517.24	440.03	616.13
16	177.73	115.77	115.77	115.77	121.81	332.73	551.26	483.61	453.65
17	163.14	82.36	82.36	82.36	83.95	261.78	475.83	433.96	268.23
18	107.28	42.20	42.20	42.20	42.20	129.88	262.59	253.27	96.73
19	4.74	2.69	2.69	2.69	2.69	4.39	7.36	7.55	4.89

B.4.1 Solar Heat Gain Factors for Transmitted Solar Heat Gain (Cont'd)

Month	Jul								
	TSHGF	(W/m2)							
LST	N	NE	E	SE	S	SW	W	NW	Hori
6	3.99	6.59	6.75	4.28	2.48	2.48	2.48	2.48	4.51
7	90.86	261.44	289.17	157.95	42.27	41.64	41.64	41.64	97.78
8	130.09	429.55	506.23	306.63	84.75	80.44	80.44	80.44	276.23
9	142.93	461.24	571.06	381.04	122.50	112.57	112.57	112.57	466.92
10	156.20	398.28	522.76	380.20	153.46	137.38	137.38	137.38	631.91
11	170.52	280.23	384.46	314.28	177.16	157.13	154.31	154.86	751.79
12	177.77	190.41	219.86	221.47	192.48	178.36	172.81	172.59	808.73
13	177.74	172.44	172.60	178.19	192.40	222.24	221.00	190.81	808.48
14	170.42	154.68	154.19	156.91	176.96	315.11	386.07	281.36	750.96
15	156.05	137.18	137.18	137.18	153.21	380.54	523.65	399.21	630.54
16	142.83	112.30	112.30	112.30	122.18	380.70	571.04	461.42	465.24
17	129.92	80.11	80.11	80.11	84.38	305.58	504.97	428.69	274.39
18	90.21	41.25	41.25	41.25	41.86	156.26	286.35	259.06	96.44
19	3.65	2.28	2.28	2.28	2.28	3.89	6.11	5.97	4.14

B.4.1 Solar Heat Gain Factors for Transmitted Solar Heat Gain (Cont'd)

Month	Aug TSHGF	(W/m2)							
LST	N	NE	E	SE	S	SW	W	NW	Hori
6	0.61	1.07	1.22	0.85	0.45	0.42	0.42	0.42	0.94
7	43.72	157.64	198.55	133.45	36.11	32.68	32.68	32.68	67.65
8	89.94	337.75	462.13	338.18	90.01	78.06	78.06	78.06	236.48
9	125.85	376.00	558.04	452.20	147.13	115.22	115.22	115.22	430.46
10	151.19	312.31	524.07	476.09	210.68	143.41	143.41	143.41	598.92
11	167.53	216.61	391.10	419.89	264.82	173.49	162.29	162.29	722.08
12	175.42	186.47	227.50	306.69	294.83	211.11	183.29	174.41	781.63
13	175.00	172.81	180.72	204.08	293.14	319.44	240.53	187.61	778.52
14	166.24	160.79	160.79	170.42	260.17	428.92	408.39	224.67	712.20
15	149.01	140.93	140.93	140.93	204.30	477.53	532.44	321.98	583.32
16	122.69	111.82	111.82	111.82	140.76	444.79	554.96	377.52	411.38
17	85.59	73.75	73.75	73.75	84.69	321.10	443.05	326.38	216.49
18	37.83	27.74	27.74	27.74	30.51	109.39	163.75	131.26	55.28
19	14.96	8.73	8.73	8.73	9.21	28.19	45.85	39.79	19.41

B.4.1 Solar Heat Gain Factors for Transmitted Solar Heat Gain (Cont'd)

Month	Sep								
	TSHGF	(W/m2)							
LST	N	NE	E	SE	S	SW	W	NW	Hori
6	0.00	0.00	0.00	0.00	0.00	0.00	0.00	0.00	0.00
7	25.86	80.96	121.75	99.85	33.21	23.76	23.76	23.76	45.77
8	76.06	232.33	397.00	352.95	131.20	73.76	73.76	73.76	199.81
9	114.64	255.64	509.03	504.07	243.97	114.64	114.64	114.64	386.89
10	144.76	203.50	482.90	548.58	345.94	154.20	144.76	144.76	547.76
11	164.09	181.04	353.83	504.90	418.90	197.92	164.09	164.09	661.97
12	172.56	174.71	211.46	391.47	452.47	313.48	189.02	172.56	713.97
13	170.08	170.08	176.72	252.54	442.54	449.79	265.63	178.36	698.71
14	156.68	156.68	156.68	175.65	390.29	534.51	422.48	182.61	617.20
15	132.46	132.46	132.46	135.95	302.47	540.45	509.17	230.19	479.72
16	98.38	97.46	97.46	97.46	192.88	449.85	478.36	259.32	303.38
17	54.68	51.88	51.88	51.88	83.21	247.11	289.47	179.19	120.59
18	4.48	4.00	4.00	4.00	5.04	10.52	12.89	9.46	7.26
19	0.00	0.00	0.00	0.00	0.00	0.00	0.00	0.00	0.00

B.4.1 Solar Heat Gain Factors for Transmitted Solar Heat Gain (Cont'd)

Month	Oct								
	TSHGF	(W/m2)							
LST	N	NE	E	SE	S	SW	W	NW	Hori
6	0.00	0.00	0.00	0.00	0.00	0.00	0.00	0.00	0.00
7	15.30	37.45	66.92	63.60	29.96	15.30	15.30	15.30	28.29
8	63.85	146.37	331.00	343.38	175.51	63.85	63.85	63.85	160.14
9	104.14	158.28	447.18	521.08	324.69	110.14	104.14	104.14	333.10
10	133.34	150.82	424.24	578.93	444.23	154.91	133.34	133.34	482.61
11	151.45	156.01	301.21	543.69	522.54	254.33	151.78	151.45	584.28
12	158.47	158.47	185.24	438.24	553.67	402.02	177.34	158.47	625.75
13	154.35	154.35	158.54	291.62	535.35	522.20	262.87	155.88	601.28
14	139.13	139.13	139.13	172.12	468.92	577.62	399.76	153.20	514.29
15	112.82	112.82	112.82	121.92	359.32	546.71	452.97	153.48	375.82
16	75.40	75.40	75.40	75.65	216.18	402.32	377.19	157.46	204.59
17	27.94	27.94	27.94	27.94	62.76	136.14	140.51	73.00	54.73
18	3.23	3.15	3.15	3.15	5.07	10.01	11.06	7.06	7.00
19	0.00	0.00	0.00	0.00	0.00	0.00	0.00	0.00	0.00

B.4.1 Solar Heat Gain Factors for Transmitted Solar Heat Gain (Cont'd)

Month	Nov								
	TSHGF	(W/m2)							
LST	N	NE	E	SE	S	SW	W	NW	Hori
6	0.00	0.00	0.00	0.00	0.00	0.00	0.00	0.00	0.00
7	7.22	12.97	23.91	24.61	14.41	7.22	7.22	7.22	13.11
8	50.57	96.73	286.97	325.26	187.25	52.09	50.57	50.57	119.33
9	87.59	110.42	415.75	533.17	362.32	96.85	87.59	87.59	280.34
10	114.61	124.03	397.03	605.47	495.00	153.16	114.61	114.61	428.05
11	131.54	131.67	276.36	577.63	580.19	282.42	132.06	131.54	528.63
12	138.29	138.29	162.37	479.14	614.65	436.32	153.82	138.29	570.50
13	134.79	134.79	139.21	332.30	596.75	553.04	230.92	134.79	548.65
14	121.08	121.08	121.08	186.83	527.35	605.80	367.02	127.47	465.78
15	97.25	97.25	97.25	110.42	409.34	569.18	423.55	112.86	331.12
16	63.38	63.38	63.38	66.64	246.76	407.75	347.04	106.44	167.80
17	20.49	20.49	20.49	20.49	57.79	107.08	101.13	43.79	38.38
18	0.00	0.00	0.00	0.00	0.00	0.00	0.00	0.00	0.00
19	0.00	0.00	0.00	0.00	0.00	0.00	0.00	0.00	0.00

B.4.1 Solar Heat Gain Factors for Transmitted Solar Heat Gain (Cont'd)

Month	Dec								
	TSHGF	(W/m2)							
LST	N	NE	E	SE	S	SW	W	NW	Hori
6	0.00	0.00	0.00	0.00	0.00	0.00	0.00	0.00	0.00
7	0.99	1.63	2.69	2.76	1.76	0.99	0.99	0.99	2.21
8	41.41	80.09	231.48	260.88	149.83	42.52	41.41	41.41	88.86
9	80.81	105.55	400.59	508.37	339.94	88.82	80.81	80.81	242.93
10	110.09	120.43	409.25	609.89	486.48	141.30	110.09	110.09	397.94
11	129.16	130.33	303.96	600.96	584.02	263.65	129.16	129.16	509.58
12	137.96	137.96	175.34	515.24	629.72	420.68	150.11	137.96	563.67
13	136.43	136.43	143.76	375.09	621.74	547.21	205.81	136.43	554.14
14	124.58	124.58	124.58	220.43	560.43	612.88	343.76	128.41	482.11
15	102.49	102.49	102.49	120.69	448.08	593.09	420.47	115.35	355.49
16	70.18	70.18	70.18	75.46	287.66	451.54	369.65	103.33	193.91
17	28.10	28.10	28.10	28.37	90.05	161.24	147.41	57.24	54.54
18	11.37	11.37	11.37	11.37	29.11	57.89	57.23	27.61	25.26
19	0.00	0.00	0.00	0.00	0.00	0.00	0.00	0.00	0.00

B.4.2 Solar Heat Gain Factors for Absorbed Solar Heat Gain

Month	Jun								
	Ni x ASHGF		(W/m2)						
LST	N	NE	E	SE	S	SW	W	NW	Hori
6	0.32	0.51	0.51	0.30	0.14	0.14	0.14	0.14	0.21
7	2.55	4.79	4.86	2.98	0.90	0.90	0.90	0.90	2.09
8	3.82	7.97	8.20	5.27	1.65	1.61	1.61	1.61	4.44
9	4.11	8.86	9.97	6.50	2.32	2.19	2.19	2.19	7.03
10	3.88	7.96	9.22	6.76	2.86	2.63	2.63	2.63	8.34
11	3.64	6.74	7.42	6.05	3.24	2.96	2.93	3.02	9.06
12	3.58	4.42	4.66	4.00	3.42	3.33	3.30	3.37	10.19
13	3.59	3.31	3.23	3.27	3.41	4.41	5.33	4.92	10.03
14	3.67	2.95	2.89	2.89	3.18	6.28	7.73	6.99	8.89
15	3.93	2.57	2.57	2.57	2.77	6.78	9.51	8.16	8.21
16	4.11	2.10	2.10	2.10	2.21	6.35	9.82	8.89	6.62
17	3.68	1.49	1.49	1.49	1.52	4.93	7.71	7.55	3.98
18	2.20	0.76	0.76	0.76	0.76	2.48	4.09	4.04	1.68
19	0.09	0.05	0.05	0.05	0.05	0.08	0.13	0.13	0.07

B.4.2 Solar Heat Gain Factors for Absorbed Solar Heat Gain (Cont'd)

Month	Jul								
	Ni x ASHGF		(W/m2)						
LST	N	NE	E	SE	S	SW	W	NW	Hori
6	0.07	0.12	0.12	0.08	0.04	0.04	0.04	0.04	0.06
7	2.05	4.28	4.45	2.93	0.77	0.75	0.75	0.75	1.74
8	3.11	7.68	8.03	5.67	1.53	1.46	1.46	1.46	4.11
9	3.08	8.49	10.11	7.08	2.22	2.04	2.04	2.04	6.82
10	2.88	7.58	9.62	7.35	2.78	2.49	2.49	2.49	8.34
11	3.09	6.30	7.63	6.79	3.36	2.84	2.79	2.80	9.00
12	3.22	3.74	4.93	4.99	3.85	3.23	3.13	3.12	10.15
13	3.22	3.12	3.13	3.23	3.84	5.01	4.97	3.76	10.14
14	3.09	2.80	2.79	2.84	3.36	6.80	7.65	6.32	8.99
15	2.88	2.48	2.48	2.48	2.77	7.35	9.64	7.59	8.33
16	3.08	2.03	2.03	2.03	2.21	7.08	10.10	8.50	6.79
17	3.10	1.45	1.45	1.45	1.53	5.65	8.00	7.66	4.08
18	2.03	0.75	0.75	0.75	0.76	2.90	4.40	4.24	1.72
19	0.07	0.04	0.04	0.04	0.04	0.07	0.11	0.11	0.06

B.4.2 Solar Heat Gain Factors for Absorbed Solar Heat Gain (Cont'd)

Month	Aug								
	Ni x ASHGF		(W/m2)						
LST	N	NE	E	SE	S	SW	W	NW	Hori
6	0.01	0.02	0.02	0.02	0.01	0.01	0.01	0.01	0.01
7	0.93	2.79	3.17	2.45	0.65	0.59	0.59	0.59	1.17
8	1.63	6.20	7.23	6.21	1.63	1.41	1.41	1.41	3.57
9	2.28	6.95	9.73	8.32	3.12	2.09	2.09	2.09	6.30
10	2.74	6.47	9.64	8.76	4.77	2.60	2.60	2.60	8.14
11	3.03	4.74	7.68	8.04	5.95	3.14	2.94	2.94	8.81
12	3.18	3.38	4.96	6.72	6.53	4.35	3.32	3.16	9.57
13	3.17	3.13	3.27	4.05	6.50	6.91	5.37	3.40	9.51
14	3.01	2.91	2.91	3.09	5.86	8.14	7.88	5.01	8.74
15	2.70	2.55	2.55	2.55	4.62	8.78	9.79	6.55	8.03
16	2.22	2.02	2.02	2.02	2.94	8.18	9.55	6.96	6.02
17	1.56	1.34	1.34	1.34	1.53	5.90	6.90	5.99	3.31
18	0.81	0.50	0.50	0.50	0.55	2.01	2.64	2.31	0.95
19	0.32	0.16	0.16	0.16	0.17	0.52	0.76	0.68	0.28

B.4.2 Solar Heat Gain Factors for Absorbed Solar Heat Gain (Cont'd)

Month	Sep								
	Ni x ASHGF		(W/m2)						
LST	N	NE	E	SE	S	SW	W	NW	Hori
6	0.00	0.00	0.00	0.00	0.00	0.00	0.00	0.00	0.00
7	0.47	1.48	1.99	1.75	0.70	0.43	0.43	0.43	0.75
8	1.38	4.30	6.30	6.10	2.92	1.34	1.34	1.34	3.07
9	2.08	5.21	9.01	8.96	5.06	2.08	2.08	2.08	5.65
10	2.62	4.48	8.87	10.05	6.76	2.79	2.62	2.62	7.74
11	2.97	3.28	7.14	9.28	7.95	3.91	2.97	2.97	8.54
12	3.12	3.16	4.27	7.71	8.50	6.72	3.42	3.12	8.83
13	3.08	3.08	3.20	5.59	8.33	8.43	5.88	3.23	8.74
14	2.84	2.84	2.84	3.18	7.48	9.82	7.92	3.43	8.29
15	2.40	2.40	2.40	2.46	6.05	9.80	9.33	5.08	6.97
16	1.78	1.76	1.76	1.76	4.14	7.87	8.02	4.97	4.45
17	0.99	0.94	0.94	0.94	1.86	4.27	4.56	3.29	1.99
18	0.08	0.07	0.07	0.07	0.09	0.19	0.23	0.17	0.11
19	0.00	0.00	0.00	0.00	0.00	0.00	0.00	0.00	0.00

B.4.2 Solar Heat Gain Factors for Absorbed Solar Heat Gain (Cont'd)

Month	Oct								
	Ni x ASHGF		(W/m2)						
LST	N	NE	E	SE	S	SW	W	NW	Hori
6	0.00	0.00	0.00	0.00	0.00	0.00	0.00	0.00	0.00
7	0.28	0.69	1.09	1.05	0.59	0.28	0.28	0.28	0.44
8	1.16	2.99	5.43	5.48	3.35	1.16	1.16	1.16	2.56
9	1.89	3.56	8.09	8.63	6.00	1.99	1.89	1.89	4.87
10	2.41	2.73	7.81	10.30	8.16	2.87	2.41	2.41	7.02
11	2.74	2.82	6.34	9.99	9.60	5.63	2.75	2.74	8.16
12	2.87	2.87	3.50	8.18	10.17	7.68	3.21	2.87	8.47
13	2.79	2.79	2.87	6.25	9.83	9.59	5.80	2.82	8.29
14	2.52	2.52	2.52	3.49	8.61	10.43	7.44	2.77	7.43
15	2.04	2.04	2.04	2.21	6.62	9.22	8.29	3.35	5.49
16	1.37	1.37	1.37	1.37	4.08	6.45	6.35	3.34	3.15
17	0.51	0.51	0.51	0.51	1.24	2.20	2.24	1.38	0.91
18	0.06	0.06	0.06	0.06	0.10	0.18	0.19	0.13	0.10
19	0.00	0.00	0.00	0.00	0.00	0.00	0.00	0.00	0.00

B.4.2 Solar Heat Gain Factors for Absorbed Solar Heat Gain (Cont'd)

Month	Nov								
	Ni x ASHGF		(W/m2)						
LST	N	NE	E	SE	S	SW	W	NW	Hori
6	0.00	0.00	0.00	0.00	0.00	0.00	0.00	0.00	0.00
7	0.13	0.24	0.41	0.42	0.27	0.13	0.13	0.13	0.19
8	0.92	2.21	4.80	5.04	3.45	0.94	0.92	0.92	2.06
9	1.59	2.31	7.58	8.36	6.67	1.75	1.59	1.59	4.19
10	2.08	2.25	7.33	10.28	9.09	3.39	2.08	2.08	6.27
11	2.38	2.38	5.97	10.55	10.59	6.05	2.39	2.38	7.68
12	2.50	2.50	3.13	8.82	11.17	8.12	2.78	2.50	8.17
13	2.44	2.44	2.52	6.70	10.87	10.17	5.30	2.44	7.93
14	2.19	2.19	2.19	4.34	9.67	10.60	6.93	2.31	6.82
15	1.76	1.76	1.76	2.00	7.53	9.09	7.79	2.09	4.87
16	1.15	1.15	1.15	1.21	4.54	6.30	6.00	2.49	2.75
17	0.37	0.37	0.37	0.37	1.07	1.70	1.64	0.89	0.62
18	0.00	0.00	0.00	0.00	0.00	0.00	0.00	0.00	0.00
19	0.00	0.00	0.00	0.00	0.00	0.00	0.00	0.00	0.00

B.4.2 Solar Heat Gain Factors for Absorbed Solar Heat Gain (Cont'd)

Month	Dec								
	Ni x ASHGF		(W/m2)						
LST	N	NE	E	SE	S	SW	W	NW	Hori
6	0.00	0.00	0.00	0.00	0.00	0.00	0.00	0.00	0.00
7	0.02	0.03	0.05	0.05	0.03	0.02	0.02	0.02	0.03
8	0.75	1.80	3.84	4.07	2.76	0.77	0.75	0.75	1.56
9	1.46	2.29	7.25	7.88	6.26	1.61	1.46	1.46	3.74
10	1.99	2.18	7.53	10.08	8.93	3.03	1.99	1.99	5.82
11	2.34	2.36	6.30	10.85	10.63	5.79	2.34	2.34	7.44
12	2.50	2.50	3.74	9.48	11.38	7.89	2.72	2.50	8.14
13	2.47	2.47	2.60	7.26	11.25	10.07	4.75	2.47	8.02
14	2.26	2.26	2.26	5.07	10.23	10.83	6.69	2.32	7.06
15	1.86	1.86	1.86	2.30	8.24	9.55	7.74	2.09	5.22
16	1.27	1.27	1.27	1.37	5.29	6.98	6.54	2.39	3.11
17	0.51	0.51	0.51	0.51	1.66	2.55	2.41	1.22	0.92
18	0.21	0.21	0.21	0.21	0.55	0.94	0.93	0.53	0.36
19	0.00	0.00	0.00	0.00	0.00	0.00	0.00	0.00	0.00